AS
36
P7X
NH

ISSN 0097-4463

ANNALS of CARNEGIE MUSEUM

SMITHSONIAN
FEB 1 6 19
LIBRARIES

THE CARNEGIE MUSEUM OF NATURAL HISTORY
4400 FORBES AVENUE • PITTSBURGH, PENNSYLVANIA 15213

VOLUME 68 11 FEBRUARY 1999 NUMBER 1

CONTENTS

ARTICLES

New karyotypes of shrews (Mammalia: Soricidae) from Cameroon and Somalia .... **Duane A. Schlitter, Rainer Hutterer, Tiziano Maddalena, and Lynn W. Robbins** 1

The head skeleton of *Amphisbaena alba* Linneaus .... **Ricardo Montero and Carl Gans** 15

Editors, ANNALS, BULLETIN and SPECIAL PUBLICATIONS:

J. L. Carter, Ph.D
B. C. Livezey, Ph.D
D. R. Watters, Ph.D
M. A. Schmidt, ELS, Assistant Editor

Manuscripts, subscriptions, orders for individual numbers, and changes of address should be sent to:

Office of Scientific Publications
Carnegie Museum of Natural History
4400 Forbes Avenue
Pittsburgh, PA 15213-4080
Phone (412) 622-3287
Fax (412) 622-8837
E-mail: scipubs@clpgh.org

ANNALS OF CARNEGIE MUSEUM is published quarterly by The Carnegie Museum of Natural History, 4400 Forbes Avenue, Pittsburgh, Pennsylvania 15213-4080, by the authority of the Board of Trustees of Carnegie Institute.

© 1999 Carnegie Institute.

♾ This paper meets the requirements of ANSI/NISO Z39.48-1992 (Permanence of Paper).

ANNALS OF CARNEGIE MUSEUM
Vol. 68, Number 1, Pp. 1–14 11 February 1999

NEW KARYOTYPES OF SHREWS (MAMMALIA: SORICIDAE) FROM CAMEROON AND SOMALIA

Duane A. Schlitter[1]
Curator, Section of Mammals

Rainer Hutterer[2]

Tiziano Maddalena[3]

Lynn W. Robbins[4]
Research Associate, Section of Mammals

Abstract

Chromosomal data are presented for 11 species of African shrews collected during field studies in Cameroon and Somalia. The karyotypes of *Sylvisorex johnstoni, S. isabellae, S. ollula, Crocidura attila, C. batesi, C. greenwoodi, C. parvipes, C. picea,* and *C. yankariensis* are reported for the first time. The karyotype of *Sylvisorex johnstoni* (2n = 30, FN = 38) represents one of the lowest and that of *Crocidura yankariensis* (2n = 68, FN = 122) the highest diploid numbers so far reported for an African shrew. The rare *Crocidura picea* has been rediscovered in the Cameroon highlands, from whence the species was known only by the holotype since 1940.

Key Words: *Sylvisorex, Crocidura,* shrews, Africa, karyotypes

Introduction

African shrews present a variety of problems taxonomically, with the diversity of species being of principal concern. Recent checklists of the African species in the genera *Sylvisorex* and *Crocidura* list ten and 104 species, respectively (Hutterer, 1993). In addition, most species are difficult to obtain in the field and maintain in a vivarium. Although comparisons of species using cytotaxonomic and biochemical techniques are desirable, they are generally unavailable. Karyotypic comparisons using differential staining methods are needed but have been difficult to obtain. For most species, even standard karyotypes are unknown.

Although standard karyotypes are of limited value in assessing chromosomal evolution and phylogenetic relationships within genera, these data may still be useful for clarifying some taxonomic issues (Baker et al., 1987), especially in detecting potential cryptic or sibling species, confirming species status, or determining general karyotypic trends.

---

[1] Current address: Executive Director, Museum Park, P. O. Box 30178, Sunnyside, Pretoria 0132, Republic of South Africa.

[2] Zoologisches Forschunginstitut und Museum Alexander Koenig, Adenauerallee 160, D-53113 Bonn, Germany.

[3] Institut de zoologie et d'ecologie animale, Université de Lausanne, CH-1005 Lausanne, Switzerland. Current address: CH-6672 Gordevio, Ticino, Switzerland.

[4] Department of Biology, Southwest Missouri State University, Springfield, Missouri 65804–0095.

Submitted 13 August 1996.

Table 1.—*Summary of karyotypic data for shrews occurring on the African continent, arranged by increasing diploid number. The nomenclature of the species as given in the original reports has been critically revised (Reumer and Meylan, 1986; Hutterer, 1993).*

Species	2n	FN	FNa	Reference—country
Crocidura				
canariensis	36	56	52	4[1]—Canary Is.
luna	36	56	52	6—Burundi
obscurior	36	56	—	6—Côte d'Ivoire
lusitania	38	74		6—Burkina
bottegi	40	60		10—Côte d'Ivoire
russula	42	60	56	4—Morocco
osorio	42	62	58	5—Canary Is.
nanilla	42	74		6—Côte d'Ivoire
ebriensis	44	66		10—Côte d'Ivoire
ebriensis	44	72		6—Côte d'Ivoire
crossei	44, 45	72, 73	68	6, 12—Côte d'Ivoire
grandiceps	46	68	64	12—Côte d'Ivoire
nigrofusca	48	78		6—Burundi
o. olivieri	50	66	62	1—Egypt
o. spurrelli	50	66	62	10—Côte d'Ivoire
o. kivu	50	66	62	9—Zaire
o. manni	50	66	62	12—Mali, Cameroon, Nigeria
o. odorata	50	66	62	6, 12—Burkina Faso
o. bueae	50	66	62	This study—Cameroon
o. cinereoaenea	50	66		15—Ethiopia
viaria	50	66	62	12—Morocco
viaria	50	66	62	6—Burkina Faso
hirta	50	66	62	8—Tanzania
greenwoodi	50	66	—	This study—Somalia
attila	50	66	62	This study—Cameroon
flavescens	50	74	70	7—South Africa
batesi	50	76	—	This study—Cameroon
nigeriae	50	76	72	12—Nigeria

The standard karyotypes of 11 species of shrews, collected during fieldwork in Cameroon and Somalia, are presented and compared to other geographic samples and species. Published karyotypic data for an additional 38 species and subspecies are presented for comparison (Table 1).

MATERIALS AND METHODS

All karyotypes were obtained from bone marrow preparations made in the field by the in vivo incubation method described by Robbins and Baker (1978) during field trips in 1978 (Cameroon) and 1982 (Somalia). Determinations of diploid numbers were based on counts of at least ten metaphases. Nomenclature of chromosome morphology used is that of Levan et al. (1964). All specimens examined were prepared as standard museum voucher specimens and are housed at the Carnegie Museum of Natural History (CM).

SPECIMENS EXAMINED

Sylvisorex johnstoni.—**Cameroon**: 4 km S, 2 km E Eseka (3°36′N, 10°48′E) (CM 58078 ♂, CM 58080 ♀).

Sylvisorex isabellae.—**Cameroon**: 11 km S, 1 km E Bamenda, 1900 m (5°51′N, 10°10′E) (CM 58081 ♀, CM 58085 ♀).

Table 1.—*Continued*

Species	2n	FN	FNa	Reference—country
Crocidura				
wimmeri	50	84	80	12—Côte d'Ivoire
theresae	50	82, 84		10—Côte d'Ivoire
?thalia	50			13—Ethiopia
parvipes	52	66	—	This study—Cameroon
lamottei	52	68	64	10—Côte d'Ivoire
poensis	52, 53	70, 72	66	10, 12—Côte d'Ivoire
hildegardeae	52	76		6—Burundi
virgata	52	86	82	12—Nigeria
fuscomurina	56	86	82	6—Burundi
picea	58	66		This study—Cameroon
"bicolor"	60	—	—	13—Ethiopia
yankariensis	68	122	118	This study—Somalia
Myosorex				
sp.	24	—	36	14—South Africa
cafer	38	—	58, 60	2, 14—South Africa
sclateri	38	—	—	2, 14—South Africa
tenuis	40	—	—	2, 14—South Africa
varius	42	—	74	2, 14—South Africa
Suncus				
murinus	40	—	—	3—Djibouti
Sylvisorex				
johnstoni	30	38	36	This study—Cameroon
isabellae	36	40	—	This study—Cameroon
morio	38	—	—	This study—Cameroon
ollula	38	64	62	This study—Cameroon
megalura	48	96	—	11—Côte d'Ivoire
lunaris	58	80	—	6—Burundi

[1] Reference codes:
1—De Hondt, 1974.
2—Dippenaar et al., 1983.
3—Hutterer and Tranier, 1990.
4—Hutterer et al., 1987.
5—Hutterer et al., 1992.
6—Maddalena, 1990*a*; Maddalena and Ruedi, 1994.
7—Maddalena et al., 1987.
8—Maddalena et al., 1989.
9—Meylan, 1967.
10—Meylan, 1971.
11—Meylan, 1975.
12—Meylan and Vogel, 1982.
13—Orlov et al., 1989.
14—Wolhuter, *in* Smithers, 1983.
15—Baskevich et al., 1995.

Sylvisorex morio.—**Cameroon**: Buea, Upper Farm, Mount Cameroon (4°10'N, 9°14'E) (CM 58098 ♀).

Sylvisorex ollula.—**Cameroon**: Buea, Upper Farm, Mount Cameroon (4°10'N, 9°14'E) (CM 58119 ♂); 30 km N, 40 km E Obala (4°22'N, 11°58'N) (CM 58120 ♂).

Crocidura attila.—**Cameroon**: 11 km S, 1 km E Bamenda, 1900 m (5°51'N, 10°10'E) (CM 58051 ♂).

Crocidura batesi.—**Cameroon**: Yaounde, Mont Febe, 1900 m (3°52′N, 11°31′E) (CM 58072 ♀).

Crocidura greenwoodi.—**Somalia**: Libsoma Farm, 6 km S, 17 km W Afgoi (2°05′N, 44°58′E) (CM 85103 ♂, CM 85105 ♀).

Crocidura olivieri.—**Cameroon**: Buea, Upper Farm, Mount Cameroon (4°10′N, 9°14′E) (CM 58017 ♀); Yaounde (3°52′N, 11°31′E) (CM 58039 ♂).

Crocidura parvipes.—**Cameroon**: 1 km S, 1 km W Ngaoundere (7°18′N, 13°34′E) (CM 58046 ♀, CM 58049 ♀).

Crocidura picea.—**Cameroon**: 11 km S, 1 km E Bamenda, 1900 m (5°51′N, 10°10′E) (CM 58050 ♀, CM 58061 ♀, CM 58065 ♀).

Crocidura yankariensis.—**Somalia**: Libsoma Farm, 6 km S, 17 km W Afgoi (2°05′N, 44°58′E) (CM 85086 ♂, CM 85088 ♀); SNAI Sugar Plantation, 1½ km S, ½ km E Giohar (2°46′N, 45°31′E) (CM 85091 ♀).

RESULTS

Representative karyotypes for the species examined in this study are presented in Figures 1–4. A summary of these data and that of the published literature on the chromosomal morphology for species of African shrews is presented in Table 1. A brief description of the karyotypes for each species reported from this study follows.

Sylvisorex johnstoni (Dobson, 1888)
(2n = 30; FN = 38; Fig. 1A)

The karyotypes of the female and male specimens of this species examined possess four pairs of submetacentric and ten pairs of acrocentric autosomes, grading from a very large pair to 13 pairs of medium-sized chromosomes. The X chromosome is a medium-sized acrocentric whereas the Y is a tiny chromosome.

Sylvisorex isabellae Heim de Balsac, 1968
(2n = 36; FN = 50; Fig. 1C)

The karyotype of the two females of this species that were examined each consisted of six pairs of large- to medium-sized metacentric and submetacentric and 12 pairs of acrocentric chromosomes. Since only females were analyzed, it is not possible to identify the sex chromosomes for this species.

Sylvisorex morio (Gray, 1862)

Although specimens of this species from Mount Cameroon were karyotyped, the quality of the preparations was too poor to obtain publishable figures. However, spreads examined from a single specimen indicate that the diploid number is probably 38.

→

Fig. 1.—Standard karyotype of: A, *Sylvisorex johnstoni* ♂ (CM 58078), 2n = 30, FN = 38 (FN includes sex chromosomes); B, *Sylvisorex ollula* ♂ (CM 58120), 2n = 38, FN = 64; C, *Sylvisorex isabellae* ♀ (CM 58081), 2n = 36, FN = 50.

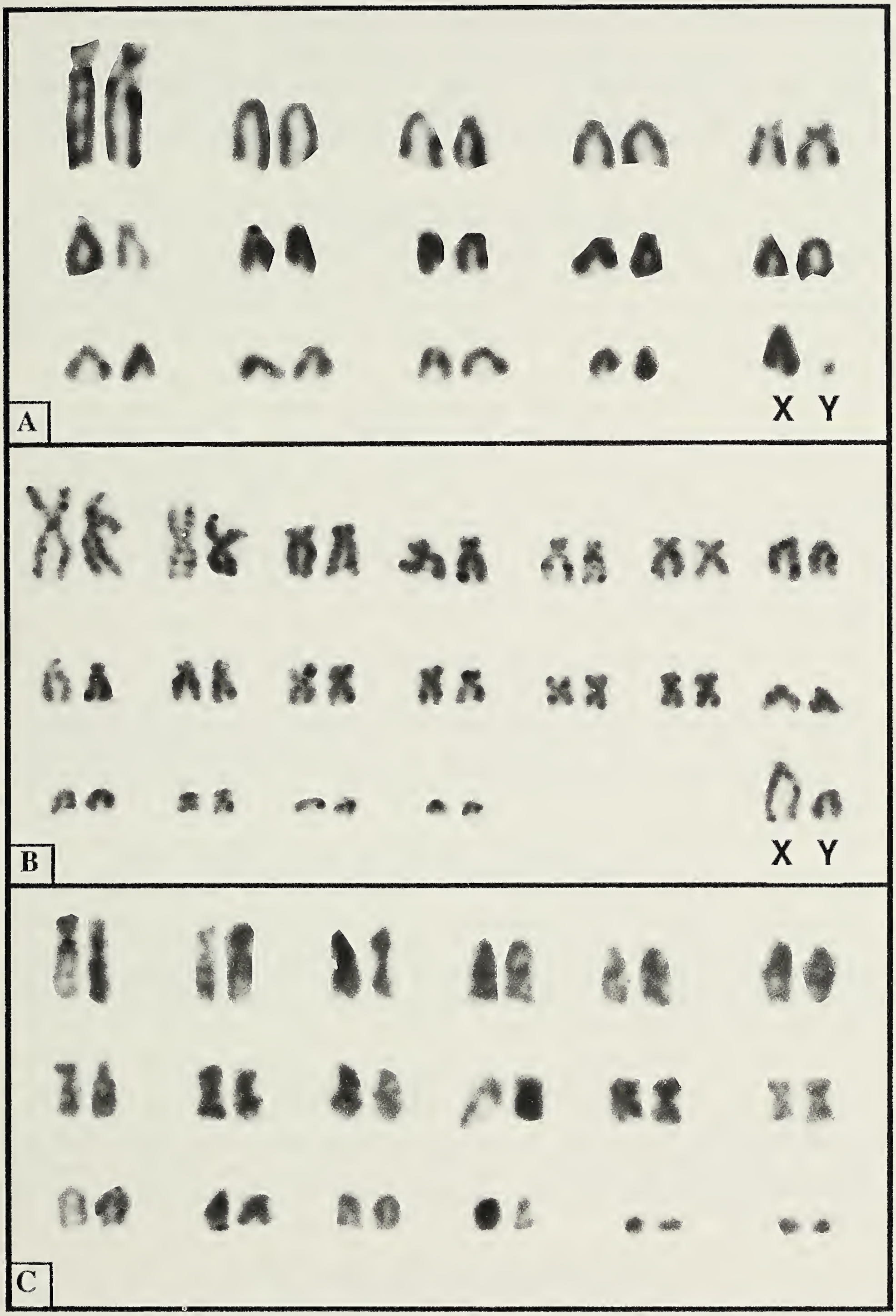
X Y
A
X Y
B
C

Sylvisorex ollula Thomas, 1913
(2n = 38; FN = 64; Fig. 1B)

The two males of this species examined indicate that the karyotype consists of 13 pairs of a graded set of large- to medium-sized metacentric and submetacentric and five pairs of small acrocentric autosomes. The X and Y chromosomes are both acrocentric.

Crocidura attila Dollman, 1915
(2n = 50; FN = 66; Fig. 2B)

The single male that was karyotyped possessed seven pairs of metacentric and submetacentric and 17 pairs of acrocentric autosomes ranging from large to small in size. The X chromosome is a medium-sized metacentric and the "Y" is a small acrocentric one.

Crocidura batesi Dollman, 1915
(2n = 50; FN = 76; Fig. 2A)

The results of an analysis of the karyotype of the single female available of this species reveals that the karyotype consists of 13 pairs of metacentric and submetacentric and 12 pairs of acrocentric chromosomes. Only a single female was available, therefore the X and Y chromosomes could not be distinguished at this time. By analogy with other species of *Crocidura,* however, the X chromosome should be a large metacentric one.

Crocidura greenwoodi Heim de Balsac, 1966
(2n = 50; FN = 66; Fig. 4B)

The karyotype of this shrew is characterized by seven pairs of large metacentric and submetacentric and 17 pairs of large- to small-sized acrocentric autosomes. The X chromosome is a large metacentric and the Y is a small acrocentric chromosome.

Crocidura olivieri bueae Heim de Balsac and Barloy, 1966
(2n = 50; FN = 66; Fig. 2C)

Of the individuals of this species that were karyotyped, a male and a female had spreads suitable for analysis. The karyotype consists of seven pairs of medium-sized metacentric and submetacentric and 17 pairs of medium- to small-sized acrocentric autosomes. The X chromosome is a large metacentric and the Y is a small acrocentric chromosome.

Crocidura parvipes Osgood, 1910
(2n = 52; FN = 66; Fig. 3B)

Suitable spreads were available only from two females. These had a chromosomal complement consisting of seven pairs of large metacentric and submetacentric and 19 pairs of acrocentric autosomes. The sex chromosomes could not be distinguished.

Crocidura picea Sanderson, 1940
(2n = 58; FN = 66; Fig. 3A)

Three females of this rare species, previously known only by the holotype (Sanderson, 1940), were available for study. From these, a karyotype consisting of four pairs of large metacentric and 25 pairs of large- to small-sized acrocentric chromosomes was developed. The sex chromosomes could not be distinguished but the X is probably one of the large metacentric chromosomes.

Crocidura yankariensis Hutterer and Jenkins, 1980
(2n = 68; FN = 122; Fig. 4A)

Spreads from a single female and male possessed 26 pairs of large- to small-sized metacentric and submetacentric chromosomes and only seven pairs of small acrocentric chromosomes in the autosomal complement. The X chromosome is a very large metacentric and the Y is an acrocentric.

DISCUSSION

Of the ten currently recognized species in the genus *Sylvisorex,* karyotypes of only two species have been reported previously: *S. megalura* from the Côte d'Ivoire (2n = 48, FN = 96) (Meylan, 1975) and *S. lunaris* from Burundi (2n = 58, FN = 80) (Maddalena, 1990*a*; Table 1). The karyotypes of the three additional species in the genus that are reported here are characterized by very low diploid and fundamental numbers, with *S. johnstoni* having one of the lowest diploid numbers of any African shrew. Although spreads obtained from specimens of *S. morio* from Mount Cameroon were unsuitable for the preparation of publishable karyotypes, a diploid number of 38 could be determined. Specimens of this taxon from Bioko were described as a new subspecies, *S. morio isabellae,* by Heim de Balsac (1968), but have been regarded recently as a full species by Hutterer (1993) based on morphological differences. Specimens from the Bamenda plateau of Cameroon, from which the karyotypes reported here were obtained, appear to be morphologically indistinguishable from the insular population described by Heim de Balsac (1968) and are regarded as representing the same species, *S. isabellae,* with *S. morio* confined to Mount Cameroon. The karyological differences between *S. isabellae* and *S. morio* support the recognition of the former as a full species.

The species of *Sylvisorex,* as currently understood (Jenkins, 1984; Hutterer, 1993), seem to fall into two groups. One group includes the two previously reported species with high diploid and fundamental numbers and the second the three newly reported species with low diploid and fundamental numbers. However, such a grouping is not congruent with Butler and Greenwood (1979), who placed *S. johnstoni* and *S. megalura* in one group, and *S. morio, S. ollula,* and *S. lunaris* in another based on morphological similarities. Maddalena (1990*a*, 1990*b*) also found considerable allozymic differences between *S. megalura* and *S. lunaris.* Results from these three data sets suggest that the genus *Sylvisorex* may be polyphyletic. In addition, some African species in the genus *Suncus* are very similar morphologically to species of *Sylvisorex.* Unfortunately, karyotypic data are unavailable for any of the species of *Suncus* native to Africa (e.g., *S. infinitesimus, S. lixus, S. remyi,* and *S. varilla*). *Suncus murinus* from Djibouti, from which a karyotype with a diploid number of 40 chromosomes was reported, originated from Asia or Arabia (Hutterer and Tranier, 1990).

Diploid numbers of African *Crocidura* range from 36 to 68. Within this grouping, a number of species with similar chromosomal formulae are now known (Table 1). The chromosomal formulae for *C. attila, C. greenwoodi,* and *C. olivieri bueae* (2n = 50, FN = 66) are the same as those previously reported for various subspecies of *C. olivieri* and the species *C. viaria* and *C. hirta* (review by Mad-

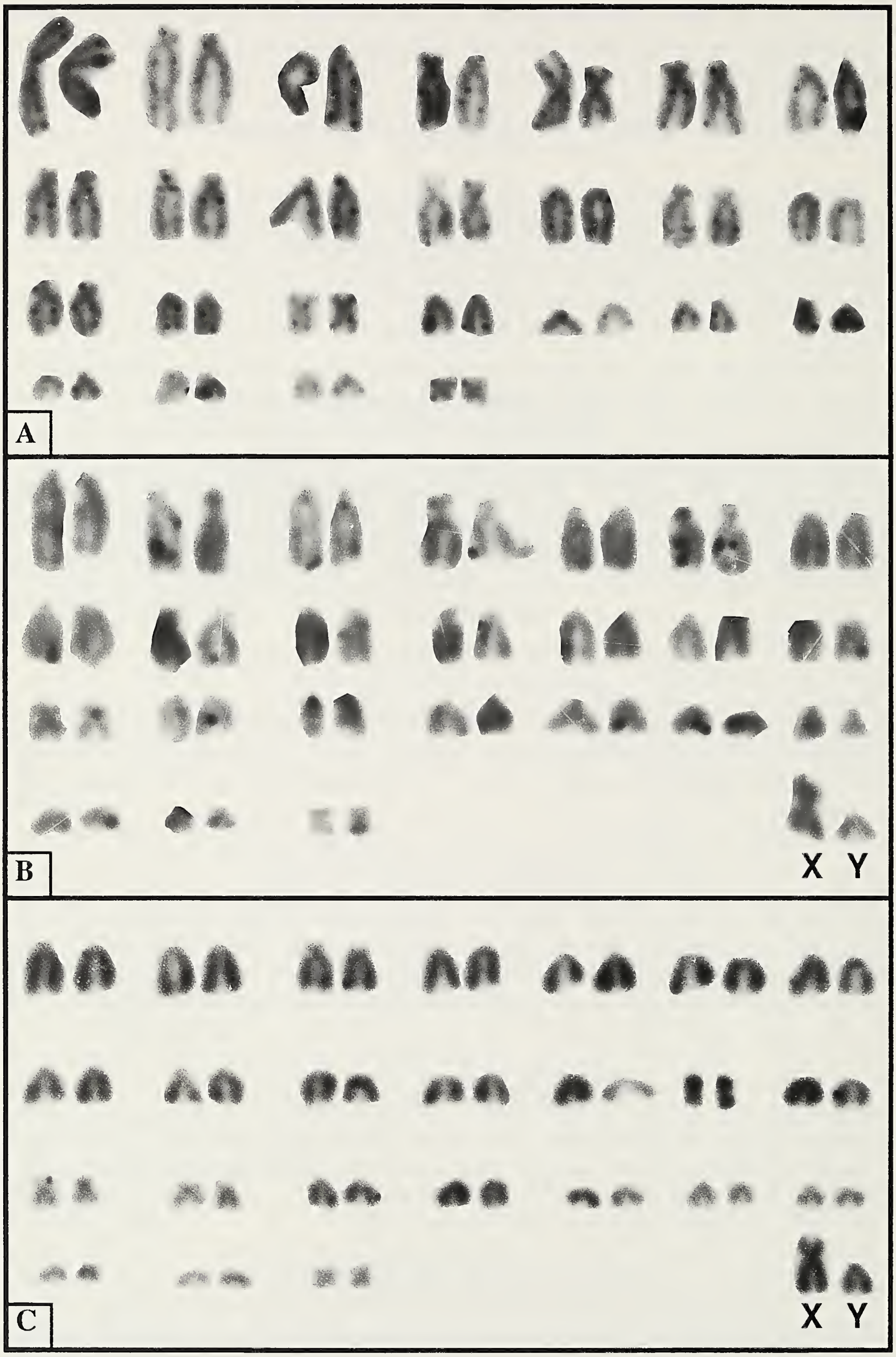
A
B
X Y
C
X Y

dalena and Ruedi, 1994; Table 1). However, in the case of *C. attila,* there are some notable differences in the morphology of the autosomes. These differences might reflect convergence of diploid and fundamental numbers. *Crocidura greenwoodi* is a little-known savanna shrew from Somalia. In describing it, Heim de Balsac (1966) emphasized the similarity of his new species to *C. hirta* and *C. fulvastra* (which he called *sericea*). The distinctiveness of *C. greenwoodi* from *C. hirta,* with which it shares the same karyotype, is still questionable and should be reassessed, as must be the relationship between *C. hirta* and *C. viaria.* In the case of *C. olivieri,* results from karyological studies of populations from various parts of Africa have revealed exactly the same chromosomal formula (Table 1). Although *C. olivieri* is a morphologically variable species, the homogeneity of the chromosomal formula confirms the wide distribution of this anthropophilic shrew.

Crocidura batesi has the same chromosomal formula as that described for *C. nigeriae* from Nigeria (Meylan and Vogel, 1982) and the two karyotypes seem initially to have a similar morphology. However, until additional data are available, especially differentially stained karyotypes, confirmation of whether this similarity is due to simple convergence or reflects close phylogenetic relationship is impossible.

Crocidura parvipes is in a group of species that is characterized by a diploid number of 52 (Table 1). This group includes such species as *C. lamottei, C. poensis, C. hildegardeae,* and *C. virgata.* In this case, however, the fundamental numbers and the morphology of the chromosomes are different. It will be necessary to compare the chromosomes of these species using banding techniques in order to identify the homologies and convergence between the karyotypes of the different species in this group.

The final two species of *Crocidura* examined are unique. *Crocidura picea* has a high diploid number accompanied by a large number of acrocentric chromosomes (Table 1). This condition is not known for any other species in the genus (Maddalena, 1990*a*, 1990*b*). In the case of *C. yankariensis* with a diploid number of 68 and a fundamental number of 122, the chromosomal formula is the highest yet reported for a species in the genus *Crocidura.*

ACKNOWLEDGMENTS

Fieldwork in Cameroon was supported by grants from the M. Graham Netting Research Fund (CM), the Loyalhanna Foundation, and the National Geographic Society. Assistance with fieldwork was provided by R. Robbins and S. Williams. Permission to conduct fieldwork and collecting permits were received from the Ministry of Agriculture. We are indebted to Victor Belinga, Director of Forestry Services, and Clement Njiti for assistance in obtaining necessary permits.

Fieldwork in Somalia was supported by grants from the M. Graham Netting Research Fund and the Hays Fund of the American Philosophical Society. Assistance in the field was provided by M. Smolen, R. Ruiz, Omar Hagi, Abdulwahab Josuf, and Mohamed Ali. Facilities and support in Somalia were graciously supplied by Mohamed Abdi Nur, Minister of Agriculture; Mohamed Abikar, Director General; and Abdulcadir Nur, Director, Department of Plant Protection and Locust Control, all in the Ministry of Agriculture. Abdullahi Ahmed Karani, General Manager, National Range Agency, issued the necessary permits to work in Somalia. John and Jonquil Ash; Bill and Sally Smythe; and Tony

←

Fig. 2.—Standard karyotype of: A, *Crocidura batesi* ♀ (CM 58072), $2n = 50$, $FN = 76$; B, *Crocidura attila* ♂ (CM 58051), $2n = 50$, $FN = 66$; C, *Crocidura olivieri* ♂ (CM 58039), $2n = 50$, $FN = 66$.

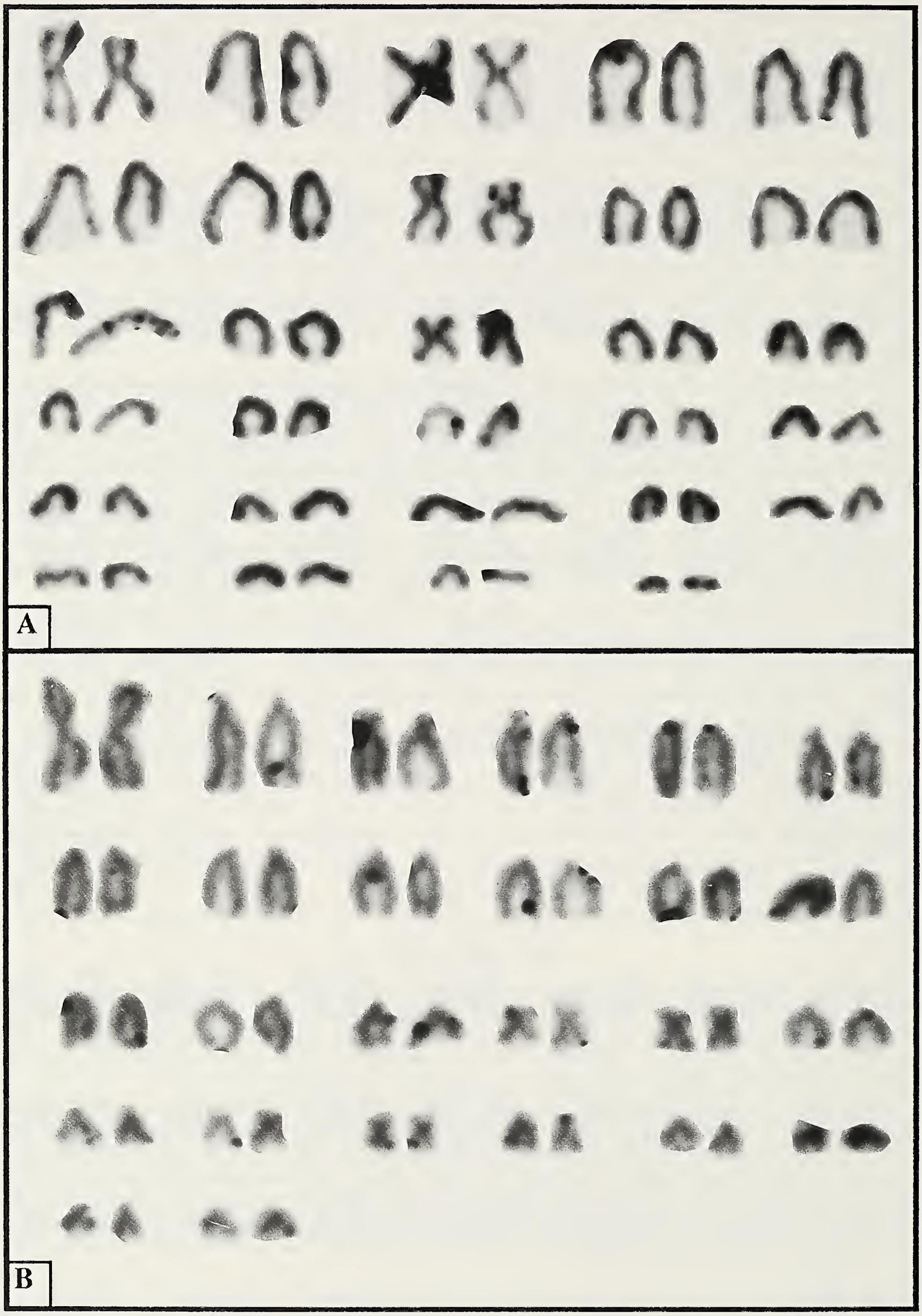

Fig. 3.—Standard karyotype of: A, *Crocidura picea* ♀ (CM 58061), 2n = 58, FN = 66; B, *Crocidura parvipes* ♀ (CM 58046), 2n = 52, FN = 66.

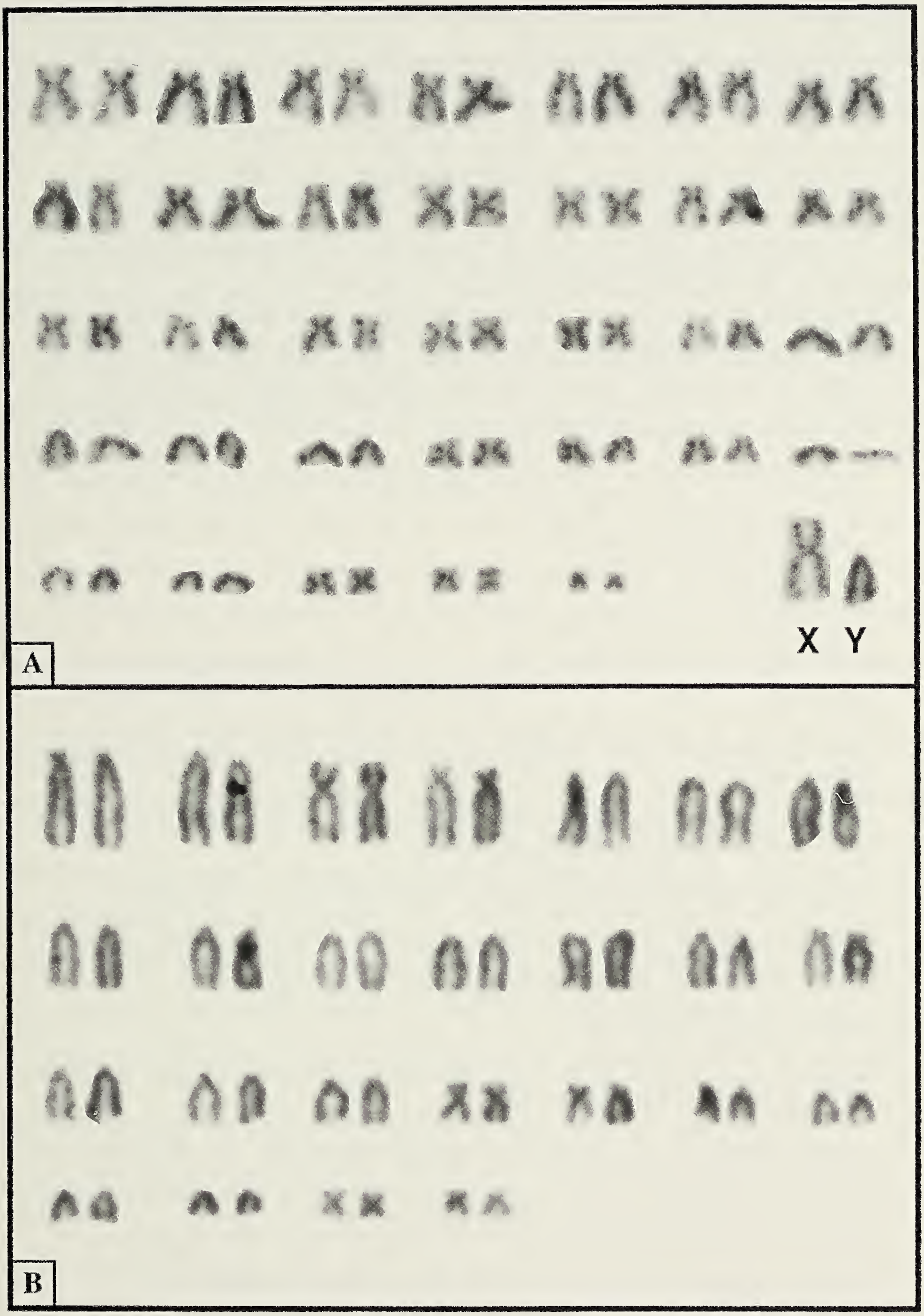

Fig. 4.—Standard karyotype of: A, *Crocidura yankariensis* ♂ (CM 85103), 2n = 68, FN = 122; B, *Crocidura greenwoodi* ♀ (CM 85088), 2n = 50, FN = 66.

and Lynette Johnston, United Nations Development Program in Somalia, graciously assisted in numerous ways.

We are grateful to A.-M. Mehmeti of the University of Lausanne for her skillful laboratory assistance. Funds for travel to the United States were received by R. Hutterer from the Museum Alexander Koenig and the Deutsche Forschungsgemeinschaft.

Literature Cited

Baker, R. J., M. B. Qumsiyeh, and C. S. Hood. 1987. Chromosomal evolution in mammals: Role of differentially-stained chromosomes. Pp. 69–96, *in* Current Mammalogy (H. H. Genoways, ed.). Plenum Press, New York, New York.

Baskevich, M. I., V. N. Orlov, A. Bekele, and A. Membrate. 1995. New data on the karyotypes of Ethiopian small mammals (Insectivora, Rodentia). Pp. 58–72, *in* Theriological Investigations in Ethiopia (V. E. Sokolov, ed.). Nauka, Moscow, Russia.

Butler, P. M., and M. Greenwood. 1979. Soricidae (Mammalia) from the Early Pleistocene of Olduvai Gorge, Tanzania. Zoological Journal of the Linnean Society, 67:329–379.

De Hondt, H. A. 1974. Karyological studies of two insectivores of Egypt. Proceedings of the Egyptian Academy of Sciences, 25:171–174.

Dippenaar, N. J., J. Meester, I. L. Rautenbach, and D. A. Wolhuter. 1983. The status of southern African mammal taxonomy. Annales Koninklijk Museum voor Midden-Afrika, Tervuren, Zoologische Wetenschappen, 237:103–107.

Heim de Balsac, H. 1966. Contribution à l'étude des Soricidae de Somalie. Monitore Zoologico Italiano, 74 (Supplemento):196–221.

———. 1968. Contribution à l'étude des Soricidae de Fernando Po et du Cameroun. Bonner Zoologische Beiträge, 19:15–42.

Heim de Balsac, H., and J. J. Barloy. 1966. Révision des Crocidures du groupe *flavescens–occidentalis–manni*. Mammalia, 30:601–633.

Heim de Balsac, H., and R. Hutterer. 1982. Les Soricidae (Mammifères Insectivores) des îles du Golfe de Guinée: Faits nouveaux et problèmes biogeographiques. Bonner Zoologische Beiträge, 33:133–150.

Hutterer, R. 1993. Order Insectivora. Pp. 69–103, *in* Mammal Species of the World, a Taxonomic and Geographic Reference (D. E. Wilson and D. M. Reeder, eds.). Smithsonian Institution Press, Washington, D.C.

Hutterer, R., and M. Tranier. 1990. The immigration of the Asian house shrew *Suncus murinus* into Africa and Madagascar. Pp. 309–319, *in* Vertebrates in the Tropics (G. Peters and R. Hutterer, eds.). Museum Alexander Koenig, Bonn, Germany.

Hutterer, R., L. F. Lopéz-Jurado, and P. Vogel. 1987. The shrews of the eastern Canary Islands: A new species (Mammalia: Soricidae). Journal of Natural History, 21:1347–1357.

Hutterer, R., T. Maddalena, and O. M. Molina. 1992. Origin and evolution of the endemic Canary Island shrews (Mammalia: Soricidae). Biological Journal of the Linnean Society, 46:49–58.

Jenkins, P. D. 1984. Description of a new species of *Sylvisorex* (Insectivora: Soricidae) from Tanzania. Bulletin of the British Museum (Natural History) (Zoology), 47:65–76.

Levan, A., K. Fredga, and A. A. Sandberg. 1964. Nomenclature for centromeric position on chromosomes. Hereditas, 52:201–220.

Maddalena, T. 1990*a*. Systématique, évolution et biogéographie des musaraigne Afrotropicales et Paléarctiques de la sous-famille des Crocidurinae: Une approche génétique. Ph.D. Dissert., Université de Lausanne, Lausanne, Switzerland.

———. 1990*b*. Systematics and biogeography of Afrotropical and Palaearctic shrews of the genus *Crocidura* (Insectivora: Soricidae): An electrophoretic approach. Pp. 297–308 *in* Vertebrates in the Tropics (G. Peters and R. Hutterer, eds.). Museum Alexander Koenig, Bonn, Germany.

Maddalena, T. and M. Ruedi. 1994. Chromosomal evolution in the genus *Crocidura* (Insectivora: Soricidae). Pp. 335–344, *in* Advances in the Biology of Shrews (J. F. Merritt, G. L. Kirkland, Jr., and R. K. Rose, eds.). Special Publication of Carnegie Museum of Natural History, no. 18.

Maddalena, T., A.-M. Mehmeti, G. Bronner, and P. Vogel. 1987. The karyotype of *Crocidura flavescens* (Mammalia, Insectivora) in South Africa. Zeitschrift für Säugetierkunde, 52:129–132.

Maddalena, T., P. Vogel, and W. N. Verheyen. 1989. The African giant shrew: Taxonomy and relationships. P. 674, *in* Abstracts of the Fifth International Theriological Congress (E. Capanna and L. Boitani, eds.). Rome, Italy.

Meylan, A. 1967. La formule chromosomique de *Crocidura occidentalis kivu* Osgood (Mammalia, Insectivora). Revue suisse de Zoologie, 74:685–691.

———. 1971. Chromosomes de Soricidés de Côte d'Ivoire (Mammalia, Insectivora). Revue suisse de Zoologie, 78:603–613.

———. 1975. Formule chromosomique de *Sylvisorex megalura* (Jentink) (Mammalia, Insectivora). Mammalia, 39:319–320.

MEYLAN, A., AND P. VOGEL. 1982. Contribution à la cytotaxonomie des Soricidés (Mammalia, Insectivora) de l'Afrique occidentale. Cytogenetics and Cell Genetics, 34:83–92.

ORLOV, V. N., N. S. BULATOVA, AND A. N. MILISHNIKOV. 1989. Karyotypes of some mammalian species (Insectivora, Rodentia) in Ethiopia. Pp. 95–109, *in* Ecological and Faunistical Studies in South-western Ethiopia (V. E. Sokolov, ed.). Nauka, Moscow, Russia. (In Russian, English summary.)

REUMER, J. W. F., AND A. MEYLAN. 1986. New developments in vertebrate cytotaxonomy. 9. Chromosome numbers in the order Insectivora (Mammalia). Genetica, 70:119–151.

ROBBINS, L. W., AND R. J. BAKER. 1978. Karyotypic data for African mammals, with a description of an *in vivo* bone marrow technique. Pp. 188–210, *in* Ecology and Taxonomy of African Small Mammals (D. A. Schlitter, ed.). Bulletin of Carnegie Museum of Natural History, no. 6.

SANDERSON, I. T. 1940. The mammals of the North Cameroons forest area being the results of the Percy Sladen Expedition to the Mamfe Division of the British Cameroons. Transactions of the Zoological Society of London, 24:623–725.

SMITHERS, R. H. N. 1983. The Mammals of the Southern Africa Subregion. University of Pretoria, Pretoria, South Africa.

ANNALS OF CARNEGIE MUSEUM
Vol. 68, Number 1, Pp. 15–80 11 February 1999

THE HEAD SKELETON OF *AMPHISBAENA ALBA* LINNEAUS

Ricardo Montero[1]

Carl Gans[2]
Research Associate, Section of Amphibians and Reptiles

Abstract

The skull of *Amphisbaena alba* Linneaus and its disarticulated components are described in detail and illustrated by photographs and labeled sketches. The cartilaginous components, particularly the adult chondrocranium are characterized in parallel. The bone formerly referred as the orbitosphenoid is considered as a distinct element nonhomologous to the synonymous element in other squamates and hence referred to as a "tabulosphenoid" (sphenoid plate). The element-X (of Zangerl) is considered to represent an epiphysis that facilitates the transmission of muscular forces to the growing skull, rather than being the remnant of an element no longer expressed. Cranial kinesis is discussed as are the general structural patterns associated with the relative distribution of spongy and dense laminar bone.

Key Words: Reptilia, Squamata, Amphisbaenia, *Amphisbaena alba*, osteology, chondrocranium, head anatomy, cranial kinesis

Introduction

Amphisbaena alba is the largest (longest and stoutest) South American amphisbaenian, reaching more than 750 mm in length (Vanzolini, 1955; Gans, 1986), and has the largest range, extending from Panamá and Trinidad, southward to Bolivia and Paraguay (Vanzolini, 1955; Gans, 1962). Indeed, the species may have the largest range of any amphisbaenian, although the range of *Amphisbaena fuliginosa* is remarkably similar (Vanzolini, 1951*b*). *Amphisbaena alba* appears to be commensal with the leaf-cutter ants, the tunnel systems of which provide it with a unique habitat (Riley et al., 1986).

The skull of *Amphisbaena alba* has been described a number of times as an entity (Cuvier, 1829–1830; Brühl, 1886; Williston, 1918*a* [illustration attributed to Alexander Ruthven], 1925; Gilmore, 1928 [after Williston, 1918*a*, poor proportions]; Vanzolini, 1951*a*; McDowell and Bogert, 1954; Romer, 1956 [after Williston 1918*a*]; Underwood, 1957; Jollie, 1960 [new 3/4 view of side]; Wu et al., 1995) and is sometimes used as a model for all amphisbaenians. These descriptions are based on articulated skulls and commonly only on those of fairly large individuals. However, amphisbaenian skulls have a plywoodlike construction; some individual bony elements overlap substantially, and significant details are lost when only the exposed portions of skulls are described.

---

[1] Instituto de Herpetología (CONICET) and Facultad de Ciencias Naturales, Universidad Nacional de Tucumán, Miguel Lillo 251, 4000 Tucumán, Argentina. ueso@unt.edu.ar

[2] Department of Zoology, The University of Texas at Austin, Austin, Texas 78746, USA. carolus@uts.cc.utexas.edu

Submitted 11 February 1997.

The present characterization of the skull of *Amphisbaena alba* is the first of a series of redescriptions of the skulls of all amphisbaenians. They are intended to serve as the basis for a reanalysis of generic and familial classifications, for which substantial material has accumulated. In addition to a description of the intact skull, this study includes descriptions of each of the cranial bones and their relationships to one another. For the sake of convenience, the descriptive account of each element is followed immediately by a brief defense of the homology and, if necessary, by comments on the literature dealing with the particular element. Beyond providing a baseline for taxonomic comparisons, the study was designed to allow identification of a series of fossil bones from Lagoa Santa (Gans and Montero, in press). The study also led to some strictly morphological conclusions. The large azygous ventral bone formerly referred to as the orbitosphenoid is considered not to be homologous to the synonymous element in other squamates. For reasons presented below it is hence referred to as a "tabulosphenoid" (sphenoid plate).

MATERIALS AND METHODS

The material of *Amphisbaena alba* used in this study includes five complete and articulated skulls; two articulated, incomplete skulls; three totally disarticulated skulls used for the description of individual cranial elements; three sets of serial sections through the head (deriving from studies with E. G. Wever); and one cleared and stained specimen (Table 1). The disarticulated skulls were obtained by soaking the heads of skinned fresh specimens in water for several weeks until they disintegrated; careful washing thereafter freed the bones. Both photographs and labeled overlays of the identical views are provided.

Whenever possible, the skull and its elements are shown in orthogonal projection (Loeb and Gans, 1986). In this the plate usually shows a central figure which is normally in one of the standard (dorsal, lateral, ventral, medial, etc.) positions, illustrating the element as seen along the major axes or planes of symmetry of the skull; however, more complex elements are shown at other angles as well. The various photographs are placed at right angles to the lines of view (i.e., normal to the surface illustrated).

It is facile to visualize orthogonal projection by considering that the bone has been placed into a transparent box, with the views shown on the plane sides paralleling the surfaces of the element. Once the individual drawings have been completed, some edges are slit, the box is unfolded, and the six or more sides placed flat, maintaining the contact lines between them. Some of the views will likely contain minimal supplementary information and can be omitted. This procedure not only shows processes and sutures in a standard fashion, but allows the comparison of adjacent figures, thus facilitating three-dimensional reconstruction.

The descriptions in this report first deal with the entire articulated skulls and mandibles and thereafter with the individual bones. Discussion of the cranial cartilages and major cranial cavities follows. Each account begins with a paragraph dealing with the general outline of the element, and then discusses its shape and foramina based on the entire bone and its exposure in serial sections. Finally, each contains a brief statement about the identification (homology) of the element and, if appropriate, about anatomical and nomenclatorial comments from the literature. However, as a list of historical treatments of the cranial elements has been

Table 1.—*Morphometric data of the analyzed specimens (in cm). See definitions and acronyms in the Morphometrics section.*

Measurements	CG 3533	CG 3537	UMMZ 149616	AMNH 73233	AMNH 17799	KM 11a	KM 11b	CG 1811	CG 1216	CG 1200	ICN 5733
1. Snout–vent length	55.2	30.9	—	—	41.8*	—	—	—	—	—	55.0
2. Tail length	4.10	2.40	—	—	3.2*	—	—	—	—	—	4.4
3. Skull length	3.18	1.82	2.12	2.79	2.66	—	—	—	—	—	3.02
4. Skull greatest height	0.97	0.48	0.55	0.71	0.75	0.89	0.73	—	—	—	0.93
5. Face length	1.09	0.63	0.78	0.98	1.01	—	—	—	—	—	1.07
6. Face width	1.10	0.55	0.74	0.96	0.99	—	—	—	—	—	1.21
7. Face height	0.60	0.34	0.39	0.50	0.46*	—	—	—	—	—	0.61
8. Maxillary length	0.75	0.43	0.52	0.69	0.69	0.79	—	0.71	0.65	0.69	0.75
9. Occipital width	1.36	0.75	0.87	1.12	1.16	—	1.15	1.32	1.20	1.25	1.29
10. Occipital height	0.75	0.45	0.50	0.62	0.66	0.70	0.64	0.73	0.67	0.73	0.74
11. Occipital condyle width	0.36	0.24	0.27	0.34	0.34	—	0.35	0.35	0.34	0.34	0.35
12. Occipital crest length	0.69	0.32	0.35	0.60	—	0.70	0.55	0.70	0.58	0.70	0.63
13. Parietal width	0.50	0.32	0.38	0.43	0.43	0.50	—	0.45	0.43	0.44	0.49
14. Parietal length	1.49	0.87	0.85	1.15	1.20	1.32	—	1.30	1.25	1.31	1.14
15. Pterygoid width	0.705	0.42	0.54	0.59	0.59	—	—	—	—	—	0.77
16. Parietal + occipital length	2.23	1.22	1.26	1.80	1.78	2.11	—	—	—	—	1.92
17. Crest width	0.12	0.08	0.09	0.12	0.15	0.14	0.12	0.16	0.11	0.13	0.16
18. Frontal segment	0.67	0.40	0.53	0.64	0.62	—	—	—	—	—	0.83
19. Medial segment	1.38	0.76	0.80	1.18	0.80	—	—	—	—	—	1.45
20. Occipital segment	0.49	0.22	0.24	0.33	0.24	—	—	—	—	—	0.63

* Measurement of vertebral column.

published (Gans, 1978), the discussion of literature has been restricted to cases posing potential problems.

Some material derives from loans of several museums, whose curators we acknowledge. The acronyms are as follows: AMNH—American Museum of Natural History, New York, New York, USA (C. J. Cole, R. G. Zweifel); CG—Carl Gans Collection (includes E. G. Wever serial sections); ICN—Instituto de Ciencias Naturales, Universidad Nacional de Colombia, Santafé de Bogota, Colombia (O. V. Castano); KM—Zoologisk Museum, University of Copenhagen, Copenhagen, Denmark (Dr. F. W. Brastrup); UMMZ—University of Michigan Museum of Zoology, Ann Arbor, Michigan, USA (G. Schneider).

The following materials were used to generate the description of the skull. Articulated skulls: CG 3533 (no data), CG 3537 (Capitania Maloca Feia, Marienopolis, Mn. de Villabela, Mato Grosso, Brazil), UMMZ 149616 (Colombia), AMNH 73233 (no data), AMNH 17799 (Trinidad, from New York Aquarium), ICN 5733 (Colombia). Incomplete, articulated skulls: KM 11a (no data), KM 11b (no data). Completely disarticulated skulls (some of the bones are articulated): CG 1811 (Leticia, Colombia). Parietal articulated with tabulosphenoid and frontals, CG 1216 (Leticia, Colombia). Occipital complex articulated with parabasisphenoid and parietal, CG 1200 (Leticia, Colombia). Cleared and stained specimen: CG 3542 (Santo Amaro, Sao Paulo, Brazil). Serially sectioned specimens (frontal sections): CG 1500, 1667, 1668 (dealers, Brazil, Venezuela; cf. Gans and Wever, 1972).

Results

Morphometrics

As most skulls of *Amphisbaena alba* in collections do not provide information about the proportions of the entire specimen, we dissected three specimens (CG 3537, 3553; ICN 5733). For AMNH 17799 the snout–vent length is estimated from the articulated vertebral column. Various measurements of the skull are listed in Table 1 and all but 1, 2, and 10 are illustrated in Figure 1. These are defined as follows:

1. Snout–vent length: Measured from the tip of the snout to the cloacal slit (vent) of the entire specimen.

2. Tail length: Measured from the vent to the caudal tip (this species never displays caudal autotomy).

3. Skull length: Measured from the tip of the snout (premaxilla) to the condyle (exposed posterior to the occipital crest).

4. Skull greatest height: Measured from the ventral point of element-X to point just anterior to the gap between parietal and ascendent process of the supraoccipital.

5. Face length: Measured from the tip of the snout to the posterior end of the maxilla.

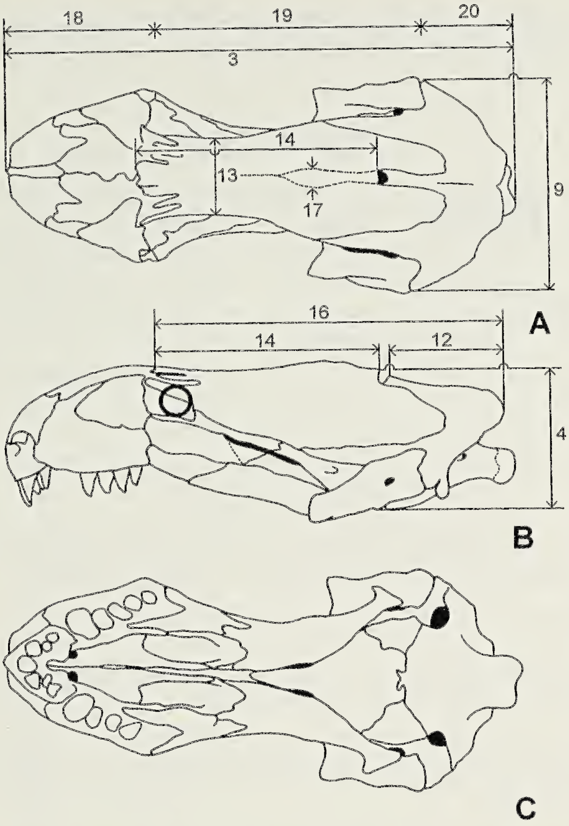

Fig. 1.—*Amphisbaena alba.* Labeled outline of skull showing the measurements in Table 1, items 3 to 20 as defined in text. Measurement 10 cannot be seen in these views. The circle (in view B) shows the approximate position of the eye in the posteriorly open orbit.

6. Face width: Measured just anterior to the maxilla–ectopterygoid joint.

7. Face height: Measured behind the last maxillary tooth, from the top of the frontals to the ventral aspect of the maxilla.

8. Maxilla length: Measured from the posterolateral border of the external nares to the posterior end of the maxilla.

9. Occipital width: Measured between the outer sides of the paroccipital processes.

10. Occipital height: Measured from the anterior end of the occipital ascendent process to the center of the basioccipital plate.

11. Occipital condyle width: Measured horizontally at the widest spot.

12. Ascendent process length: Measured from the anterior end of the occipital ascendent process to the border of the occipital crest.

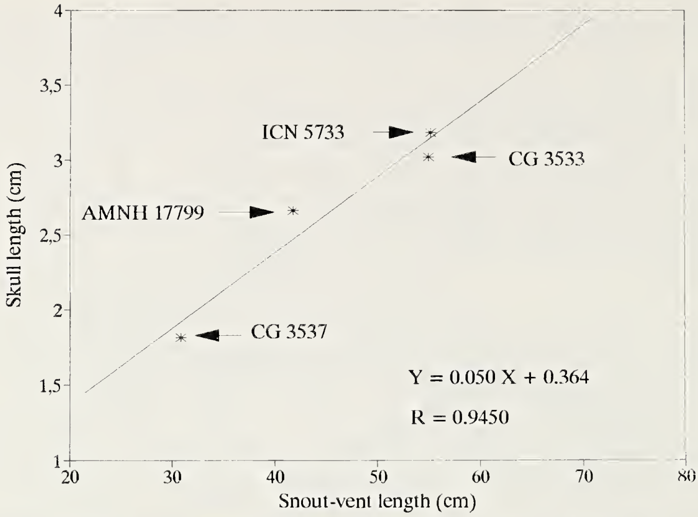

Fig. 2.—*Amphisbaena alba.* Estimated regression line of the skull length versus snout–vent length of intact animals; the asterisks refer to the cranial length of dissected specimens.

13. Parietal width: Measured as the narrowest width between the lateral borders of the parietal.

14. Parietal length: Measured from the anterior tip at the midline to the posterior end of the parietal crest.

15. Pterygoid width: Measured as the narrowest width between the lateral borders of the palato–pterygoid shelves.

16. Parietal + occipital length: Measured at the midline from the anterior tip of the parietal to the posterior end of the occipital crest.

17. Parietal crest width: Measured as the maximum width of the parietal crest.

Measurements 18 to 20 were taken from drawings made with a camera lucida; hence, they are not comparable to direct measurements. The length of the skulls may be subdivided into three portions, namely the facial segment (18), the medial segment (19), and the occipital segment (20). The facial segment extends from the tip of the premaxilla to the maxilla–ectopterygoid joint. The medial segment extends from here to the posterior tips of the quadrates. The occipital segment extends to the posterior end of the occipital condyle.

Although the number of specimens is too low to allow a statistical analysis, the raw data presented here represent a starting point for future studies (Table 1). The lengths of the available skulls (measurement 3) range from 1.82 to 3.18 cm. The width of the occipital complex (measurement 9) ranges from 0.75 to 1.36 cm, and the greatest height of the cranium (measurement 4) from 0.48 to 0.97 cm. The width of the anterior portion of the snout (measurement 6) ranges from 0.55 to 1.10 cm. Figure 2 shows that the skull length varies linearly with the snout–vent length of intact animals. The ratio of facial to cranial length of *Amphisbaena alba* (18/3) is approximately 0.28 and that of medial to cranial length is 0.46.

External View of Skull

The elongate skull of *Amphisbaena alba* (Fig. 3, 4) comprises a facial, a medial, and an occipital portion; the latter two are often referred to as a cranial portion (cf. Vanzolini, 1951*a*; Gans, 1960). In dorsal view (Fig. 3A, 4A), the articulated skull has an hourglass-shaped outline. The posterior tips of the maxillae and the occipital crest form the widest portions; whereas the medial portion is narrowest. The anterior edge of the blunt snout is defined by the nasal and premaxillary curves. More posteriorly, the maxillary edge defines the side of the face, the face gradually becomes wider to the posterior processes of the maxilla. From here the lateral extent of the skull is defined by the width of the braincase, and by the smooth edge of the palato–pterygoid shelf. From the palato–pterygoid suture with the lateralmost posterior process of the maxilla, the edge of the ectopterygoid curves toward the midline. The edge of the palato–pterygoid shelf is narrowest here, but thereafter sweeps laterally to reach the head of the inclined quadrate, which lies adjacent to the otic region, forming the widest portion of the articulated skull. The distal portion of the quadrate (and the site of the mandibular articulation) reaches anteriorly to the midlevel of the pterygoid. The lateralmost extremity of the quadrate lies parallel to the midline of the skull, although curving very slightly mediad. The posterior outline of the skull is defined by the fused occipitals. The wide bicipital occipital condyle extends just beyond the flaring occipital crest (Fig. 4, 5), which is medially notched near its contact with the ascendent process of the occipital complex.

In lateral view (Fig. 3B, 4B), the dorsal surface of the face is slightly concave, the bend beginning at the frontoparietal joint. The ventral surface is formed by the premaxillary plane and lies at an angle of about 35° below the axis of the cranial portion. More posteriorly, along the posteroventral plane of the maxilla, it lies at an angle of only 15°. The dorsal surface of the medial portion is defined by the parietal crest, which starts near the midline of the skull, and shows a widened and dorsally projecting process at the midline; this process serves as the attachment for the mass of epaxial and mandibular adductor muscles. The parietal extends far posteriorly over the compound occipital complex; however, a median notch within the parietal accommodates the ascendent process of the latter. In prepared skeletons, the tip of the ascendent process of the occipital is separated from the posteriormost portion of the medial ridge of the parietal so that a notch is seen in lateral view. Posterior to the notch, the ascendent process of the occipital extends to the level of the posteriorly projecting edge of the dorsal surface; this edge then drops ventrally and anteriorly toward the level of the quadratic articulation. From this level, the occipital condyle extends on a slender neck to form the posteriormost portion of the skull. Ventrally the medial portion of the skull is defined by the projecting palato–pterygoid shelf that angles slightly ventrally from the edge of the maxilla to the condyle of the quadrate (around which it bends). The element-X, the distal extremity of the stapes, and the paroccipital process extend posteroventral to the quadrate. More posteriorly, the skull is delimited by the surface of the ventral plate of the occipital complex.

The dorsal surface of the snout (face) (Fig. 3A, 4A) is formed by the rugose

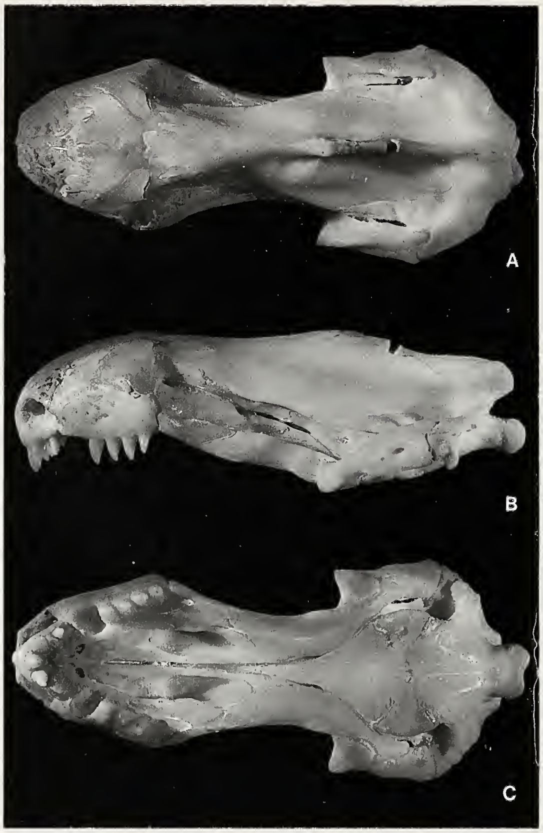

Fig. 3.—*Amphisbaena alba*. Photographs of skull (CG 3533); note that the stapes are missing. Anterior is to the left. The bar shows 0.5 cm to scale. A, dorsal view; B, lateral view; C, ventral view.

nasals, which are separated by a narrow, vertical nasal process of the azygous premaxilla. The nasals roof the external nares, which are ventromedially defined by the premaxilla, and laterally by the maxillae, and lined internally by the septomaxillae. The maxillae form the vertical walls of the snout, reaching the frontals anterodorsally. The premaxillary nasal process reaches the dorsal aspect of the medially interlocking but superficially smooth frontals (which actually extend ventrolaterally more posteriorly, forming a ring around the anterior portion of the cerebral cavity). The maxillae are separated from more posterior frontal contact by the prefrontals, which reach the orbits and partially overlap the frontals medially reducing their dorsal exposure. The maxillae and prefrontals form an important part of the sides of the face, and also of the anterior wall of the orbit. The complex posterior suture of the frontals with the parietals laterally extends as two to four fingerlike processes that form an anteriorly open angle. The parietal defines the medial and dorsal portion of the skull, posterior to prefrontals and frontals; it extends laterally and ventrally from the midline. An anterior projection of the parietal may or may not reach the prefrontal, thus narrowing the posterolateral appearance of the frontals. Authors have been confused by the multiple

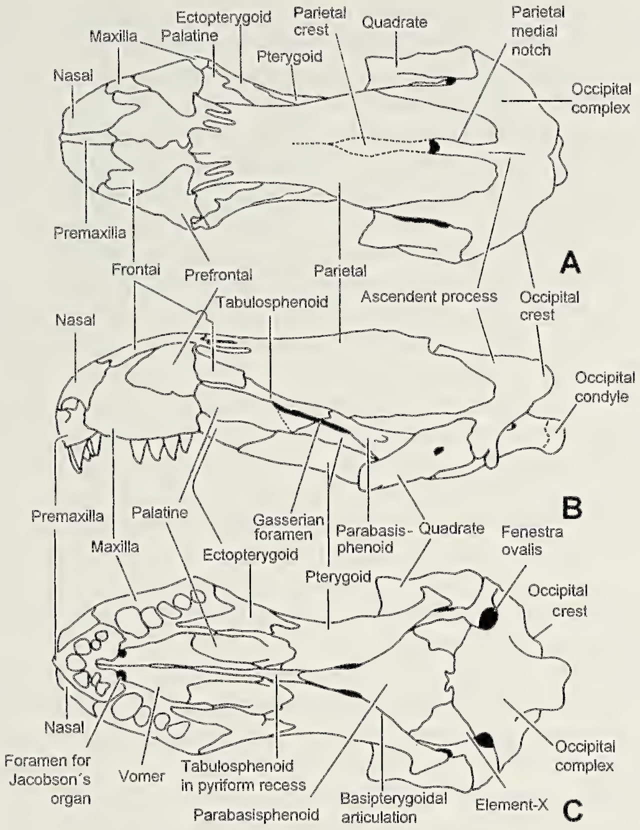

Fig. 4.—*Amphisbaena alba.* Labeled outline of skull shown in Figure 3.

and seemingly independent appearance of frontal exposures, labelling them as distinct elements (May, 1978).

The orbital space is defined anteriorly, but is posteriorly open. All of the elements that intercalate to form the anteromedial portion of the orbit show complex interdigitation so that the patterns of exposure differ among specimens and even bilaterally. The orbital spaces are formed anteriorly by the prefrontals, medially by the ventral processes of the frontals, medioventrally by the tabulosphenoid, and ventrally by the palatine shelf (palatine plus ectopterygoid). The spaces are open posteriorly and dorsally (Fig. 1B). The postorbital spaces ventral to the lateral borders of the parietal and the tabulosphenoid, and dorsal to the palato–pterygoid (and ectopterygoid) shelves, would represent the epipteric cavities; they continue as lateral concavities extending posteriorly to the quadrates and otic region of the occipitals. Posteriorly, the pterygoids are laterally adjacent and suturally joined to the parabasisphenoid; at this level the roof of the concavities is formed by the tabulosphenoid. The wide Gasserian foramen (for the trigeminal ganglion, cf. Vanzolini, 1951*a*) opens between the posterior tip of the tabulosphenoid and the parabasisphenoid. There is no trace of an epipterygoid in this region, a character reported only for *Trogonophis* among amphisbaenians (Gans, 1960).

The basal plate of the premaxilla articulates posterolaterally with the ventral plate of the paired maxillae and posteriorly with the vomers. In ventral view (Fig. 3C, 4C), the tilted basal plate of the premaxilla bears seven inclined teeth, a large median one and three pairs of smaller lateral ones. The more nearly horizontal ventral plate of the maxilla bears five larger teeth. More posteriorly lie the foramina of Jacobson's organ, bordered by the premaxilla, maxillae, and vomers. The internal nares open dorsad to the palatal plates of the maxillae and are defined by maxillae, vomers, and palatines. They open into deep troughs on the palate formed posteriorly and medially by the palatines which laterally contact the maxillae, ectopterygoids, and posteriorly the pterygoids. Anteriorly, the slender vomers have wide lateral connections with the maxillae; their posterior rod-shaped ends lie ventral to the medial edges of the palatines and extend just anterior to contact the pterygoids. In lateral view (Fig. 3B, 4B), the anterodorsal parts of the palatines are seen to contact the tabulosphenoid; however, at the level at which palatines overlap the posterior pterygoids as a shelf, a gap separates them from the tabulosphenoid (this is the anterior portion of the Gasserian foramen). The slender pterygoids diverge posteriorly from the midline (Fig. 3C, 4C). At their midportion, their medial borders start to contact the parabasisphenoid and more posteriorly they narrowly contact element-X. The lateral borders of the posterior pterygoid processes curve around the articular condyles of the quadrates; thereafter the pterygoids curve to cover the midshaft of the quadrates, medially bordering the extracolumellar passage.

A medial gap between the posterior parts of vomers and palatines (pyriform recess) allows inspection of the floor of the braincase, i.e., the contact line between the ventral processes of the frontals and of the tabulosphenoid. More posteriorly, the tabulosphenoid contacts the sharp medial point of the triangular parabasisphenoid, which tilts posteroventrally and curves laterally. The large elements-X are each wedged between the parabasisphenoid and basioccipital from which they are separated by triradiate cartilaginous plates (Fig. 55, 56). The wide, platelike basioccipital (fused into the occipital complex) forms the posterior floor of the cranium. Its posterior border is rounded and bent dorsally, forming the posterior end of the braincase. The lateral otic areas bear the openings of the fenestra ovalis, providing the seat to the stapedial footplate. The columella of the stapes lies across the ventral edge of the quadrate; the cartilaginous extracolumella, in an intact specimen, projects anteriorly along the ventral face of the quadrate to parallel the infralabial scales and end in an infralabial pad further anteriorly (Wever and Gans, 1973).

In posterior view (Fig. 5, 6), most of the area is occupied by the posterior aspect of the occipital complex; hence the fossae and foramina thus exposed can be characterized by reference to the account of this bone in the discussion of individual bony elements below. The tip of the occipital condyle is visible dorsally. Lateroventrally, there is exposure of the extreme ventral portion of the quadrate and ventral to it the posterolateral head of the pterygoid which extends around the former. As the facial portion of the skull bends ventrally, the palatal tip appears ventral to the generally concave basiventral edge.

Mandible

The mandible consists of two rami connected anteriorly and medially by a solid symphysis and each extending posteriorly as a coronoid process and terminating in a mandibular condyle, here a compound bone (Fig. 7, 8). The compound bone (that is presumed to be the fusion of several bones, i.e., articular, splenial, prearticular, and supra-angular) articulates with the ventral condyle of one of the quadrates. The anterior portion of each ramus is formed of a dentary, bearing eight teeth, and followed by the coronoid. More ventrally lies the angular, which wraps around the posteroventral edge just anterior to the condyle of the compound bone.

Lateral views show that the anteroventral border of the mandible gently curves downward at the midline symphysis, the chin slopes posteriorly to the ventral edge (Fig. 7A, 8A). The edge continues as an almost straight line to the edge of the mandibular condyle. The dorsal mandibular border is straight and its medial aspect supports the implantation sites of eight teeth. The border then ascends in a smooth curve up the coronoid process; however, the dorsal and posterior edges of the process are formed by the coronoid bone. With the mouth closed, the coronoid process of the mandible extends dorsally to the palato–pterygoid shelf. The anterior border of the apex of the coronoid process is more rounded than the posterior border, which descends more abruptly in a wavy fashion toward the articular process. The articular process of the compound bone is expanded dorsad and ventrally and the posterior articular surface (for the quadrate) is concave. The posterior part of the ramus has an almost horizontal ventral border below the articular process; the retroarticular process is reduced.

The dorsal view of the mandible (Fig. 7C) shows the broad mandibular symphysis, from which the slightly medially curved mandibular rami diverge to form a posteriorly open angle of about 15° from the central plane. Also, the rami are inclined laterally from vertical, exposing the inner sides in the truly dorsal view shown in Figure 7C. The anterior part of each ramus is thick, becoming thinner posteriorly. At the anterior tip of the coronoid process the mandibles start a medial curve that becomes sharp at the articular process, which is twisted and inclined mediad, exposing its lateral side in dorsal view.

In labial (lateral) view (Fig. 7A, 8A), each dentary forms more than half of its mandibular ramus. Anteriorly the dentaries are slender and show multiple labial (mental) foramina on the anterior half; posteriorly the dentaries become wider; dorsally and ventrally, they embrace the coronoid processes of the mandible. The coronoid processes are formed mainly by the laterally ascending compound bones; however, the coronoid forms a dorsal cap which extends medioventrally to the level of Meckel's canal. The lateral exposure of the compound bone has two foramina, one anterior near the joint with the dentary, and posteriorly another one (posterior mandibular foramen) that penetrates it from side to side anterior to the articular condyle. The mandibular condyle, formed by the compound bone, is bent medially and ventrally. The ventral borders of the coronoid process of the mandible are formed by a ventral process of the dentary and a small labial exposure of the angular.

In lingual (medial) view (Fig. 7B, 8B), each dentary has a Meckel's canal running along the midface from the medial symphysis to a mandibular central foramen of the medial face of the mandible limited by the dentary, angular, and coronoid. The posterior part of Meckel's canal is bordered dorsomedially by the coronoid and ventromedially by the angular, both bones overlapping the dentary. The labial surface of the coronoid process is formed mainly by the coronoid bone. Anteriorly the ventral borders are formed by the angulars; posteriorly they twist toward the labial face. A long, thin exposure of the compound bone lies between the angulars and coronoids; these exposures are widened posteriorly along the

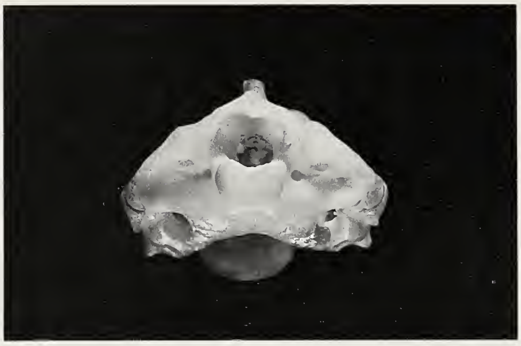

Fig. 5.—*Amphisbaena alba.* Posterior photographic view of skull (CG 3533).

articular process. The labial opening of the posterior mandibular foramen is partially bordered by the posterior end of the coronoid.

The several bony elements of the mandible form a longitudinal tunnel (Meckel's canal) that extends from the posterior mandibular foramen to the anterior part of the dentary. Posteriorly, the tunnel opens at the posterior mandibular foramen; at the middle of its length it opens at the mandibular central foramen and anteriorly it branches to end in several minor foramina on the labial side of the dentary. Some other small foramina of the compound bone and angular also terminate in this tunnel.

Descriptions of Individual Bony Elements

Premaxilla.—The U-shaped basal plate of the unpaired premaxilla terminates in a lateral process on each side (Fig. 9, 10). A medial and vertical nasal process (Jollie, 1960) arises from its middle; its dorsal edge curves smoothly and dorsoposteriorly. The nasal process passes posteriorly between and over the nasals and just reaches the frontals. The lateral aspects of the basal plate articulate with the maxillae, the posteromedial aspects with the vomers, septomaxillae, and nasal septum. Ventrally, the basal plate bears seven "subpleurodont" teeth (Gans, 1957), based in a single U-shaped dental groove with a higher labial than medial wall (Fig. 9C, 10C). The dry teeth tend to split along their axis of symmetry. The labial face of each tooth is in contact with the labial wall; the medial or posteromedial face is free and has a hollow pit, the nutritive foramen, at its base (Fig. 9C, 10C) along which bone reabsorption appears to take place in association with tooth replacement. Some empty "sockets" show a foramen at the bottom. The azygous tooth is the largest, the first paired teeth are more slender but almost as tall as the median one; the next two pairs are shorter. The first three teeth are aligned normal to the curved anterior edge of the premaxilla and the second and third pairs of teeth lie posteriorly in the dental groove at a more acute angle to the medial plane.

The top of each side of the basal plate forms the floor of the external nares. The more posterior lateral processes are covered by the maxillae. The joint surfaces with the maxillae are almost one-third as long as the horizontal edge of the premaxilla; the areas in contact are increased by rugose and longitudinal folding. Ventrally, a vertical wall borders the inner side of the U-shaped lateral processes that contact the vomers and septomaxillae.

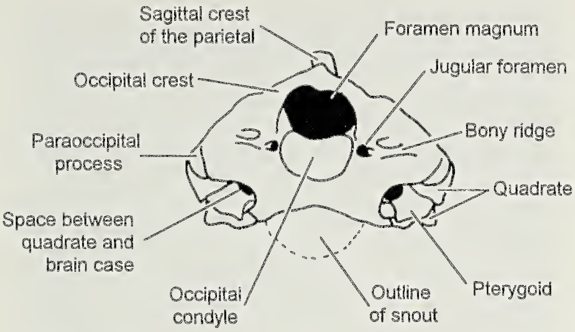

Fig. 6.—*Amphisbaena alba.* Labeled outline of posterior view of the skull shown in Figure 5.

Each side of the base of the nasal process bears a wide longitudinal canal. Its anterior end opens at the side of the vertical blade (Fig. 9A, 10A); anteriorly, the thickened nasal process protects the openings (Fig. 9D, 10D). The posterior end of this canal (see Bellairs and Kamal, 1981) opens directly posteriorly at the articulating surface of the premaxilla and septomaxilla (in which the canal continues), being separated from that of the opposite side by a thin vertical blade (Fig. 9C, 10C). The serial sections show that a narrow vertical canal extends ventrally just before the posterior end. That canal pierces the basal plate and subdivides, terminating at the nutritive foramen at the base of each tooth; a horizontal canal parallel to the dental groove interconnects the vertical canals.

The vertical portion of the nasal process is wide and forms the anterior extent of the snout. After bending horizontally, the posterior extension of the process becomes compressed into a blade, the surface extension of which separates the nasals which meet ventral to it. The rodlike termination of the nasal process lies at the anterior edge of the frontals.

The premaxilla is identified by general homology to the median tooth-bearing bone(s) of other reptiles (Romer, 1956; Fiorini, 1962). See Smith et al. (1953) about comments on the relation and innervation of the azygous median tooth with the egg-tooth.

Maxilla.—In cross section of the head, each of the paired maxillae (Fig. 11, 12) is roughly L-shaped, although the two surfaces join in a curve rather than an angle (Fig. 11E, 12E). The vertical lateral plate forms the lateral surface of the skull and its base gives rise to the teeth at the site at which it bends horizontally to form the palatal plate. Anteriorly, each maxilla contacts the premaxilla; medially the septomaxilla, vomer, and palatine; posteriorly the ectopterygoid; and dorsally the nasal, frontal, and prefrontal.

Anteriorly the lateral plate rises in a dorsovertical line. Posteriorly the lateral plate terminates vertically just posterior to the last tooth. The anterior portion of the dorsal border extends furthest dorsad; a triangular posteromedially directed frontal process (Kritzinger, 1946) arises from its anterior fifth and reaches past the nasal to extend between the frontal and prefrontal which overlaps it. More posteriorly, the dorsal border of the lateral plate terminates roughly in parallel to the ventral edge.

The posteriorly extending frontal process bends toward the midline (Fig. 11A–E, 12A–E). Only the anterior part of the process is visible in an intact skull

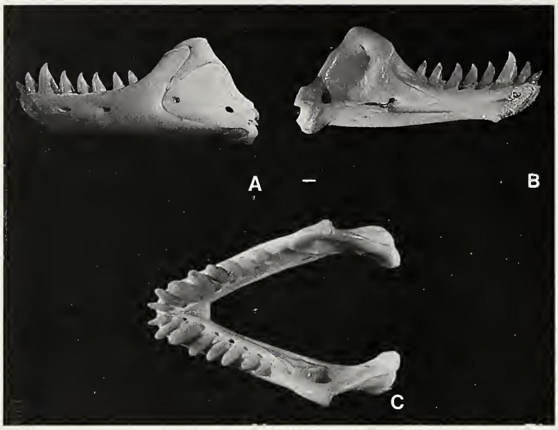

Fig. 7.—*Amphisbaena alba.* Photographs of isolated left mandibular ramus (CG 3533). The bar shows 1 mm to scale. A, lateral view; B, medial view; C, dorsal view of articulated mandible.

because the prefrontal overlaps a triangular portion along the posteroventral edge of the lateral surface.

One or two foramina open at the anteroventral corner of the vertical lateral plate. Here its surface folds inwards to form the side of the external nares. Two to four smaller foramina extend in a row from here to the center of the lateral plate, where one or two large foramina open. The posterodorsal corner of the vertical plate extends dorsally and posteriorly to overlap the maxillo–prefrontal junction; the prefrontal here abuts the medial surface.

The palatal plate of each maxilla extends medially from its ventral edge as a horizontal palatal process lying at an inner angle of about 90° anteriorly but becoming obtuse posteriorly (Fig. 11E, 12E); here it articulates with the ectopterygoid, which forms a continuation of the shelf. Ventrally, the palatal plate bears five posteriorly and medially curved subpleurodont teeth, the surfaces of which are smooth and not ridged (Fig. 11C, 12C); the labial faces of the teeth are curved but the medial ones are straight. The first maxillary tooth is the largest, the posterior ones smaller and subequal. Whereas all of the posterior teeth are smaller than the first, there is also a general trend to anterior to posterior reductions. However, the pattern is disjunct and several generations of tooth replacements may sometimes be involved in a tooth row. The medial wall of the dental groove is wide; from here the palatal process of the maxilla extends toward the midline, forming (with the vomer) a structure analogous to a secondary palate (Fig. 13, 14). A peglike premaxillary process departs just dorsal to the anteriormost maxillary tooth, from the ventral edge of the anterior end of the palatal process of the maxilla. This process overlaps the premaxilla dorsally and is overlapped, in turn, by the septomaxilla (therefore this process is masked in the articulated skull); its ventral articulating surface is folded and rugose as is the premaxillary counterpart. Posteriorly, the palatal plate expands medially and the anteromedial process of the ectopterygoid lies in a ventral groove; however, a tiny lateral process of the maxilla overlaps the ventral surface of the ectopterygoid.

The dorsal face of the palatal plate of the maxilla has two distinct areas of

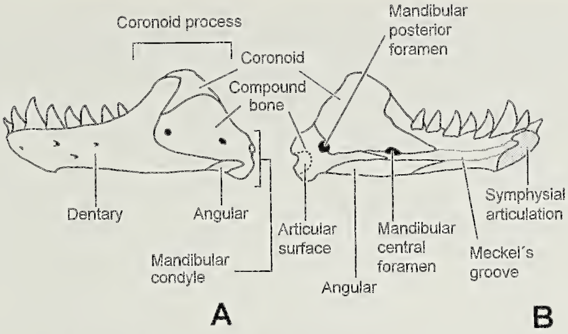

Fig. 8.—*Amphisbaena alba.* Labeled outline of mandible shown in Figure 7. A, lateral view; B, medial view.

different thickness; a maxillary step marks the boundary between these (Fig. 11A, 11D, 12A, 12D). The anterior and thicker area is overlapped dorsally and medially by the septomaxilla and forms the lateral part of the floor of the nares (Fig. 13A, 14A). Anteriorly, the medial edge of this portion forms the bony ventrolateral wall of the capsule of the organ of Jacobson (Fig. 13B, 14B).

The posterior area of the palatal plate of the maxilla forms part of the ventral floor of the nasal passage (Fig. 13A, 14A). The lateral wing of the vomer contacts the maxilla along part of the step that runs along a lateral and posterior diagonal; the joint between vomer and maxilla allows a connection between the opening of Jacobson's organ and the internal choanal opening through which passes the lacrimal duct. A large foramen opens at the inner angle formed by the vertical wall of the step (Fig. 11E, 12E); its canal passes from the dorsal surface of the posterior area of the palatal process to the lateral side of the vertical lateral plate. Here also it meets the posterior end of a canal that runs anteriorly to the lateral side of the nares (deep to the implantation site of the first tooth). A groove along the inner angle of the maxilla extends from the middle to the posterior end of this bone (Fig. 11D, 12D). The lacrimal duct lies in the groove.

The maxilla is identified as being homologous to the paired lateral tooth-bearing cranial bones of other reptiles (Romer, 1956).

Septomaxilla.—The paired septomaxillae (Fig. 15, 16) are exposed only on the inside of the nares. Each septomaxilla forms the roof of an organ of Jacobson and lines the floor of an anterior nasal passage (Fig. 13, 14). The complexly shaped bone lies dorsal to a vomer (Fig. 13B, 14B) and to the palatine process of the maxilla; whereas its posterior aspect contacts the wing of the vomer, the lateral border of the septomaxilla overlaps the palatal plate of the maxilla. The flattened dorsal surface is slightly concave.

The medial flat face of the septomaxilla contacts the medial cartilage of the nasal septum. However, the anteroventral corners of the paired bones pass ventral to the nasal septum and contact the opposite septomaxilla. The high anterior end contacts the premaxilla; posteriorly the medial face is ventrally arched (Fig. 15C, 16C) so that only its anterior and posterior ends make ventral contact with the vomer. At the midlevel of the septomaxilla there is a gap between the ventral concavity of the medial face and the underlying vomer (Fig. 13B, 14B). In medial view, the vertical flat face reaches less than half the height of the nasal cavity; a

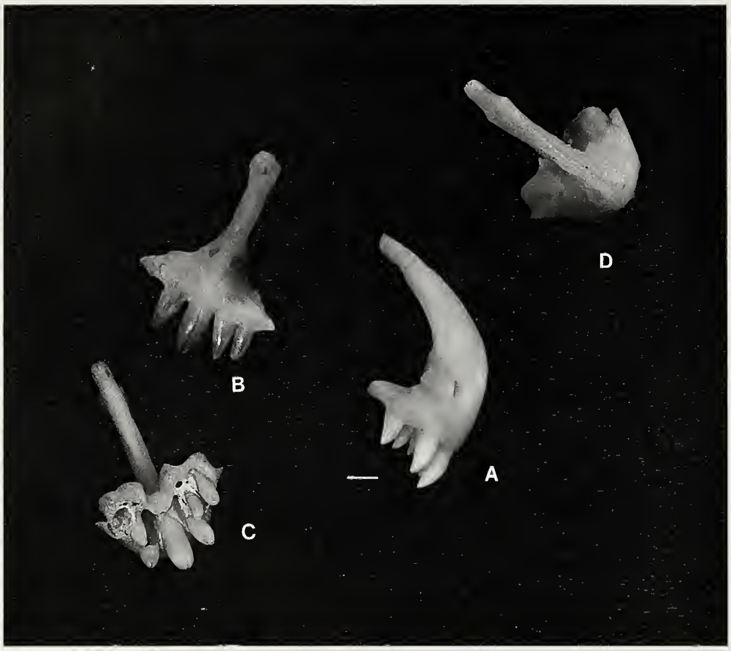

Fig. 9.—*Amphisbaena alba.* Photographs of premaxilla (CG 1811). The bar shows 1 mm to scale. A, lateral view (top of figure is dorsal, right is anterior); B, posterodorsal view; C, posteroventral view; D, dorsal view.

cartilaginous sheet (the nasal septum) rises between the medial borders of the septomaxillae, extending dorsally to the nasals. This medial sheet provides medial closure of the nasal capsules and partial separation of Jacobson's organs.

The straight medial border of the flattened septomaxilla is higher than the lateral one, so that the dorsal surface of the bone is inclined ventrolaterally. The anterior border continues laterally as a slender lateral process (Fig. 15A, 16A). Posteriorly, the thin lateral septomaxillary border expands over the maxilla and the wide U-shaped posterior border overlaps the vomer.

The anterior face of the septomaxilla is thicker at the medial side and becomes thinner laterally. Its medial region makes full contact with the premaxilla. The lateral anterior border overlaps the premaxillary process of the maxilla. At the anterolateral edge, a slim lateral process extends over the anterior palatine plate of the maxilla reaching to the border of the external nares; here the process bends dorsally to follow the shape of the nares. Near the midline, the septomaxilla is penetrated by a longitudinal passage (Fig. 15B, 16B); anteriorly, the larger medial opening faces the posterior foramen of the longitudinal canal of the premaxilla and a lateral opening faces anteriorly to reach the external nares dorsal to the premaxillary plate. In *Monopeltis,* the passage carries the medial nasal branch (of the olfactory nerve) and a small artery (Kritzinger, 1946).

In medial view of the septomaxilla (Fig. 13B, 14B), the thin anteromedial corner matches the inner concavity of the nasal process; more posteriorly the medial border is straight. The dorsal face is saddle-shaped, having a convex longitudinal axis and a concave transversal one (Fig. 15A, 16A). Anteriorly and

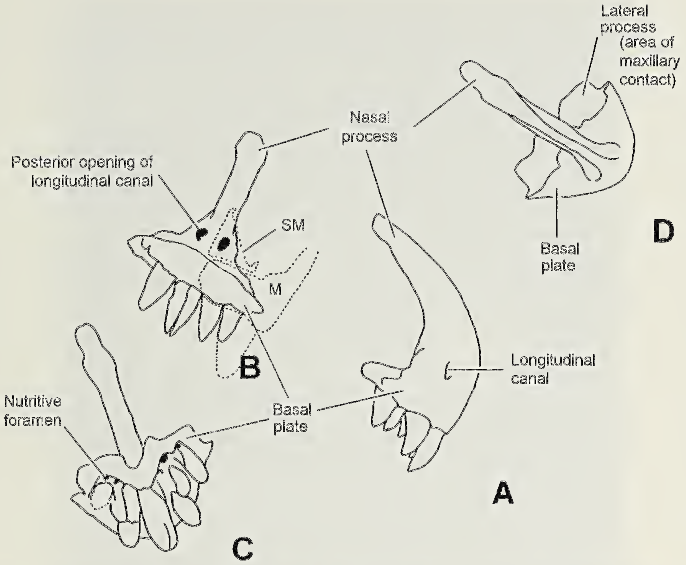
Lateral process (area of maxillary contact)
Nasal process
Posterior opening of longitudinal canal
SM
M
D
Basal plate
Longitudinal canal
B
Nutritive foramen
Basal plate
A
C

Fig. 10.—*Amphisbaena alba.* Labeled outline of premaxilla shown in Figure 9.

medially it is defined by slightly elevated borders; the posterior border is bent ventrally and contacts the vomer. The canal that pierces the septomaxilla opens posteriorly near the end of the dorsal middle border.

In ventral view (Fig. 14A, 15A) the concavity of the septomaxilla forms an inverted cup that roofs Jacobson's organ. The anterior and medial sides of the cup are bordered by a high ridge. The lateral flat border contacts the dorsal face of the palatine process of the maxilla and the thin U-shaped posterior border overlaps the anterior border of the vomerine wing; it thus encloses the posterior aspect of the organ of Jacobson. Some specimens show an elliptical foramen displaced to the midline at the dorsal edge of the cup; this foramen represents a medial opening of the longitudinal passage.

The septomaxilla is identified as the paired element that forms the base of each naris and roof of the vomeronasal system.

Vomer.—The complex, very elongate paired vomer has an elongate medial portion that parallels the midline of the palatal roof of the mouth (Fig. 17, 18) and from which arises a lateral wing. Anteriorly, the vomer lies ventral to the septomaxilla (Fig. 13B, 14B) and a slender anterior process of its medial portion contacts the premaxilla. More posteriorly there is a lateral wing, the edge of which abuts, and extends partially dorsal to, the palatal plate of the maxilla. The very slender posterior process of the medial portion extends ventral to the medial border of the palatine, ending just anterior to the contact of the latter with the pterygoid. The two vomers contact one another at the midline for the anterior third of their length; a medial gap separates them posteriorly (this is the anterior part of the pyriform recess). The anterior medial portion forms a vertical flat wall that rises dorsally from the straight medial edge; more posteriorly, the ventral edge of this wall inclines laterally, rotating to expose its surface in a ventral view. An-

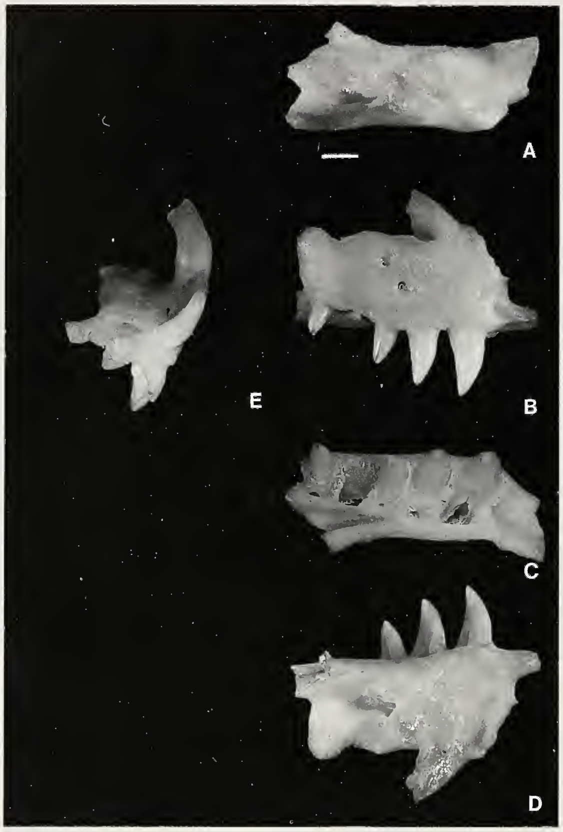

Fig. 11.—*Amphisbaena alba.* Photographs of right maxilla (CG 1811), anterior to the right. The bar shows 1 mm to scale. A, dorsal view; B, lateral view; C, ventral view; D, medial view; E, posterior view.

teriorly, this medial face is high and flat; it becomes gradually lower posteriorly with the posterior process terminating in a point (Fig. 17B, 18B).

The slender anterior process of the vomer contacts the posterior concavity of the premaxilla. At its middle, a triangular lateral expansion of the process forms part of the anterior border of the palatal opening of Jacobson's organ. The expansion is pierced by a foramen that extends from the medial face, to open on the anterolateral one. Here the foramen faces anteriorly and ventrally; in intact skulls, the foramen lies just anterior to the opening of Jacobson's organ. The anterior process is ventrally inclined from the plane of the rest of the vomer; it forms an angle at its base (Fig. 17B, 18B). This inclination reflects the inclination of the premaxillary basal plate relative to the rest of the skull (Fig. 13B, 14B).

The anterior border of the lateral wing of the vomer forms the posterior border of the bony frame for Jacobson's organ. Dorsally, the middle of the anterior border of the wing rises as a dorsal anterior ridge that converges posteriorly onto the medial wall (Fig. 17A, 18A), delimiting the posterior floor of the cavity of Jacobson's organ; the floor terminates posteriorly forming a narrow groove, whereas the adjacent and concave septomaxilla shapes the dorsal closure (Fig. 13B, 14B).

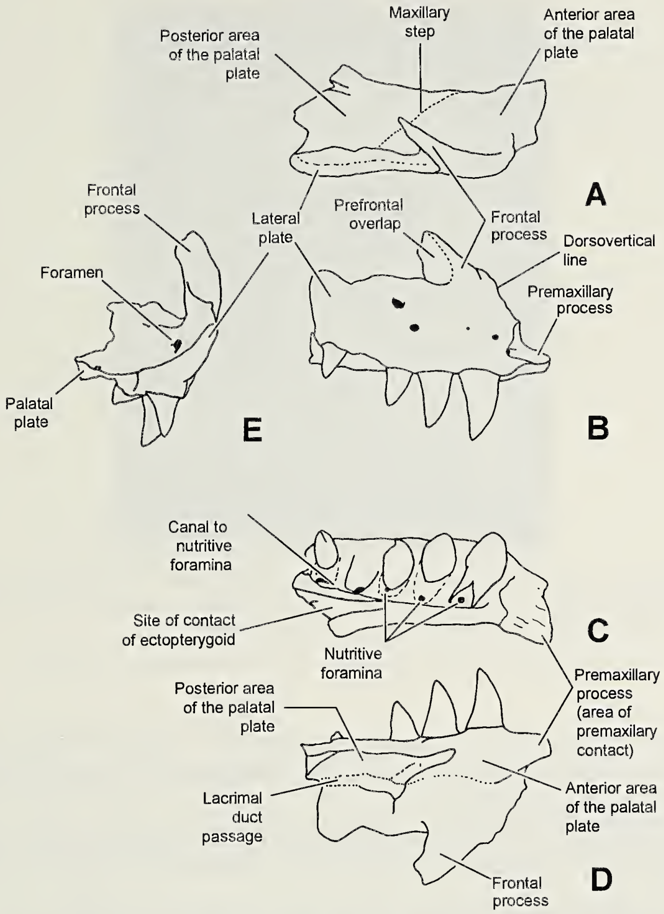
Posterior area of the palatal plate
Maxillary step
Anterior area of the palatal plate
A
Frontal process
Foramen
Palatal plate
E
Lateral plate
Prefrontal overlap
Frontal process
Dorsovertical line
Premaxillary process
B
Canal to nutritive foramina
Site of contact of ectopterygoid
Nutritive foramina
C
Premaxillary process (area of premaxilary contact)
Posterior area of the palatal plate
Lacrimal duct passage
Anterior area of the palatal plate
Frontal process
D

Fig. 12.—*Amphisbaena alba.* Labeled outline of maxilla shown in Figure 11.

At the center of the vomerine floor opens a canal which extends to the tip of the anterior process of the palatine (not illustrated). The smooth posterodorsal surface of the vomerine wings forms the floor of the nasal passage. At the base of the posterior vomerine process (the parasagittal plate), an anterior process of the palatine overlaps the vomer.

In dorsal view, the surface of the lateral wing shows an anterior ridge that diverges posteriorly from the midline and is paralleled by the median border of the maxillary shelf (Fig. 17A, 18A), thus forming an intermediate channel for the lacrimal duct (see Maxilla). Posteriorly, the dorsal surface of the lateral wings is smooth. The lateral border lies dorsad to the posterior surface of the palatal process of the maxilla, without touching it; the gap between them shapes the internal choana. Posteriorly, the thin vomerine margin is in ventral contact with the anterior border of the palatine.

Anteriorly, the vomers form a tunnel along the sagittal plane that leads to foramina piercing the medial vertical plates just anterior to their divergence. The foramina emerge at the tips of the anterior process of the palatine. A posterodorsal

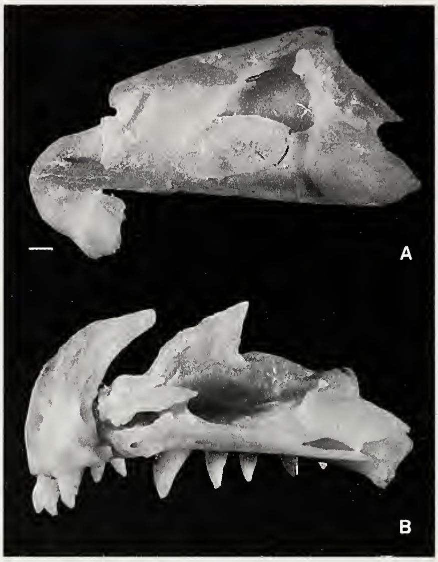

Fig. 13.—*Amphisbaena alba.* Photographs of partially disarticulated tip of snout (without the nasals and frontals) (CG 1811). Note that the posterior palatine process and the ectopterygoid are broken. The bar shows 1 mm to scale. A, dorsal view; B, medial view.

groove extends along the inner angle between the medial vertical plate and the horizontal wing. The anterior process of the palatine closes the dorsolateral aspect of the groove to form a canal.

The vomer is identified as the element that lies anteriorly on the palatal surface and extends laterally to form portions of the vomeronasal system and the internal choanae.

Palatine.—Each paired palatine roofs the posterior portion of a deep and inverted, posteriorly flattened palatal trough (Fig. 19, 20). The ventral edges of the palatines thus lie on the surface of the buccal palate, although the two medial edges of the bones are separated from each other by a narrow pyriform recess. Anterolaterally, each palatine contacts a vomer; laterally (posterior to the internal choana) each lies dorsal to the maxilla and the ectopterygoid, posteriorly each overlaps the pterygoid and dorsally each contacts the frontal, the (azygous) tabulosphenoid, and the prefrontal.

The center of the palatine forms a high vault, the palatal trough, that continues the choana posteriorly. The anteriormost portion of the trough is clearly highest (deepest), the palatine becoming shallower and flattening posteriorly at its articulation with the pterygoid. In dorsal view (Fig. 19A, 20A), the roof is triangular. The anterior high border forms the posteroventral closure of the nasal passage (Fig. 13, 14); the medial straight border is vertical but the lateral border extends laterally shaping the ventral wall of the orbital space as the anterior portion of the palato—pterygoid shelf (Fig. 3B, 4B). Anteriorly, the flattened dorsal surface of the bottom of the trough (the roof of the palatine) just contacts the frontal; more posteriorly it is in broader contact with the tabulosphenoid (Fig. 19A, 20A). Whereas these bones are adjacent, rather than forming an articulation, sections show ligamentous connections between them. The tabulosphenoid contact termi-

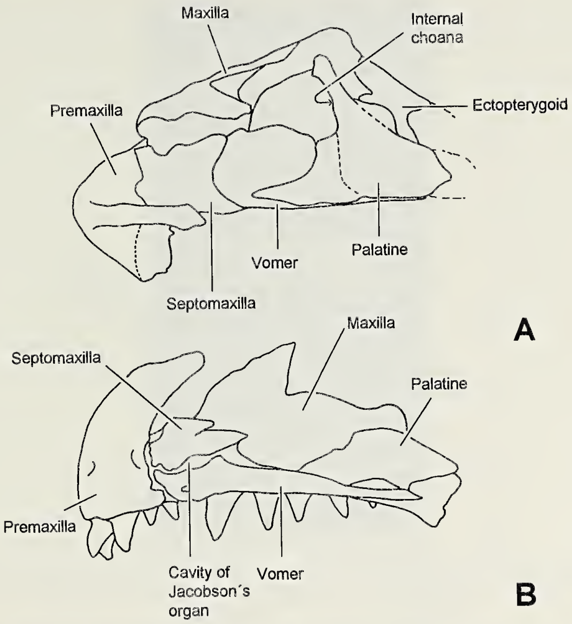

Fig. 14.—*Amphisbaena alba.* Labeled outline of Figure 13.

nates anterior to the dorsal overlap of the palatine with the pterygoid and the gap between these bones forms the anterior border of the Gasserian foramen.

The straight medial border of each palatine is formed anteriorly by a high concave parasagittal plate; posteriorly the border is formed by the medial edge of the choanal trough. The most lateral projection of the palatine plate is a triangular lateral process, the anterodorsal edge of which forms the posterior edge of the internal choana; the lateral projection then bends posteroventrally and recurves toward the midline, defining the internal choana. The posterior edge of the choana overlaps the dorsal surface of the maxilla and, posteriorly, of the ectopterygoid (Fig. 19C; also 3C, 4C). Anteriorly, the medial edge of the projection lies parallel to the medial border of the palatine (on the other edge of the trough). The lateral border is widest anteriorly; more posteriorly, it approaches the midline, narrowing the bone. The thin and flat posterior edge of the palatine overlaps the dorsal edge of the pterygoid.

Although the palatines do not show foramina, four horizontal canals pass through the sutures of each palatine with adjacent elements. Anteromedially, the dorsal contact of the palatine roof with both tabulosphenoid and frontals is interrupted by a canal that runs alongside the lateral process of the frontal from the inner side of the orbit to the medial nasal septum. Anterolaterally, the suture of the dorsal face of the palatine with the ectopterygoid is perforated by another canal extending from the ventrolateral side of the orbit to the groove along the inner angle of the maxilla. Posterodorsally, the posterior end of the suture between the tabulosphenoid and palatine shows a third canal that runs from the lateral gap between the parietal and the palato–pterygoid shelf to the medial gap between palatines. The fourth canal lies posterolaterally and can be double; it is shaped

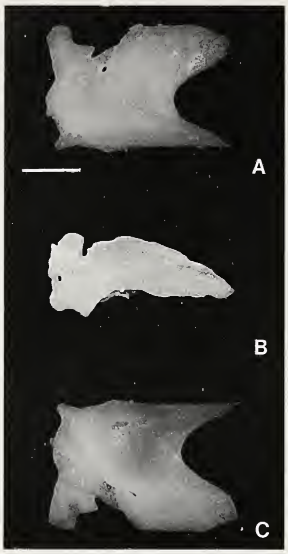

Fig. 15.—*Amphisbaena alba.* Photographs of right septomaxilla (CG 1811), anterior to the left. The bar shows 1 mm to scale. A, dorsal view; B, medial view; C, ventral view.

through the junction of palatine, pterygoid, and ectopterygoid, connecting the dorsal and ventral surfaces of the palato–pterygoid shelf; in smaller skulls (shorter than 1.8 cm) this gap is relatively wider. Could this be a reduced infraorbital fenestra that is otherwise common in other squamates (Jollie, 1960)?

The palatal trough provides posterior continuation of the air passage to the mouth. Moreover, in unskinned specimens the ventral aspect of each palatal trough is closed by a triangular projection of connective tissue that extends laterally from the medioventral border of the palatine. The free border of the tissue touches the lateral triangular process of the palatine. Thusly, it forms a closed canal, more posteriorly displacing the internal choana toward the posterior end of the palatine. This neochoanate condition (in the sense of Lakjer, 1927) of *Amphisbaena alba* is similar to that of *Monopeltis* (Kritzinger, 1946); the amphisbaenian secondary palate would be analogous to those of scincids (Greer, 1970) and some gymnophthalmids (Gans, 1978; Presch, 1976).

The palatine is here identified as the element that lies anteriorly on the palatal surface, that forms the frame of the palatal trough, and that extends posteriorly onto the pterygoid surface.

Ectopterygoid.—The paired triangular ectopterygoid (Fig. 21, 22) connects anteriorly to the maxilla and posteriorly to the pterygoid (Fig. 3B, 3C, 4B, 4C); ventrally it has a triangular (triradiate) exposure on the palato–pterygoid shelf and dorsally it reaches the lateral fold of the palatine (Fig. 3B, 4B). Each ectopterygoid is doubly forked. Anteriorly it has lateral and medial processes (Fig. 21A, and 22A), and posteriorly it has dorsal and ventral ones (Fig. 21D, 22D).

In a dorsal view, the ectopterygoid is Y-shaped (Fig. 21A, 22A); the widely separating anterior arms of the Y enclose the posterior aspect of the maxilla. The short and blunt anterolateral process contacts the posterior tip of the maxilla at the level of the back of the last maxillary tooth. This laterally compressed process

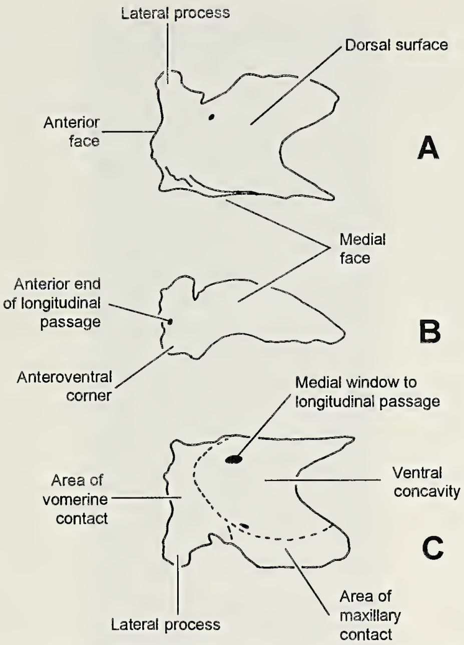

Fig. 16.—*Amphisbaena alba.* Labelled outline of septomaxilla shown in Figure 15.

extends posteriorly as a dorsal blade to reach the posterodorsal process (Fig. 21D, 22D), and forms the side of the palato–pterygoid shelf. The slender anteromedial process is longer than the anterolateral one and rests in a ventral groove of the palatal process of the maxilla.

The midline of the concave dorsal surface of the body of the ectopterygoid bears a faint ridge that just fits the lateral border of the palatine. The joint with the palatine runs posteriorly from the middle point between the anterior processes. It parallels the lateral line of the ectopterygoid; thus, the mediodorsal area of the ectopterygoid is covered by the palatine, whereas the lateral one is free.

The posterodorsal and posteroventral processes of the ectopterygoid interlock with the lateral anterior process of the pterygoid; the posterodorsal process attaches to the medial face of the lateral dorsal ridge of the pterygoid and the posteroventral process attaches to the ventral face of the pterygoid. Both processes are compressed. The base of the posteroventral process lies anterior to the posterodorsal one; in lateral view, they are parallel (Fig. 21D, 22D). In ventral view, the posteroventral process is slightly medial in relation to the posterodorsal one (Fig. 21C, 22C). The posteroventral process is more slender and shorter than the posterodorsal one. A small foramen perforates the base of the posteroventral process.

The ectopterygoid is identified as the element that completes the lateral edge of the palatal surface between the maxilla and the palato–pterygoid shelf. Lakjer (1927) incorrectly labeled this bone as a jugal, because a jugal usually forms the ventral and posterior margins of the orbit; a true jugal may be present in some amphisbaenian fossils of the family Hyporhinidae (Estes, 1983).

Pterygoid.—Each flat Y-shaped pterygoid (Fig. 23, 24) extends from anterior

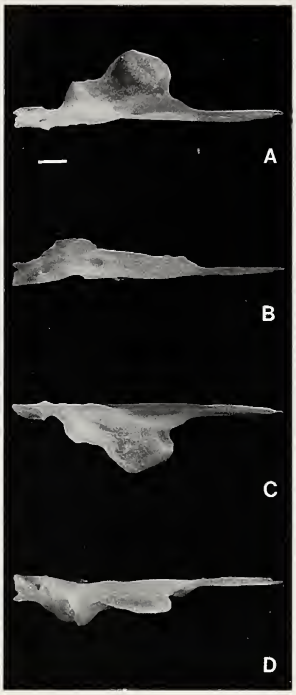

Fig. 17.—*Amphisbaena alba.* Photographs of right vomer (CG 1811), anterior to the left. The bar shows 1 mm to scale. A, dorsal view; B, medial view; C, ventral view; D, lateral view (angle of this view is slightly off horizontal).

contact with the palatine and ectopterygoid to pass ventrolaterally at the level of the cranial base where its lips rise and curve around the medial face of the ventral extent of the quadrate. The pterygoid abuts on the parabasisphenoid, but there is no clearly marked basipterygoid articulation (see below).

The main plate of the pterygoid is strongly dorsally inclined toward the midline (Fig. 3C, 4C), forming the posterior part of the palato–pterygoid shelf. The anterolateral process articulates with the ectopterygoid, the anteromedial process contacts the palatine, and its posterior process extends to reach and curve about the distal head of the quadrate. Medially the pterygoid parallels the lateral edges of the parabasisphenoid. The paired pterygoid is subtriangular in ventral view from the articulation with the palatine to the posterior apex where the bone curves around the quadrate. The lateral portion of the pterygoid is triangular in cross section, rising into a lateral dorsal ridge. This portion is anteriorly open, forming a deep pocket (not illustrated) which articulates with the posterodorsal process of the ectopterygoid. Medially, the bone is extended by a wide, thin flange that anteriorly articulates with the palatine and then abuts or parallels the edge of the parabasisphenoid.

The concavity of the anterior border of the pterygoid, between the anteromedial and anterolateral processes, is displaced to the midline; thus, the border of the base of the medial process is shorter than those of the longer lateral one. Most of the anterior border and the entire medial process are dorsally covered by the

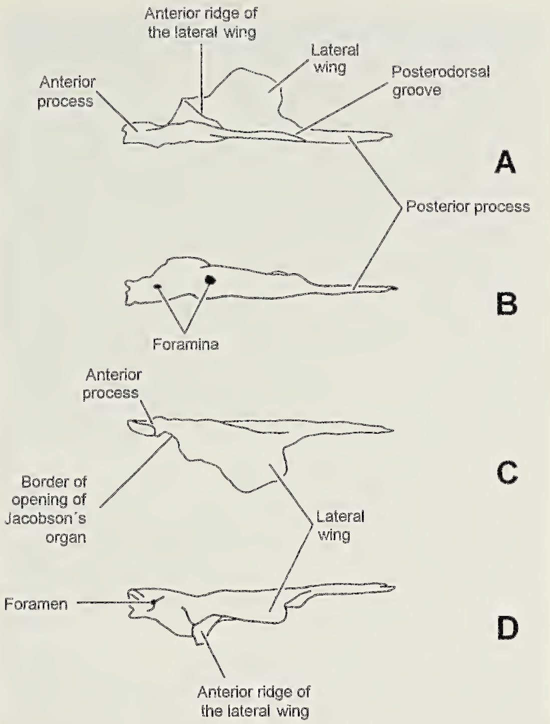

Fig. 18.—*Amphisbaena alba.* Labelled outline of vomer shown in Figure 17.

palatine that extends posteriorly at the midline. The articular surface bears short, shallow anteroposterior ridges.

Anteriorly, the medial border of the pterygoid lies ventral to and lacks contact with the tabulosphenoid and the parabasisphenoid, thus forming a longitudinal gap; more posteriorly it makes a loose medial contact with the parabasisphenoid (basipterygoid articulation) and may contact the edge of element-X. The portion of the pterygoid just opposite to the basipterygoid articulation can show (in section) a scattering of cartilaginous cells (Fig. 55B, 56B); these are not involved in production of a cartilaginous pad. The posterior portion of the medial border is free where it bridges the gap that separates the anterior part of the quadrate from the braincase (the posterior extension of the postorbital space).

In ventral view, the slim anterolateral process is covered by the posteroventral process of the ectopterygoid. At the lateral border, the pterygoid is a curved solid structure that is triangular in cross section; its ventral surface forms the base of the medial extension of the bone (the pterygoidal plate) that reaches to contact the parabasisphenoid. In dorsal view (Fig. 23A, 24A), one sees that the laterodorsal ridge and main plate of the pterygoid are separated by a narrow groove anteriorly; posteriorly, the groove ends in a pocket, into which fits the posterodorsal process of the ectopterygoid. Posteriorly to the anterolateral groove, the medial face of the lateral plate is continuous with the main one, shaping a step as a railing marks the ventrolateral border of the postorbital space. At the posterior end, the pterygoid is twisted laterally and sends a process around the medial and

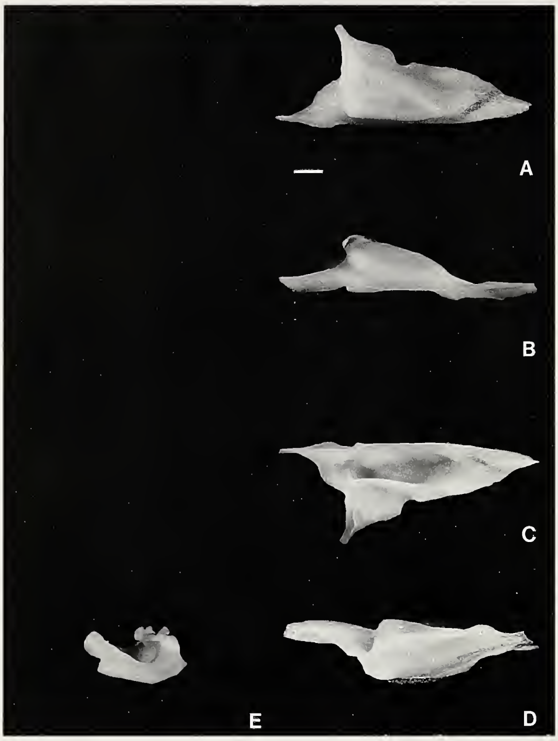

Fig. 19.—*Amphisbaena alba.* Photographs of right palatine (CG 1200), anterior to the left. The bar shows 1 mm to scale. A, dorsal view; B, medial view; C, ventral view; D, lateral view; E, anterior view.

posterior sides of the distal articular head of the quadrate (see also Fig. 55B, 56B). Here, the pterygoid shows a dorsolateral groove which fits the contour of the distal head of the quadrate. The posterior process of the pterygoid overlaps the medial and posterior borders of the ventral exposure of the anterior head of the quadrate. The articulated posterior process, ventral to the midbody of the quadrate, borders the extracolumellar path. The center of the posterior process shows spongy bone surrounded by a lamellar shell (Fig. 55, 56).

This large bone is identified as the pterygoid by its size, position, and anterior contact with the palatines and posterior articulation with the ventral shaft of the quadrate.

Nasal.—Each thick nasal (Fig. 25, 26) forms a subtriangular roofing over a naris, its typically rugose dorsal surface being incurved both in the anteroposterior and transverse planes. During skinning one can see that parallel ligamentous slips leave the foramina and connect the nasal to the thickened anterior integument. The anteromedial corner curves ventrally. The anterior side of the triangle forms a smooth curve marking the concave anterior narial edge. The lateral corner is truncated near its contact with the maxilla; it may slightly overlap the maxilla or embrace the maxillary anterodorsal edge. More posteriorly, the border angles more medially and forms a similar junction with the maxillary frontal process. The posterior side is concave and forms a complex series of articular shelves that

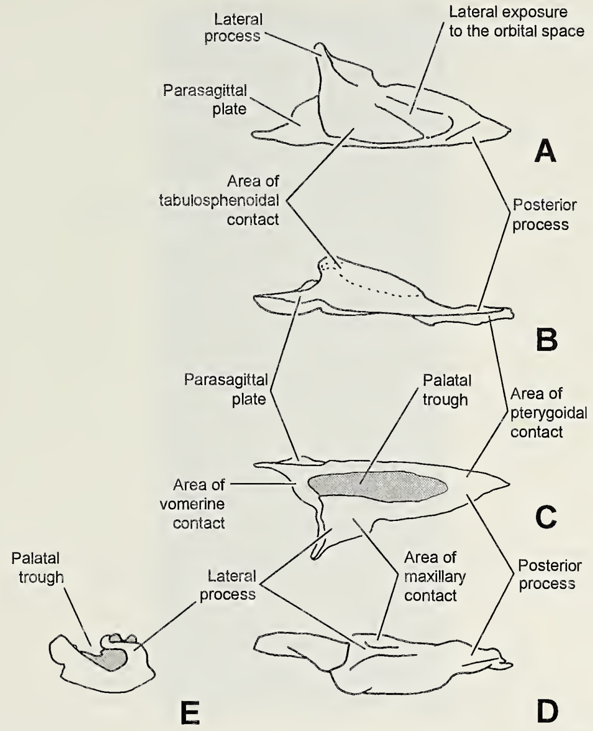

Fig. 20.—*Amphisbaena alba.* Labeled outline of palatine shown in Figure 19.

embrace the edge of the frontal. The medial border projects ventrally a concave bony medial sheet that embraces the nasal process of the premaxilla. The ventral portion of the medial sheet contacts that of the opposite nasal ventral to the nasal process of the premaxilla.

In ventral view, the internal surface of the nasal is concave and smooth (Fig. 25C, 26C); it defines the roof of the nasal passage. The medial border of each nasal is anteriorly curved where it fits around one side of the nasal process and descends parallel to this to form the dorsomedial roof of the nares. Ventrally, the thin, concave medial sheet contacts that of the opposite nasal near the midline. It is continuous with the cartilaginous nasal septum. Although the length of the ventral and dorsal borders of the medial sheet are similar, the ventral one is shifted posteriorly and its end is bent ventrally more markedly than the dorsal one. The concave anterior end of the medial sheet is wider than the posterior one, thus fitting the ventral widening of the premaxillary process and anteriorly having a ventral point of contact with the septomaxilla.

Posteriorly, at the middle of the joint with the frontals, the nasal has a narrow wedgelike frontal process. Between the frontal process and the posteromedial corner of the nasal, a thin, rugose (frontal) plate ventrally underlies the frontal. Lateral to the frontal process, the posterior border of the nasal bears two foramina that face into a notch of the frontal (not illustrated). Inside the bone, these foramina divide and connect to the numerous foramina that open onto the dorsal surface. The dorsal foraminal pattern has a centrifugal disposition from the center of the

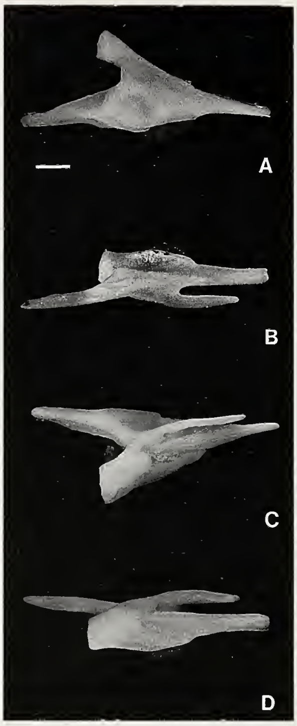

Fig. 21.—*Amphisbaena alba*. Photographs of right ectopterygoid (CG 1811), anterior to the left. The bar shows 1 mm to scale. A, dorsal view; B, medial view; C, ventral view; D, lateral view.

nasal (where the foramina pass perpendicular to the surface) toward the borders (where they lie more tangential to the surface and are continued by open grooves) (Fig. 25A, 26A).

The bone is identified as the roofing element of the naris and by its association with the premaxilla and maxilla.

Prefrontal.—The paired subtriangular prefrontal (Fig. 27, 28) forms the posterior part of the roof and posterolateral closure of the nasal passage. Laterally it extends the cheek dorsally above the maxilla, and forms the anterior wall of the orbit. The bone is not penetrated by any foramina; however, the lacrimal duct reaches the posterior face, lying either in a V-shaped groove or in an incomplete canal. The prefrontal is bordered anteriorly and ventrolaterally by the maxilla; dorsomedially it contacts the frontal and posteroventrally the palatine. The parietal sends anterior processes that sometimes contact the prefrontal.

In dorsal view, the lateral border of the prefrontal articulates ventrally with the lateral plate of the maxilla (Fig. 27A, 28A). The straight medial border articulates with the frontal process of the maxilla (the prefrontal lies external to the posterior part of this process) and the dorsal plate of the frontal; the posteromedial process of the prefrontal bends medially and lies in a groove of the frontal which usually does not reach the anterior process of the parietal (in AMNH 73233 the anterior process of the parietal contacts the prefrontal on one side; also see Jollie, 1960). Laterally, the posterior border bends ventrally. It contacts the ventral process of the frontal and the dorsal surface of the palatine. A concave, smooth surface faces

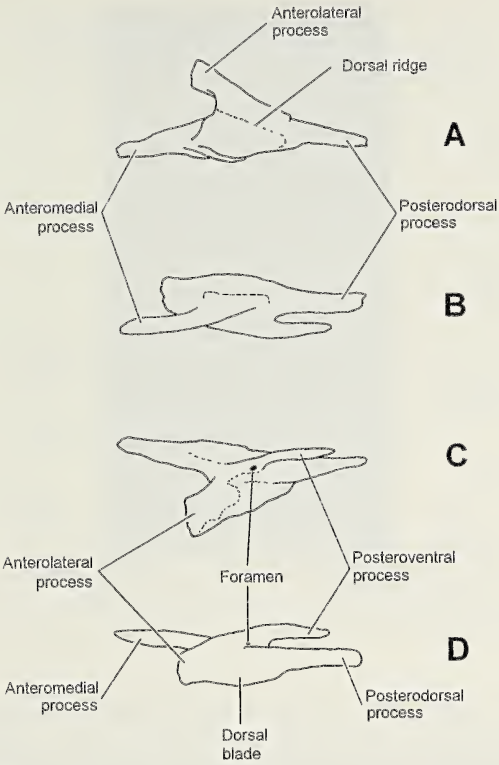

Fig. 22.—*Amphisbaena alba.* Labeled outline of ectopterygoid shown in Figure 21.

posteriorly to form the anterior wall of the open orbit (Fig. 1B, 27A, 28A). The bifurcate ventrolateral extent contacts the inner side of the lateral maxillary wall; the gap formed by the bifurcation (for the passage of the lacrimal duct) is laterally closed by the maxilla.

The prefrontal is identified as the element dorsal to the posterior aspect of the maxilla and in articulation with the frontal. However, as the lacrimal duct is closely associated with this bone, Kesteven (1957) proposed that it was the lacrimal, a bone penetrated by the duct which only lies adjacent to it in *Amphisbaena*. However, the lacrimal has frequently been lost in squamates; the prefrontal has not.

Frontal.—Each paired frontal (Fig. 29, 30) has a thick dorsal horizontal plate that articulates with that of the opposite side. Along the middle of its extent, the plate gives rise to a ventrolateral process that passes ventrad around the anterior end of the cerebral chamber and that ventrally contacts the frontal of the opposite side; the two frontals thus form a frontal ring (frontal fenestra) around the anterior end of the cerebral chamber (Fig. 31C, 32C). The horizontal dorsal plate of the frontal articulates anteriorly with the premaxilla, nasal, maxilla, and prefrontal, and posteriorly with the parietal. The lateral process has lateral contact with the prefrontal and ventral contact with the palatine and tabulosphenoid. All portions of the frontal are relatively thick; serial sections show that the centers of both the dorsal and lateral plates show scattered lacunae, suggesting spongy bone. The

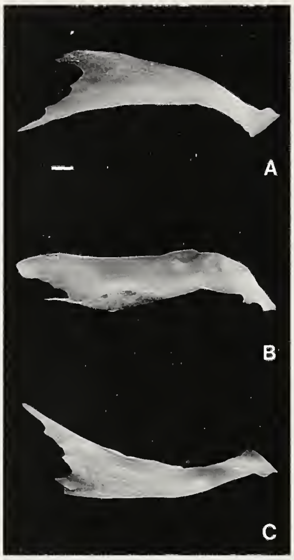

Fig. 23.—*Amphisbaena alba.* Photographs of right pterygoid (CG 1200), anterior to the left. The bar shows 1 mm to scale. A, ventral view; B, lateral view; C, dorsal view.

articulations consist of complex linear interdigitations within the articulating surfaces; these bones provide a rigid frame for the anterior braincase, connecting it firmly to the facial elements. The exposure of sutures along the external surface of the skull gives a poor indication of this complexity of internal sutures.

In situ, the anterior half of the dorsal plate of the frontal is ventrally inclined (Fig. 29B, 30B) beginning the profile of the snout. The truncated anteromedial corner fits the nasal process of the premaxilla. The anterior border joins with the nasal. A deep notch at the middle of the anterior frontal border is entered by the frontal process of the nasal (Fig. 29A, 30A). More laterally, one or two smaller notches sometimes mark the joint with the nasal. Anteriorly, the lateral border of the frontal contacts the frontal process of the maxilla. More posteriorly, the frontal has a deep, medially curved groove that embraces the posteromedial process of the prefrontal.

The medial border of the dorsal plate is thick. The median suture of the two frontals is marked along the cranial surface; however, the bone shows two or three layers. Whereas each layer articulates with that of the opposite side, the articulating curves, although matching those of the opposite side, are not congruent between layers (Fig. 29A, 30A). The asymmetrical arched folds and grooves of the medial surfaces fit those of the opposite side. They lock the dorsal interfrontal joint and prevent anteroposterior sliding along the midline.

Posteriorly, each frontal sends an articular plate ventral to the anterior edge of the parietal. The posterior border of this plate widens laterally. A thin, ventral projection of the adjacent (ventral) surface of the parietal keeps the simple medial edges of the articular plates from medial contact. More laterally, the articular plate of each frontal has a complicated suture with the overlying parietal. These lateral portions of the articular plates bear finger-shaped dorsal flutings and ridges that are oriented posteriorly and medially (Fig. 29A, 30A). Most of the ridges are

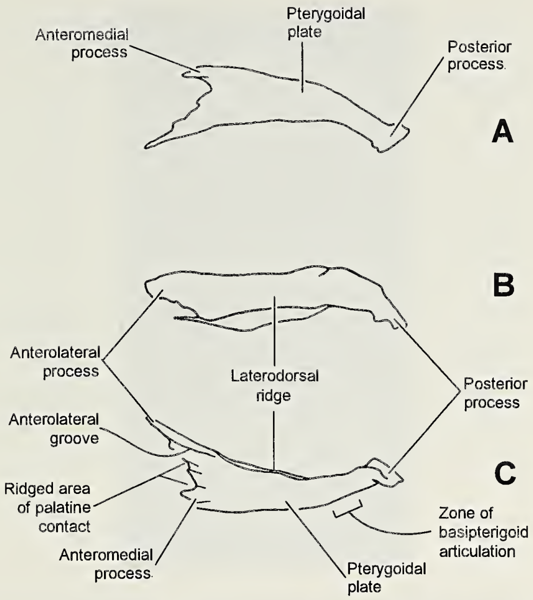

Fig. 24.—*Amphisbaena alba.* Labeled outline of pterygoid shown in Figure 23.

covered by the parietal surface; however, some of the larger ridges extend to and perforate the parietal to reach its dorsal surface (Fig. 31A, 32A).

At the level of the posterior end of the prefrontal, each frontal forms a lateral process; ventral to this, the ventral process then bends medially to form the floor of the anterior braincase. The sides of the ventral process of the frontal extend posteriorly to form a triangular exposure, dorsally with the anteroventral surface of the parietal and ventrally with the anterior curve of the tabulosphenoid (Fig. 2B, 2C, 3B, 3C, 31B, 32).

The ventral process of the frontals makes an elongated ring, the "frontal fenestra" (in CG 1811, reaching approximately 2.2 mm horizontally and only 1.5 mm vertically) (Fig. 31C, 32C). This fenestra is anteriorly closed by sheets of connective tissues pierced by nerves deriving from the anterior brain.

The thick, ventral end of each frontal has a grooved medial articular surface. Anteriorly, one or two processes interweave with those of the opposite side forming a lock-and-key junction that fixes the frontals relative to each other in a pattern similar to that of the dorsal interfrontal articulation. The anteroventral face of the ventral process contacts the palatine; posteriorly, this process contacts the azygous tabulosphenoid, of which two anterolateral processes embrace the interfrontal medial suture (Fig. 29, 30, 31C, 32C). The interdigitations of the wide contact surface with the tabulosphenoid are much shallower than those of the dorsal junction with the parietal.

Anteriorly, the lateral side of the ventral process gives rise to a vertical plate, the lateral process that extends ventrally below the frontal floor. This plate forms part of the posteroventral closure of the nasal cavity (Fig. 29D, 30D, 33, 34). The frontal is in contact with the palatine and tabulosphenoid at the ventral junction of the vertical plate with the frontal lateral wall. This is the site of the aforemen-

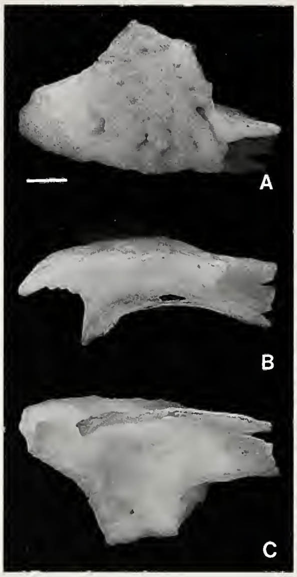

Fig. 25.—*Amphisbaena alba.* Photographs of right nasal (CG 1811), anterior to the left. The bar shows 1 mm to scale. A, dorsal view; B, medial view; C, ventral view.

tioned (see palatine) gap connecting the medial side of the orbit with the nasal capsules.

These unique bones are referred to as the frontals because in amphisbaenians they surround the olfactory passage anterior to the forebrain. Unlike those of most other reptiles, they preclude the formation of an interorbital septum. Bellairs (1949) specifically concluded that this aspect of amphisbaenian frontals is unique. However a similar ventral closure of the frontals is seen in other lizards, such as some Geckkonidae (Jollie, 1960).

Parietal.—The azygous medial parietal (Fig. 33, 34; also 3, 4, 31, 32) provides most of the roof and sides of the braincase. Anteriorly, the parietal forms an overlapping articulation with the frontals and posteriorly with the supraoccipital area of the occipital complex. A triangular, dorsal planar area includes the zone of frontal articulation (Fig. 31A, 32A). Its apex joins smoothly to a long medial crest that rises as it extends posteriorly and then widens to a dorsal boss after which the parietal splits to form a deep medial notch. Two wide and slightly convex lateral plates extend ventrally, thus shaping the lateral sides of the braincase; they contact the frontals, the tabulosphenoid, and the anterolateral processes of the occipital complex.

The development of the anterior part of the sagittal crest is variable depending on the size of the skull; on smaller skulls it may be only a slightly raised ridge. On larger skulls, it is represented by a higher and thickened blade. Posterior to the middle of the parietal length, the sagittal crest rises more sharply in a concave outline to a site at which it is broader and forms a flat dorsal facet (Fig. 31A, 32A); more posteriorly, a deep medial notch in the parietal forms around the continuation of the crest, seen as an ascendent process arising from the dorsal plate of the occipital region. The medial edges of the parietal, adjacent to the

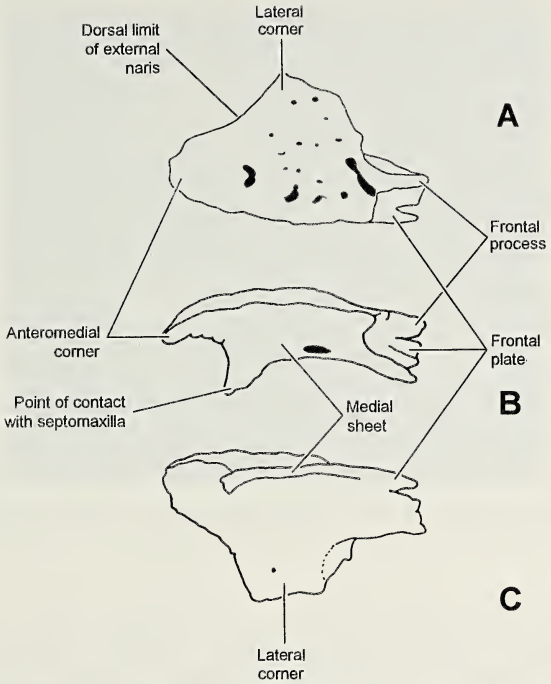

Fig. 26.—*Amphisbaena alba.* Labeled outline of nasal shown in Figure 25.

process, become thinner posteriorly. The posterior end of the sagittal crest of the parietal bears a concave articular facet. There is a vertical cartilaginous rod (the processus ascendens tecti synotici, Gaupp, in Kritzinger, 1946) between the facet and the ascendent process of the supraoccipital area.

Anteroventrally, the parietal articulates with the frontals at a complex, deeply notched, surface suture. The wide ventral articular surface of the anterior portion of the parietal shows long grooves that match the frontal ridges (Fig. 33A, 34). A tiny longitudinal blade at the sagittal line keeps the posterior ends of the frontals from contact. The parietal, and hence the cranium, is narrowest near the posteriormost extent of the frontal. More laterally the parietal edge inclines posteroventrally and forms a simple junction with the ventral process of the frontal.

The sharp ventrolateral borders of the parietals laterally overlap the vertical paired dorsal processes of the azygous tabulosphenoid. The inner (medial) surface of the ventrolateral borders of the parietal show elongate ridges that match those of the tabulosphenoid (Fig. 33B). Posteriorly, as the vertical dorsal processes of the tabulosphenoid are shallower, the parietal border becomes flat.

The parietal reaches its greatest width at the site of the flat lateral facets; here it is in dorsolateral contact with the dorsal anterolateral processes of the occipital complex. The inner surface of the parietal bears scalelike posterior projections (Fig. 33B) that fit into grooves on the anterior tips of the occipital. Posteriorly, the posterior plate of the parietal widely overlaps the dorsal plate of the occipital complex. The ventral face of the overlapping area is gently and longitudinally grooved; anteriorly, and laterally from the midline, it shows a short flap that

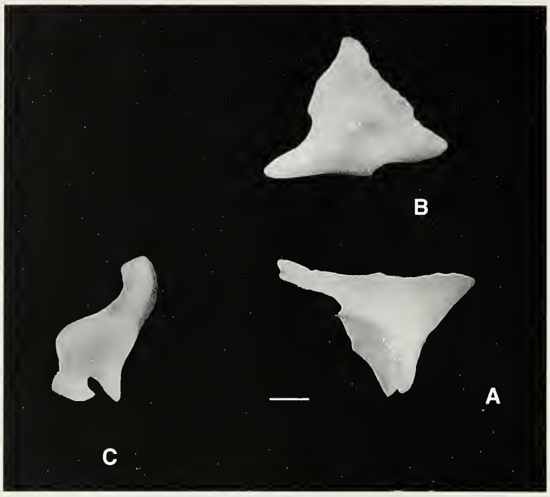

Fig. 27.—*Amphisbaena alba.* Photographs of right prefrontal (CG 1200), top is dorsal, anterior to the right. The bar shows 1 mm to scale. A, lateral view; B, medial view; C, posterior view.

embraces part of the occipital anterior edge. A medial elongated notch extends posteriorly from the sagittal crest accommodating the dorsal ascendent process of the supraoccipital area that posteriorly prolongs the sagittal crest. The lateral borders of the medial notch turn slightly dorsad, covering the base of the lateral faces of the occipital process.

The smooth inner surface of the parietal roofs and forms the sidewalls of most of the cranial cavity. Its dorsomedial line shows a shallow groove that marks the base of the sagittal crest.

The parietal is identified as the very large element roofing the braincase anterior to the occipital region. Although paired in many squamates, it is azygous in amphisbaenians.

Tabulosphenoid (ex Orbitosphenoid).—The unpaired tabulosphenoid (Fig. 35, 36) forms an elongated section of the floor of the anterior braincase between the frontals and the parabasisphenoid. The concave lateral borders of the tabulosphenoid articulate dorsally with the parietal, their closure shapes the sides of the braincase. Anteriorly, the most external portion of the tabulosphenoid extends dorsally to the palatines. Posteriorly, its posterior border medially overlaps the parabasisphenoid; more laterally it forms the anterior border of the Gasserian foramen.

The center of the tabulosphenoid is thick; however, each of the edges tends to be thinned, its medial surfaces being extended laterally and anteriorly and its peripheral surfaces being extended posteriorly. The curved grooves on the surface thus interlock with those on the adjacent elements.

The processes on the anterior edge of the tabulosphenoid lie ventral and external to those of the frontals, and are thinner than the body of the tabulosphenoid. The V- or U-shaped split between the anterior processes embraces the sides of the posterior part of the ventral interfrontal suture (Fig. 31C, 32C). In dorsal view, the anterolateral processes show shallow grooves that diverge posteriorly (Fig. 35A, 36A); the dorsal surfaces of the anterolateral processes are delimited pos-

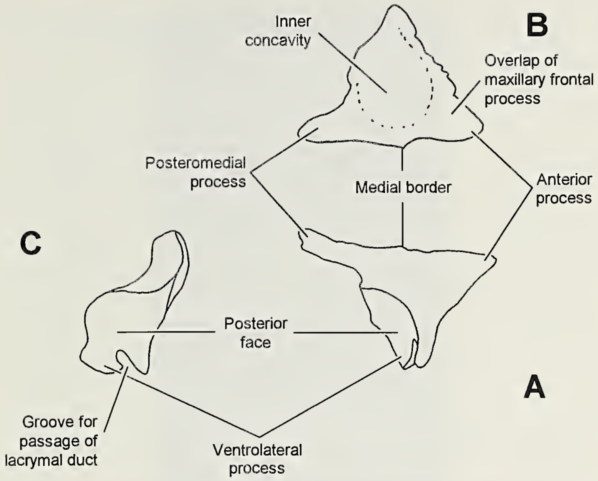

Fig. 28.—*Amphisbaena alba.* Labeled outline of prefrontal shown in Figure 27.

teriorly by a step which supports the posterior ventral ends of the frontals. Ventrally, each process abuts, without suture, the dorsal surface of a palatine.

The ventral surface of the tabulosphenoid (Fig. 35C, 36C) bears a slight and round medial keel, extending posteriorly from the anterior zone between the palatines to the level of the anterior tip of the parabasisphenoid. Here, the medial keel of the tabulosphenoid divides and the halves diverge posteriorly, forming a triangular medial groove, in which rests the rostrum of the parabasisphenoid. The posterior ends of the ridges are grooved, matching the ridges of the parabasisphenoid. The bottom of the medial groove may show a narrow posterior slit, or a scar, that could be evidence of a medial fusion of the posterior part of the tabulosphenoid (cf. Bellairs and Gans, 1983).

Each lateral portion of the posterior border of the tabulosphenoid contacts the most anterior point of the anterolateral processes of the occipital complex. Medial to this, the posterior border forms a small concave section of the most anterior border of each Gasserian foramen. The medial portion of the posterior border of the tabulosphenoid, between the posterior projections of the ventral ridges, is variable in shape and in its relationship with the parabasisphenoid. The center may be V-shaped and rest upon the dorsal surface of the anterior rostrum of the parabasisphenoid, or in other specimens it may be straighter and articulate with a step of the dorsal face of the parabasisphenoid.

In dorsal view, the vertical dorsolateral processes rise a little inward of the lateral borders and run posteriorly parallel to them. They are highest in their anterior third; posteriorly they descend gradually almost to nothing. The internal (medial) faces of the dorsal processes are straight and vertical, but the external (lateral) processes are inclined to the lateral border until they meet with the ventral face, and jointly form the sharp lateral border of the bone. The lateral faces of the dorsolateral processes contact the ventrolateral sides of the parietal; anteriorly, they show ridges that match the grooves on this bone. Posteriorly, the vertical blades of the tabulosphenoid are lower and the lateral borders just support the borders of the parietal.

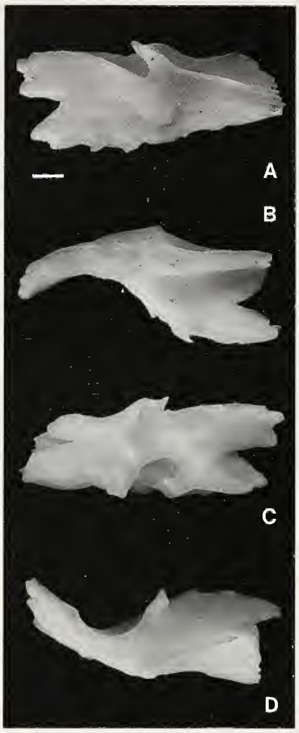

Fig. 29.—*Amphisbaena alba.* Photographs of right frontal (CG 1200), anterior to the left. The bar shows 1 mm to scale. A, dorsal view; B, medial view; C, ventral view; D, lateral view (this view is slightly tilted relative to view B so that their outlines differ).

The dorsal medial surface of the tabulosphenoid is smooth and concave (Fig. 35A, 36A). The posterior ventral groove for the parabasisphenoid does not modify the inner floor of the cranial cavity. On either side, midway between midline and lateral margin, open the ducts for the optic nerves (Kritzinger, 1946). These run anterolaterally and end beside the base of the ventral ridges at the tip of the articulation with the parabasisphenoid.

In lizards, the orbitosphenoid generally is a small, paired cartilage replacement bone. However, the analysis of embryonic material of the amphisbaenian genus *Leposternon* suggests that the elements of this region are paired membranous ossifications combined with the remnants of cartilages that fuse to produce the adult condition (Bellairs and Gans, 1983); clearly, this embryonic pattern suggests that we are dealing with the occurrence of a different, perhaps a compound bone. Hence, we depart from Bellairs and Gans (1983) and modify the name to tabulosphenoid (platelike sphenoid), to emphasize the distinction and to encourage examination of more and particularly embryonic material of possibly related outgroup forms.

Parabasisphenoid.—The azygous parabasisphenoid (Fig. 37, 38) is a wide, spearhead-shaped plate, with a thickened, roughly rectangular medial portion the dorsal surface of which forms the floor of the braincase. The ventral surface of the portion extends thin flanges that form the posterior part of the palate. Anter-

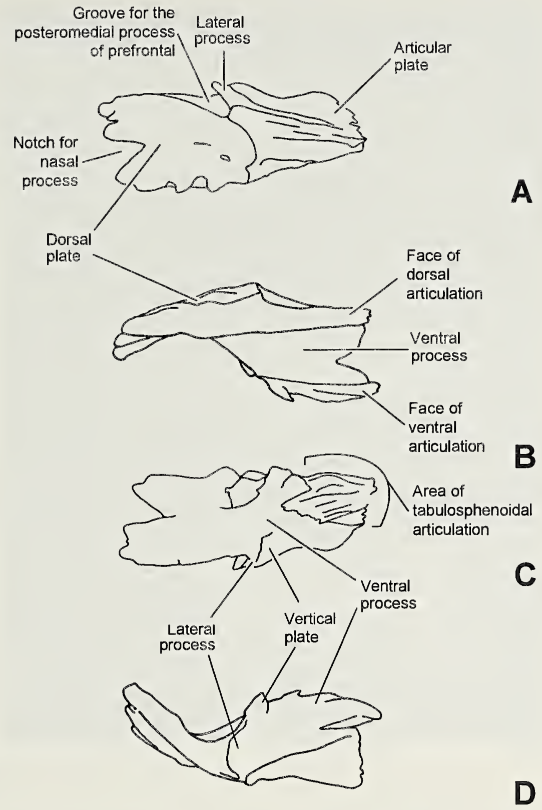
Groove for the posteromedial process of prefrontal
Lateral process
Articular plate
Notch for nasal process
A
Dorsal plate
Face of dorsal articulation
Ventral process
Face of ventral articulation
B
Area of tabulosphenoidal articulation
C
Ventral process
Lateral process
Vertical plate
D

Fig. 30.—*Amphisbaena alba.* Labeled outline of frontal shown in Figure 29.

odorsally, a blunt connection with some wedged projections inserts into the tabulosphenoid, and anteroventrally a sharp rostrum rests in a ventral groove of this bone. Posteriorly, the parabasisphenoid is ventrally inclined and articulates with the basioccipital area of the occipital complex. The parabasisphenoid is in lateral contact with a pterygoid on each side. Laterally the posterior border contacts an element-X on each side. Medially, the parabasisphenoid–basioccipital suture forms an irregular interdigitation either on the dorsal or ventral level of the bone.

The lateral edges of the parabasisphenoid angle outward evenly from their anterior rostrum up to the site at which the braincase starts; thereafter, the lateral edges of the parabasisphenoid flare more widely. A lateral concavity defines the volume between dorsal and ventral surface (Fig. 37B, 38B).

The medial axis of the ventral face of the parabasisphenoid is straight (Fig. 37B, 38B). Posterior to the middle of the parabasisphenoid length, the posterior borders of the ventral face extend into wide lateral plates (basipterygoid processes, Jollie, 1960; basipterygoid shoulders or angles, Vanzolini, 1951*a*) that are inclined ventrally; the plates laterally contact the medial borders of the pterygoids. These plates each bear a cartilaginous nodule shown mainly in the sections (Fig. 55B,

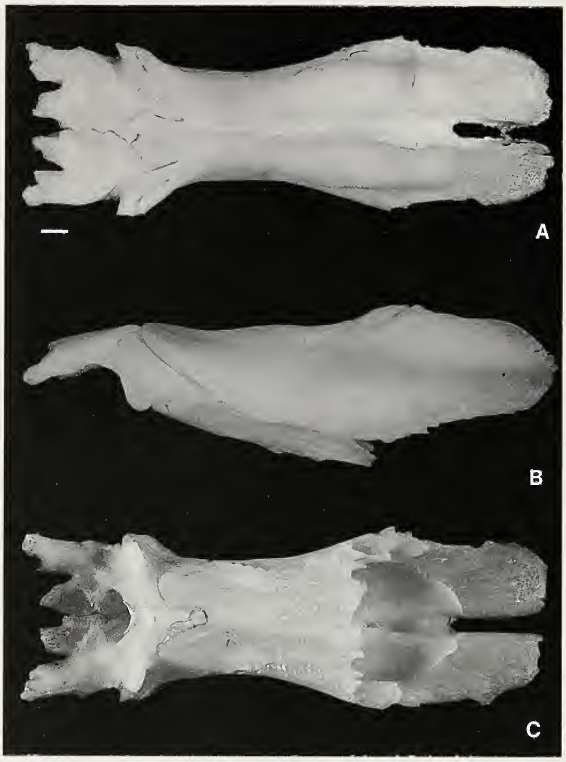

Fig. 31.—*Amphisbaena alba.* Photographs of articulated frontals, tabulosphenoid, and parietal (CG 1811), anterior to the left. The bar shows 1 mm to scale. A, dorsal view; B, lateral view; C, ventral view.

56B). Posteriorly the lateral plates are joined with the elements-X by a synchondrotic joint.

Each concave lateral face of the parabasisphenoid forms a groove that is open to the gaps left between palato–pterygoid shelves ventrally, and parietal and lateral sphenoid areas of the occipital complex dorsally. A large foramen enters the lateral side of the parabasisphenoid, near the midlength of the brain cavity (the anterior end of the parabasal canals; Jollie, 1960).

The thin dorsal surface of the anterior rostrum of the parabasisphenoid that contacts the tabulosphenoid seems to be formed mainly by the projection of the dense ventral layer of bone. At the posterior end of this contact surface there is either a smooth slope to the posterior and thicker area of the parabasisphenoid, or a more or less transversal and dentate step bordering the posterior edge of the tabulosphenoid. More posteriorly the concave dorsal face forms a shallow medial "basin" (best seen in histological section and representing the sella turcica) that is rounded posteriorly and elongated anteriorly. Its posteriorly displaced bottom is the thinnest region of the bone. There is no special depression for the hypophysis. The high and thick dorsolateral borders of the basin form the ventral borders of the Gasserian foramina. Anteriorly, the lateral dorsal borders project as small tabulosphenoid processes, dorsal to the anterior tip of the bone, that fit into grooves on the posterior ridges of the tabulosphenoid.

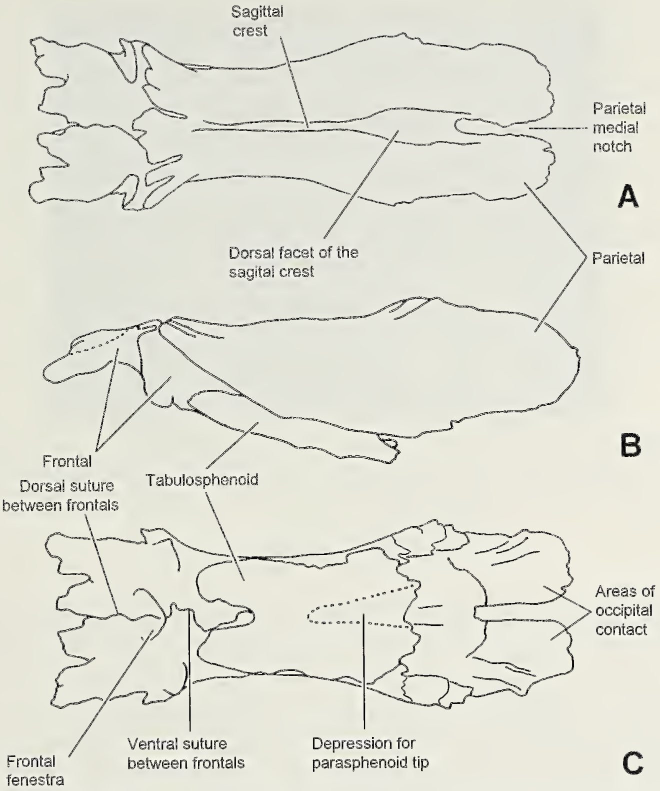
Sagittal crest
Parietal medial notch
A
Dorsal facet of the sagital crest
Parietal
B
Frontal
Dorsal suture between frontals
Tabulosphenoid
Areas of occipital contact
Frontal fenestra
Ventral suture between frontals
Depression for parasphenoid tip
C

Fig. 32.—*Amphisbaena alba.* Labeled outline of anterior braincase shown in Figure 31.

The thick posterolateral borders of the parabasisphenoid form flat contact faces for chondral articulation with the element-X of each side. A parabasal (Jollie, 1960) or Vidian (after Rieppel, 1993; Fig. 36C, 38C) canal opens at the base of the ventrolateral plate, just between the facets of articulation with element-X and the basioccipital area. Through this canal passes the internal carotid artery and the palatine branch of the facial nerve; anteriorly it opens on the lateral side of the parabasisphenoid. At its middle, the canal branches off to a canal that opens at the dorsal basin, carrying the internal carotid. The ventral side of the anterior foramen of each parabasal canal may bear a narrow and short fissure or a tiny scar marking the base of the ventrolateral plate; some specimens lack this scar (CG 1216, CG 1811, CG 3534, AMNH 73233, KM 11).

Medially between the elements-X of the two sides, the posterior border of the parabasisphenoid contacts the basioccipital area. Three areas of contact can be distinguished (Fig. 37D, 38D): at the midline there is a narrow zone, concave in the basioccipital area, with a thin articulation of dense connective tissue; more laterally the gap with the basioccipital is wider and each lateral area of the parabasisphenoid articulation shows rugose, or porous, convex surfaces that are faced with corresponding articulation faces of the basioccipital area. These lateral articular faces are covered with one leg of the triradiate cartilaginous plate (Fig. 55A, 56A). The frontal sectional slides show that the parabasisphenoid bone at the base

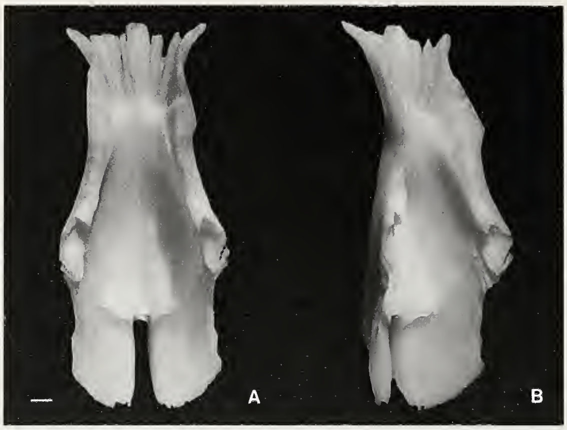

Fig. 33.—*Amphisbaena alba.* Photographs of parietal (CG 1200), anterior to the top. The bar shows 1 mm to scale. A, ventral view; B, ventrolateral view to show the ridges of the ventrolateral border. For dorsal and lateral views of this bone see Figures 2, 3, 31, and 32.

of the rostrum anterior process is spongy and there are spongy regions in the posterolateral corners deep to the lateral articular faces with the occipital complex (Fig. 55A, 56A). Large adults tend to show fusion of the sutures between parabasisphenoid, basioccipital, and elements-X (Fig. 55B, 56B).

The literature suggests that the parabasisphenoid is compound. The portion of the floor of the cranium that lies anterior to the basioccipital and extends laterally and ventrally to contact the pterygoids is considered to derive from the basisphenoid. The triangular anteroventral portion that contacts the tabulosphenoid is considered to be a fused anterior parasphenoid. This interpretation follows Zangerl (1944) and Jollie (1960). Kesteven (1957) stated that reptiles lack a parasphenoid, and that the amphisbaenian parabasisphenoid represents only the basisphenoid. Moreover, Zangerl (1944) discussed the possibility that juveniles of *Leposternon* may have two sutures, an anterior one between the basisphenoid and parasphenoid and a posterior one between the basioccipital and basisphenoid. Regardless of the situation in other species, our specimens of *Amphisbaena alba* show only the posterior one. Zangerl also mentioned separation of a presphenoid in the extreme anterior tip of the parabasisphenoid; no such separation appears in our material.

Element-X.—The elements-X (Fig. 39, 40) are small, massive bones (defined by the triradiate cartilaginous plates), each fitting into a lateral socket between the parabasisphenoid and the basioccipital and prootic areas of the occipital complex (Fig. 55, 56). In large specimens, the elements-X tend to fuse as the plates close.

In ventral view, each element-X has a subtriangular shape. The apex faces the midline and the rounded lateral side (Fig. 39C, 40C) faces to the fenestra ovalis; the anterior side forms a synchondrosis with the parabasisphenoid and the posterior side with the lateral expansion of the basioccipital plate. The anterior and posterior faces are flat; whereas the anterior area of articulation has an oval outline, the shape of the posterior one is subtriangular.

A thickening at the center of the dorsal face (Fig. 39B, 40B) embraces the end of the prootic process. The internal carotid artery passes ventral to the stapes to

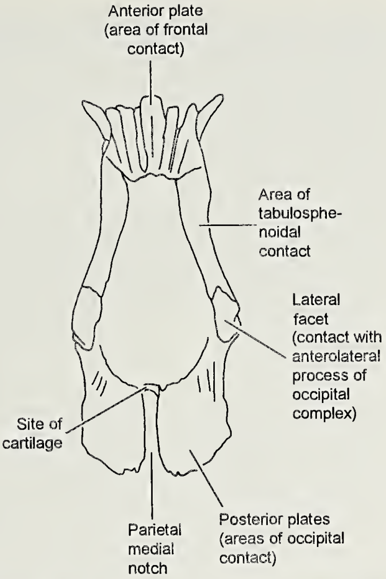
Anterior plate (area of frontal contact)
Area of tabulosphenoidal contact
Lateral facet (contact with anterolateral process of occipital complex)
Site of cartilage
Parietal medial notch
Posterior plates (areas of occipital contact)

Fig. 34.—*Amphisbaena alba.* Labeled outline of parietal shown in Figure 33A.

enter the skull through the parabasal canal defined by the prootic process, the lateral expansions of the basioccipital area and (ventrally) the element-X. The parabasal canal is continued anteriorly into the parabasisphenoid. The element-X is entirely spongy and its articulations are cartilaginous (Fig. 55, 56).

The nature of the element-X as an element of the amphisbaenian skull has been discussed in the previous literature but there is no agreement among authors. Zangerl (1944) cites Williston (1917) as having labeled the elements as "paroccipitals," but our copy of the paper lacked such a figure; however, in Williston (1918*a*) the element is coded "pc." Williston, 1918*a,* only included the view of the skull to illustrate the vertebrae of the head joint and does not identify the abbreviation; however, in the next paper in the journal (Williston, 1918*b*) and in his summary book (1925) the abbreviation "pc" is coded as prootic. Diverse alternative interpretations can be found: Lakjer (1927) and Jollie (1960) called them sphenoccipital epiphyses; Zangerl (1944) found no certain homologies to any reptilian bone, calling them "elements X"; Vanzolini (1951*a*) suggested homology to the basitemporal of birds and crocodilians; and Kesteven (1957) considered them as reduced prootics. Gans (1960, 1978) considered these elements as bony epiphyses suitable for muscular attachment, a position supported by our histological evidence. Hence we accept the position of Lakjer (1927) and Jollie (1960). However, the double synchondroses generate uncertainty as to whether the epiphyses pertain to the basioccipital or the parabasisphenoid. For this reason the term element-X remains suitable.

Stapes.—The paired stapes (Fig. 41, 42) have a subcircular, thick footplate that fits into each fenestra ovalis of the occipital complex; both faces of each footplate are quite concave. Its distal face gives origin to a bladelike stapedial columella (Fig. 41A, 42A) that projects ventrolaterally toward the quadrate. The anterior edge of the columella forms an articulation for the cartilaginous extracolumella

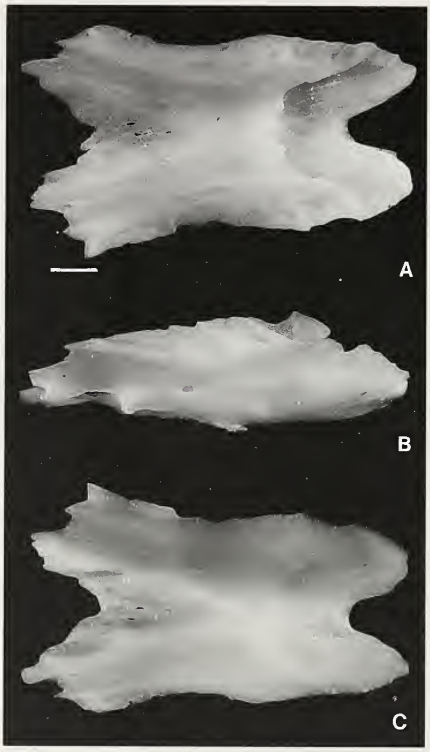

Fig. 35.—*Amphisbaena alba.* Photographs of tabulosphenoid (CG 1200), anterior to the right. The bar shows 1 mm to scale. A, dorsal view; B, lateral view; C, ventral view.

just before its distal end. The footplate, but not the columella, is formed of spongy bone.

The footplate fits exactly into the fenestra ovalis as a plug; the outline of the proximal (inner) face of the footplate follows the almost circular shape of the transverse section of the auditory tube. A step or ridge of the otic capsule (seen only internally) passes half around the auditory tube; on the lateral side, it supports the border of the proximal stapedial face. At the opening of the auditory tube the inclined anterior border of the footplate is thicker than the posterior one (Fig. 41A, 42A). The distal face extends anteriorly, overlapping the anterior border of the tube, covering part of the facial canal of the occipital complex.

The compressed columella (Fig. 41B, 42B) ascends perpendicularly from the center or from the anterolateral side of the distal face of the stapedial footplate, as a projection of the border. Both faces of the base of the columella show tiny foramina. The posterior border of the columella shows an S-curvature, with the distal tip rounded; the anterior border of the columella rises almost straight. Its distal end bears an anteriorly oriented articular face that connects with the extracolumella.

The stapes are recognized as being the bones that close the fenestra ovalis and distally contact the cartilaginous extracolumellae (Wever, 1978).

Quadrate.—The quadrate (Fig. 43, 44) is a paired, complexly shaped long bone that links the side of the cranium (paroccipital process) to the posterior end of

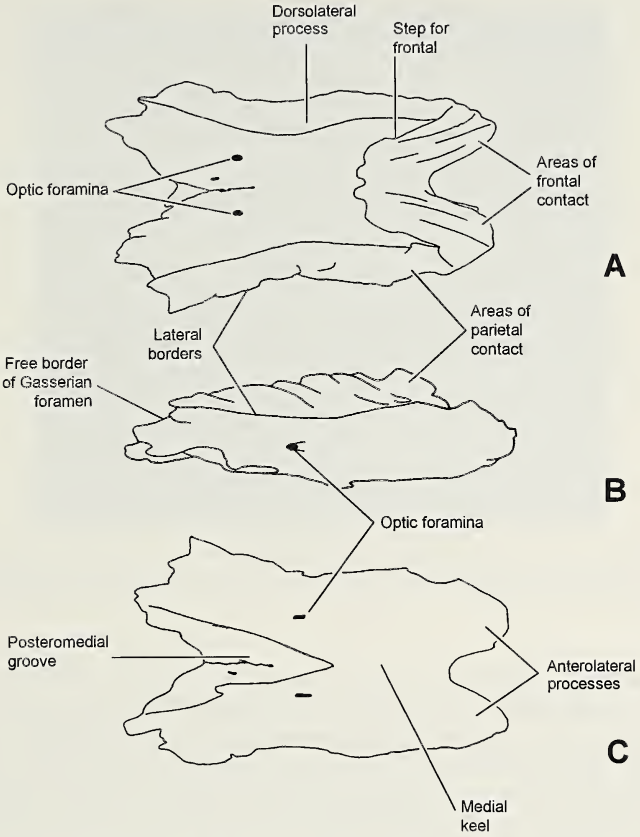

Fig. 36.—*Amphisbaena alba.* Labeled outline of tabulosphenoid shown in Figure 35.

the mandibular ramus (articular process of the compound bone). Anteriorly, its longitudinal axis slightly approaches the sagittal plane (at an angle less than 10°) and is vertically inclined at an angle of approximately 30°. The posterior continuation of the postorbital space, which is continued to the otic region, separates the medial face of the quadrate from the braincase. Anteriorly (distally), the medial and ventral sides are embraced by the posterior end of the pterygoid; posteriorly it contacts the columellar tip and the extracolumella swings around its ventral exposure.

The quadratic proximal articulation with the paroccipital process is subcircular in shape, and its surface is strongly concave (Fig. 43E, 44E). The distal articular head of the quadrate is slightly wider and higher than the shaft of the bone and the articular surface is saddle-shaped; its convexity is vertical and its concavity horizontal. The ventral side of the articular head protrudes, leaving a marked posterior ridge (Fig. 43B, 44B) that is embraced by the posterior process of the pterygoid. The lateral sides of the distal end are flat and vertical (Fig. 43A, 44A).

A lateral plate emerging tangentially from the shaft shapes a wide and flat lateral face of the quadrate, the center of which has a hollow concavity, the bottom of which is pierced by a lateral foramen (Fig. 43A, 44A). The lateral plate extends

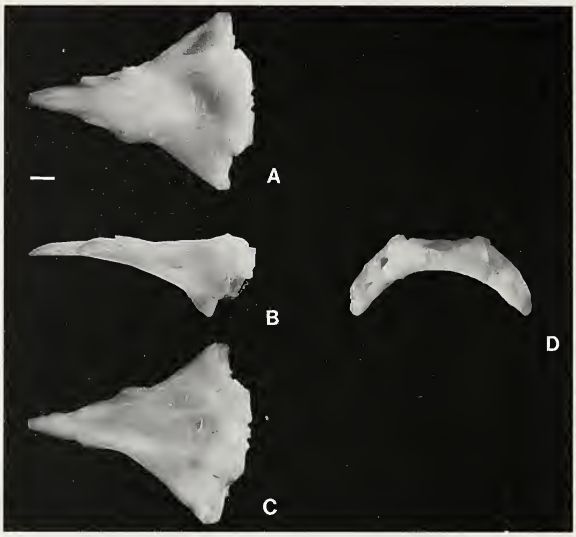

Fig. 37.—*Amphisbaena alba*. Photographs of parabasisphenoid (CG 1200), anterior to the left. The bar shows 1 mm to scale. A, dorsal view; B, lateral view; C, ventral view; D, posterior view.

ventrally, projecting slightly below the ventral quadratic face. The posterior part of the lateral plate extends dorsally beyond the dorsal border of the proximal articulation; it maintains its height, dorsally greater than that of the body of the bone, along the posterior half of the quadrate, but becomes lower anteriorly.

The dorsal surface of the quadrate is flat and narrow, being limited at the sides by the lateral plate and by a smaller medial border (Fig. 43D, 44D) that extends from the anterior half of the quadrate (where the opposite lateral plate becomes lower). These two projections form an intermediate concave dorsal canal along the quadrate. A distinct dorsal foramen pierces the base of the lateral plate; its canal ends at the center of the lateral plate (lateral foramen).

The ventral view of the quadrate (Fig. 43B, 44B) shows a narrow, flat corridor along which runs the extracolumella. This corridor passes anteriorly from the ventral posterior end of the quadrate and spirals laterally to end at the lateral face of the distal end.

The medial side of the distal head and the posteroventral border of the quadrate shaft contact the posterior process of the pterygoid; its expanded head rests next to the ventral extracolumellar corridor. One or two tiny foramina appear just dorsal to the attachment of the pterygoid. Both proximal and distal heads of the quadrate are formed of spongy bone. However, the shaft and the projecting plates represent dense laminar ossification (Fig. 55, 56).

The quadrates are identified as the bones that provide articulation of the mandible to the braincase.

Occipital Complex.—The occipital complex (Fig. 5, 6, 45, 46) represents the posteriormost aspect of the skull. Several cranial elements appear to have fused, making the structure most complex, geometrically and developmentally. Several of its elements remain as anteriorly reaching processes, making the occipital complex easiest to describe from back to front. It consists primarily of the fused four-element (supraoccipital, exoccipitals, basioccipital) ring framing the foramen mag-

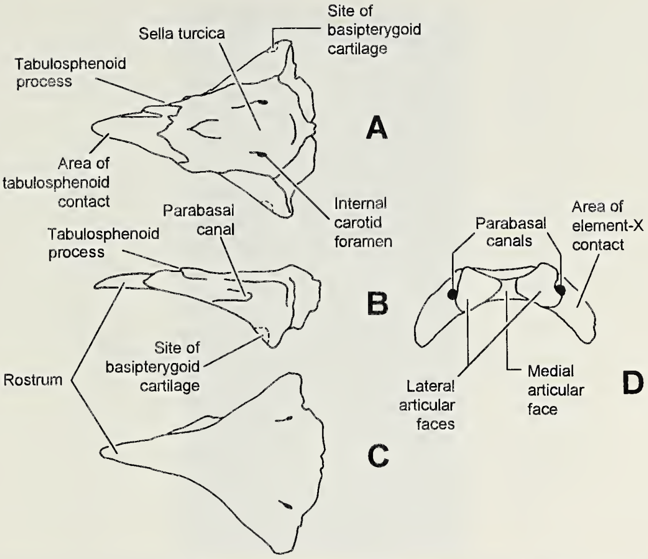

Fig. 38.—*Amphisbaena alba.* Labeled outline of parabasisphenoid shown in Figure 37.

num, and extending as a pair of lateral wedges in posterior view. Dorsally there is a pronounced and flaring occipital crest that provides a domed roof anteriorly underlying the parietal and extending laterally to the quadrate articulation. Ventral to the foramen lies the occipital condyle, the base of which reaches anteriorly into the basioccipital plate (Fig. 45C, 46C). This plate extends anteriorly to the contact zone with the parabasisphenoid and laterally to the cup-shaped articulation with the elements-X. Somewhat anterior to the foramen magnum, the occipital complex broadens and sends lateral branches to the paroccipital processes. The thick zone between the dorsal and basioccipital plates is complicated by fusion of the multiple elements that comprise the internal portions of the otic apparatus. The auditory canal emerges through the ventrolaterally placed fenestra ovalis which holds the stapedial footplates.

The occipital condyle is double knobbed (bicipital) and formed of spongy bone. The articular surfaces are smooth (and seen in section to be covered with hyaline cartilage), whereas the rest of the surface is rougher. In posterior view, the condyle has the shape of a kidney resting on its side. As the anterior part of the bicipital occipital condyle is narrower than the posterior head, it shapes a "neck." The bicipital knobs project further dorsally than ventrally; they are more widely separated by the midventral border of the foramen magnum (Fig. 5, 6). The atlantal vertebra surrounds the condyle like a ring; its dorsal projection reaches the inner face of the dorsal roof of the foramen magnum which constrains its opening. The condylar articulation is unique in having a meniscus.

The foramen magnum opens in the center of the posterior face of the occipital complex immediately dorsal to the occipital condyle (Fig. 5, 6). The posterior face is delimited dorsally by the occipital crest, laterally by the paroccipital processes, and ventrally by the ventral plate of the occipital. Lateral to the foramen magnum, the surface of the posterior face is concave. Lateral to the base of the

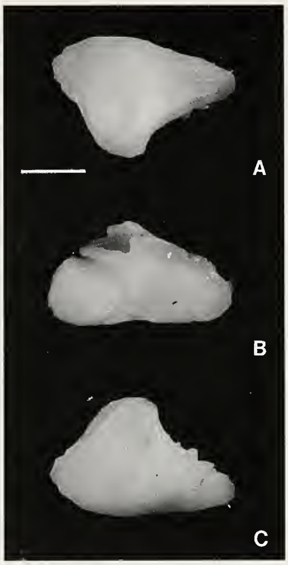

Fig. 39.—*Amphisbaena alba.* Photographs of right element-X (CG 1200), anterior to the left. The bar shows 1 mm to scale. A, dorsal view; B, medial view; C, ventral view.

occipital condyle appear two large jugular foramina; they open into a chamber from which five foramina radiate. The largest foramen passes to the cranial cavity; the internal opening lies just posterior to the otic capsule. Two of the four smaller foramina enter from the ventral surface, one enters medially, and the last one dorsally. Two bony ridges extend laterally along the posterior face from the level of the jugular foramen to the posterior part of the paroccipital process.

The posterior border of the dorsal plate is elevated into a transverse occipital crest that projects beyond the posterior aspect of the cranium and reaches almost to the end of the middle of the occipital condyle. The extent of crest and condyle in dorsal view are affected by slight allometric differences and angulation of the long axis. In dorsal view, the border of the occipital crest is generally medially notched.

The dorsal plate roofs the foramen magnum. There is a wide transverse occipital crest that curves from the quadratic articulations to the midline. The most striking feature of the dorsal plate is the high and thick sagittal ascendent process, which fits into the median notch of the parietal and thus continues the sagittal crest of the parietal posteriorly (Fig. 45A, 46A). In lateral view (Fig. 45B, 46B), the anterior part of the process has a baseline that runs parallel to the dorsal border; however, the posterior end of the baseline rises to meet the dorsal border of the occipital crest. The dorsal plate spreads laterally and anteriorly from the base of the ascendent process forming a doubly crescentic element, the posterior crescent deriving from the occipital crest and the more anterior one from the flared edge between the anterolateral processes. The plate roofs the posterior part of the braincase and the otic capsules. The roof of the otic capsules shows some spongy bone. The anterior part of the dorsal plate thins and its surface shows a pattern of ridging that provides an interlocking articulation with the posterior portion of the overlapping parietal. Two slim anterolateral processes extend the dorsal plate, as their

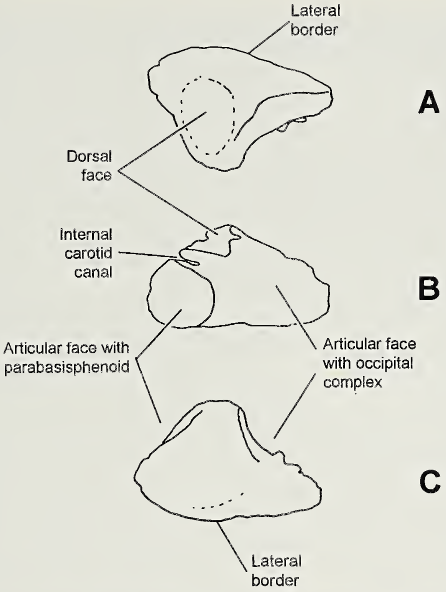
Lateral border
A
Dorsal face
Internal carotid canal
B
Articular face with parabasisphenoid
Articular face with occipital complex
C
Lateral border

Fig. 40.—*Amphisbaena alba.* Labeled outline of element-X shown in Figure 39.

ventral border forms the dorsal edge of the postorbital gap and the Gasserian foramina. More posteriorly, the lateral border of the dorsal occipital plate is continuous with the paired anteroventrally projecting paroccipital processes.

The basioccipital plate is smaller than the dorsal one (Fig. 45C, 46C); its concave anterior border articulates medially with the parabasisphenoid. Lateral to this, wide, paired ventral anteroventral processes (tuberculum sphenoccipitale; Jollie, 1960) contact the element-X of each side via a thick synchondrosis and bend ventrally, thus shaping a concavity between them. Laterally, a notch on each side of the ventral plate forms the medial border of the auditory canals into which fit the stapes. More posteriorly, the paroccipital process gives rise to a vertical plate. The posterior aspect of the basioccipital plate is inclined dorsally; its posterolateral borders are rounded whereas the flat medial region extends posteriorly to the condylar neck.

The lateral paroccipital processes are short and massive. Anteriorly, each ends in a blunt and hemispheric quadratic articulation that faces lateroventrally, reflecting the inclination of the quadrate (Fig. 45B, 46B). All paroccipital processes are formed of spongy bone as are the adjacent areas of the contacting plates (Fig. 55, 56).

The fenestra ovalis lies medial to the paroccipital process. The medial border of the process is connected to the basioccipital plate by a curved plate. This plate delimits the posterior and medial aspects of the externally open middle-ear cavity; the paroccipital process and the quadrate delimit the cavity laterally. The stapedial footplate fits on a narrow step in the wall of the auditory tube, just internal to the fenestra ovalis, which it then occludes. The step lies mainly on the medial surface of the auditory tube, but also continues slightly around the anterior and

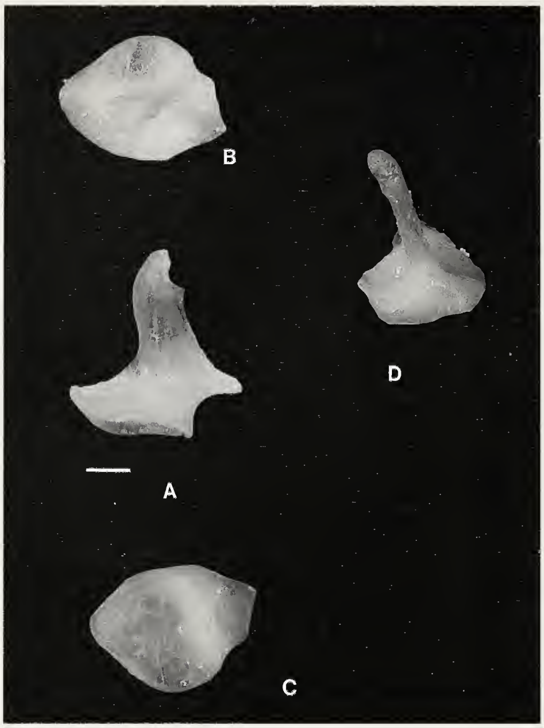

Fig. 41.—*Amphisbaena alba.* Photographs of right stapes (CG 1811); the orthogonally presented pictures are all rotated from the lateral view. The bar shows 1 mm to scale. A, lateral view; B, distal view; C, proximal view; D, anterior view.

posterior area. At the ventral side of the step, a foramen opens from the region dorsal to the posterior face of the auditory canal.

Anterior to the fenestra ovalis arises a wide facial canal, defined at each side between the dorsad base of the anterolateral process and the ventral prootic process. The anterior end of this canal shapes the posterior border of the Gasserian foramen. The facial canal is partially overlapped by the stapedial footplate. Just anterior to each stapes, one (or two) foramina pierce the bone to open at the inner ventrolateral angle of the braincase (not illustrated). Ventral to the facial canal, a prismatic prootic process contacts the element-X. The internal carotid passes through a canal between this prootic process and the anteroventral lateral one.

Internally, the complex forms the smooth posterior aspect of the braincase. Also, its lateral wings house the internal portions of the otic apparatus (Wever and Gans, 1973; Baird, 1978) which are discernible only in section although they may be visualized by treating the bone with essential oils. As the structure is unitary and shows almost no sutures, homology of the components remains a problem. In a frontal view (Fig. 45D, 46D), the inner roof of the braincase is formed by the ventral surface of the dorsal plate. Anteriorly, the dorsal occipital part of the braincase is wide, but posteriorly the roof of the braincase is narrowed by the projection of the otic capsules that are bulky on the sides and fuse dorsally with the dorsal occipital plate. More posteriorly, the braincase expands slightly in the lateral dimension but is constrained again by the foramen magnum. Two

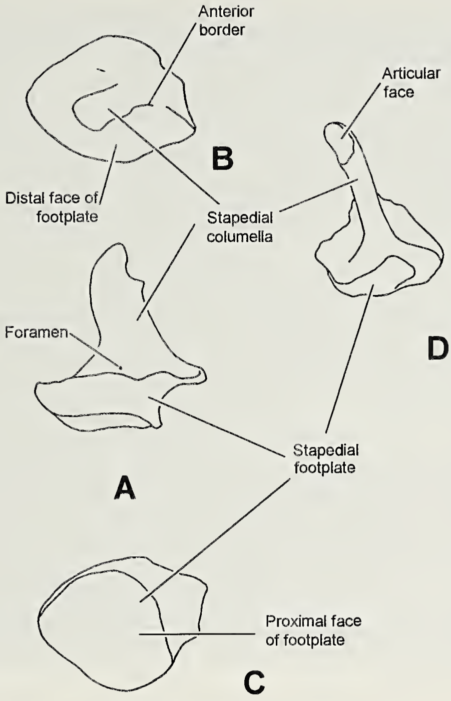

Fig. 42.—*Amphisbaena alba.* Labeled outline of stapes shown in Figure 41.

large, anteriorly facing foramina pierce the inner surface of each otic capsule. One of these opens from the bottom of the otic capsule near the floor of the brain cavity. The other opens more anteriorly and dorsally. The floor of the braincase is concave, shaping a basin supporting the cerebellum. Posteriorly, the base of the occipital condyle forms a rising edge from the basin.

Whereas a comparison with other reptiles makes it reasonably clear that the amphisbaenian occipital complex is compound, it is difficult to decide which elements are included. Certainly it includes the occipitals (cf. Gans, 1960). The anterolateral processes have been described as separate pleurosphenoids by Zangerl (1944), but Rieppel (1993) presumed them to be homologous with the alar processes of the prootic; also, a series of elements of the otic complex are presumably fused within this area. One of the skulls (CG 1216) shows that the anterolateral processes of the occipital complex are bifid. The sutures could be interpreted, with reservation, to represent the boundaries between the supraoccipital and laterosphenoid; if so, these processes are compound. However, until embryos are available for description, this pattern remains to be confirmed.

Dentary.—The dentary (Fig. 47, 48) is the main bone of each mandibular ramus. Anteriorly it is joined with the opposite dentary by means of a complex symphyseal articulation, diverging posteriorly in an angle of 15° from the medial axis (Fig. 7C); posteriorly the dentaries are divided into pointed posterodorsal and posteroventral processes. The dorsal border of each dentary bears eight teeth and posteriorly curves dorsally and then horizontally in a continuation that forms the anterior border of the coronoid processes of the mandible. The ventral border of

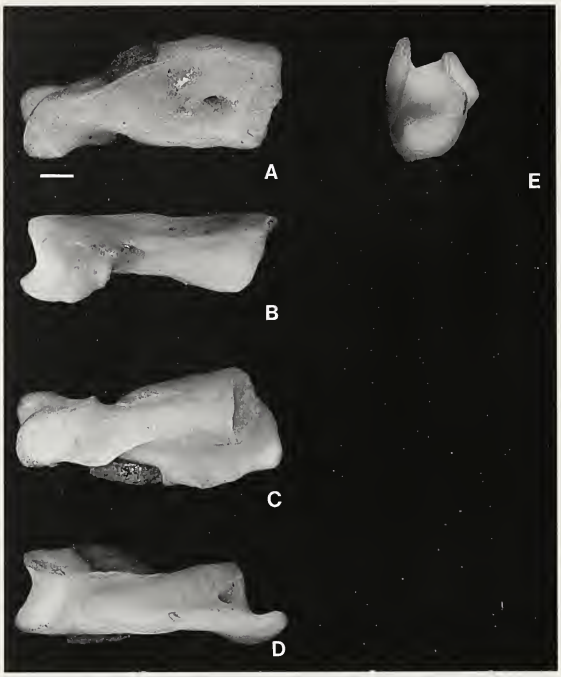

Fig. 43.—*Amphisbaena alba.* Photographs of right quadrate (CG 1811), anterior to the left. The bar shows 1 mm to scale. A, lateral view; B, ventral view; C, medial view; D, dorsal view; E, posterior view (slightly tilted to the right).

the dentary leaves the symphyseal surface in a sharp dorsomedial curve then gradually curves ventrally and horizontally. The angular prevents contact of the dentary with the articular process of the compound bone. The dorsal and ventral processes are separated by a wide, hollow posterior cavity into which fits the dentary point of the compound bone. On the labial side the dentary lies labial to the coronoid, but more ventrally the sliver of the compound bone lies lingual to it. On the lingual side, the posterodorsal process is covered by the coronoid and angular; the ventral process is covered by the angular.

The symphyseal surface is flat, elongated, and separated from that covered by a thin layer of hyaline cartilage. The longest axis of the symphysis is oriented ventrally and posteriorly; the articulation surface expands dorsally and ventrally, so that it is wider than the cross section of the dentary. A notch on the posterior (inner) side is shaped by the extension of Meckel's canal.

In a lateral (labial) view (Fig. 47B, 48B), the dentary shows two longitudinal rows of mental foramina which perforate to the posterior cavity. The dorsal row begins posteriorly with a large foramen at the center of the lateral face, and is prolonged anteriorly by two to four smaller foramina. The ventral row begins more anteriorly and is composed of two to four small foramina in a dorsally angled line that meets the dorsal row anteriorly.

The solid posterodorsal process shapes the anterior border of the coronoid processes of the mandible, reaching almost to its top; here it bends posteriorly, fitting

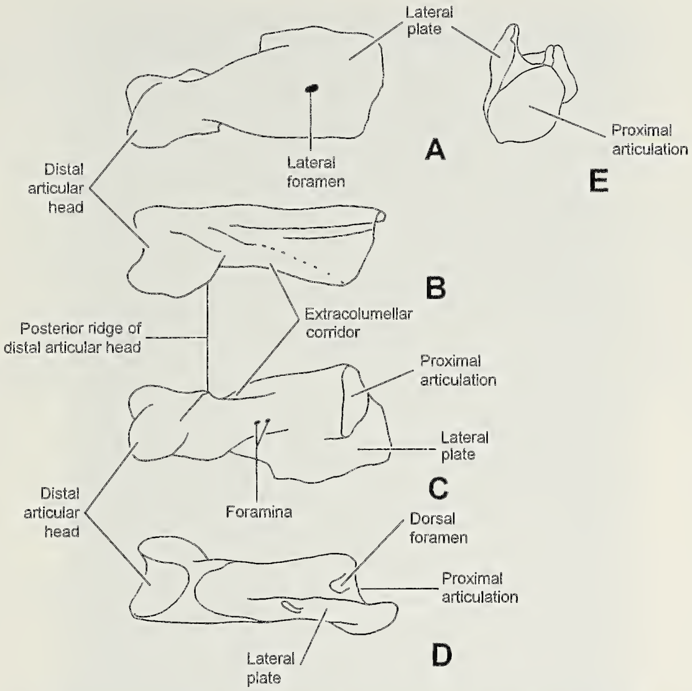

Fig. 44.—*Amphisbaena alba.* Labeled outline of quadrate shown in Figure 43.

into a lateral groove of the coronoid. A flat posterior face of the posterodorsal process contacts the coronoid; at its base begins the posterior cavity of the dentary.

Between the two processes opens a wide and deep posterior cavity into which the compound bone fits. Two thin plates, lateral and medial, shape its lateral walls. The posterior cavity is vertically elongated; anteriorly it narrows into a branching tunnel that runs anteriorly and opens to the foramina of the lateral face of the dentary. The coronoid and angular fit into a triangular depression on the lingual surface of the medial plate.

Meckel's canal is open along the medial face of the dentary. Anteriorly it extends to the mandibular symphysis; posteriorly it reaches the mandibular central labial foramen that is formed between the dentary, compound bone, and coronoid (in the articulated mandible this aperture seems to be shaped only by coronoid and dentary). A rod of cartilage (Meckel's cartilage) runs along the entire canal and extends posteriorly, lying lateral to the angular and penetrating the mandible by its central foramen; the cartilage ends in a sharp point in the anterior part of the longitudinal tunnel of the compound bone. The posterior part of Meckel's canal is bordered dorsally by the coronoid and ventrally by the angular borders; its posterior end is limited by the posterior overlapping sliver of the compound bone.

In dorsal view (Fig. 47C, 48C), the dentary shows a slight inclination toward the medial plane. The dorsal border is labially widened, supporting the bases of the teeth in subpleurodont tooth implantation (Gans, 1957). The conical teeth are inclined anteriorly and laterally; however, the points are curved medially and

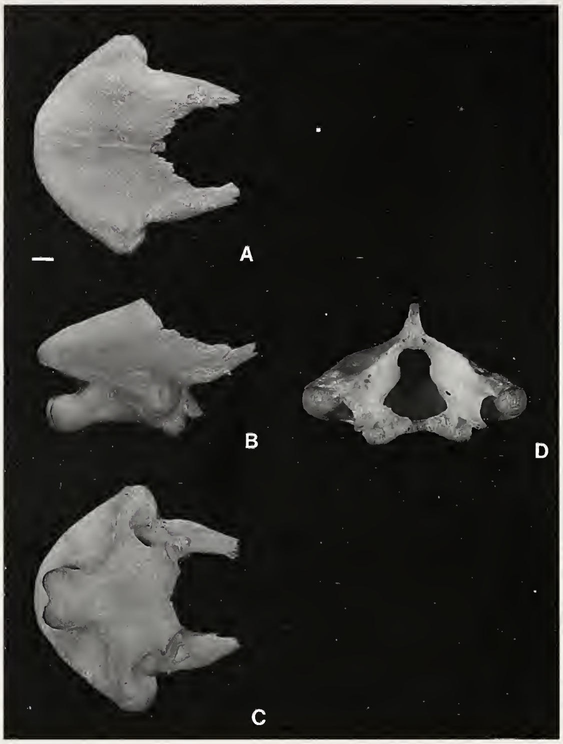

Fig. 45.—*Amphisbaena alba.* Photographs of occipital complex (CG 1811). The dorsal and ventral views are tilted as they are perpendicular to the dorsal and ventral plates respectively, and not to the horizontal plane of the bone; anterior to the right. The bar shows 1 mm to scale. A, dorsal view; B, lateral view; C, ventral view; D, anterior view.

posteriorly. The anterior teeth are further inclined than the posterior ones, which are more straight. The most anterior tooth is relatively small, the second is larger, and the third the largest of the mandibular series, exceeding the height of the other teeth by one-third. Posteriorly, the other teeth become smaller, but the level of their tips is maintained as the dentary base rises posteriorly. On the lingual side, the bases of the teeth show nutritive foramina on the plane of the curvature. Each tooth appears to have a plane of weakness beginning at the basal foramina; several teeth are split along this plane which is coincident with the plane of curvature. The bases of the teeth are ankylosed to their sockets by a ring of cement.

The dentary is recognized as the sole tooth-bearing bone of the mandible.

Compound Bone.—The complex compound bone (Fig. 49, 50) is the most posterior bone of the mandible and bears the mandibular articulation with the quadrate (Fig. 55, 56). Its anterior point (the dentary process) is inserted into the posterior cavity of the dentary. Below this it is in contact with the posterior ventral processes of the dentary and with the angular; dorsomedially the compound bone contacts the coronoid. Its medial (lingual) side is mostly covered by the coronoid and angular. The disarticulated compound bone bears three processes: a posterior

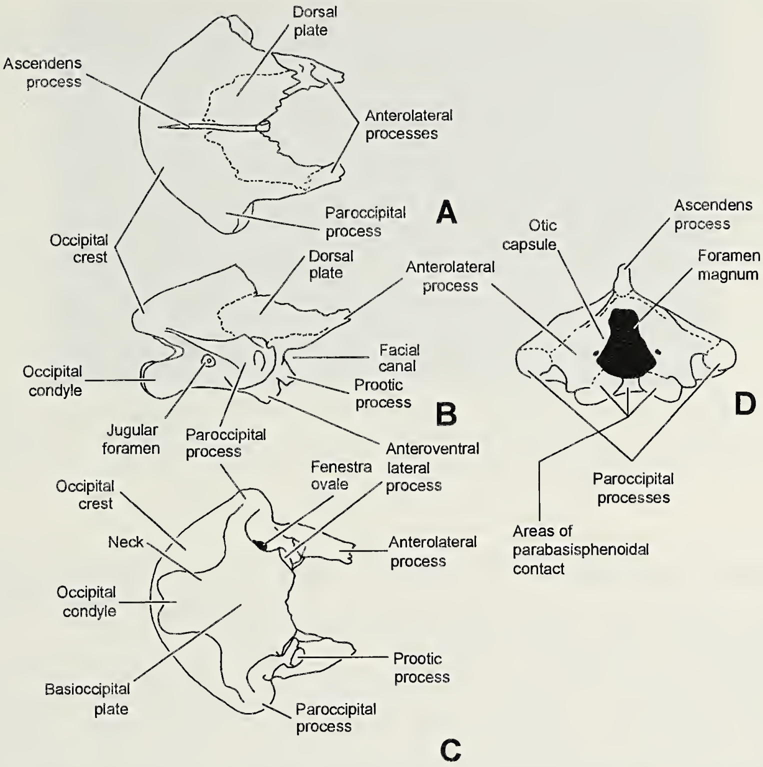

Fig. 46.—*Amphisbaena alba.* Labeled outline of the occipital complex shown in Figure 45.

articular process, a wide triangular lateral plate terminating in a dentary process, and a ventromedial sliver.

The articular process is bent medially, more dorsally than ventrally (i.e., its dorsal borders are closer to the medial plane than the ventral ones). This inclination compensates for the lateral inclination of the articulated mandible (Fig. 7C). The articular and quadrate are equivalently displaced and the entire mandible can close into the V-shaped angle between the maxillae. The posterior articulating head is massive and is ventrally thickened by the base of the ventromedial sliver (Fig. 49B, 50B). The vertical concavity of the articulation surface faces posteriorly and medially, matching the anterior articulation of the quadrate. The articular process is composed of spongy bone (Fig. 55B, 56B), as is an anterior branch extending along the ventral side. The other bony tissues are dense.

The lateral plate of the compound bone comprises most of the lateral side of the posterior mandible (Fig. 49B, 50B). Its concave ventral surface rests upon the ventral process of the dentary (Fig. 49C, 50C). The anterior dentary process extends the labial plate to fit deeply into the posterior cavity of the dentary at the site at which the dorsal border of the lateral plate overlaps the coronoid. Anteriorly to the articular process, the lateral plate is pierced by a posterior mandibular foramen; medially (Fig. 49A, 50A), the aperture opens to the posterior portion of Meckel's canal in the compound bone. The posterior foramen of the lingual side lies dorsal to the posterior base of the ventromedial sliver; in the articulated

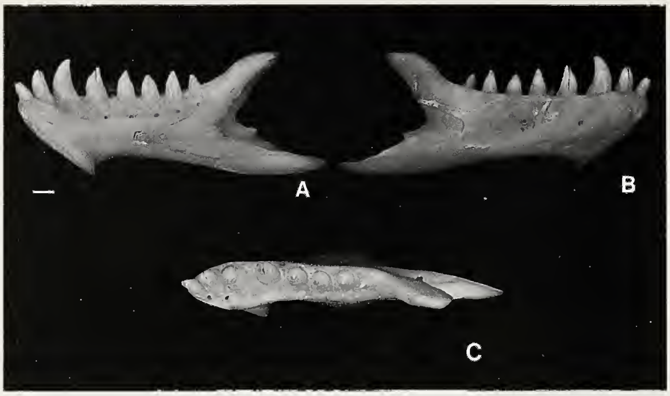

Fig. 47.—*Amphisbaena alba.* Photographs of right dentary (CG 1811). The bar shows 1 mm to scale. A, medial (or lingual) view; B, lateral (or labial) view; C, view at right angle to its longitudinal axis.

mandible this lingual opening is closed partially by the coronoid. In addition to the posterior foramen near the articulation, the labial plate shows a smaller foramen the other end of which opens anteriorly to Meckel's canal.

The medial sliver projects anteriorly from the articular process, just ventral to the posterior foramen. Ventrally it is fused with the lateral plate along the ventral border (Fig. 49B, 50B). Anteriorly the ventral face of the sliver is separated from the lateral plate as a thin and sharp point; it does not enter in the dentary pocket as the lateral plate, but overlaps the medial face of the dentary, covering Meckel's canal posteriorly. The dorsal border of the medial sliver contacts the center of the medial face of the lateral plate (Fig. 49A, 50A), with which has a suture line; the dorsal space left between the sliver and the lateral plate defines a wide longitudinal canal (Meckel's canal) that connects the posterior and central foramina of the medial side of the mandible. The canal of the compound bone is closed lingually by the coronoid and ventrally by the angular.

The compound bone seems to result from fusion of the supra-angular (the labial sliver), the articular (posterior articulation head), the splenial (the labial plate), and the prearticular (the ventral face that joins the supra-angular and splenial). This issue needs further analysis as the bone shows only two dermal ossification centers in embryos of *Amphisbaena darwini* (Montero et al., 1999).

Coronoid.—The flat rectangular coronoid (Fig. 51, 52) shapes the lingual aspect of most of the coronoid process of the mandible. On the lateral face of the mandible it is almost fully covered by the compound bone and dentary. However, it is completely exposed on the medial face of mandible, and anteriorly contacts the dentary, ventrally Meckel's canal (which separates it from the angular), and posteriorly the compound bone. The dentary contact includes a slender anteroventral coronoid process resting upon the medial face of this bone.

The concave medial surface of the coronoid shapes a wide and shallow central cup (Fig. 51A, 52A). The high and broad anterodorsal border of the central cup represents the bottom of the lateral groove that embraces the posterodorsal process of the dentary. The thin ventral border of the coronoid covers the compound bone medially; anteriorly the border contributes to the closure of the central foramina

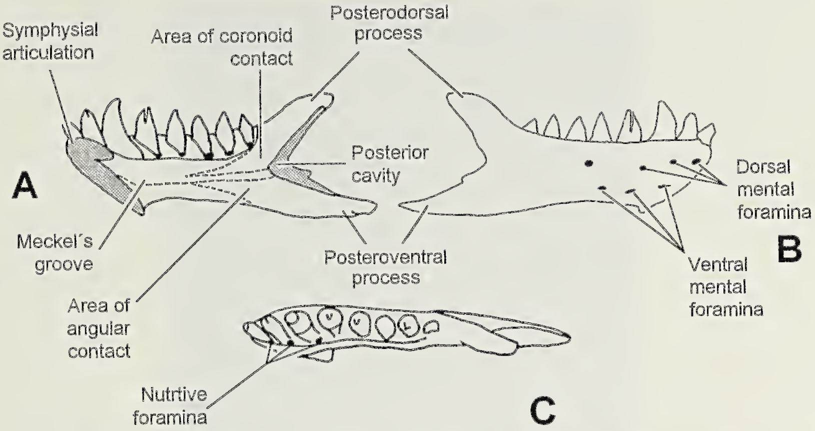

Fig. 48.—*Amphisbaena alba.* Labeled outline of dentary shown in Figure 47.

of the medial face of the dentary and posteriorly it forms the anterior edge of the posterior mandibular foramen.

In lateral view (Fig. 51B, 52B), the anterodorsal side of the coronoid bears a deep groove into which fits the dorsal process of the dentary. The prominent posterior border of that groove is higher than the anterior one, and presents a flat posterior surface; at the middle of its base, a tiny foramen (not illustrated) pierces the coronoid to the bottom of the lingual cup. Labially the canal is continued ventrally by a narrow and deep groove that runs along the posterior border of the lateral groove, ending at the central labial foramina of the mandible.

The anteroventral process of the coronoid is a thin, spear-shaped blade that rests on the labial face of the dentary. The anterodorsal border is straight; the ventral one bears a constriction that is shaped by the dorsal border of the central labial foramina (forming a neck). The ventral border extends straight anteriorly meeting acutely with the dorsal border at the point.

The densely boned coronoid is so identified as it is the main component of the dorsal coronoid process of the mandible.

Angular.—Most of the slender rod-shaped angular (Fig. 53, 54) lies on the medial face of the ventral process of the dentary. Posteriorly the angular twists from the lingual face toward the labial one, passing ventrally along the posterior border of the mandible.

The anterior end of the angular is sharp and acute. At the middle, the angular has a triangular cross section, showing a dorsal border (that anteriorly shapes the ventral border of Meckel's canal, and that posteriorly underlies the compound bone; Fig. 53B, 54B), a lateral face (that rests upon the dentary; Fig. 53C, 54C), and a medial free face (Fig. 53B, 54B). Posteriorly, the medial and lateral faces are obliterated by a ventral face that twists from the lingual to labial side of the mandible (Fig. 53A, 54A). Near the middle of the angular, it is pierced by a foramen from the medial to the dorsal surface; it connects the internal longitudinal canal of the compound bone with the labial surface. As the canal of the angular bifurcates, its labial surface shows two foramina.

The angular is identified with some diffidence as the ventral bony element of the mandibular ramus.

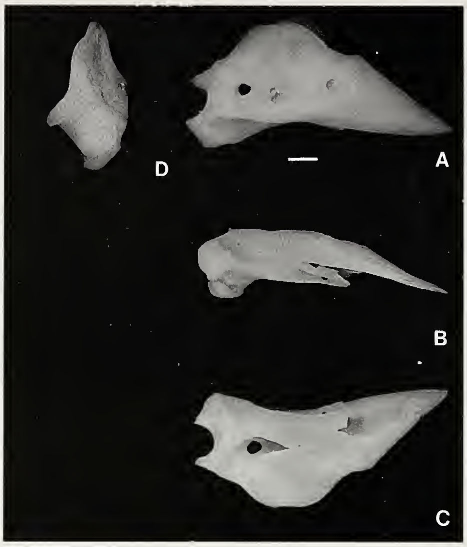

Fig. 49.—*Amphisbaena alba.* Photographs of right compound bone (CG 1811), anterior to the right. The bar shows 1 mm to scale. A, lateral view; B, ventral view; C, medial view; D, posterior view.

Cartilages

Although descriptions of the cranial skeleton commonly emphasize the osseous elements, we here add a short supplemental description of the cartilaginous elements. These are important because of the role of the chondrocranial elements in development, because they have a functional role even in adults, and because cartilages are critical for mechanical function during growth. Consequently, their characterization completes the description of the skeletal structures of the skull. We follow the terminology of Bellairs and Kamal (1981) and Pratt (1948). The following description is based entirely on the serial sections.

The well-developed nasal septum is a narrow (two to five cells wide) plate that lies along at the sagittal plane of the snout, beginning at the level of the premaxilla and nasals anteriorly to terminate posteriorly at a level just anterior to the frontal fenestra. The septum extends dorsoventrally, from the dorsal roof of the snout to the ventral midline between the vomers and palatines. Dorsally, it meets the internasal suture with the premaxillary septum and expands laterally thus forming the parietotectal cartilage which comprises the roof of the nasal capsule.

Anteriorly, the nasal septum sends off anterior branches at the site of contact between the nasals and each branch projects anteroventrally and is continuous with the nasal cupula that surrounds the external nares. The nasal process of the premaxilla separates these branches. The extreme tip of the nasal septum bends ventrally and projects as two posterior rodlike cartilages that are continuous with a cartilaginous concha and an anterodorsal cup inside the cavity of Jacobson's organ.

The nasal capsule is roofed by a poorly developed cartilage that has a large fenestra superior. Laterally, this parietotectal cartilage is continuous with the paranasal cartilage, a cup-shaped lateral plate that forms the lateral wall of the olfactory chamber. The medial cup-shaped projection of the paranasal generates the

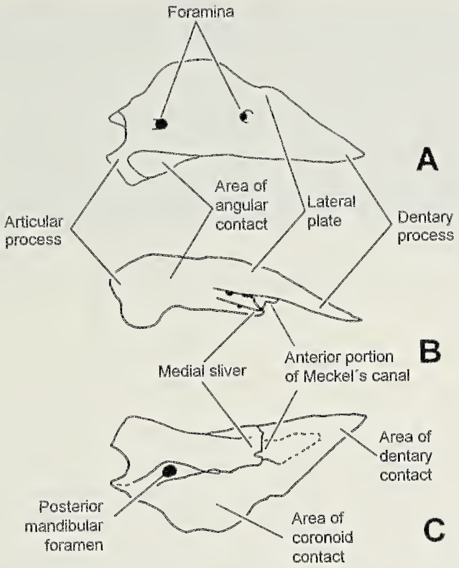

Fig. 50.—*Amphisbaena alba.* Labeled outline of compound bone shown in Figure 49.

hemispherical concha around which lies the very large and anteroposteriorly elongated olfactory chamber. The posterior wall of the olfactory chamber is formed partially by a posterior cartilaginous plate (planum anteorbitale). Medially, the ventral corner of this plate has a rod-shaped paraseptal cartilage that passes anteroventrally, thus running along the medial sides of the vomer to the level of the middle of Jacobson's organ. However, it does not contact the cartilages of Jacobson's organ. Only a sheet of connective tissue separates the brain cavity from the nasal cavities in the frontal fenestra; the cartilaginous planum anteorbitale lies lateral to the frontal fenestra.

Posteriorly, the nasal septum is continued as a thick medial rod, the trabecula communis. This passes between the palatines, just ventral to the frontals; the medial contact of these bones precludes formation of an interorbital septum (Bellairs, 1949), a character unique in amphisbaenians among squamate reptiles. More posteriorly, the trabecula communis passes ventral to the tabulosphenoid. Just anterior to the anterior tip of the parabasisphenoid (that underlies the posterior part of the tabulosphenoid) the trabecula communis splits posterolaterally to form the paired trabeculae. These trabeculae run posteriorly at the sides of the anterior tip of the parabasisphenoid, but terminate just anterior to the posterior border of the tabulosphenoid.

The elements thus far defined are adult remnants of the embryonic chondrocranium. More posteriorly, there are two additional kinds of cartilages, those of the basisphenoid–pterygoid junction, and the epiphyseal ones (Fig. 55, 56).

Sections show that the cartilage of the basisphenoid–pterygoid junction forms a nodule that lies within the former bone at the site at which the shoulders of the pterygoid bend laterally around the latter bone. Whereas the wall of this nodule bulges into the gap between the bones, adult specimens show most of the gap filled by dense connective tissues.

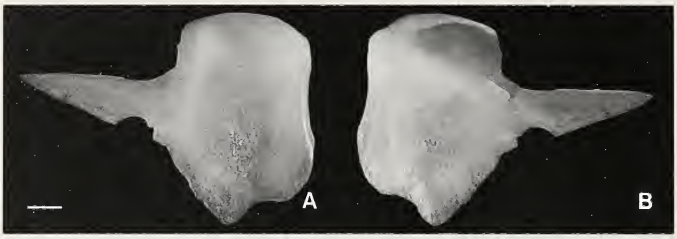

Fig. 51.—*Amphisbaena alba.* Photographs of right coronoid (CG 1811). The bar shows 1 mm to scale. A, medial view (anterior to upper left corner of the photograph); B, lateral view (anterior to upper right corner of the photograph).

The epiphyseal cartilages sheathe the surfaces of the synovial junctions and are generally underlain by spongy bone. Such tissues are seen at the connection of the occipital condyle with the vertebrae forming the head joint, the junction of the paroccipital process and the quadrate, the junction of the quadrate with the mandibular compound bone, and the symphyseal junction of the mandibles (which lacks a synovial cavity). Only the head joint shows cartilaginous or connective tissue menisci.

Cartilage also sheathes the articular surface of the element-X, as seen in sections by the elaborate triradiate synchondrosis (Fig. 55, 56). Together with its spongy internal structure, and the observation of fusion to the parabasisphenoid and the basioccipital plate in the largest adult, this supports the above-mentioned concept that these elements function as epiphyses.

DISCUSSION

Mechanical Framework

The structural pattern of the skull is seen less adequately on the basis of general exposure of the several cranial elements than on three-dimensional reconstruction based on serial sections and consideration of the individual disarticulated bones. The preceding analysis documents that examination only of the surface exposure of the individual cranial elements does not provide sufficient understanding of amphisbaenian skull architecture. Sections and drawings indicate both the nature of inter-element articulations and the pattern of the internal ossifications. Particularly the former is critical as almost all bones form junctions that not only provide abutment with or without minor interconnection but complexly overlap portions of the adjacent bones. This aspect of the cranial architecture of amphisbaenians is characteristic and differs profoundly from that of other squamates.

As noted in earlier papers (cf. Gans, 1974, 1978), the skull is strong and seemingly simple. However, rather than having major cranial elements being composed of single bones that articulate by simple joints involving the edges of plates, the bones overlap and commonly interdigitate; the junctions tend to be three-dimensional and extremely complex. Many of the skeletal elements (premaxilla, tabulosphenoid, parietal, occipital, compound bone) are azygous either due to their intrinsically azygous nature or due to fusion during ontogeny. The anterior portions of the skull are comprised of paired bones; however, these also show a

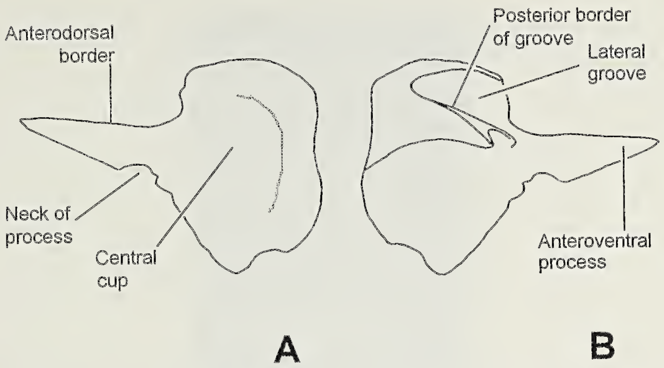

Fig. 52.—*Amphisbaena alba.* Labeled outline of coronoid shown in Figure 51.

complex interlocking that may proceed on several levels within a single junction; interlocking ensures minimal potential of midline slippage.

In some sites one sees junctions of subparallel plates that overlap widely with the contact fields fitted with lands and grooves the axes of which are likely important, as the arrangement thereof (angles between, rather than number of grooves) has low variance. This phenomenon is well demonstrated by the contact zone between parietal and supraoccipital. Simultaneously one sees joints in zones at which the edges of the articulating bones are swollen, and in which the surface of articulation curves and bulges in a three-dimensional array. These curves shift semi-irregularly, with those of the sides being asymmetrical. The surfaces of bony intercalation furthermore may lie near either the deep or superficial surfaces of the bones being joined; they may reach the free surface or be placed within the depth of the bones. The intrinsic irregularity accounts for the differing numbers of projecting fingers on the two sides of the skull (e.g., at the frontal parietal joint).

Unlike the articulation of the elements of the ophidian snout, which provide edge-to-edge or end-to-end contact, the entire elements of the snout of *Amphisbaena alba* tend to be complexly bent. Therefore, one rarely sees simple planar lines that parallel much of the edge between bones (i.e., in the nasomaxillary joint), lines that would mark sites of potential inter-element slippage. Furthermore, this trend is emphasized by the complex bending and projection of the elements. For instance, cranial sections prove to be difficult to interpret, as processes of particular elements may show up multiple times in a sequence, e.g., the frontal–prefrontal–maxilla and the tabulosphenoid–parietal–frontal sequences.

Many of the zones of articulation are narrow and filled with dense, collagenous connective tissue which should preclude significant sliding movements. This is the most common pattern; for instance, it is seen in the frontal–parietal and the medial basisphenoid–basioccipital junctions. In some other cases the crevices are filled with a much wider band of connective tissue; whereas this also may limit slippage, the width of such articulations should be reduced whenever they are loaded in compression. This is seen between the vomer and premaxilla, and in the more lateral part of the basisphenoid–basioccipital junction including its continuation into the edges of the elements-X.

A relatively few articulation zones of adult animals have cartilage (details be-

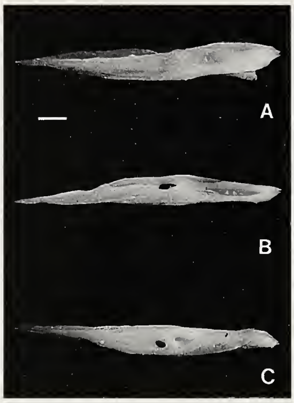

Fig. 53.—*Amphisbaena alba*. Photographs of right angular (CG 1811). Anterior to the left. The bar shows 1 mm to scale. A, ventral view; B, medial view; C, lateral view.

low). This cartilage may be in nodular form as in the zone in which the pterygoid contacts the basisphenoid. Also, several joint surfaces may be lined with a thin layer of hyaline cartilage. Such areas occur whenever the joints involve synovial cavities and probably contribute to the addition of lubricating fluids. Beyond this, the compressibility of the cartilage assures congruence (parallel shape) of the sliding surfaces as the rotating elements move past each other. Consequently, cartilaginous areas facilitate rotational movements in zones being loaded in compression normal to the surface. The three main sets of synovial cavities are that at the head joint between the vertebrae and the occipital condyle, that between the paroccipital process and the quadrate, and that between the quadrate and the articular surface of the mandible.

What is even more critical is that most of the sites involving the application of normal compressive forces are, in all but the largest specimens, underlain by spongy bone. This suggests that throughout the process of growth the combination of synovial cavity, cartilage, and spongy bone represents a complex that permits joints to be loaded during rotation.

An overview of the skull thus indicates that it represents a tubular structure which is approximately six times as long as its narrowest dorsoventral or lateral extent. The anterior elements consist of solid lamellar bones that are interlocked as described above. In several cases these bones show local thickenings with the deep and superficial surfaces providing projecting processes that overlap adjacent elements (e.g., maxilla and prefrontal, nasal with premaxilla anteriorly and with frontal posteriorly). Hence the snout forms a compression-resistant wedge, although its articulation at the frontal level is looser than at other sites.

From the frontal to the occipital levels all elements form a heavily walled tube, with the walls approximately parallel to the long axis. The bones are dense and lamellar and even at their complex sites of interlocking (e.g., dorsoventral between parietal and tabulosphenoid, anteroposterior between frontals and parietal) have almost no sponginess. Such a heavily walled tube has substantial resistance to compressive and torsional loading, as well as to the associated buckling. The noncircular construction of the tube increases its resistance to bending about the

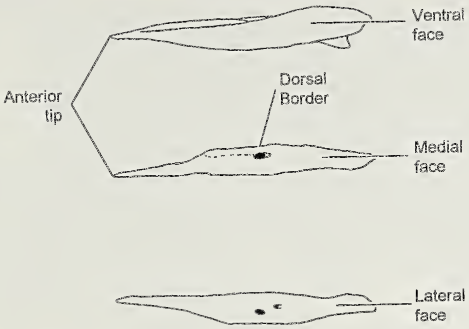

Fig. 54.—*Amphisbaena alba.* Labeled outline of right angular shown in Figure 53.

dorsoventral axis. A supplemental resistance to bending is produced both by the parietal–occipital keel and by the firmly associated pterygoids.

The complex occipito–otic element shows the combination of multiple influences. The central zone serves as a shell for the central nervous system and the lateral elements for the otic complex. In terms of mechanical function the central–medial zone involves a posterior prolongation of the compression-resistant tube. This would allow transmission of straight tunneling forces. The laterally flaring paroccipital processes allow some of the backward-directed compressive forces resulting from a push of mandible against the substratum to be opposed by forces acting on the occipital condyles. The angulations of the bilateral sutures allow resistance to rotational forces whenever torsion is imposed by the trunk and exerted by the snout. As noted in earlier reports (cf. Gans, 1974), the skull is also capable of resisting bending along the nasal–frontal level during bites. It is clear that we are here dealing with a primary chain of sequential compressive elements, as documented by the occurrence of three sequential synovial joints and three sets of cartilage plates.

Cranial Kinesis

Various authors (Versluys, 1898; Kritzinger, 1946; Vanzolini, 1955; Romer, 1956) have referred to cranial kinesis in the amphisbaenians; in some cases, there is reference to the conditions in juvenile skulls. However, other studies (e.g., Gans, 1960) have suggested that adult kinesis is most unlikely, in part because the articulation of the fronto–parietal joint involves two axes. However the possible degrees of freedom are greatest at the naso–frontal junction which, however, is stabilized by the complex prefrontal.

The present observations do not eliminate the possibility of some cranial flexibility in adults, but severely restrict it. The fronto–parietal joint is very solid and the possibility of slippage between parietal and tabulosphenoid is limited by the sturdy anterior, lateral, and posterior articulations. The nasal capsule does not permit significant internal movement nor does it allow much movement on the frontals. The premaxilla, nasals, maxillae, and prefrontals are solidly interlocked with each articulation folded to involve two or more planes. Ventrally, the palatines are overlapped by vomers and frontals. Also, the palato–pterygoid joints overlap significantly; their fluted interdigitation may allow only a most limited anterior–posterior sliding.

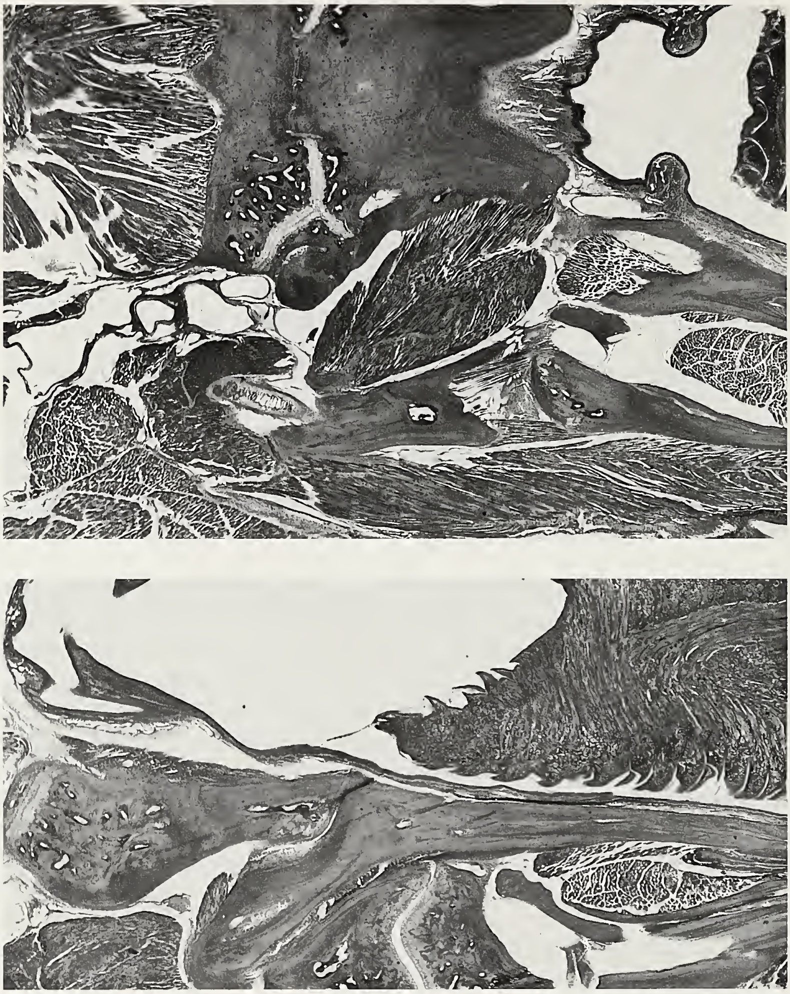

Fig. 55.—*Amphisbaena alba.* Details of horizontal serial sections to show cartilaginous contributions to various joints (E. G. Wever slide set 1667). A, detail of basipterygoid (slide 173); B, detail of tight joint between basioccipital and basisphenoid, as well as more lateral chondrosis, splitting to form the outline of the element-X (slide 194). Use Figure 56 for scale.

The anterior attachment of the vomers is relatively loose and ligamentous, which might allow some minor slippage that could be transmitted to the quadrate by the palato–pterygoid chain. Consequently, the slippage likely would be transmitted to the shaft of the quadrate and some equivalent movement would have to permit rotation of the parabasi–pterygoid joint. This slippage could be lateral instead of anteroposterior; however, examination of the serial sections suggests that flexibility of the connective tissues in the narrow slit would be limited (Fig. 55, 56). The issue is complicated because the vomer is much more slender than the other bones in the chain; flexibility might involve bending and rotation within elements. The bending of the vomer could press on the capsule of Jacobson's

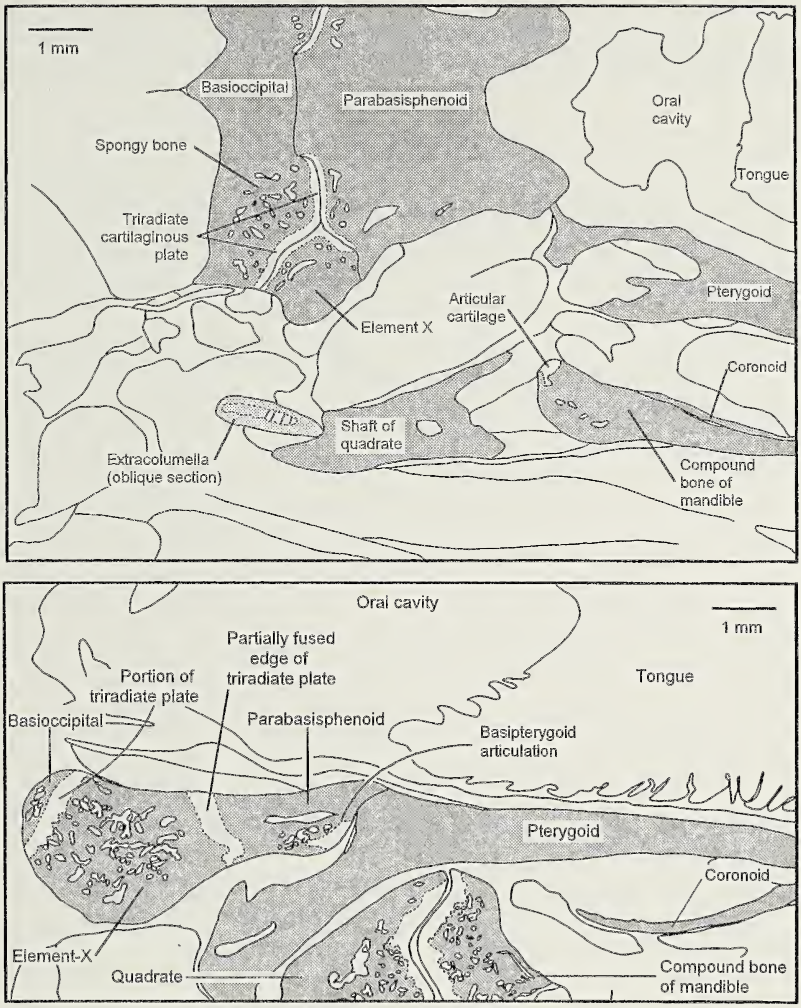

Fig. 56.—*Amphisbaena alba.* Labeled outline of horizontal serial sections shown in Figure 55.

Organ and tend to extrude its contents, as postulated for Monopeltis by Kritzinger (1946).

Rather than considering kinesis to be involved primarily in anteroposterior displacements within parasagittal planes, it may be useful to consider lateral movements. For example, rotation of the head of the quadrate might laterally displace the posterior wing of the pterygoid; however, the symphyseal fusion of the mandibles would limit this and would also limit the facility of the edges of the pterygoid in assisting ingestion and swallowing.

ACKNOWLEDGMENTS

We thank David Bay for assistance with some of the photography. David Canatella and several anonymous reviewers provided useful comments. The initial visit of RM to Ann Arbor was possible thanks to a fellowship of the Universidad Nacional de Tucumán, funds from CIUNT and Instituto de Herpetología, and the help of N. Palermo, M. Campastro, and E. Lavilla. Funding for the visit of RM to Austin and the visit of CG to San Miguel de Tucumán were supported by a grant from the Leo Leeser Foundation.

LITERATURE CITED

BAIRD, I. L. 1978. The anatomy of the reptilian ear. Pp. 193–275, *in* Biology of the Reptilia, Volume 2 (C. Gans and T. S. Parsons, eds.). Academic Press, London, United Kingdom.

BELLAIRS, A. D'A. 1949. The anterior braincase and interorbital septum of Sauropsida, with a consideration of the origin of snakes. Journal of Anatomy (London), 83:116–146.

BELLAIRS, A. D'A., AND C. GANS. 1983. The reinterpretation of the amphisbaenian orbitosphenoid. Nature, 302:243–244.

BELLAIRS, A. D'A., AND A. M. KAMAL. 1981. The chondrocranium and the development of the skull in Recent reptiles. Pp. 1–263, *in* Biology of the Reptilia, Volume 11 (C. Gans and T. S. Parsons, eds.). Academic Press, London, United Kingdom.

BRÜHL, C. B. 1886. Zootomie aller Thierklassen für Lernende, nach Autopsien, skizziert. Hoelderer, Vienna, Austria.

CUVIER, G. L. C. F. D. 1829–1830. La règne animale, distribué d'après son organisation, Volumes 2 and 3, Nouvelle édition. Deterville, Paris, France.

ESTES, R. 1983. Sauria Terrestria, Amphisbaenia. Handbuch der Paläoherpetologie/Encyclopedia of Paleoherpetology, Part 10A. Gustav Fischer Verlag, Stuttgart, Germany.

FIORINI, P. 1962. Der Eizahn und die Eischwiele der Reptilien. Eine zusammenfassende Darstellung. Acta Anatomica, 49:328–366.

GANS, C. 1957. "Anguimorph" tooth replacement in *Amphisbaena alba* Linnaeus, 1758 (Reptilia: Amphisbaenidae). Breviora, 70:1–12.

———. 1960. Studies on amphisbaenids (Amphisbaenia: Reptilia). 1. A taxonomic revision of the Trogonophinae and a functional interpretation of the amphisbaenid adaptive pattern. Bulletin of the American Museum of Natural History, 119:129–204.

———. 1962. Notes on amphisbaenids (Amphisbaenia: Reptilia). 5. A re-definition and a bibliography of *Amphisbaena alba* Linné. American Museum Novitates, 2105:1–31.

———. 1974. Biomechanics. Approach to Vertebrate Biology. J. P. Lippincott, Philadelphia, Pennsylvania.

———. 1978. The characteristics and affinities of the Amphisbaenia. Transactions of the Zoological Society of London, 34:347–416.

GANS, C., AND R. MONTERO. In press. Two new fossil amphisbaenids from the Pleistocene of Lagoa Santa (Minas Gerais, Brasil). Steenstrupia (Copenhagen).

GANS, C., AND E. G. WEVER. 1972. The ear and hearing in Amphisbaenia (Reptilia). Journal of Experimental Zoology, 179:17–34.

GILMORE, C. W. 1928. Fossil lizards of North America. Memoirs of the National Academy of Sciences, 22:1–201.

GREER, A. 1970. A subfamilial classification of scincid lizards. Bulletin of the Museum of Comparative Zoology, 139:151–184.

JOLLIE, M. T. 1960. The head skeleton of the lizard. Acta Zoologica, 41:1–64.

KESTEVEN, L. 1957. Notes on the skull and cephalic muscles of the Amphisbaenia. Proceedings of the Linnean Society of New South Wales, 82:109–116.

KRITZINGER, C. C. 1946. The cranial anatomy and kinesis of the south African amphisbaenid *Monopeltis capensis* Smith. South African Journal of Science, 42:175–204.

LAKJER, T. 1927. Studien über die Gaumenregion bei Sauriern im Vergleich mit Anamniern und primitiven Sauropsiden. Zoologische Jahrbücher, Abteilung für Anatomie und Ontogenie der Thiere, 49:57–356.

LOEB, G. E., AND C. GANS. 1986. Electromyography for Experimentalists. University of Chicago Press, Chicago, Illinois.

MAY, E. 1978. Zur Kenntnis der Entwicklung des Schaedels von *Leposternon microcephalum* Wagler, 1824 (Reptilia: Amphisbaenia). Senckenbergiana biologie, 59:41–69.

MCDOWELL, S. B., AND C. M. BOGERT. 1954. The systematic position of *Lanthanotus* and the affinities of the anguinomorphan lizards. Bulletin of the American Museum of Natural History, 105:1–142.

MONTERO, R., C. GANS, AND M. L. LIONS. 1999. Embryonic development of the skeleton of *Amphisbaena darwini heterozonata* (Squamata: Amphisbaenidae). Journal of Morphology, 239:1–25.

PRATT, C. W. 1948. The morphology of the ethmoidal region of *Sphenodon* and lizards. Proceedings of the Royal Society of London, 118:171–201.

PRESCH, W. 1976. Secondary palate formation in microteiid lizards (Teiidae: Lacertilia). Bulletin of the Southern California Academy of Science, 75:281–283.

RIEPPEL, O. 1993. Patterns of diversity in the reptilian skull. Pp. 344–390, *in* The Skull. Volume 2: Patterns of Structural and Systematic Diversity (J. Hanken and B. K. Hall, eds.). University of Chicago Press, Chicago, Illinois.

RILEY, J., J. M. WINCH, A. F. STIMSON, AND R. D. POPE. 1986. The association of *Amphisbaena alba* (Reptilia: Amphisbaenia) with the leaf-cutting ant *Atta cephalotes* in Trinidad. Journal of Natural History, 20:459–470.

ROMER, A. S. 1956. Osteology of the Reptiles. University of Chicago Press, Chicago, Illinois.

SMITH, M. A., A. D'A. BELLAIRS, AND A. E. W. MILES. 1953. Observations on the premaxillary dentition of snakes with special reference to the egg-tooth. Journal of the Linnean Society (Zoology), 42:260–268.

UNDERWOOD, G. 1957. *Lanthanotus* and the anguinomorphan lizards: A critical review. Copeia, 1957: 20–30.

VANZOLINI, P. E. 1951*a*. Evolution, adaptation and distribution of the amphisbaenid lizards (Sauria: Amphisbaenidae). Unpublished Ph.D. Dissert., Harvard University, Cambridge, Massachusetts.

———. 1951*b*. *Amphisbaena fuliginosa*. Contribution to the knowledge of the brazilian lizards of the family Amphisbaenidae Gray 1825. 6. On the geographical distribution and differentiation of *Amphisbaena fuliginosa* Linné. Bulletin of the Museum of Comparative Zoology, 106:1–67.

———. 1955. Contribuiçoes ao conhecimento dos lagartos brasileiros da familia Amphisbaenidae Gray, 1825. 5. Distribuiçao geografica e biometrica de *Amphisbaena alba*. Arquivos do Museo Nacional Rio de Janeiro, 42:683–705.

VERSLUYS, J. 1898. Die mittlere und äussere Ohrsphäre der Lacertilia und Rhynchocephalia. Inaugural-Dissert., University of Giessen, Jena, Germany.

WEVER, E. G. 1978. The Reptilian Ear. Princeton University Press, Princeton, New Jersey.

WEVER, E. G., AND C. GANS. 1973. The ear in Amphisbaenia (Reptilia): Further anatomical observations. Journal of Zoology (London), 171:189–206.

WILLISTON, S. W. 1917. The phylogeny and classification of reptiles. Contributions from the Walker Museum, University of Chicago, 2:61–71.

———. 1918*a*. The evolution of vertebrae. Contributions from the Walker Museum, University of Chicago, 2:75–85.

———. 1918*b*. The osteology of some American Permian vertebrates. III. Contributions from the Walker Museum, University of Chicago, 2:87–112.

———. 1925. Osteology of Reptiles. Harvard University Press, Cambridge, Massachusetts.

WU, X.-C., D. B. BRINKMAN, AND A. P. RUSSELL. 1996. *Sineoamphisbaena hexatabularis*, an amphisbaenian (Diapsida: Squamata) from the Upper Cretaceous redbeds at Bayan Mandahu (Inner Mongolia, People's Republic of China), and comments on the phylogenetic relationships of the Amphisbaenia. Canadian Journal of Earth Sciences, 33:541–577.

ZANGERL, R. 1944. Contributions to the osteology of the skull of the Amphisbenidae. American Midland Naturalist, 31:417–454.

INSTRUCTIONS FOR AUTHORS

ANNALS OF CARNEGIE MUSEUM consist of contributions to the earth sciences (including paleontology), life sciences, and anthropology, in 30 by 46 picas format (127 by 195 mm or 5 by 7⅝ inches). Submit all manuscripts to the Office of Scientific Publications. Authors should give particular attention to scientific content, format, and general style for the ANNALS. **Manuscripts that do not conform to the style of the ANNALS will be returned to the author immediately.** Every manuscript will be subjected to external peer review. Authors should submit the names, addresses, phone and fax numbers, and e-mail addresses of at least four qualified potential reviewers for each manuscript. Authors will be asked to subsidize, if funds are available, any or all costs of publication (approximately $100/page printed). A detailed set of instructions to authors may be requested from the Office of Scientific Publications.

Manuscript Style.—Articles should include the following items in this order: title page, abstract, text (with desired headings), acknowledgments, literature cited, tables, figure captions, and copies of illustrations. All manuscripts must be typed ***double-spaced*** on standard 8½ by 11-inch white bond paper, with at least one-inch margins all around, and submitted ***in quadruplicate***—an original for the editors, and three review copies. All pages should be numbered, including tables, literature cited, and the list of figure captions. Only correspondence quality or better dot matrix printouts will be accepted; draft mode is unacceptable. A monospaced font, (e.g., Courier) is required. A disk in WordPerfect x.x or ASCII is helpful.

Title Page. The title should be brief, include the animal or plant group involved, be placed on a separate page, and appear two to three inches below the top margin. Include the author's name(s) and the affiliations of non-CMNH authors. In the case of multiple authorship, indicate the address to which proofs should be sent.

Abstracts. Abstracts should be short, but substantive, and included at the head of the first page of text.

Text. Do not right justify text or break (hyphenate) a word at the end of a line. ***Footnotes and acknowledgments as footnotes are unacceptable.*** All text is double-spaced in a monospaced font (e.g., Courier).

Tables and Figure Legends. The list of figure legends and each table should be typed consecutively on individual pages separate from the text. Tables must be double-spaced throughout with **no vertical lines**.

Measurements. Metric units should be used, if possible.

Literature Cited. All references to literature in text must appear in the Literature Cited section. The data (author, date, and page) in both citations must agree. ***Do not abbreviate the titles of periodicals or serials.*** The following style, double-spaced, should be used in Literature Cited:

1) Two authors in a journal series:
   Soltis, D. E., and P. S. Soltis. 1992. The distribution of selfing rates in homosporous ferns. American Journal of Botany, 79:97–100.
2) Same authors repeated—use three-em dash:
   ———. 1923. The fauna of the Ardyn Obo Formation. American Museum of Natural History Novitates, 98:1–5.
3) Same authors plus a third author—repeat all authors:
   Knutson, L. V., R. E. Orth, and W. L. Murphy. 1986. Catalog of Sciomyzidae (Diptera) of America north of Mexico. Entomography, 4: 1–53.
4) Chapter in an edited volume:
   Rausch, R. L. 1963. A review of the distribution of Holarctic mammals. Pp. 29–43, *in* Pacific Basin Biogeography (J. L. Gressitt, ed.). Bishop Museum Press, Honolulu, Hawaii.
5) Unpublished dissertation:
   Smith, J. P. 1976. Review of Eocene Mammals. Unpublished Ph.D. Dissert., University of California, Berkeley, California.
6) Book:
   White, M. J. D. 1961. The Chromosomes. Metheuen and Co., Ltd., London, United Kingdom.
7) Journal articles with usual volume and issue number:
   Anderson, W. I. 1969. Lower Mississippian conodonts from northern Iowa. Journal of Paleontology, 43:916–928.

Figures. Including all illustrative materials (line art, halftones, photographs), figures are to be numbered in Arabic numerals. Four sets of figures are required, one (original artwork) for reproduction, three for reviewers. Photocopies of photographs for reviewers are usually not acceptable but are adequate for line drawing review copies. Figures may not be larger than 17 by 12 inches. Reducing figures is the responsibility of the author. All figures must be reducible to a maximum of 127 by 195 mm (30 by 46 picas) without loss of clarity. Line copy should be designed for reduction to ⅔ or ½ or actual size. Typewritten figure copy will not be accepted. Photographic figures should be submitted at **actual reproduction size**, if possible.

Rectangular halftone figures should be abutted, without intervening spaces. The printer will insert narrow white spaces during the reproduction process. All figures must have **minimally** one-inch borders all around. Each figure should be given a protective cover and identified on the back side.

Lettering and/or a magnification scale (linear metric scale) for rectangular halftone figures should be placed directly on the photo, not in a blank space between photos. The scale or lettering for closely cropped photos can be placed in blank areas close to the figure.

Proof.—The author should answer all queried proof marks and check the entire proof copy. Return corrected page proof with the edited manuscript ***promptly*** to the Office of Scientific Publications.

If an author chooses to make extensive alterations to a paper in proof stage, the author will bear the cost. Original manuscripts will not be returned unless requested. Figures will be returned to the author only if requested prior to publication.

AS
36
P7X
NH

W

ISSN 0097-4463

SMITHSONIAN
SEP 07 1999
LIBRARIES

ANNALS of CARNEGIE MUSEUM

THE CARNEGIE MUSEUM OF NATURAL HISTORY
4400 FORBES AVENUE • PITTSBURGH, PENNSYLVANIA 15213

VOLUME 68 14 MAY 1999 NUMBER 2

CONTENTS

ARTICLES

New species and immature instars of crane flies of subgenus *Tipulodina* Enderlein from Sulawesi (Insecta: Diptera: Tipulidae: *Tipula*) .... **Chen W. Young** 81

Tournaisian (early Osagean) brachiopods from a bioherm in the St. Joe Formation near Kenwood, Oklahoma .... **John L. Carter** 91

Editors, ANNALS, BULLETIN and SPECIAL PUBLICATIONS:

J. L. Carter, Ph.D
B. C. Livezey, Ph.D
D. R. Watters, Ph.D
M. A. Schmidt, ELS, Assistant Editor

Manuscripts, subscriptions, orders for individual numbers, and changes of address should be sent to:

Office of Scientific Publications
Carnegie Museum of Natural History
4400 Forbes Avenue
Pittsburgh, PA 15213-4080
Phone (412) 622-3287
Fax (412) 622-8837
E-mail: scipubs@clpgh.org

ANNALS OF CARNEGIE MUSEUM is published quarterly by The Carnegie Museum of Natural History, 4400 Forbes Avenue, Pittsburgh, Pennsylvania 15213-4080, by the authority of the Board of Trustees of Carnegie Institute.

© 1999 Carnegie Institute.

♾ This paper meets the requirements of ANSI/NISO Z39.48-1992 (Permanence of Paper).

ANNALS OF CARNEGIE MUSEUM
Vol. 68, Number 2, Pp. 81–90 14 May 1999

NEW SPECIES AND IMMATURE INSTARS OF CRANE FLIES OF SUBGENUS *TIPULODINA* ENDERLEIN FROM SULAWESI (INSECTA: DIPTERA: TIPULIDAE: *TIPULA*)

Chen W. Young
Associate Curator, Section of Invertebrate Zoology
youngc@clpgh.org

Abstract

Tipula (*Tipulodina*) *nettingi* and *T.* (*T.*) *phasmatodes*, the first two species of subgenus *Tipulodina* recorded from Sulawesi, Indonesia, are described and figured. The external anatomy of the last instar larva and pupa of *T. nettingi* is described and illustrated. Comments concerning habitats of the larva and the mate-searching behavior of the adult male are provided.

Key Words: *Tipulodina*, Tipulidae, larva, pupa, Sulawesi

Introduction

Crane flies of the subgenus *Tipulodina* (Enderlein, 1912) (Diptera: Tipulidae: Tipulinae: *Tipula*) have a predominantly Oriental distribution; of the 47 recorded species, 42 are strictly Oriental (Alexander and Alexander, 1973), with two species occurring in the Australasian region (Oosterbroek, 1989), and at least three species recorded from northern China and Japan (Ishida, 1956; Oosterbroek and Theowald, 1992). There is also one undescribed species from Korea (George Byers, personal communication). In Indonesia, nine species of this subgenus have been reported from Borneo, Java, and Sumatra. In 1985, two undescribed species of *Tipula* (*Tipulodina*) were collected on Sulawesi, the first record of this subgenus from that island. Species of *Tipulodina* can be separated morphologically from those of other subgenera of *Tipula* by having a conspicuous dark mark at the tip of the wings on the costal margin, and by having elongate legs with snowy-white rings on the femora, tibiae, or tarsi. *Tipulodinodes* and a few species of *Dolichopeza* also exhibit the white rings on the tarsi, but can be separated from *Tipulodina* by absence of the dark mark at the tip of the wings.

A pupal skin from Salatiga, Java, was sent to de Meijere and subsequently determined and briefly described as *Tipula* (*Tipulodina*) *pedata* Wiedemann (de Meijere, 1911). This was later translated and commented upon by Alexander (1915). A female pupa of an unknown species (Alexander, 1931) and larvae of two undetermined species (Alexander, 1931; Savchenko, 1983), all from Java, also have been supposed to belong to the subgenus *Tipulodina*. Both Alexander and Savchenko were guarded in their conclusions because of the lack of associated adult flies. Based on the current investigation, it is clear that the larval specimens involved in both Alexander's and Savchenko's papers show significant differences from the larva of the new species in having relatively small spiracular discs, unequal spiracular lobes, and six anal gills. The pupal specimen from Buitenzorg, Java (Alexander, 1931), does agree with pupae of the new species. However, a

Submitted 26 February 1998.

pupal specimen from Tallulah Falls, Georgia (Alexander, 1915:185), most likely belongs to *Leptotarsus* (*Longurio*) *testaceus* Loew (Gelhaus and Young, 1995).

The successful rearing of several larvae into adults allows the present study to contribute the first complete descriptions and illustrations of the last instar larva and pupa for the subgenus *Tipulodina*, as well as additional knowledge regarding the biology and behavior of the larvae and adults. Terminology of larval, pupal, and adult characters follows that of Byers (1961), McAlpine (1981), and Gelhaus (1986).

SYSTEMATICS

Tipula (*Tipulodina*) *nettingi* Young, **new species**

(Fig. 1A, B, E)

Description.—Body length: male, 17 mm; female, 27 mm. Wing length: male, 19 mm; female, 22 mm.

Head: rostrum short, grayish brown, sides with dark brown median stripe. Nasus distinct, about two-thirds length of rostrum. Occiput brown with dark brown median line extending from base to anterior vertex. Palpi yellowish brown. Antenna 9 mm in male, 4.5 mm in female; antenna with scape, pedicel, and first flagellomere pale brown, other flagellomeres dark brown, basal enlargements conspicuous with four to five verticils; in female, verticils longer than corresponding flagellomeres.

Thorax: pronotum dark brown medially, yellowish brown laterally. Prescutum yellowish brown with three distinct dark brown stripes; central stripe broad, with dark, narrow median line; lateral stripes shorter, extending from pseudosutural fovea to transverse suture. Scutum yellowish brown with dark brown center, bordered with brown. Scutellum and parascutellum grayish brown, former with dark brown median vitta. Postscutellum grayish brown. Wings grayish subhyaline, with dark brown area including apex in outer radial cells and with conspicuous dark seams on anterior and posterior cord; outer medial veins narrowly seamed with brown; stigma dark brown, confluent with brown seam at cord; a faint light brown quadrate spot before middle of cell bm along vein CuA. Halteres dark brown. Legs with coxae and trochanters light yellow; femora brownish yellow with short, conspicuously darkened apex; outer one-fifth of fore femora whitened to form long diffuse ring; tibiae brownish black with long, white, subterminal ring, subequal in length to darkened apex; basitarsi white with dark brown proximal and distal ends; remaining tarsomeres white except dark brown pretarsi.

Abdomen: terga chestnut brown with brownish black subterminal band, extreme posterior borders narrowly yellow; sterna yellowish brown.

Male hypopygium: external structures as in Figures 1A and B. Posterior border of tergum IX slightly emarginate, with small, median glabrous lobe; broadly rounded, lateral lobes of tergum setiferous. Outer dististyle oval, flattened. Inner dististyle with beak slender in dorsal aspect, directed anteriorly; lower basal lobe of inner dististyle fingerlike, with long, dark apical setae; outer basal lobe of inner dististyle small, hook-shaped, apex a sharp black spine directed inward. Sternum VIII with posterior border short, rounded sides.

Ovipositor: external structures as in Figure 1E. Cerci slightly longer than tergum X, broad at base, tapered posteriorly toward slightly upcurved apex. Basal portion of cerci expanded dorsally. Hypovalves extending to about half length of cerci. Sternum IX with distinct, sclerotized lateral lobes and median fused valvulae. Sternum X with long setae.

Type Material.—Holotype: male, Carnegie Museum of Natural History (CMNH). Verbatim text of three pin labels: INDONESIA Sulawesi Utarra Dumoga-Bone N. P. 6 Sept. 1985 Coll. Chen Young / R2 Toraut 211 m PROJECT WALLACE / HOLOTYPE *Tipula* (*Tipulodina*) *nettingi* Young [red paper]. Paratypes: three males and one female, topotypic, males collected on 25 August and 3 September 1985; female emerged on 4 September 1985.

Other Material.—One male specimen, topotypic, emerged on 3 September 1985, preserved in 80% ethanol and deposited in CMNH.

Etymology.—This species is named in honor of the late Dr. Graham Netting for his wisdom and foresight in establishing an endowed fund for research at the Carnegie Museum of Natural History. This fund has greatly aided field research programs in entomology over the years.

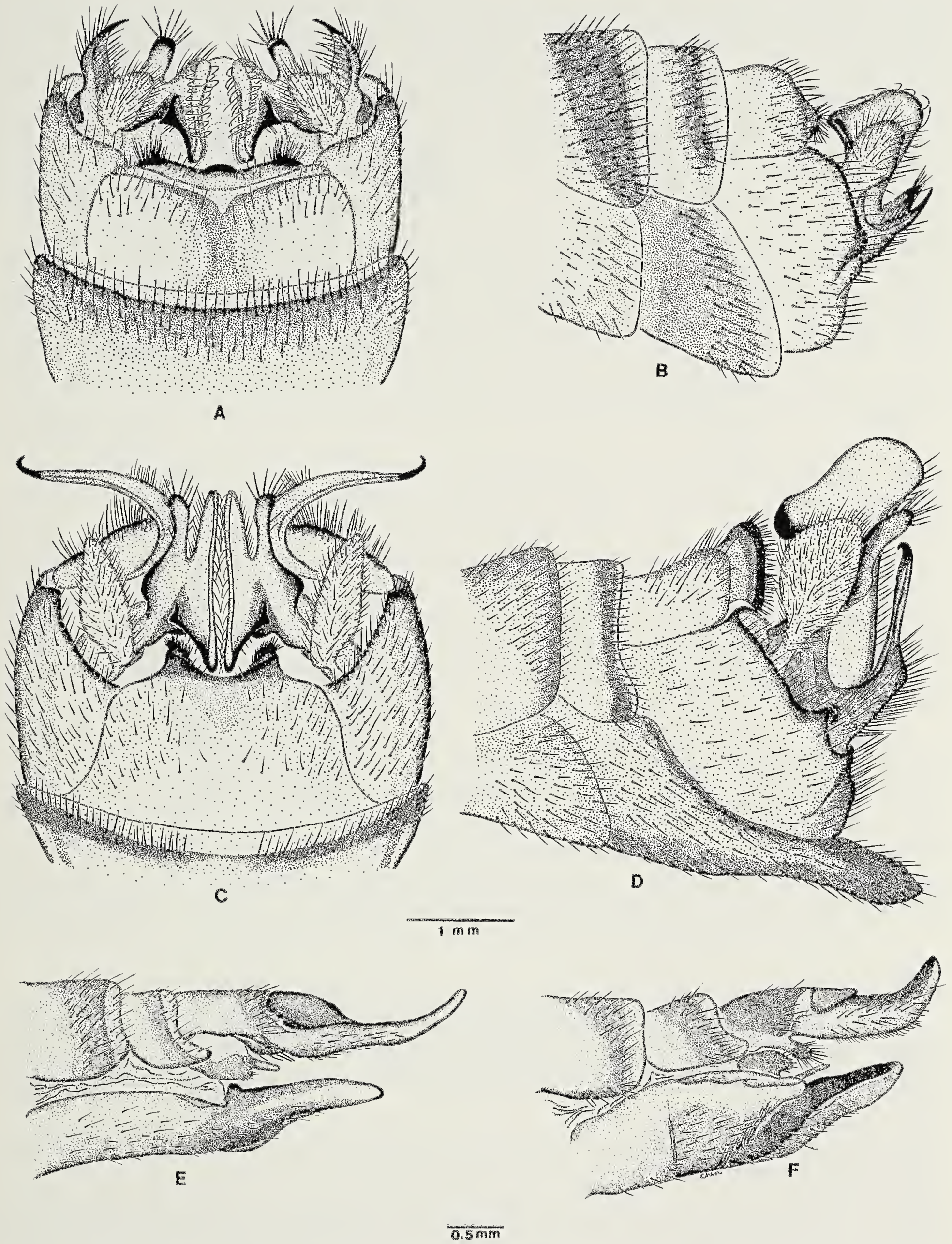

Fig. 1.—A, B. Adult male hypopygium of *Tipula* (*Tipulodina*) *nettingi:* A, dorsal view; B, lateral view. C, D. Adult male hypopygium of *T.* (*T.*) *phasmatodes:* C, dorsal view; D, lateral view. E. *Tipula* (*T.*) *nettingi* female ovipositor, lateral view. F. *Tipula* (*T.*) *phasmatodes* female ovipositor, lateral view.

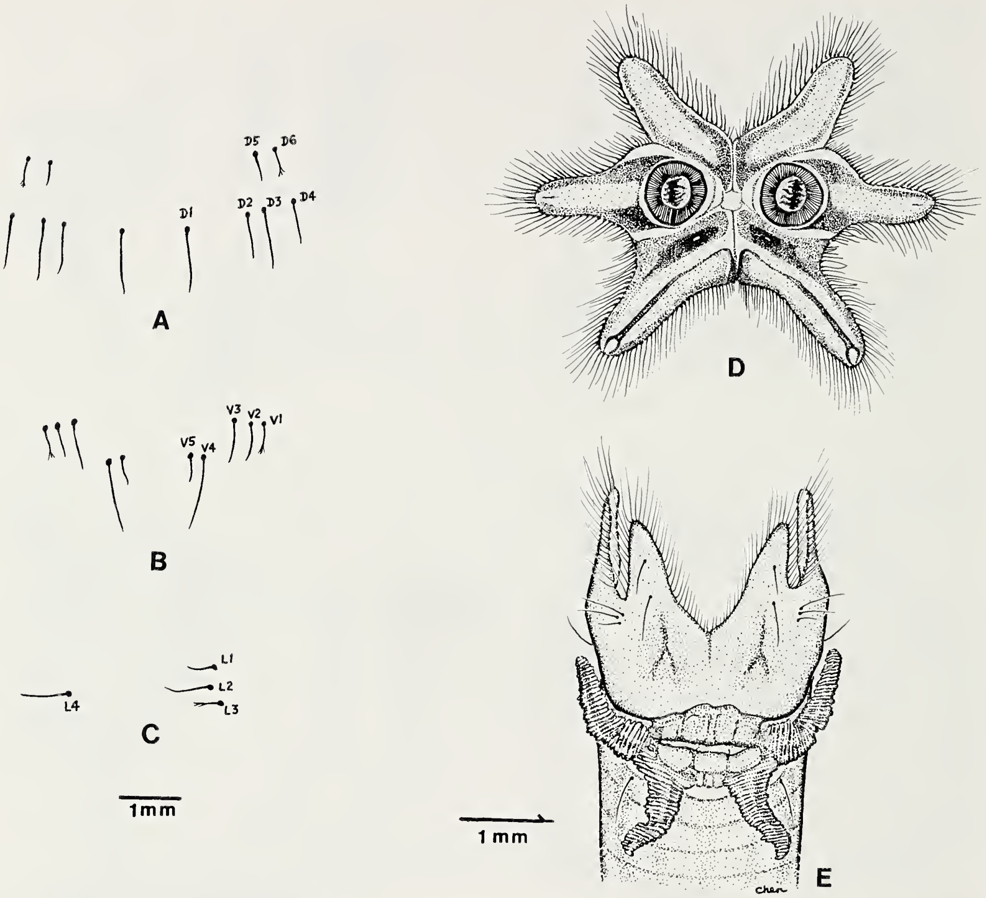

Fig. 2.—Larva of *T.* (*Tipulodina*) *nettingi.* A, C. Abdominal macrosetal arrangements. A, dorsal setae. B, ventral setae. C, lateral setae. D, spiracular disc. E, anal papillae, ventral view.

Comparative Notes.—*Tipula nettingi* is closely related to *T. albiprivata* Edwards and *T. dyak* Alexander on the basis of male hypopygium, including especially the short outer basal lobes and the posterior border of eighth sternum simple with short, rounded sides.

Larval Description.—Fourth (final) instar larva: body 46.0–48.0 mm long and 5.5–6.0 mm wide. Body sordid yellow, paler laterally.

Head: broad, massive, a well-sclerotized, typical tipuline head capsule (Byers, 1961; Young, 1981; Gelhaus and Young, 1991). Mandible with one large tooth near base and three to four smaller teeth apically along inner margin. Maxilla with hairy galea and lacinia. Hypopharynx with five short, rounded teeth. Hypostomal bridge with one large, blunt central tooth and four smaller ones on each side.

Body: body of last instar larva stout and terete, tapering gradually toward both ends. Both thorax and abdomen covered with long microscopic hairs perpendicular to body. Thoracic segments also densely covered with fine, shorter microscopic hairs appressed to body. Dark macrosetae located in all segments, with placement as in Figures 2A–C. All setae except L4 are situated on posterior annuli. L4 situated on anterior annulus. Setae D1, D2, D3, D4, V2, V3, V4, L2, and L4 long; D5, L1, and V5 short. Setae D6, L3, and V1 short and branched.

Spiracular disk: surrounded by six subequal spiracular lobes (Fig. 2D), slightly longer than width at base, ventral pair slightly longer than others, lateral pair equidistant from dorsal and ventral pairs. All lobes with well-developed border of setae, margined with brown adjacent to setal bases. Discal surface of upper four lobes sordid yellow, paler along middle of each lobe; ventral lobes each with dark, median longitudinal streak, approximately as long as lobe; below each spiracle one fairly conspicuous black spot. Spiracles large, fuscous brown with blackish centers, separated by distance slightly more than transverse diameter of a spiracle. Four elongate anal papillae (Fig. 2E) with many constrictions along their length; all papillae single; two longer ones curled dorsad around abdomen; two shorter ones extending ventrad.

Remarks.—The larvae of *T.* (*T.*) *nettingi* resemble superficially those of Nearctic species of the subgenera *Angarotipula, Bellardina, Nobilotipula, Platytipula,* and *Yamatotipula.* They all share the following morphological characters: subequal, long spiracular lobes with long setae; single, dark, median longitudinal streak on ventral lobes; elongate, constricted anal papillae; and branched setae (Gelhaus, 1986). The distinctive difference is the number of anal papillae. Larvae of all the aforementioned subgenera have six anal papillae, while *T.* (*T.*) *nettingi* has only four.

Within the genus *Tipula,* the number and shape of the anal papillae provide a characteristic, synapomorphic feature for some subgenera which otherwise display much diversity in larval morphology (Gelhaus, 1986). The current study shows that larvae of *T. nettingi* have a reduced number of four anal papillae compared to six in most aquatic species. Studies of larvae of additional *Tipulodina* species and species belonging to other subgenera are needed to determine the homology of the anal papillae and establish the polarity of the character. One can speculate that a derived feature of *Tipulodina* may well be the apomorphic loss of two anal papillae, and such studies may make it possible to determine which two have been lost.

The size, form, and number of anal papillae are distinctly correlated with larval habitats. They are large, elongate, and more numerous in aquatic species, reduced in size and number in semiaquatic/terrestrial species (Gelhaus, 1986). It has been postulated that the anal papillae provide osmoregulatory and/or locomotory functions (Chiswell, 1956; Brindle, 1957, 1960; Pritchard, 1983). The reduced number of anal papillae found in *T. nettingi* could result from the fluctuation in the amount of water in the larval habitats, as described below in the biology section.

Pupal Description.—Male: length 21–23 mm, width 3.9–4.1 mm. Female: length 29.8–30.2 mm, width 4.8–5.1 mm. Body coloration overall light yellowish brown, slightly darker on tarsal sheaths.

Head: antennal sheath slightly expanded at base (Fig. 3A), apex of sheath reaching about two-thirds length of mesothoracic tibia. Paired short, wrinkled ridges lying between bases of antennal sheaths, with pair of small dorsal papillae. Maxillary palpal sheath short, apex of sheath recurved, reaching sheath of prothoracic femur.

Thorax: respiratory horn (Fig. 3B) length 7.0 mm in male, 10.0 mm in female; minute annulations along entire length of horn; apex flat and rounded. Dorsum of thorax densely wrinkled. Four pairs of short setae on thoracic dorsum above base of wing sheath. Apex of wing sheath nearly reaching end of abdominal segment II. Leg sheaths reaching to posterior venter of abdominal segment IV in male, to anterior venter of abdominal segment IV in female. Apices of all leg sheaths in transverse alignment.

Abdomen: segments II–VII with well-defined anterior and posterior annuli (Fig. 3A, B). Small forked spines present laterally, along posterodorsal margins of all segments, and along basal margins of posterior annuli of segments V–VII. Posteroventral margins of segments III–VII with larger curved spines. Terminal segment (VIII and IX in male; VIII–X in female) with five pairs of elongate spines: two pairs directed dorsally, one pair directed laterally, one pair directed posteriorly, and one pair directed ventrally. Single, short pair of genital sheaths ventral to large posterior spines in male (Fig. 3D). Two pairs of slightly curved, closely appressed genital sheaths between and below posterior spines in female (Fig. 3C).

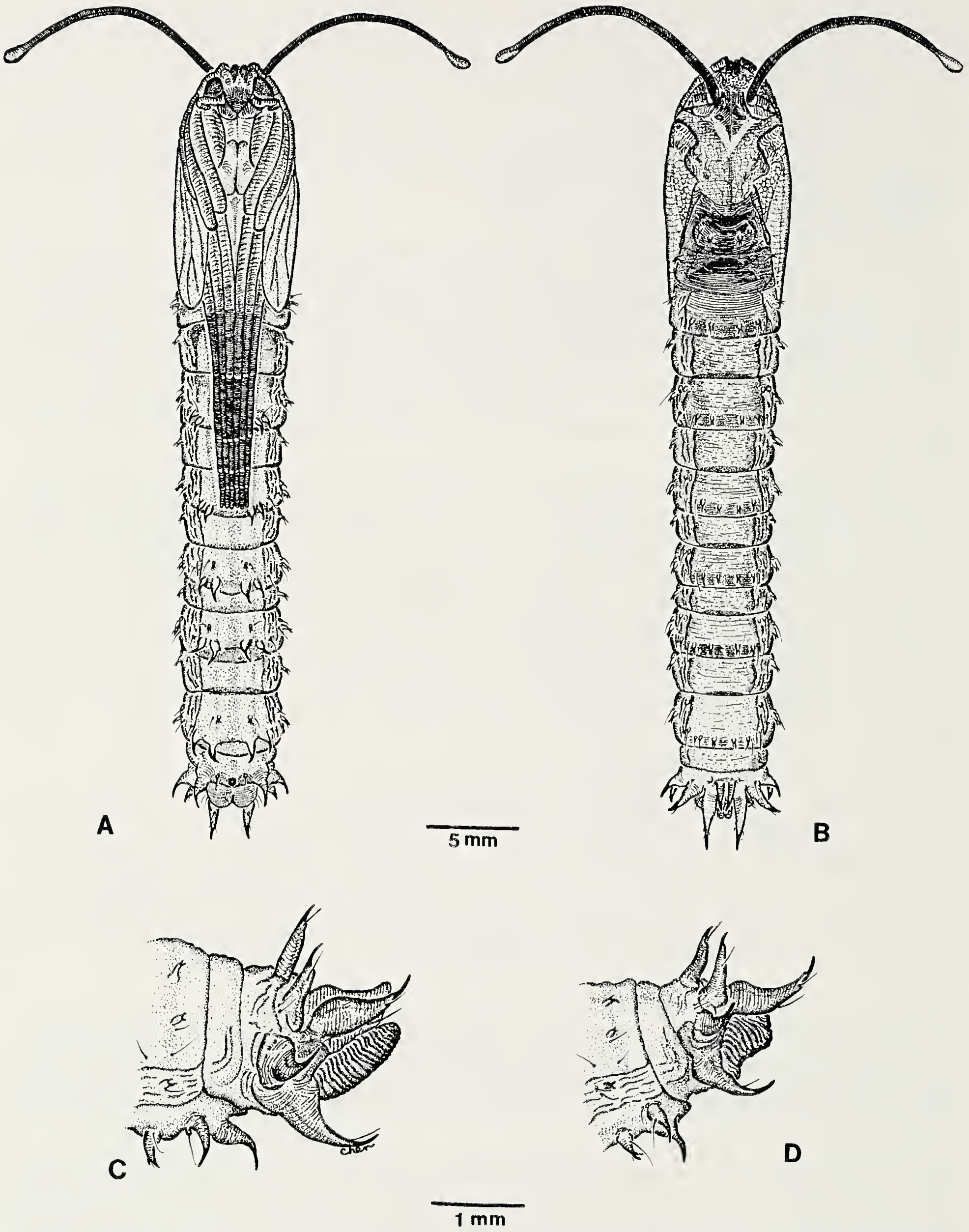

Fig. 3.—Pupae of *T.* (*Tipulodina*) *nettingi*. A, ventral view. B, dorsal view. C, female terminal segments, lateral view. D, male terminal segments, lateral view.

Remarks.—The shape of the maxillary palpal sheath, the length of the distal section of the antennal sheath, and the position of the antennal sheath have been analyzed by previous workers attempting to place various lineages of crane flies within the Tipulinae. A straight or curved maxillary palpal sheath, short distal section of antennal sheath, and apices of antennal and palpal sheaths closely approximated (for example, *Megistocera, Brachypremna,* and *Leptotarsus*) are considered plesiomorphic within the Tipulinae (Oosterbroek and Theowald, 1991; Gelhaus and Young, 1995). A strongly recurved apex of the maxillary palpal sheath, an extended distal section of the antennal sheath, and apices of antennal and palpal sheaths widely separated (for example, *Dolichopeza, Nobilotipula, Platytipula,* and most other Tipulinae) are considered apomorphic (Gelhaus and Young, 1995). The present study of the pupal characters of *T. nettingi* shows its resemblance to most of the species of the advanced lineages of Tipulinae.

The size and form of the respiratory horns of the pupa of *T. nettingi* are probably specifically associated with pupal habitats. Elongate respiratory horns are also present in several other unrelated aquatic species of *Angarotipula* and *Leptotarsus,* within Tipulinae.

Biology.—All specimens used in this study were collected at a rain-forest site within the Dumoga-Bone National Park on the northern peninsula of Sulawesi. The National Park is located just north of the equator (0°38′N, 124°06′E). The vegetation of the site is primary lowland forest at approximately 200 m elevation. Larvae were collected in rotted stumps of the palm *Livistona rotundifolia.* The palm stumps were about 1 m high with small pools of water in the center. Many of the stumps showed evidence of habitation by termites in the more basal parts. Larvae could be located when they opened the spiracular lobes and exposed the caudal end to the surface of the water for breathing. They moved quite swiftly by extension and contraction of the body. When the outside wall of the stump was tapped gently, the larvae withdrew both the spiracular lobes and the head capsule and remained motionless for several minutes. Larvae withdrew and moved briskly by undulation when the stump was suddenly, vigorously vibrated. In one of the stumps, where the water inside had receded, larvae were found buried to about 8–12 cm below the surface where the substrate was still very wet.

Larvae for rearing were transported back to the field laboratory and kept in a 32 × 24 × 11-cm transparent plastic box. Water and organic substances from the natural habitat were mixed and covered the bottom of the box to a depth of 5 cm. Broken pieces of decomposed palm pith were added to one end of the box to simulate the natural habitat. Pupae attached themselves vertically to the wall of the palm with the tips of the respiratory horns protruding out of the water. When disturbed, they wriggled vigorously and withdrew completely into the water. They resumed their partially emergent posture when left undisturbed for a few minutes. Duration of the pupal stage was about ten days.

Pupae of other *Tipulodina* species have also been reported from other kinds of phytotelmata in similar habitats. Pupae of *T.* (*T.*) *brunettiella* Alexander were collected from bamboo stumps in India (Edwards, 1932). I collected one callow female of *T.* (*T.*) *taiwanica* (Alexander) from a hollow bamboo stump in Taiwan. Within the study area, one female of the new species described below, *Tipula* (*Tipulodina*) *phasmatodes,* was observed to deposit eggs in a flooded cavity in a fig tree. Larvae and pupae of an undescribed species were also collected by Byers from a tree hole in Korea. Byers speculated that the larvae of *Tipulodina* in Korea probably fed on mosquito larvae which inhabited the same tree hole (George Byers, personal communication), since these larvae quickly disappeared from a laboratory jar also containing *Tipulodina.* It is conceivable that with limited accessible food resources in a phytotelmaton, the usually herbivorous larvae will occasionally become carnivorous opportunists.

Tipula (*Tipulodina*) *phasmatodes* Young, **new species**
(Fig. 1C, D, F)

Description.—Body length: male, 20 mm; female, 26 mm. Wing length: male, 19 mm; female, 20 mm.

Head: rostrum short, grayish brown, sides with dark brown stripe. Nasus distinct, about one-half length of rostrum. Occiput brown, anterior vertex with a small, dark brown, erect median tubercle between eyes. Palpi yellowish brown. Antenna 6 mm in male, 3.5 mm in female; scape, pedicel pale brown, flagellomeres dark brown, basal enlargements conspicuous with four to five verticils; verticils subequal to segment length in both sexes.

Thorax: pronotum dark brown medially, yellowish brown laterally. Prescutum yellowish brown with three poorly defined stripes; central stripe with dark, narrow median line. Scutum, scutellum, and parascutellum grayish brown. Postscutellum grayish brown. Wings grayish subhyaline, with dark brown area including apex in outer radial cells and with conspicuous dark seams on anterior and posterior cord; outer medial veins narrowly seamed with brown; stigma dark brown, confluent with seam at cord; a distinct, large, brown quadrate spot before middle of cell bm along vein CuA. Halteres dark brown. Legs with coxae and trochanters light yellow; femora brownish yellow, outer one-fourth more whitened to form long diffuse ring; fore and middle tibiae brownish black with long white ring at midlength; hind tibiae black with two white rings between proximal and terminal dark rings; basitarsi with basal half brown and terminal half white; remaining tarsomeres white except pretarsi brown.

Abdomen: terga chestnut brown with brownish black subterminal band, extreme posterior borders narrowly yellow; sterna yellowish brown.

Male hypopygium: external structures as in Figures 1C and D. Posterior border of tergum IX slightly emarginate with lateral angles produced as flat lobes bearing abundant black setae. Outer dististyle large, oval, flattened. Inner dististyle with beak flattened, slender, directed anteriorly; lower basal lobe of inner dististyle fingerlike, apex with long, dark setae; outer basal lobe long, curved outward from base, gradually into long, recurved, black terminal spine. Sternum VIII with posterior border produced into long, triangular blade.

Ovipositor: external structures as in Figure 1F. Cerci subequal in length to tergum X, broad from base to midlength and then narrowed toward upwardly curved apex. Hypovalvae reaching to about midlength of cerci, base of hypovalvae expanded upward. Sternum IX with distinct, sclerotized side lobes and median fused valvulae. Sternum X with long, dense setae.

Type Material.—Holotype: male, CMNH. Verbatim text of three pin labels: INDONESIA Sulawesi Utarra Dumoga-Bone N. P. 4 Sept. 1985 Coll. Chen Young / R2 Toraut 211 m PROJECT WALLACE / HOLOTYPE *Tipula* (*Tipulodina*) *phasmatodes* Young [red paper]. Paratypes: two males and one female, topotypic, males collected on 24 August and 3 September 1985; female collected on 7 September 1985; one male, 21 January 1985, collected by J. Holloway.

Etymology.—The name of this species is the Greek adjective phasmatodes, meaning phantomlike, and refers to the ghostly appearance that the black-and-white banded legs give to the adult flies when on the wing.

Comparative Notes.—The general appearance of *T.* (*T.*) *phasmatodes* is similar to that of *T. nettingi.* These two species can be distinguished by color pattern of hind tibia. In *T. phasmatodes* the hind tibia with black center between two white rings, while in *T. nettingi* it is white center between two black rings. The nearest relatives of the present fly include *T. felicita* Alexander, *T. fuscitarsis* Edwards, and *T. pedata* Wiedemann, each with the structure of the male hypopygium distinct, including especially the elongated outer basal lobes and the posterior border of eighth sternum produced into long, triangular blade.

Mate-searching Behavior.—Mate-searching behavior of adult males of Tipulinae has been described as walking or flying over the ground, up tree trunks, or among vegetation (Pritchard, 1983). Attraction to the same resting area and swarming also brings males and females into close proximity (Byers, 1961). Males of both species in this study performed a downward, searching behavior on tree trunks. The male started its search on the tree trunk about two meters off the ground and performed a series of vertical oscillating flights around and toward the base of the trunk. It then flew to the next tree trunk and repeated the same search pattern. Males do not limit their searches to trunks or stumps of the palm *Livistona rotundifolia* usually inhabited by the larvae and pupae. Actual copulation was not observed in nature.

ACKNOWLEDGMENTS

This paper is Project Wallace Paper No. 145 and is based on specimens collected by the author on Project Wallace, sponsored by the Indonesian Institute of Science and the Royal Entomological Society of London. The research was supported by a grant from the M. Graham Netting Field Research Fund, the Carnegie Museum of Natural History, Pittsburgh, Pennsylvania. I would like to thank J. E. Rawlins and R. L. Davidson for suggestions on the manuscript; thanks also to three anonymous reviewers for their comments.

LITERATURE CITED

ALEXANDER, C. P. 1915. On a collection of Javanese crane-flies (Tipulidae, Diptera) in the United States National Museum. Proceedings of the United States National Museum, 49:157–193.

———. 1931. Deutsche Limnologische Sunda-Expedition. The crane-flies (Tipulidae, Diptera). Archiv für Hydrobiologie, 9:135–191.

ALEXANDER, C. P., AND M. M. ALEXANDER. 1973. Family Tipulidae. Volume 1:10–224, *in* A Catalog of the Diptera of the Oriental Region (M. D. Delfinado and D. E. Hardy, eds.). The University Press of Hawaii, Honolulu, Hawaii.

BRINDLE, A. 1957. The ecological significance of the anal papillae of *Tipula* larvae (Diptera, Tipulidae). Entomologist's Monthly Magazine, 93:202–204.

———. 1960. Notes on the larvae of the British Tipulinae (Diptera, Tipulidae). Part 6. The larvae of the *Tipula oleracea* group. Entomologist's Monthly Magazine, 95:176–177.

BYERS, G. W. 1961. The crane fly genus *Dolichopeza* in North America. The University of Kansas Science Bulletin, 42:665–924.

CHISWELL, J. R. 1956. A taxonomic account of the last instar larvae of some British Tipulinae (Diptera: Tipulidae). Transactions of the Royal Entomological Society of London, 108:409–484.

DE MEIJERE, J. C. H. 1911. Studien über Südostasiatische Dipteren V. Ostindische Tipulidae. Tijdschrift voor Entomologie, 54:21–79.

EDWARDS, F. W. 1932. The Indian species of *Tipula* (Diptera, Tipulidae). Part I. Stylops, 1:180–184.

ENDERLEIN, G. 1912. Studien über die Tipuliden, Limoniiden, Cylindrotomiden und Ptychopteriden. Zoologische Jahrbücher (Systematik), 32:1–88.

GELHAUS, J. K. 1986. Larvae of the crane fly genus *Tipula* in North America (Diptera: Tipulidae). University of Kansas Science Bulletin, 53:121–182.

GELHAUS, J. K., AND C. W. YOUNG. 1991. The immature instars and biology of the crane fly genus *Brachypremna* Osten Sacken (Diptera: Tipulidae). Proceedings of the Entomological Society of Washington, 93:613–621.

———. 1995. Pupae of the crane fly genus *Leptotarsus* (Diptera: Tipulidae) in the New World, with discussion of the monophyly of the genus. Annals of the Carnegie Museum, 64:135–145.

ISHIDA, H. 1956. The catalogue of the Japanese Tipulidae, with the keys to the genera and subgenera. II. *Tipula* (part) and Cylindrotominae. Annual Report of Hyogo Agricultural College, 5:59–77.

MCALPINE, J. F. 1981. Morphology and terminology—adults. Pp. 9–63, *in* Manual of Nearctic Diptera, Volume 1 (J. F. McAlpine, B. V. Peterson, G. E. Shewell, H. J. Teskey, J. R. Vockeroth, and D. M. Wood, eds.). Agriculture Canada Monograph, no. 27.

OOSTERBROEK, P. 1989. Tipulidae. Pp. 53–116 *in* Catalog of the Diptera of the Australasian and Oceanian Regions (N. L. Evenhuis, ed.). Bishop Museum Press, Honolulu, Hawaii.

OOSTERBROEK, P., AND BR. THEOWALD. 1991. Phylogeny of the Tipuloidea based on characters of larvae and pupae (Diptera, Nematocera), with an index to the literature except Tipulidae. Tijdschrift voor Entomologie, 134:211–267.

———. 1992. Family Tipulidae. Volume 1:56–178, *in* Catalogue of Palaearctic Diptera (A. Soós, L. Papp, and P. Oosterbroek, eds.). Hungarian Natural History Museum, Budapest, Hungary.

PRITCHARD, G. 1983. Biology of Tipulidae. Annual Review of Entomology, 28:1–22.

SAVCHENKO, E. N. 1983. Crane-flies (Family Tipulidae), Introduction, Subfamily Dolichopezinae, subfamily Tipulinae. Fauna USSR, Diptera, Volume 2, Parts 1–2, New Series, 127:1–584. [in Russian]

YOUNG, C. W. 1981. The immature instars of *Tipula* (*Platytipula*) *ultima* Alexander (Tipulidae, Diptera). Journal of the Kansas Entomological Society, 54:409–415.

ANNALS OF CARNEGIE MUSEUM
VOL. 68, NUMBER 2, PP. 91–149 14 MAY 1999

TOURNAISIAN (EARLY OSAGEAN) BRACHIOPODS FROM A BIOHERM IN THE ST. JOE FORMATION NEAR KENWOOD, OKLAHOMA

JOHN L. CARTER
Curator, Invertebrate Paleontology
jlcarter@nauticom.net

ABSTRACT

A diverse early Osagean (Upper Tournaisian) brachiopod fauna from a carbonate buildup in the St. Joe Formation near Kenwood, Mayes County, northeastern Oklahoma, is described. This is the earliest Lower Carboniferous, and perhaps only, Tournaisian biohermal brachiopod fauna described in North America, although potentially earlier unknown faunas could occur in mid-Kinderhookian bioherms of southwestern Missouri. It consists of 40 species in 34 genera and is characterized by unusually robust specimens of several species. New species are *Geniculifera siphuncula, Pustula kenwoodensis, Pustula oklahomae, Schizophoria mayesensis, Rhynchopora kollari, Cranaena salinensis,* and *Dielasma oklahomensis.*

KEY WORDS: brachiopods, Tournaisian, Osagean, bioherm, St. Joe Formation, Oklahoma, Mississippian, Lower Carboniferous

INTRODUCTION

Lower Carboniferous North American brachiopod faunas from either bioherms or framework-supported reefs have never been described and illustrated. This report consists of the description of such a fauna from the unbedded biosparite core, not flanking beds, of a biohermal mound in northeastern Oklahoma.

The term bioherm is used here in the sense of Wilson (1975:23), that is, a "buildup whose internal composition shows it to be largely derived from in situ production of organisms or as framework or encrusting growth as opposed to mainly mechanical (hydrodynamical) piling." Wilson further characterized Waulsortian mounds as being composed of massive lime mudstones with scattered crinoidal and bryozoan fragments which form lenslike buildups or mounds.

After the end of the great Frasnian extinction event true reefs were absent from the world's oceans for a considerable period of time. Although organic framework-supported reefs possibly did not reappear until the Viséan, carbonate buildups started appearing in North America along the margins of the Burlington Shelf of Lane (1978) during the Tournaisian (late Kinderhookian and early Osagean) as bioherms and Waulsortian mounds. The former generally have a thick, crinoidal, nonbedded inner core and the latter have a fine-grained micritic core. The earliest known North American buildups are in the late Kinderhookian Compton Limestone of southwestern Missouri (Thompson and Fellows, 1970). According to Lane (1982) the basal beds of the Swimming Woman Canyon carbonate mound in central Montana, as described by Cotter (1965), bear late Kinderhookian conodonts.

Lower Carboniferous bioherms and other carbonate buildups have been described in the Tri-State District (Missouri, Oklahoma, and Kansas) mining area from the St. Joe and Keokuk formations of northeastern Oklahoma by Harbaugh (1957), from the St. Joe Formation of southwest Misssouri and northwest Arkan-

Submitted 19 March 1998.

sas by Troell (1962), from the Reeds Spring Formation of northeastern Oklahoma by McKnight and Fischer (1970), and from the Compton Limestone of southwestern Missouri by Thompson and Fellows (1970). Lane (1982) summarizes the distribution of early Carboniferous carbonate buildups in North America, which he terms the "Waulsortian facies."

Brachiopods or other macrofossils have been rarely reported or described from carbonate buildups in the early Carboniferous. Demanet (1923) described the Early Viséan faunas from the flank beds of the Waulsortian mounds near Sosoye, Belgium. Gordon, in McKnight and Fischer (1970), listed fossils, mostly brachiopods, from a bioherm in the Reeds Spring Formation of northeast Oklahoma. Mundy and Brunton (1985) and Brunton and Mundy (1988) described diverse brachiopod faunas from Upper Viséan reefs in England. An undescribed brachiopod fauna of late Kinderhookian or early Osagean age was collected by Glenister and his students (personal communication) from a thick buildup in the Lodgepole Formation of Montana, as described by Cotter (1965).

The general features of the carbonate buildup that is the subject of this report were described by Harbaugh (1957). The massive nonbedded core facies described and illustrated by Harbaugh (1957) from the west end of the Kenwood bioherm was subsequently penetrated by a small quarry, which yielded the exceptionally well-preserved fauna described below. About six to eight meters of limestone are exposed in the quarry, all in the core facies. Presumably, the floor is normal bedded limestone but it is cluttered with debris and large blocks from the quarrying operation and examination of the floor is difficult.

In the Folk (1962) classification scheme the limestone of virtually the entire core would be termed a fine to coarse biosparite. Virtually no micrite was observed in numerous hand samples. There is no indication of stratification of the core. Vugs occur sparsely throughout the core, although being most numerous near large biogenic clasts. Brachiopods, rare bivalves, and very rare corals are the largest clasts observed although occasional crinoid plates and columnals were found intact. Fossils are sparsely and irregularly distributed throughout the core facies in this small quarry.

The paleoecological setting for this assemblage is unknown and undescribed in the literature. Lane (1982) interpreted the carbonate buildups of Osagean age in the Kenwood region as being formed at the outer shelf edge, presumably on the slope and in water of moderate depth. The excellent preservation, with no signs of abrasion from transport, suggests that the fossils were found more or less in situ. If that is indeed the case then one could conclude that the brachiopods and other large faunal elements were buried by rapidly accumulating crinoid debris in a thriving crinoid thicket. The water must have been of sufficient depth to prevent comminution of the crinoid plates, ossicles, and other clasts that make up the biogenic portion of the biosparite.

Orientation of specimens appears to have been random although geopetal accumulations of carbonate sand in the ventral umbonal regions of several of the spiriferoid brachiopods were noted. The interiors of most of the complete specimens are completely or partially filled with calcite spar. Wilson (1975:146) warned against interpreting sparry in-fillings as an indicator of high-energy environments.

Stratigraphic Setting

The name St. Joe was first used by Hopkins (1893) for extensive exposures at St. Joe, Searcy County, Arkansas, wherein he designated it as the basal unit of the Boone Formation. Cline (1934) raised the St. Joe of Oklahoma to formational rank and Clarke and Beveridge (1952) raised the St. Joe of Missouri to group rank, including the Compton Limestone, Northview Formation, and the Pierson Formation, in ascending order.

In northeastern Oklahoma, according to Huffman (1958), the St. Joe Formation generally consists of about ten feet of thin-bedded, gray nodular limestone at the base, a middle portion composed of several feet of soft, limy green shale, and an upper portion of about 25 feet of gray, thick-bedded, coarse-grained crinoidal limestone. It rests unconformably on the Chattanooga Shale which is absent in some areas and is conformably overlain by the Reeds Spring Limestone (Moore, 1928). McKnight and Fischer (1970) reassigned the St. Joe of northeastern Oklahoma to the Boone Formation and reduced it to member level. However, most recently Fay (1987) used the term St. Joe Group in the COSUNA correlation chart for this region. Following Thompson and Fellows (1970), the St. Joe is referred to in the present report as a formation. The bioherm that is the subject of this paper occurs within the upper unit, which is coeval with the upper St. Joe at its type section in Arkansas and the Pierson Formation of southwestern Missouri.

BIOSTRATIGRAPHY

This Kenwood fauna is clearly of early Osagean age and can be correlated readily with similar faunas from the upper St. Joe Formation of northcentral Arkansas, the Pierson Formation of southwestern Missouri, the lower Burlington Limestone of eastern Missouri, and the Fern Glen Formation of eastern Missouri and western Illinois.

Girty (1915) described or discussed a total of 39 species of invertebrates collected from the upper beds of the St. Joe at or near its type section near St. Joe, Searcy County, Arkansas. This included six corals, nine bryozoans, 23 brachiopods, and one gastropod. Following Weller (1909) he correlated this fauna with that of the Fern Glen Formation of eastern Missouri, a general correlation that stands today. Neither Weller (1909) nor Girty (1915) collected faunas from the basal beds of the St. Joe which were not exposed at that time. A subsequent quarrying operation revealed the lower St. Joe. By digging a trench at this locality I have recovered the following fauna from thin limestone beds one to two feet above the base of the St. Joe:

Leptagonia sp.
"*Chonetes*" sp.
Productina sampsoni (Weller, 1909)
Magnumbonella newarkensis (Moore, 1928)
Magnumbonella sp.
"*Avonia*" *honeycreekensis* Carter, 1967
Rhytiophora blairi (Miller, 1881)
Rhipidomella sp.
Macropotamorhynchus tuta (Miller, 1881)
Macropotamorhynchus chouteauensis (Weller, 1914)
Shumardella obsolescens Weller, 1910
Cleiothyridina n. sp.
Crurithyris parva (Weller, 1899)
Prospira latior (Swallow, 1863)

Voiseyella sp.
Brachythyris sp.
Cyrtina sp.
Cranaena sp.

This fauna is indicative of a late Kinderhookian age, which is in agreement with the conodonts recovered at this locality by Thompson and Fellows (1970).

In addition to the fauna reported by Girty (1915) from the upper St. Joe at the type section, I found at this same locality specimens of *Marginatia fernglenensis* (Weller, 1909), *Eomartiniopsis rostrata* (Girty, 1899), *Crinisarina prouti* (Swallow, 1860), and *Fernglenia vernonensis* (Swallow, 1860). These occurrences further confirm the correlations discussed above.

Huffman (1958), in summarizing the paleontology of the St. Joe of northeastern Oklahoma, listed the following ten brachiopod species:

Rhipidomella oweni Hall and Clarke
"*Dictyoclostus*" *fernglenensis* (Weller)
Spirifer rowleyi Weller
Spirifer vernonensis Swallow
Brachythyris suborbicularis (Hall)
Athyris lamellosa (Léveillé)
Cliothyridina prouti (Swallow)
Pseudosyrinx missouriensis Weller
Allorhynchus sp.
Leptaenella analoga (Phillips)

It is evident from this list that these collections were made from the upper, early Osagean portion of the St. Joe.

THE KENWOOD, OKLAHOMA, LOCALITY

A large collection of well-preserved brachiopods was made in a small, abandoned quarry in a massive biohermal core on the north side of the Salina–Kenwood Road, about two miles west of Kenwood, Mayes County, Oklahoma (SE ¼, SE ¼, Sec. 11, T 21 N, R 21 E). The database number of this collection is SL407. There is another sizable collection of this material in the National Museum of Natural History, made by G. A. Cooper in the 1960s.

FAUNAL COMPOSITION

Most Lower Carboniferous articulate brachiopod groups are represented in this fauna. Inarticulates are conspicuously absent. All major groups are represented by at least two genera except for the impunctate rhynchonellids with only one genus, *Macropotamorhynchus* Sartenaer. Table 1 shows the occurrences of the Kenwood brachiopod species in the Pierson Formation of southwestern Missouri, the upper St. Joe at its type section in Arkansas, the Lower Burlington Limestone of eastern Missouri, and the Fern Glen Formation of eastern Missouri.

This fauna is notable for the unusually large specimens of several species, including *Leptagonia analoga* (Phillips), *Pustula kenwoodensis* n. sp., *Lamellosathyris lamellosa* (Léveillé), *Eomartiniopsis* n. sp., *Brachythyris chouteauensis* (Weller), ?*Torynifer* sp., *Cranaena globosa* Weller, *Cranaena salinensis* n. sp., and *Dielasma oklahomensis* n. sp. In addition, several other large species are a

Table 1.—*Occurrences of Kenwood brachiopod species also found in the Pierson Formation of southwestern Missouri, the upper St. Joe Formation in northcentral Arkansas, the lower Burlington Limestone in eastern Missouri, and the Fern Glen Formation in eastern Missouri. New and indeterminate Kenwood species are not included.*

Species	Kenwood Loc.	Pierson Fm.	St. Joe of Ark	L. Burl. Ls.	Ferm Glen Fm.
Leptagonia analoga	X	X	X	X	X
Rugosochonetes multicostus	X	X	X	X	X
Caenanoplia burlingtonenesis	X	X		X	X
Breileenia minnewankensis	X			X	
S. (Seminucella) semicostata	X			X	
Marginatia magna	X			X	
Scutepustula arctifossa	X	X		X	
Ovatia laevicosta	X	X	X	X	
Rhipidomella diminutiva	X	X	X	X	X
Macropotamorhynchus tuta	X			X	
Rhynchopora persinuata	X	X		X	X
Coledium simulans	X		X		
Rowleyella fabulites	X			X	
Lamellosathyris lamellosa	X	X	X	X	X
Crinisarina prouti	X	X	X		X
Cleiothyridina cf. *glenparkensis*	X	X		X	X
Eomartiniopsis rostrata	X		X		
S. (Mesochorispira grimesi	X	X	X	X	
Fernglenia vernonensis	X	X	X		X
Tegulocrea incerta	X			X	
Voiseyella novamexicana	X	X		X	X
Brachythyris chouteauensis	X	X	X	X	X
Kitakamithyris cooperensis	X	X	X	X	
Pseudosyrinx missouriensis	X	X	X	X	
Punctospirifer subtexta	X	X		X	X
Cranaena globosa	X			X	

conspicuous constituent of this fauna, including *Marginatia magna* Carter and *Spirifer* (*Mesochorispira*) *grimesi* (Hall).

Although Girty (1915) listed 23 brachiopod species in the St. Joe at the type section many of his identifications were queried or indeterminate and a much less diverse fauna is the norm for the St. Joe Formation. Huffman (1958) reported only ten species in the normally bedded St. Joe of northeastern Oklahoma, as compiled from the literature, and Gordon (in McKnight and Fischer, 1970) identified 12 species from six collections. This contrasts sharply with the 40 species identified in this report from a single collection.

Mundy and Brunton (1985) and Brunton and Mundy (1988) documented more than 45 genera of brachiopods in the Upper Viséan (mostly Asbian) reefs of the Craven Reef Belt in England. At least some of these reefs were partially framework-supported.

Although not the most numerous elements of their faunas, strophalosioids and aulostegoids formed an important epifaunal constituent, as in the Permian reefs of West Texas described by Grant (1971). Neither of these groups are present in the Kenwood St. Joe fauna which seemingly provided no obvious firm attachment substrate, except for the sparsely distributed coarse skeletal material including other brachiopods. However, there were primitive aulostegoids at about this time in the midcontinent. Carter (1991*b*) described the aulostegoid *Archaiosteges* Carter, 1991, from the upper, early Osagean beds of the Gilmore City Limestone of northern Iowa. The specimens of this genus were collected from a lagoonal oolite but were clearly transported and their provenance in life is unknown. It is possible that the pedunculate Kenwood brachiopods were attached to living crinoids which buried the brachiopods in coarse debris when they died and disarticulated.

Comparison of the Kenwood fauna with other biohermal faunas of the same age is not possible at the present time due to a dearth of information. However, one can conclude that although the diversity of the Kenwood bioherm is comparable to younger framework-supported reefs the characteristic epifaunal and cemented groups had not yet exploited these early Carboniferous buildups, possibly due to a lack of suitable substrates.

SYSTEMATIC PALEONTOLOGY

In the following treatment generic diagnoses are not provided if they are essentially correct in the "Treatise on Invertebrate Paleontology" or can be found in the recent literature (see Literature Cited). Higher classification generally follows that proposed by Carter et al. (1994), Brunton et al. (1995), Brunton and Cocks (1996), Savage (1996), and Williams et al. (1996). Types and figured specimens are deposited in the Section of Invertebrate Paleontology, Carnegie Museum of Natural History (CM), Pittsburgh, Pennsylvania.

Phylum Brachiopoda Duméril, 1806
Subphylum Rhynchonelliformea Williams, Carlson, Brunton, Holmer, and Popov, 1996
Class Strophomenata Williams, Carlson, Brunton, Holmer, and Popov, 1996
Order Strophomenida Öpik, 1932
Suborder Strophomenidina Öpik, 1932
Superfamily Strophomenoidea King, 1846
Family Leptaenidae Hall and Clarke, 1894
Genus *Leptagonia* M'Coy, 1844
Leptagonia analoga (Phillips, 1836)
(Fig. 1A–E)

1836 *Producta analoga* Phillips: p. 116, pl. 7, fig. 10.
1968 *Leptagonia analoga* (Phillips): Brunton, pp. 29–31, pl. 3, fig. 26–31, pl. 4, fig. 1–9; textfig. 6–17.
1972 *Leptagonia analoga* (Phillips): Brand, pp. 59–61, pl. 8, fig. 1–6.

Diagnosis.—From Brunton (1968:29): "Subquadrate to semicircular *Leptagonia* with adult disc about one-half as long as wide, outline commonly modified by emargination medianly and less commonly laterally; immature shells planoconvex, adult shells biconvex, about one-half as deep as long, commonly uniplicate, rarely parasulcate; dorsally directed trail variably developed; visceral region with 14–18 regular rugae having mean wavelengths of 1.0 mm and 1.4 mm for the fifth and tenth rugae; rounded costae, commonly 5 or 6 in 2 mm, 10 mm anteromedianly of umbones; pseudospondylium subcircular, seven-tenths as long as wide and about one-third as long as length of disc; dorsal muscle field one-half as long as wide; median septum extending forward for about two-fifths length of disc."

Comments.—This species does not occur above the Upper Tournaisian in North America. The genus *Leptagonia* does not reappear in North America until the end of the Chesterian (late Serpukhovian) where it occurs as undescribed new species in the Imo Formation of Arkansas and the Chainman Shale of Utah.

This species appears to be highly variable in the development of a high ridge at the margin of the ventral disc, maximum depth of the visceral area of the conjoined valves, and development of a pseudospondylium. For example, the specimens considered here from the Kenwood locality are rarely, if ever, half as thick as long. On the other hand, similar specimens from the Nunn Member of the Lake Valley Formation of New Mexico generally are more than half as thick as long but are otherwise closely similar to the Kenwood specimens. The development of a pseudospondylium has not been observed. If it existed in juveniles, as in Brunton's specimens, the existence of this structure awaits description.

The costation density of these Kenwood specimens of 19–21 per 5 mm at a distance of 1 cm anterior to the umbones falls within the range of 15–22 as given by Brand (1972).

Material.—In addition to the illustrated specimens there are seven more or less complete specimens and five disarticulated valves.

Suborder Orthotetidina Waagen, 1884
Superfamily Orthotetoidea Waagen, 1884
Family Schuchertellidae Williams, 1953
Genus *Schuchertella* Girty, 1904
Schuchertella sp.
(Fig. 1F, G)

Comments.—Orthotetoids are rare in this fauna and are invariably disarticulated and generally fragmentary. The only two complete valves are figured here (Fig. 1). Figure 1F is a nearly complete, flat dorsal valve. The umbo is spalled, revealing a very low, bilobed cardinal process and short diverging sockets. The other specimen (Fig. 1G) is a thicker, more-inflated ventral valve which lacks any evidence of internal plates. Thus, there seems to be little doubt about assignment of these specimens to the genus *Schuchertella*, but the paucity of material obviates a species assignment.

Suborder Chonetidina Muir-Wood, 1955
Superfamily Chonetoidea Bronn, 1862
Family Rugosochonetidae Muir-Wood, 1962
Genus *Rugosochonetes* Sokolskaya, 1950
Rugosochonetes multicostus (Winchell, 1863)
(Fig. 1H–J)

1863 *Chonetes multicosta* Winchell: p. 5.

Diagnosis.—Transversely subquadrate *Rugosochonetes* generally with greatest width at hingeline, about two-thirds as long as wide; ventral valve with shallow medial sinus or flattening in anterior two-thirds of valve; hingeline with six or seven fine spines on each side of beak; large specimens with about five capillae per millimeter at medial anterior margin.

Comments.—The specimen selected by Weller (1914:pl. 8, fig. 12, University of Michigan number 1343) as the most typical of Winchell's eight syntypes is hereby designated as the lectotype. This specimen is from the lower Burlington Limestone at Burlington, Iowa, hence from the Dolbee Creek Member. Selection of a lectotype is necessary for the purposes of nomenclatorial stability because the syntype suite includes several species ranging in age from earliest Kinder-

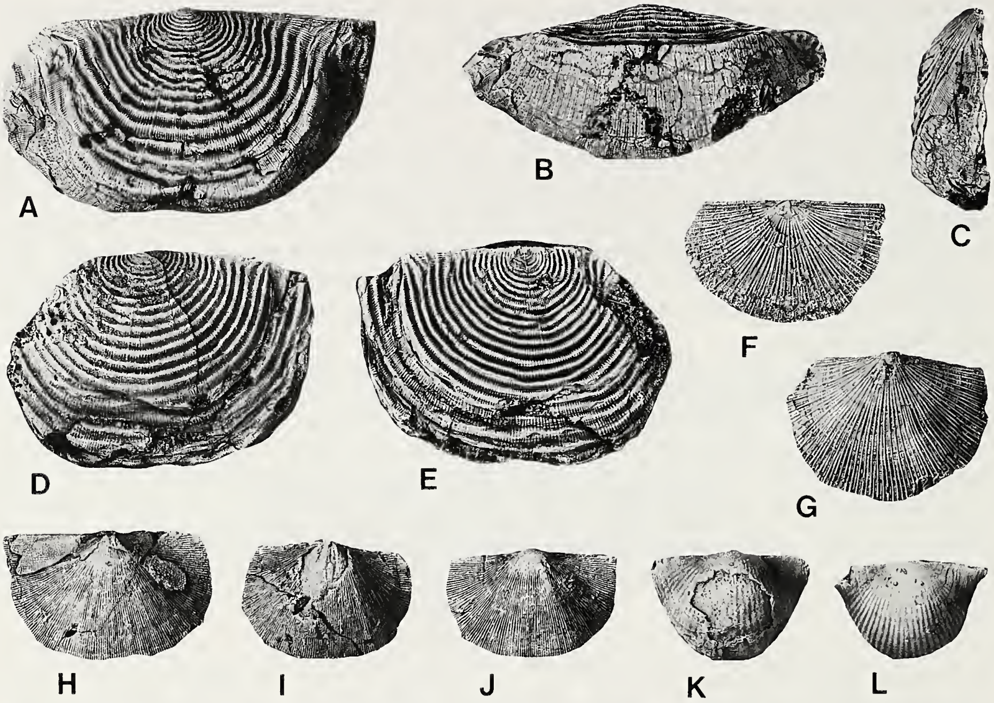

Fig. 1.—Strophomenids and chonetids. A–E, *Leptagonia analoga* (Phillips); A–C, ventral, anterior, and lateral views of large ventral valve, CM 45000; D, E, ventral and dorsal valves of nearly complete specimen, CM 45001, both × 1. F, G, *Schuchertella* sp., ventral and dorsal valves, CM 45002, 45003, both × 1. H–J, *Rugosochonetes multicostus* (Winchell), three ventral valves, CM 45004–45006, all × 2. K, L, *Caenanoplia burlingtonensis* Carter, two ventral valves, CM 45007, 45008, × 2.

hookian through the middle Osagean. *Rugosochonetes multicostus* apparently ranges from the late Kinderhookian into the middle Osagean, but a thorough revision is needed in order to establish this range with confidence.

Material.—In addition to the illustrated specimens there are five ventral valves.

Family Anopliidae Muir-Wood, 1962
Genus *Caenanoplia* Carter, 1968
Caenanoplia burlingtonensis Carter, 1968
(Fig. 1K, L)

1968 *Caenanoplia burlingtonensis* Carter: p. 1144, pl. 145, fig. 1–26.

Diagnosis.—Strongly concavo-convex *Caenanoplia* with large, well-defined subangular auriculations, faintly capillate ornament, coarsely lamellose growth lamellae, and two spines on each side of beak inclined at high angle to hingeline.

Comments.—This species has previously only been reported from the lower Burlington white chert at Louisiana, Missouri. It is most similar to *Retichonetes*? *gibberula* Carter, 1967, from the Chappel Limestone of central Texas. The latter differs in being more transverse, having smaller ears, a less inflated, more poorly differentiated umbonal region, only one spine on each side of the beak, and a shorter ventral septum.

Small specimens of *Caenanoplia logani* (Norwood and Pratten, 1855) are similar in outline to *C. burlingtonensis* but the former can be readily differentiated by its smaller ears. Normal adults of this species are much larger than *C. burlingtonensis.*

Material.—In addition to the illustrated specimens there are three ventral valves.

Suborder Productidina Waagen, 1883
Superfamily Productoidea Gray, 1840
Family Productellidae Schuchert, 1929
Subfamily Marginiferinae Stehli, 1954
Tribe Breileeniini Brunton, 1997
Genus *Breileenia* Brunton, 1997
Breileenia minnewankensis (Shimer, 1926)
(Fig. 2A–N)

1926 *Productus minnewankensis* Shimer: p. 40, pl. 1, fig. 6a–c, 7.
1942 *Avonia linospinosa* Sutton: p. 466, pl. 71, fig. 5–7.
1942 *Avonia minuta* Sutton: pp. 466–467, pl. 71, fig. 3, 4.
1987 *Avonia minnewankensis* (Shimer): Carter, p. 31, pl. 6, fig. 1–14.

Diagnosis.—Small, narrow, very strongly concavo-convex, with narrow ventral umbonal region; spine bases elongate, scattered in umbonal region; spine bases forming continuous costellae anterior to umbo and on moderately long trails of both valves; spines arranged roughly concentrically in widely spaced rows anterior to umbonal region.

Comments.—This species is similar to *Breileenia williamsana* (Girty, 1931) from the Keokuk Limestone (early and possibly middle Viséan) and *Avonia batchatica* (Tolmachev, 1924) from the Tournaisian of the Kuznets Basin. *Breileenia williamsana* (Girty) is larger, broader, and has much shorter trails in both valves. *Avonia batchatica* (Tolmachev) is more similar to *B. williamsana*, being larger, with short trails, and in addition, it has weak dorsal ribbing.

Carter (1987) placed the two Burlington Limestone species proposed by Sutton (1942) in synonymy with *B. minnewankensis*, being unable to differentiate them morphologically or biostratigraphically.

Material.—In addition to the illustrated specimens there are 130 specimens, mostly disarticulated ventral valves.

Subfamily Plicatiferinae Muir-Wood and Cooper, 1960
Tribe Levitusiini Muir-Wood and Cooper, 1960
Genus *Geniculifera* Muir-Wood and Cooper, 1960
Geniculifera siphuncula, **new species**
(Fig. 2O–T)

Holotype.—CM 45013, Fig. 2S, 2T, a nearly complete shell with conjoined valves and narrow, nasute elongation.

Paratype.—CM 45012, Fig. 2O–R, a ventral valve.

Diagnosis.—Medium-size *Geniculifera* with short trail in both valves forming narrow, nearly complete, medial anterior siphon.

Description.—Medium size for genus, transversely subquadrate in ventral view; cardinal extremities angular, but maximum width anterior to hingeline; umbonal region not much inflated, ventral visceral disc weakly to moderately convex; trails short, medially extended by narrow nasute constriction; body cavity moderately shallow.

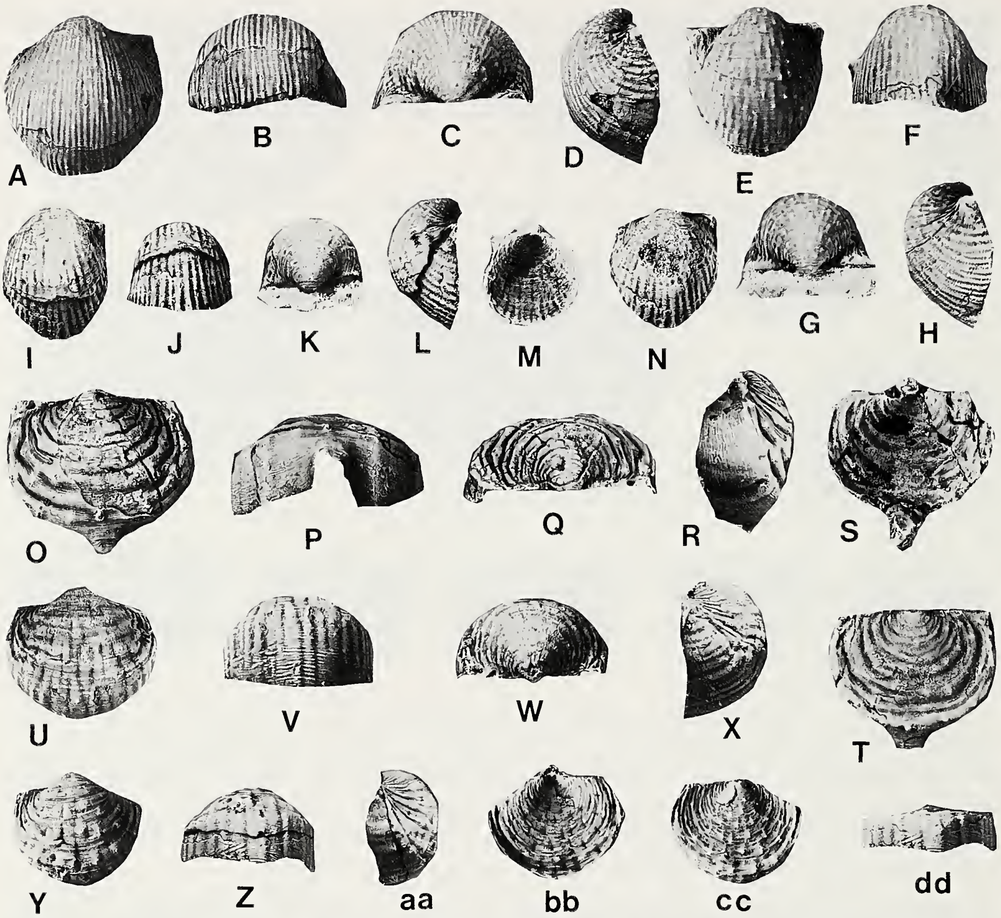

Fig. 2.—Productoids. A–N, *Breileenia minnewankensis* (Shimer); A–H, ventral, anterior, posterior, and lateral views of two ventral valves, CM 45009 and 45010, × 2; I–N, ventral, anterior, posterior, lateral, and dorsal views, and dorsal mold of a complete specimen, CM 45011, × 2. O–T, *Geniculifera siphuncula* n. sp.; O–R, ventral, anterior, posterior, and lateral views of a large ventral valve paratype, CM 45012, × 2; S, T, dorsal valve and dorsal mold of the holotype, a nearly complete specimen, CM 45013, × 2. U–dd, *Spinocarinifera* (*Seminucella*) *semicostata* (Girty); U–X, ventral, anterior, posterior, and lateral views of a large ventral valve, CM 45014; Y–dd, ventral, anterior, lateral, dorsal, dorsal views of dorsal valve mold, and anterior view of same mold, CM 45015, all × 1.5.

Ventral valve weakly convex in umbonal region, strongly geniculated; ears small, well delimited by concave flexures; flanks steep, normal to plane of articulation; anteromedial portion of trail narrowly constricted into anteriorly directed gap; beak small, projecting posteriorly slightly; hinge spines rare, only one or two at most on each side of beak, but with several erect or clasping spines just anterior to hingeline; visceral disc with several, generally 20 or more, widely spaced erect spine bases with single median spine just posterior to siphon on all three ventral valves in this collection; no spines on trail; concentric ornament of several, generally about seven or eight, irregular rugae on visceral disc; radial ornament lacking; interior unknown.

Dorsal valve weakly concave on visceral disc except for convex flexures defining ears; strongly geniculate; protegulal node at hingeline; trail short, with elongate medial extension matching that of opposite valve; ornament complementary to opposite valve with scattered shallow pits more or less opposite ventral spines and rugae on visceral disc; spines absent; interior unknown.

Measurements of Types.—See Table 2.

Table 2.—*Measurements (in mm) of the types of* Geniculifera siphuncula, *n. sp.*

Number	Length	Width	Thickness	Surface measure
CM 45013	11.0	11.2	2.4	13.2
CM 45012	10.9	12.7	—	13.0

Comparisons.—The nearly complete narrow siphon of this new species differentiates it from the other species assigned to the genus *Geniculifera.* The type species, *Avonia boonensis* Branson, 1938, is from the Chouteau Limestone of Missouri. Although the trail of this species is lobate, it lacks the nearly complete siphon seen in this new species. *Geniculifera brevicula* Carter, 1967, from the Chappel Limestone of central Texas, can be differentiated in the same manner.

Comments.—The development of a narrow, nasute elongation on a short trail appears to be the only difference between this St. Joe species and its predecessors. The anterior lobation seen in the earlier two species is a precursor to this distinctive modification.

Material.—Types only.

Family Productidae Gray, 1840
Subfamily Leioproductinae Muir-Wood and Cooper, 1960
Tribe Semiproductini McKellar, 1970
Genus *Spinocarinifera* Roberts, 1971
Subgenus *Seminucella* Carter, 1987
Spinocarinifera (*Seminucella*) *semicostata* (Girty, 1915)
(Fig. 2U–dd)

?1888 *Productus rushvillensis* Herrick: p. 22, pl. 3, fig. 15.
1915 *Productella semicostata* Girty: p. 12, pl. 1, fig. 6–7c.

Diagnosis.—Medium-sized geniculate *Seminucella* with transversely subovate outline in ventral view, coarsely costellate, moderately short trails, and generally convex lateral extremities with few spines.

Comments.—Hyde (1953:234) considered Girty's species *Productella semicostata*, from the St. Joe Formation of Arkansas, to be a subjective synonym of *Productus rushvillensis* Herrick, 1888, from the Rushville Formation of Ohio. The early Osagean age of the St. Joe is well established as is that of the Rushville (Thompson et al., 1971:705). Unfortunately, Herrick's collection of *P. rushvillensis* is long lost, leaving us with only a crude line drawing of the type (Herrick, 1888:pl. 3, fig. 15). Hyde (1953) must have seen specimens of this species in order to be confident of the synonymy of the two taxa but his collections of this species are also lost and he did not illustrate the species. No specimens of *Productus rushvillensis* are known to be extant.

Girty's types from the St. Joe of Arkansas are preserved in the National Museum of Natural History, Washington, D.C. They clearly represent the species found in the St. Joe of the Kenwood bioherm. For these reasons Girty's species name is used here with the full realization that Herrick's name may be valid and have seniority.

This species is generally similar to *Spinocarinifera* (*Seminucella*) *pustulifera* (Moore, 1928) from the lower Burlington Limestone of Missouri. The latter differs in being slightly smaller, more evenly convex in profile, more finely ribbed, and it has more numerous spines on the lateral extremities, sometimes forming a brush. *Spinocarinifera* (*Seminucella*) *parva* Carter, 1987, from the Banff Formation of Alberta, is much smaller, more elongate, and more finely ribbed with pinched concave lateral extremities generally bearing a brush of fine spines.

Material.—In addition to the illustrated specimens there are 13 other specimens including four with conjoined valves.

Subfamily Buxtoniinae Muir-Wood and Cooper, 1960
Tribe Tolmatchoffiini Sarycheva, 1963
Genus *Marginatia* Muir-Wood and Cooper, 1960
Marginatia magna Carter, 1968
(Fig. 3A–I)

1968 *Marginatia magna* Carter: p. 1147, pl. 147, fig. 1–9.

Diagnosis.—Large elongate *Marginatia* with long, irregularly fluted, sometimes spreading trail and shallow fold and sulcus; internally with large trilobate cardinal process with long, deep antron.

Comments.—This distinctive species is easily differentiated from other species of *Marginatia* by its large size alone. *Marginatia fernglenensis* (Weller) is a widely distributed species found in several formations of slightly greater age than *M. magna*. It differs in being smaller with a weaker fold-sulcus and internally has a very small antron, or lacks one altogether. *Marginatia burlingtonensis* (Hall), of slightly younger age, differs in being smaller, much more finely ribbed, and having a stronger fold-sulcus.

Material.—In addition to the illustrated specimens there are 43 other specimens, including many with conjoined valves.

Superfamily Echinoconchoidea Stehli, 1954
Family Echinoconchidae Stehli, 1954
Subfamily Pustulinae Waterhouse, 1981
Genus *Pustula* Thomas, 1914
Pustula kenwoodensis, **new species**
(Fig. 4A–D, O; 5A–C)

Holotype.—CM 45018, Fig. 4A–D, a large ventral valve.

Paratypes.—CM 450022, Fig. 4O, natural mold of a dorsal exterior; CM 45023, Fig. 5A–C, a large ventral valve.

Diagnosis.—Large, transverse, strongly inflated *Pustula* with shallow, wide, rounded fold and sulcus, strongly rugose visceral region, and flared marginal rim.

Description.—Large for genus, ventral valve strongly convex, transversely subquadrate to transversely subovate in outline; greatest width generally near midlength (excluding marginal rim); ears small, subangular, well delimited by strongly concave flexures; body cavity deep.

Ventral valve strongly convex in lateral profile, generally not geniculate, most convex in umbonal region; lateral slopes dropping steeply to lateral margins; sulcus broad, shallow, wide, originating just anterior to umbonal region as flattened venter and becoming rounded and deeper anteriorly; anterior profile subtrapezoidal to subquadrate; umbonal region moderately broad, posteriorly overhanging

→

Fig. 3.—Productoids. *Marginatia magna* Carter; A–D, ventral, anterior, posterior, and lateral views of a very large specimen showing the anterior spreading of the trail, CM 45016; E–I, ventral, anterior, lateral, posterior, and dorsal views of a nearly complete shell, CM 45017; all × 1.

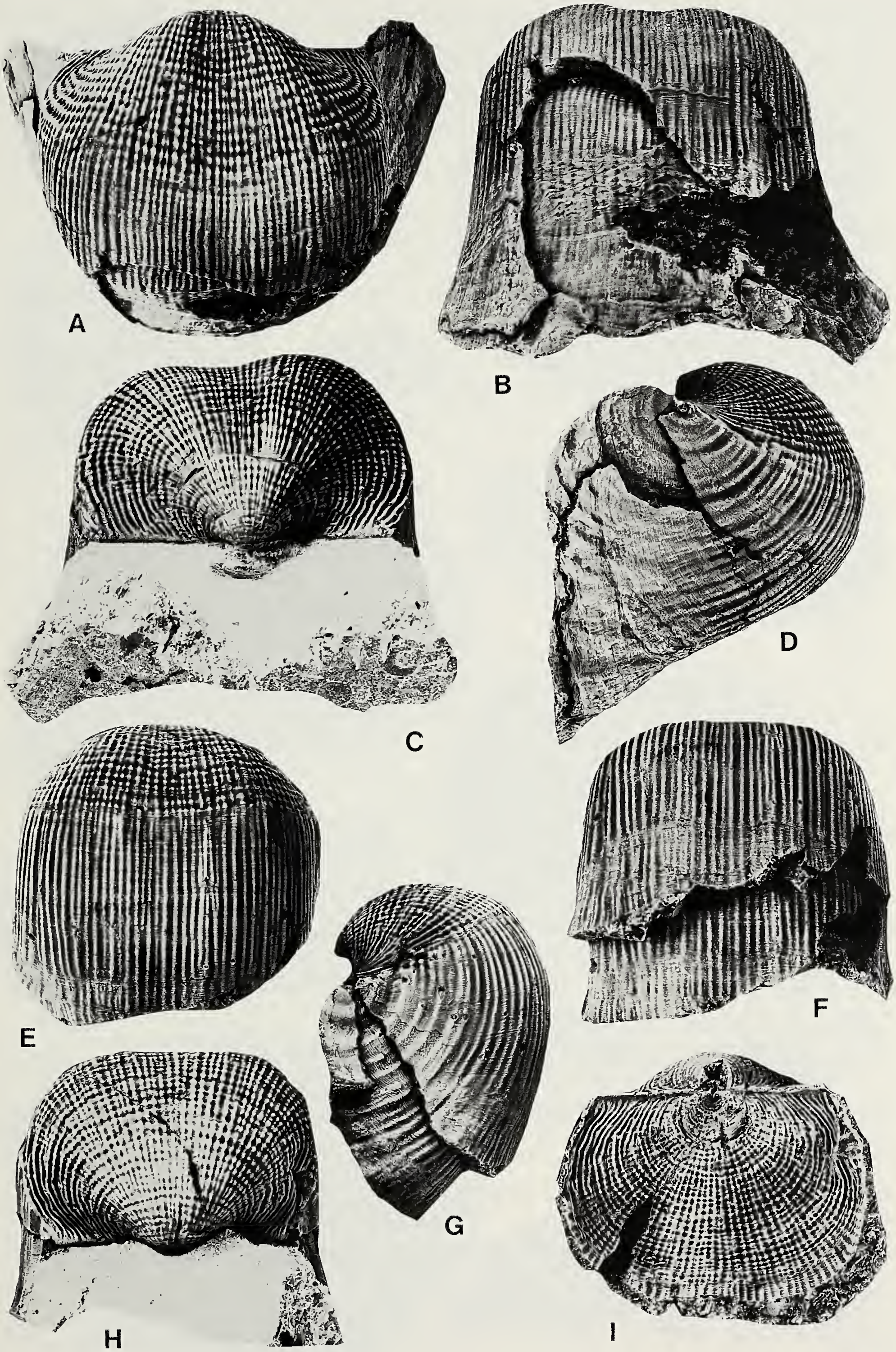
A
B
C
D
E
F
G
H
I

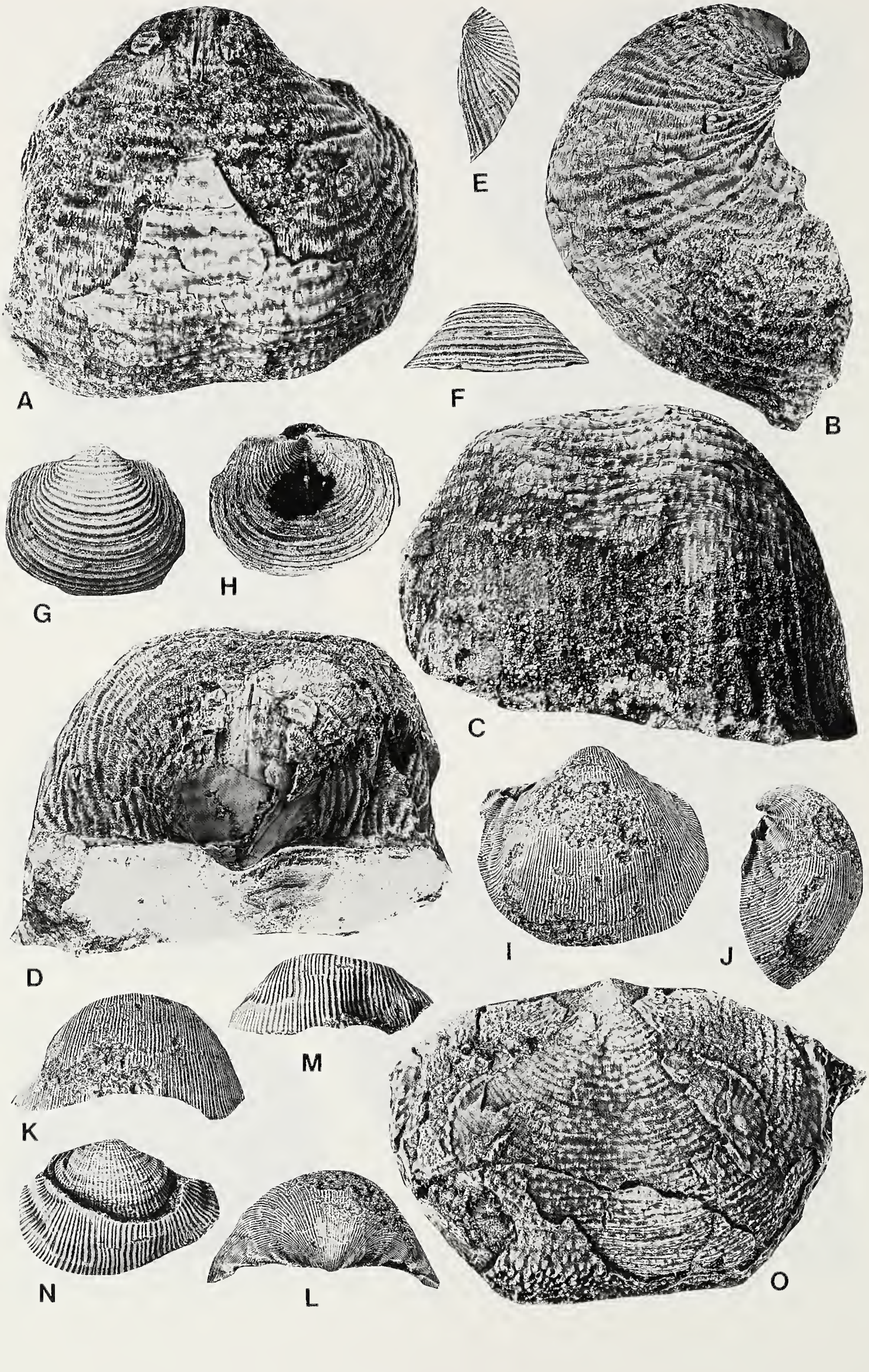
A
B
C
D
E
F
G
H
I
J
K
L
M
N
O

hingeline; beak incurved; ornament of numerous moderately irregular rugae over entire surface and many elongate spine ridges roughly arranged in quincunx generally on rugae; near anterior margin spine ridges occasionally forming short costae or coarse irregular fluting; interior not observed.

Dorsal valve with weakly concave visceral disc and short geniculate trail with flared marginal rim; fold low, moderately narrow, originating in umbonal region, becoming only moderately higher anteriorly; ears delimited by weakly convex flexures; ornament of somewhat finer rugae than those of ventral valve and shallow rounded pits; numerous fine, apparently erect spine bases scattered over valve in both pits and on rugae; internal details not observed.

Measurements of Types.—See Table 3.

Comparisons.—This new species is most similar to *Pustula pyxidiformis* (Koninck, 1847) from the Lower Viséan of Belgium and the British Isles. The latter is substantially larger, broader, with a narrower deeper fold-sulcus, and coarser ornament and spine bases.

Comments.—This large, strongly convex true *Pustula* is the first such form reported in the United States. As Carter (1987) pointed out, most species referred to this genus have subsequently been reassigned to other genera. He described a true *Pustula* from the Banff Formation of Alberta as *Pustula* cf. *P. pustulosa* (Phillips). This is a much smaller, less transverse species with spreading flanks and is probably not closely related to the present biohermal species.

Material.—In addition to the types there is one large ventral valve in the collection. Several large specimens were left in situ at the quarry. Being found on large, solid blocks they could not be removed with conventional collecting gear except at great expense of time.

Pustula oklahomae, **new species**
(Fig. 5D–L)

Holotype.—A nearly complete ventral valve, CM 45024, Fig. 5F–I.

Paratypes.—A nearly complete ventral valve, CM 45025, Fig. 5J–L; two natural molds of dorsal exteriors, CM 45026 and 45027, Fig. 5D, E.

Diagnosis.—Medium size, outline transversely subovate, venter flattened but sulcus lacking or very weak, cincture on anterior part of ventral valve of mature specimens, spine ridges regularly arranged in quincunx on ventral valve, becoming elongated anterior to cincture, rugae moderately strong posteriorly, much weaker anterior to cincture, dorsal valve with rugae similar to opposite valve with regular quincuntially arranged, rounded pits and fine, slightly elongated spine bases within pits.

Description.—Medium size for genus, transversely subovate in outline, moderately concavo-convex; maximum width near midlength; fold and sulcus absent or very weak; lateral profile subsemicircular; ears moderately developed, cardinal extremities rounded; trails short; body cavity (corpus) moderately deep.

Ventral valve moderately well inflated, most convex in umbonal region, almost evenly convex in profile except for slight geniculation anterior to cincture; venter flattened or with faint sulcus, flanks

---

←

Fig. 4.—Productoids. A–D, O, *Pustula kenwoodensis* n. sp.; A–D, ventral, lateral, anterior, and posterior views of the holotype, a ventral valve, CM 45018, × 1; O, natural mold of the dorsal exterior, CM 45022, × 1. E–H, *Scutepustula arctifossa* (Moore), lateral, anterior, ventral, and dorsal views, CM 45019, × 1. I–N, *Ovatia laevicosta* (White); I–L, ventral, lateral, anterior, and posterior views of a large ventral valve, CM 45020, × 1; M, N, anterior and ventral views of a dorsal valve and partial ventral valve, CM 45021, × 1.5.

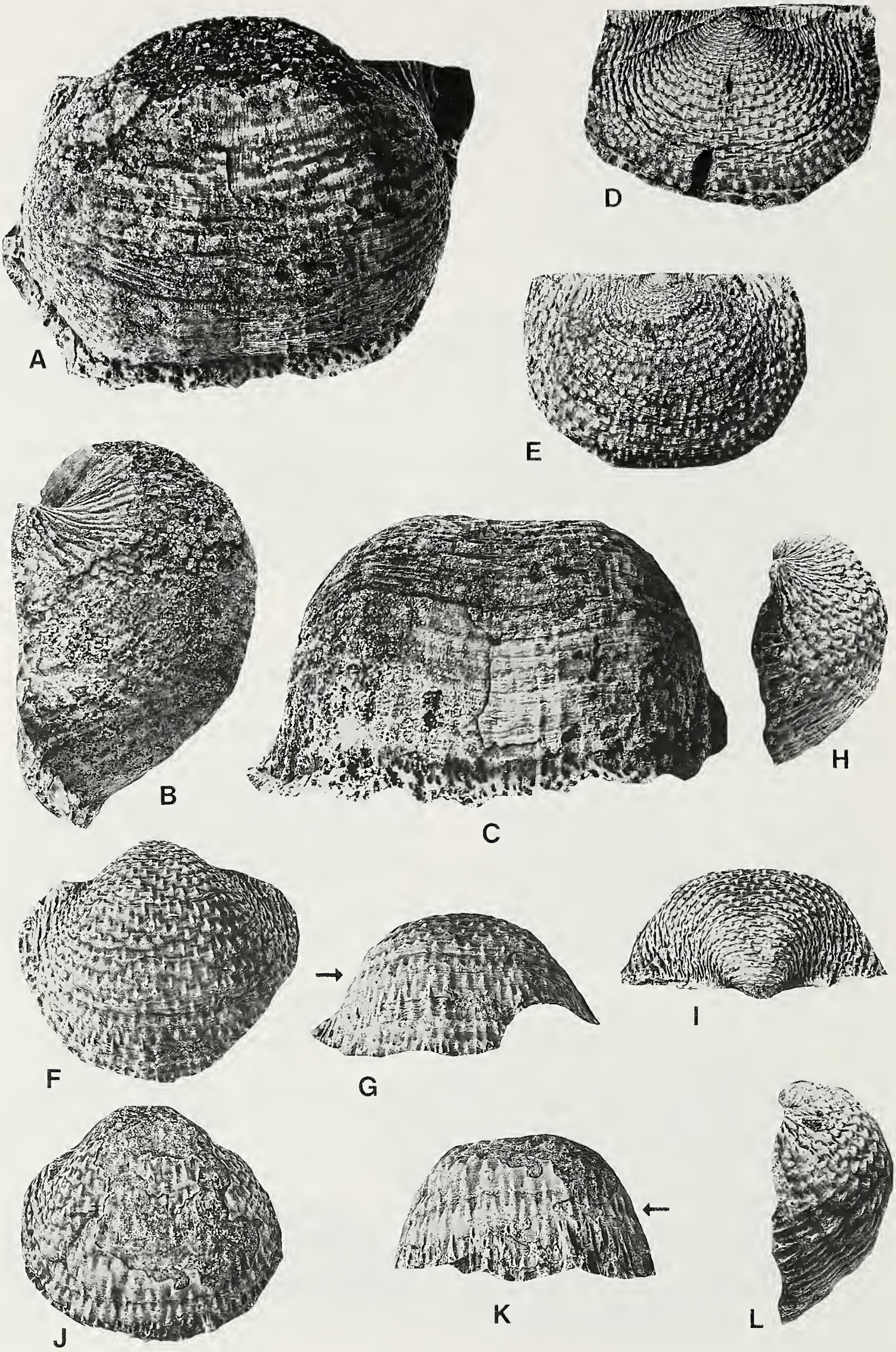
A
B
C
D
E
F
G
H
I
J
K
L

Table 3.—*Measurements (in mm) of the types of* Pustula kenwoodensis, *n. sp. DV = dorsal valve.*

Number	Length	Width	Height	Surface measure
CM 45018	66.7	+71.7	41.7	118.5
CM 45023	59.8	74.5	32.9	101.5
CM 45022 (DV)	50.7	76.5	13.1	—

sloping moderately steeply to lateral margins; ears small, compressed, delimited by strongly concave flexures; umbonal region of moderate breadth, beak small, incurved, slightly overhanging hingeline; visceral region delimited by distinct cincture in large adults; ornament consisting of numerous low, irregular, discontinuous rugae on visceral region with elongate spine ridges regularly arranged in quincunx; rugae weaker anterior to cincture, spine ridges becoming more elongate, almost costalike; interior not observed.

Dorsal valve weakly to moderately concave, most concave near front margin; ears larger than on ventral valve, defined by convex flexures; dorsum with slight fold, lateral slopes weakly concave; ornament consisting of numerous rugae similar to those of opposite valve and numerous fine, rounded pits arranged in quincunx that become elongated anteriorly; fine spine bases generally disposed in pits, becoming elongated anteriorly; interior with trilobed, dorsally directed cardinal process and low lateral ridges at hingeline; other internal details not observed.

Measurements of Types.—See Table 4.

Comparisons.—This species is similar in size and outline to *Pustula rugata* (Phillips, 1836), from the Viséan of the British Isles and *Pustula pustulosiformis* Rotai, 1931, from the Upper Tournaisian of the Ukraine. It can be differentiated from both of these species by its cincture on the ventral valve of large, mature specimens. In addition, *Pustula rugata* has a more irregular disposition of spine bases on the visceral region of the ventral valve and a stronger fold and sulcus. The specimen of *Pustula pustulosiformis* illustrated by Aizenverg and Poletaev (1971) is similar to this St. Joe species in size and ornament but differs in having a subquadrate outline with larger ears, a slightly less inflated lateral profile, and a shallow sulcus. The specimen of *P. pustulosiformis* illustrated by Fotieva (1964) has a smaller ventral umbo and finer, more costate ornament than *P. oklahomae.* Sarycheva (1963) illustrated a large specimen of *P. pustulosiformis* that is clearly geniculate with a finer, weaker ornament than in the St. Joe species. The specimens of *P. pustulosiformis* illustrated by Kalashnikov (1974) are also geniculate with more closely spaced spine ridges than in our species.

Comments.—Many of the species assigned by Thomas (1914) to his new genus *Pustula* have been assigned to other genera by subsequent authors. The remaining Thomas species are easily differentiated from this St. Joe species in having a distinct fold and sulcus in adult specimens or in obvious differences in outline or ornamentation, with the notable exception of *P. rugata,* as noted above.

Material.—In addition to the types there are 12 other specimens, including two with conjoined valves.

←

Fig. 5.—Productoids. A–C, *Pustula kenwoodensis* n. sp., ventral, lateral, and anterior views of a large ventral valve paratype showing the marginal rim, CM 45023. D–L, *Pustula oklahomae* n. sp. D, E, two dorsal valve molds, CM 45026 and 45027; F–H, ventral, anterior, lateral, and posterior views of a ventral valve, the holotype, CM 45024; J–L, ventral, anterior, and lateral views of a ventral valve, CM 45025; all × 1. The small arrows point to the slight cincture on the ventral valves.

Table 4.—*Measurements (in mm) of the types of* Pustula oklahomae, *n. sp. DV = dorsal valve.*

Number	Length	Width	Thickness	Surface measure
CM 45024	31.7	42.9	20.0	52.8
CM 45025	37.4	39.6	19.6	58.5
CM 45026 (DV)	30.1	+43.9	±6.9	—
CM 45027 (DV)	29.4	42.9	±8.2	—

Genus *Scutepustula* Sarycheva, 1963

Scutepustula arctifossa (Moore, 1928)

(Fig. 4E–H)

1928 *Pustula arctifossa* Moore: p. 269, pl. 10, fig. 7–11.

Diagnosis.—The material at hand does not permit differentiation from the type species. Therefore a description of the Kenwood species follows.

Description.—Medium size for genus; transversely subovate in outline, moderately inflated; fold and sulcus absent; greatest width near midlength; lateral profile low, subguttate; ears well developed, cardinal extremities subangular, hinge width slightly less than maximum width; body cavity shallow to moderately deep; trails lacking.

Ventral valve moderately inflated, most convex in umbonal region; venter rounded or slightly flattened, flanks sloping evenly to lateral margins; beak small, narrow, incurved over hingeline; ears delimited by concave flexures; ornament of numerous regular, low, rounded rugae; radial ornament absent; each ruga with single row of closely spaced, fine spines set on narrow, elongated spine ridges that produce striated appearance; ears with dense brush of fine spines; interior not observed.

Dorsal valve weakly concave; ears large, well defined by convex flexures on each side of triangular posteromedial depression; ornament similar to that of opposite valve but rugae finer and more numerous; interior not observed in Kenwood specimens.

Comparisons.—This species is the only representative of this genus in the Lower Carboniferous of North America. It is closely similar to the type species, *Scutepustula scutelata* (Balashova, 1955), from the Tournaisian of the southern Urals. The latter also is described and illustrated by Sarycheva (1963:166, pl. 20, fig. 1–5, text-fig. 670-70) from specimens from the Kuznets Basin. These specimens are almost impossible to differentiate from Moore's types of *S. arctifossa*, the Kenwood specimen illustrated here in Figure 4, and several specimens from the lower Burlington Limestone of Pike County, Missouri. These two species clearly typify the genus. Sarycheva (1963) suggested that several species with unknown interiors might belong here including the species described here. The form described as *Productus* (*Pustula*) *fredericksianus* Paeckelmann, 1931, seems to have a pitted dorsal valve as in true *Pustula* and may not belong in *Scutepustula*. The other species mentioned by Sarycheva (1963) is *Productus fournieri* Demanet, 1923, from the Waulsortian facies of Belgium. This species has very coarse, regular rugae with faint radial "striations" which may represent spine bases. Without better material, assignment of this species to the genus *Scutepustula* would be speculative at best.

Comments.—Moore's holotype and paratypes are from the "lower Burlington white chert" of eastern Missouri and Pierson Formation of southwestern Missouri. These are judged to be about the same age as the St. Joe bioherm at Kenwood. The specimen figured (Fig. 4) is the only mature representative of this species in our Kenwood collection. The species is rare. Besides Moore's types and these Kenwood specimens I have seen only three other specimens from the lower Burlington at Louisiana, Missouri, one of which bears a cardinal process closely similar to that of the type species.

Material.—In addition to the illustrated specimens there are three other specimens, including one ventral valve and two with conjoined valves.

Superfamily Linoproductoidea Stehli, 1954
Family Monticuliferidae Muir-Wood and Cooper, 1960
Subfamily Auriculispinae Waterhouse, 1975
Genus *Ovatia* Muir-Wood and Cooper, 1960
Ovatia laevicosta (White, 1860)
(Fig. 4I–N)

1860 *Productus laevicostus* White: p. 230.

Diagnosis.—Medium-sized, shallow-bodied *Ovatia* with moderately inflated, moderately broad ventral umbo, long trail, and 20–27 ribs per centimeter at surface measure of 2.5 cm from ventral beak.

Comments.—This species was originally described from the late Kinderhookian Wassonville Dolomite of southeastern Iowa. It is moderately common in the late Kinderhookian and early Osagean of the North American midcontinent. It also has been reported at many other localities in the Cordilleran region and the former Soviet Union.

Material.—In addition to the illustrated specimens there are four other specimens, including three ventral valves and one with conjoined valves.

Class Rhynchonellata Williams, Carlson, Brunton, Holmer, and Popov, 1996
Order Orthida Woodward, 1852
Superfamily Enteletoidea Waagen, 1884
Family Schizophoriidae Schuchert, 1929
Subfamily Schizophoriinae Schuchert, 1929
Genus *Schizophoria* King, 1850
Schizophoria mayesensis, **new species**
(Fig. 6A–nn, tt; 7)

Holotype.—CM 45029, Fig. 6F–J.

Paratypes.—CM 45028, 45030–45035, Fig. 6A–D, 6K–nn, seven complete specimens; CM 45037, a large dorsal valve, Fig. 6tt.

Diagnosis.—Transverse, nearly equivalve, medium-sized, thin-bodied *Schizophoria* with greatest width usually slightly posterior to midlength; folds and sulci generally lacking but ventral valve often medially flattened anteriorly; ventral interarea very low, forming very acute isosceles triangle.

Description.—Medium size for genus, transversely subelliptical in outline, cardinal extremities rounded, greatest width generally posterior to midlength; subequally biconvex, body thin for genus; lateral profile guttate; hingeline about one-half to two-thirds maximum width.

Ventral valve weakly to moderately convex, most convex in umbonal region with compressed, weakly concave lateral extremities; venter generally flattened to slightly sulcate, anterior commissure straight to weakly uniplicate; umbonal region narrow, extending slightly posterior to hingeline; beak small, pointed, incurved; ventral interarea low, acutely triangular, defined by subangular beak ridges, weakly concave, apsacline, marked by indistinct transverse ridges; delthyrium forming equilateral triangle; interior with short, stout, slightly divergent dental plates and low, thick median ridge that extends forward beyond dental plates; other internal details not observed in thin section.

Dorsal valve thin for genus, about same thickness as ventral valve, rarely thicker or thinner, most

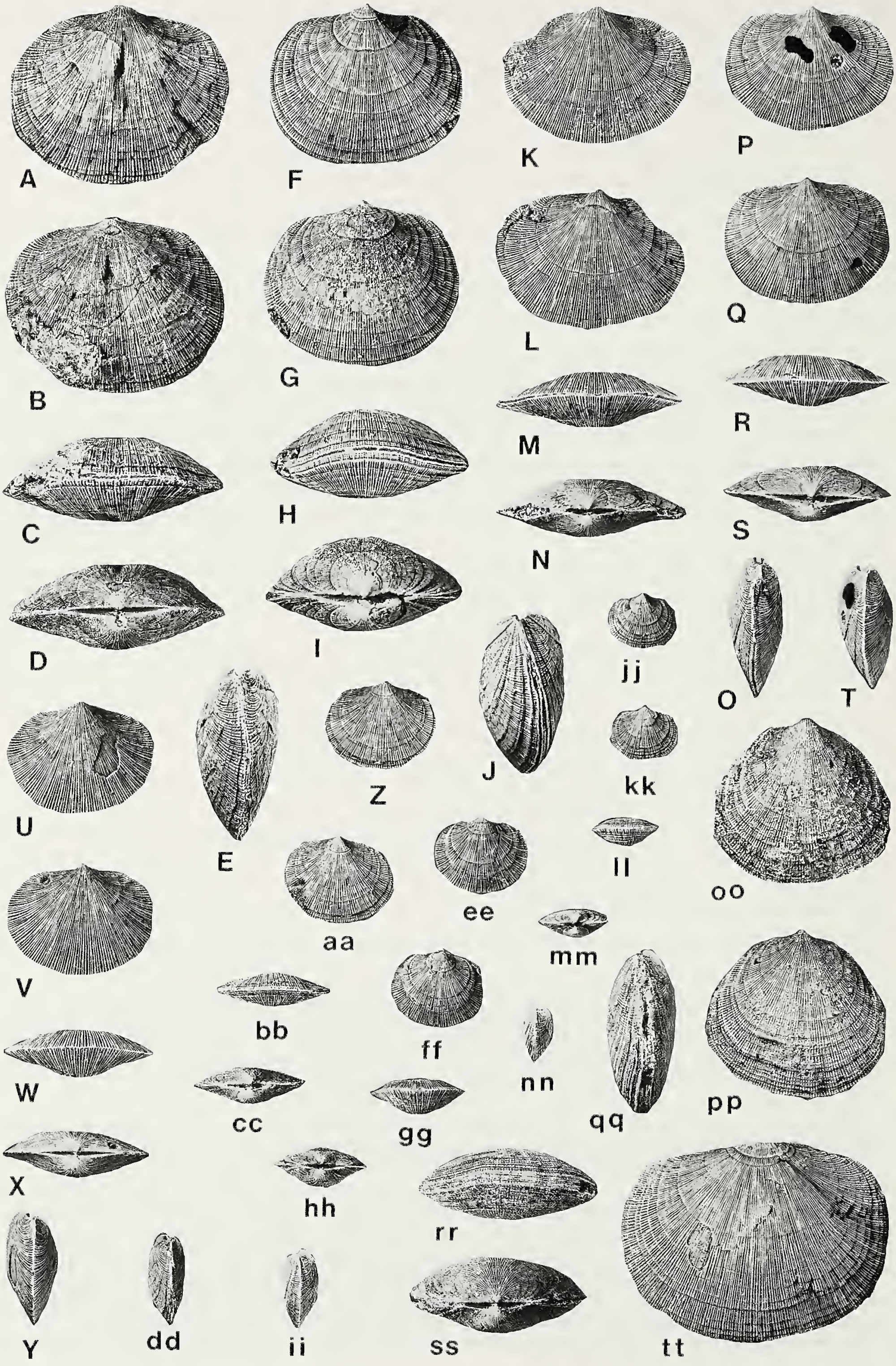
A
F
K
P
B
G
L
Q
M
R
C
H
N
S
D
I
jj
O
T
U
E
Z
J
kk
ll
oo
V
aa
ee
mm
bb
ff
nn
qq
pp
W
cc
gg
X
hh
rr
Y
dd
ii
ss
tt

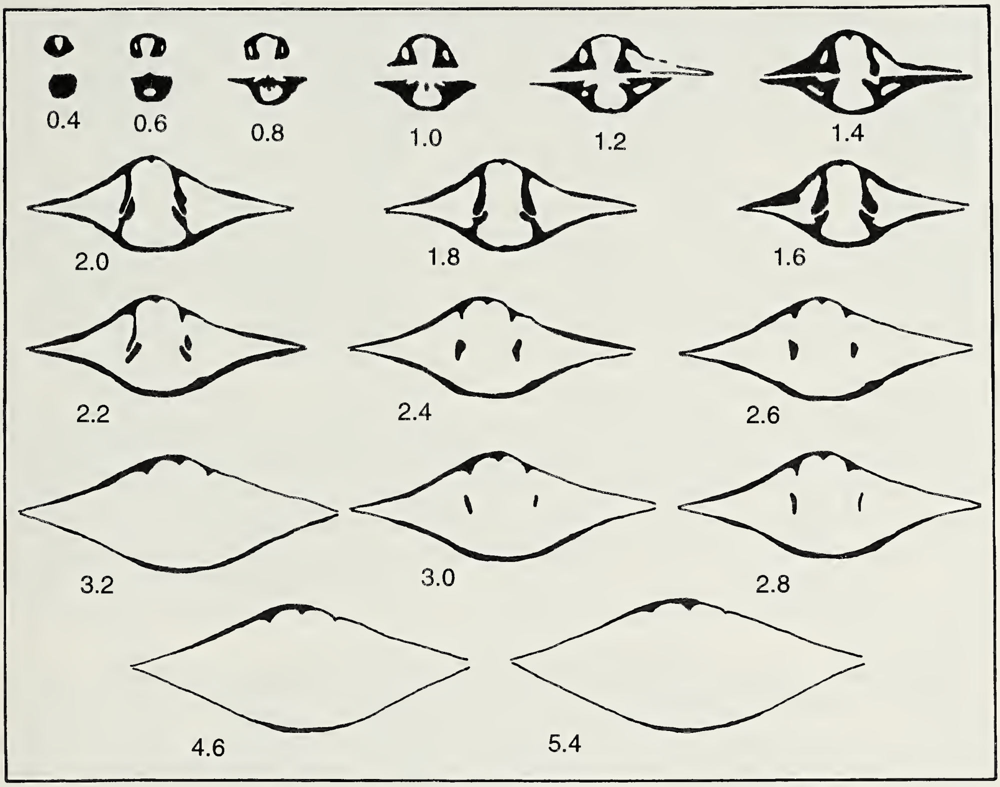

Fig. 7.—Transverse serial sections of *Schizophoria mayesensis* n. sp., CM 45038, × 1.5. Numbers refer to distance from ventral beak (in mm).

convex on dorsum, becoming slightly less convex on flanks, lateral extremities slightly compressed and weakly concave; dorsum generally rounded, rarely with faint sulcus; umbonal region narrow, weakly inflated, with short, acute beak that projects slightly posterior to hingeline; dorsal interarea very low, orthocline to weakly anacline; interior with stout sockets, high and strong inner socket-ridges, thick brachiophores and short, stout brachiophore plates; other internal details not observed from thin sections.

Measurements.—See Table 5.

Comparisons.—This distinctive new species is most similar to *Schizophoria subelliptica* (White and Whitfield, 1862) from the Starr's Cave Oolite of Iowa, *Schizophoria chouteauensis* Weller, 1914, from the Chouteau Limestone of Missouri, and *Schizophoria sedaliensis* Weller, 1914, from the Sedalia Dolomite of central Missouri, all of Kinderhookian or middle Tournaisian age. These species are similar to this new one in being thin-bodied for the genus with a lenticular

---

←

Fig. 6.—Punctate orthids. A–nn, tt, *Schizophoria mayesensis* n. sp. A–nn, ventral, dorsal, anterior, posterior, and lateral views of eight specimens including the holotype (F–J), CM 45029, and eight paratypes CM 45028, 45030–45035; tt, very large disarticulated dorsal valve paratype, CM 45037. oo–ss, *Rhipidomella diminutiva* Rowley, ventral, lateral, dorsal, anterior, and posterior views, CM 45036. All figures × 1.

Table 5.—*Measurements (in mm) of the types of* Schiophoria mayesensis, *n. sp. DV = dorsal valve.*

Number	Length	Width	Thickness
CM 45037 (DV)	29.5	40.3	±7.7
CM 45028	26.2	32.3	12.8
CM 45029	24.3	29.0	13.2
CM 45030	20.5	27.9	8.7
CM 45031	18.5	24.7	8.2
CM 45032	16.7	21.7	7.4
CM 45033	13.0	16.5	5.5
CM 45034	11.6	13.8	5.2
CM 45035	8.2	10.0	4.1

profile. *Schizophoria mayesensis* differs from the first species in its much larger size, smaller ventral umbo, and nearly equally biconvex profile, and the maximum width is generally attained posterior to midlength. It is similar in size to *S. chouteauensis* Weller but can be differentiated by its more transverse outline, more convex ventral valve, almost equally biconvex profile, narrower ventral umbo, and a more posteriorly placed maximum width. It differs from *S. sedaliensis* in being slightly thinner with narrower umbones and a more posteriorly placed maximum width.

Comments.—It seems reasonable to conclude that these four species are closely related. *Schizophoria subelliptica* and *S. chouteauensis* are about the same age and may be sister species. Neither is morphologically well known, internal information completely lacking for both species, so it is impossible to determine which might have given rise to *S. sedaliensis* or *S. mayesensis.* A more germane question concerns the origin of these four relatively thin-bodied schizophorias. There are no similar species in the early Kinderhookian of North America. In the Famennian of North America only *Schizophoria williamsi* Rodriguez and Gutschick, 1978, from the Leatham Formation (Late Famennian) of Utah bears much similarity. Its transverse outline, subequally biconvex valves, and moderately inflated valves suggest a possible relationship with these much younger species.

Material.—In addition to the types there are 52 additional specimens, including 37 articulated specimens.

Superfamily Dalmanelloidea Schuchert, 1913
Family Rhipidomellidae Schuchert, 1913
Subfamily Rhipidomellinae Schuchert, 1913
Genus *Rhipidomella* Oehlert, 1890
Rhipidomella diminutiva Rowley, 1900
(Fig. 6oo–ss)

1900 *Rhipidomella diminutiva* Rowley: p. 261, pl. 5, fig. 41–43.

Diagnosis.—Medium-sized *Rhipidomella* with subovate outline, maximum width invariably anterior to midlength, small, narrow ventral umbo, apsacline ventral interarea of less than half maximum width, generally with very weak ventral sulcus and shallow, narrow dorsal sulcus that originates in dorsal umbo, being lost anteriorly in some specimens.

Comparisons.—*Rhipidomella diminutiva* Rowley is readily differentiated from species of similar age such as *R. jerseyensis* Weller, 1914, or *R. burlingtonensis*

Hall, 1858, by its small, narrow ventral umbo and narrow, shallow dorsal sulcus which often is confined to the umbonal region. *Rhipidomella jerseyensis* is much smaller, has a broad ventral umbo, and a broader, deeper dorsal sulcus forming an emarginate anterior commissure. *Rhipidomella burlingtonensis* has a larger, broader ventral umbo, a better-developed ventral sulcus, a weaker dorsal sulcus, if any, and the maximum width is attained near midlength.

Comments.—This species is rare in the Kenwood collection, consisting of only eight specimens, only one of which is illustrated here. This illustrated specimen is not typical for the species in lacking a clear dorsal sulcus in the umbonal region.

Weller (1914) illustrated several specimens he assigned to this species that are either not typical or misidentified. The specimens he illustrated on his plate 20, figures 9–13 from the lower Burlington white chert are more elongate than any specimens from the same horizon and locality in our collections. The specimen illustrated in figures 16–18 on this same plate do not appear to be assignable to this species, being subquadrate in outline, too thick, and lacking any indication of a narrow, shallow dorsal sulcus. The specimen Weller referred to as *Rhipidomella* sp. in figures 19–21 appears to be an almost typical, if misshapen, *R. diminutiva.*

Material.—In addition to the illustrated specimens there are three articulated and three disarticulated specimens.

Order Rhynchonellida Kuhn, 1949
Superfamily Rhynchotrematoidea Schuchert, 1913
Family Trigonirhynchiidae Schmidt, 1965
Subfamily Trigonirhynchiinae Schmidt, 1965
Genus *Macropotamorhynchus* Sartenaer, 1970
Macropotamorhynchus tuta (Miller, 1881)
(Fig. 8A–D)

1881 *Rhynchonella tuta* Miller: p. 315, pl. 7, fig. 11.

Diagnosis.—Small, strongly inflated, outline subtrigonal to subovate, length and width subequal or slightly longer than wide, maximum width anterior to midlength; lateral profile subovate; cardinal margins not compressed; ventral beak erect to suberect; ventral valve strongly and evenly convex in profile; dorsal valve moderately thicker with subtrigonal profile; fold and sulcus moderately produced, flattened; fold with five costae, sulcus with four costae, flanks generally with six costae, rarely five.

Comparisons.—This small, rotund species with four costae in the sulcus and six on the flanks is distinctive and easily differentiated from most other species of this genus. It is similar to some specimens of *Macropotamorhynchus insolitus* Carter, 1987, from the Banff Formation of Alberta. That species differs in having compressed cardinal margins, a variable number of ribs on the fold-sulcus and flanks, a more rounded anterior margin, and generally a thinner, less convex ventral valve.

Comments.—This species was named from the Nunn Member of the Lake Valley Formation of New Mexico. It also has been widely identified in North America and the former Soviet Union. If Weller's (1914) identification of this species in the Chouteau Limestone of Missouri is correct, the species ranges from the middle Kinderhookian through the early Osagean in North America.

Material.—The illustrated specimen is the only one in the collection.

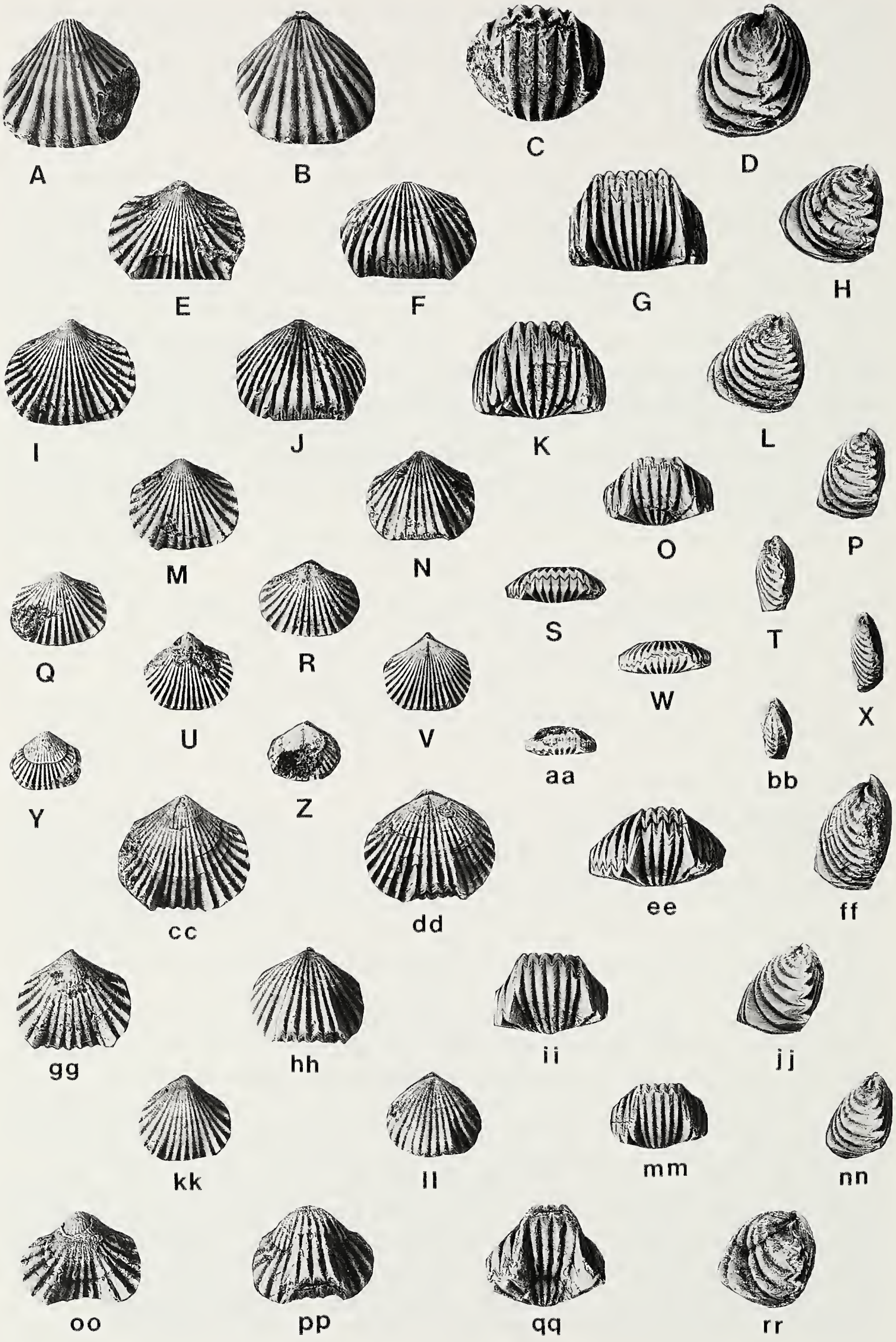
A
B
C
D
E
F
G
H
I
J
K
L
M
N
O
P
Q
R
S
T
U
V
W
X
Y
Z
aa
bb
cc
dd
ee
ff
gg
hh
ii
jj
kk
ll
mm
nn
oo
pp
qq
rr

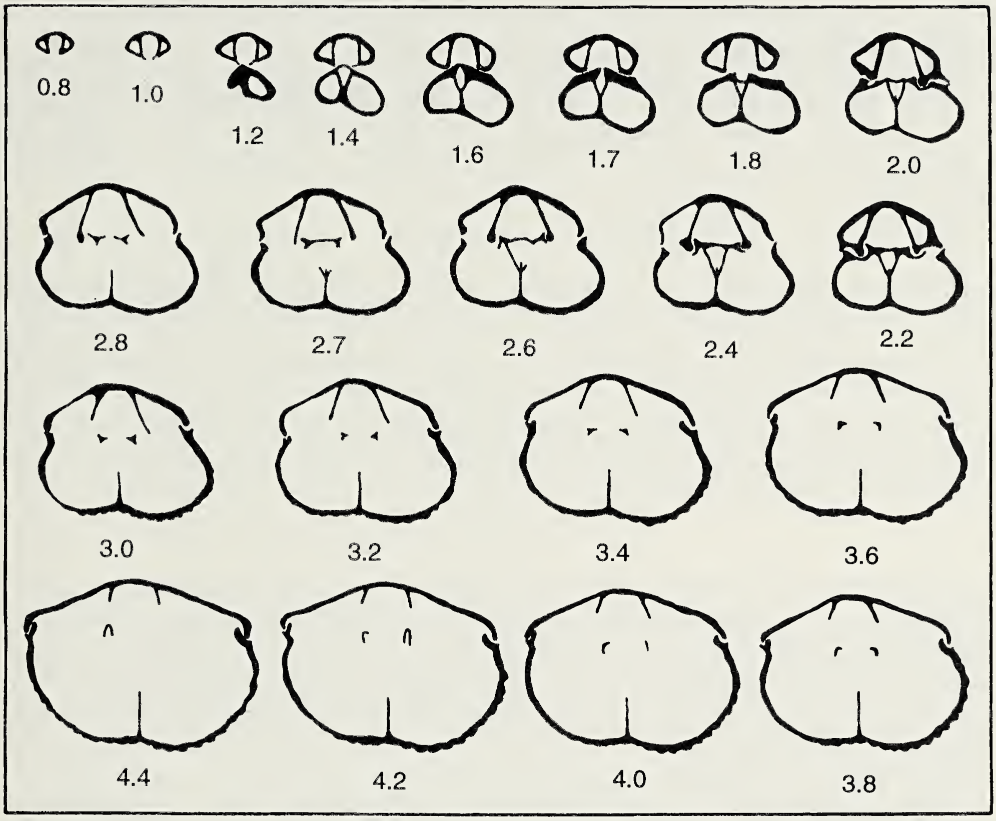

Fig. 9.—Transverse serial sections of *Rhynchopora persinuata* (Winchell), CM 45050, × 2. Numbers refer to distance from ventral beak (in mm).

Superfamily Rhynchoporoidea Muir-Wood, 1955
Family Rhynchoporidae Muir-Wood, 1955
Genus *Rhynchopora* King, 1865
Rhynchopora persinuata (Winchell, 1865)
(Fig. 8E–bb; 9)

1865 *Rhynchonella persinuata* Winchell: p. 121.

Diagnosis.—Medium-sized, transversely subquadrate to subovate *Rhynchopora* with five to nine costae, generally six to eight, in the sulcus and six to ten costae, generally eight or nine, on the flanks of mature shells for a total of about 22–25 ribs per valve.

←

Fig. 8.—Rhynchonellids. A–D, *Macropotamorhynchus tuta* (Miller); ventral, dorsal, anterior, and lateral views, CM 45039, × 3. E–bb, *Rhynchopora persinuata* (Winchell), ventral, dorsal, anterior, and lateral views of six specimens, CM 45040–45045, × 1. cc–nn, *Rhynchopora kollari* n. sp., ventral, dorsal, anterior, and lateral views of three specimens including the holotype (cc–ff, CM 45046) and two paratypes CM 45047 and 45048, × 1.5. oo–rr, *Rhynchopora* sp. A, ventral, dorsal, anterior, and lateral views, CM 45049, × 1.5.

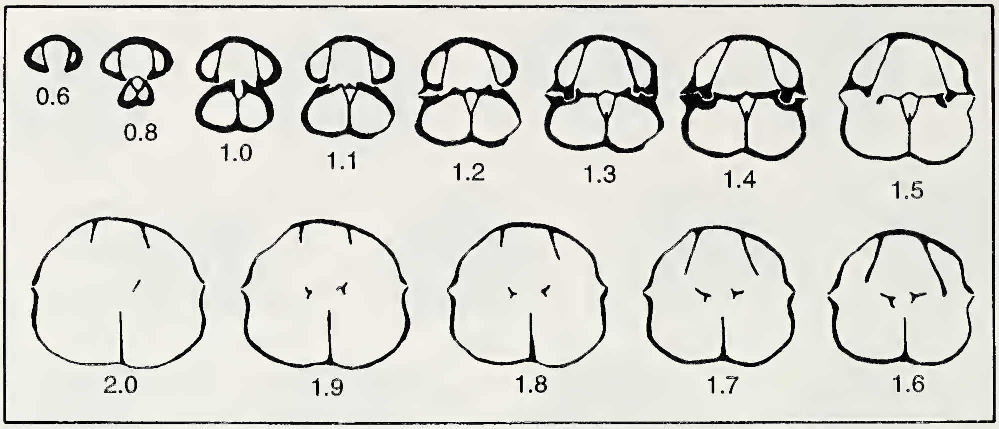

Fig. 10.—Transverse serial sections of *Rhynchopora kollari* n. sp., CM 45051, × 4. Numbers refer to distance from ventral beak (in mm).

Comments.—This species was originally found in the Wassonville Dolomite at Burlington, Iowa, but is common in the Nunn Member of the Lake Valley Formation of New Mexico and Fern Glen Formation of Missouri and Illinois. Weller's (1914) description of the interior did not include an illustration of serial sections and no mention was made of the crura. The interior of a Kenwood specimen of this species shows the rodlike subtrigonal crura that terminate in narrowly arcuate anterior processes (Fig. 9).

This species is similar to *Rhynchopora sansabensis* Carter, 1967, from the Chappel Limestone of central Texas. The latter differs in having more numerous sulcal ribs and fewer lateral ribs with a total of about 18–21 per valve. The stratigraphic range of *R. persinuata* is from the late Kinderhookian through the early Osagean.

Material.—In addition to the illustrated specimens there are 151 articulated specimens.

Rhynchopora kollari, **new species**
(Fig. 8cc–nn; 10)

Holotype.—CM 45046, Fig. 8cc–ff.

Paratypes.—CM 45047 and 45048, Fig. 8gg–nn.

Diagnosis.—Small *Rhynchopora* with transversely subovate outline, moderately wide, flattened fold and sulcus; four to six costae in sulcus, generally five; flanks with six to nine costae, generally six or seven; about 16–21 total costae per valve, generally 18 or 19.

Description.—Small for genus, transversely subovate in outline, dorsibiconvex; fold low, moderately broad, flattened; sulcus shallow, moderately broad, with dorsally directed linguiform extension; surface multicostate with four to six ribs in sulcus, generally five, and six to nine on flanks, generally six or seven; total number of costae about 18 or 19; front margin serrate; shell substance punctate.

Ventral valve much thinner than opposite valve, moderately and evenly convex in lateral profile; umbonal region broad, posterior margins slightly concave in ventral view; beak small, acute, nearly straight or slightly inclined, foramen not observed; flanks weakly convex posteriorly, becoming weakly concave anteriorly; sulcus originating near or anterior to midlength, becoming moderately deep and

Table 6.—*Measurements (in mm) of the types of* Rhynchopora kollari, *n. sp.*

Number	Length	Width	Thickness	Ribs/Sulcus	Ribs/Fold
CM 45046	11.4	12.9	7.1	9	4
CM 45047	10.3	11.3	7.3	6	6
CM 45048	9.0	9.3	5.8	7	5

flattened anteriorly, and forming short to medium, dorsally directed tongue; beak ridges short, subangular, posterior margins compressed; interior with moderately long divergent dental plates; teeth bladelike.

Dorsal valve much more inflated than opposite valve, most inflated anteriorly, forming subtrigonal lateral profile; umbonal region moderately broad with medial depression, dorsal beak inconspicuous, obscured by opposite valve; posterior margins compressed as in opposite valve, forming short flanges on each side of umbones; fold originating near midlength, rising moderately toward front of valve, flattened or weakly concave throughout; moderately convex flanks sloping evenly to lateral margins, steeply to anterior margin; interior with moderately long, deep septalium covered by ventrally convex connectivium; septum long, high, extending well past cardinalia; crura short, broadly to narrowly trigonal in section from rear to front, bladelike anteriorly.

Measurements of Types.—See Table 6.

Comparisons.—This new species is similar in size to *Rhynchopora hamburgensis* Weller, 1910, from the Glen Park Formation (earliest Kinderhookian) of Illinois and Missouri. That species, however, is easily differentiated by its subtrigonal to subpentagonal outline and moderately rounded, not well-flattened, fold and sulcus. Another small species, *Rhynchopora pustulosa* (White, 1860) from the McCraney Limestone (middle Kinderhookian) of southeastern Iowa, is easily differentiated from *R. kollari* n. sp. by its fewer, coarser costae and rounded fold.

Material.—In addition to the types there are 25 articulated specimens.

Rhynchopora species A

(Fig. 8oo–rr)

Description.—Small for genus, transversely subovate in outline, strongly dorsibiconvex with dorsal valve strongly gibbous and longer than ventral valve; lateral profile subovate, globose; fold and sulcus well developed, flattened, narrow; four costae in sulcus, five or six on each flank for a total of 15 per valve; front margin serrate; shell substance finely punctate.

Ventral valve much thinner than dorsal valve, most convex in umbonal region; umbonal region moderately narrow for genus, posterior margins moderately concave in ventral view; beak small, acute, tightly apposed to dorsal umbo; flanks weakly convex; sulcus originating in posterior third of valve, becoming moderately deep anteriorly, forming dorsally directed tongue; beak ridges short, rounded; posterior margins slightly compressed; interior with moderately long, slightly divergent dental plates.

Dorsal valve longer than ventral valve, strongly inflated, with gibbous umbonal region; umbonal region moderately broad, with medial depression, dorsal beak obscured by ventral beak; posterior margins compressed as in opposite valve, forming short flanges on each side of umbo; fold originating posterior to midlength, becoming flattened and moderately high anteriorly; flanks moderately convex posteriorly, sloping steeply to anterolateral margins; interior unknown.

Comments.—This description is based on a single specimen. It is indubitably punctate but quite unlike any *Rhynchopora* I previously have seen. It is possible that it is an aberrant *Rhynchopora kollari* n. sp., as described above, even though it differs in most respects from typical individuals of that species.

Superfamily Stenoscismatoidea Oehlert, 1887
Family Atriboniidae Grant, 1965
Subfamily Atriboniinae Grant, 1965
Genus *Atribonium* Grant, 1965
Atribonium species cf. "*Coledium*" *evexum* Grant 1965
(Fig. 11I–P)

1965 *Coledium evexum* Grant: p. 112, pl. 15, fig. 1–10, text-fig. 26.

Comments.—There are four specimens of stenoscismatoids in the Kenwood collection that are assignable to the genus *Atribonium* Grant, 1965. Two of these specimens have the vertically opposing lateral marginal slopes and a sulcal tongue normal to the lateral margins that are externally characteristic of that genus. All of the specimens also have several fine, weak ribs on the fold and sulcus and on the lateral slopes, which is also typical of *Atribonium.* Only the largest specimen (Fig. 11I–L) would have been suitable for sectioning, leaving no large, well-preserved specimen available for other purposes. In any case the interiors of *Atribonium* are not much different from those of several species of the genus *Coledium* Grant, 1965, the only other likely genus. Assignment to a known species of *Atribonium* is much more difficult.

The only previously described North American species of *Atribonium* of early Mississippian age in the literature are *Atribonium bisinuata* (Rowley, 1900) from the lower Burlington Limestone of eastern Missouri, and the species described by Shaw (1962) as *Stenoscisma obesa* (Clarke, 1917) from the Lodgepole Limestone of Montana. The latter is closely similar to *A. bisinuata*, as Shaw noted (1962: 634), and, as Grant (1965:40) pointed out, is not assignable to *Camarophoria obesa* Clarke, 1917. These species bear a single rib in the sulcus and have smooth lateral slopes, unlike these Kenwood specimens.

The type suite of *Coledium evexum* Grant, 1965, from the Chappel Limestone of central Texas includes two specimens (Grant, 1965:pl. 15, fig. 3, 6) with vertical lateral slopes and tongues as in the genus *Atribonium.* This species also commonly has several weak ribs on the fold and sulcus and lateral slopes as found in these Kenwood specimens. It seems possible that these two specimens were misidentified and belong in *Atribonium*, not *Coledium.* In the meantime this Kenwood specimen can be said to be externally similar to some of Grant's paratyes of *Coledium evexum.*

Material.—In addition to the illustrated specimens there are two small specimens.

Family Stenoscismatidae Oehlert, 1887
Subfamily Stenoscismatinae Oehlert, 1887
Genus *Coledium* Grant, 1965
Coledium simulans (Girty, 1915)
(Fig. 11A–H; 12)

1915 *Camarophoria simulans* Girty, p. 35, pl. 2, fig. 10a–11b.

Diagnosis.—Larger than average for genus, strongly dorsibiconvex *Coledium* with subovate to transversely subelliptical outline; moderately inflated ventral valve; strongly inflated dorsal valve; smooth flanks; narrow fold and deep sulcus, each with one or more weak ribs, generally about four in adults; short suberect beak; rounded beak ridges; moderately long spondylium; moderately long, strongly curved camarophorium; and long, anteriorly free intercamarophorial plate.

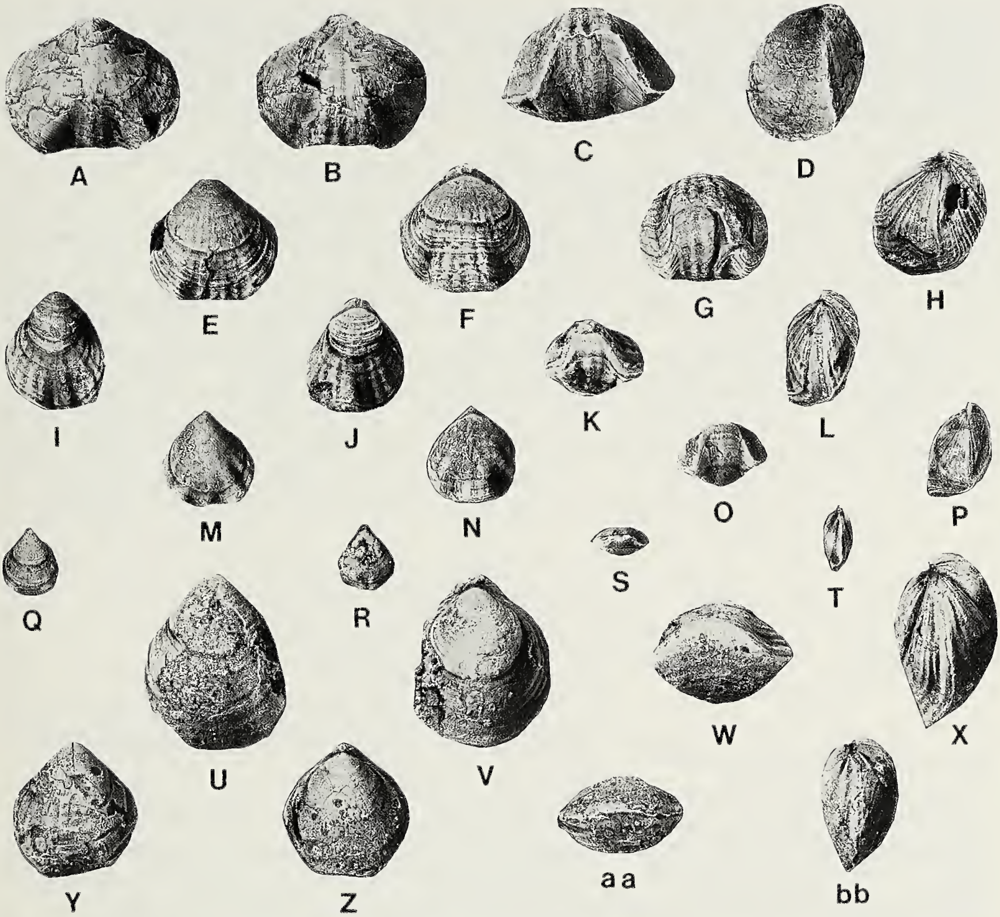

Fig. 11.—Stenoscismatoids and athyridids. A–H, *Coledium simulans* (Girty, 1915), ventral, dorsal, anterior, and lateral views of two specimens, CM 45052 and 45053, × 2. I–P, *Atribonium* sp. cf. *Coledium evexum* Grant 1965, ventral, dorsal, anterior, and lateral views of two specimens, CM 45054 and 45055, × 2. Q–T, ventral, dorsal, anterior, and lateral views of an indeterminate stenoscismatoid juvenile lacking generic characters, CM 45056, × 2. U–bb, *Rowleyella fabulites* (Rowley), ventral, dorsal, anterior, and lateral views of two specimens, CM 45057 and 45058, × 2.

Comments.—This identification is based on three specimens, one of which was sectioned in order to verify the generic identification and prepare Figure 12. The large specimen (Fig. 11A–D) differs from Girty's largest syntype in being considerably more transverse. However, the other specimen in this small Kenwood collection (Fig. 11E–H) is nearly equidimensional and more similar in outline to the smallest of Girty's syntypes although it is proportionally thicker.

In his monograph on the Stenoscismatacea, Grant (1965) did not assign *Camarophoria simulans* (Girty, 1915) to any of his genera. He probably missed it in his search of the stenoscismatoid literature. It is assigned here to the genus *Coledium* Grant on the basis of its angular lateral margins, smooth flanks, and deep, ventrally curving camarophorium.

Coledium simulans is not closely similar to any other known species in this

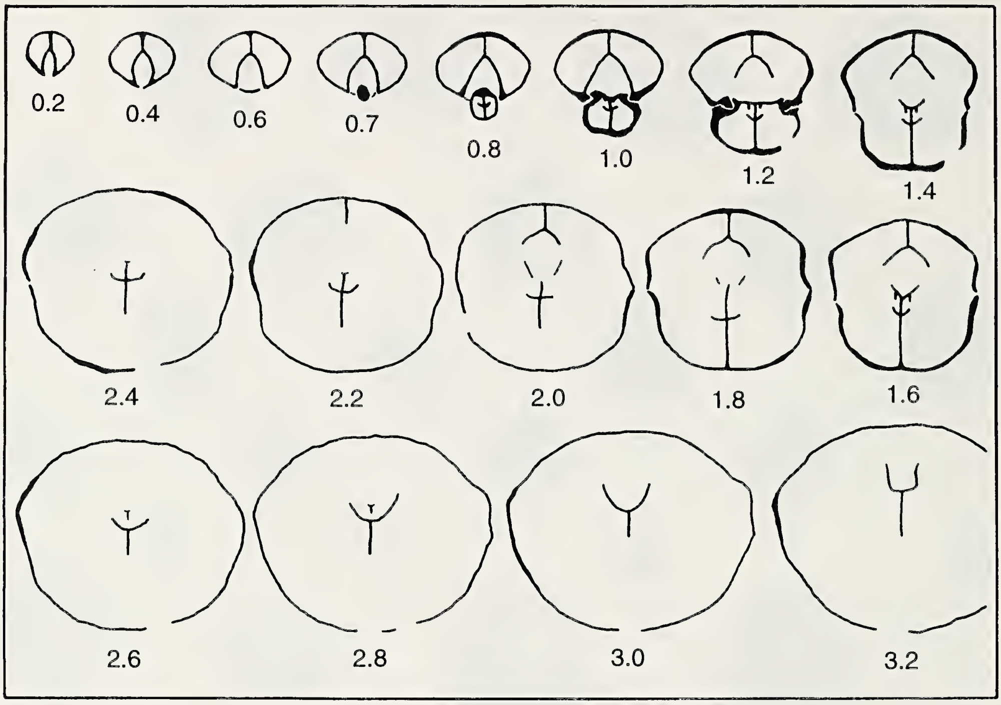

Fig. 12.—Transverse serial sections of *Coledium simulans* (Girty), CM 45059, × 4. Numbers refer to distance from ventral beak (in mm).

genus. *Coledium altisulcatum* Carter, 1967, from the Chappel Limestone of central Texas is similar in size and general shape but differs in having a much more inflated dorsal umbo and a stronger, wider, more rounded fold and sulcus.

Material.—In addition to the illustrated specimens there are nine other smaller immature specimens of this genus, presumably assignable to this species.

Order Athyridida Boucot, Johnson, and Staton, 1965
Suborder Athyridina Boucot, Johnson, and Staton, 1965
Superfamily Meristelloidea Waagen, 1883
Family Camarophorellidae Schuchert, 1929
Subfamily Camarophorellinae Schuchert, 1929
Genus *Camarophorella* Hall and Clarke, 1893
Camarophorella species
(Fig. 13I–L)

Comments.—There is a single complete specimen of the genus *Camarophorella* in this collection. It is medium in size, transversely subovate in outline, and relatively thin-bodied. There is a weak, shallow ventral sulcus and a faint dorsal, medial groove anteriorly that produces a slight anterior emargination. Internally there are distinct median septa as seen through the translucent shell material. Also apparent is a dorsal shoe-lifter process originating less than one millimeter in front of the hingeplate.

Identification of this species is not possible from a single specimen. It is similar in outline to smaller specimens of *Camarophorella dorsata* Carter, 1967, from the Chappel Limestone of central Texas but differs in being much thinner and has a longer ventral beak. *Camarophorella mutabilis* Hyde, 1908, from the Waverly of Ohio differs in being larger and thicker, and has a better developed ventral sulcus.

Subfamily Rowleyellinae Alvarez and Brunton, 1995
Genus *Rowleyella* Weller, 1911
Rowleyella fabulites (Rowley, 1900)
(Fig. 11U–bb)

1900 *Terebratula fabulites* Rowley: p. 265.
1991*a* *Rowleyella fabulites* (Rowley): Carter, p. 84, fig. 1C–Q; fig. 2.

Diagnosis (for Both Genus and Species).—Small elongate terebratuliform camarophorellids with weak fold-sulcus externally and short shoelifter process with long cruralium in dorsal valve.

Comments.—This rare species is previously known only from the lower Burlington Limestone of Pike County, Missouri.

Material.—Only the illustrated specimens were recovered.

Family Athyrididae Davidson, 1881
Subfamily Athyrididae Davidson, 1881
Genus *Lamellosathyris* Jin and Fang, 1983
Lamellosathyris lamellosa (Léveillé, 1835)
(Fig. 13A–H; 14)

1835 *Spirifer lamellosus* Léveillé: p. 39, pl. 2, fig. 21–23.
1980 *Actinoconchus lamellosus* (Léveillé): Brunton, p. 225, fig. 15–17.

Diagnosis.—Large transverse *Lamellosathyris* with subovate to subelliptical outline, ventral sulcus well developed anteriorly in adults, dorsal fold which may be rounded or have weak medial sulcus, rounded uniplicate anterior commissure and well-defined rugae with corrugated lamellar extensions.

Comments.—Brunton (1980) selected and illustrated a neotype for this species from the Upper Tournaisian (Tn3b) of Belgium. This neotype differs from the specimens illustrated here only in being about half their size. *Lamellosathyris lamellosa* is readily differentiated from *L. bradyensis* (Carter, 1967) from the Chappel Limestone of central Texas by its much larger size, stronger fold-sulcus, and narrower, more rounded cardinal extremities.

Material.—In addition to the illustrated specimens there are 24 articulated specimens.

Genus *Crinisarina* Cooper and Dutro, 1982
Crinisarina prouti (Swallow, 1860)
(Fig. 13M–P)

1860 *Spirigera proutii* Swallow: p. 649.

Diagnosis.—Transverse, strongly and almost equally biconvex medium-sized *Crinisarina* with strong, moderately narrow fold and sulcus.

Comments.—This species is readily distinguished from most Devonian representatives of this genus by its transverse outline and well-developed fold and sulcus. In this respect it is similar to *C. reticulata* (Stainbrook) from the Rhodes Canyon Formation (Famennian) of New Mexico, which can be differentiated by its less transverse outline and much wider fold-sulcus.

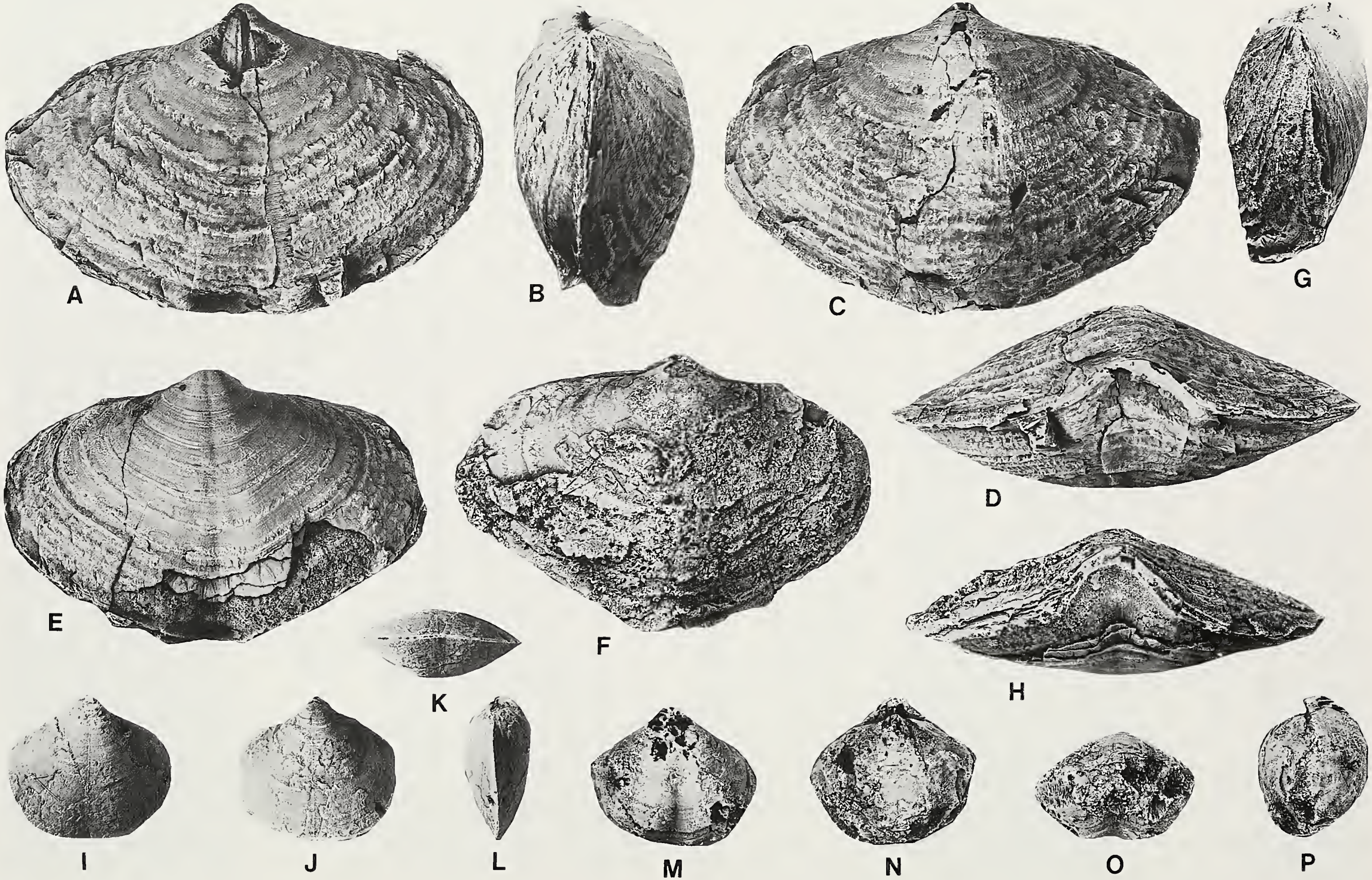
A
B
C
G
D
E
F
K
H
I
J
L
M
N
O
P

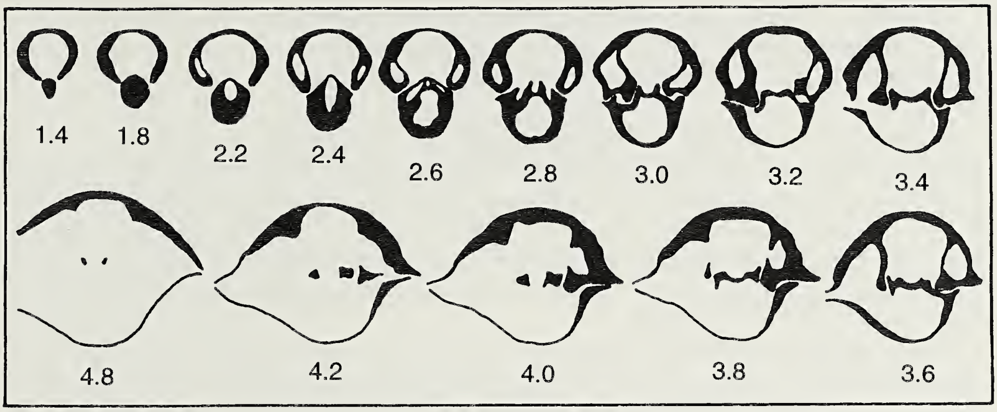

Fig. 14.—Transverse serial sections of *Lamellosathyris lamellosa* (Léveillé), CM 45064, × 1.5. Numbers refer to distance from ventral beak (in mm).

Material.—In addition to the illustrated specimen there is one small complete specimen and one ventral valve.

Genus *Cleiothyridina* Buckman, 1906
Cleiothyridina cf. *C. glenparkensis* Weller, 1914

1914 *Cleiothyridina glenparkensis* Weller: p. 473, pl. 78, fig. 21–24.

Comments.—In this collection there are three poor athyridid specimens with closely spaced growth lamellae fringed with flattened spines characteristic of the genus *Cleiothyridina* Buckman. The best of these specimens is of medium size, transversely subovate in outline, and thin-bodied. In size and outline it resembles *Cleiothyridina glenparkensis* Weller but differs in being much less inflated. One other, more incomplete specimen is slightly thicker but still less thick than *C. glenparkensis.*

Order Spiriferida Waagen, 1883
Suborder Spiriferidina Waagen, 1883
Superfamily Martinioidea Waagen, 1883
Family Martiniidae Waagen, 1883
Subfamily Eomartiniopsinae Carter, 1994
Genus *Eomartiniopsis* Sokolskaya, 1941
Eomartiniopsis rostrata (Girty, 1899)
(Fig. 15E–X; 16)

1899 *Martinia rostrata* Girty: p. 553–554, pl. 70, fig. 5a–g.
1972 *Eomartiniopsis rostrata* Girty: Carter, p. 487, pl. 2, fig. 1–11; text-fig. 6.
1987 *Eomartiniopsis rostrata* Girty: Carter, p. 85, pl. 2, fig. 30; pl. 27, fig. 27–42; text-fig. 25.

←

Fig. 13.—Athyridids. A–H, *Lamellosathyris lamellosa* (Léveillé), ventral, lateral, dorsal, and anterior, views of two large specimens, CM 45060 and 45061, × 1. I–M, *Camarophorella* sp., ventral, dorsal, anterior, and lateral views, CM 45062, × 1.5. M–P, *Crinisarina prouti* (Swallow), ventral, dorsal, anterior, and lateral views, CM 45063, × 1.5.

Diagnosis.—Medium to large, generally transversely subovate *Eomartiniopsis* with noncostate lateral slopes, rounded fold-sulcus, narrow, poorly delineated ventral interarea, moderately produced ventral umbonal region, and lacking crural plates.

Comments.—This species was described from the Lodgepole Formation of the Madison Group in Yellowstone National Park. Carter (1972, 1987) subsequently described specimens assigned to this species from the latest Kinderhookian Gilmore City Formation of Iowa and the Banff Formation of Alberta where it ranges from late Kinderhookian into the early Osagean. The interior of these Kenwood specimens (Fig. 16) is closely similar to the specimens sectioned by Carter (1972, 1987) from Iowa and Alberta.

Eomartiniopsis tscherepeti Sokolskaya, 1941, from the Upper Tournaisian of the Russian Platform and *Eomartiniopsis grandiformis* Plodowski, 1968, from the Viséan of Afghanistan are similar in size and outline to *E. rostrata*. Sokolskaya's (1941:pl. 7, fig. 7–9) types differ little from medium-sized specimens of *E. rostrata* and it may be a junior synonym of this species. However, dorsal valves of *E. tscherepeti* were not known to Sokolskaya nor was an entire shell sectioned so the interior is poorly known. *Eomartiniopsis grandiformis* Plodowski differs from *E. rostrata* in its larger, more extended ventral umbonal region and the presence of crural plates inside the dorsal valve.

Material.—In addition to the illustrated specimens there are 33 other specimens, including 11 articulated and 21 single valves.

Eomartiniopsis, **new species**

(Fig. 15A–D)

Comments.—A single large specimen of martiniid is assigned to the genus *Eomartiniopsis* on the basis of having a smooth shell with dental adminicula in the ventral valve. This unique specimen is unlike any other species of *Eomartiniopsis* known to me in its unusually large size, transversely subelliptical outline, and rather broad, flattened fold-sulcus. The ventral beak is broken, revealing thickened dental adminicula of indeterminate length and the dorsal umbo is spalled (Fig. 15D). A pair of thick, low ridges can be seen extending forward and defining an impressed dorsal muscle field. These ridges do not appear to be true plates but such ridges are not known in other *Eomartiniopsis* to my knowledge.

Family Gerkispiridae Carter, 1985

Genus *Punctothyris* Hyde, 1953

Punctothyris kenwoodensis Carter, 1985

(Fig. 20C–F)

1985 *Punctothyris kenwoodensis* Carter: p. 387, fig. 2E, 5–7.

Diagnosis.—Medium-sized *Punctothyris* with subcircular outline, rotund profile, eight to 11 lateral costae and zero to three sulcal costae.

Comments.—This is a common element in the Kenwood fauna there being in excess of 20 more-or-less complete specimens. It was illustrated and diagnosed by Carter (1985).

Superfamily Spiriferoidea King, 1846
Family Spiriferidae King, 1846
Subfamily Spiriferinae King, 1846
Genus *Spirifer* Sowerby, 1818
Subgenus *Mesochorispira* Carter, 1992
Spirifer (*Mesochorispira*) *grimesi* (Hall, 1858)
(Fig. 17A–D)

1858 *Spirifer grimesi* Hall: p. 604, pl. 14, fig. 1–5.

Diagnosis.—Large transverse *Mesochorispira* with moderately broad, well-developed, rounded fold-sulcus, greatest width at or near midlength and moderately coarse costae.

Comments.—This species is commonly identified from many localities and Osagean horizons in North America and abroad. It is characteristic of the Burlington Limestone and ranges throughout much of that formation and coeval strata in the midcontinent and the Cordilleran region. It is commonly confused with *Spirifer* (*Mesochorispira*) *logani* Hall, 1858, of Lower Viséan age, which generally has somewhat coarser costae and well-developed auriculations forming a wide hinge-line.

Material.—In addition to the illustrated specimen there are 15 articulated shells and seven disarticulated valves.

Family Imbrexiidae Carter, 1992
Genus *Fernglenia* Carter, 1992
Fernglenia vernonensis (Swallow, 1860)
(Fig. 17E, F)

1860 *Spirifer vernonensis* Swallow: p. 644.
1992 *Fernglenia vernonensis* Swallow: Carter, p. 329, fig. 1.1–1.11, 2.

Diagnosis.—Medium-sized transverse *Fernglenia* with strong, well-defined, moderately broad fold-sulcus, moderately coarse costae with few bifurcations, long dental adminicula, and protuberant stegidium or stegidial plates.

Comments.—This species was described from the Fern Glen Formation of eastern Missouri but also occurs in the Pierson Formation of southwestern Missouri, the St. Joe Formation of northern Arkansas and northeastern Oklahoma, the New Providence Shale of Kentucky, the Lake Valley and Keating formations of New Mexico, and the Redwall Limestone of Arizona. Related but undescribed species occur in the Caballero Formation of New Mexico and Banff Formation of Alberta.

Material.—In addition to the illustrated specimen there are two other ventral valves.

Genus *Tegulocrea* Carter, 1992
Tegulocrea incerta (Hall, 1858)
(Fig. 18A–D)

1858 *Spirifer incertus* Hall: p. 602, pl. 13, fig. 3.
1992 *Tegulocrea incerta* (Hall): Carter, p. 331, fig. 3.1–3.34, 4.

Diagnosis.—Medium-sized transverse subsemicircular *Tegulocrea* with mucronate lateral extremities in adults, with numerous bifurcating or trifurcating medium-coarse costae or costellae, and with very short dental adminicula and little apical callus internally.

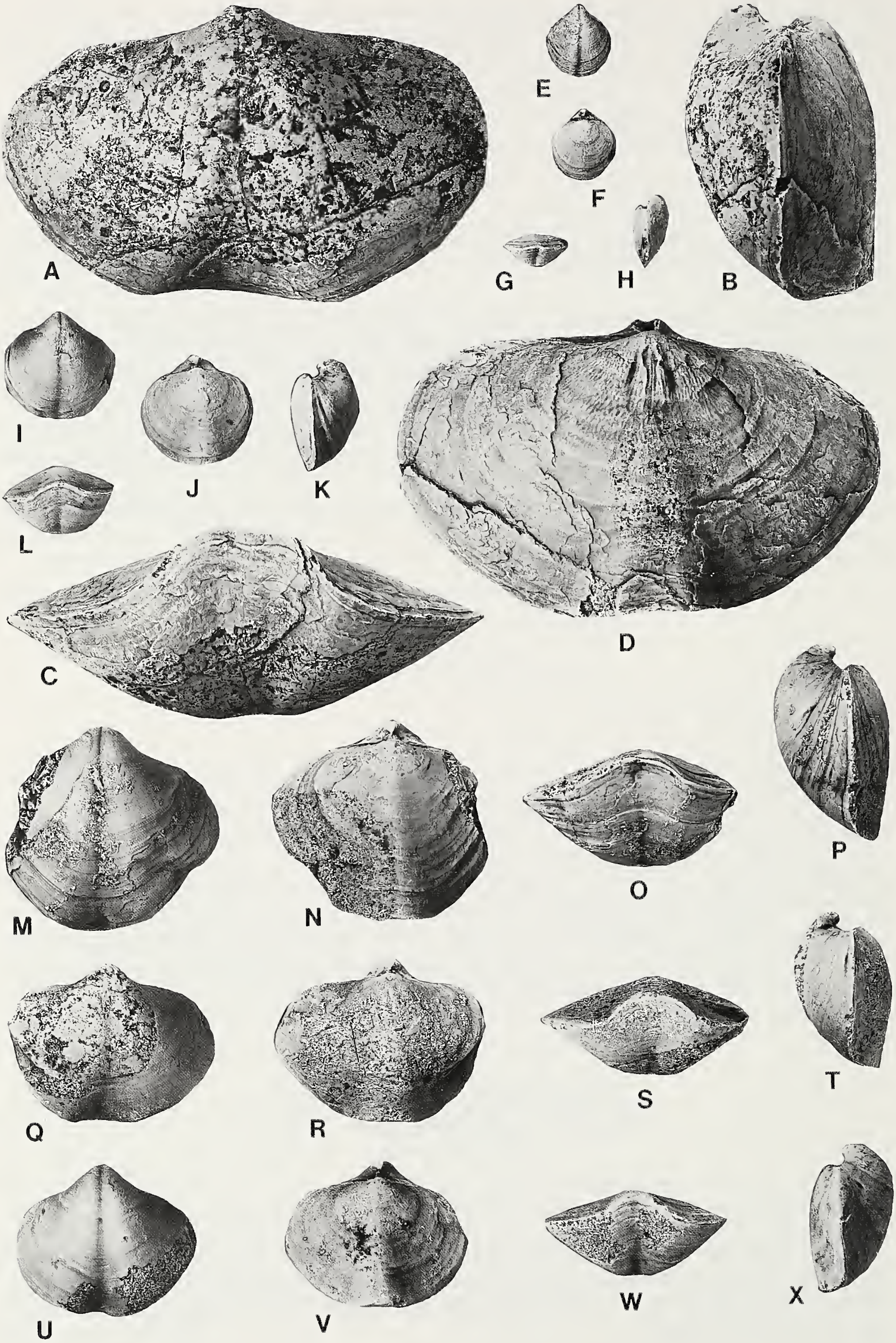
A
B
C
D
E
F
G
H
I
J
K
L
M
N
O
P
Q
R
S
T
U
V
W
X

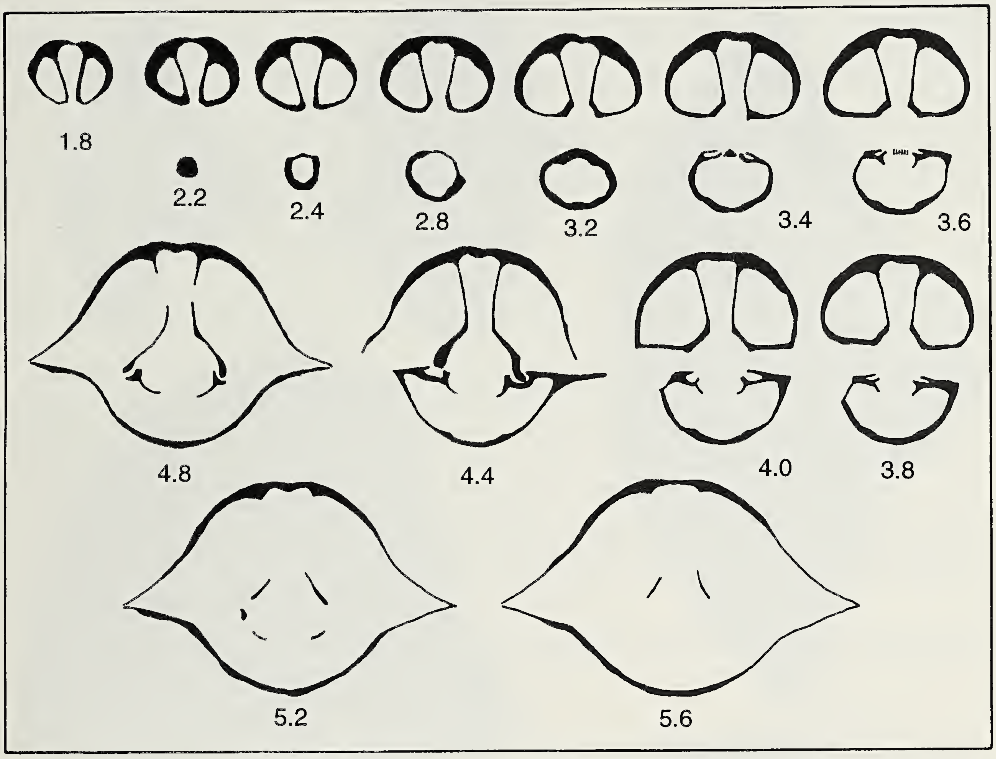

Fig. 16.—Transverse serial sections of *Eomartiniopsis rostrata* (Girty), CM 45071, × 1.5. Numbers refer to distance from ventral beak (in mm).

Comments.—Hall's (1858) type of this species is from the Burlington Limestone at Burlington, Iowa. The horizon within the Burlington is not known and, despite Weller's (1914) contention that it is a common Burlington element, is rare in my collections except for these Kenwood specimens. Most of Hall's (1858) Burlington brachiopod types are from the lowest subdivision, the Dolbee Creek Member, and provenience at that level would be in agreement with the occurrence of these St. Joe specimens.

Carter (1992) assigned *Spirifer tenuicostatus* Hall, 1858, and *Spirifer tenuimarginatus* Hall, 1858, to the genus *Tegulocrea.* The former differs from *T. incerta* in being finer-ribbed and having longer dental adminicula with a thick apical callus. The latter is known only from Hall's type which is small, rounded in outline, only moderately transverse, and with finer ribbing than *T. incerta.* Weller (1914) suggested that the type of *T. tenuimarginatus* might represent an aberrant individual of *T. tenuicostus.*

Material.—In addition to the illustrated specimen there are ten articulated and

---

←

Fig. 15.—Martinioids. A–D, *Eomartiniopsis* n. sp., ventral, lateral, anterior, and dorsal views, CM 45065. E–X, *Eomartiniopsis rostrata* (Girty), ventral, dorsal, anterior, and lateral views of five specimens, CM 45066–45070. All figures × 1.

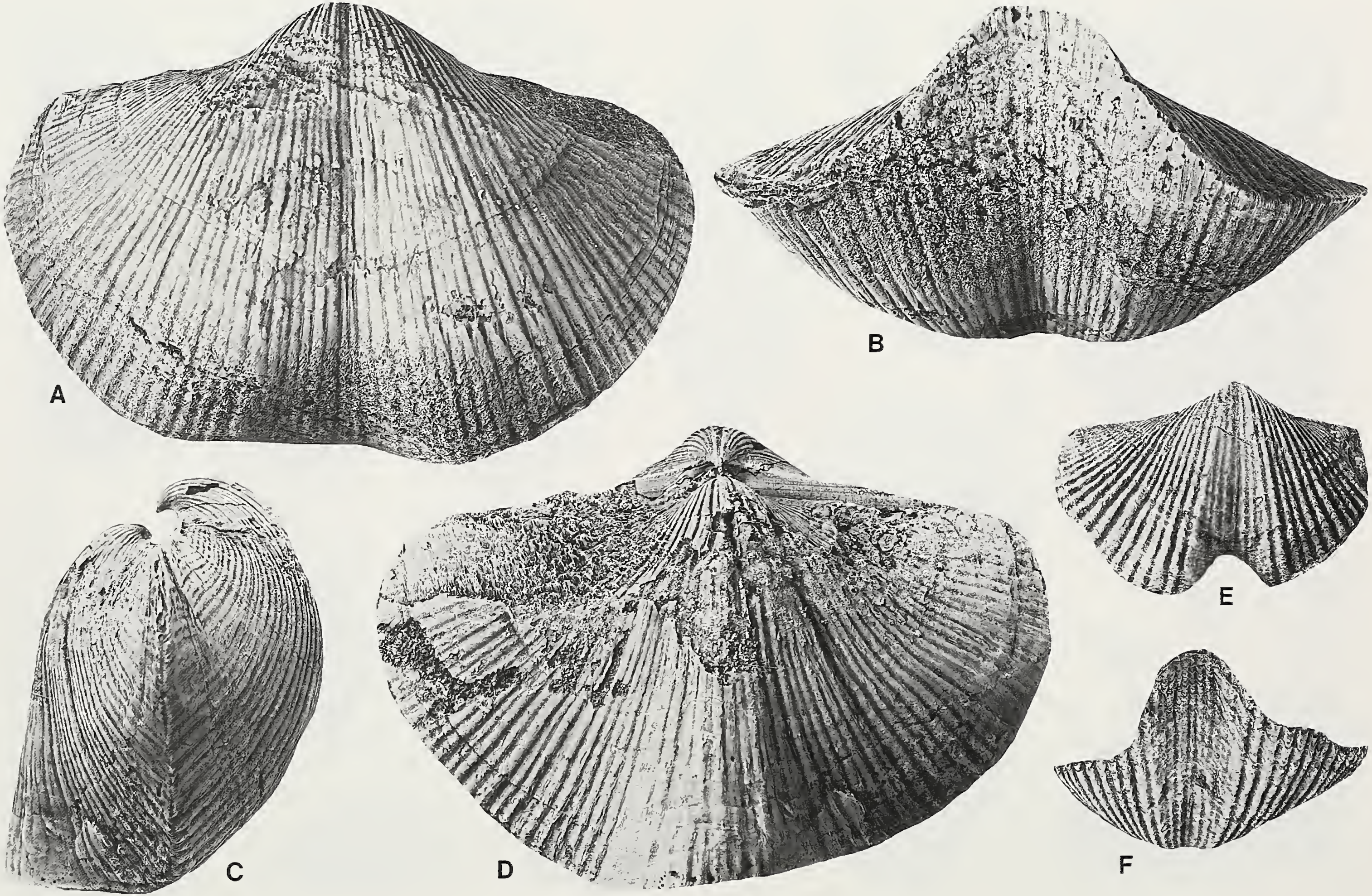
A
B
E
C
D
F

eight ventral valves. Carter (1992) illustrated a growth series of seven specimens from this collection.

Superfamily Paeckelmannelloidea Ivanova, 1972
Family Strophopleuridae Carter, 1974
Subfamily Strophopleurinae Carter, 1974
Genus *Voiseyella* Roberts, 1963
Voiseyella novamexicana (Miller, 1881)
(Fig. 18E–L; 19)

1881 *Spirifera novamexicana* Miller: p. 314, fig. 10–10b.
1967 *Amesopleura novamexicana* (Miller): Carter, p. 366, pl. 33, fig. 9–12, text-fig. 29.

Diagnosis.—Alate to slightly mucronate, gerontically geniculate *Voiseyella* with seven to nine costae on each flank and procline to catacline ventral interarea; internally with a dorsal umbonal callus and short dental adminicula.

Comments.—*Voiseyella texana* (Carter, 1967) from the Chappel Limestone of central Texas, the only other North American Osagean species, differs in its less transverse outline, apsacline ventral interarea, nongeniculate growth form, and thickened dental adminicula. The type species, *Voiseyella anterosa* (Campbell, 1957) from the Middle Viséan of eastern Australia, is smaller, has fewer ribs, and lacks a median dorsal groove.

Material.—In addition to the illustrated specimens there are five articulated and three disarticulated specimens.

Superfamily Brachythyridoidea Frederiks, 1924
Family Brachythyrididae Frederiks, 1924
Genus *Brachythyris* McCoy, 1844
Brachythyris chouteauensis Weller, 1909
(Fig. 18M–X)

1909 *Brachythyris chouteauensis* Weller: p. 305, pl. 13, fig. 11.

Diagnosis.—Medium-sized *Brachythyris* of rounded outline, proximate beaks, slightly compressed ventral umbonal region, low, wide ventral interarea that is well defined by subangular beak ridges, seven to 11 costae per flank, and one or two pairs of weak or very faint costae on the sides of the sulcus.

Comments.—In this continent there are two Lower Mississippian species of the genus *Brachythyris* that are similar in profile and outline to *B. chouteauensis* Weller. These are *Brachythyris suborbicularis* (Hall, 1858) from the upper Burlington and Keokuk limestones of the midcontinent and *Brachythyris hortonensis* Carter, 1988, from the Glen Park Formation of east-central Missouri and adjacent portions of Illinois. *Brachythyris suborbicularis* is much larger than *B. chouteauensis* and has correspondingly coarser ribbing and wider hingeline. *Brachythyris hortonensis* has a transversely subovate outline, broader umbonal region, three sulcal costae, and a median groove on the dorsal fold.

←

Fig. 17.—Spiriferoids. A–D, *Spirifer* (*Mesochorispira*) *grimesi* (Hall), ventral, anterior, lateral, and dorsal views of a large specimen, CM 45072. E, F, *Fernglenia vernonensis* (Swallow), ventral and anterior views of a large ventral valve, CM 45073. All figures × 1.

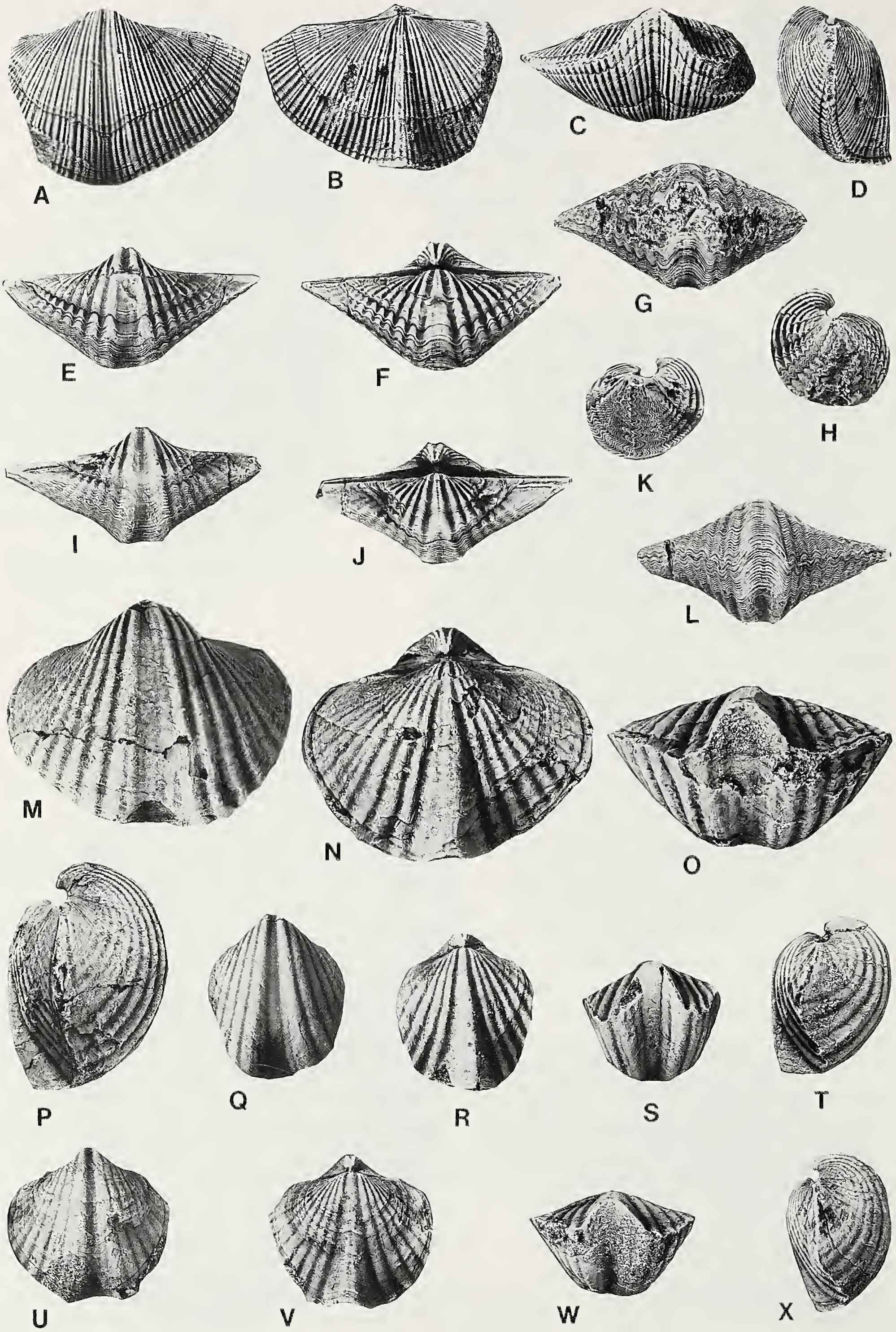
A
B
C
D
G
E
F
H
K
I
J
L
M
N
O
P
Q
R
S
T
U
V
W
X

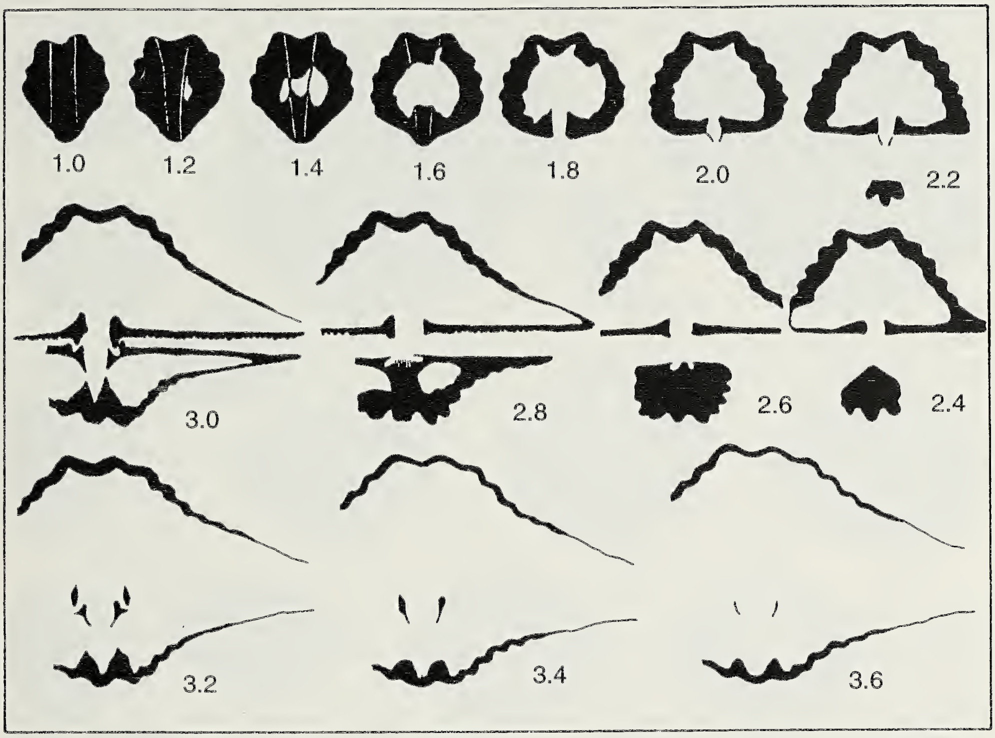

Fig. 19.—Transverse serial section of *Voiseyella novamexicana* (Miller), CM 45080, × 3. Numbers refer to distance from ventral beak (in mm).

Material.—In addition to the illustrated specimens there are ten articulated and 21 disarticulated specimens.

Suborder Delthyridina Ivanova, 1972
Superfamily Reticularioidea Waagen, 1883
Family Elythidae Frederiks, 1924
Subfamily Elythinae Frederiks, 1924
Genus *Kitakamithyris* Minato, 1951
Kitakamithyris cooperensis (Swallow, 1860)
(Fig. 20G–Z)

1860 *Spirifer cooperensis* Swallow: p. 643.
1967 *Reticularia*? *cooperensis* (Swallow): Carter, p. 405, pl. 40, fig. 1–7, text-fig. 41.

Diagnosis.—Medium-sized transverse elythins with a subelliptical outline, weakly developed fold-sulcus, and moderately narrow, ventral umbonal region

---

←

Fig. 18.—Spiriferoids, paeckelmanelloids, and brachythyridoids. A–D, *Tegulocrea incerta* (Hall), ventral, dorsal, anterior, and lateral views, CM 45074, × 1. E–L, *Voiseyella novamexicana* (Miller), ventral, dorsal, anterior, and lateral views of two specimens, CM 45075 and 45076, × 1.5. M–X, *Brachythyris chouteauensis* (Weller), ventral, dorsal, anterior, and lateral views of three specimens, CM 45077–45079, × 1.

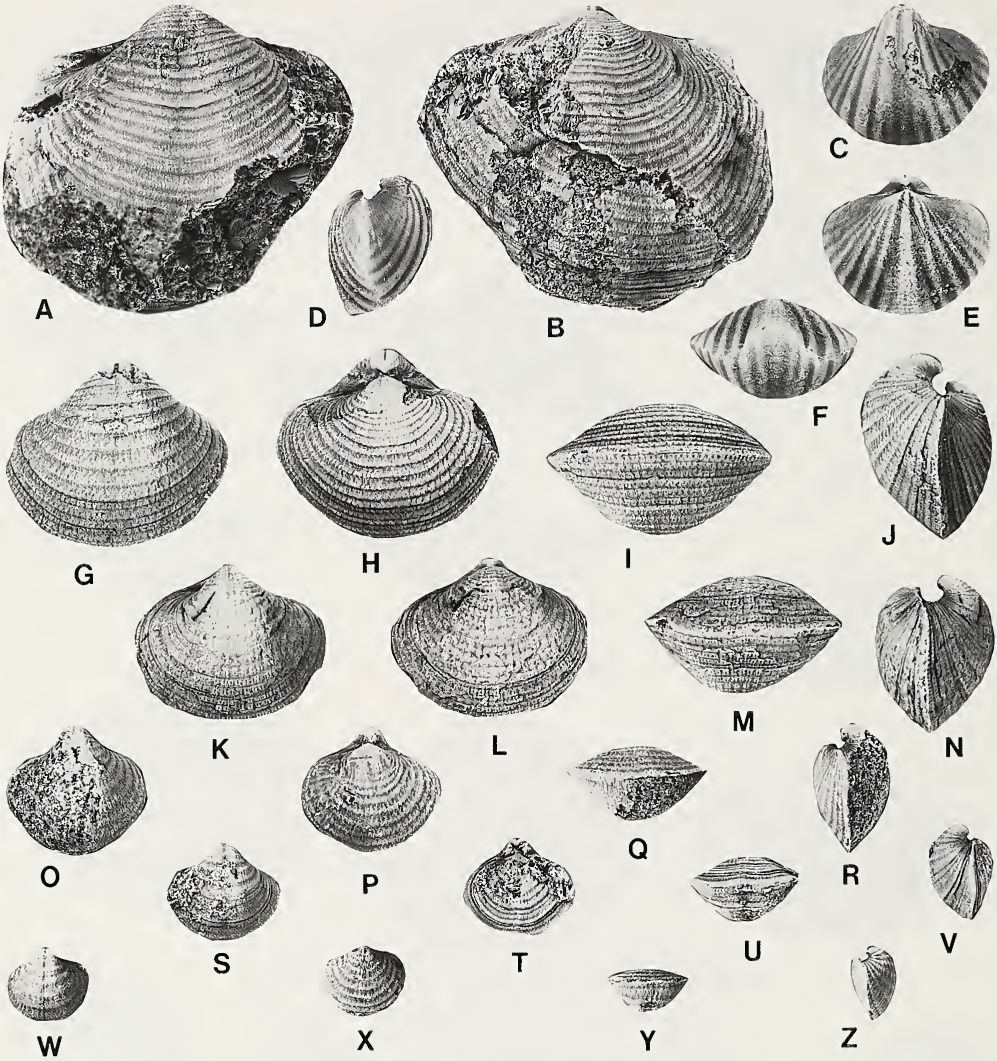

Fig. 20.—Reticularioids. A, B, ?*Torynifer* sp., ventral and dorsal views of a large specimen, CM 45081, × 1. C–F, *Punctothyris kenwoodensis* Carter, ventral, lateral, dorsal, and anterior views, CM 45082, × 1.5. G–Z, *Kitakamithyris cooperensis* (Swallow), ventral, dorsal, anterior, and lateral views of five specimens, CM 45083–45087, × 1.5.

that extends slightly posterior to the hingeline; internally with short, slightly divergent dental adminicula and low, thin median ridges in both valves that extend to about midlength.

Comments.—There are few other representatives of this genus in North America. *Reticularia setigera* var. *internascens* Girty, 1928, from the silicious middle Boone Formation (Lower or Middle Viséan) of northeastern Arkansas, may belong in this genus. It differs from *K. cooperensis* (Swallow) in being larger and more transverse and seems to lack a dorsal median ridge although, as Girty (1929:

92) pointed out, that character cannot be confirmed in better-preserved calcareous specimens.

Material.—The illustrated specimens constitute the entire collection of this species.

Subfamily Toryniferinae Carter, 1994
Genus *Torynifer* Hall and Clarke, 1893
?*Torynifer* species
(Fig. 20A, B)

Description.—[This description is based on the specimen illustrated in Figure 20 plus a crushed ventral valve.] Medium-sized to large for the subfamily, transversely subovate in outline, subequally biconvex with proximate beaks; fold and sulcus moderately well delimited but weakly developed; cardinal extremities probably well rounded but poorly preserved in both specimens; ventral interarea low, concave, vertically striated, moderately narrow, apsacline; dorsal interarea not preserved; micro-ornament spinous but not well preserved; surfaces of both valves almost regularly rugose; ventral interior with short dental adminicula and very low median ridge; dorsal interior with either median ridge or septum, ascertainable only by destructive examination; other internal details unknown.

Comments.—Assignment to the genus *Torynifer* cannot be confirmed without additional information about the micro-ornament and dorsal interior. These Kenwood specimens are similar in size and outline to typical *Torynifer pseudolineatus* (Hall, 1858), from the upper Burlington and Keokuk limestones of the midcontinent, but differ in having more closely spaced, rugose growth lamellae.

Order Spiriferinida Ivanova, 1972
Suborder Spiriferinidina Ivanova, 1972
Superfamily Syrinothyridoidea Frederiks, 1926
Family Syringothyrididae Frederiks, 1926
Subfamily Permasyrinxinae Waterhouse, 1986
Genus *Pseudosyrinx* Weller, 1914
Pseudosyrinx cf. *P. missouriensis* Weller, 1914
(Fig. 21A–D)

1914 *Pseudosyrinx missouriensis* Weller: p. 406, pl. 65, fig. 5–9; pl. 66, fig. 11–13.

Diagnosis.—Medium-sized strongly transverse *Pseudosyrinx* with narrowly rounded cardinal extremities, rounded beak ridges, 16–18 costae on each flank, strongly procline, long, flattened ventral interarea, and long tongue in ventral sulcus.

Comments.—The specimen illustrated here differs from typical *Pseudosyrinx missouriensis* in having a shorter ventral interarea, a much shorter tongue in the sulcus, a proportionately longer dorsal valve, and shorter ventral valve with an even more strongly procline ventral interarea. An incomplete ventral valve provides no additional insight into the nature of this species, which may well represent an undescribed species.

Pseudosyrinx missouriensis Weller, 1914, is widely distributed in the lower Burlington Limestone, Meppen Formation, Fern Glen Formation, Pierson Formation, and St. Joe Formation, all from the midcontinent. It is readily differentiated from *Pseudosyrinx gigas* Weller, 1914, from the Keokuk Limestone, by its

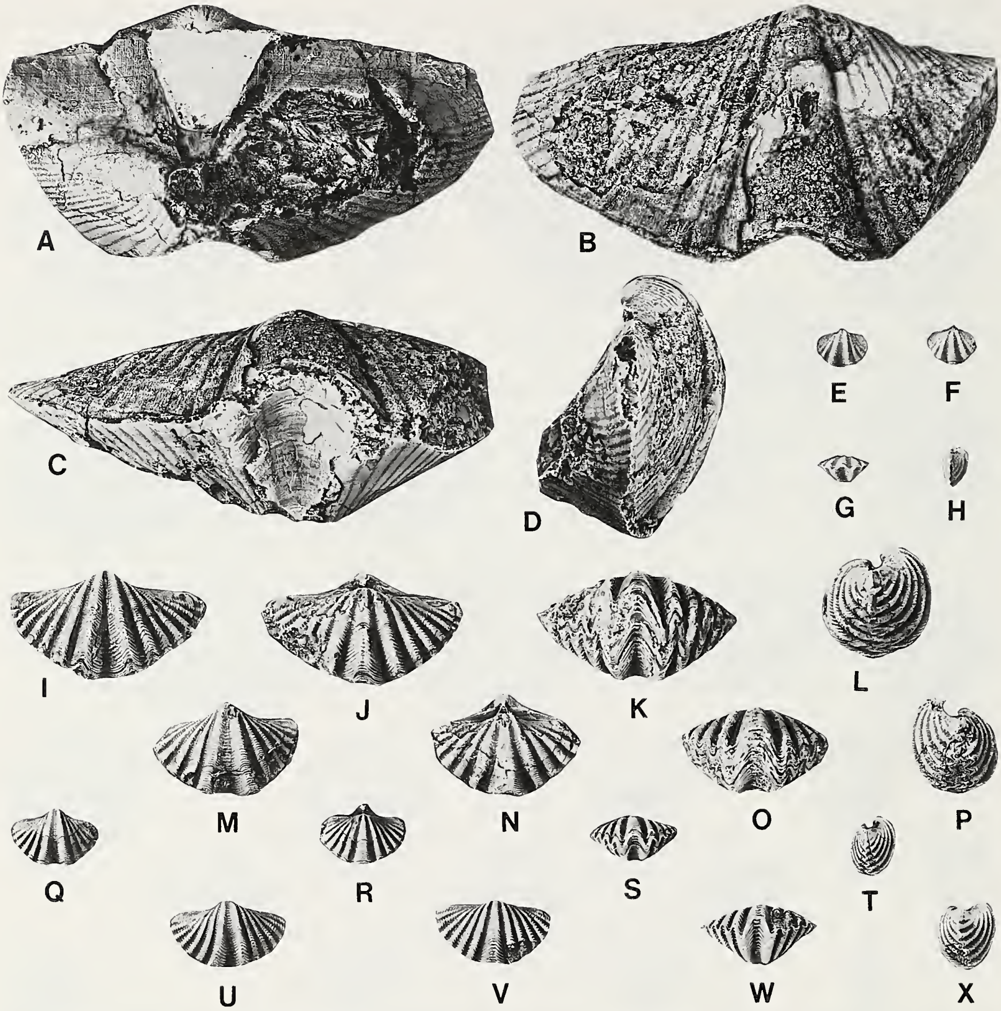

Fig. 21.—Punctate spiriferids. A–D, *Pseudosyrinx* cf. *P. missouriensis* Weller, ventral, dorsal, anterior, and lateral views, CM 45088. E–X, *Punctospirifer*? *subtexta* (White), ventral, dorsal, anterior, and lateral views of five specimens, CM 45089–45093. The specimens in Figures E–T bear a short spondylium, whereas the specimen in Figures U–X has discrete apical plates. All figures × 1.

rounded beak ridges, longer tongue, more strongly procline ventral interarea, and smaller size.

Superfamily Pennospiriferoidea Dagis, 1972
Family Punctospiriferidae Waterhouse, 1975
Genus *Punctospirifer* North, 1920

Type Species.—*Punctospirifer scabricosta* North, 1920, by original designation.

Diagnosis.—Small to medium size; outline variable, usually transverse; cardinal extremities subangular, rounded, or rarely slightly mucronate; fold-sulcus narrow to moderately wide, rounded, smooth or with single medial rib, often slightly flaring anteriorly; ventral interarea moderately high, weakly concave, usually apsacline; lateral slopes with moderately numerous strong, rounded plicae separated by narrow subangular interspaces; growth varices irregularly spaced; micro-ornament of closely spaced imbricate growth laminae and fine, discontinuous capillae which rise and become wider with imbrications anteriorly as tiny U-shaped crenulations of lamellae in the type species and sometimes terminating in minute semi-erect pseudospines in others; dental adminicula short, slightly divergent; median septum long, high, slender; apical callus variably thick; ctenophoridium large, supported by short callus; dorsal adminicula absent or very short; adductors separated by long myophragm and bounded laterally in some species by low ridges; punctae moderately coarse; jugum probably absent.

Comments.—Recognition of this genus was problematical until the type species, *Punctospirifer scabricosta* North, 1920, was redescribed in great detail by Campbell (1959). In this paper the capillate micro-ornament was made known for the first time, however, the U-shaped minute crenulations forming pseudospinules or semi-erect nodes fringing the growth lamellae were described by Campbell (1959:353) as "extremely minute projections, causing an almost imperceptible serration of the lamellar edge." Campbell did not detect spines or spine bases per se.

The question then is—do the North American species with minute but distinct semi-erect pseudospinules fringing the growth lamellae, as described below, belong in the genus *Punctospirifer*? I think that they do because perfect and complete preservation of such delicate minuscule structures is bound to be rare. At least in North America representatives of this genus very rarely seem to be well preserved. In the unusually well-preserved specimens at hand any attempt to free the pseudospinules from the soft matrix for photographic purposes results in their destruction. They are best observed in finely silicified specimens, as occur in the white cherts of the lower Burlington Limestone, or in calcareous specimens preserved with a thin layer of soft marly matrix exposing the rows of pseudospinules, as occur in the Kenwood fauna.

Punctospirifer? *subtexta* (White, 1862)
(Fig. 21E–X, 22, 23)

1862 *Spiriferina*? *subtexta* White: p. 25.
1914 *Spiriferina subtexta* White: Weller, p. 291, pl. 36, fig. 35–40.

Diagnosis.—Small transverse punctospiriferids with smooth fold-sulcus, six to nine simple costae on each flank, sulcus bounded by disproportionately large costae, ventral interarea commonly flattened, weakly apsacline to almost catacline, dental adminicula and ventral septum converging and either discrete or forming short spondylium, and imbricate, discontinuously capillate growth lamellae fringed with moderately coarse, semi-erect pseudospinules.

Description.—Medium-sized for genus, subequally biconvex, transversely subelliptical to acutely subtrigonal in outline; greatest width just anterior to hingeline; lateral profile subovate to subcircular; cardinal extremities extended, acutely rounded in all growth stages, generally slightly compressed; fold-sulcus moderately well developed, narrow, rounded; flanks with six to nine, usually seven, rounded simple costae separated by equally wide interspaces in adult specimens, those bounding the ventral sulcus being disproportionately large; growth lamellae regularly imbricate; micro-ornament consisting of fine discontinuous capillae, rising anteriorly and terminating in fine semi-erect pseudospinules; shell substance moderately coarsely punctate.

Ventral valve strongly and almost evenly convex except at beak, slightly to moderately thicker than opposite valve; most convex in umbonal region; flanks moderately convex, sloping evenly to anterolateral margins; beak small, slightly laterally compressed, incurved; interarea moderately high, acutely

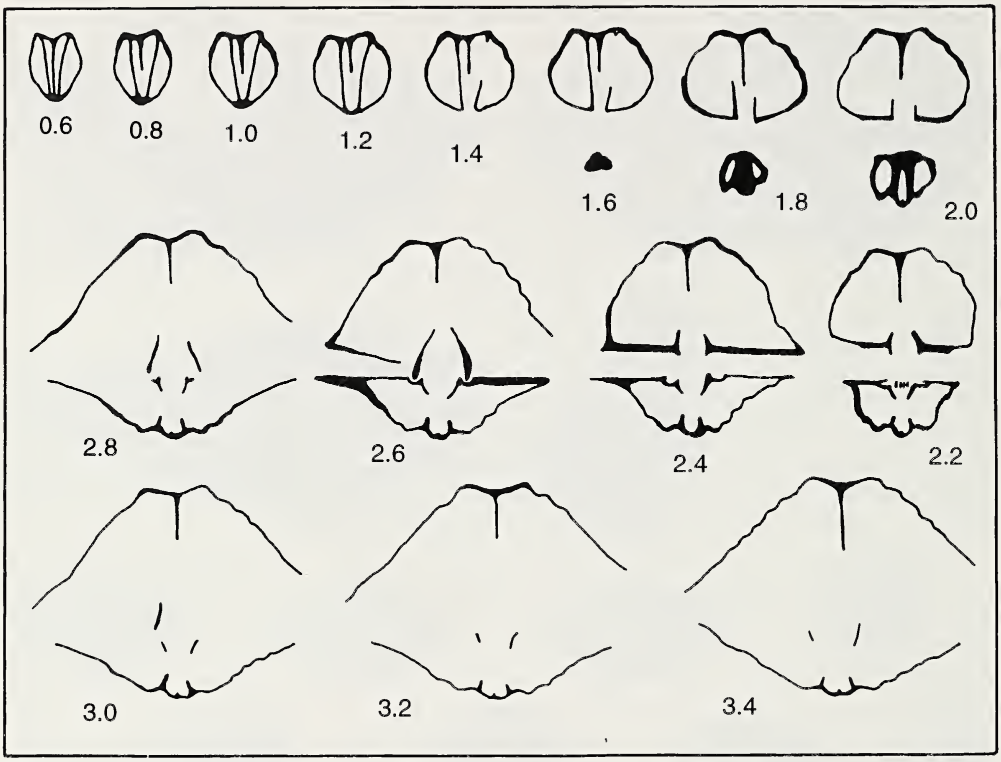

Fig. 22.—Transverse serial sections of *Punctospirifer*? *subtexta* (White) with discrete apical plates, CM 45094, × 3. Numbers refer to distance from ventral beak (in mm).

triangular, slightly concave, generally apsacline, rarely almost catacline; delthyrium much longer than wide; beak ridges acutely rounded to subangular; sulcus originating at beak, becoming gradually wider and deeper anteriorly, smooth and rounded except for imbricate ornament; interior with long, high median septum originating at beak, much shorter thin dental adminicula which converge in beak, fusing with septum in beak region to form short spondylium in some populations; teeth small, blade-like.

Dorsal valve moderately convex, most convex in umbonal region; lateral slopes evenly and weakly to moderately convex, sloping evenly to margins; ears as in opposite valve; dorsal interarea very short, orthocline to slightly anacline; fold low, smooth, rounded, rising above flanks only near anterior margin, defined by fold-bounding interspaces slightly deeper than those on lateral slopes; dorsum rounded or, in rare specimens, slightly flattened or marked by faint medial groove; interior with small ctenophoridium supported by short apical callus; muscle field well defined by prominently thickened bounding ridges on interior crests of fold-bounding interspaces; medial myophragm present in anterior portion of muscle field; sockets small, crural bases attached to mediodorsal edges of inner socket ridges; spiralia consisting of at least five whorls; presence or absence of jugum not ascertained.

Comments.—Tentative assignment to the genus *Punctospirifer* North is based on overall similarity to the type species. To my knowledge, a spondylium, albeit a very short one, has never been reported in this family. In fact, a spondylium is known from only two other genera in the suborder Spiriferinidina. For this reason the generic assignment is queried.

The collection on which this description is based consists of 25 complete specimens and several disarticulated valves but only a few have a well-preserved micro-ornament. Six of these specimens have discrete dental adminicula and median septa (Fig. 22), the remaining specimens having a short spondylium (Fig. 23A, B). No other morphological difference can be discerned between these groups of specimens, and, in light of their mutual occurrence within the Kenwood bioherm, it is assumed that those with a spondylium represent an unusual variant of the same species. Two of the illustrated specimens (Fig. 21E–T) have a spondylium whereas the other one (Fig. 21U–X) has discrete plates. Specimens of this species with a spondylium are also known from the Pierson Formation of Stone County, Missouri. The significance of the short spondylium (Fig. 23) is not known for it is an unusual, if not unknown, feature in members of this superfamily.

This is a moderately common species in the lower Burlington Limestone at Louisiana, Missouri, but seems to be less common elsewhere in the early Osagean. A capillate-fimbriate micro-ornament has not been previously observed or reported in this species.

Material.—In addition to the illustrated specimens there are 17 complete specimens and 12 disarticulated valves.

Order Terebratulida Waagen, 1883
Suborder Terebratulidina Waagen, 1883
Superfamily Dielasmatoidea Schuchert, 1913
Family Cranaenidae Cloud, 1942
Subfamily Cranaeninae Cloud, 1942
Genus *Cranaena* Hall and Clarke, 1893
Cranaena globosa Weller, 1914
(Fig. 24A–ff)

1914 *Cranaena globosa* Weller: 249, pl. 34, fig. 60–66; text-fig. 25.

Diagnosis.—Small elongate *Cranaena* with subovate rounded outline and thickly lenticular profile in adults, commonly with geniculate anterior margin of both valves in gerontic specimens; maximum width generally attained anterior to midlength in large adults; ventral beak erect or slightly incurved; venter and dorsum flattened anteriorly in large adults, forming straight or slightly emarginate anterior commissure; rarely with weak ventral sulcus; dental plates short; hingeplate concave, dorsally situated; crural processes high, ventrally directed; loop short with posteriorly directed jugum.

Comments.—This species is moderately common in the lower Burlington white chert at Louisiana, Missouri, but has not been described from elsewhere in North America. Weller's (1914) holotype is purportedly from the "upper Burlington limestone" near Springfield, Missouri. A large, complete adult specimen was serially sectioned for this report (Fig. 25). Weller (1914) illustrated only the posterior portion of a dorsal valve.

Cranaena texana Carter, 1967, is similar to *C. globosa* Weller in outline, growth form, and general proportions but differs in being smaller with a less inflated lateral profile, the maximum width in large specimens is at midlength, the anterior portions of the valves are less flattened and thus lacking an emarginate anterior commissure in large adults. *Cranaena occidentalis* (Miller, 1892) from the Chouteau Limestone of Missouri is smaller and less inflated than *C. globosa* Weller

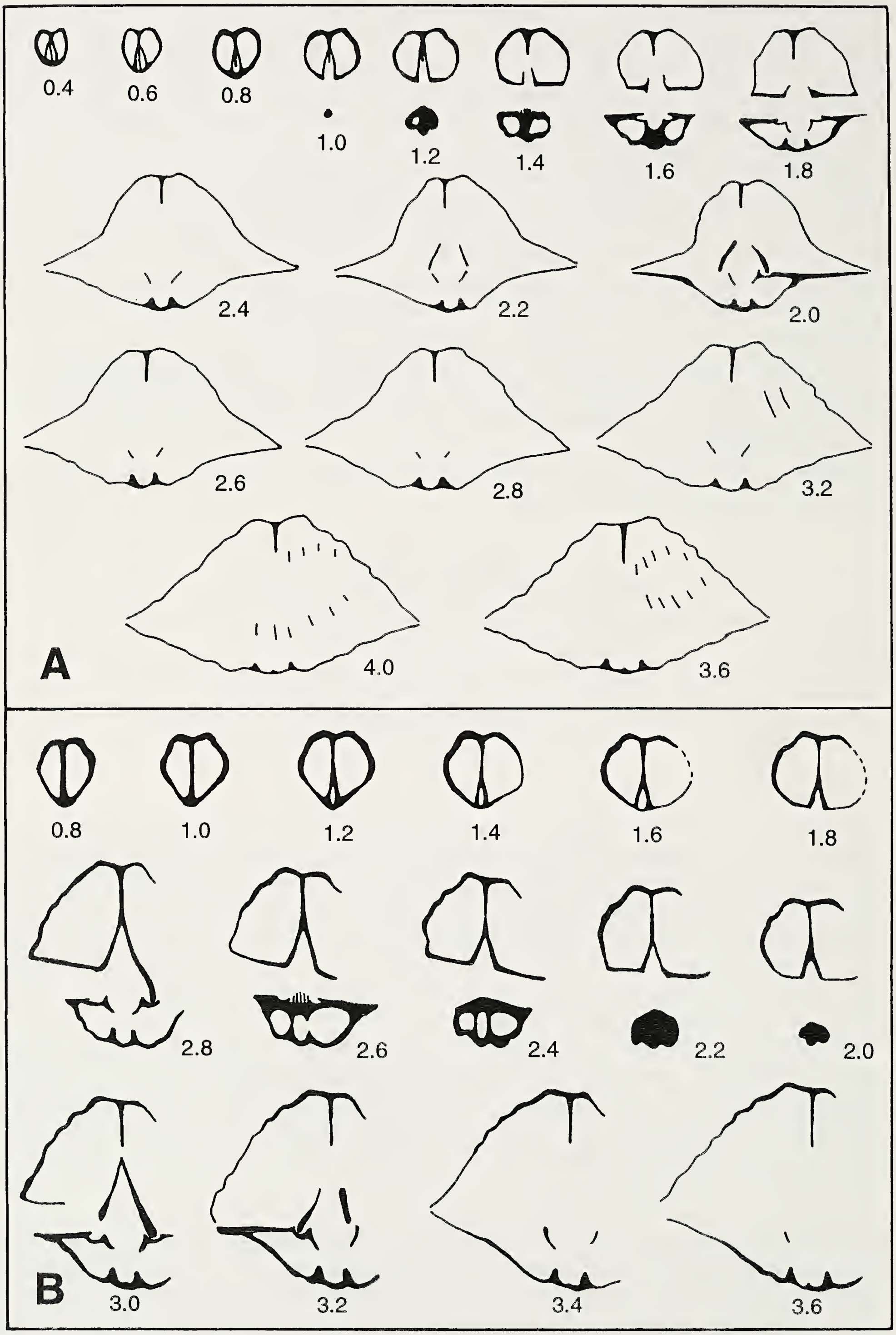
0.4
0.6
0.8
1.0
1.2
1.4
1.6
1.8
2.4
2.2
2.0
2.6
2.8
3.2
4.0
3.6
A
0.8
1.0
1.2
1.4
1.6
1.8
2.8
2.6
2.4
2.2
2.0
B
3.0
3.2
3.4
3.6

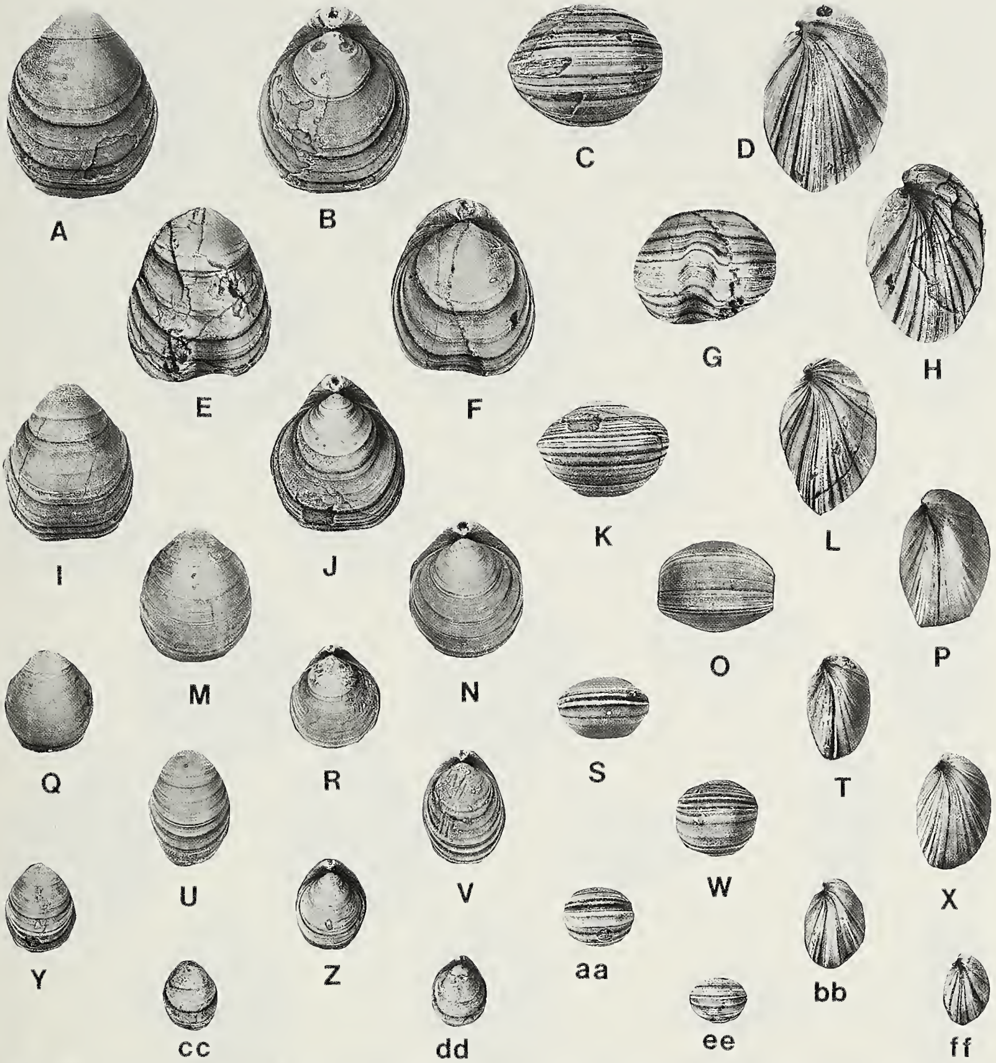

Fig. 24.—Terebratulids. A–ff, *Cranaena globosa* Weller, ventral, dorsal, anterior, and lateral views of eight specimens, CM 45097–45104, × 1.5.

and has nearly straight posterolateral margins, unlike the rounded posterior margins in the latter.

Material.—In addition to the illustrated specimens there are 269 complete specimens.

←

Fig. 23.—Transverse serial sections of two specimens of *Punctospirifer*? *subtexta* (White) with short spondylia. A, a small specimen, CM 45095; B, a larger specimen, CM 45096, both × 3. Numbers refer to distance from ventral beak (in mm).

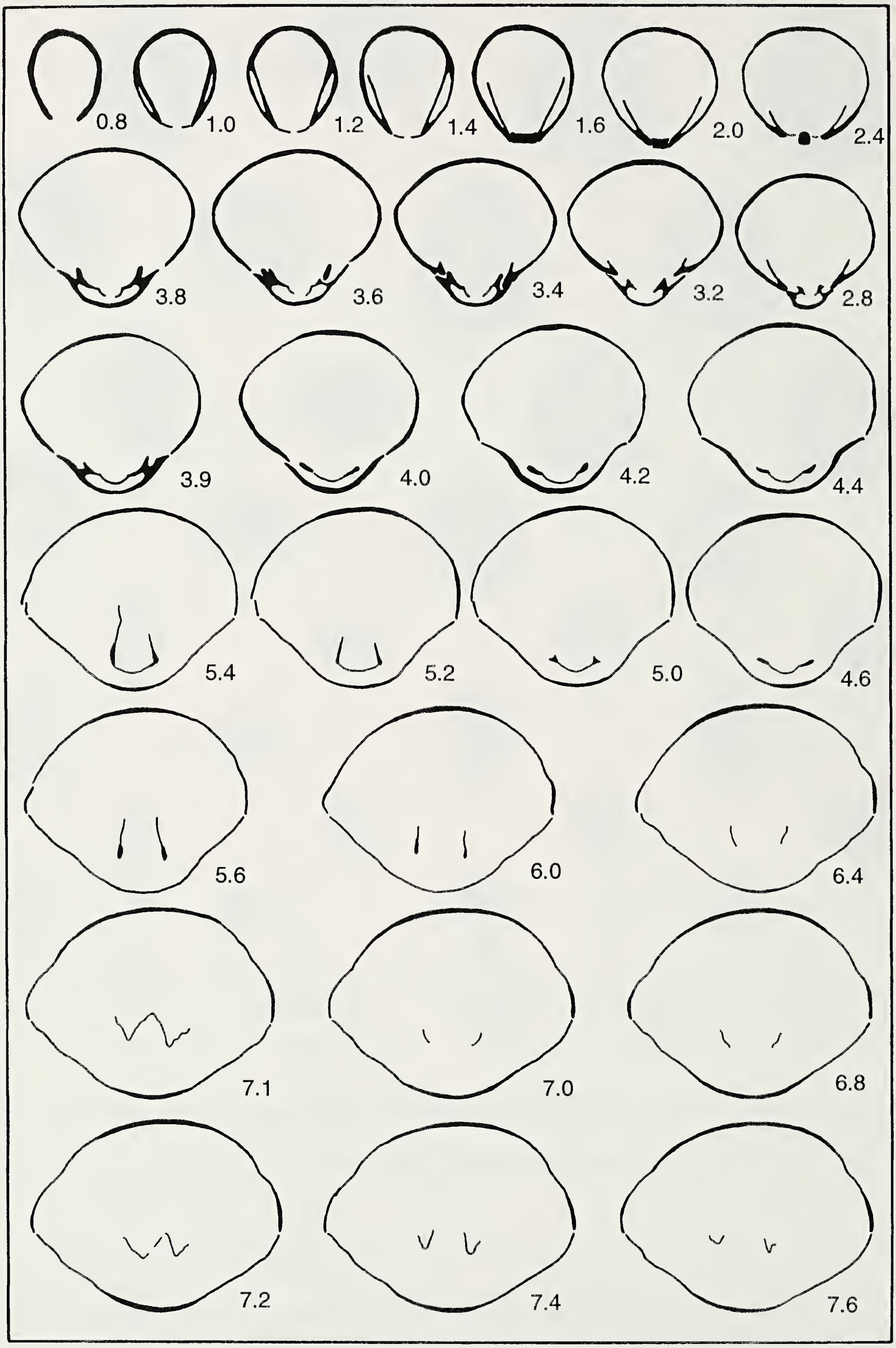
0.8
1.0
1.2
1.4
1.6
2.0
2.4
3.8
3.6
3.4
3.2
2.8
3.9
4.0
4.2
4.4
5.4
5.2
5.0
4.6
5.6
6.0
6.4
7.1
7.0
6.8
7.2
7.4
7.6

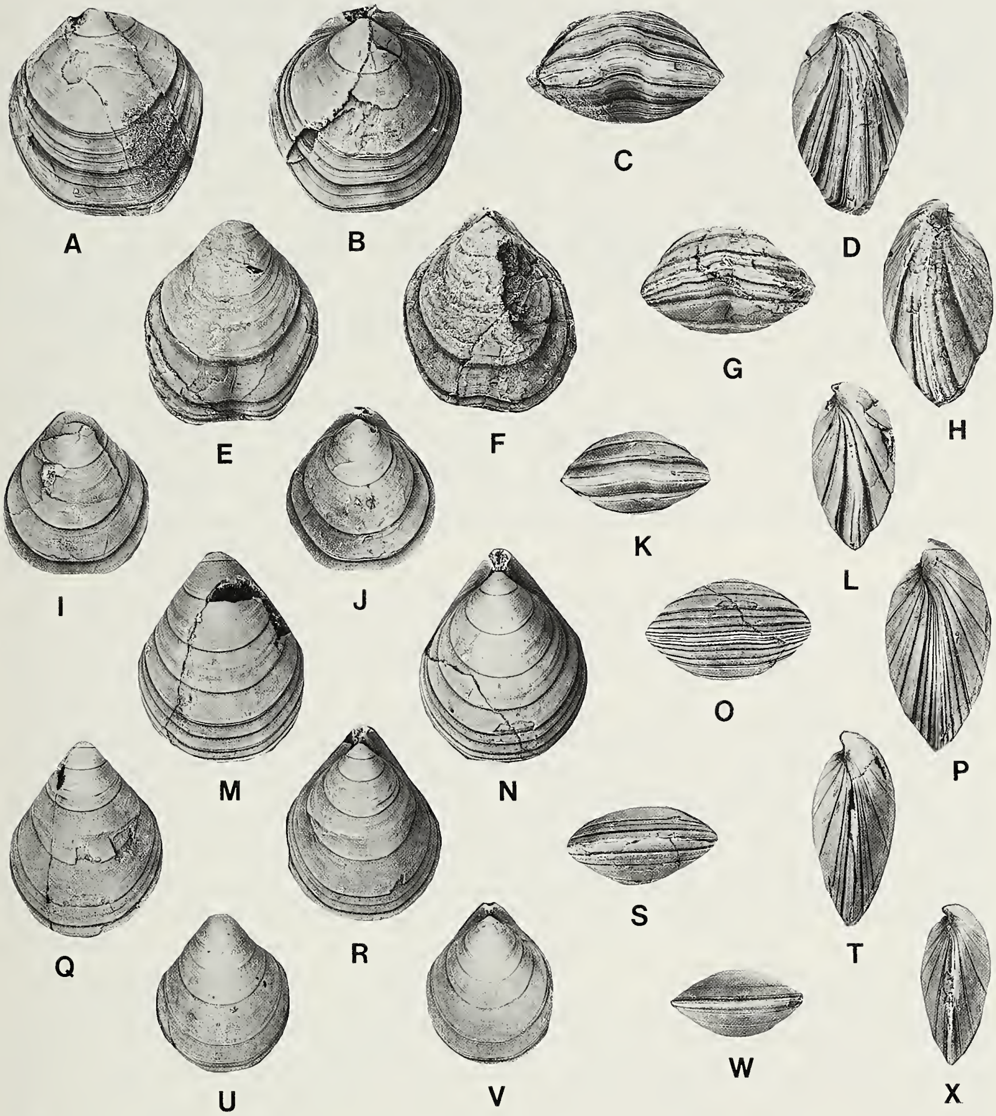

Fig. 26.—Terebratulids. A–L, *Dielasma oklahomensis* n. sp., ventral, dorsal, anterior, and lateral views of three specimens including the holotype (Fig. E–H, CM 450107) and two paratypes (CM 45106 and 45108), × 1. M–X, *Cranaena salinensis* n. sp., ventral, dorsal, anterior, and lateral views of three specimens, including the holotype (Fig. M–P, CM 45109) and two paratypes (CM 45110 and 45111), × 1.

←

Fig. 25.—Transverse serial sections of *Cranaena globosa* Weller, CM 45105, × 3. Numbers refer to distance from ventral beak (in mm).

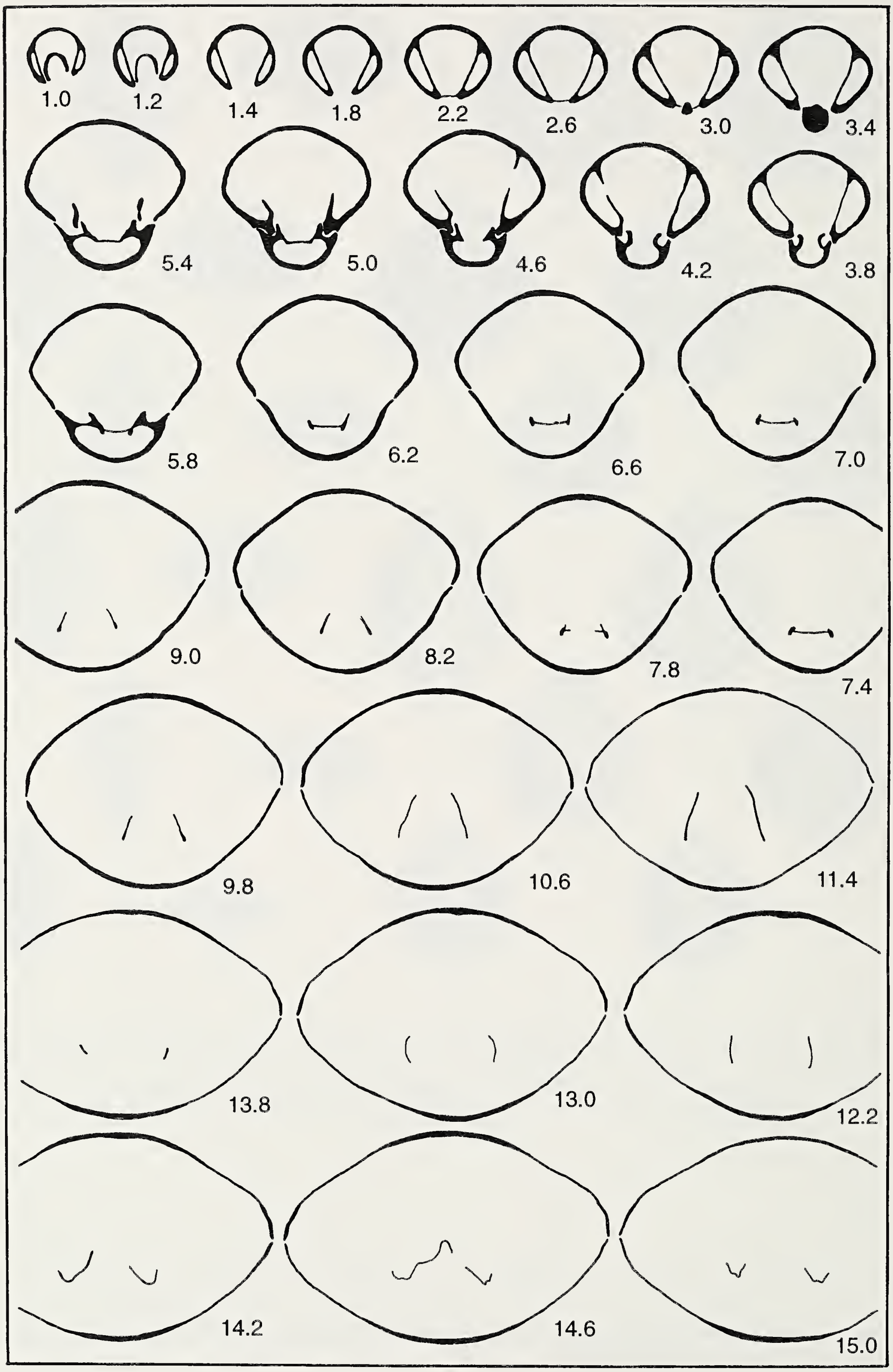
1.0
1.2
1.4
1.8
2.2
2.6
3.0
3.4
5.4
5.0
4.6
4.2
3.8
5.8
6.2
6.6
7.0
9.0
8.2
7.8
7.4
9.8
10.6
11.4
13.8
13.0
12.2
14.2
14.6
15.0

Table 7.—*Measurements (in mm) of the types of* Cranaena salinensis, *n. sp.*

Number	Length	Width	Thickness
CM 45109	28.0	22.3	14.2
CM 45110	25.8	20.7	11.3
CM 45111	21.3	17.5	9.3

Cranaena salinensis, **new species**
(Fig. 26M–X; 27)

Holotype.—CM 45109, Fig. 26M–P.

Paratypes.—CM 45010 and 45011, Fig. 26Q–X.

Diagnosis.—Medium-sized, nearly equally biconvex, moderately well-inflated *Cranaena* having guttate outline with straight posterolateral margins, maximum width anterior to midlength in large adults, rounded dorsum and venter with rectimarginate anterior commissure, and suberect beak angle; internally with well-developed, moderately long dental plates; hingeplate slightly concave anteriorly, nearly flat posteriorly, loop long.

Description.—Medium size for genus, subequally biconvex, longitudinally guttate in outline in adults, subovate to subelliptical in juveniles; greatest width attained anterior to midlength in adults, near midlength in juveniles; anterior profile lenticular; lateral profile lenticular to subguttate; fold and sulcus absent, both valves nearly evenly convex; anterior commissure rectimarginate; growth varices strong, widely spaced.

Ventral valve evenly convex in lateral profile or slightly more convex umbonally; lateral slopes weakly convex, venter more convex, arched; beak suberect, rarely erect; foramen ovate, permesothyridid, slightly labiate; beak ridges narrowly rounded, forming poorly defined, moderately concave palintropes; interior with pedicle collar and moderately long, diverging dental plates; teeth small.

Dorsal valve about as thick as opposite valve, evenly convex in lateral profile or slightly more convex posteriorly near umbo; lateral slopes weakly and evenly convex, dorsum more convex, arched as in opposite valve; interior with apically perforated, weakly concave or flattened hingeplate; crura attached to dorsal edges of inner socket ridges; crural processes strongly developed, projecting ventrally into body cavity; loop moderately long for genus; jugum ventrally arched and directed slightly posteriorly.

Measurements of Types.—See Table 7.

Comments.—This new species is most similar in size, outline, and dorsal interior to the species described as *Cranaena* cf. *C. hannibalensis* Moore, 1928, by Carter (1967) from the Chappel Limestone of central Texas. This Chappel species differs in being smaller, with a subovate to nearly circular outline and with the maximum width attained at midlength. *Cranaena hannibalensis* Moore, 1928, was described from the Hannibal Formation (middle Kinderhookian) of Pike County, Missouri, and Moore's types are not very similar to this new species, being smaller and less elongated, with a subovate outline and maximum width at midlength. In addition, the dorsum is flattened in some specimens. Unfortunately, the dorsal interior is unknown.

Material.—In addition to the illustrated types there are 23 articulated specimens and four disarticulated valves.

←

Fig. 27.—Transverse serial section of *Cranaena salinensis* n. sp., CM 45112, × 2. Numbers refer to distance from ventral beak (in mm).

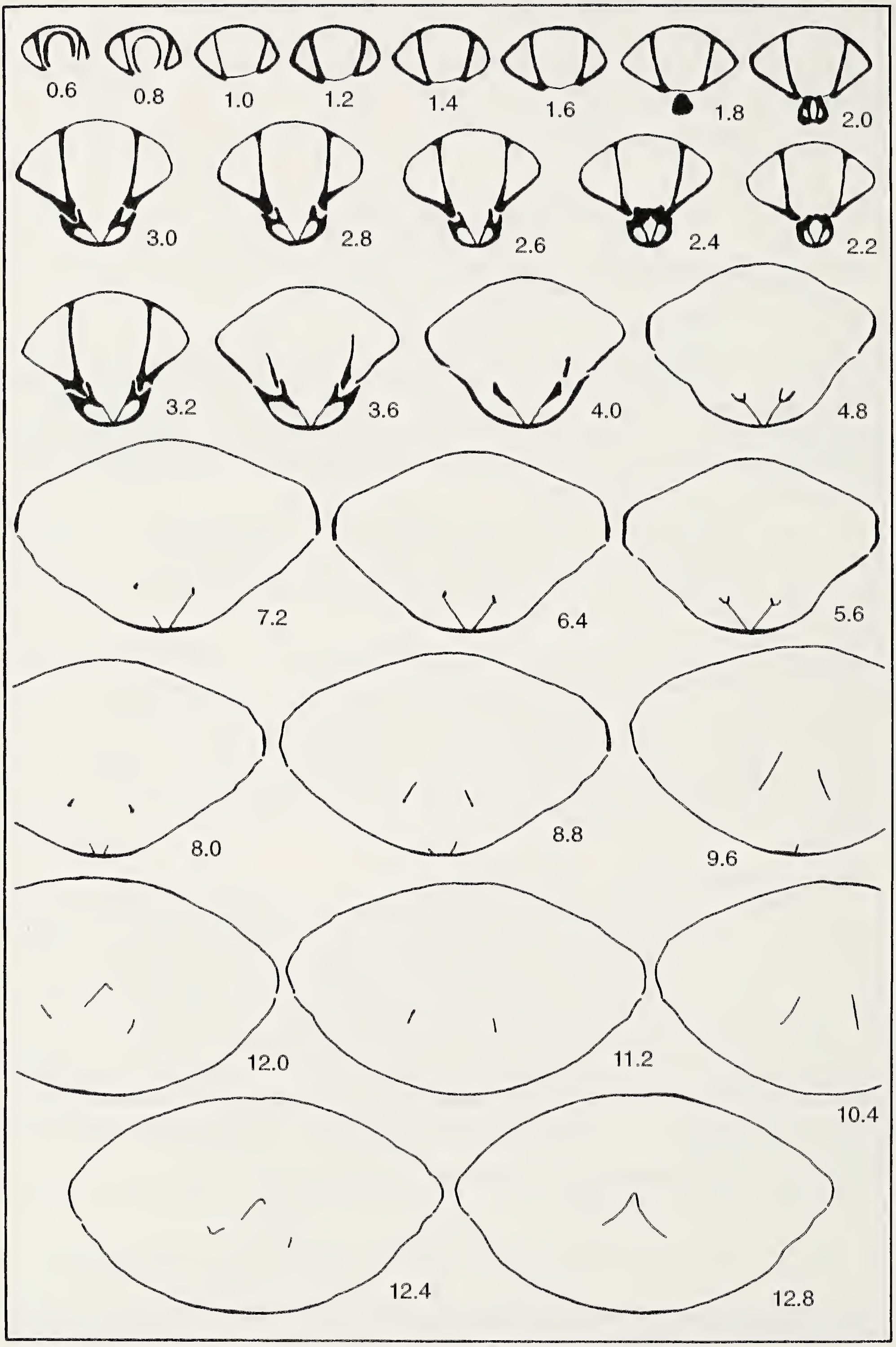
0.6
0.8
1.0
1.2
1.4
1.6
1.8
2.0
3.0
2.8
2.6
2.4
2.2
3.2
3.6
4.0
4.8
7.2
6.4
5.6
8.0
8.8
9.6
12.0
11.2
10.4
12.4
12.8

Table 8.—*Measurements (in mm) of the types of* Dielasma oklahomensis, *n. sp.*

Number	Length	Width	Thickness
CM 45106	+27.8	26.4	15.9
CM 45107	27.4	23.0	14.9
CM 45108	22.1	19.7	11.5

Family Dielasmatidae Schuchert, 1913
Subfamily Dielasmatinae Schuchert, 1913
Genus *Dielasma* King, 1859
Dielasma oklahomensis, **new species**
(Fig. 26A–L; 28)

Holotype.—CM 45107, Fig. 26E–H.

Paratypes.—CM 45106 and 45108, Fig. 26A–D, 26I–L.

Diagnosis.—Large, moderately elongate, subequally biconvex *Dielasma* with subpentagonal outline; narrow, shallow sulcus in ventral valve; and very weakly uniplicate anterior commissure.

Description.—Medium to large for genus, subequally biconvex, longitudinally subpentagonal in outline; greatest width and thickness near or posterior to midlength; anterior profile dorsibiconvex, lateral profile subequally lenticular; anterior commissure weakly uniplicate; fold absent or very weakly developed and narrow anteriorly, scarcely detectable; shallow, narrow sulcus present in anterior third or half of large specimens only, forming truncated front margin or slight emargination; growth varices strong on anterior half of shell, irregularly spaced; growth lines finely and regularly spaced; fine punctae densely arranged in quincunx.

Ventral valve moderately and evenly convex, most convex in umbo; posterolateral margins nearly straight; venter slightly arched posteriorly, with shallow, narrow sulcus in anterior half or third of shell; lateral slopes weakly convex; umbo broad, generally subtending an angle slightly greater than 90° in large specimens; beak ridges narrowly rounded, extending anteriorly and defining broad weakly concave palintropes; beak small, suberect; foramen subovate, moderately labiate, epithyrid; deltidium flattened or slightly convex; interior with pedicle collar and short dental plates, diverging slightly both anteriorly and laterally; teeth delicate, bladelike.

Dorsal valve slightly thicker than opposite valve, almost evenly convex in lateral profile, medially arched in anterior profile; lateral slopes moderately convex; most convex in slightly inflated umbonal region which is well defined by anterolateral concave flexures; beak small, protruding into delthyrium; fold generally absent, rarely present as weak, low prominence near anterior margin; interior with inner hingeplates nearly joining at floor of valve, diverging moderately anteriorly; crural bases originating at dorsal edges of inner socket ridges, attached to ventral edges of inner hinge plates and extending forward as rounded rods; crural processes moderately high converging ventrally; jugum projecting anteriorly.

Measurements of Types.—See Table 8.

Comments.—This new species is not similar to other Lower Mississippian *Dielasma* in North America. *Dielasma* is rare in the Lower Carboniferous of North America, there being documented occurrences noted only by Carter (1967, 1987) and Rodriguez and Gutschick (1968), the latter being tentatively referred to *Terebratula utah* Hall and Whitfield, 1877, which is unknown internally. The other

---

←

Fig. 28.—Transverse serial sections of *Dielasma oklahomensis* n. sp., CM 45113, × 2. Numbers refer to distance from ventral beak (in mm).

descriptions by Carter (1967, 1987) were inadequate for species assignment but the interiors and generic assignment were ascertained by means of serial sections.

Material.—In addition to the types there are five articulated specimens.

ACKNOWLEDGMENTS

The fieldwork for this report was supported by the M. Graham Netting Research Fund of the Carnegie Museum of Natural History and a grant from the Amoco Production Company. Albert Kollar provided valuable field assistance for which I am grateful.

LITERATURE CITED

AIZENVERG, D. E., AND V. I. POLETAEV. 1971. Brakhiopoda. Pp. 66–91, *in* [Atlas of the Tournaisian Fauna in the Donets Basin] (D. E. Aizenverg, ed.). Akademiia Nauk Ukrainskoi SSR, Institut Geologicheskikh Nauk, Naukova Dumka, Kiev. [In Russian]

BALASHOVA, E. A. 1955. Produktidy Turneiskikh otlozhenii Ber-Chogura (Mugodzhary). Uchenie Zapiski Leningradskogo Gosudarstvennogo Universiteta (LGU), Seriia Geologo-Pochvenno-Geograficheskaia, Vypusk 6, 189:124–156.

BRAND, P. J. 1972. Some British Carboniferous species of the brachiopod genus *Leptagonia* McCoy. Bulletin of the Geological Survey of Great Britain, 39:57–79.

BRUNTON, C. H. C. 1968. Silicified brachiopods from the Visean of County Fermanagh (II). Bulletin of the British Museum (Natural History), Geology Series, 16:1–70.

———. 1980. Type specimens of some Upper Palaeozoic Athyridide brachiopods. Bulletin of the British Museum (Natural History), Geology Series, 34:219–234.

BRUNTON, C. H. C., AND L. R. M. COCKS. 1996. The classification of the brachiopod order Strophomenida. Pp. 47–51, *in* Brachiopods, Proceedings of the Third International Brachiopod Congress, Sudbury, Ontario, Canada, 2–5 September 1995 (P. Copper and J. Jin, eds.). A. A. Balkema, Rotterdam, The Netherlands.

BRUNTON, C. H. C., AND D. C. MUNDY. 1988. Strophalosiacean and aulostegacean productoids (Brachiopoda) from the Craven Reef Belt (late Viséan) of North Yorkshire. Proceedings of the Yorkshire Geological Society, 47:55–88.

BRUNTON, C. H. C., S. S. LAZAREV, AND R. E. GRANT. 1995. A review and classification of the brachiopod order Productida. Palaeontology, 38:915–936.

CAMPBELL, K. S. W. 1957. A Lower Carboniferous brachiopod-coral fauna from New South Wales. Journal of Paleontology, 31:34–98.

———. 1959. The type species of three Upper Palaeozoic punctate spiriferoids. Palaeontology, 1: 351–363.

CARTER, J. L. 1967. Mississippian brachiopods from the Chappel Limestone of central Texas. Bulletins of American Paleontology, 53:253–488.

———. 1968. New genera and species of Mississippian brachiopods from the Burlington Limestone. Journal of Paleontology, 42:1140–1152.

———. 1972. Early Mississippian brachiopods from the Gilmore City Limestone of Iowa. Journal of Paleontology, 46:473–491.

———. 1985. The Lower Mississippian brachiopod genus *Punctothyris* Hyde is not endopunctate. Annals of Carnegie Museum, 54:375–391.

———. 1987. Lower Carboniferous brachiopods from the Banff Formation of western Alberta. Geological Survey of Canada Bulletin, 378:1–183.

———. 1991*a*. Validation of the genus *Rowleyella* Weller, 1911, and description of a new genus (Brachiopoda: Athyridida). Annals of Carnegie Museum, 60:83–91.

———. 1991*b*. A new aulostegid (Brachiopoda: Aulostegoidea) from the Lower Mississippian of northcentral Iowa. Annals of Carnegie Museum, 60:359–363.

———. 1992. New genera of Lower Carboniferous spiriferid brachiopods (Brachiopoda: Spiriferida). Annals of Carnegie Museum, 61:327–338.

CARTER, J. L., J. G. JOHNSON, R. GOURVENNEC, AND H.-F. HOU. 1994. A revised classification of the spiriferid brachiopods. Annals of Carnegie Museum, 63:327–374.

CLARKE, E. L., AND T. R. BEVERIDGE. 1952. A revision of the Early Mississippian nomenclature in western Missouri. Missouri Geological Survey and Water Resources, Report of Investigations, 13: 71–77.

CLARKE, T. H. 1917. New blastoids and brachiopods from the Rocky Mountains. Bulletin of the Museum of Comparative Zoology, 61:361–380.

Cline, L. C. 1934. Osage formations of southern Ozark region, Missouri, Arkansas, and Oklahoma. Bulletin of the American Association of Petroleum Geologists, 18:1132–1159.

Cotter, E. 1965. Waulsortian-type carbonate banks in the Mississippian Lodgepole Formation of central Montana. Journal of Geology, 73:881–888.

Demanet, F. 1923. Le Waulsortien de Sosoye et ses rapports fauniques avec le Waulsortien d'age Tournaisien Supérieur. Mémoirs de l'Institut Géologique de l'Université de Louvain, 11:39–284.

Fay, R. O. 1987. Columns 1–4, 6–12, 14–16, *in* Correlation of Stratigraphic Units in North America (cosuna) Project. Texas–Oklahoma Region (F. A. Lindberg, ed.). American Association of Petroleum Geologists, Tulsa, Oklahoma.

Folk, R. L. 1962. Spectral subdivision of limestone types. Pp. 62–84, *in* Classification of Carbonate Rocks (W. E. Ham, ed.). American Association of Petroleum Geologists, Memoir 1.

Fotieva, N. N. 1964. Turneiskie produktidy raiona pechory. Pp. 3–12, *in* Biostratigrafiia Neftegazonosnykh Oblastei SSSR (M. M. Aliev, ed.). Akademiia Nauk SSSR, Nauka, Moscow.

Girty, G. H. 1899. Geology of the Yellowstone National Park, part 2, section 2, Devonian and Carboniferous fossils. U.S. Geological Survey Monograph 32, Part 2:479–599.

———. 1915. Faunas of the Boone Limestone at St. Joe, Arkansas. U.S. Geological Survey Bulletin, 598:1–50.

———. 1929. The fauna of the middle Boone near Batesville, Arkansas. U.S. Geological Survey, Professional Paper, 154B:73–103.

———. 1931. New Carboniferous invertebrates—III. Journal of the Washington Academy of Sciences, 21:390–397.

Grant, R. E. 1965. The brachiopod superfamily Stenoscismatacea. Smithsonian Miscellaneous Collections, 148:1–192.

———. 1971. Brachiopods in the Permian reef environment of West Texas. Proceedings of the North American Paleontological Convention, Chicago, Illinois, September 1969, Part J:1444–1481.

Hall, J. 1858. Part 2, Paleontology. Pp. 473–724, *in* Report on the Geological Survey of the State of Iowa (J. Hall and J. D. Whitney). Volume 1.

Hall, J., and R. P. Whitfield. 1877. Paleontology. Part 2. U.S. Geological Exploration of the 40th parallel, Volume 4.

Harbaugh, J. W. 1957. Mississippian bioherms in northeast Oklahoma. Bulletin of the American Association of Petroleum Geologists, 41:2530–2544.

Herrick, C. L. 1888. The geology of Licking County, Ohio. Part 4. List of Waverly fossils continued. Bulletin of the Geology Laboratory of Denison University, 4:11–60.

Hopkins, T. C. 1893. Marbles and other limestones. Pp. 253–349, *in* Arkansas Geological Survey, Annual Report for 1890, Volume 4.

Huffman, G. C. 1958. Geology of the flanks of the Ozark Uplift. Oklahoma Geological Survey Bulletin, 77:1–281.

Hyde, J. E. 1953. The Mississippian Formations of Central and Southern Ohio. Ohio Geological Survey Bulletin 51.

Kalashnikov, N. V. 1974. Rannekamenougol'nye brakhiopody pechorskogo urala. Akademiya Nauk SSSR, Komi Filial, Institut Geologii, "Nauka," Leningrad, USSR.

Lane, H. R. 1978. The Burlington shelf (Mississippian, north-central United States). Geologica et Palaeontologica, 12:165–175.

———. 1982. The distribution of the Waulsortian facies in North America as exemplified in the Sacramento Mountains of New Mexico. Pp. 96–114, *in* Symposium on the Paleoenvironmental Setting and Distribution of the Waulsortian Facies (K. Bolton, H. R. Lane, and D. V. LeMone, eds.). El Paso Geological Society and the University of Texas at El Paso, El Paso, Texas.

Léveillé, C. 1835. Aperçu géologique de quelques localités trés riche en coquilles sur les frontières de France et de Belgique. Memoires Societé géologique de France, 2:29–40.

McKnight, E. T., and R. P. Fischer. 1970. Geology and ore deposits of the Picher Field Oklahoma and Kansas. U.S. Geological Survey Professional Paper, 588:1–163.

Miller, S. A. 1881. Subcarboniferous fossils from the Lake Valley mining district of New Mexico, with descriptions of new species. Journal of the Cincinnati Society of Natural History, 4:306–315.

———. 1892. Palaeontology. Advance Sheets, 18th Report on the Geological Survey of Indiana.

Moore, R. C. 1928. Early Mississippian formations in Missouri. Missouri Bureau of Geology and Mines, 2nd Series, 21:1–283.

Mundy, D. J. C., and C. H. C. Brunton. 1985. Morphological similarities in some British Dinantian and Texas Permian reef brachipods. Neuvième Congrès International de Stratigraphie et de Géologie du Carbonifère, Compte Rendu, 5:225–232.

NORTH, F. J. 1920. On *Syringothyris* Winchell, and certain Carboniferous Brachiopoda referred to *Spiriferina* D'Orbigny. Quarterly Journal of the Geological Society, 76:162–227.

PAECKELMANN, W. 1931. Die Brachiopoden des deutschen Unterkarbons. 2. Teil: Die Productinae und Productus-ähnlichen Chonetinae. Jahrbuch der Preussichen Geologischen Landesanstalt (neue Folge), 136:1–440.

PHILLIPS, J. 1836. Illustrations of the geology of Yorkshire. Part II. The Mountain Limestone district. London, England.

RODRIGUEZ, J., AND R. C. GUTSCHICK. 1968. *Productina, Cyrtina,* and *Dielasma* (Brachiopoda), from the Lodgepole Limestone (Mississippian) of southwestern Montana. Journal of Paleontology, 42: 1027–1032.

———. 1978. A new shallow water *Schizophoria* from the Leatham Formation (Late Famennian), northeastern Utah. Journal of Paleontology, 52:1346–1355.

ROTAI, A. P. 1931. Brakhiopody i stragrigrafiia nizhnego karbona Donetskogo basseina. Trudy Glavnogo Geologo-Razvedochnogo Ypravleniya, 73:35–144.

ROWLEY, R. R. 1900. Descriptions of new species of fossils from the Devonian and sub-Carboniferous rocks of Missouri. American Geologist, 25:261–273.

SARYCHEVA, T. G. 1963. Productacea. Pp. 124–237, pl. 13–38, *in* Brakhiopody i paleogeografiya karbon Kuznetskoi kotloviny (T. G. Sarycheva, A. N. Sokolskaya, G. A. Beznosova, and S. V. Maksimova). Akademiya Nauk SSSR, Paleontologicheskii Institut, Moscow, USSR, Trudy 95.

SAVAGE, N. M. 1996. Classification of Paleozoic rhynchonellid brachiopods. Pp. 249–260, *in* Brachiopods, Proceedings of the Third International Brachiopod Congress, Sudbury, Ontario, Canada, 2–5 September 1995 (P. Copper and J. Jin, eds.). A. A. Balkema, Rotterdam, The Netherlands.

SHAW, A. B. 1962. Rhynchonellid brachiopods and a *Torynifer* from the Madison Group (Mississippian). Journal of Paleontology, 36:630–637.

SHIMER, H. S. 1926. Upper Paleozoic faunas of the Lake Minnewanka section, near Banff, Alberta. Geological Survey of Canada, Bulletin 42.

SOKOLSKAYA, A. N. 1941. Lower Carboniferious and Devonian–Carboniferous brachiopods of the Moscow Basin (Tschernyschino, Upa and Malevka–Murajevnia beds), Part 1, Spiriferidae. Akademiia Nauk SSSR, Paleontologicheskogo Instituta, Trudy, 12:1–139.

SUTTON, A. H. 1942. *Worthenella, Setigerella,* and new productid species. Journal of Paleontology, 16:464–470.

SWALLOW, G. C. 1860. Descriptions of some new fossils from the Carboniferous and Devonian rocks of Missouri. Academy of Science of St. Louis Transactions, 1:635–659.

THOMAS, I. 1914. The British Carboniferous Producti. I. Genera *Pustula* and *Overtonia.* Geological Survey of Great Britain, Palaeontology, Memoirs, 1:197–366.

THOMPSON, T. L., AND L. D. FELLOWS. 1970. Stratigraphy and conodont biostratigraphy of Kinderhookian and Osagean rocks of southwestern Missouri and adjacent areas. Missouri Geological Survey and Water Resources, Report of Investigations, 45:1–263.

THOMPSON, T. L., N. S. FORD, AND W. C. SWEET. 1971. Conodonts from the Rushville Formation of Ohio. Journal of Paleontology, 45:704–712.

TROELL, A. R. 1962. Lower Mississippian bioherms of southwestern Missouri and northwestern Arkansas. Journal of Sedimentary Petrology, 32:629–664.

WELLER, S. 1909. Kinderhook faunal studies. 5. The fauna of the Fern Glen Formation. Geological Society of America Bulletin, 20:265–332.

———. 1910. Internal characters of some Mississippian rhynchonelliform shells. Geological Society of America Bulletin, 21:497–516.

———. 1914. The Mississippian Brachiopoda of the Mississippi Valley Basin. Illinois Geological Survey Monograph, 1:1–508.

WHITE, C. A. 1860. Observations upon the geology and paleontology of Burlington, Iowa, and its vicinity. Boston Society of Natural History Journal, 7:209–235.

———. 1862. Descriptions of new species of fossils from the Devonian and Carboniferous rocks of the Mississippi Valley. Boston Society of Natural History Proceedings, 9:8–33.

WHITE, C. A., AND R. P. WHITFIELD. 1862. Observations upon the rocks of the Mississippi Valley, which have been referred to the Chemung Group of New York, together with descriptions of new species of fossils from the same horizon at Burlington, Iowa. Boston Society of Natural History Proceedings, 3:289–306.

WILLIAMS, A., S. J. CARLSON, C. H. C. BRUNTON, L. E. HOLMER, AND L. POPOV. 1996. A supra-ordinal classification of the Brachiopoda. Philosophical Transactions of the Royal Society of London (B), 351:1171–1193.

WILSON, J. L. 1975. Carbonate facies in geologic history. Springer-Verlag, New York, New York.

WINCHELL, A. 1863. Descriptions of fossils from the yellow sandstones lying beneath the "Burlington Limestone" at Burlington, Iowa. Academy of Sciences of Philadelphia Proceedings:2–25.

———. 1865. Descriptions of new species of fossils, from the Marshall Group of Michigan, and its supposed equivalent in other states; with notes on some fossils of the same age previously described. Academy of Natural Sciences of Philadelphia Proceedings, Series 2, 17:109–133.

INSTRUCTIONS FOR AUTHORS

ANNALS OF CARNEGIE MUSEUM consist of contributions to the earth sciences (including paleontology), life sciences, and anthropology, in 30 by 46 picas format (127 by 195 mm or 5 by 7⅝ inches). Submit all manuscripts to the Office of Scientific Publications. Authors should give particular attention to scientific content, format, and general style for the ANNALS. **Manuscripts that do not conform to the style of the ANNALS will be returned to the author immediately.** Every manuscript will be subjected to external peer review. Authors should submit the names, addresses, phone and fax numbers, and e-mail addresses of at least four qualified potential reviewers for each manuscript. Authors will be asked to subsidize, if funds are available, any or all costs of publication (approximately $100/page printed). A detailed set of instructions to authors may be requested from the Office of Scientific Publications.

Manuscript Style.—Articles should include the following items in this order: title page, abstract, text (with desired headings), acknowledgments, literature cited, tables, figure captions, and copies of illustrations. All manuscripts must be typed ***double-spaced*** on standard 8½ by 11-inch white bond paper, with at least one-inch margins all around, and submitted ***in quadruplicate***—an original for the editors, and three review copies. All pages should be numbered, including tables, literature cited, and the list of figure captions. Only correspondence quality or better dot matrix printouts will be accepted; draft mode is unacceptable. A monospaced font, (e.g., Courier) is required. A disk in WordPerfect x.x or ASCII is helpful.

Title Page. The title should be brief, include the animal or plant group involved, be placed on a separate page, and appear two to three inches below the top margin. Include the author's name(s) and the affiliations of non-CMNH authors. In the case of multiple authorship, indicate the address to which proofs should be sent.

Abstracts. Abstracts should be short, but substantive, and included at the head of the first page of text.

Text. Do not right justify text or break (hyphenate) a word at the end of a line. ***Footnotes and acknowledgments as footnotes are unacceptable.*** All text is double-spaced in a monospaced font (e.g., Courier).

Tables and Figure Legends. The list of figure legends and each table should be typed consecutively on individual pages separate from the text. Tables must be double-spaced throughout with **no vertical lines.**

Measurements. Metric units should be used, if possible.

Literature Cited. All references to literature in text must appear in the Literature Cited section. The data (author, date, and page) in both citations must agree. ***Do not abbreviate the titles of periodicals or serials.*** The following style, double-spaced, should be used in Literature Cited:

1) Two authors in a journal series:
    Soltis, D. E., and P. S. Soltis. 1992. The distribution of selfing rates in homosporous ferns. American Journal of Botany, 79:97–100.
2) Same authors repeated—use three-em dash:
    ———. 1923. The fauna of the Ardyn Obo Formation. American Museum of Natural History Novitates, 98:1–5.
3) Same authors plus a third author—repeat all authors:
    Knutson, L. V., R. E. Orth, and W. L. Murphy. 1986. Catalog of Sciomyzidae (Diptera) of America north of Mexico. Entomography, 4: 1–53.
4) Chapter in an edited volume:
    Rausch, R. L. 1963. A review of the distribution of Holarctic mammals. Pp. 29–43, *in* Pacific Basin Biogeography (J. L. Gressitt, ed.). Bishop Museum Press, Honolulu, Hawaii.
5) Unpublished dissertation:
    Smith, J. P. 1976. Review of Eocene Mammals. Unpublished Ph.D. Dissert., University of California, Berkeley, California.
6) Book:
    White, M. J. D. 1961. The Chromosomes. Metheuen and Co., Ltd., London, United Kingdom.
7) Journal articles with usual volume and issue number:
    Anderson, W. I. 1969. Lower Mississippian conodonts from northern Iowa. Journal of Paleontology, 43:916–928.

Figures. Including all illustrative materials (line art, halftones, photographs), figures are to be numbered in Arabic numerals. Four sets of figures are required, one (original artwork) for reproduction, three for reviewers. Photocopies of photographs for reviewers are usually not acceptable but are adequate for line drawing review copies. Figures may not be larger than 17 by 12 inches. Reducing figures is the responsibility of the author. All figures must be reducible to a maximum of 127 by 195 mm (30 by 46 picas) without loss of clarity. Line copy should be designed for reduction to ⅔ or ½ or actual size. Typewritten figure copy will not be accepted. Photographic figures should be submitted at **actual reproduction size**, if possible.

Rectangular halftone figures should be abutted, without intervening spaces. The printer will insert narrow white spaces during the reproduction process. All figures must have **minimally** one-inch borders all around. Each figure should be given a protective cover and identified on the back side.

Lettering and/or a magnification scale (linear metric scale) for rectangular halftone figures should be placed directly on the photo, not in a blank space between photos. The scale or lettering for closely cropped photos can be placed in blank areas close to the figure.

Proof.—The author should answer all queried proof marks and check the entire proof copy. Return corrected page proof with the edited manuscript ***promptly*** to the Office of Scientific Publications.

If an author chooses to make extensive alterations to a paper in proof stage, the author will bear the cost. Original manuscripts will not be returned unless requested. Figures will be returned to the author only if requested prior to publication.

AS
36
P7X
NH

ISSN 0097-4463

SMITHSONIAN
AUG 17 1999
LIBRARIES

ANNALS of CARNEGIE MUSEUM

THE CARNEGIE MUSEUM OF NATURAL HISTORY
4400 FORBES AVENUE • PITTSBURGH, PENNSYLVANIA 15213

VOLUME 68 12 AUGUST 1999 NUMBER 3

CONTENTS

ARTICLES

Biology and immature stages of snail-killing flies belonging to the genus *Tetanocera* (Insecta: Diptera: Sciomyzidae). III. Life histories of the predators of aquatic snails . . . . **B. A. Foote** 151

Revision of the Wind River faunas, Early Eocene of central Wyoming. Part 14. Postcranium of *Shoshonius cooperi* (Mammalia: Primates) . . . . **Marian Dagosto, Daniel L. Gebo, and K. Christopher Beard** 175

REVIEW

Rattlesnake: Portrait of a Predator (Manny Rubio) . . . . . . **Travis J. Laduc** 213

Editors, ANNALS, BULLETIN and SPECIAL PUBLICATIONS:

J. L. Carter, Ph.D
B. C. Livezey, Ph.D
D. R. Watters, Ph.D
M. A. Schmidt, ELS, Assistant Editor

Manuscripts, subscriptions, orders for individual numbers, and changes of address should be sent to:

Office of Scientific Publications
Carnegie Museum of Natural History
4400 Forbes Avenue
Pittsburgh, PA 15213-4080
Phone (412) 622-3287
Fax (412) 622-8837
E-mail: scipubs@clpgh.org

ANNALS OF CARNEGIE MUSEUM is published quarterly by The Carnegie Museum of Natural History, 4400 Forbes Avenue, Pittsburgh, Pennsylvania 15213-4080, by the authority of the Board of Trustees of Carnegie Institute.

© 1999 Carnegie Institute.

♾ This paper meets the requirements of ANSI/NISO Z39.48-1992 (Permanence of Paper).

ANNALS OF CARNEGIE MUSEUM
VOL. 68, NUMBER 3, PP. 151–174 12 AUGUST 1999

BIOLOGY AND IMMATURE STAGES OF SNAIL-KILLING FLIES BELONGING TO THE GENUS *TETANOCERA* (INSECTA: DIPTERA: SCIOMYZIDAE)

III. LIFE HISTORIES OF THE PREDATORS OF AQUATIC SNAILS

B. A. FOOTE[1]
Research Associate, Section of Invertebrate Zoology

ABSTRACT

The geographic distribution, life history, and larval feeding habits of ten species of*Tetanocera* that prey on aquatic pulmonate snails are presented. All species are generalist predators of a broad mix of aquatic pulmonate snails. Differences in phenologies are apparent. Seven species are univoltine, whereas three are multivoltine. Three species overwinter as pupae, one species overwinters as partially grown larvae, and four species pass the winter months as diapausing first-instar larvae within eggs.

KEY WORDS: Diptera, Sciomyzidae, *Tetanocera*, aquatic snails, life histories

INTRODUCTION

This is the third paper in a series devoted to the biology and immature stages of Nearctic species of malacophagous *Tetanocera*. The first paper (Foote, 1996*a*) reviewed the literature, presented materials and methods, and gave natural history information for two species, *T. fuscinervis* (Zetterstedt) and *T. silvatica* Meigen, associated with shoreline snails. The second paper (Foote, 1996*b*) gave natural history information on four species, *T. melanostigma* Steyskal, *T. oxia* Steyskal, *T. rotundicornis* Loew, and *T. spirifera* Melander, that feed on succineid snails. The present paper focuses on the natural history of ten species, *T. annae* Steyskal, *T. ferruginea* Fallén, *T. latifibula* Frey, *T. loewi* Steyskal, *T. mesopora* Steyskal, *T. montana* Day, *T. obtusifibula* Melander, *T. robusta* Loew, *T. spreta* Wulp, and *T. vicina* Macquart, whose larvae prey on pulmonate aquatic snails.

LIFE HISTORIES

Tetanocera annae Steyskal

Steyskal, 1938. Occasional Papers of the Museum of Zoology of the University of Michigan, 386:5.

Tetanocera annae is a Nearctic species (Knutson et al., 1986) that has been recorded from Ontario and New Hampshire, west to British Columbia and Montana, and south to North Carolina and Ohio (Fig. 1). In central New York and northeastern Ohio, adults were found most commonly in partially wooded swamps that contained some standing water throughout the year. They were rarely collected in swampy woodlands containing only vernal pools, and were relatively uncommon in open grass-sedge and cattail marshes. Further evidence that this species prefers more wooded sites is that all of the field-collected puparia were found floating at the water's surface in small stands of alders or willows bordering

---

[1] Department of Biological Sciences, Kent State University, Kent, Ohio 44242. Submitted 28 October 1996.

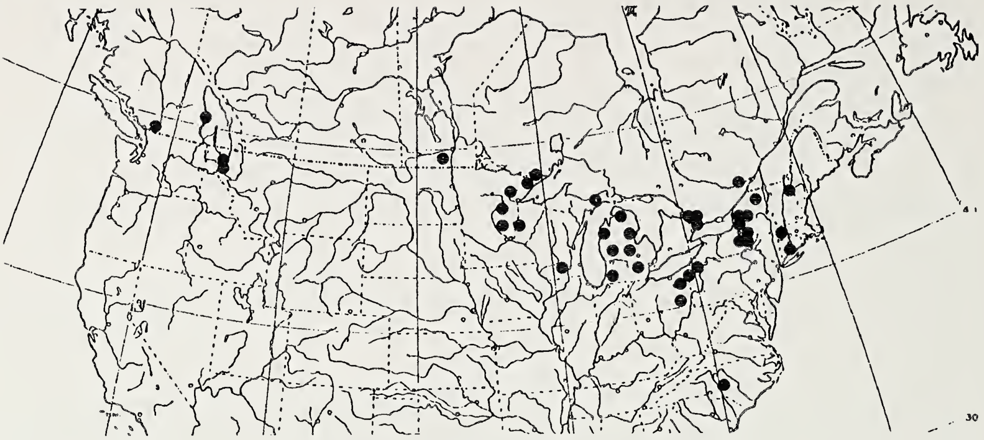

Fig. 1.—Distribution of *T. annae*.

open marshes. In contrast, the similar puparia of *T. ferruginea* were nearly always found in wetlands dominated by herbaceous vegetation.

Rearings of this species were initiated from two females collected on 21 August from the shaded marshy borders of a small woodland stream located near Oswego (Oswego County), New York. A more complete rearing was obtained from a female collected at the White Church marsh (Tompkins County) south of Ithaca on 3 July. Additional rearings were established from puparia collected in late March in an alder swamp near Ithaca.

Most of the nearly 500 eggs obtained in the laboratory rearings were scattered singly over the glass walls of the breeding jars, although a few were affixed to the cheesecloth covers. No eggs were placed on living or dead snails or on the peat moss that lined the bottom of the jars. The single female collected on 3 July deposited 379 eggs before dying on 11 August. Her last ten eggs were laid on 10 August. The incubation period lasted three to four days (n = 51).

In the rearing dishes, newly hatched larvae moved down to the water surface and broke through the surface film. The dichotomously branched interspiracular processes (float hairs) were obviously hydrofuge and served to keep the posterior end of the larvae in contact with the surface film. Therefore, the larvae are best considered to be infraneustic. Bubbles of air within the larval gut added buoyancy, and larvae held underwater quickly floated back to the surface film when released. A larva that was held continuously below the surface died within 20 minutes, suggesting that newly hatched larvae are not capable of foraging below the water surface.

At the surface film, larvae always came to rest against some support, usually the walls of the rearing dishes. Although they readily moved around the edges of the dish, they rarely ventured out into the open water. When larvae were placed in the open water, they quickly moved toward the dish edge by rapid downstrokes of the anterior half of the body. These observations suggest that in nature, the larvae lie in contact with floating debris or rest against emergent vegetation penetrating the water surface.

Larvae were predacious and showed no obvious preference for any particular species of pulmonate snail. They readily consumed numerous individuals of *Lym-*

naea palustris (Müller), *Helisoma trivolvis* (Say), *Biomphalaria glabrata* (Say), *Physella gyrina* (Say), and *Oxyloma effusa* (Pfeiffer). Newly hatched larvae easily overcame small snails that were less than 5.0 mm in length but were usually unsuccessful in attacking larger individuals. In contrast, third-instar larvae attacked and consumed the largest individuals of *L. palustris* available (shell length, 20.5 mm).

Larvae seemed to locate potential prey by a series of random movements. When a larva came in contact with a living snail, it quickly located the exposed foot and attacked the flesh with swift downward thrusts of its mandibles (mouth hooks). Shortly thereafter, a dark mass of ingested food appeared in the larva's gut. Unless disturbed, the larva fed to repletion before abandoning its prey. If the snail was less than 10 mm in length and the larva in the second or third instar, the flesh of the prey was usually consumed entirely. On the other hand, smaller larvae feeding on larger snails frequently left some flesh in the shell. No snail that had suffered feeding damage was seen to recover, even when only a small fraction of its flesh had been consumed.

The first larval stadium lasted an average of five days; the second, about seven days; and the third, from eight to ten days ($n = 13$). Shortly before forming puparia at the water surface, larvae voided the gut, became quite inactive, and did not feed for at least two days before pupariating. Although 16 puparia were obtained in the laboratory rearings, only two adults emerged. One adult emerged in 17 days, but the second one required 37 days. The remaining pupae apparently entered diapause, as they did not produce adults during the two months they were held at room temperature.

The discovery of puparia in the field on 29 March (two) and 3 April (three) coupled with my failure to obtain emergence from puparia formed in the laboratory during the summer months is strong evidence that overwintering occurs as diapausing pupae. This is probably a univoltine species.

One of three puparia collected on 2 April in the alder swamp near Ithaca produced a female of an undetermined species of Ichneumonidae on 14 April.

Tetanocera ferruginea Fallén

Fallén. 1820. Sciomyzides Sveciae, 9.

Tetanocera ferruginea is a common species in both Europe (Rozkošný and Elberg, 1984) and North America (Knutson et al., 1986). In the Nearctic region it occurs across the continent from Newfoundland to Alaska and south to New Jersey, Illinois, and California (Fig. 2).

In central New York and in Idaho, this species occurred most commonly in emergent or shoreline vegetation bordering permanent ponds and marshes, and was especially abundant in unshaded grass-sedge and cattail marshes. It was uncommon in marshes whose standing water disappeared during the summer and was very rare in woodland swamps. In northeastern Ohio, this was a common species in open marshes that retained water throughout the year.

At Ithaca, rearings were initiated from material collected at Boole's Backwater and at the Inlet Valley, Floral Avenue, and White Church marshes (Tompkins County). In southern Idaho, a rearing was obtained from adults collected in an open grass-sedge-cattail marsh located near Hagerman (Gooding County). Ohio rearings were initiated from three females collected in a stand of emergent veg-

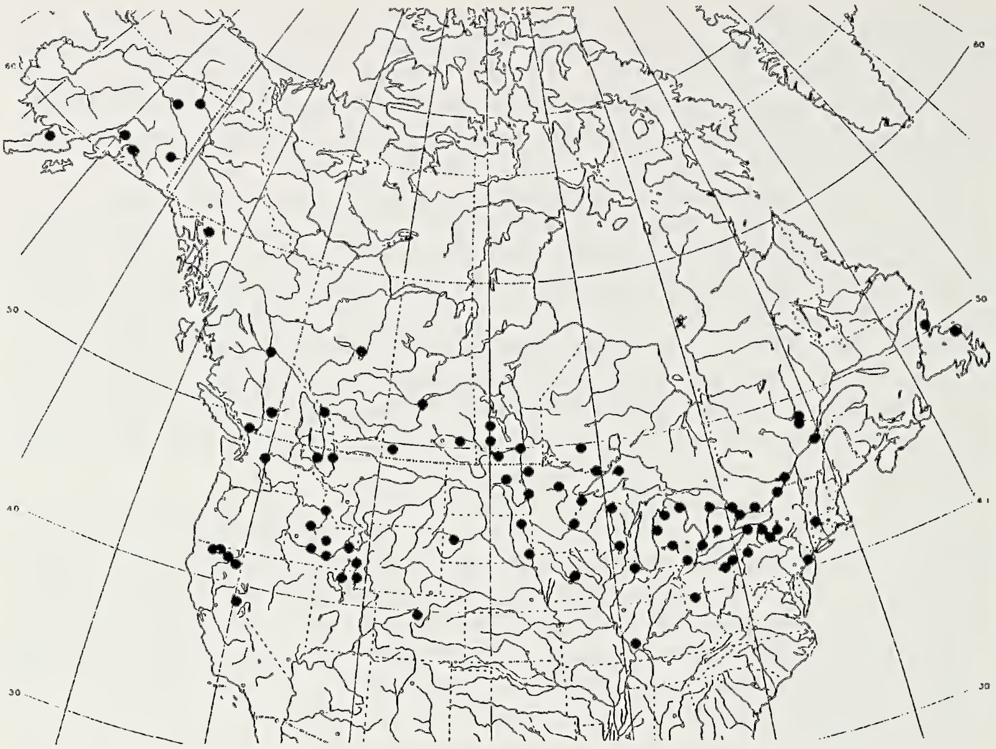

Fig. 2.—Distribution of *T. ferruginea.*

etation (*Sparganium, Juncus, Typha, Scirpus, Pontederia*) growing in the shallow water bordering Lake Hodgson (Portage County).

Females scattered most of their eggs singly over the glass walls of the breeding jars, but other eggs were placed on fragments of cattail and on projecting bits of sphagnum moss. A few were placed on the cheesecloth covers and a very few were laid on shells of living *Lymnaea* and *Helisoma* snails. Under laboratory conditions eggs hatched in four to six days (n = 100: Ithaca, 45; Hagerman, 40, Lake Hodgson, 15). Newly hatched larvae moved down the substrate until they encountered the surface film of the water in the breeding container. They then broke through the film and assumed a position on the underside of the film, retaining contact with atmospheric air via their spiracles that penetrated the film. No evidence was obtained that suggested that larvae can leave the surface to prey on completely immersed aquatic snails.

Larvae in nature were generalized predators of pulmonate aquatic snails. At Boole's Backwater, third-instar larvae were seen feeding on *Lymnaea palustris* and *Helisoma* sp. Laboratory-reared larvae consumed many individuals of *Lymnaea humilis* (Say), *L. obrussa* (Say), *L. palustris, Gyraulus parvus* (Say), *Helisoma anceps* (Menke), *H. subcrenata* Carpenter, *H. trivolvis, Biomphalaria glabrata, Planorbula armigera* (Say), *Physella gyrina* (Say), and *Aplexa hypnorum* (L.), as well as the terrestrial snails *Cionella lubrica* (Müller), *Zonitoides arboreus* (Say), *Catinella avara* (Say), and *Oxyloma effusa* (Pfeiffer).

Very few snails were able to evade an attacking larva. Occasionally a smaller larva became trapped in the mucus produced by a large snail as it retreated into its shell, but larger second- and third-instar larvae were never observed to be trapped by this secretion. A specimen of *Biomphalaria glabrata* (diameter, 10.2 mm) showed a progressive slowing of the heartbeat during an attack by a nearly mature third-instar larva, and the heart action ceased within 18 minutes. Many large individuals of *Helisoma* bled profusely shortly after being attacked, indicating that their hemocoeles had been ruptured. Bleeding snails never recovered, even if the attacking larva was removed.

In the laboratory, the first larval stadium lasted four to six days; the second, three to four days; and the third, ten to 14 days (*n* = 44: Ithaca, 30; Hagerman, 14).

Fully grown larvae did not move into drier situations prior to pupation, and many puparia were obtained from larvae developing in dishes that contained only water and snails. When the substrate was moist paper toweling, as many puparia were formed above the toweling as below it. Very few of the larvae reared on moist sphagnum moss burrowed into it before pupation. The presence of float hairs and the upturned condition of the posterior end of the puparium indicate that this stage is adapted for floating. In nature puparia frequently were found floating in water several centimeters deep, usually in contact with debris or emergent vegetation. Adults crawled up onto the floating material or onto the vegetation before undergoing hardening of the body.

The pupal stage lasted nine to 12 days during the spring and summer breeding season (*n* = 33: Ithaca, 21; Hagerman, 12).

Mating began within a few days after females emerged from puparia. Females accepted males repeatedly, and copulation lasted from a few minutes to more than two hours. Mated, laboratory-reared females usually began ovipositing six to eight days after emerging. A female that emerged and mated on 13 May began ovipositing on 19 May. She laid from zero to 102 eggs daily between 19 May and 10 June, depositing a total of 535 eggs. There was a gradual decline in productivity after the first five days. Thus, between 19 May and 22 May an average of 60 eggs was laid daily, but from 23 May to 10 June the average dropped to 18 daily. The female died on 12 June, having lived for 30 days.

During oviposition, females moved slowly over the substrate while frequently applying the tip of the abdomen to the moss, cattail, or glass wall. Eggs were laid individually, and each egg-laying act took less than two seconds. Eggs were not laid in compact masses as has been observed for *Sepedon* (Neff and Berg, 1966), but were scattered over the substrate.

In central New York, the earliest seasonal record for adults was obtained on 13 May; the latest, on 28 August, and capture records are nearly continuous between those dates. Larvae were collected on 25 June and 1 August at Boole's Backwater in Ithaca, on 12 August at the Inlet Valley marsh, and on 29 October at the Floral Avenue marsh. Puparia were taken during February, March, April, May, and November. In laboratory rearings during the summer season, one generation followed another with no delays in development, each life cycle requiring approximately 40 days. Adults frequently lived at least until the first of their progeny emerged as adults. There is no reason to suppose that longevity of adults is appreciably less or that development is much slower in nature, and these observations establish beyond doubt that this species should be placed in Group 1 of Soós (1958)—eurychrone species having long, interrupted flight periods and breeding continuously to produce several generations per year. However, Soós placed *T. ferruginea* in Group 3 because he noted an interruption in the capture records of the pinned specimens in certain European museums. Interruptions in capture records may result merely from interruptions in collecting efforts, not from actual interruptions in the occurrence of adults in nature. This is the correct explanation of data presented by Soós on *T. ferruginea.*

This species overwinters in the pupal stage. The pupae evidently can survive even when frozen in the ice cover of ponds and marshes. Seventy-eight puparia collected from marshes in central New York during February, March, and early April produced adults in nine to 11 days after being brought into the heated laboratory. All of these were taken at least one month before the first adult was collected in the area, and some were taken more than three months before that date. The earliest record for puparia that produced adults was made on 10 February, 1955, at the Inlet Valley marsh. Although ice still covered the marsh, it became soft and flexible under an unseasonably warm sun during that afternoon. As the ice sagged under my weight, water collected on top of it, and six puparia of *T. ferruginea* (plus 18 puparia of other species) were found floating in this water. Undoubtedly the water that was forced up onto the ice as the ice was depressed must have escaped through the holes that had formed around the stems of emergent vegetation, as melting occurred first around these dark objects. Puparia typically float into contact with any object which thus breaks the surface film, and they must have been concentrated in such situations before the marsh froze.

Six species of Ichneumonidae, *Theroscopus pumilis* (Cresson), *Theroscopus* sp. A, *Theroscopus* sp. B, *Theroscopus* sp. C, *Mesoleptus* sp., and *Phygadeuon* sp., were reared from puparia collected in marshes near Ithaca. Each infested puparium produced only one wasp. During the spring of 1958, information was obtained on the percentage of puparia infested with ichneumonids. Forty-five puparia collected on 28 February at the Inlet Valley marsh produced 33 flies and seven wasps. Fifteen collected on 30 March at the Floral Avenue marsh produced seven flies and five wasps. Twenty-one collected on 2 April at the same marsh produced 11 flies and seven wasps. Eighteen taken on 3 April at the same marsh produced 12 flies and three wasps. Sixty-two collected on 5 April 5 at the Inlet Valley marsh produced 45 flies and 13 wasps. Thus, ichneumonid larvae infested 16 to 33% of the overwintering puparia. From the total of 161 puparia, 35 wasps were reared (21%). In each sample, the adult wasps emerged two to six days after the last emergence of flies.

Tetanocera latifibula Frey (= *hespera* Steyskal, 1959)

Frey, 1924. Notulae Entomologicae, 4:51.

Steyskal (1959) described *T. hespera* from material taken in western North America, but this author placed it in synonymy with *T. latifibula* (Steyskal, 1965). It is now known to occur both in Europe (Rozkošný and Elberg, 1984) and North America (Knutson et al., 1986), where it ranges from Iowa to California and north to Alaska (Fig. 3). Adults were taken most commonly in Idaho and Washington by sweeping emergent and shoreline vegetation bordering open, permanent ponds and lakes, but a few specimens were collected also from unshaded vernal marshes that became dry by midsummer.

A rearing was initiated with a female swept on 17 August from a dense stand of *Scirpus* sp. growing in about seven centimeters of water at a small, permanent

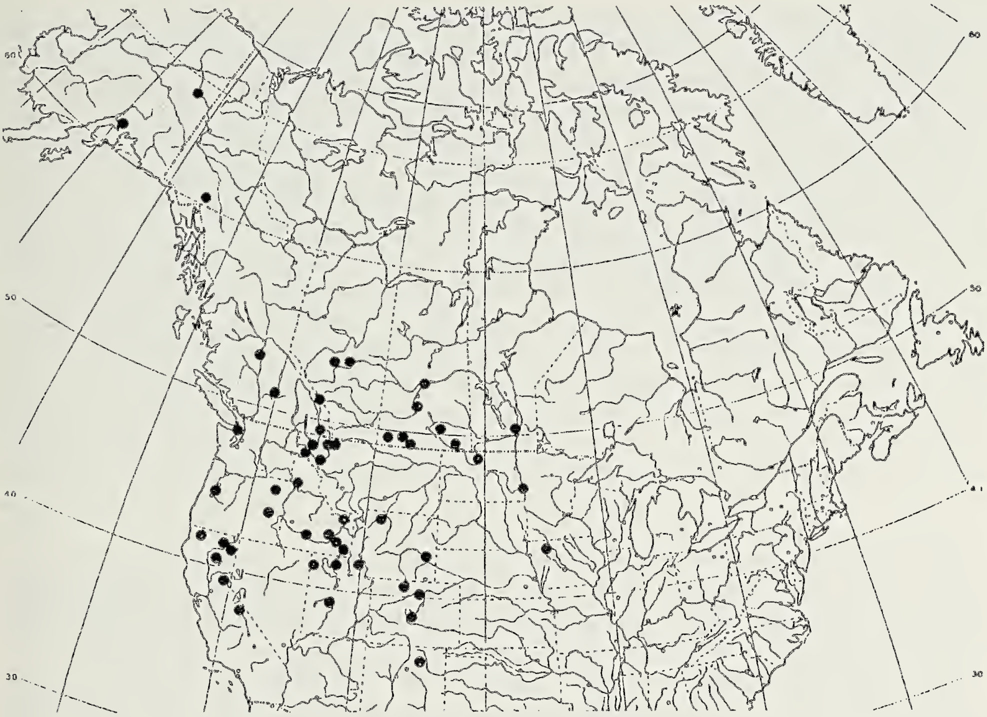

Fig. 3.—Distribution of *T. latifibula*.

lake located along State Route 18 about 33 km south of Sprague (Whitman County), Washington. She deposited 37 eggs on the cheesecloth cover of the breeding jar between 18 and 31 August.

Well-formed, living larvae were found when six eggs laid on 18 August were dissected on 31 August. These were transferred to a small amount of water and provided with several small *Helisoma* snails, but all remained very sluggish, did not feed, and died within five days. Hatching still had not occurred by 11 September, when the remaining 31 eggs were placed in a refrigerator and held at 7°C. Six apparently viable eggs were removed from the refrigerator and returned to the heated laboratory on 13 February. One egg dissected contained a living, first-instar larvae, which was placed in water and given a small *Physella*. The larva had not fed by 14 February, and was returned to the refrigerator. When checked on 16 February, this larva had consumed a 1.4- and a 2.7-mm-long *Physella* in the refrigerator. It was returned to the heated laboratory on 19 February, where it continued to feed on small *Physella*, consuming eight snails (1.4–5.0 mm long) while in the first instar, six (4.0–5.0 mm long) in the second, and 24 (2.9–10.0 mm long) in the third, for a total of 38 snails as a larva. The larva molted into the second instar on 24 February, into the third on 1 March, and finally formed a puparium on 20 March, 35 days after it was removed from the egg. During the four days preceding pupation the larva did not feed and remained relatively inactive. None of the other five eggs removed from the refrigerator on 13 February hatched, and all contained decaying remains of first-instar larvae when dissected on 1 March.

The remaining 25 eggs, only nine of which appeared viable, were removed from the refrigerator on 24 February. Two eggs were covered by mold and obviously dead. Fourteen had hatched in the refrigerator, but the larvae had not fed on the small, living snails included in the rearing dishes and were dead and badly decayed. Seven of the viable eggs were floated on a small amount of water and left at room temperature. The remaining two were dissected, and the larvae were removed. One of these first instars consumed six *Physella* (1.8–3.1 mm long) before molting into the second instar on 2 March. This larva fed on one additional snail before dying on 4 March. The second larva consumed five *Physella* (1.8–2.7 mm long) before dying on 1 March while molting into the second instar.

Two larvae that began to hatch on 24 February died before escaping from the egg envelopes. Three eggs hatched on 25 and 26 February, and on 2 March, but the remaining two never hatched and became covered by mold within ten days. Two of the three larvae that successfully emerged died while still in the first instar, although each fed at least once on small *Physella.* The larva that hatched on 26 February fed readily on *Physella*, molted into the second instar on 3 March, but died on 9 March. It consumed four snails (1.8–2.8 mm long) as a first instar and five more (1.5–2.6 mm long) as a second instar.

The only larva that pupated in the laboratory left the water on the preceding day, crawled up to the lid of the rearing dish, where it pupariated. The posterior end of the puparium was upturned, and the puparium floated when placed in water. A male emerged on 29 March, nine days after the puparium was formed.

The fragmentary rearing results indicate that *T. latifibula* has seasonal aspects similar to those of *T. loewi* (see below)—only one generation per year, with overwintering occurring either as eggs or as young larvae. Adults were taken in Idaho between 19 June and 3 August, but these dates probably do not indicate the entire flying season.

Tetanocera loewi Steyskal

Steyskal, 1959. Papers of the Michigan Academy of Science, Arts, and Letters, 44:68.

Restricted to the Nearctic Region (Knutson et al., 1986), *Tetanocera loewi* ranges from Ontario to North Carolina and Kansas west to Alberta and northern California (Fig. 4). In central New York and northeastern Ohio, adults and larvae were found most commonly in woodland swamps that contained vernal ponds. Although taken occasionally in open, vernal marshes, they rarely were collected in permanent marshes or along the marshy borders of unshaded lakes and streams.

Rearings were obtained from material collected in New York at the Inlet Valley marsh in Ithaca during early April (larvae taken by C. O. Berg), in a floodplain swamp along the outlet stream at Cayuta Lake (Schuyler County) during late August (adults), along the marshy borders of a sluggish woodland stream located near Oswego during August (adults), in a swamp woods near Albion (Orleans County) during April (larvae), and in the Manchester swamp (Ontario County) during April (larvae). Ohio rearings were initiated from three females collected on 20 September in a wooded swamp near Twin Lakes (Portage County).

In the breeding jars, eggs were scattered over the leaves of moss, the glass walls, and the cheesecloth covers. Very few of the eggs hatched, apparently being in diapause. Six eggs were laid on 29 August by a female collected on 24 August at Cayuta Lake. A larva that began to hatch from one of these on 10 September still had not escaped the egg on 12 September, when it was removed and placed

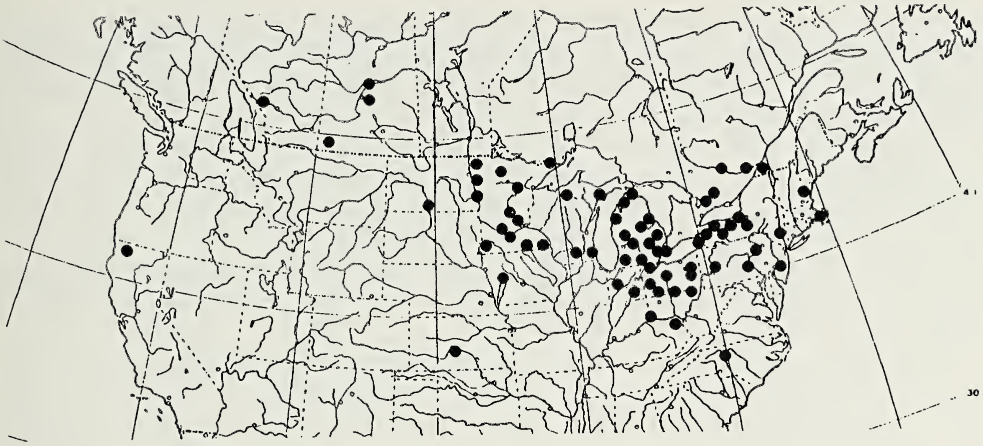

Fig. 4.—Distribution of *T. loewi*.

in several milliliters of water with several small *Helisoma* snails. The larva was very sluggish, did not feed even when placed on the expanded foot of a snail, and finally died on 18 September. On 18 September, the remaining five eggs were dissected, and four well-developed, living larvae were found. These larvae also refused to feed and all died within ten days. Twenty eggs laid on 17 September by another female from Cayuta Lake similarly failed to hatch, even though 16 of them contained well-formed, first-instar larvae when dissected on 5 October. These larvae remained inactive and failed to feed. During September, two females collected on 18 August near Oswego laid 55 eggs. A single larva emerged on 23 October, but did not feed and died on 29 October. No additional hatching was obtained, although many eggs contained living first- instar larvae when dissected on 1 November. None of these larvae fed on the small *Biomphalaria* and *Lymnaea* snails provided. Similar results were obtained with eggs deposited by females collected in late September in northeastern Ohio. The 57 eggs obtained were held at room temperature until fully formed, first-instar larvae were present. They were then treated in various ways in an effort to obtain hatching and feeding. Three eggs held continuously at room temperature for 107 days did not hatch. Ten eggs were placed in a refrigerator at 5–7°C for 15 days and then returned to room temperature. No hatching was obtained during the 50 days they were held at room temperature, and all had collapsed by mid-December. Additional sets of ten eggs were held in the refrigerator at 5–7°C for 30, 60, 90, and 129 days, respectively, before being returned to room temperature. No hatching occurred, although three larvae partially escaped the egg membranes. These larvae did not feed when extracted from the membranes and placed with small *Gyraulus* and *Physella* snails.

From the preceding results, it appears that embryogeny proceeds normally in eggs deposited in late summer and early fall, but the first-instar larvae remain within the egg membranes for an undetermined length of time. Hatching probably does not occur in nature until the larvae have been exposed to an extended period of low temperatures. Apparently, extended exposure to temperatures as low as 5°C is not sufficient to break the first-instar larval diapause.

Five first-instar and nine second-instar larvae were taken at the Manchester swamp on 17 April. In contrast to the larvae obtained from laboratory-reared eggs, these free-living larvae fed voraciously on *Lymnaea palustris, Helisoma* sp., *Biomphalaria glabrata, Planorbula armigera*, and *Physella* sp., grew rapidly, and formed several puparia in the rearing dishes.

The five first-instar larvae molted into the second instar on 21 and 22 April, giving a first larval stadium lasting at least four or five days. The actual time spent as free-living, first instars probably was considerably longer as there was no way of determining when hatching had occurred. All five larvae molted into the third instar on 26 and 27 April, giving a second larval stadium lasting four to six days. Three larvae formed puparia on 9 May, giving a third larval stadium lasting about 12 days.

Although all puparia were formed beneath a layer of moist paper toweling, they floated at the surface when placed in water. The posterior end of the puparium was strongly upturned and float hairs were present, indicating that the puparia were adapted to floating. In the laboratory, the pupal stage lasted 15 to 19 days, adults being produced in late May ($n = 10$, Manchester swamp).

Females taken in the field during August, September, and early November accepted males repeatedly, with each copulation lasting five to 60 minutes. Six feral females collected in August and September each deposited seven to 40 eggs a few days after being confined to the breeding jars, but a lone female collected on 9 November at the Manchester swamp did not oviposit and died on 14 November. In contrast to females collected in late summer, laboratory-reared females and those taken in nature during June and July did not oviposit during the ten to 25 days they were in confinement.

Laboratory-reared females lived only ten to 15 days, but mortality could have been due to faulty rearing techniques. Feral adults collected in the summer months lived 20 to 25 days.

In central New York, adults were encountered between 5 June and 9 November. Flies were collected repeatedly between early June and late September. Overwintering apparently takes place either as first-instar larvae within eggs or as free-living, early-instar larvae. The earliest record for larvae was obtained by C. O. Berg on 9 April at the Inlet Valley marsh, and other first instar larvae were found as early as 17 April at the Manchester marsh.

The evidence summarized above demonstrates that *T. loewi* is univoltine. Second- and third-instar larvae and puparia develop in April and May, requiring averages of 5, 12, and 17 days for a total of 34 days to pass through these stadia. Adults emerge in late spring but apparently do not mate or oviposit until three months or more have passed. Although there might still be time for a second generation if the eggs produced in late summer and autumn developed directly, most of them do not and those that do develop produce only listless larvae that do not feed. A diapause seems to intervene usually just before, but apparently sometimes just after, hatching, and the first-instar larvae which are formed in August and September remain in that stadium until the following April (seven or eight months). Thus, the life cycle, which may be completed in as little as 45 days in multivoltine species of *Tetanocera*, is extended in *T. loewi* to several months. This extension is due to two long periods of suspended activity—the delay before adult flies mate and oviposit and the long period (either before or after hatching) during which the first-instar larvae do not feed.

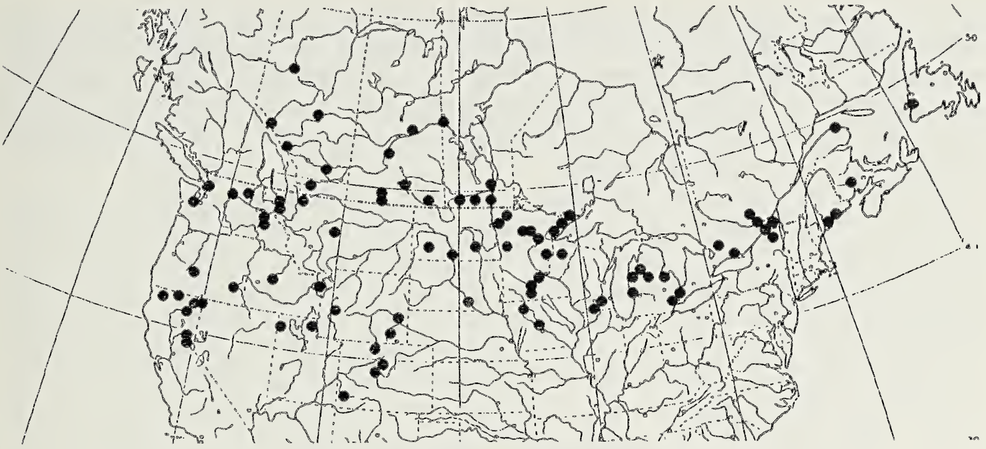

Fig. 5.—Distribution of *T. mesopora.*

Tetanocera mesopora Steyskal

Steyskal, 1959. Papers of the Michigan Academy of Science, Arts, and Letters, 44:70.

The known range of this strictly Nearctic species (Knutson et al., 1986) is transcontinental, extending from Newfoundland to British Columbia and south to New York, Colorado, and California (Fig. 5).

In northwestern Montana, adults were collected most commonly in open or partly shaded marshes dominated by species of *Carex.* In all marshes, there was a steady decline in water levels as summer progressed, and the habitats frequently lacked any standing water by late July. A few specimens were taken in more-permanent sedge marshes. Snails were abundant in all habitats and included species of *Gyraulus, Planorbula, Aplexa, Physella, Lymnaea,* and *Oxyloma.* Other species of Sciomyzidae commonly occurring with *T. mesopora* were *Atrichomelina pubera* (Loew), *Pherbellia anubis* Knutson, *P. griseola* (Fallén), *P. argyra* Verbeke, *Pteromicra siskiyouensis* Fisher and Orth, *Renocera cyathiformis* Melander, *Hedria mixta* Steyskal, *T. latifibula,* and *T. plebeja* Loew.

Rearings were initiated by a female collected on 10 August from a *Carex* marsh located along the Swan River about 8.8 km east of Big Fork (Flathead County), Montana, and by three females and two males collected on 25 August in a nearly dry sedge marsh situated some 11 km north of Deary (Latah County), Idaho.

The females collected on 10 August survived in the laboratory until 17 November but oviposited only on 19 August (nine eggs) and 13 September (12 eggs). Thirteen of these eggs were scattered over the cheesecloth covering the jars, and the remaining eight were attached to projecting sprigs of peat moss in the breeding jar. One egg hatched on 10 September, but the other 20 still had not hatched on 28 September when they were transferred to a constant- temperature chamber and maintained at a temperature of 22°C and long-day photoperiod (15 hours of light). Removal of the chorion of one egg of 29 September revealed a fully formed, first-instar larva. The larva was excised from the remaining egg membranes and placed in a small petri dish containing water and a few small aquatic snails. The larva remained sluggish, did not feed, and died on 5 October. Four of the remaining 19 eggs that had been placed at constant temperatures hatched within ten days, and three newly hatched larvae began to feed on small aquatic snails. One larva did not feed and died seven days after hatching. The remaining 15 eggs had not hatched by 20 November when it was noted that all had collapsed, indicating death of the larvae. The scanty results presented here indicate that embryogeny proceeds normally in this species in eggs laid in late summer but that hatching is delayed until the following spring.

The three larvae that hatched in the constant temperature cabinet fed as overt predators on *Gyraulus parvus, Helisoma* sp., *Physella* sp., and *Lymnaea obrussa.* Each larva killed between nine and 13 snails (2.5–4.0 mm) as first instars, three to five (3.2–9.0 mm) as second instars, and seven to 15 (3.4–10.0 mm) as third instars. A few of the newly hatched larvae left the surface film to seek out submerged snails, but most maintained contact with the surface film via their posterior spiracles. The first stadium lasted seven to nine days; the second, four to five days; and the third, 28 to 33 days. No larva fed during the last two to three weeks of the third stadium and remained relatively inactive within the rearing dishes. One larva did not feed for 25 days prior to pupariation, and another did not feed for 18 days. The third larva died before forming a puparium. This long cessation of feeding by third-instar larvae is reminiscent of *T. plumosa* except that overwintering occurs as larvae in that species, with pupariation being delayed until the following spring.

One puparium was formed on 25 October; the other, on 13 November. Both puparia were held at room temperature until 2 December when they became moldy. Subsequent dissection determined that both pupae had died.

Two of the females collected on 25 August died on 11 September; the third female, on 20 September. They deposited a total of 142 eggs between 4 and 11 September. Very few of the eggs hatched, and no larva fed on the snails provided.

The rearing data are too few to allow definitive conclusions about the life cycle of this species, but it appears that there is only a single generation a year. Eggs probably are not deposited until mid- to late August; a lengthy diapause affects the fully formed, first-instar larvae within the eggs; and hatching in nature may be delayed until the following spring. The earliest collection date for adults was obtained on 5 June (Eaglebend, Minnesota); the latest, on 3 October (Mille Lacs, Minnesota).

Tetanocera montana Day

Day, 1881. Canadian Entomologist, 13:87.

Tetanocera montana is a Holarctic species (Knutson et al., 1986) that ranges in North America from Ontario west to Alaska and south to New York, Michigan, and Wyoming (Fig. 6). Adults and larvae were collected in central New York only at the Manchester swamp, where they were abundant among the emergent vegetation and floating plant debris of a vernal pond. In Idaho, adults were swept from emergent herbage and low shoreline shrubs bordering two small, shallow, but permanent, lakes that were partially shaded by overhanging trees.

Rearings were obtained from larvae taken at the Manchester swamp during April and from adults collected in a *Carex* sedge marsh bordering a small lake located some 11 km north of Fortine (Lincoln County), Montana, on 6 July.

Eggs laid in the laboratory always were scattered on the cheesecloth covers or on the upper three centimeters of the glass jars. The incubation period was strik-

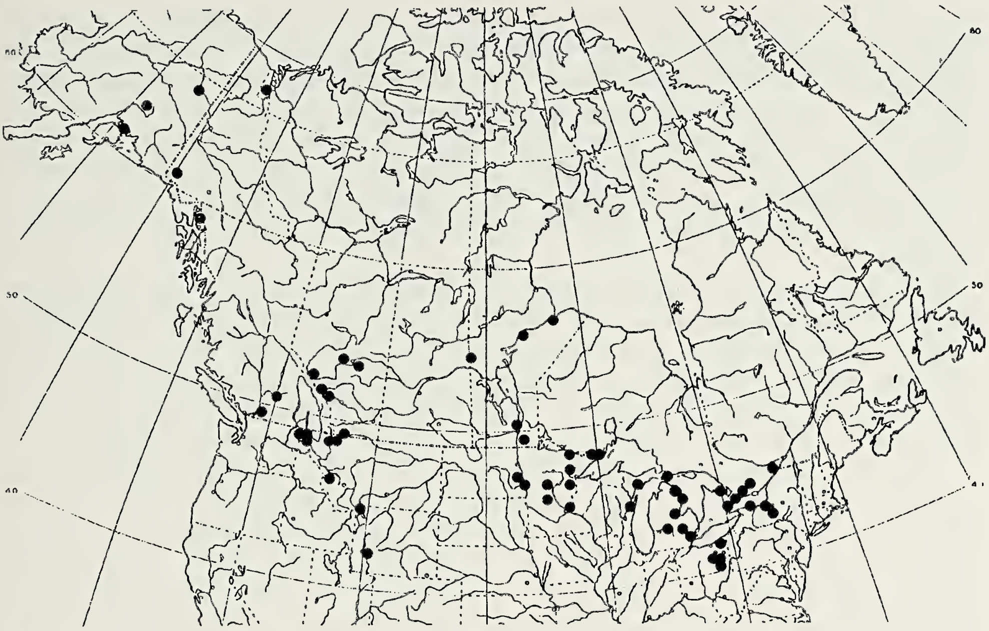

Fig. 6.—Distribution of *T. montana.*

ingly extended, and it appeared that eggs or, more likely, the first-instar larvae underwent diapause within the egg membranes before hatching.

On 13 June, 16 eggs laid by laboratory-reared females that had developed from larvae taken at the Manchester swamp were placed in small Stender dishes and left at room temperatures. Although embryogeny took place, only three larvae emerged. One of these emerged 23 days after the eggs were deposited, another after 25 days, and the third after 28 days. The three larvae were very sluggish, fed sparingly on *Australorbis*, and died within five days. Dissection of the remaining 13 unhatched eggs during late July disclosed that six contained well-developed, living, first-instar larvae, but the remaining seven eggs contained no larvae and were covered with mold. The six larvae excised from eggs were also very sluggish, rarely fed, and died within a few days. The unusually long incubation period of this species was very similar to other species developing in vernal woodland ponds (e.g., *T. loewi*).

Twenty-three eggs laid by females collected at the lake in Lincoln County, Montana, also failed to hatch during the 95 days they were held at room temperature, although one larva partially escaped from an egg before dying. All of the remaining eggs eventually became covered with fungi, an indication that the larvae had perished. Another 25 eggs were held at room temperature for 15 days and then transferred to a refrigerator where they were held for an additional 183 days. No hatching was obtained, although many eggs contained first instars.

Larvae collected in the field in New York were predacious and destroyed many individuals of *Lymnaea palustris, Helisoma* sp., *Australorbis glabratus, Planorbula armigera, Gyraulus parvus*, and *Physella* sp. At the Manchester swamp, second- and third-instar larvae were very abundant on the decaying leaves and stems of a coarse sedge floating in approximately 0.3 m of water during April.

Associated with them were many individuals of *T. loewi* and a few of *T. plumosa.* Aquatic snails such as *Lymnaea palustris, Physella* sp., *Planorbula armigera, Aplexa hypnorum*, and the succineid *Catinella avara* were abundant. Many of the *T. montana* larvae collected on 17 April were in the second instar, but most of the 30 larvae taken on 20 April were in the third instar. These larvae completed development rapidly in the laboratory and began pupariating during late April.

Under laboratory conditions the first larval stadium lasted three to four days; the second, four to seven days; the third, eight to 12 days (*n* = 6, Manchester swamp).

During the day preceding pupariation, many larvae ceased feeding, emptied the remaining gut contents, and became relatively inactive. They made little attempt to reach a drier situation, and most formed puparia in water that was five to ten millimeters deep. (The spiracular float hairs and the upturned posterior end of the puparium indicate that this stage is adapted for floating.) Under laboratory conditions, the pupal stage lasted 16 to 20 days (*n* = 15, Manchester swamp).

Three females that emerged on 17 and 18 May from material collected at the Manchester swamp were first seen copulating on 23 May. Copulation was repeated frequently thereafter, and each act lasted from 30 to 60 minutes. Two females began ovipositing on 20 June, the third on 23 June, 33 to 37 days after emerging. Before I killed them on 2 July, they each deposited between 23 and 30 eggs. A female collected at Westmond (Bonner County), Idaho, on 8 July began ovipositing on 10 July and laid a total of 116 eggs before dying on 18 July.

Larvae were collected only at the Manchester Swamp on 17 and 20 April. Adults were taken there during July and August. Because the laboratory-reared females delayed oviposition more than a month after emerging, it is probable that *T. montana* is univoltine. Overwintering probably occurs as unhatched eggs or young larvae, larval feeding occurs during late winter and spring, pupariation occurs in late April and May, and adults emerge in late May and early June.

Tetanocera obtusifibula Melander

Melander, 1920. Annals of the Entomological Society of America, 13:328.

Except for a doubtful record from the province of Quebec in eastern Canada, *Tetanocera obtusifibula* is known only from Idaho, Washington, Oregon, California, and British Columbia (Fig. 7). In Idaho, the only locality where the biology was studied, adults were found exclusively in vernal marshes that became dry by midsummer. Near Moscow in Latah County, they were swept in late summer from emergent plants (sedges, grasses, rushes) growing in unshaded, dry marshes. These marshes contained water up to 0.3 m in depth during the early spring, but as summer advanced, the water level dropped until by mid-July they lacked standing water.

On 7 April, two third-instar larvae were observed crawling about on floating plant debris in a very small, unshaded, vernal pond located just east of Moscow. Another third instar was taken on 20 April. The pond was only 3.1 m long and not more than 1.0 m wide at its broadest point. At the time of collection it was filled with water to a depth of 25 cm and was choked with immersed and emergent vegetation, mostly sedges and rushes, and supported a large population of *Lymnaea* sp. snails. The water level receded steadily during May, and by late June the depression was dry.

The two larvae collected on 7 April were placed in a refrigerator at 10°C and

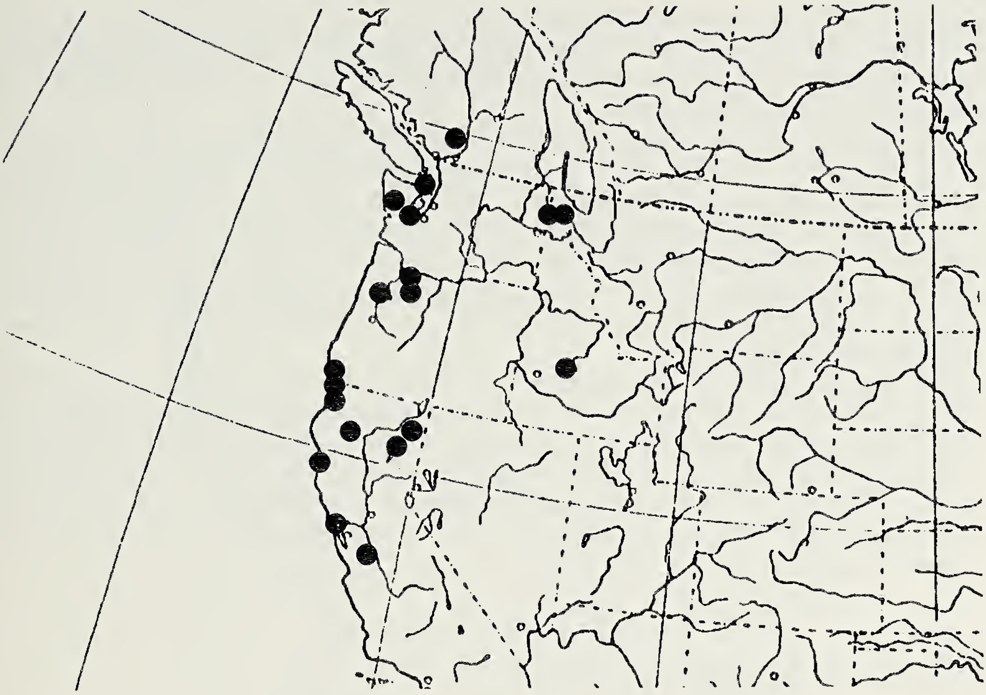

Fig. 7.—Distribution of *T. obtusifibula.*

left there until 18 April when they were returned to room temperature. The larva collected on 20 April was not subjected to this cold treatment. At room temperature all three larvae were very active and fed daily on small *Lymnaea* taken at the pond. They ceased feeding on 28 April, emptied their gut contents, and became relatively inactive. They did not attempt to reach a drier situation, and on 29 April all pupariated at the water surface. Males emerged on 13 and 14 May and a female on 16 May, giving a pupal stage lasting 14 to 17 days. All three adults died within three days without copulating.

Females taken from June to early August did not contain recognizable eggs, but a female taken on 21 August contained a large number of well-developed eggs when examined on 8 September, the day she died. Two females collected in marshes near Deary (Latah County), Idaho, on 25 August were placed in breeding jars with males. Copulation was first observed on 26 August and was repeated frequently during the next ten days. They deposited 166 eggs on 4 September on the cheesecloth cover of the breeding jar. Thirty-seven of these eggs were held continuously at room temperature for 141 days. Eleven larvae attempted to hatch during this period, but only one larva completely escaped the egg membranes. It fed twice on small *Physella* snails before dying 15 days later. The remaining 26 eggs underwent embryogeny, with fully formed, first-instar larvae being formed, which never hatched and eventually collapsed. Another 85 eggs were held at room temperature for ten days without hatching and were then transferred to a refrigerator where they were held at 5–7°C for varying periods of time before being returned to room temperature or placed in a freezer at 0°C. Of 40 eggs held at 5–7°C for 170 days, 18 hatched while still in the refrigerator. However, none of the newly emerged larvae fed. None of the remaining 22 eggs hatched after they had been returned to room temperature. No hatching occurred in 45 eggs that were subjected to 5–7°C for 40 days and to 0°C for 89 to 121 days before being returned to room temperature.

The records indicate that there is only one generation per year with overwintering occurring as larvae. Puparia are formed in late April or May, and adults emerge in late spring or early summer. Adults remain active throughout the summer, but do not begin ovipositing until late summer or early fall. Eggs undergo embryogeny and become first-instar larvae within a few days. However, larvae then go into diapause and do not escape the egg membranes until the diapause has been completed. Hatching possibly occurs in late autumn, but probably is delayed until early spring.

Parasitism by unidentified roundworms (Nematoda) was noted in two females of *T. obtusifibula* collected on 26 June in a small sedge meadow located two kilometers north of Deary, Idaho. Both females had greatly distended abdomens when collected. Four roundworms emerged from the abdomen of one female on 29 June; two, from the second female on 30 June. The abdomens of both females collapsed shortly after the worms had emerged, and both died a day later without ovipositing.

Tetanocera robusta Loew

Loew, 1847. Stettiner Entomologische Zeitung, 8:197.

Tetanocera robusta is Holarctic in distribution (Knutson et al., 1986), ranging in North America from Michigan and Ontario west to Alaska, and south to Utah and New Mexico (Fig. 8). In Idaho, adults were taken most abundantly in open, permanent marshes and along the unshaded borders of lakes. A few were swept from open, vernal marshes and a very few were taken in shaded marshes bordering small ponds.

A rearing was initiated on 8 August from eggs laid by a female collected the same day at Robinson's Lake, 15 km east of Moscow in Latah County, Idaho. Of the 175 eggs obtained from this female, 92 were laid on the glass wall of the breeding jar, 72 were affixed to the cheesecloth cover, and 11 were attached to a short length of *Typha* leaf. They were scattered over the substrate, and no clusters contained more than five eggs. Hatching occurred in three (n = 44) or four days (n = 29) under laboratory conditions.

Groups of eggs were subjected to different hatching conditions in efforts to determine whether eggs immersed in, or floating on, water will hatch and whether the eggs can withstand prolonged chilling. All but two of 24 eggs placed on a short length of microscope slide projecting above the water hatched. In contrast, only six of 24 that were floated on water produced larvae, and only one of 14 newly laid eggs that were completely immersed hatched. No hatching was obtained in 20 eggs that were immersed after being exposed to air for 48 hours. None of 20 eggs held in a refrigerator at 7°C for four months hatched when returned to room temperature. These results indicate that *T. robusta* eggs are not resistant to prolonged exposure to either wetting or low temperatures.

Records were kept of the number and dimensions of snails killed by the predacious larvae. Individual larvae in small, plastic petri dishes containing a small amount of water were given three or four living snails daily. Snails used were

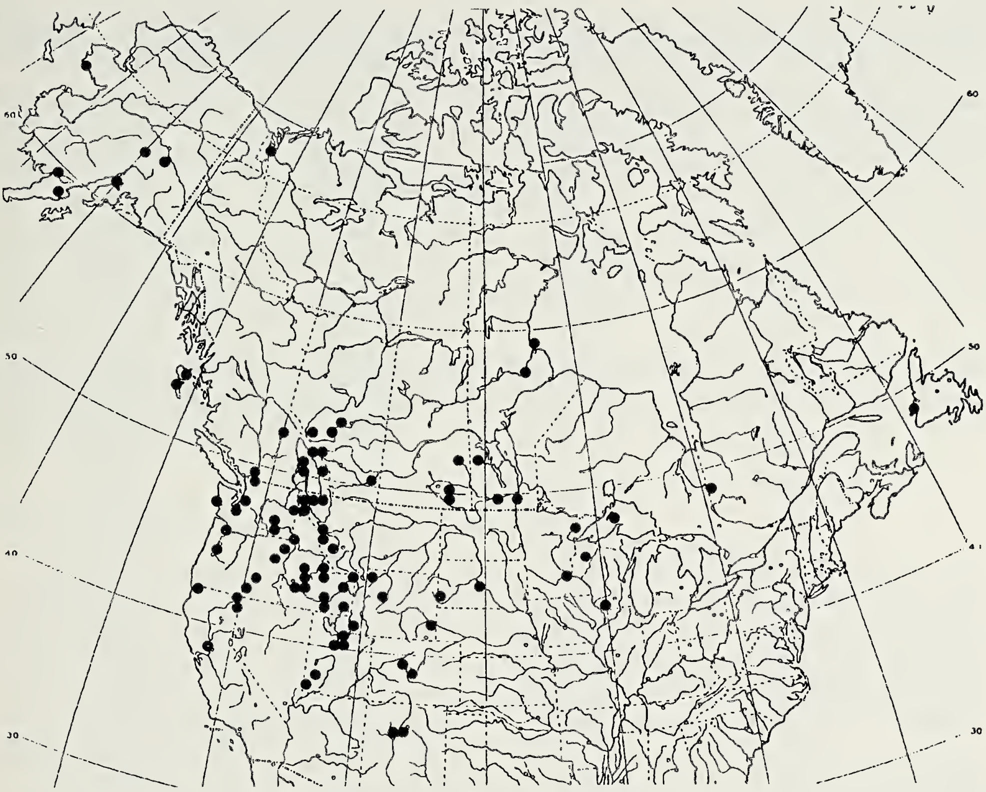

Fig. 8.—Distribution of *T. robusta.*

Gyraulus parvus, Helisoma subcrenatum, Lymnaea obrussa, and *Physella* sp. (Table 1).

Apparently the species of snail available does not influence the total number consumed by the larvae unless one species is considerably larger than the others. Larvae killed from 20 to 26 small *Gyraulus, Lymnaea*, and *Helisoma*, but only 12 to 16 larger *Lymnaea* and *Physella.* Larvae were placed individually in petri dishes containing different-sized *Lymnaea obrussa* or *Helisoma subcrenatum.* One snail was given to each larva. Larvae killed and fed upon *Lymnaea* that were five, eight, and ten millimeters long and *Helisoma* that were two, five, and six millimeters in diameter. These small larvae had considerable difficulty attacking snails greater than about eight millimeters in greatest dimension. To determine how long newly hatched larvae could survive without food, five larvae were placed on 28 August in small dishes containing only a slight amount of water. Four of these larvae died on 1 September, but the remaining larva lived until 3 September.

Larvae developed normally in water considerably deeper than their body lengths. They fed several times on *Gyraulus* in water that was ten and 20.0 mm deep. Mortality of larvae was no higher in the deep water than in water that was only two to five millimeters deep.

Under laboratory conditions the first larval stadium lasted from four to six days; the second, from two to seven days; the third, from six to 11 days ($n = 19$). The

Table 1.—*Numbers and dimensions (lengths of* Lymnaea *and* Physella, *diameters of* Gyraulus *and* Helisoma *in millimeters) of snails killed by larvae of* T. robusta. *Species of snail killed:* G. = Gyraulus parvus, H. = Helisoma subcrenatum, L. = Lymnaea obrussa, P. = Physella *sp.*

	Snails consumed during			
Larva	First instar	Second instar	Third instar	Total number of snails killed
1	7 *G.*	6 *L.*	12 *L.*	25
	(2.2–2.8)	(4.5–6.1)	(5.0–9.2)	(2.2–9.2)
2	10 *G.*	5 *L.*	8 *L.*	23
	(1.6–2.6)	(4.5-8.0)	(4.5–7.0)	(1.6–8.0)
3	11 *G.*	4 *L.*	8 *L.*	23
	(1.7–3.0)	(5.0–9.0)	6.0–8.0)	(1.7–9.0)
4	10 *G.*	6 *L.*	8 *L.*	24
	(1.7–3.0)	(5.8–8.4)	5.8–8.5)	(1.7–8.5)
5	9 *G.*	4 *L.*	10 *L.*	23
	(1.7–3.2)	(5.5–7.0)	(5.2–13.2)	(1.7–13.2)
6	8 *G.*	7 *L.*	10 *L.*	25
	(1.8–2.4)	(4.0–7.0)	(4.0–7.0)	(1.8–7.5)
7	10 *G.*	4 *L.*	12 *L.*	26
	(1.9–2.4)	(4.0–7.0)	(5.0–9.0)	(1.9–9.0)
8	7 *G.*	5 *L.*	12 *L.*	24
	(1.6–2.6)	(4.0–7.0)	(5.0–9.0)	(1.6–9.0)
9	8 *G.*	2 *H.*	10 *H.*	20
	(1.9–5.0)	(3.0–4.8)	(3.8–10.0)	(1.9–10.0)
10	8 *G.*	5 *H.*	9 *H.*	22
	(1.7–2.4)	(1.8–3.3)	(4.8–8.0)	(1.7–8.0)
11	8 *G.*	6 *H.*	10 *H.*	24
	(1.5–5.0)	(3.0–6.2)	(3.5–8.5)	(1.5–8.5)
12	3 *L.*	6 *L.*	7 *L.*	16
	(3.4–4.2)	(3.2–8.0)	(6.1–9.8)	(3.2–9.8)
13	2 *L.*	2 *L.*	8 *L.*	12
	(3.8–5.0)	(5.4–6.0)	(6.8–9.2)	(3.8–9.2)
14	2 *P.*	5 *P.*	8 *P.*	15
	(3.4–4.2)	(4.9–9.4)	(7.0–9.0)	(3.4–9.4)
15	3 *P.*	5 *P.*	7 *P.*	15
	(2.8–5.5)	(5.3–8.0)	(7.0–10.0)	(2.8–10.0)
16	3 *P.*	5 *P.*	7 *P.*	15
	(3.4–5.5)	(5.5–9.0)	(6.2–9.0)	(3.4–9.0)

day preceding pupariation, many larvae ceased feeding and became relatively inactive. Of the 22 puparia obtained in the laboratory, 12 were formed above the water on the walls of the rearing dishes and ten were floating at the water surface. Several adults were obtained from puparia formed in both situations. The pupal stage lasted from 12 to 16 days ($n = 7$). Records were not obtained on the number of eggs laid by laboratory-reared adults, but two field- caught females deposited 60 and 175 eggs, respectively, during the nine and eight days they lived in the breeding jars.

Information on seasonal aspects of *T. robusta* comes in part from subarctic regions. In Iceland, Nielsen et al. (1954) found young larvae on 20 July and in August; older larvae from 10 July to 12 August; mature larvae in August; and puparia in July, in August, and on 13 April. They suggested that "the species winters as mature larvae or puparia." A floating puparium collected at Fire Lake, near Anchorage, Alaska, on 26 June 1952, produced an adult fly on 1 July. Adults were taken commonly throughout the summer in Idaho. The earliest record is 17 May; the latest, 25 September. The entire life cycle was completed in 40 days in

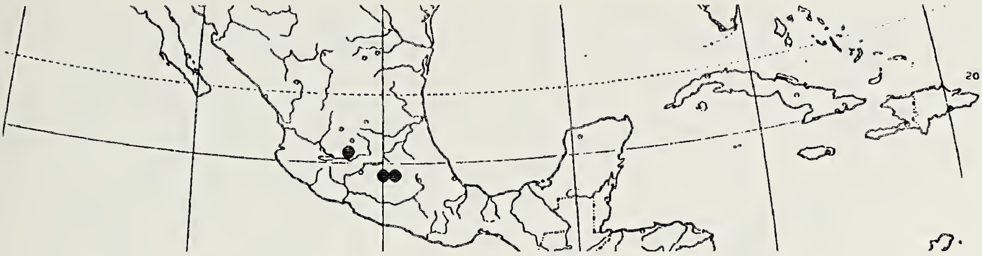

Fig. 9.—Distribution of *T. spreta*.

Idaho, with no delays in development. This indicates that *T. robusta* has more than one generation per year at that latitude, although it probably is univoltine in more northern parts of its range.

Tetanocera spreta Wulp

Wulp, 1897. Biologia Centrali-Americana. Diptera, 2:358.

Tetanocera spreta is known only from southcentral Mexico (Knutson et al., 1986), where it has been recorded from Toluca (Michoacan), Jalisco (Jalisco), and Mexico City (District Federal) (Fig. 9). I am indebted to S. E. Neff for information on the biology of this species. A rearing was initiated from two females collected on 22 August 1958, by sweeping water hyacinth, cattails, and sedges growing abundantly in the shallow water of a roadside ditch located along Route 190 near Kilometer 15, District Federal, Mexico.

The females deposited 77 eggs between August 25 and September 15, with over half of the eggs being laid before August 28. Nearly all eggs were placed on the leaves and rhizoids of the moss present in the jar, but a few were attached to the glass walls of the container. Hatching occurred in three to five days under laboratory conditions. The larvae possessed sizeable float hairs and were obviously adapted to an aquatic existence. They fed upon the aquatic snails *Helisoma* sp., *Biomphalaria glabrata*, and *Physella* sp. In the laboratory the first larval stadium lasted six or seven days; the second stadium, from two to six days; and the third stadium, from five to 11 days ($n = 5$). The larvae made no attempt to reach a drier situation before pupating and all puparia were formed at the water surface in the breeding dishes. The pupal stage lasted from nine to ten days ($n = 4$).

On 25 September, a first generation female that had emerged during the preceding day was placed with two males in a breeding jar. Copulation was not observed until 14 October, but was seen frequently during the next several days. Each copulation lasted from a few minutes to over an hour. The female had not oviposited by 22 October when she was exposed to the light emitted by a 75-watt incandescent lamp. Oviposition first occurred on 27 October, when the female deposited five eggs between 1130 and 1300. Between then and 7 November, 39 eggs were deposited, with the daily count varying from zero to nine. She did not oviposit again until 21 November, but between then and 29 December, she laid an additional 67 eggs. Thus, only 106 eggs were laid by this one female between 27 October and 29 December. Several eggs, especially those laid in December, did not hatch. The female died on 4 February 1959, having lived for 129 days.

Because the laboratory-reared female did not oviposit until nearly a month had

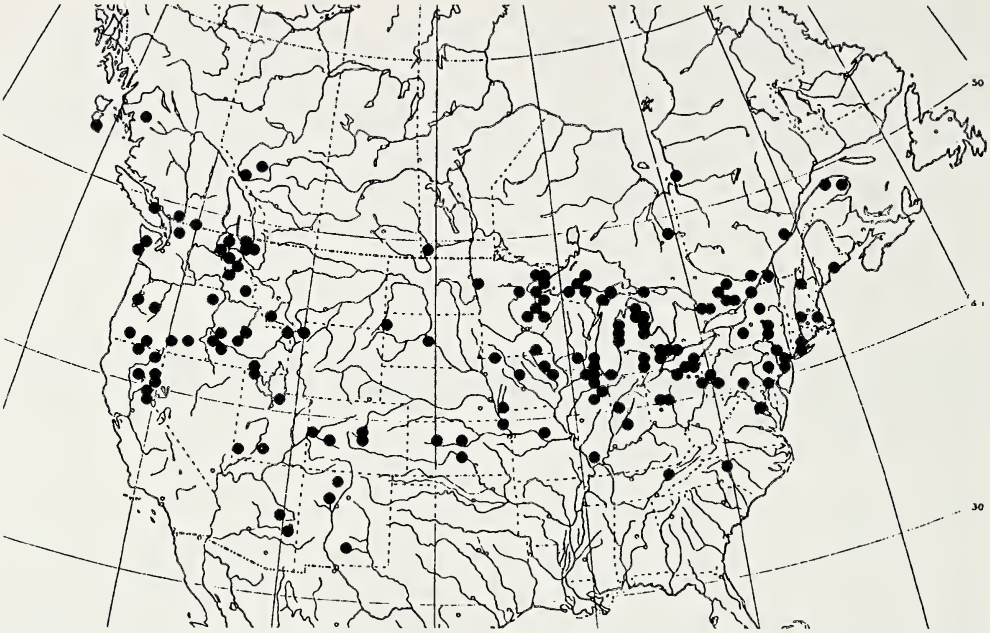

Fig. 10.—Distribution of *T. vicina.*

elapsed from the date of her emergence, it is possible that *T. spreta* has only one generation per year, but additional data are needed before any definite conclusion can be made as to seasonal distribution. Eggs laid by the feral and laboratory-reared females hatched quickly, and neither the larvae nor the pupae showed any unusual delays in development.

Tetanocera vicina Macquart

Macquart, 1843. Diptères exotiques noveaux ou peu connus, 2(3):337.

Tetanocera vicina is restricted to the Nearctic region (Knutson et al., 1986), where it is recorded from New Brunswick west to British Columbia, and south to North Carolina, Tennessee, Kansas, and Arizona (Fig. 10). In central New York and Idaho, adults were swept most abundantly in unshaded vernal marshes. Although several specimens were collected in open marshy land bordering permanent lakes and a very few were swept from wooded swamps and along woodland streams, it appears that *T. vicina* is best adapted to open, vernal marshes containing lush stands of grasses and sedges. In central New York, rearings were obtained from material collected at the Inlet Valley, Floral Avenue, and White Church marshes (Tomkins County). In Idaho, a rearing was initiated from adults taken at a small vernal marsh located near Moscow (Latah County). Additional rearings were obtained from material collected near Kent (Portage County), Ohio.

Adults of *T. vicina* collected in nature during May, June, and early July did not oviposit during the ten to 40 days they were held in the breeding jars, but those taken in August and early September began ovipositing a few days after being confined. Laboratory-reared females remained alive for more than a month before ovipositing, indicating that the eggs had an unusually long maturation period. One female that emerged on 22 November did not begin ovipositing until 7 January, 46 days later. Another that emerged in early May did not lay her first eggs until late July. It is evident that *T. vicina* is a univoltine species in which the adults emerging in late spring and early summer do not begin ovipositing until late summer and early autumn. In contrast to those of other univoltine species (e.g., *T. loewi*), the eggs of *T. vicina* hatch within a few days. The newly hatched larvae begin feeding on aquatic snails and continue to grow until their activity is slowed and finally stopped by lowering water temperatures. With the return of warm weather and melting of the ice, the larvae again become active and attain their full growth during the late spring. Pupation occurs in late spring, with adults emerging in 18 to 20 days.

The only rearing of this species from adult to adult was initiated from eggs laid on 1 October by two females that were collected on 29 September at the Inlet Valley marsh. All eggs were deposited on the leaves and stems of the moss used as a substrate in the breeding jar. Fifteen larvae hatched in seven to nine days. The aquatic larvae were highly predacious and fed voraciously on a wide variety of nonoperculate aquatic snails. The first larval stadium lasted four to five days; the second, five to six days; and the third, from nine to 12 days ($n = 4$). The only puparium that produced an adult was formed on the surface of shredded peat moss on 29 October. The adult emerged on 16 November, after a pupal period of 18 days.

On 23 August, a second rearing was initiated from eggs laid by two females collected on 18 August at a small vernal marsh located 8.8 km north of Moscow (Latah County), Idaho. Between 23 and 29 August, 166 eggs were deposited followed by death of the female. Of these eggs, 85 were attached to projecting sprigs of peat moss, 59 were placed at various places on the shells of living and dead *Lymnaea* and *Helisoma*, and 22 were laid on the lower 2.5 cm of the glass walls of the breeding jar. Of those eggs placed on peat moss, 35 were clustered together in one compact mass at the tip of a projecting sprig, while the other 50 were scattered over the moss surface. Most eggs laid on shells were placed in the sutures separating the body whorls, but several were attached to the parietal lips or onto convex surfaces. Those laid on the glass walls were scattered, and only rarely were eggs touching each other. Hatching occurred in nine to 14 days, with most larvae emerging in ten to 12 days ($n = 44$). Records were maintained on the number of snails eaten by the first- and second-instar larvae. Each of six first-instar larvae destroyed between six and eight *Gyraulus parvus*, ranging in diameter from 1.3 to 2.9 mm. Two second instar larvae consumed eight and nine *Lymnaea obrussa*, ranging in length from 2.3 to 7.0 mm, respectively. A third-instar larva consumed five *L. obrussa* (5.0–7.0 mm long) before dying. The first larval stadium in this rearing lasted from two to five days; the second, from seven to nine days ($n = 6$). As larvae died before forming puparia, the length of time spent in the third instar could not be determined.

Puparia obtained from larvae collected in nature were frequently formed on peat moss or within empty snail shells. Although a few puparia were formed at the water surface in dishes lacking moss, many larvae in such dishes died, apparently while pupariating. The posterior end of the puparium was only slightly upturned, and it is probable that the larvae either move to the shore or enter hollow stems before pupariating. The fact that puparia were not found in nature, even in marshes where larvae were abundant earlier, is additional evidence that the larvae leave the water prior to forming puparia. The pupal stage lasted from 18 to 20 days ($n = 8$).

Reared females did not accept males until ten to 15 days after emerging from puparia. Copulation was repeated frequently throughout the life of the females, with each act lasting from a few minutes to over an hour. A female that was collected at the Inlet Valley marsh on 29 September laid 42 eggs before dying on 9 October. Another female that emerged in the laboratory on 21 September produced 27 eggs before dying on 19 February. Feral adults collected in August and September laid from 40 to 81 eggs. A few reared adults remained alive in the breeding jars for as long as 100 days, but most died within 25 days.

In central New York, the first seasonal record for adults was made on 31 May; the latest, on 29 September. In Idaho, the earliest record was made on 19 June; the latest, on 1 October. In both states adults were collected commonly throughout the summer months. Larvae were taken at the White Church marsh on 6 November, at the Inlet Valley marsh on 1 January, and in several marshes between February and early May. Probably both second- and third-instar larvae can overwinter as one of the larvae taken on 6 November was in the earlier instar. Other second-instar larvae were collected during the early spring, but most of those collected in winter and early spring as well as one of the two collected on 6 November were in the third instar. Larvae taken in midwinter and early spring readily attacked, killed, and fed on snails and quickly completed development, but the two taken on 6 November did not feed and died a few days after being brought into the heated laboratory. Although this observation might suggest that the larvae are in diapause during early winter, the rearing of larvae through to pupation from eggs laid during September provides evidence to the contrary.

No parasitoid wasps were obtained from the scores of puparia collected in nature. Perhaps *T. vicina* evades hymenopterous enemies because its larvae develop in seasons when wasp activity is at a minimum.

DISCUSSION

Species comprising the aquatic predator guild possess certain behavioral and morphological features in common. Larvae of all ten species are overt, generalized predators of aquatic pulmonate snails, kill quickly, consume several snails their during larval life, and usually form puparia at the water's surface. The larvae prey on aquatic snails at or near the water's surface and do not forage below the surface to any extent. They lie just beneath the surface film in shallow water, commonly near shorelines, and keep their posterior spiracles in contact with the atmosphere. In general, the larvae are dark in color, have wrinkled integuments, elongate lobes around the posterior spiracular disc, and four well-developed, branching spiracular processes (float hairs) on the posterior spiracles.

Although the guild of aquatic predators in the genus *Tetanocera* is sizeable, consisting of at least ten species in North America, resource partitioning probably reduces competitive interactions. There does not appear to be much partitioning of the trophic axis, as all species are generalized predators of a variety of aquatic pulmonate snails. The spatial axis is partitioned to some extent, as certain species have fairly distinct geographic distributions. *Tetanocera robusta* and *T. obtusifibula* are largely western, *T. spreta* is known only from the central plateau area of Mexico, and *T. annae* is most commonly found in the northeastern states, whereas the remaining six species are more widely distributed.

Table 2.—*Habitat utilization in ten species of malacophagous* Tetanocera.

Species	Habitat
T. annae	Permanent woodland swamps
T. ferruginea	Permanent unshaded marshes
T. latifibula	Permanent unshaded marshes
T. loewi	Vernal woodland pools
T. mesopora	Vernal unshaded marshes
T. montana	Permanent and vernal woodland pools
T. obtusifibula	Vernal unshaded marshes
T. robusta	Permanent unshaded marshes
T. spreta	Vernal unshaded marshes
T. vicina	Vernal unshaded marshes

Differences in habitat occurrence are also recognizable (Table 2). *Tetanocera ferruginea, T. latifibula*, and *T. robusta* are found in unshaded permanent marshes, dominated by herbaceous vegetation, in which water is present throughout the year. In contrast, *T. mesopora, T. obtusifibula, T. vicina*, and probably *T. spreta* occur in more ephemeral marshes that contain water only during the spring and early summer months. Permanently flooded woodland swamps are occupied by *T. annae* and possibly *T. montana*, whereas wooded sites containing only vernal pools that dry up as summer progresses are the home of *T. vicina* and *T. montana*.

Perhaps the niche axis that is most obviously partitioned is the temporal one, as different species have rather specific feeding times and phenologies (Table 3). *Tetanocera obtusifibula* and *T. vicina* are univoltine, overwinter as partly grown larvae in diapause, and do most of their feeding during the autumn and spring months. *Tetanocera latifibula, T. loewi, T. mesopora*, and *T. montana* are also univoltine, but pass the winter as fully embryonated but diapausing eggs. Hatching in those species probably occurs in early spring, and larval feeding is largely completed by late April. In contrast, *T. ferruginea* and *T. robusta* are multivoltine, overwinter as pupae, and have successive generations of larvae feeding throughout the warm season. *Tetanocera annae* is somewhat unusual in that it appears to be univoltine, overwinters as pupae in diapause, and completes its larval life in early summer.

No conclusions can be drawn as to the forces that drove resource partitioning in this guild, but the idea of interspecific competition is an appealing one. One interesting possibility is the concept of the "ghost of competition past" (Connell,

Table 3.—*Phenology of ten species of malacophagous Tetanocera.*

Species	Overwintering stage	Voltinism	Larval feeding time
T. annae	Pupa	Univoltine	Early summer
T. ferruginea	Pupa	Multivoltine	Summer
T. latifibula	"Egg"	Univoltine	Spring
T. loewi	"Egg"	Univoltine	Spring
T. mesopora	"Egg"	Univoltine	Spring
T. montana	"Egg"	Univoltine	Spring
T. obtusifibula	Larva	Univoltine	Spring
T. robusta	Pupa	Multivoltine	Summer
T. spreta	NA	Multivoltine?	NA
T. vicina	Larva	Univoltine	Autumn, spring

1980) which suggests that partitioning resulted from intense competition for resources during times of increased environmental stress. Certainly drought can reduce aquatic habitats dramatically which, in turn, would result in significantly lower snail populations. As a result, competition for one or more limiting resources (habitats, snails) would intensify. Any phenological or habitat shift on the part of *Tetanocera* species would have selective value.

ACKNOWLEDGMENTS

Research was supported by grants from the National Science Foundation, National Institute of Allergy and Infectious Diseases, National Geographic Society, and the American Philosophical Society. Deep appreciation is expressed to G. C. Steyskal of Gainesville, Florida, for his expert help in determining species of *Tetanocera*.

Specimens of species reared in this study have been deposited in the insect collections of Cornell University and Carnegie Museum of Natural History.

This paper is dedicated to the fond memory of Dr. C. O. Berg, Department of Entomology at Cornell University, who inspired numerous students throughout the world to initiate studies of the biology of the Sciomyzidae.

LITERATURE CITED

CONNELL, J. H. 1980. Diversity and the coevolution of communities, or the ghost of competition past. Oikos, 35:131–138.

FOOTE, B. A. 1996*a*. Biology and immature stages of snail-killing flies belonging to the genus *Tetanocera* (Insecta: Diptera: Sciomyzidae). I. Introduction and life histories of predators of shoreline snails. Annals of Carnegie Museum, 65:1–12.

———. 1996*b*. Biology and immature stages of snail- killing flies belonging to the genus *Tetanocera* (Insecta: Diptera: Sciomyzidae). II. Life histories of predators of snails of the family Succineidae. Annals of Carnegie Museum, 65:153–166.

KNUTSON, L. V., R. E. ORTH, T. W. FISHER, AND W. L. MURPHY. 1986. Catalog of Sciomyzidae (Diptera) of America north of Mexico. Entomography, 4:1–53

NEFF, S. E., AND C. O. BERG. 1966. Biology and immature stages of malacophagous Diptera of the genus *Sepedon*. Bulletin of the Virginia Agricultural Experiment Station, 566:1–113.

NIELSEN, P. O., O. RINGDAHL, AND S. L. TUXEN. 1954. The Zoology of Iceland. Volume III, Part 48a: Diptera I. Ejnar Munksgaard, Copenhagen, Denmark.

ROZKOŠNÝ, R., AND K. ELBERG. 1984. Family Sciomyzidae. Pp. 167–193, *in* (Á. Soós and L. Papp, eds.). Catalogue of Palaearctic Diptera, Volume 9. Micropezidae—Agromyzidae. Akademie Kiado, Budapest, Hungary.

SOÓS, Á. 1958. Ist das Insektenmaterial der Museen für ethologische und ökologische Untersuchungen verwandbar? Angaben über Flugzeit und die Generationszahl der Sciomyziden (Diptera). Acta Entomologische Museum National Prague, 32:101–150.

STEYSKAL, G. C. 1959. The American species of the genus *Tetanocera* Dumeril (Diptera). Papers of the Michigan Academy Sciences, Arts, and Letters, 44:59–91.

———. 1965. Family Sciomyzidae. Pp. 686–695, *in* A Catalog of the Diptera of America North of Mexico (A. Stone, C. W. Sabrosky, W. W. Wirth, R. H. Foote, and J. R. Coulson, eds.). United States Department of Agriculture Handbook, 276.

ANNALS OF CARNEGIE MUSEUM
Vol. 68, Number 3, Pp. 175–211 12 August 1999

REVISION OF THE WIND RIVER FAUNAS, EARLY EOCENE OF CENTRAL WYOMING. PART 14. POSTCRANIUM OF *SHOSHONIUS COOPERI* (MAMMALIA: PRIMATES)

Marian Dagosto[1]

Daniel L. Gebo[2]

K. Christopher Beard
Associate Curator, Section of Vertebrate Paleontology
beardc@clpgh.org

Abstract

Postcranial elements of the omomyid primate *Shoshonius cooperi* are described from the late early Eocene (Lostcabinian) Buck Spring Quarries, Wind River Formation, central Wyoming. A complete right humerus, left femur, and nearly complete right tibia are among the remains. These allow several limb indices of functional importance to be estimated for the first time in the Omomyidae. Comparative functional analysis of the skeletal anatomy of *Shoshonius* indicates that leaping was an important part of its locomotor repertoire, but that *Shoshonius* was less specialized for leaping than is living *Tarsius* or those galagines classified as vertical clingers and leapers. Rather, *Shoshonius* more closely resembles cheirogaleids, *Otolemur*, and *Galagoides demidovii*, prosimian taxa in which quadrupedalism and climbing are as important components of the locomotor repertoire as is leaping. *Shoshonius* differs from specialized vertical clingers and leapers and resembles leaper-quadrupeds particularly in its relatively short, robust femur, high humerofemoral index, spherical humeral head, and long, low humeral trochlea. Although postcranial elements are known for only a small fraction of North American omomyids, *Shoshonius* closely resembles these taxa in most aspects of postcranial morphology, indicating that they too were likely more generalized than specialized in positional behavior.

Phylogenetic analysis of postcranial characters provides modest support for the monophyly of Tarsiiformes, which includes Eocene- Recent Tarsiidae, Eocene Omomyidae, and Eocene Microchoeridae. The hypothesis that tarsiids are more closely related to anthropoids than to Eocene omomyids and/or microchoerids requires much more homoplasy in the postcranial skeleton and is not supported by available evidence.

Key Words: Eocene, Primates, Postcranium, *Shoshonius*

Introduction

From 1985 to 1991, field crews from the Carnegie Museum of Natural History collected 13 limb elements of an omomyid primate from the Buck Spring Quarries, Wind River Basin, Wyoming (Table 1). The specimens are late Lostcabinian in age, dating to roughly 50.5 Ma (Stucky et al., 1990; Beard et al., 1991). Although none of these omomyid postcranial elements was found in articulation or in direct association with craniodental remains, they are attributed here to *Shoshonius cooperi*, a species that is represented at this locality by numerous skulls, jaws, and teeth (Stucky et al., 1990; Beard et al., 1991; Beard and MacPhee, 1994). The bones are identified as omomyid on the basis of their great similarity

---

[1] Department of Cell and Molecular Biology, Northwestern University, 303 East Chicago Avenue, Chicago, Illinois 60611. m-dagosto@nwu.edu
[2] Department of Anthropology, Northern Illinois University, DeKalb, Illinois 60115.
Submitted 5 June 1998.

Table 1.—*Postcranial elements of* Shoshonius cooperi *from the Buck Spring Quarries, Wind River Formation, Wind River Basin, Wyoming.*

Specimen	CM locality	Description
CM 67297	2404: K6, Quarry 6	left talus, complete
CM 67298	2404: K6, Quarry 6	left talus, virtually complete (slightly damaged posteroplantarly)
CM 67299	2404: K6, Quarry 6	right calcaneus, virtually complete (slightly damaged distomedially)
CM 69753	2409: K6, Quarry 11	left femur, proximal end (missing lesser trochanter)
CM 69754	2409: K6, Quarry 11	right metatarsal I, proximal end
CM 69755	2404: K6, Quarry 6	right humerus, complete
CM 69756	2404: K6, Quarry 6	left talus, complete
CM 69757	2404: K6, Quarry 6	right tibia, virtually complete (missing proximal end)
CM 69758	2404: K6, Quarry 6	left humerus, virtually complete but dorsoventrally crushed (missing distal part of supinator crest, capitulum)
CM 69759	3219: K6, surface	right tibia, distal end
CM 69760	2404: K6, Quarry 6	right femur, proximal end (missing lesser trochanter)
CM 69764	2404: K6, Quarry 6	left femur, complete (head slightly damaged)
CM 69765	2409: K6, Quarry 11	left calcaneus, complete

to homologous bones of other primates, especially omomyids. Their small size precludes assignment to Adapidae. Cranial and dental remains of *Shoshonius* far outnumber those of any other primate at this locality (Stucky et al., 1990). *Shoshonius* has traditionally been classified among the washakiin omomyines (Szalay, 1976; Honey, 1990). Among omomyids, *Shoshonius* is noteworthy because its cranial anatomy has been interpreted as evidence for a close phylogenetic relationship between this genus (and possibly other omomyids for which skulls remain unknown) and extant *Tarsius* (Beard et al., 1991; Beard and MacPhee, 1994).

Among the recovered postcranial elements are several virtually complete limb bones. Entire limb bones are extremely rare in the fossil record of tarsiiform primates, the only other examples being the nearly complete humeri, femora, and tibiofibulae of certain European microchoerids (Schlosser, 1907; Weigelt, 1933; Szalay and Dagosto, 1980; Dagosto, 1985; Dagosto and Schmid, 1996). The new material described here allows several limb indices of functional importance to be estimated for the first time in North American Omomyidae. Functional analysis of the postcranial anatomy of *Shoshonius* indicates that, although leaping was an important part of its locomotor repertoire, *Shoshonius* was not as anatomically specialized for this behavior as is living *Tarsius* or those galagines classified as vertical clingers and leapers (*G. senegalensis, G. moholi, G. gallarum*). Rather, *Shoshonius* most closely resembles those prosimian primates in which quadrupedalism and climbing are as important components of the locomotor repertoire as is leaping. This group of primates includes living cheirogaleids, *Galagoides demidovii*, and *Otolemur*. *Shoshonius* differs from specialized vertical clingers and leapers (VCLs) and resembles leaper/quadrupeds (LQs) in its relatively short, robust femur, high humerofemoral index, spherical humeral head, and long, low humeral trochlea.

Institutional acronyms are as follows: CM, Carnegie Museum of Natural History (Pittsburgh, Pennsylvania); FMNH, Field Museum of Natural History (Chicago, Illinois); UCMP, University of California Museum of Paleontology (Berkeley, California); USNM, National Museum of Natural History (Washington, D.C.).

ANATOMY OF *SHOSHONIUS COOPERI*

The limb bones of *Shoshonius* were compared with those of small prosimian primates, particularly cheirogaleids, galagos, and tarsiers, as well as those of other omomyids. Measurements of postcranial elements of *Shoshonius* are provided in Table 2. Definitions of limb measurements (and indices derived from these measurements) are provided by Szalay and Dagosto (1980), McArdle (1981), Dagosto (1985), Gebo (1988), Gebo et al. (1991), Dagosto and Schmid (1996), and Schmitt (1996).

Body Size.—The limb elements of *Shoshonius* are comparable in size to those of *Microcebus* and *G. demidovii* (50–70 g), but are much smaller than those of *Tarsius* (100–130 g) (Bearder, 1987; Rickart et al., 1993) (Table 3; Fig. 1). This suggests a body weight for *Shoshonius* well below estimates based on molar size, which range from 103–122 g (Conroy, 1987) to 155 g (Fleagle, 1988). Instead, regression equations based on postcranial dimensions (Table 4) suggest a body weight for *Shoshonius* conservatively estimated at 60–90 g. This discordance between weight estimates based on teeth and postcranial elements is common among omomyid primates (Dagosto and Terranova, 1992), and indicates relative megadonty in these small animals.

Limb Indices.—The humerofemoral index (HFI) of *Shoshonius* calculated from the mean of the two humeri (CM 69755 and CM 69788) and the single femur (CM 69764) is 64.6. Calculating the HFI separately for each humerus yields values of 63.3 and 65.9. These long bones are probably not all derived from the same individual. However, these values are very reasonable approximations of HFI in *Shoshonius* for the following reasons. (1) The probability of mixing long bones from two omomyid species of different body size is extremely low, because other omomyids are rare at this site (Stucky et al., 1990). (2) The size range observed in the skulls, dentitions, and limb bones of *Shoshonius* indicate that there was not a great degree of intraspecific variation in size. (3) The correlation between species mean HFI and HFI estimated from mean humerus length and mean femoral length is high ($r = 0.997$) in a sample consisting of 13 species of galagos, cheirogaleids, and tarsiers (Table 5). (4) In extant species with low HFIs, one cannot derive an HFI as high as that of *Shoshonius*, even if the index is constructed using the shortest femur and the longest humerus (Table 5). Conversely, in species with high HFIs, one cannot derive a particularly low HFI, even if the shortest humerus and longest femur are compared. (5) Finally, HFIs were constructed by having the computer randomly select a humerus and a femur from each species sample 100 times and averaging the values. The values obtained were not significantly different from the mean species HFI.

An HFI of 64.6 is quite high compared to specialized VCL primates (*Tarsius, Galago*: HFI 45–50), but similar to the proportions of the more frequently quadrupedal galagos (*Otolemur, Galagoides*) and cheirogaleids (Table 6). Figure 2 shows the disparity in humerofemoral lengths in *Tarsius* and *Shoshonius* (see Figure 1 for a comparison of *Shoshonius* and *Microcebus*). The estimated HFI of *Microchoerus* is 59 (Dagosto, 1993), indicating a greater degree of hind-limb dominance in this microchoerid than in *Shoshonius*.

The HFI is highly correlated ($r = 0.977$) with the intermembral index (IMI) in a sample composed of galagos, tarsiers, and cheirogaleids (although this may not be the case among primates generally; Jungers, 1985). This allows the intermem-

Table 2.—*Measurements (in mm) of postcranial elements of* Shoshonius cooperi.

	Specimen			
Element: dimension	CM 69755	CM 69758		Mean
Humerus	CM 69755	CM 69758		
length	24.87	23.90		24.39
proximal width	4.11	4.19		4.15
proximodistal chordal length of head	3.49	3.16		3.33
inferior mediolateral width of head	2.97	2.83		2.90
length of deltopectoral crest	10.03	9.50		9.77
anteroposterior width of midshaft	1.94			1.94
mediolateral width of midshaft	1.98			1.98
width of trochlea	2.03	2.26		2.15
height of trochlea	1.56	1.70		1.63
width of capitulum	1.40			1.40
width of capitulum + tail	1.93			1.93
width of distal articular surface	4.29			4.29
width of medial epicondyle	2.15	1.75		1.95
bicondylar width	6.12			6.12
length of brachial flange	10.00	9.22		9.61
Femur	CM 69764	CM 69760	CM 69753	
length	37.76			37.76
breadth of shaft distal to lesser trochanter (BSDLT)[1]	2.59	2.36	2.31	2.42
neck length 1[1]		3.63	3.93	3.78
neck length 2[1]	2.17	1.57	1.60	1.78
neck angle, in degrees[1]	70	63	68	67
fossa length[1]	2.50	3.04	2.97	2.84
width of lesser trochanter	2.00			2.00
height of lesser trochanter[1]	3.27			3.27
height of third trochanter[1]	1.62	2.42	2.38	2.14
width of third trochanter	1.34	1.19	1.16	1.23
anteroposterior width of midshaft	2.15			2.15
mediolateral width of midshaft	2.46			2.46
height of lateral condyle	5.63			5.63
bicondylar width	5.05			5.05
Tibia	CM 69757	CM 69759		
length (estimate)	38.00			38.00
height of cnemial crest	3.49			3.49
anteroposterior width of midshaft	2.04			2.04
mediolateral width of midshaft	1.90			1.90
length of distal facet	2.74	2.99		2.87
width of distal facet	2.33	2.57		2.45
malleolar rotation, in degrees	18	13		15.5
Talus	CM 67297	CM 67298	CM 69756	
length (A1)[2]	5.24	5.66	5.66	5.52
width (A2)[2]	2.66	2.90	2.84	2.80
neck length (A5)[2]	2.75	3.12	2.81	2.89
length of trochlea (A3)[2]	2.66	2.78	2.64	2.69
width of trochlea (A4)[2]	2.04	2.01	2.09	2.05
lateral height (A7)[2]	2.37		2.37	2.37
width of head	1.87	1.94	2.20	2.00
height of head	1.84	1.81	1.60	1.75
Calcaneus	CM 69765	CM 67299		
length (C1)[2]	9.82	9.76		9.79
width (C2)[2]	2.97	3.53		3.25

Table 2.—*Continued.*

Element: dimension	Specimen		Mean
	CM 69755	CM 69758	
length of posterior talocalcaneal facet (C3)[2]	2.27	2.18	2.23
width of posterior talocalcaneal facet (C4)[2]	1.37	1.13	1.25
heel length (C7)[2]	2.15	2.28	2.22
anterior length	5.00	5.19	5.10
width of cuboid facet (C6)[2]	2.29	2.34	2.32
height of cuboid facet (C5)[2]	1.56	1.53	1.55

[1] See Dagosto and Schmid (1996) for explanation of measurements of the proximal femur.

[2] See Dagosto and Terranova (1992) for explanation of tarsal measurements.

Table 3.—*Measurements (in mm unless noted otherwise; species means are given) of postcranial elements in* Shoshonius *and some extant prosimians. See Dagosto and Terranova (1992) for definition of tarsal measurements used here.*

Measure	*Shoshonius cooperi*	*Microcebus murinus*	*Galagoides demidovii*	*Tarsius syrichta*	*Galago moholi*	*Galago senegalensis*	*Cheirogaleus medius*
weight, in g	?	50	70	125	160	215	233
area of M_1, in mm^2	3.40	2.22	3.37	7.01	4.11	4.83	4.87
area of M^1, in mm^2	5.25	3.70	5.50	11.69	7.30	8.02	6.37
Talus							
A1	5.52	5.46	5.54	6.73	8.01	8.37	6.62
A2	2.80	2.71	3.40	4.13	5.11	5.38	3.84
A3	2.69	2.49	2.94	3.93	4.31	4.18	3.62
A4	1.97	1.85	2.10	3.13	3.28	3.28	2.60
Calcaneus							
C1	9.79	9.87	21.05	26.10	28.19	29.82	9.88
C2	3.25	2.52	3.05	3.58	4.33	4.70	3.58
C3	2.25	1.85	2.24	3.15	3.29	3.47	2.88
C4	1.25	1.17	1.35	1.70	2.18	2.13	1.68
C5	1.55	1.68	1.90	2.30	2.43	3.00	2.10
Humerus							
length	24.38	20.89	25.64	28.38	31.27	32.10	27.01
anteroposterior width of midshaft	1.89	1.70	1.79	2.30	2.51	2.69	2.57
mediolateral width of midshaft	1.98	1.71	1.61	2.12	2.47	2.69	2.55
bicondylar width	6.12	4.92	5.76	7.91	8.12	8.53	8.29
Tibia							
length	38.00	33.40	42.38	57.13	57.52	60.38	40.50
Femur							
length	37.76	29.41	38.39	56.65	62.83	68.10	39.90
anteroposterior width of midshaft	2.15	2.00	2.16	2.76	3.81	4.38	2.78
mediolateral width of midshaft	2.46	3.14	2.05	2.43	3.18	3.68	2.76
bicondylar width	5.05	4.47	4.55	6.10	7.30	7.74	7.37

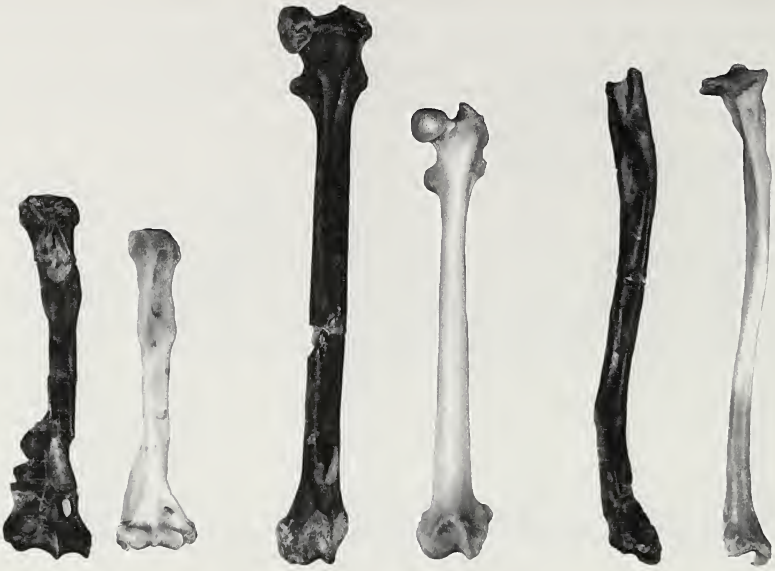

Fig. 1.—Postcranial elements of *Shoshonius cooperi* (left of each pair) compared with those of *Microcebus murinus* (right of each pair).

bral index of *Shoshonius* to be estimated as 66 (95% confidence intervals = 64–68).

McArdle (1981) ranked galagos into three groups based on the IMI. Those with the highest IMI (> 66) (*Otolemur, G. demidovii*) use quadrupedalism most frequently; the intermediate group (IMI = 62–64: *Euoticus, G. alleni, G. zanzibaricus*) uses quadrupedalism less frequently; and the third group (IMI < 60: *G. moholi, G. senegalensis, G. gallarum*) includes the most frequent leapers. This scheme works fairly well for other prosimians as well. Cheirogaleids, most lemurids, and *Daubentonia* fall into group 1; *Hapalemur, Lepilemur*, and most indriids in group 2; and tarsiers and *Avahi* in group 3. Distribution of these taxa on the basis of HFI follows an identical pattern. *Shoshonius* falls at the junction of groups 1 and 2, with the leaper/quadrupedal forms, not the most specialized leapers.

The humerotibial index (HTI) of *Shoshonius* is estimated at 64. The distribution of this index is quite similar to that of the HFI and IMI, and thus *Shoshonius* again groups with the non-VCL forms. The HTI of *Necrolemur* is estimated at 53 (Dagosto, 1993), which is lower than *Shoshonius*, but still higher than in extant VCL forms.

The crural index of approximately 100 is typical for prosimians (Table 6). This index shows few correlations with locomotor groups, but *Shoshonius* likely did not have the unusually high crural index of *G. demidovii* or *Microcebus*. Given its humerus length of roughly 24 mm, the unknown radius of *Shoshonius* would have been unusually long to achieve a brachial index greater than 100, values that are typical for tarsiers and indriids (but not galagos).

Table 4.—*Estimation of body mass (in g) of* Shoshonius cooperi *derived from dental and postcranial measures. Prediction equations are based on least squares regression of a strepsirhine dataset. Sources of equations used to predict body mass are as follows:* [1] Dagosto and Terranova (1992); [2] Conroy (1987); and [3] Terranova (1994).

Measure	Mean predicted body mass	95% confidence intervals (lower–upper)
M^1 area[1]	113	77–165
M_1 area[1,2]	120, 103	92–158
humerus length[3]	69	
anteroposterior width of humeral midshaft[3]	64	
mediolateral width of humeral midshaft[3]	73	
femur length[3]	72	
anteroposterior width of femoral midshaft[3]	60	
mediolateral width of femoral midshaft[3]	106	
A1[1]	90	84–96
A2[1]	61	57–66
A3[1]	66	62–70
A4[1]	72	67–77
A7[1]	84	79–89
C2[1]	121	115–128
C3[1]	97	91–103
C4[1]	53	49–58
C5[1]	50	45–55
C6[1]	102	97–107
C7[1]	107	94–122
Index 1[1]	83	78–88
Index 4[1]	69	65–73
Index 6[1]	69	65–74
minimum	50	45–55
maximum	121	115–128
mean	78	75–86

Table 5.—*Estimation of the humerofemoral index (HFI) in some extant prosimians.*

Locomotor category/taxon	Species mean HFI	mean humerus/ mean femur	shortest humerus/ longest femur	longest humerus/ shortest femur	randomly generated HFI
Specialized leapers					
Tarsius bancanus	45.9	45.7	42.9	51.1	45.5
Galago senegalensis	47.1	47.1	40.5	53.4	48.0
Galago gallarum	49.0	48.1	43.1	54.2	47.4
Galago moholi	49.6	49.6	43.4	54.6	50.1
Tarsius syrichta	50.8	50.1	42.0	61.0	49.4
Intermediates					
Euoticus elegantulus	59.1	58.8	53.8	69.4	59.2
Galago alleni	60.1	60.0	57.7	62.3	60.1
Leaper/Quadrupeds					
Otolemur garnetti	64.1	64.0	54.7	75.6	64.1
Cheirogaleus medius	65.8	65.8	62.0	69.6	65.8
Otolemur crassicaudatus	66.1	66.0	60.5	76.4	65.4
Galagoides demidovii	66.6	66.5	58.4	79.0	66.7
Microcebus murinus	71.1	71.0	56.3	90.0	71.2
Cheirogaleus major	71.4	71.5	53.3	92.4	70.8

Table 6.—*Limb indices in* Shoshonius cooperi *and some extant prosimians. Humerofemoral index (HFI) = (100)(humerus length)/femur length; intermembral index (IMI) = (100)(humerus length + radius length)/(femur length + tibia length); crural index (CI) = (100)(tibia length)/femur length; brachial index (BI) = (100)(radius length)/humerus length.*

Locomotor category/taxon	*n*	mean HFI, *s.d.*	mean IMI, *s.d.*	mean CI, *s.d.*	mean BI, *s.d.*
Shoshonius cooperi	1	64.6	~66	~100	?
Leaper/quadrupeds					
Microcebus murinus	19	71, 1.19	71, 0.95	112, 4.36	111, 5.88
Cheirogaleus medius	6	68, 2.7	68, 0.09	101, 1.7	103, 1.5
Cheirogaleus major	9	71, 2.41	70, 1.09	101, 2.96	98, 4.89
Otolemur crassicaudatus	9	66, 1.84	71, 0.59	95, 1.96	106, 2.28
Otolemur garnetti	10	64, 1.68	67, 1.39	94, 2.08	103, 4.73
Galagoides demidovii	12	66, 2.25	67, 0.7	109, 2.98	113, 2.38
Specialized leapers					
Galago moholi	9	50, 1.25	53, 0.35	91, 0.94	106, 3.13
Galago senegalensis	6	47, 0.56	53, 2.03	89, 0.79	103, 0
Galago gallarum	4	49, 1.6	51, 1.21	95, 0.71	103, 1.07
Tarsius syrichta	11	51, 0.88	57, 0.71	101, 1.39	126, 1.47
Tarsius bancanus	8	46, 2.19	52, 0.25	99, 0.84	126, 3.97

In summary, the new postcranial elements show that *Shoshonius* likely did not have the low HFI and IMI, nor the high brachial index typical of extant specialized vertical clingers and leapers, but was more comparable to less specialized leaper/quadrupeds in its limb proportions.

Limb Scaling.—The relationship between body mass and limb length in primates has been studied by several investigators (Jungers, 1985; Terranova, 1994). Assuming *Shoshonius* followed the scaling relationships of extant cheirogaleids, limb lengths yield body mass estimates higher than what most other postcranial dimensions would suggest (Table 7). Galagid equations yield reasonable weight estimates from humerus length, but low estimates from femur length. These observations suggest that *Shoshonius* likely had longer humeri and femora than would be expected in a cheirogaleid of its mass, while its femur was shorter than that of a comparably sized galago.

Another way to examine this is to predict long-bone lengths for *Shoshonius* assuming body weights of 60–100 g (Table 7). Humerus length is better predicted by the galago than the cheirogaleid equation; the cheirogaleid model grossly underestimates femur length, while the galago equation overestimates femur length. The relationship between body mass and humerus and femur length in *Shoshonius* does not appear to be significantly different from the average for strepsirhine primates. *Shoshonius* does not have the extremely elongated hind limbs typical of specialized leapers.

Humerus.—CM 69755 is the only complete humerus known from a North American omomyid (Fig. 3). It exhibits minor breakage along the deltopectoral crest and has eroded areas on the humeral head. Cracks run through the shaft and brachial flange. In a second specimen (CM 69758), the proximal part of the shaft is crushed, and the capitulum, lateral epicondyle, and lateral half of the brachial flange are missing.

The humeral head extends slightly above the greater tuberosity. The head is relatively round, being only moderately taller than wide (inferior width to prox-

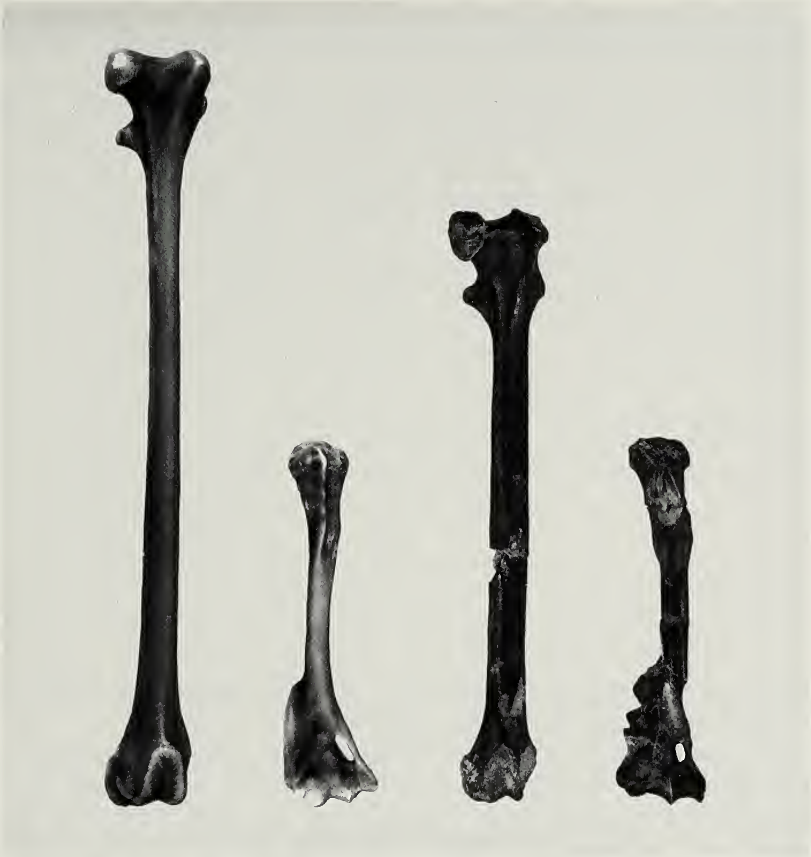

Fig. 2.—Femur and humerus of *Tarsius* (left) and *Shoshonius* (right), scaled to the same humeral length. Note the greater relative length of the femur in *Tarsius*.

imodistal length index, Table 8; Fig. 4), and thus is more similar in shape to quadrupedal primates than to specialized vertical clingers and leapers, which have narrower humeral heads with limited mediolateral mobility distally (Schmitt, 1996). VCL primates also increase the range of flexion and extension possible at the shoulder joint by inflating the anterior-posterior dimensions of the humeral head (Schmitt, 1996). Our estimate of this feature (Table 8:ap extension index) indicates that *Shoshonius* again groups with the leaper/quadrupeds, not the specialized VCLs. In contrast, *Microchoerus* exhibits a narrower, anteroposteriorly extended humeral head similar to that of VCL primates.

The attachment areas for the shoulder muscles are better developed in *Shoshonius* than in most extant prosimians (Fig. 1–4). The lesser tuberosity is prominent, as is the attachment area for latissimus dorsi. The deltopectoral crest comprises 40% of the total length of the humerus, which is typical for extant primates, and is quite extensive anteriorly. The brachial flange, the area for attachment of the brachial and brachioradialis muscles, is also prominent and curves back along the shaft proximally. The flange covers 39% of the length of the humerus. The

Table 7.—*Scaling of body mass (in g) and humerus and femur length (in mm) in* Shoshonius cooperi. *Sources of equations used to predict body mass are as follows:* [1] *Terranova (1994);* [2] *Jungers (1985).*

Element/scaling model	Actual value	Predicted weight	Predicted limb length at 60 g	Predicted limb length at 80 g	Predicted limb length at 100 g
Humerus	24.38				
Cheirogaleid model					
length/mass[1]		111.7	13.4	15.9	18.1
length/mass[2]		112.9	18.8	21.2	23.1
Galagine model					
length/mass[1]		80.8	22.3	24.7	26.8
length/mass[2]		68.9	23.1	25.6	27.7
Strepsirhine model					
length/mass		69.3	23.2	25.6	27.7
Femur	37.76				
Cheirogaleid model					
length/mass[1]		126.6	18.8	22.3	25.5
length/mass[2]		143.2	26.2	29.5	32.4
Galagine model					
length/mass[1]		52.0	51.7	54.8	57.3
length/mass[2]		45.8	41.1	45.1	48.4
Strepsirhine model					
length/mass		72.8	35.2	39.1	42.3

lateral extent of the flange is similar to that of many prosimian primates, including *Tarsius*, but is wider than in *Microchoerus*.

The capitulum is very round and ball-like compared to the more proximodistally elongated, mediolaterally restricted capituli of *Absarokius* and *Hemiacodon* (Fig. 5). In this feature, *Shoshonius* is more like *Tarsius* than are other omomyids. *Shoshonius* has a capitular tail that is similar in relative length to a variety of prosimian primates (Gebo et al., 1994). As in other omomyids the trochlea is long

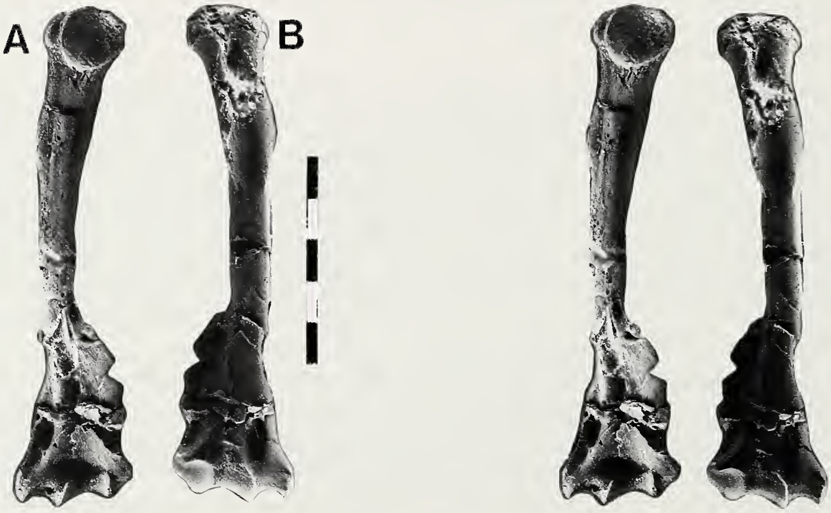

Fig. 3.—Right humerus of *Shoshonius cooperi* (CM 69755) in posterior (A) and anterior (B) views. Both views are stereopairs. Scale = 10 mm.

(47% of articular width), and lower (76% of trochlear length) than in extant vertical clingers and leapers. Thus, the elbow joint of *Shoshonius* is more similar to that of leaper/quadrupeds (Szalay and Dagosto, 1980). As in other haplorhines, the trochlea is downturned (i.e., the medial edge extends further distally than does the lateral edge). A large entepicondylar foramen is present. The medial epicondyle is broad and medially directed, and thus does not differ from the configuration typical of most prosimian primates, including other omomyids. Posteriorly, the olecranon fossa is shallow, with low crests running along the rims of the trochlea. A shallow dorsoepitrochlear fossa is present as in other omomyids and microchoerids. *Tarsius* lacks this fossa. *Shoshonius* lacks the distally tapered, anteroposteriorly extended humeral head and high, short humeral trochlea typical of extant vertical clingers and leapers. The humerus is quite similar to that of less specialized leaper/quadrupeds, except for having more prominent muscle scars.

Femur.—CM 69764 is the most nearly complete femur ever recovered of an omomyid primate (Fig. 6). The head is damaged, especially medially, the shaft is cracked in several places, and the greater trochanter, lateral condyle, and patellar facet are slightly eroded. The head is well preserved in two other proximal femora (CM 69753 and CM 69760).

As in other omomyids, tarsiers, and galagos, the joint surface of the femoral head is extended onto the posterodorsal aspect of the femoral neck, and the posterior surface of the head is slightly flat (Fig. 7). Like *Hemiacodon* and other North American omomyids, the femoral head is only moderately flat medially and somewhat rounded dorsally. This semicylindrical shape of the femoral head in *Shoshonius* and *Hemiacodon* contrasts with the more fully cylindrical shape observed in galagos and tarsiers. The femoral neck and head are aligned to the shaft at an angle of 67° (Table 9), which is slightly less perpendicular than observed in other omomyids, galagos, or tarsiers. The neck is also relatively longer than in other North American omomyids, galagos, or tarsiers, but still fairly short compared to lemurids, indriids, and platyrrhines.

The entire proximal part of the femur is bowed anteriorly relative to the shaft. The greater trochanter overhangs the anterior part of the shaft and extends slightly proximal to the head. The anterior region of the proximal femur possesses an especially prominent lateral pillar extending from the greater trochanter, forming a central triangular fossa on the proximoanterior surface of the femur for the attachment of vastus lateralis. In all of these features, *Shoshonius* resembles other omomyids and tarsiers. The lesser trochanter is fairly broad (high projection index) and protrudes from the shaft at an angle of 30°, which is a more posterior orientation than in other omomyids, galagos, or tarsiers. *Necrolemur* resembles *Shoshonius* in terms of orientation of the lesser trochanter. The third trochanter is laterally prominent, and more similar in its size, morphology, and placement to *Tarsius* and other omomyids than to galagos, in which the third trochanter is incorporated into a crest extending distally from the greater trochanter (Burr et al., 1982; Dagosto and Schmid, 1996). The third trochanter is proximal to the lesser trochanter. A paratrochanteric crest is present. The trochanteric fossa is deep but short as in other omomyids (and in contrast to *Necrolemur*), although not quite as short as in galagos or tarsiers. There is no intertrochanteric crest.

The robusticity of the femoral shaft of *Shoshonius* is more comparable to leaper/quadrupeds than to specialized leapers, and is likely an additional reflection of a relatively short femur in this omomyid. In contrast to most extant strepsirhines and *Tarsius* (except *Otolemur crassicaudatus* and some cheirogaleids; Terranova,

Table 8.—*Indices of the humerus in* Shoshonius cooperi, *other fossil tarsiiforms, and some extant prosimians. Mean values are provided first, with ranges in parentheses. Abbreviations are as follows:* N *(x,y), sample sizes of proximal and distal humeri, respectively; INFW, width of inferior quadrant of humeral head; PD CHORD, proximodistal chordal length of humeral head; AP EXT, central anteroposterior chord from PD CHORD/INFW; DPCL, maximum deltopectoral crest length; HL, humerus length; BFL, brachial flange length; TH, trochlear height; TW, trochlear width; AW, width of distal articular surface of humerus; CTW, capitular tail width; CW, capitular width. Humeral head measurements after Schmitt (1996); due to the small size of* Shoshonius, *the same method of measuring could not be adopted. Instead, PD CHORD (corresponds to Schmitt's measurement PD central) and INFW (corresponds to Schmitt's measurement ML inf) were measured directly from the specimens with calipers, AP EXT was measured by tracing the proximodistal arc of the humeral head with a camera lucida, and measuring the perpendicular distance from the highest point of the arc to the implicit PD CHORD (corresponds to Schmitt's measurement AP cent). Distal humerus measurements after Szalay and Dagosto (1980) and Gebo et al. (1994).* Absarokius *data are from Covert and Hamrick (1993).*

		Humeral head		Humeral shaft		Elbow joint		
Taxon	*N* (x,y)	INFW/PD CHORD	AP EXT	DPCL/HL	BFL/HL	TW/AW	TH/TW	CTW/CW
Shoshonius cooperi	2, 1	87.3 (85.1–89.6)	56.7 (55.8–57.6)	40 (39.7–40.3)	39.4 (38.6–40.2)	47.3	76 (75.2–76.8)	37.8
Hemiacodon gracilis	0, 3					45.8 (42.9–47.8)	69.2 (67.8–73.8)	33.5 (29.4–37.6)
?*Tetonius* (UCMP)	0, 1					35.4	78.2	
UCMP 113301	0, 1					44.3	61.9	
Absarokius	0, 1					42.4	70.7	28.4
Necrolemur sp.	0, 2					49.1 (47.1–51.2)	81.2 (79.0–83.5)	46.6 (46.0–47.2)
Microchoerus sp.	1, 2	72.5	84.5	46.2	39.1	49.0 (47.1–50.8)	70.2 (68.0–72.4)	38
Leaper/quadrupeds								
Microcebus murinus	6, 18	73.4 (70.6–77.0)	71.4 (65.2–79.0)	41.8 (39.4–45.5)	36.1 (32.1–38.4)	48.4 (43.5–55.2)	77 (66.7–85.8)	
Cheirogaleus medius	3, 3	75.8 (70.1–81.9)	62.5 (58.3–66.8)	46.4 (45.4–48.4)	39.5 (36.0–43.5)	49.8 (44.4–53.8)	77.8 (64.1–88.7)	25.6 (22.5–25.6)
Cheirogaleus major	2, 6	80.7 (73.7–87.8)	71.8 (69.5–74.1)	43.2 (42.2–44.3)	43.1 (42.4–43.9)	46.4 (43.2–50.0)	78.3 (71.0–92.5)	58.2 (44.5–72.0)
Otolemur crassicaudatus	3, 7	77.0 (74.9–79.0)	57.4 (54.1–60.6)	41.9 (40.8–42.4)	37.8 (35.5–39.5)	44.8 (41.8–48.9)	90.1 (82.7–102.1)	42.2 (41.7–42.7)
Otolemur garnetti	3, 6	74.2 (64.6–81.2)	64.6 (47.7–83.6)	42.7 (41.0–44.8)	38.3 (35.6–39.9)	44.1 (42.0–47.8)	81.7 (74.1–95.9)	41.1 (33.3–48.8)
Galagoides demidovii	4, 7	70 (66.6–74.1)	76 (69.7–77.9)	39.7 (36.5–40.9)	41.5 (34.4–44.7)	45.0 (41.2–49.2)	91.7 (78.4–101.5)	

Table 8.—*Continued.*.

		Humeral head		Humeral shaft		Elbow joint		
Taxon	*N* (x,y)	INFW/PD CHORD	AP EXT	DPCL/HL	BFL/HL	TW/AW	TH/TW	CTW/CW
Specialized leapers								
Galago moholi	6, 7	68 (62.7–73.5)	84.6 (77.7–98.1	40.1 (37.8–43.2)	43.3 (41.9–45.6)	44.6 (42.8–45.4)	99.1 (93.8–105.5)	
Galago senegalensis	2, 2	69.0 (68.7–69.3)	70.4 (68.1–72.8)	41.1 (40.3–41.8)	47.9 (47.4–48.5)	36.2 (33.4–39.0)	109.2 (108.7–109.7)	48.7 (45.9–51.5)
Galago gallarum	5, 5	65.6 (62.2–70.4)	92.8 (80.6–102.3)	42.5 (41.5–42.9)	43.2 (41.5–45.9)	41.8 (39.2–44.7)	103.3 (91.4–121.0)	
Tarsius syrichta	6, 10	70.6 (62.6–77.3)	81.7 (73.3–82.0)	38.8 (33.4–41.9)	34 (31–37)	41.9 (37.8–47.9)	101.9 (86.5–121.0)	39.3 (17.2–53.3)
Tarsius bancanus	7, 6	66 (59.3–76.3)	86 (75.6–115.8)	40.1 (32.9–44.4)	38 (34–44)	38.4 (33.3–43.7)	113.4 (96.6–135.1)	41 (16.5–70.0)

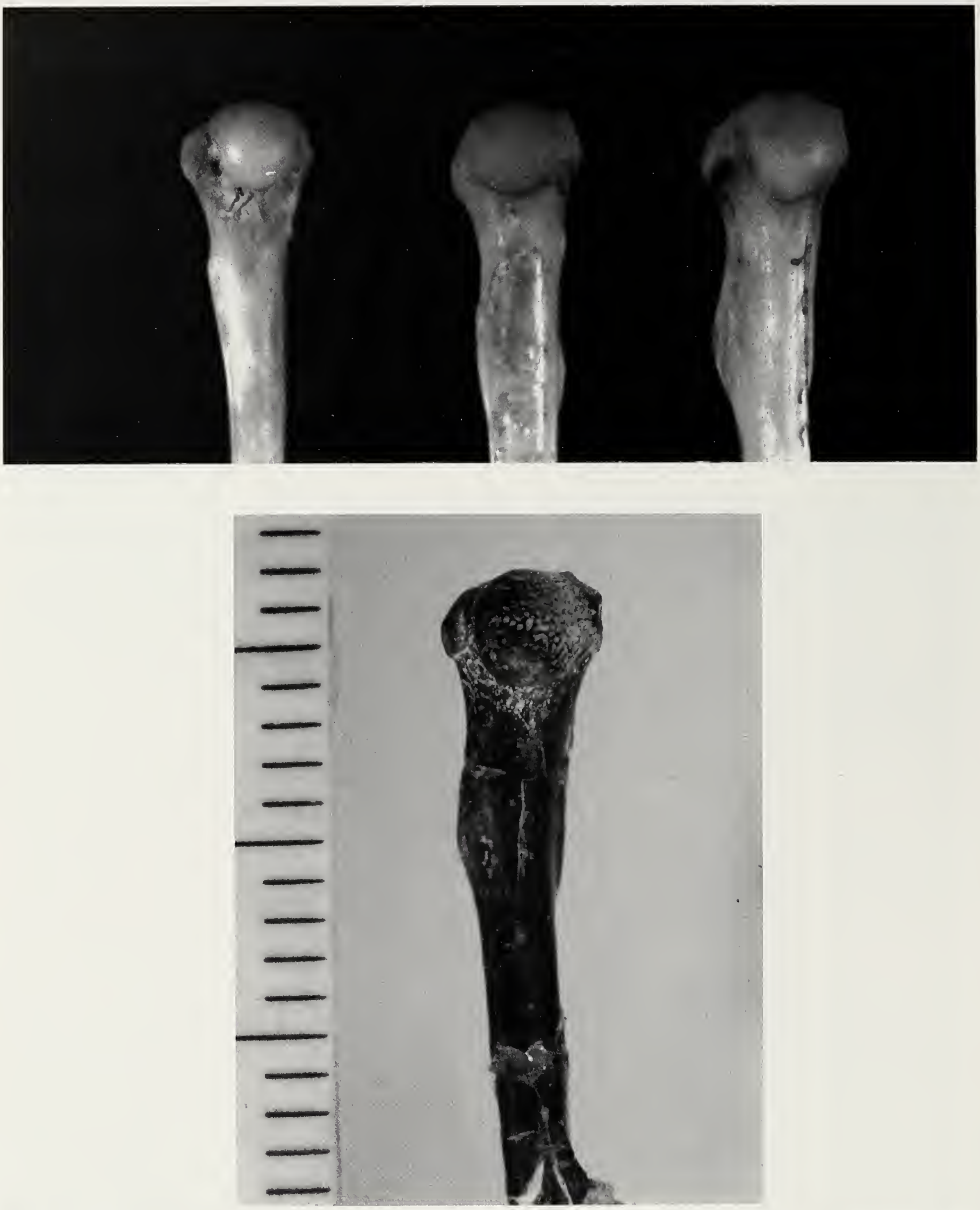

Fig. 4.—Proximal humeri of extant prosimians (top) and *Shoshonius* (bottom), all in posterior view. From left to right, extant taxa are as follows: *Tarsius syrichta* (FMNH 129379), *Cheirogaleus medius* (FMNH 85146), and *Galago senegalensis albipes* (FMNH 153087). Note the relatively narrower distal part of the humeral head in *Tarsius* and *Galago* compared to *Cheirogaleus* and *Shoshonius*. Scale in mm.

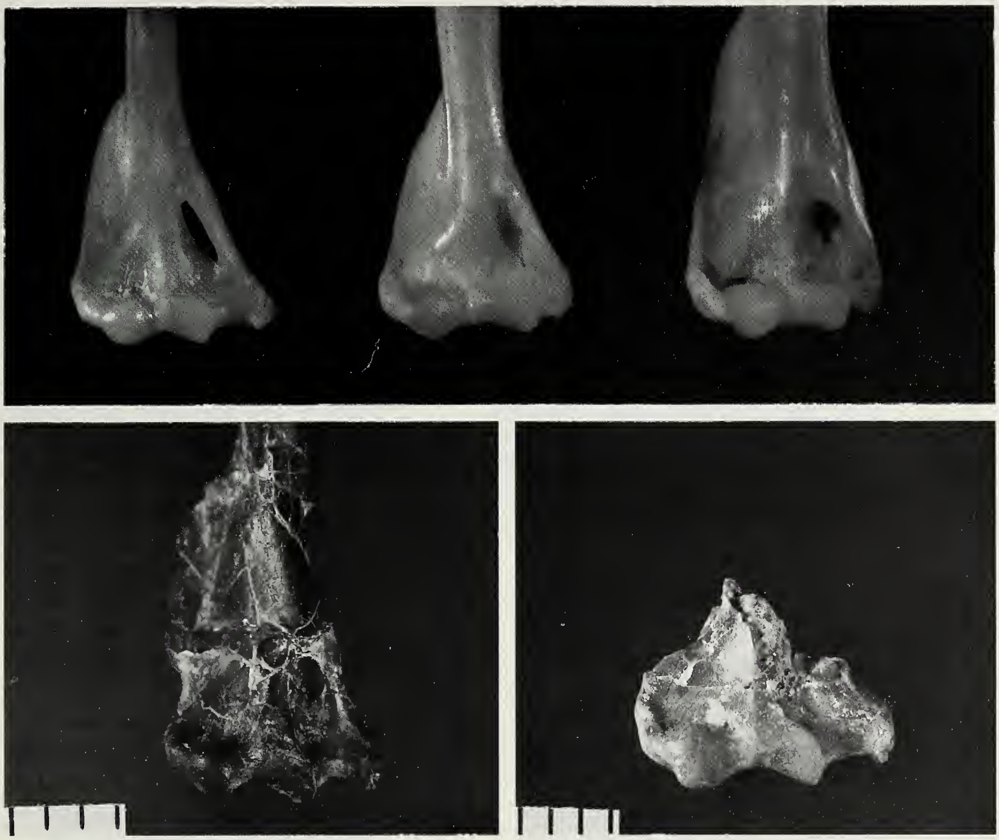

Fig. 5.—Distal humeri of extant prosimians (top) and Eocene omomyids (bottom), all in anterior view. From left to right, extant taxa are as follows: *Tarsius, Cheirogaleus*, and *Galago senegalensis*. Eocene omomyids are *Shoshonius cooperi* (left, CM 69755) and *Hemiacodon gracilis* (right, AMNH 126722). Note that the trochlea is relatively longer in *Shoshonius* and *Hemiacodon* than in *Tarsius* and that the capitulum is more spherical in *Shoshonius* and *Tarsius* than in *Hemiacodon*. Scale in mm.

1994), in *Shoshonius* the external mediolateral diameter of the femoral midshaft exceeds the anteroposterior diameter. *Otolemur crassicaudatus* and *O. garnettii* also have relatively lower ratios of ap to ml bending strength than other galagos (Demes and Jungers, 1993; Terranova, 1994). This suggests that in *Shoshonius*, the femur was not subjected to the high anteroposterior bending moments experienced by specialized leapers (Schaffler et al., 1985).

Specialized leapers are also distinguished by humeral/femoral contrasts in bone cross-sectional properties (Schaffler et al., 1985; Ruff and Runestad, 1992; Demes and Jungers, 1993; Terranova, 1994). Contrasts of external dimensions parallel the observed differences in bone cross-sectional properties. An index of humeral to femoral midshaft areas (external ap dimension multiplied by the ml dimension; Table 9) shows that specialized leapers (with the exception of *Tarsius*) have low indices (femoral area greatly exceeds humeral area), while leaper/quadrupeds have higher indices. The index of *Shoshonius* is higher than is usual in the specialized leapers, and more comparable to the leaper/quadruped group.

The knee is very tall and narrow, with an elevated and rounded lateral patellar

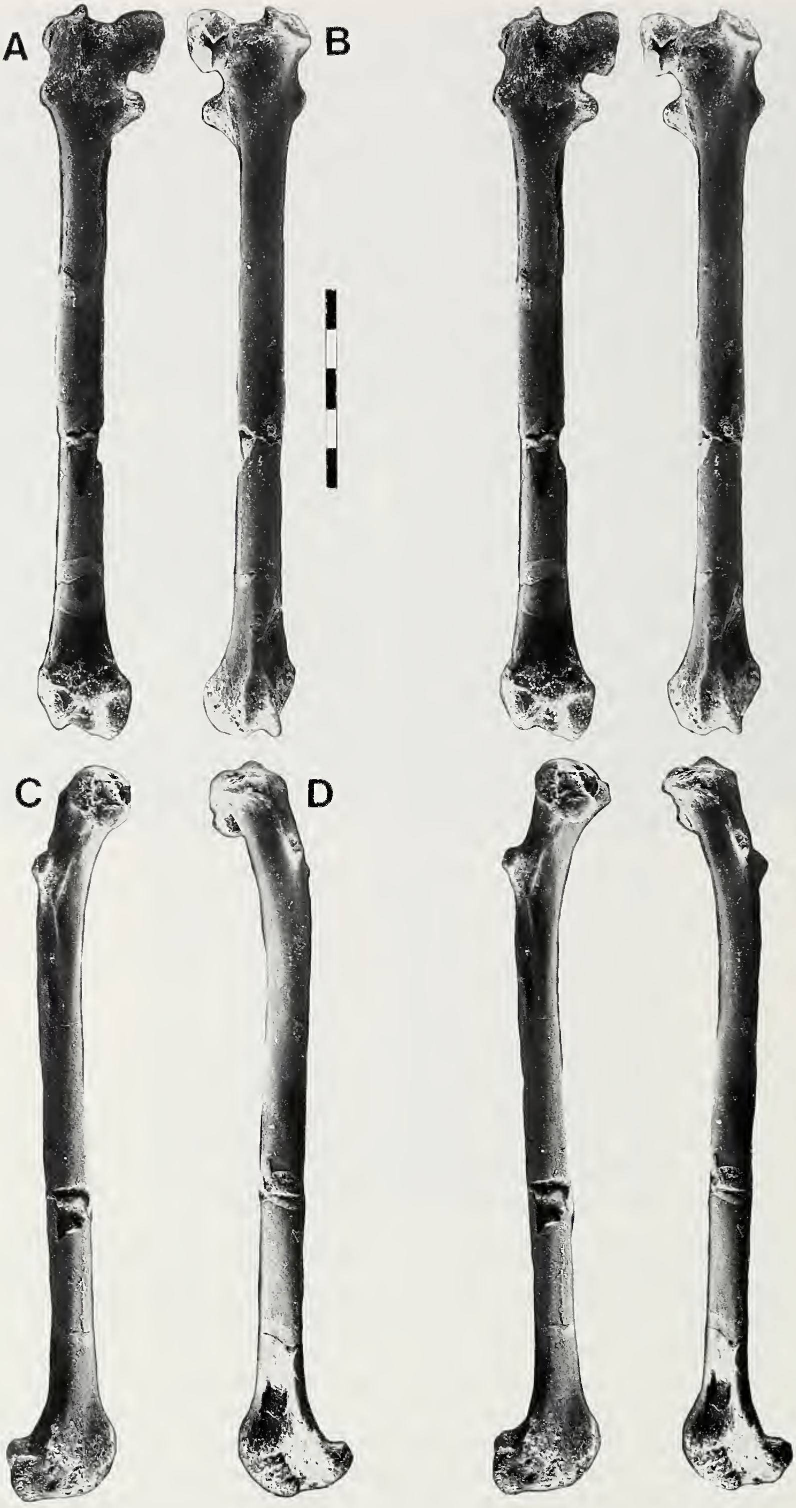

Fig. 6.—Left femur of *Shoshonius cooperi* (CM 69764) in posterior (A), anterior (B), medial (C), and lateral (D) views. All views are stereopairs. Scale = 10 mm.

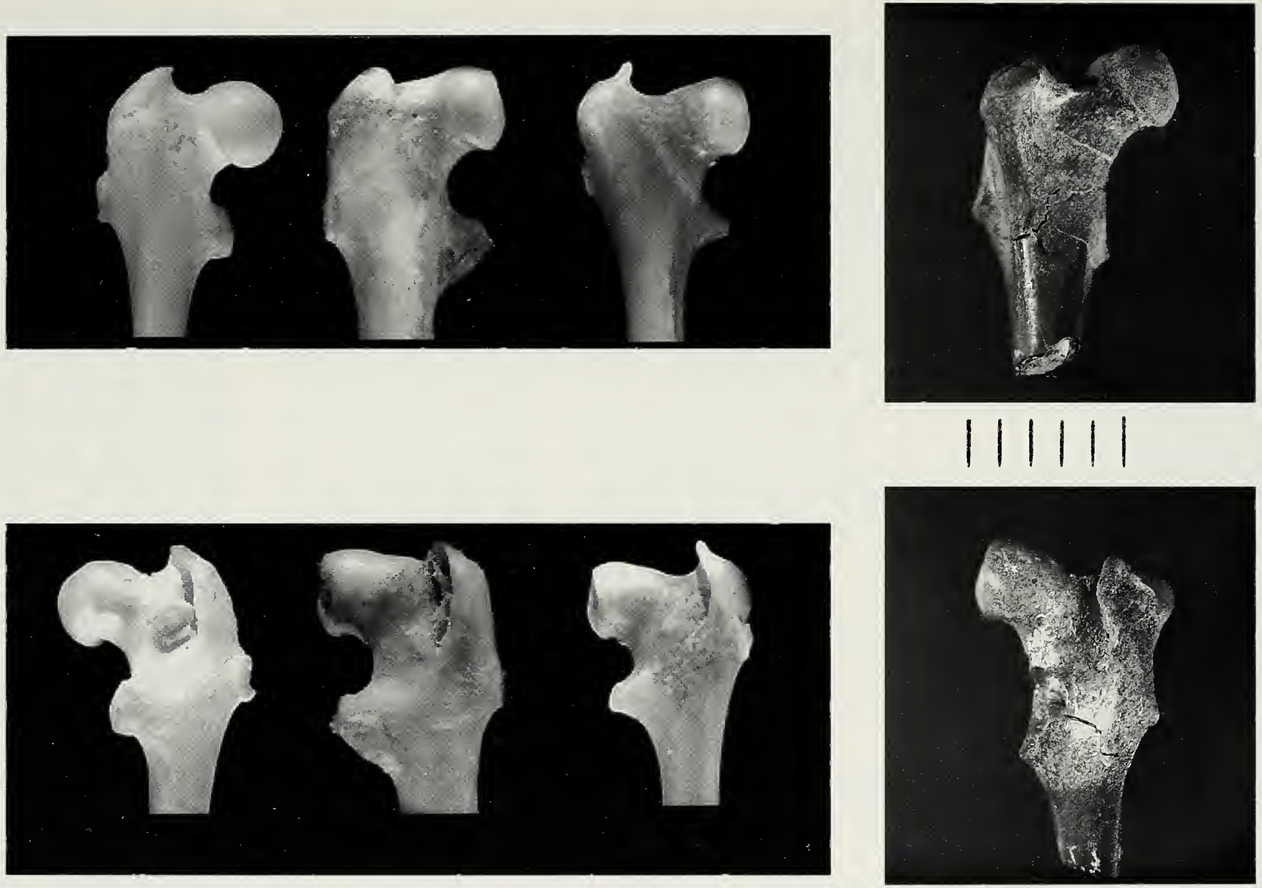

Fig. 7.—Proximal femora of extant prosimians and *Shoshonius* in anterior (top) and posterior (bottom) views. From left to right, specimens illustrated are as follows: *Cheirogaleus major* (FMNH 85144), *Otolemur ?garnetti* (FMNH 53066), *Tarsius syrichta* (FMNH 142007), and *Shoshonius cooperi* (CM 69760). Note the nearly spherical shape of the femoral head in *Cheirogaleus*, the semicylindrical shape of the femoral head in *Shoshonius*, and the more fully cylindrical shape of the femoral head in galagos and tarsiers. Scale in mm.

Table 9.—*Measurements and indices of the femur and tibia in* Shoshonius cooperi, *other fossil tarsiiforms, and some extant prosimians. Mean values are provided first, with ranges in parentheses.* N *(x,y,z) = sample sizes at proximal femora, distal femora, and tibiae, respectively. Femoral robusticity = (100)(femoral midshaft anteroposterior diameter + femoral midshaft mediolateral diameter)/femoral length. Other femoral measurements are defined in Dagosto and Schmid (1996). Distal tibial measurements are defined in Dagosto (1985).*

Taxon	*N* (x,y,z)	Lesser trochanter		Femoral neck	
		Projection	Angle	Length 1	Angle
Shoshonius cooperi	3, 1, 2	77.2	30	162.0 (153.8–170.1)	67 (63–70)
Hemiacodon gracilis	3, 1, 1	42.8	23 (20–27)	129.1	73.5 (72–75)
USNM 336187	1, 0, 0	69.7	20	137.6	74
?Omomys	1, 1, 3	38.9	12	129.3	71
Necrolemur sp.	1, 0, 1		47	179.2	65
Microchoerus sp.	1, 1, 0	72.7			
Leaper/quadrupeds					
Microcebus murinus	6, 14, 18	65.5 (38.3–88.9)	17 (9–23)	168.2 (142.3–193.2)	68 (65–75)
Cheirogaleus medius	3, 3, 3	62.1 (64.1–66.6)	11 (9–13)	174.4 (170.0–178.8)	62 (63–68)
Cheirogaleus major	6, 7, 7	62.1 (52.0–70.5)	16 (11–19)	183.0 (174.7–193.5)	64 (59–71)
Otolemur crassicaudatus	6, 6, 5	80.3 (70.3–93.0)	13 (8–16)	138.9 (120.1–154.2)	70.8 (65–76)
Otolemur garnetti	3, 6, 6	67.3 (57.5–79.8)	9 (5–14)	126.9 (122.0–130.3)	71.7 (65–80)
Galagoides demidovii	4, 4, 4	69.2 (60.3–78.7)	11 (7–14)	143.1 (127.0–154.1)	73 (67–79)
Specialized leapers					
Galago moholi	5, 5, 5	55.6 (52.2–66.9)	12 (10–15)	134.6 (119.4–152.7)	74.2 (72–80)
Galago senegalensis	3, 1, 2	62 (46–74.4)	11 (8–14)	141.8 (137.9–144.1)	74 (66–83)
Galago gallarum	5, 5, 4	64.6 (54.9–79.2)	8 (5–13)	153.6 (136.2–174.3)	77.5 (68–81)
Tarsius syrichta	6, 11, 6	79.3 (69.4–90.9)	9 (6–13)	152.2 (149.0–161.6)	78 (67–88)
Tarsius bancanus	4, 7, 7	69 (42.6–86.8)	10 (8–12)	149.0 (140.7–157.8)	71 (68–76)

rim (Fig. 6, 8). The ratio of condylar depth (anteroposterior dimension) to bicondylar width equals 111 in *Shoshonius*. Like *Hemiacodon, Shoshonius* compares best with specialized leapers such as *Tarsius, Galago*, and *Avahi* in this feature (Dagosto, 1993). As in extant frequent leapers, the patellar groove projects further anteriorly than the femoral shaft (Rose and Walker, 1985; Anemone, 1990, 1993). Unlike specialized leapers, however, the medial epicondyle exhibits only a slight anterior bulge and the distal articular surface of the medial epicondyle is only slightly indented (Dagosto, 1993). In these aspects of condylar shape, *Shoshonius* resembles *Hemiacodon* and *Microchoerus* and differs from tarsiers and galagos.

The femur of *Shoshonius* shares some features with extant specialized small-bodied leapers like the semicylindrical femoral head, the relatively perpendicular and short femoral neck, the enlarged, anteriorly prominent greater trochanter, the

Table 9.—*Extended.*

Fossa length	Femoral shaft ap/ml	Femoral robusticity	Humeral ap*ml/ femoral ap*ml	Lateral condyle height	Tibia	
					Rotation	Distal ap/ml
112.7	87.4	12.2	70.1	111.5	15.5	117
(96.5–128.8)					(13–18)	(116.3–117.6)
115				116		120.6
113.3						
101.7				108.9	16	125.3
					(12–21)	(118.2–131.3)
152.2					20	129.2
107.8				>99		
132.3	105.7	12.8	77	98.9	29.3	134.8
(119.4–148)	(90.1–118.6)	(11.2–13.9)	(67–96)	(84.6–113.1)	(22–36)	(115–160)
137.8	100.9	13.5	86.4	90.6	31	131.5
(130.3–145)	(91.8–107.3)	(12.7–15.0)	(73.1–93.3)	(87.3–96.0)	(30–33)	(114–161)
125.2	106.6	13.6	93.1	98.5	32	125.1
(106.9–143)	(99.5–112.5)	(12.8–14.5)	(79.3–102.4)	(91.3–104.0)	(20–44)	(115.3–144.0)
101.0	99.7	12.2	71	102.5	28.8	123.5
(77.0–113.2)	(94–105)	(11.6–13.3)	(69.4–72.6)	(99.3–107.5)	(25–34)	(121.0–126.1)
89.8	97.7	12.3	71.7	97	34	112.1
(73.8–101.5)	(84–112)	(10.9–13.3)	(60.6–77.6)	(91.9–102.1)		(103.8–122.6)
91.8	110	11	67	105	21.6	126.6
(80.7–105.8)	(93–120)	(10.3–11.5)	(57–74)	(98.5–111)	(15–28)	(105.1–162.7)
84.5	121	11.2	50.7	111.8	23	115.9
(71.9–90.0)	(112–127)	(10.7–11.7)	(43–68)	(107.7–115.3)	(15–31)	(107.7–124.3)
94.3	119	11.6		112.7	20	135
(88.1–99.5)						(131.6–138.5)
94.9	112	10.8	52.2	114.4	21.5	100.4
(92.9–99.7)	(103–122)	(10.5–11.6)	(44–64)	(110.7–117.5)	(19–25)	(97.7–104.5)
97.5	114.1	9.3	74	116.3	14	104.9
(84.4–108.7)	(93.4–124.5)	(8.8–10.0)	(67–80)	(106.4–130.5)	(10–20)	(100.0–109.3)
98.5	124.9	9.2	74	118.5	18	117.2
(91.6–108.3)	(109–147)	(9.2–9.3)	(64–88)	(113.1–124.4)	(15–21)	(114.2–120.2)

short intertrochanteric fossa, and the deep knee. However, it differs from specialized leapers in its relatively short and robust femur, and the fact that the femoral shaft is broader mediolaterally than anteroposteriorly.

Tibia.—CM 69757 is a right tibia complete from the distal joint surface up to the tibial tuberosity (Fig. 9). It exhibits a marked anteroposterior S-shaped curvature, much greater than in *Tarsius*. The cnemial crest is prominent in *Shoshonius*, showing a height to midshaft height ratio of 1.71. The cnemial crest extends down about 15% of the estimated length of the tibia. In contrast to *Tarsius*, the tibia is not fused to the fibula. The bones were, however, in relatively close contact as demonstrated by the proximodistally extensive (approximately 25–35% of tibial length) tibiofibular scar. This degree of tibiofibular apposition is similar to that reported for the early Eocene anaptomorphine omomyid *Absa-*

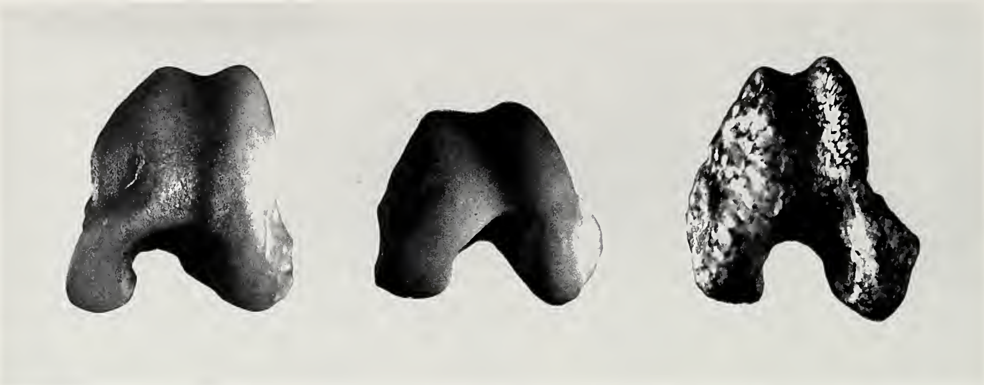

Fig. 8.—Distal femora of extant prosimians and *Shoshonius* in distal view. From left to right, specimens illustrated are as follows: *Tarsius syrichta* (FMNH 142007), *Cheirogaleus medius* (FMNH 57521), and *Shoshonius cooperi* (CM 69764). Femora are scaled to the same mediolateral width. Note the anteroposterior depth of the knee in *Tarsius* and *Shoshonius*.

rokius (Covert and Hamrick, 1993) but is much greater than that in at least some middle Eocene omomyids from the Bridger Formation (Dagosto, 1985).

The talar facet is slightly longer than wide (Table 9), only moderately grooved, and its anterior and posterior edges are parallel. The tibial malleolus is long, pyramidally shaped, and rotated only 15° from a parasagittal plane. An anterior process is present. The groove for tibialis posterior courses across the posterior edge of the malleolus. In all of these features, *Shoshonius* is quite similar to other North American omomyids for which the relevant anatomy is known (Dagosto, 1985; Covert and Hamrick, 1993). *Necrolemur* differs in having a more highly grooved articular surface for the talus and a tibialis groove that curves around the medial edge of the malleolus (Dagosto, 1985).

Talus.—Three tali of *Shoshonius* were recovered (Fig. 10). The talus of *Shoshonius* is much like those of other omomyids. It exhibits a long talar neck, a high talar body, and a trochlea that is longer than wide (Table 10; Fig. 10). In these proportions, it is much like nonlorisine strepsirhine primates and other tarsiiforms, with the notable exceptions of *Necrolemur*, which has a short talar neck, and *Tarsius*, which is distinguished by its short talar neck and low body (Godinot and Dagosto, 1983). The posterior trochlear shelf is fairly prominent, a feature in which *Shoshonius* more closely resembles anaptomorphine omomyids than other omomyines (Gebo, 1988). As in other haplorhines, the groove for the tendon of flexor tibialis is centrally positioned relative to the tibial facet, and the fibular articulation is steep-sided and ends in a short process plantarly (Beard et al., 1988). The medial tibial facet extends to the plantar edge of the body. The talar head is much wider than high, suggesting considerable abduction/adduction movement at the transverse tarsal joint.

The talus of *Shoshonius*, like those of other omomyids, is distinguished from *Necrolemur* (Godinot and Dagosto, 1983) by its longer neck, lower body, and smaller posterior trochlear shelf. *Shoshonius* is also markedly different from *Tarsius* in its possession of a long talar neck, a round talar head, and its long, nonwedged trochlear body (Gebo, 1988). No features of the talus clearly distinguish extant vertical clingers and leapers from leaper/quadrupeds.

Calcaneus.—The calcaneus of *Shoshonius* is very similar to those of other

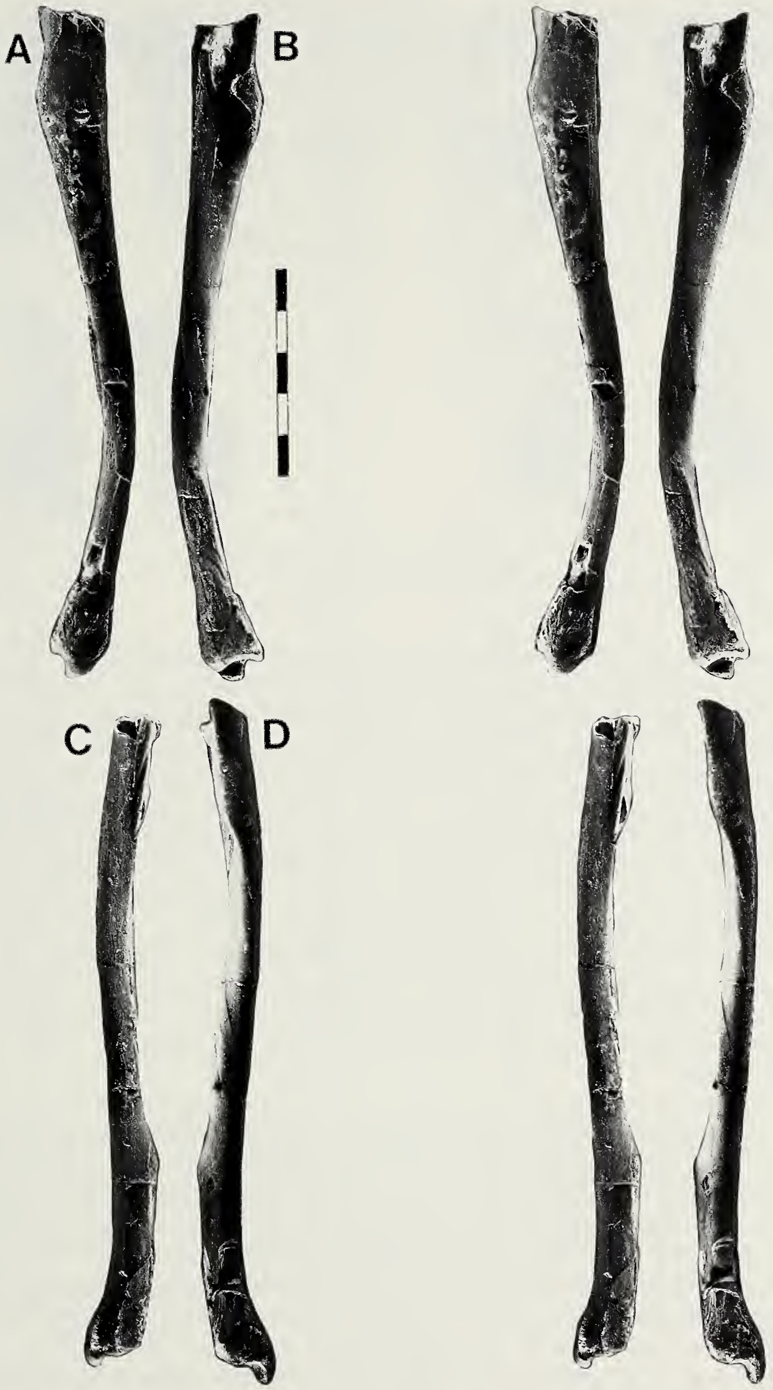

Fig. 9.—Right tibia of *Shoshonius cooperi* (CM 69757) in medial (A), lateral (B), posterior (C), and anterior (D) views. All views are stereopairs. Specimen is complete aside from the missing proximal end and the adjacent part of the shaft. Note the proximodistal extent of tibiofibular apposition. Scale = 10 mm.

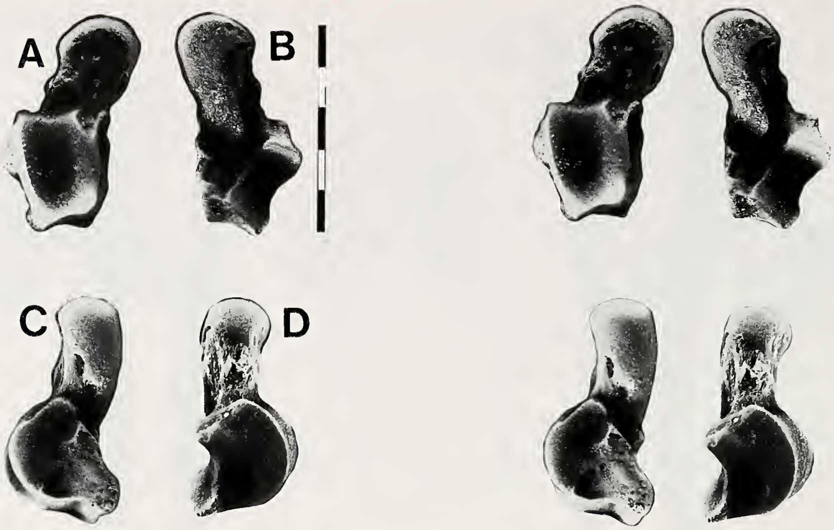

Fig. 10.—Left talus of *Shoshonius cooperi* (CM 67297) in dorsal (A), plantar (B), medial (C), and lateral (D) views. All views are stereopairs. Scale = 5 mm.

omomyines and anaptomorphines (Fig. 11). The proportions of the proximal (heel), middle (posterior talar facet), and distal regions of the calcaneus relative to total length do not distinguish *Shoshonius* from other North American omomyids (Table 11; Gebo, 1988). *Necrolemur, Microchoerus,* and *Tarsius* differ from *Shoshonius* (and other omomyids) in showing greater anterior elongation of the calcaneus (Schmid 1979; Gebo, 1988). *Shoshonius* and other omomyids also differ from *Tarsius* in several other ways. The peroneal tubercle is more anteriorly located in omomyids than in *Tarsius.* The calcaneocuboid joint of *Tarsius* is nearly as long as wide and is flat, lacking the well-developed pivot typical of other prosimian primates, including omomyids (Jouffroy et al., 1984; Gebo, 1987*a*). No features of the calcaneus clearly distinguish extant leaper/quadrupeds from VCLs. Although *Otolemur* has a relatively shorter anterior calcaneus than *Galago, G. demidovii* has an extremely elongated anterior calcaneus that is comparable to *Tarsius* (Jouffroy et al., 1984; Jouffroy and Gunther, 1985; Berge and Jouffroy, 1986).

First Metatarsal.—The proximal end of the first metatarsal of *Shoshonius* (Fig. 12) is very similar to that of *Hemiacodon* and other omomyids (Simpson, 1940; Szalay and Dagosto, 1988). *Shoshonius* and *Hemiacodon* both possess proximodistally long and dorsoplantarly tall peroneal tubercles that are unreduced, in contrast to the smaller peroneal tubercle of *Tarsius* (Table 12:c/d and h/g; Fig. 13). The great dorsoplantar height and mediolateral narrowness of the omomyid peroneal tubercle (Table 12:a/b; Fig. 13) contrasts with the dorsoplantarly shallower and mediolaterally broader peroneal tubercles of adapids (Fig. 14:a, e). In omomyids, the base of the peroneal tubercle is located in the midline, transverse to the proximal joint surface (Fig. 14:a). The peroneal tubercle is dorsoplantarly deep, mediolaterally narrow, flat on its medial and lateral sides, and rounded along its end. In adapids the peroneal tubercle is more nearly conical in appearance, being rough and irregular mediolaterally, and it begins off to one side and twists to a point. Further, the amount of bone lateral to the articular facet is much greater

Table 10.—*Measurements and indices of the talus in* Shoshonius cooperi, *other fossil tarsiiforms, and some extant prosimians. Mean values are provided first, with ranges in parentheses. Measurements are defined in Gebo (1988) and Gebo et al. (1991).*

Taxon	*n*	Trochlea width/length	Neck length/ total length	Talar head width/height	Body height/ trochlea width
Shoshonius cooperi	3	73.2 (70.1–79.2)	52.4 (49.6–55.1)	114.5 (101.6–137.5)	115.8 (113.4–116.2)
?*Hemiacodon*	6	75.4 (67.6–82.0)	51.2 (48.1–56.7)	122.3 (111.7–132.9)	110 (95.7–118.4)
?*Omomys*	8	82 (74.9–91.4)	50.8 (48.6–53.5)	124.3 (118.1–135.4)	107.3 (98.4–118.8)
Washakius	1	66.1	52.4		117.7
Tetonius	3	74.7 (66.7–78.7)	54.9 (53.8–56.7)		116.5 (115–118)
Absarokius	1	100	53.7		90.5
Necrolemur	1	82.2	44.9	112.2	110.1
Leaper/quadrupeds					
Microcebus murinus	19	74.7 (64.0–90.9)	50.2 (40.6–58.8)	116.2 (75.0–140.5)	113.5 (100.0–135.5)
Cheirogaleus medius	5	71.9 (66.7–78.1)	48.7 (45.9–54.9)	126.3	101.3 (96.5–103.8)
Cheirogaleus major	7	72.2 (63.0–76.6)	50.4 (47.8–55.2)	130.8 (120.0–137.7)	114 (105.6–123.5)
Otolemur crassicaudatus	4	64.3 (52.4–74.7)	52.6 (47.7–58.6)	120.2 (115.8–126.0)	130.4 (112.9–152.3)
Otolemur garnetti	7	65.9 (58.1–82.4)	49.6 (45.8–55.8)	119.8 (110.2–125.0)	124.9 (113.3–139.5)
Galagoides demidovii	10	73.5 (61.8–91.5)	50.1 (43.7–55.4)	119.9 (114.3–124.9)	107.2 (94.8–119.0)
Specialized leapers					
Galago moholi	9	76.4 (67.4–89.5)	52.9 (50.0–54.8)	119.2 (111.8–125.0)	102.5 (88.2–112.9)
Galago senegalensis	6	78.7 (68.2–88.1)	52.5 (44.3–57.1)	124.7 (124.1–125.2)	106.1 (88.9–123.3)
Galago gallarum	2	69.5 (64.6–74.5)	52.2 (50.0–54.3)	104.3 (86.8–121.8)	109.5 (102.9–116.1)
Tarsius syrichta	9	88.9 (71.4–103.8)	48.8 (39.8–61.4)	118.1 (114.3–123.9)	74.7 (67.5–87.1)
Tarsius bancanus	5	91.5 (83.8–110.8)	49.2 (45.1–54.1)	123.8 (122.7–125.0)	79.8 (67.6–96.2)

in adapids than in North American omomyids (Fig. 14:d). The shape of the joint surface also differs in the two groups. Part of the proximal articular surface of the first metatarsal wraps around the lateral surface of the peroneal tubercle and is obliquely oriented relative to the long axis of the joint surface in omomyids (Fig. 14:b). In adapids this surface is aligned mediolaterally. The joint surface in adapids also encompasses a much wider arc than that of omomyids (Fig. 14:c, f; Szalay and Dagosto, 1988).

DISCUSSION

Functional Anatomy and Locomotor Adaptations.—The rounded shape of the humeral head and its projection above the tuberosities implies a considerable amount of mobility at the shoulder (Gebo, 1987*b*). *Shoshonius* does not share the distally narrow, anteriorly inflated humeral head of VCL primates (Schmitt, 1996).

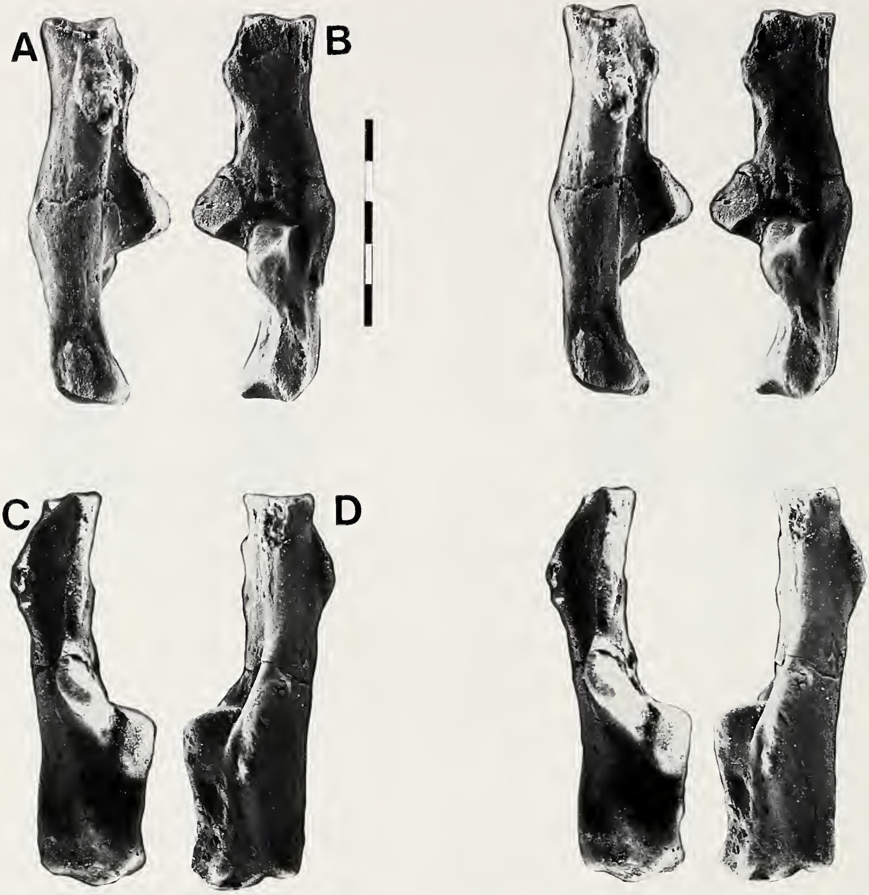

Fig. 11.—Right calcaneus of *Shoshonius cooperi* (CM 67299) in plantar (A), dorsal (B), medial (C), and lateral (D) views. All views are stereopairs. Scale = 5 mm.

The attachment areas for the muscles of the shoulder and forearm are larger than in most extant prosimian primates. The lesser tuberosity is very wide and prominent, suggesting a well-developed subscapularis, a muscle important for medial rotation of the humerus. Likewise, the deltopectoral crest and the brachial flange are wide and long relative to humeral length, suggesting well-developed and powerful deltoid, brachial, and brachioradialis muscles. The prominent medial ridge along the deltopectoral crest for latissimus dorsi suggests forceful adduction and medial rotation of the humerus. The medial and lateral epicondyles are very prominent, implying large forearm flexors and extensors, respectively.

The spherical shape of the capitulum on the distal humerus suggests extensive rotational abilities at the forearm and wrist. Likewise, the shallow olecranon fossa suggests that the forearm was never fully extended. The long, low trochlea on the distal humerus implies that clinging postures in which the elbow is highly flexed were not extensively utilized (Szalay and Dagosto, 1980).

The well-marked and frequently enlarged areas for muscular attachment, the overall robusticity of the humerus, and the mobility at the shoulder and elbow joints of *Shoshonius* imply that climbing and quadrupedalism were important

Table 11.—*Measurements and indices of the calcaneus in* Shoshonius cooperi, *other fossil tarsiiforms, and some extant prosimians. Mean values are provided first, with ranges in parentheses. Measurements are defined in Gebo (1988) and Gebo et al. (1991).*

Taxon	*n*	Heel length/ total length	Facet length/ total length	Anterior length/ total length	Cuboid facet width/height
Shoshonius cooperi	2	22.6 (21.9–23.4)	22.7 (22.3–23.1)	53.1 (52.9–53.4)	149.8 (146.8–152.9)
?*Hemiacodon*	10	28.7 (26.8–30.2)	19.6 (18.3–21.0)	52.3 (49.5–54.3)	125.3 (119.5–131.6)
?*Omomys*	8	26.3 (25.7–27.1)	18.5 (17.7–19.9)	52.6 (49.9–54.6)	134.2 (128.1–149.6)
Washakius	1	23.7	25.6	52.4	111.6
Absarokius	1	23.3	19.9	56.4	
Teilhardina	3	26.3 (25.7–26.8)	23.1 (20.3–26.5)	51.1 (47.1–54.1)	
Leaper/quadrupeds					
Microcebus murinus	18	19.3 (15.9–21.7)	18.9 (16.0–21.9)	61.4 (56.3–67.3)	104.1 (77.8–121.4)
Cheirogaleus medius	5	22.6 (18.7–25.3)	27.8 (21.1–31.0)	50.3 (46.5–52.3)	126.1 (116.5–133.3)
Cheirogaleus major	7	25.9 (20.0–29.8)	26.3 (24.1–28.6)	48.2 (46.1–50.0)	123.5 (103.7–155.0)
Otolemur crassicaudatus	6	19.7 (18.2–20.9)	16.8 (15.3–18.8)	64.7 (64.5–65.4)	118.7 (95.0–128.3)
Otolemur garnetti	7	20.2 (19.0–21.5)	15.3 (14.4–17.2)	64.6 (63.8–66.3)	116.7 (102.3–130.5)
Galagoides demidovii	10	12.6 (11.5–14.0)	10 (5.7–11.9)	77.2 (75.1–78.6)	115.3 (109.6–126.3)
Specialized leapers					
Galago moholi	9	16.2 (15.3–17.7)	11.7 (11.1–12.6)	72.2 (70.8–72.9)	124.5 (107.7–160.0)
Galago senegalensis	6	16.8 (13.5–18.2)	11.6 (9.3–12.8)	72.3 (70.5–76.2)	102.2 (97.6–106.7)
Galago gallarum	1	14.4	10.6	75	130.8
Tarsius syrichta	9	12.3 (11.1–13.6)	11.8 (10.2–12.9)	76.5 (76.2–77.4)	102.9 (82.3–125.1)
Tarsius bancanus	5	12.6 (11.2–13.9)	12.2 (11.6–12.9)	76.1 (76.1–76.9)	102.6 (81.9–121.7)

components of its locomotor repertoire. Extant specialized vertical clinging and leaping primates have humeri that are less heavily scarred by muscular attachments, and show modifications of the shoulder and elbow joint that are lacking in *Shoshonius*.

The semicylindrical femoral head indicates an emphasis on flexion and extension movements at the hip. The perpendicular angle of the femoral neck and the shortness of the head and neck also suggest a reduced emphasis on hip abduction. The anteriorly prominent greater trochanter reflects the increased size of the muscles governing knee extension. Likewise, the tall and narrow knee with its elevated and rounded lateral patellar rim and narrow patellar facet implies increased leverage for the quadriceps musculature. These features of *Shoshonius* are shared with frequently leaping primates.

As in leapers, the femur of *Shoshonius* is moderately long, but probably not as long relative to body size as in VCL galagos or tarsiers. The femoral shaft is more robust than in specialized VCL primates, and is particularly unusual in being

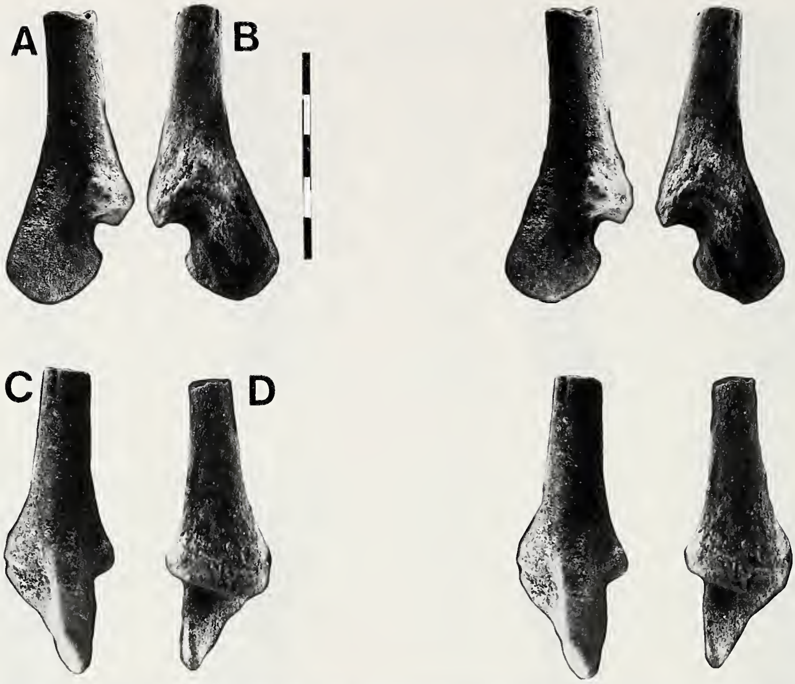

Fig. 12.—Right proximal first metatarsal of *Shoshonius cooperi* (CM 69754) in lateral (A), medial (B), plantar (C), and dorsal (D) views. All views are stereopairs. Scale = 5 mm.

wider mediolaterally than anteroposteriorly, suggesting more resistance to mediolaterally directed than anteroposteriorly directed bending forces. This arrangement is more typical of climbing than leaping primates (Burr et al., 1982).

The long, S-shaped tibia with its prominent cnemial crest, tightly apposed fibula, and only slightly medially rotated medial malleolus also imply that leaping

Table 12.—*Measurements and indices of first metatarsals (in mm). See Figure 13 for explanation of measurements.*

Measurement/index	*Notharctus*	*Adapis*	*Leptadapis*	*Hemiacodon*	*Shoshonius*
Mediolateral width of base of tubercle (a)	3.36	2.50	4.57	1.18	0.86
Mediolateral width of proximal metatarsal (b)	7.73	5.47	11.52	4.16	2.59
Dorsoplantar depth of tubercle (c)	9.81	5.75	11.79	6.28	3.30
Dorsoplantar depth of proximal metatarsal (d)	4.05	2.50	5.10	4.26	2.03
Dorsal length of metatarsal (e)	22.49	15.88	32.62	14.40	
Total length of metatarsal (f)	24.40	17.05	35.62	16.25	
Tubercle length (g)	5.34	2.99	5.80	4.59	2.36
Tubercle height (h)	4.37	2.22	4.89	4.50	2.23
a/b	43.5	45.7	43.8	28.4	33.2
c/d	41.3	43.5	43.3	67.8	61.8
e/f	92.2	93.1	91.6	88.6	
h/g	81.9	74.2	84.0	98.0	94.5

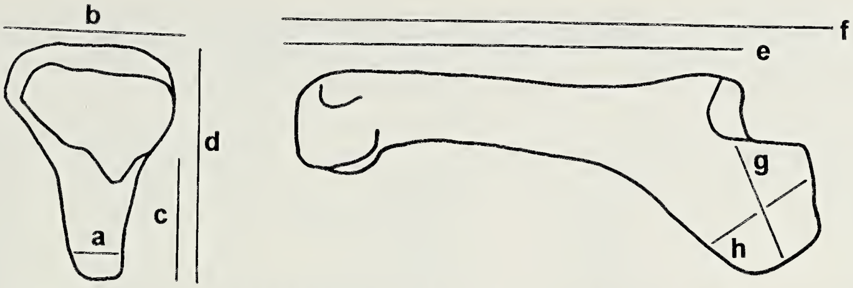

Fig. 13.—Measurements of the first metatarsal used to construct ratios provided in Table 12.

was an important component of the locomotor repertoire of *Shoshonius*. The long talar neck, the short and high talar body, the rectangular trochlea, the large posterior trochlear shelf, and elongated distal calcaneus all support an emphasis on flexion/extension movements at the upper ankle joint. In contrast, the large and round talar head, as well as the subtalar and calcaneocuboid joint surfaces, suggest a quite mobile tarsus and foot (Szalay, 1976; Dagosto, 1986; Gebo, 1988). The prominent peroneal tubercle on the first metatarsal implies an important role for peroneus longus in pedal grasping and/or a buttressing mechanism to deal with loads during leaping (Szalay and Dagosto, 1988).

Although *Shoshonius* has many characters of the hind limb (hip joint, knee joint, upper ankle joint) that suggest that leaping was an important part of its locomotor repertoire, living, small-bodied VCL primates like *Galago senegalensis, G. moholi*, and *Tarsius* show numerous specializations for leaping that are

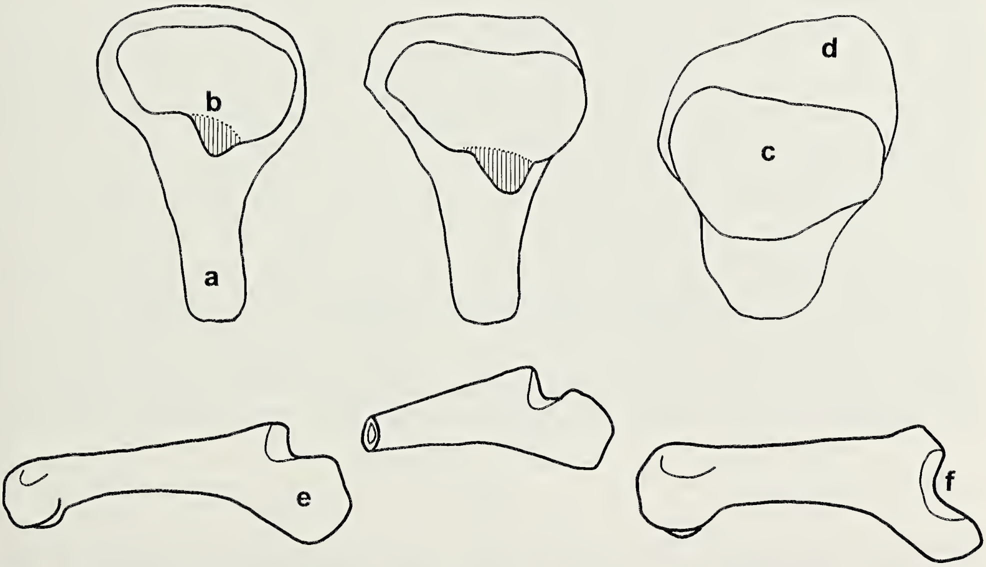

Fig. 14.—Proximal (top) and lateral (bottom) views of first metatarsals. Left to right: *Hemiacodon* (AMNH 12613), ***Shoshonius*** (CM 69754), and *Notharctus* (AMNH 11474). The letters a–f refer to features discussed in the text. The shaded area indicates the oblique direction of this region of the proximal articular facet in omomyids.

Table 13.—*Indices that distinguish leaper/quadrupeds (*Microcebus, Cheirogaleus, Otolemur, *and* Galagoides demidovii*) from specialized vertical clingers and leapers (*Tarsius, Galago senegalensis, G. gallarum, *and* G. moholi*) at* p < *0.05. The* p *values are derived either from comparison of species means or individual specimens.*

Anatomical region	Source of data	Index	*p* values, species means	*p* values, individuals
Shoulder	Table 8	AP EXT	0.010	0.002
Shoulder	Table 8	INFW/PD CHORD	0.003	0.000
Elbow	Table 8	TH/TW	0.000	0.000
Elbow	Table 8	TW/AW	0.012	0.000
Femur	Table 9	Femoral shaft ap/ml	0.001	0.000
Femur	Table 9	Femoral robusticity	0.009	0.000
Humerus and femur	Table 6	HFI	0.000	0.000
Knee	Table 9	Lateral condyle height	0.000	0.000

absent in *Shoshonius*. Like other omomyid primates, *Shoshonius* shows significant differences from *Galago senegalensis, G. moholi*, and *Tarsius* in terms of limb proportions, shoulder joint shape, elbow joint shape, degree of forelimb muscularity, and calcaneal proportions. In these features, *Shoshonius* and other omomyids are more like small, extant strepsirhine primates in which quadrupedalism and climbing remain important parts of the locomotor repertoire. Our conclusions therefore echo and support the observations of Simpson (1940), Szalay (1976), and Gebo (1988), all of whom stressed the generalized, nontarsierlike nature of the postcranium of omomyids.

Eight of the indices considered in this analysis distinguish extant vertical clingers and leapers from leaper/quadrupeds (Table 13). In all of these indices except the height of the lateral femoral condyle relative to biepicondylar breadth, *Shoshonius* groups with the LQs and not with the VCLs. The variables used to construct these indices were subjected to a principal coordinates analysis (after the raw data were "adjusted" for size by subtraction of the geometric mean [Falsetti et al., 1993; Jungers et al., 1995]). Figure 15A shows the results. The first three axes account for 87% of the variation, and the correlation between the distances implied by the first three axes and the original distance matrix is 0.99, suggesting that these axes adequately characterize relationships among the taxa. Axis 1 (64%) separates the extant VCLs from the LQs. *Shoshonius* falls with the LQs on this axis, and the minimum spanning tree (Fig. 15A) shows that it is linked to members of the LQ group rather than any of the VCL group. A cluster analysis of this data is provided in Figure 15B. The cophenetic correlation of this tree with the original distance matrix is 0.79. Features that contribute most to the positive values of the VCLs on the first principal coordinate axis are femoral length, the ap diameter of the femoral shaft, and lateral condyle height (Table 14). The negative values of the LQs result from the width of the humeral head and

→

Fig. 15.—A. Principal coordinates analysis of variables contributing to indices separating leaper/quadrupeds from vertical clingers and leapers (see Table 13). The correlations between variables and axes is given in Table 14. The dotted line is the minimum spanning tree. B. A cluster analysis (UPGMA) of the same data. C. A principal components analysis of the raw data. Factor 1 (not shown) is likely a size vector; Factors 2 and 3 separate taxa in much the same way as the principal coordinates analysis. Eigenvectors are given in Table 14.

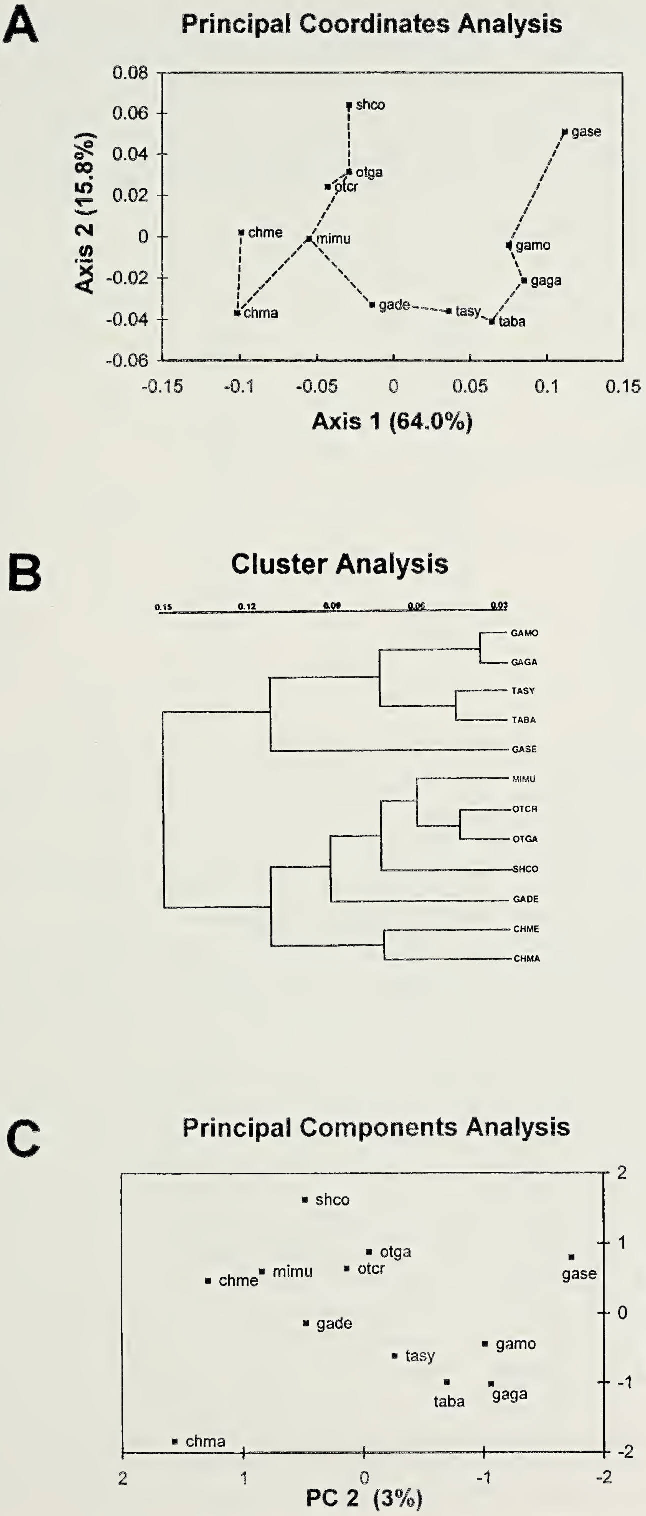
A
Principal Coordinates Analysis
Axis 2 (15.8%)
Axis 1 (64.0%)
0.08
0.06
0.04
0.02
0
-0.02
-0.04
-0.06
-0.15
-0.1
-0.05
0
0.05
0.1
0.15
shco
gase
otga
otcr
chme
mimu
gamo
gaga
gade
tasy
taba
chma
B
Cluster Analysis
0.15
0.12
0.09
0.06
0.03
GAMO
GAGA
TASY
TABA
GASE
MIMU
OTCR
OTGA
SHCO
GADE
CHME
CHMA
C
Principal Components Analysis
shco
otga
otcr
chme
mimu
gase
gade
tasy
gamo
taba
gaga
chma
2
1
0
-1
-2
PC 3 (.9%)
PC 2 (3%)

Table 14.—*Relationship of variables to axes in principal coordinates and principal components analysis (Fig. 15). For the principal coordinates analysis,* r *is the correlation coefficient and* p *is given for those variables showing a significant* ($p < 0.05$) *correlation with the axes. For the principal components analysis, the loadings of the factors are given. Measurements are defined in Tables 8 and 9. Abbreviations are as follows: HUMAP, anteroposterior diameter of humeral midshaft; HUMML, mediolateral diameter of humeral midshaft; FL, femoral shaft length; FEMAP, anteroposterior diameter of femoral midshaft; FEMML, mediolateral diameter of femoral midshaft; BEW, biepicondylar width of femoral condyles; LCONHT, height of lateral femoral condyle.*

		Principal coordinates					
		Axis 1		Axis 2		Principal components	
Anatomical region	Measurement	*r*	*p*	*r*	*p*	Factor 2	Factor 3
Humerus	HL	−0.029		0.262		0.003	0.090
Humerus	HUMAP	−0.447		0.036		0.045	0.002
Humerus	HUMML	−0.800	0.002	0.379		0.115	0.049
Shoulder	APEXT	0.031		−0.936	0.000	0.074	−0.293
Shoulder	INFW	−0.943	0.000	0.145		0.211	0.036
Shoulder	PD CHORD	−0.595	0.041	−0.425		0.090	−0.012
Elbow	AW	−0.789		−0.154		0.114	−0.006
Elbow	TH	0.120		−0.615	0.033	0.009	−0.038
Elbow	TW	−0.932	0.000	0.025		0.276	0.036
Femur	FL	0.965	0.000	−0.046		−0.411	−0.021
Femur	FEMAP	0.880	0.000	0.091		−0.281	−0.015
Femur	FEMML	0.374		0.835	0.001	−0.108	0.129
Knee	BEW	−0.048		0.451		0.004	0.041
Knee	LCONHT	0.096	0.000	0.138		−0.177	−0.009

width of the humeral trochlea. Both locomotor groups are widely spread on the second and third axes. A principal components analysis of raw data (no size "correction"; Fig. 15C) yields a similar positioning of taxa and relative loadings of variables on axes (Table 14).

Insofar as comparable elements exist, the postcranial morphology of *Shoshonius* is not significantly different from that of other North American anaptomorphine and omomyine omomyids. This similarity suggests that these other species were also leaper/quadrupeds rather than specialized vertical clingers and leapers, although in the absence of information on limb lengths it is difficult to distinguish small-bodied VCLs from LQs. The considerable similarity among North American omomyids in known postcranial elements suggests that the postcranium was relatively conservative in this group, despite its high species-level diversity and long stratigraphic range. Middle–late Eocene European microchoerids (*Necrolemur* and *Microchoerus*) differ from the North American forms in many anatomical features (Godinot and Dagosto, 1983; Dagosto, 1985; Dagosto and Schmid, 1996), some of which (lower humerofemoral and humerotibial indices, narrower humeral head, greatly elongated calcaneus) suggest a greater anatomical commitment to leaping than was the case in North American omomyids.

Phylogenetic Implications.—All omomyids and microchoerids for which the relevant anatomy is known are less derived postcranially than is *Tarsius*. Despite this fact, both omomyids and microchoerids share derived postcranial characters with tarsiers. For example, omomyids resemble tarsiers in having a short, perpendicularly oriented femoral neck, a semicylindrical femoral head that approaches the more fully cylindrical shape found in *Tarsius*, and a high knee (Dagosto and Schmid, 1996). On the other hand, microchoerids and tarsiers are derived in sharing distal tibiofibular fusion and anterior elongation of the calcaneus (Schmid,

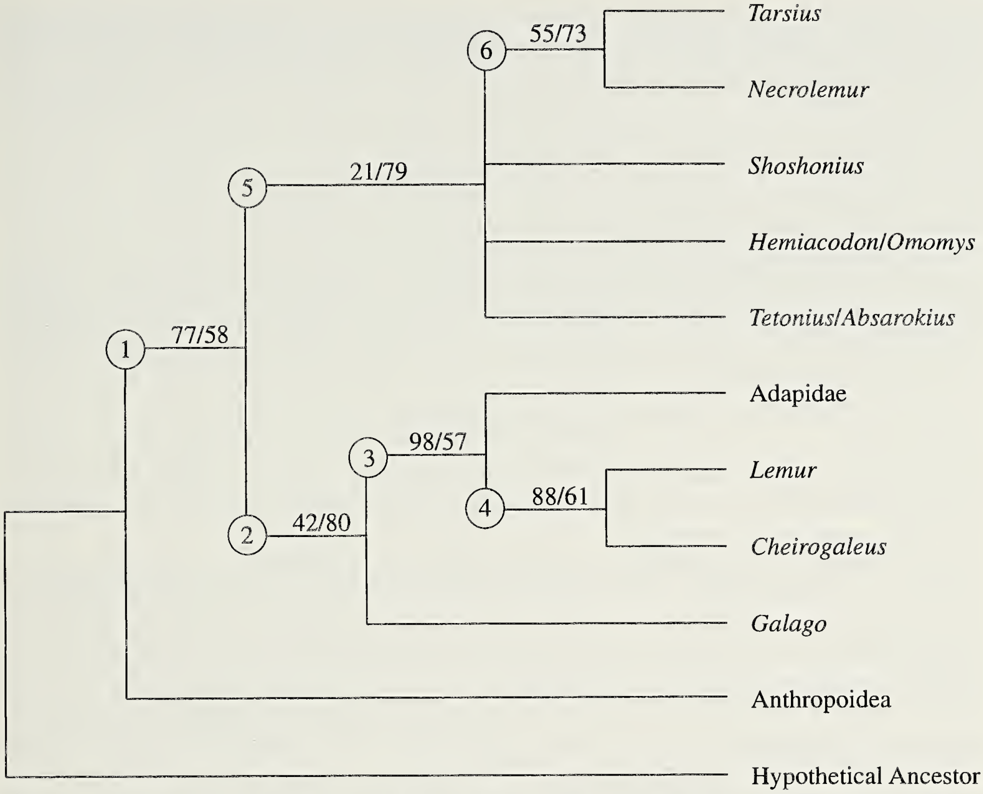

Fig. 16.—Strict consensus tree resulting from parsimony analyses of character-taxon matrix in Appendix 2 using PAUP 3.1.1 (Swofford, 1993). Characters were scaled for equal weighting regardless of number of character states. Characters 1, 2, 4, 5, 6, 9, 11, 13, 14, 20, 22, 25, 26 and 33 were treated as "ordered"; all other characters were treated as "unordered." The topology of the strict consensus tree was unaffected by separate analyses of postcranial characters alone and a combined dataset of both cranial and postcranial characters. Numerical values above stems of clades indicate percent frequency with which particular clades were supported in 1,000 bootstrapped trees. In each case, the number to the left indicates percent by which that clade was supported in bootstrapped trees derived from postcranial characters only, while the number to the right indicates percent by which that clade was supported in bootstrapped trees derived from the combined dataset.

Character transformations supporting each node are as follows (see Appendix 1 for description of character states): Node 1, Character 2 (0→1), Character 5 (0→2), Character 15 (0→1), Character 20 (0→1), Character 26 (0→1), Character 33 (0→1); Node 2, Character 12 (1→0), Character 13 (1→2), Character 14 (1→2), Character 17 (0→1), Character 18 (0→1), Character 25 (1→2), Character 26 (1→2), Character 34 (0→1), Character 44 (0→1); Node 3, Character 5 (2→1), Character 9 (1→0), Character 11 (1→0), Character 20 (1→2), Character 37 (0→1), Character 39 (0→1); Node 4, Character 19 (0→1), Character 23 (1→2), Character 52 (0→1); Node 5 (Tarsiiformes), Character 1 (1→0), Character 2 (1→2), Character 6 (0→1), Character 7 (0→1), Character 8 (0→1), Character 11 (1→2), Character 22 (1→2), Character 33 (1→2), Character 45 (0→1), Character 48 (0→1), Character 50 (0→1), Character 51 (0→1); Node 6, Character 11 (2→3), Character 15 (1→0), Character 16 (0→1), Character 21 (1→0), Character 22 (2→3), Character 24 (0→1), Character 30 (0→1), Character 38 (0→1), Character 42 (0→1).

1979; Dagosto, 1985; Gebo, 1987*a*). This pattern of crossing synapomorphies complicates attempts to reconstruct phylogenetic relationships and implies that at least some of these postcranial characters are the result of homoplasy (cf. Dagosto, 1985). Nevertheless, a recent phylogenetic analysis of primates based on postcranial characters (Dagosto and Gebo, 1994) supported the monophyly of Tarsiiformes (Tarsiidae + Omomyidae + Microchoeridae). This result agrees with some (Rosenberger, 1985; Beard et al., 1991; Beard and MacPhee, 1994), but by no means all, recent phylogenetic analyses based on cranial anatomy.

A conflicting phylogenetic reconstruction holds that tarsiers share more recent common ancestry with anthropoids than they do with either omomyids or microchoerids (Cartmill and Kay, 1978; Cartmill, 1980; Cartmill et al., 1981; MacPhee and Cartmill, 1986; Ross, 1994; Kay et al., 1997). The monophyly of such a restricted tarsier–anthropoid clade rests largely on certain features of cranial anatomy, the homology of which has been fiercely contested (Simons and Rasmussen, 1989; Beard et al., 1991; Beard and MacPhee, 1994; MacPhee et al., 1995). Because the cranial anatomy of *Shoshonius* has played such a critical role in these debates, the addition of new data regarding the postcranial anatomy of this genus may help resolve the question.

We modified the postcranial dataset published by Dagosto and Gebo (1994: table 2) by incorporating new anatomical data for *Shoshonius*, adding additional strepsirhine taxa (*Cheirogaleus* and *Galago*), and including additional characters (Appendices 1, 2). Phylogenetic analysis of this enhanced postcranial dataset continues to support tarsiiform monophyly (Fig. 16). Omomyids, microchoerids, and tarsiers form a clade in all 14 of the most parsimonious trees found for postcranial features (220 steps), but this is not a robust link. The tarsiiform clade is evident in only 21% of bootstrapped trees. Trees only one step longer (0.4%) fail to support tarsiiform monophyly. Trees with *Galago* linked to *Tarsius* or within tarsiiforms are among the most parsimonious of these solutions, and are found in 39% of bootstrapped trees. Trees linking *Tarsius* to anthropoids, however, are considerably longer (34 additional steps or 15%), and this grouping is never encountered in bootstrapped trees.

Combining postcranial and cranial datasets (Beard and MacPhee, 1994) yields stronger support for tarsiiform monophyly. *Tarsius*, omomyids, and microchoerids form a clade in all 15 of the most parsimonious trees (336 steps), and this clade occurs in 79% of bootstrapped trees (Fig. 16). However, it takes only five additional steps (1.5%) to break apart the tarsiiform clade, although a *Tarsius* + *Necrolemur* clade is retained in the first 255 MPTs. Trees that fail to support a *Tarsius* + *Necrolemur* clade are at least 12 steps (3.6%) longer than the most parsimonious solutions. A strict tarsier–anthropoid clade requires 44 more steps (13%) and is never encountered in bootstrapped trees.

To summarize, considerable new information regarding the postcranial anatomy of *Shoshonius* corroborates a previous phylogenetic analysis of primates based on postcranial characters (Dagosto and Gebo, 1994). That is, although postcranial characters provide support for the monophyly of tarsiiforms, the degree of support for this clade is weak when postcranial characters alone form the basis for analysis. Small, vertical clinging and leaping strepsirhines such as *Galago* share numerous derived postcranial characters with *Tarsius*, thereby increasing homoplasy and reducing the level of character support for Tarsiiformes. However, the alternative hypothesis of a strict tarsier–anthropoid clade is clearly at odds with postcranial datasets. Given that studies of the cranial anatomy of *Shoshonius* and other

Eocene omomyids and microchoerids also support the monophyly of Tarsiiformes (Rosenberger, 1985; Beard et al., 1991; Beard and MacPhee, 1994), we conclude that tarsiers are more closely related to these extinct taxa than to living and fossil anthropoids.

ACKNOWLEDGMENTS

These fossils were collected during the course of a long-standing program of fieldwork in the Wind River Formation that was initiated by our colleagues, L. Krishtalka and R. K. Stucky. For his skillful preparation of the postcranial elements of *Shoshonius* described here, we thank Alan R. Tabrum. Mark Klingler rendered some of the figures. We thank the American Museum of Natural History, the Field Museum of Natural History, and the National Museum of Natural History for access to their collections of living and fossil mammals. This research was funded by National Science Foundation grant 9020276 to KCB and National Science Foundation grant 8719126 and Wenner-Gren Foundation grant 4931 to MD.

LITERATURE CITED

ANEMONE, R. L. 1990. The VCL hypothesis revisited: Patterns of femoral morphology among quadrupedal and saltatorial prosimian primates. American Journal of Physical Anthropology, 83:373–393.

———. 1993. The functional anatomy of the hip and thigh in primates. Pp. 150–174, *in* Postcranial Adaptation in Nonhuman Primates (D. L. Gebo, ed.). Northern Illinois University Press, DeKalb, Illinois.

BEARD, K. C., AND R. D. E. MACPHEE. 1994. Cranial anatomy of *Shoshonius* and the antiquity of Anthropoidea. Pp. 55–97, *in* Anthropoid Origins (J. G. Fleagle and R. F. Kay, eds.). Plenum Press, New York, New York.

BEARD, K. C., M. DAGOSTO, D. L. GEBO, AND M. GODINOT. 1988. Interrelationships among primate higher taxa. Nature, 331:712–714.

BEARD, K. C., L. KRISHTALKA, AND R. K. STUCKY. 1991. First skulls of the early Eocene primate *Shoshonius cooperi* and the anthropoid–tarsier dichotomy. Nature, 349:64–67.

BEARDER, S. K. 1987. Lorises, bushbabies, and tarsiers: Diverse societies in solitary foragers. Pp. 11–24, *in* Primate Societies (B. B. Smuts, D. Cheney, R. M. Seyfarth, R. W. Wrangham, and T. T. Struhsaker, eds.). University of Chicago Press, Chicago, Illinois.

BERGE, C., AND F. K. JOUFFROY. 1986. Morpho-functional study of *Tarsius*' foot as compared to the galagines's: What does an "elongate calcaneus" mean? Pp. 146–158, *in* Current Perspectives in Primate Biology (D. Taub and F. King, eds.). Van Nostrand Reinhold Company, New York, New York.

BURR, D. B., G. PIOTROWSKI, R. B. MARTIN, AND P. NONG COOK. 1982. Femoral mechanics in the lesser bushbaby (*Galago senegalensis*): Structural adaptations to leaping in primates. Anatomical Record, 202:419–429.

CARTMILL, M. 1980. Morphology, function, and evolution of the anthropoid postorbital septum. Pp. 243–274, *in* Evolutionary Biology of the New World Monkeys and Continental Drift (R. L. Ciochon and A. B. Chiarelli, eds.). Plenum Press, New York, New York.

CARTMILL, M., AND R. F. KAY. 1978. Cranio-dental morphology, tarsier affinities, and primate suborders. Pp. 205–214, *in* Recent Advances in Primatology, Volume 3. Evolution (D. J. Chivers and K. A. Joysey, eds.). Academic Press, London, United Kingdom.

CARTMILL, M., R. D. E. MACPHEE, AND E. L. SIMONS. 1981. Anatomy of the temporal bone in early anthropoids, with remarks on the problem of anthropoid origins. American Journal of Physical Anthropology, 56:3–21.

CONROY, G. C. 1987. Problems of body-weight estimation in fossil primates. International Journal of Primatology, 8:115–137.

COVERT, H. H., AND M. W. HAMRICK. 1993. Description of new skeletal remains of the early Eocene anaptomorphine primate *Absarokius* (Omomyidae) and a discussion about its adaptive profile. Journal of Human Evolution, 25:351–362.

DAGOSTO, M. 1985. The distal tibia of primates with special reference to the Omomyidae. International Journal of Primatology, 6:45–75.

———. 1986. The joints of the tarsus in the strepsirhine primates. Unpublished Ph.D. Dissert., City University of New York, New York, New York.

———. 1993. Postcranial anatomy and locomotor behavior in Eocene primates. Pp. 199–219, *in*

Postcranial Adaptation in Nonhuman Primates (D. L. Gebo, ed.). Northern Illinois University Press, DeKalb, Illinois.

DAGOSTO, M., AND D. L. GEBO. 1994. Postcranial anatomy and the origin of the Anthropoidea. Pp. 567–593, *in* Anthropoid Origins (J. G. Fleagle and R. F. Kay, eds.). Plenum Press, New York, New York.

DAGOSTO, M., AND P. SCHMID. 1996. Proximal femoral anatomy of omomyiform primates. Journal of Human Evolution, 30:29–56.

DAGOSTO, M., AND C. J. TERRANOVA. 1992. Estimating the body size of Eocene primates: A comparison of results from dental and postcranial variables. International Journal of Primatology, 13: 307–344.

DEMES, B., AND W. L. JUNGERS. 1993. Long bone cross- sectional dimensions, locomotor adaptations and body size in prosimian primates. Journal of Human Evolution, 25:57–74.

FALSETTI, A. B., W. L. JUNGERS, AND T. M. COLE III. 1993. Morphometrics of the callitrichid forelimb: A case study in size and shape. International Journal of Primatology, 14:551–572.

FLEAGLE, J. G. 1988. Primate Adaptation and Evolution. Academic Press, New York, New York.

GEBO, D. L. 1987*a*. Functional anatomy of the tarsier foot. American Journal of Physical Anthropology, 73:9–31.

———. 1987*b*. Humeral morphology of *Cantius*, an early Eocene adapid. Folia Primatologica, 49: 52–56.

———. 1988. Foot morphology and locomotor adaptation in Eocene primates. Folia Primatologica, 50:3–41.

GEBO, D. L., M. DAGOSTO, AND K. D. ROSE. 1991. Foot morphology and evolution in early Eocene *Cantius*. American Journal of Physical Anthropology, 86:51–73.

GEBO, D. L., E. L. SIMONS, D. T. RASMUSSEN, AND M. DAGOSTO. 1994. Eocene anthropoid postcrania from the Fayum, Egypt. Pp. 203–233, *in* Anthropoid Origins (J. G. Fleagle and R. F. Kay, eds.). Plenum Press, New York, New York.

GODINOT, M., AND M. DAGOSTO. 1983. The astragalus of *Necrolemur* (Primates, Microchoerinae). Journal of Paleontology, 57:1321–1324.

HONEY, J. G. 1990. New washakiin primates (Omomyidae) from the Eocene of Wyoming and Colorado, and comments on the evolution of the Washakiini. Journal of Vertebrate Paleontology, 10: 206–221.

JOUFFROY, F. K., AND M. GUNTHER. 1985. Interdependence of morphology and behavior in the locomotion of galagines. Pp. 201–234, *in* Primate Morphophysiology, Locomotor Analyses and Human Bipedalism (S. Kondo, ed.). University of Tokyo Press, Tokyo, Japan.

JOUFFROY, F. K., C. BERGE, AND C. NIEMITZ. 1984. Comparative study of the lower extremity in the genus *Tarsius*. Pp. 167–190, *in* Biology of Tarsiers (C. Niemitz, ed.). Gustav Fischer Verlag, Stuttgart, Germany.

JUNGERS, W. L. 1985. Body size and scaling of limb proportions in primates. Pp. 345–381, *in* Size and Scaling in Primate Biology (W. L. Jungers, ed.). Plenum Press, New York, New York.

JUNGERS, W. L., A. B. FALSETTI, AND C. E. WALL. 1995. Shape, relative size, and size-adjustments in morphometrics. Yearbook of Physical Anthroplogy, 38:137–161.

KAY, R. F., C. ROSS, AND B. A. WILLIAMS. 1997. Anthropoid origins. Science, 275:797–804.

MACPHEE, R. D. E., AND M. CARTMILL. 1986. Basicranial structures and primate systematics. Pp. 219–275, *in* Comparative Primate Biology, Volume 1: Systematics, Evolution, and Anatomy (D. R. Swindler and J. Erwin, eds.). Alan R. Liss, New York, New York.

MACPHEE, R. D. E., K. C. BEARD, AND T. QI. 1995. Significance of primate petrosal from middle Eocene fissure-fillings at Shanghuang, Jiangsu Province, People's Republic of China. Journal of Human Evolution, 29:501–514.

MCARDLE, J. E. 1981. Functional morphology of the hip and thigh of the Lorisiformes. Contributions to Primatology, 17:1–132.

RICKART, E. A., L. R. HEANEY, P. D. HEIDEMAN, AND R. C. B. UTZURRUM. 1993. The distribution and ecology of mammals on Leyte, Biliran, and Maripipi islands, Philippines. Fieldiana: Zoology, 72: 1–62.

ROSE, K. D., AND A. C. WALKER. 1985. The skeleton of early Eocene *Cantius*, oldest lemuriform primate. American Journal of Physical Anthropology, 66:73–90.

ROSENBERGER, A. L. 1985. In favor of the necrolemur- tarsier hypothesis. Folia Primatologica, 45: 179–194.

ROSS, C. 1994. The craniofacial evidence for anthropoid and tarsier relationships. Pp. 469–547, *in* Anthropoid Origins (J. G. Fleagle and R. F. Kay, eds.). Plenum Press, New York, New York.

RUFF, C. B., AND J. A. RUNESTAD. 1992. Primate limb bone structural adaptations. Annual Review of Anthropology, 21:407–433.

SCHAFFLER, M. B., D. B. BURR, W. L. JUNGERS, AND C. B. RUFF. 1985. Structural and mechanical indicators of limb specialization in primates. Folia Primatologica, 45:61–75.

SCHLOSSER, M. 1907. Bietrag zur Osteologie und systematischen Stellung der Gattung *Necrolemur*, sowie zur Stammesgeschicte der Primaten überhaupt. Neuen Jahrbuch für Mineralogie, Geologie und Paläontologie, 1907:197–226.

SCHMID, P. 1979. Evidence of microchoerine evolution from Dielsdorf (Zurich region, Switzerland)—A preliminary report. Folia Primatologica, 31:301–311.

SCHMITT, D. 1996. Humeral head shape as an indicator of locomotor behavior in extant strepsirhines and Eocene adapids. Folia Primatologica, 67:137–151.

SIMONS, E. L., AND D. T. RASMUSSEN. 1989. Cranial anatomy of *Aegyptopithecus* and *Tarsius* and the question of the tarsier anthropoidean clade. American Journal of Physical Anthropology, 79:1–23.

SIMPSON, G. G. 1940. Studies on the earliest primates. Bulletin of the American Museum of Natural History, 77:185–212.

STUCKY, R. K., L. KRISHTALKA, AND A. D. REDLINE. 1990. Geology, vertebrate fauna, and paleoecology of the Buck Spring Quarries (early Eocene, Wind River Formation), Wyoming. Pp. 169–186, *in* Dawn of the Age of Mammals in the Northern Part of the Rocky Mountain Interior, North America (T. M. Bown and K. D. Rose, eds.). Geological Society of America Special Paper 243, Boulder, Colorado.

SWOFFORD, D. L. 1993. PAUP: Phylogenetic Analysis Using Parsimony, version 3.1.1. Computer program distributed by the Illinois Natural History Survey, Champaign, Illinois.

SZALAY, F. S. 1976. Systematics of the Omomyidae (Tarsiiformes, Primates): Taxonomy, phylogeny, and adaptations. Bulletin of the American Museum of Natural History, 156:157–450.

SZALAY, F. S., AND M. DAGOSTO. 1980. Locomotor adaptations as reflected on the humerus of Paleogene primates. Folia Primatologica, 34:1–45.

———. 1988. Evolution of hallucial grasping in the primates. Journal of Human Evolution, 17:1–33.

TERRANOVA, C. 1994. Leaping behaviors and cross-sectional properties of strepsirhine primate long bones. Unpublished Ph.D. Dissert., Northwestern University, Chicago, Illinois.

WEIGELT, J. 1933. Neue Primaten aus mitteleozänen (oberlutetischen) Braunkhole des Geiseltals. Nova Acta Leopolda, 1:97–156.

APPENDIX 1

Character Descriptions

1. Femoral neck length short (0); medium (1); or long (2).[1–3]

2. Angle of femoral neck < 60° (0); 60–70° (1); or > 70° (2).[1–3]

3. Angle of lesser trochanter medial (0–30°) (0); or posterior (> 30°) (1).[2, 3]

4. Size of third trochanter large (0); small (1); or crestlike or absent (2).[1–3]

5. Knee index < 90 (shallow knee) (0); 90–100 (1); or > 100 (deep knee) (2).[1, 2]

6. Femoral head shape spherical (0); semicylindrical (1); or cylindrical (2).[1–3]

7. No anterior extension of greater trochanter (0); or greater trochanter extends anteriorly beyond proximal femoral shaft (1).[2, 3]

8. Proximal femur not bent anteriorly (0); or bent anteriorly (1).[2, 3]

9. Relative length of trochanteric fossa > 125 (long) (0); 110–125 (moderate) (1); or < 100 (very short) (2).[1–3]

10. "Intertrochanteric crest" absent (0); or present (1).[2, 3]

11. Distal tibiofibular articulation unfused, synovial facet present (0); close apposition, facet present (1); close apposition, no facet (2); or fused (3).[1, 2]

12. Distal surface of tibia square in outline (0); or triangular (1).[2, 4]

13. No rotation of medial malleolus of tibia (0); slight medial rotation (1); or strong medial rotation (2).[1, 2, 4]

14. Medial malleolus of tibia flat (0); anteriorly convex, posteriorly flat (1); or all convex (2).[1, 2, 4]

15. Distal tibial shaft round in cross section (0); or anteroposteriorly compressed (1).[2]

16. Tibialis posterior groove located on medial side of malleolus (0); or on posterior side of malleolus (1).[2]

17. Flexor fibularis groove medially located with respect to trochlear articular surface (0); or laterally located (1).[2, 5]

18. Facet for fibula on talus vertical (0); or laterally flaring (1).[2, 5]

19. Trochlea on talus relatively short (0); or long (1).[2]

20. Posterior shelf on talus absent (0); present and small in size (1); or present and large in size (2).[1,2]

21. Relative length of talar neck < 100 (short) (0); or > 100 (long) (1).[2]

22. Degree of relative elongation of anterior part of calcaneus < 40 (short); 40–45 (moderate) (1); or > 45 (long).[1,2,6]

23. Peroneal tubercle on calcaneus distally located with respect to posterior talocalcaneal joint (0); located at joint (1); or located proximal to joint (2).[2]

24. Calcaneal bowing absent (0); or present (1).[2]

25. Trochlea on humerus conical in shape (0); cylindrical in shape, distal edge forms oblique angle to long axis of shaft (1); or cylindrical in shape, distal edge perpendicular to long axis of shaft (2).[1,2]

26. Dorsoepitrochlear pit on humerus present and conspicuous (0); small and shallow (1); or absent (2).[1,2]

27. Humeral head index infw/pdchord > 70 (0); < 70 (1).

28. Humeral head index ap/ext < 75 (0); > 75 (1).

29. Capitulum shape attenuated (0); round (1).

30. Relative hind limb length IMI or HFI > 60 (0); < 60 (1).

31. Relative height of humeral trochlea (index Th/TW) < 100 (0); > 100 (1).

32. Relative width of humeral trochlea (index TW/AW) > 45 (0); < 45 (1).

33. Length of navicular relative to width < 90 (short) (0); 100–150 (moderate) (1); or > 150 (long) (2).[1,2]

34. Facet for cuboid on navicular lateral in position (0); or plantar (1).[2,5]

35. Facet for first metatarsal on entocuneiform relatively flat, mediolaterally narrow, and restricted to distal end of entocuneiform (0); sellar-shaped and extensive (1); nonsellar-shaped and extensive.[2,7]

36. Auditory bulla separated from petrosal bone by a suture (0); bulla formed by petrosal (1).[8]

37. Ectotympanic expanded relative to ontogenetically early condition (0); ectotympanic not expanded and "ringlike" (1).[8]

38. External acoustic meatus not extended as a tube (0); tubelike (1).[8]

39. Annular bridge present and complete (0); present but incomplete (recessus dehiscence present) (1); annular bridge absent (2).[8]

40. Bony canals for proximal divisions of internal carotid artery absent (0); or present (1).[8]

41. Posterior carotid foramen posterolateral in position (0); posteromedial (1); or anterolateral (2).[8]

42. Suprameatal foramen absent (0); or present (1).[8]

43. Internal carotid artery unreduced in size (0); reduced, with function assumed by ascending pharyngeal artery (1); reduced, with function assumed by vertebrobasilar system or vessels other than the ascending pharyngeal (2).[8]

44. Parotic fissure present (0); or absent (1).[8]

45. Basioccipital flange overlapping bulla absent (0); or present (1).[8]

46. Apical aditus of anterior accessory cavity absent (0); or present (1).[8]

47. Central stem of basicranium broad (0); or narrow (1).[8]

48. Alisphenoid flange overlapping bulla trivial or absent (0); extensive (1).[8]

49. Postorbital septum absent (0); or present (1).[8]

50. Choanae broad in shape (0); or very narrow and "peaked" (1).[8]

51. Snout unreduced (0); or reduced (1).[8]

52. Toothcomb absent (0); or present (1).[8]

53. Postorbital bar absent (0); or present (1).[8]

[1] Multistate character treated as "ordered."

[2] Character from Dagosto and Gebo (1994:table 1).

[3] For further description of character, see Dagosto and Schmid (1996).

[4] For further description of character, see Dagosto (1985).

[5] For further description of character, see Beard et al. (1988).

[6] For further description of character, see Gebo (1988).

[7] For further description of character, see Szalay and Dagosto (1988).

[8] Character from Beard and MacPhee (1984).

APPENDIX 2

Taxon-Character Matrix Used in Parsimony Analysis

Hypothetical ancestor	10000	00010	0?000	0?000	10000	?0000	00000	00000	00000	00000	000
Galago	02022	21020	11221	01101	13102	21101	11211	10020	10110	00000	011
Cheirogaleus	11001	00000	01221	01112	12202	20000	00111	11010	00110	00000	011
Adapidae	11001	00000	01221	01102	11102	20000	00011	11011	00010	00000	001
Lemur	11001	00000	01221	01112	11202	20000	00111	11011	00010	00000	011
Anthropoidea	20110	0000(0,1)	10110	00010	11101	00000	00002	10021	10010	10010	001
Tarsius	02002	21120	30110	10000	03111	21111	11201	10121	21001	11111	101
Necrolemur	2111?	01101	30110	10002	03111	1??01	00???	10101	11001	00101	001
Shoshonius	02002	11110	20111	00001	12101	10010	00???	10001	00001	01101	101
Hemiacodon/Omomys	02002	11110	20111	00001	12101	1??0?	00101	?????	?????	?????	?0?
Tetonius/Absarokius	?????	?????	20111	00001	12101	1??0?	00???	1???1	??0??	??101	101

ANNALS OF CARNEGIE MUSEUM
Vol. 68, Number 3, Pp. 213–214 12 August 1999

REVIEW

Rattlesnake: Portrait of a Predator. Manny Rubio. 1998. Smithsonian Institution Press, Washington and London. xxxi + 240 pp. ISBN 1-56098-808-8 (cloth). $39.95.

When I was a teenager first cultivating an interest in reptiles, one of the first books I discovered was the abridged version of Klauber's 1956 classic treatise on rattlesnakes. I devoured that book, reading it cover to cover in one sitting. The knowledge and excitement in Klauber's work was contagious and that book was my impetus to learn all I could about rattlesnakes. I can only imagine the excitement and passion that will be translated to young herpetologists who pick up Manny Rubio's "Rattlesnake."

Never before have so many rattlesnake taxa been given center stage in such beautiful and detailed color pictures, all of which were taken by the author. The photographs of many taxa, including *Crotalus molossus nigrescens, C. scutulatus salvini*, and *Sistrurus ravus* are simply amazing. Pictures of various behaviors, such as *C. lepidus klauberi* consuming a centipede, and *S. miliarius barbouri* giving birth, are equally spectacular. Rubio's photography is inspiring and anyone would be hard pressed not to see the absolute beauty of these venomous snakes. Headlong into my own morphological analysis of the group, I found myself counting head scales on quite a few snakes in the book.

The book is organized into 14 chapters with the first nine addressing various aspects of rattlesnake biology ranging from morphology to reproduction, physiology to taxonomy and systematics. The text, though not exhaustive, is factually correct and provides a good summary for many aspects of rattlesnake natural history. Rubio keeps the text at a moderate academic level, maintaining the interests of both amateur and professional herpetologists alike by describing recent research coupled with long-standing facts about rattlesnake biology. The text flows smoothly as Rubio's style of writing is quite personal, making the book easy to read, though the spectacular photographs can understandably interrupt one's train of thought!

The latter chapters deal with the rattlesnake–human interface, and the unfortunate, yet predictable consequences for the rattlesnake. Here the reader finds the most passionate of Rubio's writing as his descriptions of both the rattlesnake roundups and the economic value of the snakes reveal the disappointing nature of man. The text complements the visually disturbing pictures found in these latter chapters. Successive chapters dealing with the use of rattlesnakes in religion and in folklore are equally as engaging. Rubio's final chapter champions those who study rattlesnakes (especially those in the field) and concludes with his pleas for conservation and research.

The glossary and the three appendices (two concerning scientific and common nomenclature, one listing North American regional and professional herpetological societies) make the book accessible to readers of all academic levels and the "working" bibliography is a fine springboard for anyone interested in learning more about these snakes.

A few inconsistencies are present in the book; these problems range from incorrect facts and citations to small errors in figure legends and simple misspellings. These minor problems are indeed few and do not detract from the overall quality of the book. All of the chapters, especially those on physiology, pigmentation, and locomotion, are factual, current, and well written.

Rubio doesn't pull any punches when it comes to expressing his thoughts and feelings about rattlesnakes. Lamenting that much of the previous research with rattlesnakes took place in the laboratory, he points out that only with studies focused on learning about the natural history of rattlesnakes can we start to understand the importance of rattlesnakes in nature. I strongly agree with him on the importance of field studies, but I don't share his enthusiasm that molecular studies are the panacea of all taxonomic problems among the rattlesnakes. His repeated statements that only molecular and DNA analyses will solve many of the ongoing taxonomic debates are stated almost as fact. For the sections on systematics and taxonomy, he takes a fairly objective approach by presenting both sides of the current debate. In later sections and with certain pictures, however, he unabashedly enters portions of the taxonomic debate by showing or listing taxon names that were recently synonymized, indicating his belief that these populations warrant independent taxonomic status.

Rubio prefaces his book by stating that it was not intended to take the place of the volumes of Gloyd (1940) or Klauber (1956), but instead it was to be "a visually exciting, readable book composed of current factual, interesting information." To his credit, he has produced a book that will surely fuel the fires of inspiring young herpetologists (as well as rekindle the flames within older herpetologists) with his spectacular pictures and engaging, narrative text. The affordable price and the high quality pictures make this book a valuable addition to anyone's bookshelf.

LITERATURE CITED

GLOYD, H. K. 1940. The rattlesnakes, genera *Sistrurus* and *Crotalus*. Chicago Academy of Sciences Special Publication no. 4, Chicago Academy of Sciences, Chicago, Illinois.

KLAUBER, L. M. 1956. Rattlesnakes, Their Habits, Life Histories, and Influence on Mankind. Two volumes. University of California Press, Berkeley, California.

TRAVIS J. LaDUC, *Department of Zoology and the Texas Memorial Museum, The University of Texas at Austin, Austin, Texas 78712-1064.*

INSTRUCTIONS FOR AUTHORS

ANNALS OF CARNEGIE MUSEUM consist of contributions to the earth sciences (including paleontology), life sciences, and anthropology, in 30 by 46 picas format (127 by 195 mm or 5 by 7⅝ inches). Submit all manuscripts to the Office of Scientific Publications. Authors should give particular attention to scientific content, format, and general style for the ANNALS. **Manuscripts that do not conform to the style of the ANNALS will be returned to the author immediately.** Every manuscript will be subjected to external peer review. Authors should submit the names, addresses, phone and fax numbers, and e-mail addresses of at least four qualified potential reviewers for each manuscript. Authors will be asked to subsidize, if funds are available, any or all costs of publication (approximately $100/page printed). A detailed set of instructions to authors may be requested from the Office of Scientific Publications.

Manuscript Style.—Articles should include the following items in this order: title page, abstract, text (with desired headings), acknowledgments, literature cited, tables, figure captions, and copies of illustrations. All manuscripts must be typed ***double-spaced*** on standard 8½ by 11-inch white bond paper, with at least one-inch margins all around, and submitted ***in quadruplicate***—an original for the editors, and three review copies. All pages should be numbered, including tables, literature cited, and the list of figure captions. Only correspondence quality or better dot matrix printouts will be accepted; draft mode is unacceptable. A monospaced font, (e.g., Courier) is required. A disk in WordPerfect x.x or ASCII is helpful.

Title Page. The title should be brief, include the animal or plant group involved, be placed on a separate page, and appear two to three inches below the top margin. Include the author's name(s) and the affiliations of non-CMNH authors. In the case of multiple authorship, indicate the address to which proofs should be sent.

Abstracts. Abstracts should be short, but substantive, and included at the head of the first page of text.

Text. Do not right justify text or break (hyphenate) a word at the end of a line. ***Footnotes and acknowledgments as footnotes are unacceptable.*** All text is double-spaced in a monospaced font (e.g., Courier).

Tables and Figure Legends. The list of figure legends and each table should be typed consecutively on individual pages separate from the text. Tables must be double-spaced throughout with **no vertical lines**.

Measurements. Metric units should be used, if possible.

Literature Cited. All references to literature in text must appear in the Literature Cited section. The data (author, date, and page) in both citations must agree. ***Do not abbreviate the titles of periodicals or serials.*** The following style, double-spaced, should be used in Literature Cited:

1) Two authors in a journal series:
    SOLTIS, D. E., AND P. S. SOLTIS. 1992. The distribution of selfing rates in homosporous ferns. American Journal of Botany, 79:97–100.
2) Same authors repeated—use three-em dash:
    _____. 1923. The fauna of the Ardyn Obo Formation. American Museum of Natural History Novitates, 98:1–5.
3) Same authors plus a third author—repeat all authors:
    KNUTSON, L. V., R. E. ORTH, AND W. L. MURPHY. 1986. Catalog of Sciomyzidae (Diptera) of America north of Mexico. Entomography, 4: 1–53.
4) Chapter in an edited volume:
    RAUSCH, R. L. 1963. A review of the distribution of Holarctic mammals. Pp. 29–43, *in* Pacific Basin Biogeography (J. L. Gressitt, ed.). Bishop Museum Press, Honolulu, Hawaii.
5) Unpublished dissertation:
    SMITH, J. P. 1976. Review of Eocene Mammals. Unpublished Ph.D. Dissert., University of California, Berkeley, California.
6) Book:
    WHITE, M. J. D. 1961. The Chromosomes. Metheuen and Co., Ltd., London, United Kingdom.
7) Journal articles with usual volume and issue number:
    ANDERSON, W. I. 1969. Lower Mississippian conodonts from northern Iowa. Journal of Paleontology, 43:916–928.

Figures. Including all illustrative materials (line art, halftones, photographs), figures are to be numbered in Arabic numerals. Four sets of figures are required, one (original artwork) for reproduction, three for reviewers. Photocopies of photographs for reviewers are usually not acceptable but are adequate for line drawing review copies. Figures may not be larger than 17 by 12 inches. Reducing figures is the responsibility of the author. All figures must be reducible to a maximum of 127 by 195 mm (30 by 46 picas) without loss of clarity. Line copy should be designed for reduction to ⅔ or ½ or actual size. Typewritten figure copy will not be accepted. Photographic figures should be submitted at **actual reproduction size**, if possible.

Rectangular halftone figures should be abutted, without intervening spaces. The printer will insert narrow white spaces during the reproduction process. All figures must have **minimally** one-inch borders all around. Each figure should be given a protective cover and identified on the back side.

Lettering and/or a magnification scale (linear metric scale) for rectangular halftone figures should be placed directly on the photo, not in a blank space between photos. The scale or lettering for closely cropped photos can be placed in blank areas close to the figure.

Proof.—The author should answer all queried proof marks and check the entire proof copy. Return corrected page proof with the edited manuscript ***promptly*** to the Office of Scientific Publications.

If an author chooses to make extensive alterations to a paper in proof stage, the author will bear the cost. Original manuscripts will not be returned unless requested. Figures will be returned to the author only if requested prior to publication.

AS
36
P7X
NH

W

SMITHSONIAN
NOV 23 1999
LIBRARIES

ISSN 0097-4463

ANNALS of CARNEGIE MUSEUM

THE CARNEGIE MUSEUM OF NATURAL HISTORY
4400 FORBES AVENUE • PITTSBURGH, PENNSYLVANIA 15213

VOLUME 68 18 NOVEMBER 1999 NUMBER 4

CONTENTS

ARTICLES

Fossil decapod crustaceans from the late Oligocene to early Miocene Pysht Formation and late Eocene Quimper Sandstone, Olympic Peninsula, Washington . . . . . . **Carrie E. Schweitzer and Rodney M. Feldmann** 215

Archaeology of Trants, Montserrat. Part 5. Prehistoric avifauna . . . . **Kelley R. Reis and David W. Steadman** 275

Index 289

Editors, ANNALS, BULLETIN and SPECIAL PUBLICATIONS:

D. S. Berman, Ph.D.
D. R. Watters, Ph.D.
J. R. Wible, Ph.D.
M. A. Schmidt, ELS, Managing Editor

Manuscripts, subscriptions, orders for individual numbers, and changes of address should be sent to:

Office of Scientific Publications
Carnegie Museum of Natural History
4400 Forbes Avenue
Pittsburgh, PA 15213-4080
Phone (412) 622-3287
Fax (412) 622-8837
E-mail: scipubs@clpgh.org

ANNALS OF CARNEGIE MUSEUM is published quarterly by The Carnegie Museum of Natural History, 4400 Forbes Avenue, Pittsburgh, Pennsylvania 15213-4080, by the authority of the Board of Trustees of Carnegie Institute.

© 1999 Carnegie Institute.

♾ This paper meets the requirements of ANSI/NISO Z39.48-1992 (Permanence of Paper).

ANNALS OF CARNEGIE MUSEUM
VOL. 68, NUMBER 4, PP. 215–273 18 NOVEMBER 1999

FOSSIL DECAPOD CRUSTACEANS FROM THE LATE OLIGOCENE TO EARLY MIOCENE PYSHT FORMATION AND LATE EOCENE QUIMPER SANDSTONE, OLYMPIC PENINSULA, WASHINGTON

CARRIE E. SCHWEITZER[1]

RODNEY M. FELDMANN[1]
Research Associate, Section of Invertebrate Paleontology

ABSTRACT

Fossil decapod crustaceans of the Twin River Group, including the Hoko River, Makah, and Pysht formations, of the Olympic Peninsula, Washington, have received little systematic attention since Rathbun's work in 1926. The current study provides emended descriptions of several taxa that were previously described by Rathbun as occurring in rocks that are now referrable to the Pysht Formation. Two new species are described from the Pysht Formation, *Trichopeltarion berglundorum* and *Asthenognathus cornishorum*. This marks the first notice of both *Trichopeltarion* and *Asthenognathus* on the west coast of North America. *Macrocheira longirostra*, new species from the late Eocene Quimper Sandstone, Olympic Peninsula, Washington, marks the earliest known occurrence of the genus *Macrocheira*, previously known from the Oligocene of Washington and the Miocene, Pliocene, and Recent of Japan. Decapod occurrences corroborate previously reported depths for the Pysht Formation, deposited in bathyal conditions that shallowed to inner sublittoral depths, and the Quimper Sandstone, deposited in littoral to sublittoral depths.

Decapods of the Pysht and Makah formations and the Quimper Sandstone are remarkably similar to Cenozoic decapods described from Japan. This evidence provides a biogeographic link between the east and west North Pacific decapod faunas that appears to have existed as early as the late Eocene. This link persists in the Recent because five genera from the Twin River Group and Quimper Sandstone are represented among extant decapods of the North Pacific Ocean.

KEY WORDS: Decapoda, Brachyura, Anomura, Oligocene, Miocene, Washington

INTRODUCTION

This study describes several decapod taxa, including two new species collected from the late Oligocene to early Miocene Pysht Formation of the late Eocene to early Miocene Twin River Group and one new decapod species collected from the late Eocene Quimper Sandstone.

Fossil decapod crustaceans of the northwest coast of North America were originally described in the 19th and early 20th centuries by such workers as Dana (1849), Gabb (1864), Rathbun (1916, 1926), and Withers (1924). In 1926, Rathbun described several decapod taxa, some of which were collected from rocks that have since been assigned to the Twin River Group. Subsequently, decapod crustaceans of the Twin River Group, specifically the Pysht Formation, have received little additional systematic attention until recently. Lasmanis and Berglund (1991) figured taxa from the Pysht Formation. Feldmann et al. (1991) provided a general discussion of the decapod fauna of the Twin River Group, and Tucker (1995) conducted a comprehensive study of the Raninidae including those of the

---

[1] Department of Geology, Kent State University, Kent, Ohio 44242.
Submitted 17 January 1997.

Twin River Group. Hopkins and Feldmann (1997) evaluated ctenochelids of the late Eocene to early Oligocene Makah Formation in the Twin River Group as well as the late Oligocene to early Miocene Pysht Formation.

The decapod fauna of the Pysht Formation is dominated in number of individuals by the ctenochelid *Callianopsis clallamensis* (Withers) but includes genera in several other families including the Callianassidae, Calappidae, Atelecyclidae, Portunidae, Majidae, and Pinnotheridae. In addition, the Pysht Formation has yielded an extremely large claw (CM 39690, deposited in the Carnegie Museum of Natural History) that is insufficiently complete to provide an identification or description. The Pysht Formation decapods differ from those of the other formations of the Twin River Group, the Hoko River and Makah formations. The Hoko River decapod fauna is dominated by raninids and goneplacids (Feldmann et al., 1991; Tucker, 1995). No species and only one genus, *Portunites* Bell, are shared between the Hoko River Formation and the Pysht Formation as far as is known. The Makah Formation and the Pysht Formation share the species *Callianopsis clallamensis*, but the two formations do not share any other species and only one other genus, *Portunites.* The decapod fauna of the Pysht Formation is remarkably similar to the Cenozoic, especially the early Miocene, decapod fauna from Japan (Karasawa, 1993; among others). Every decapod species herein identified from the Pysht Formation, with the exception of the callianassid taxa, has a Miocene congener in Japan.

Within this paper, several taxa originally named and described by Rathbun and others have been redescribed based upon the availability of more complete fossil material. Additionally, three new species have been recognized, and affinities with the Miocene Japanese decapod fauna are also discussed.

STRATIGRAPHY AND GEOLOGIC SETTING

The study area for the Twin River Group is located along the north coast of the Olympic Peninsula, Washington (Fig. 1). The Olympic Peninsula is composed of several terranes, some of which are considered to have been accreted, probably in the Paleocene to early Eocene, when the Kula and Farallon plates were moving obliquely northeast along the North American plate (Snavely, 1987). These accreted rocks as well as some deep marine sediments and volcanics are believed to comprise most of the core rocks of the northern Olympic Peninsula (Babcock et al., 1994). The core complex consists of metamorphic rocks and turbidites with interbeds of basalt and is overlain by the Crescent "Terrane" (Fig. 1), which is primarily composed of autochthonous sedimentary rocks (Babcock et al., 1994). The Crescent "Terrane" is separated from the core rocks of the peninsula by faults.

The lowermost unit of the Crescent "Terrane" on the northern Olympic Coast is the Blue Mountain Unit, composed of early Eocene marine turbidite sediments thought to have been a submarine fan (Babcock et al., 1994). The Blue Mountain unit is overlain by the volcanic Crescent Formation, which is itself overlain by the marine Aldwell Formation, composed of siltstones, sandstones, and conglomerates (Babcock et al., 1994). The Eocene Aldwell Formation is believed to have been deposited in cold, deep water and to represent landslides or mudflows (Babcock et al., 1994). Overlying the Aldwell Formation is the late Eocene Lyre Formation (Snavely, 1987), composed of breccias and sandstones deposited in shallow to deep water conditions (Babcock et al., 1994). Apparently the basin in

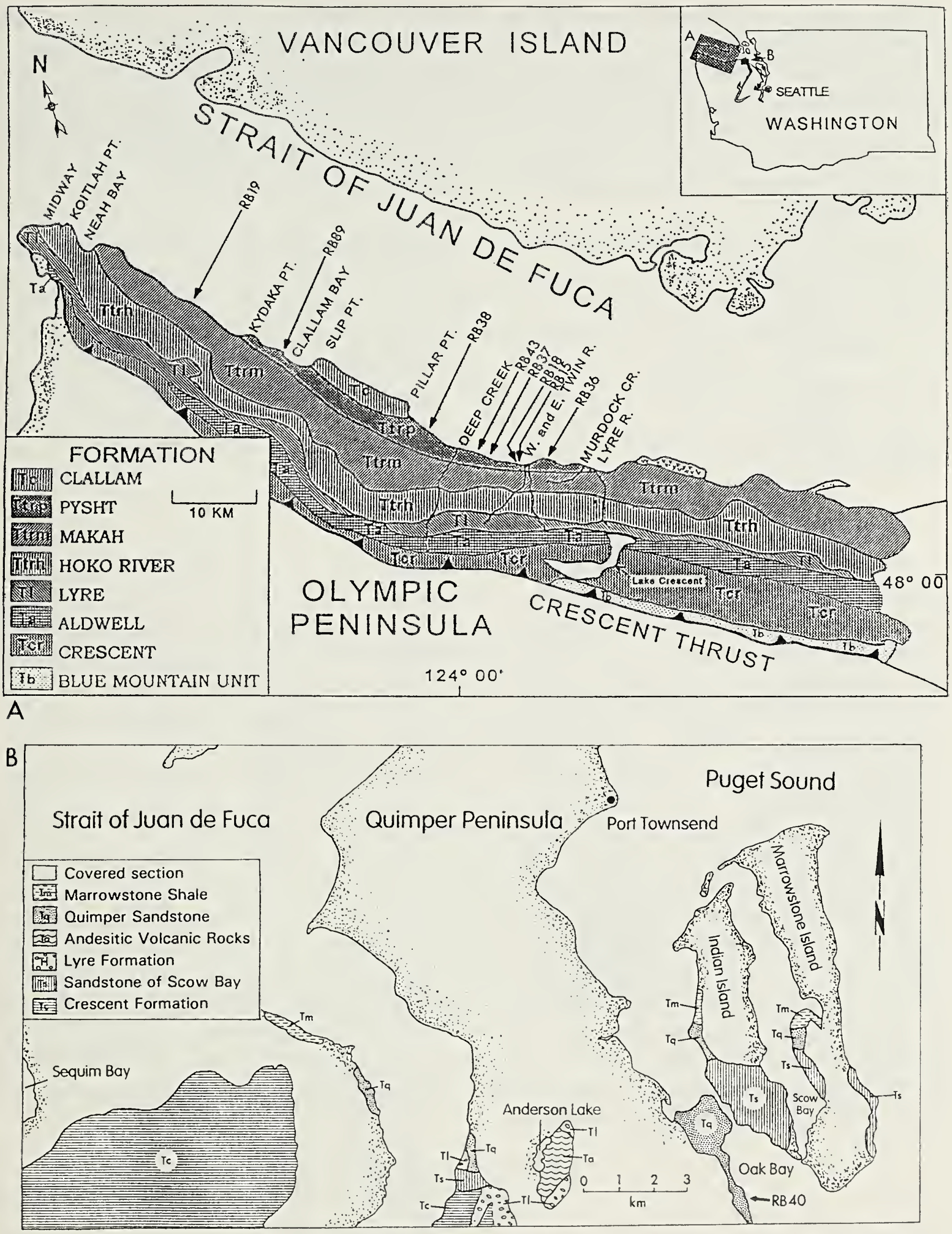

Fig. 1.—Map showing geology and collecting localities of the northern Olympic Peninsula, Washington. Enlarged area A depicts geology and collecting localities for the Twin River Group (map modified from Tucker [1995]). Enlarged area B depicts geology and collecting locality for the Quimper Sandstone (map modified from Armentrout and Berta [1977] and Babcock et al. [1994]).

which the Lyre Formation was being deposited deepened over the course of deposition (Babcock et al., 1994). Rapid subsidence was initiated in the late Eocene, and the Hoko River Formation was deposited in the deepening Tofino–Fuca basin paralleling the north coast of the Olympic Peninsula (Snavely, 1987). The Makah Formation was deposited when this basin was at its deepest during the late Eocene to Oligocene, and the late Oligocene to early Miocene Pysht and the Miocene Clallam formations were deposited as this basin shallowed into the Miocene (Snavely, 1987).

The Quimper Sandstone crops out on the Quimper Peninsula and Marrowstone and Indian islands which are located on the east coast of the Olympic Peninsula (Fig. 1). The Quimper Sandstone is underlain by the middle Eocene sandstones of Scow Bay which probably represent midfan channel fill deposits (Babcock et al., 1994). The Quimper Sandstone is separated from the Scow Bay sandstones by an angular unconformity in most areas, and in other areas, the Quimper Sandstone overlies the Lyre Formation (Babcock et al., 1994). The overlying Marrowstone Shale was deposited in a deep, rapidly subsiding basin (Babcock et al., 1994).

QUIMPER SANDSTONE

The Quimper Peninsula, located at the east end of the Olympic Peninsula, contains a section of Eocene marine sedimentary rocks (Fig. 2). Included in this sequence is the late Eocene Quimper Sandstone, believed to be approximately the same age as the Makah Formation (Babcock et al., 1994). The Quimper Sandstone has been assigned a Refugian age based upon molluscs and foraminifera (Armentrout and Berta, 1977). The lower part of the Quimper Sandstone contains amalgamated sandstone with crossbedding that indicates a shallow-water depositional environment while the upper part of the formation contains laminated siltstone and shale deposited below wave base (Babcock et al., 1994). The unit shows fining upward representing a deepening sequence from inner to outer shelf environments (Babcock et al., 1994). The provenance of this formation was likely Vancouver Island, the Coast Plutonic Complex, and the North Cascades (Babcock et al., 1994). Megafossils collected from the base of the Quimper Sandstone suggest that it was deposited on an inner shelf in littoral to sublittoral, warm temperate water conditions (Armentrout and Berta, 1977). Benthic foraminifera collected from the upper part of the formation indicate shelf deposition in sublittoral to upper bathyal, warm temperate water conditions (Armentrout and Berta, 1977). Material referred to *Macrocheira longirostra* was collected from locality RB40 in the Quimper Sandstone, located along the west shoreline of Oak Bay, south of Port Townsend, Washington (Fig. 1).

TWIN RIVER GROUP

Overview

The Twin River Group was originally named the Twin River Formation by Arnold and Hannibal (1913:584–585) who recognized it as a sequence of "soft clay shales and intercalated beds of sandstone" of late Oligocene and Miocene age that cropped out on the northern Olympic Peninsula along the Strait of Juan de Fuca from about five kilometers east of Twin Rivers to Pysht Bay. Arnold and Hannibal's definition of the upper and lower contacts as well as the areal extent of the Twin River Formation was rather ill-defined and arbitrary. In 1958, Brown

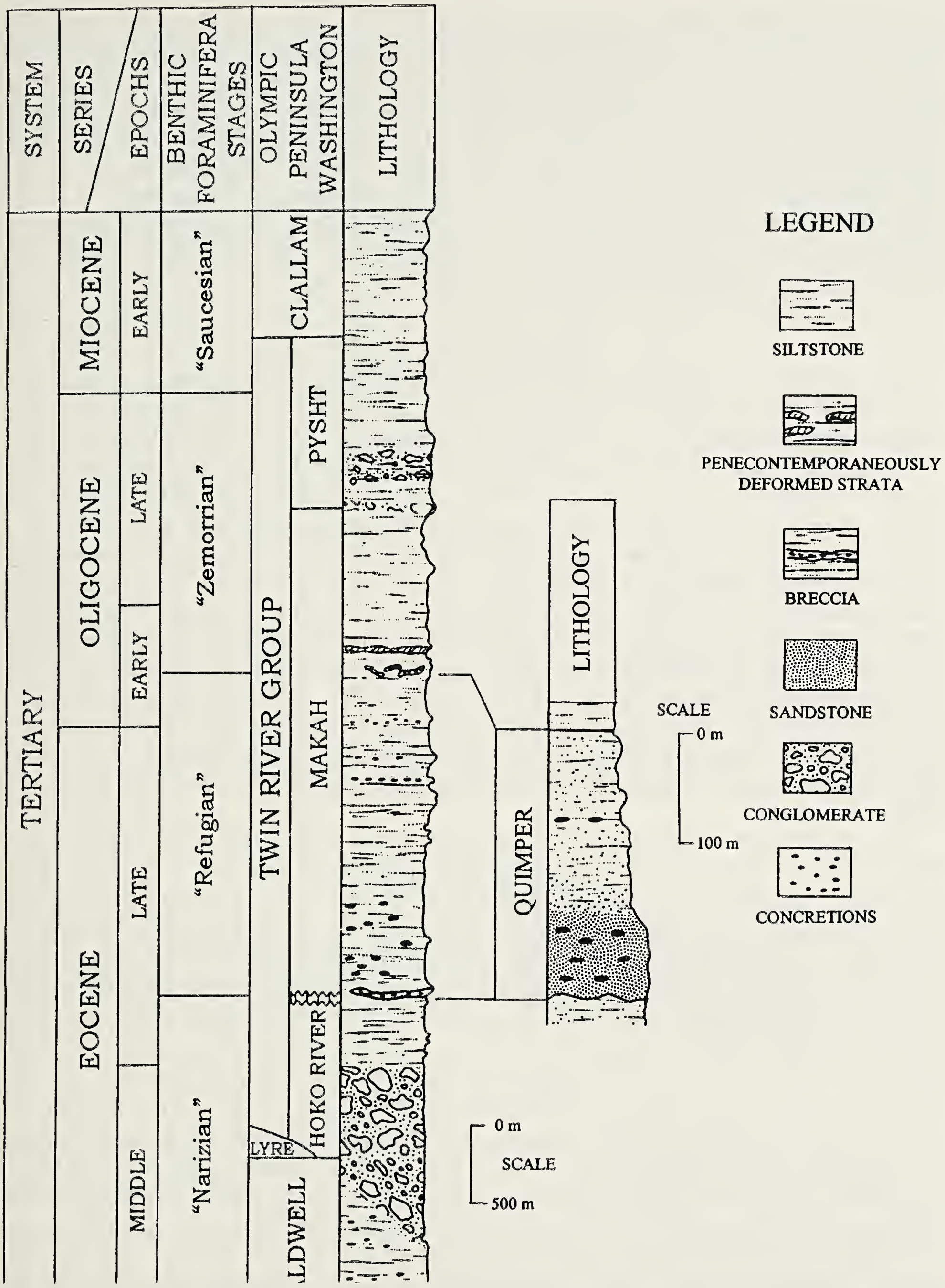

Fig. 2.—Generalized stratigraphic column of the Twin River Group and stratigraphic column of the Quimper Sandstone on West Marrowstone Island. Twin River Group column modified from Tucker (1995:370) and Quimper Sandstone column modified from Armentrout and Berta (1977:222).

and Gower redefined the formation to include up to 5300 m of sandstones, siltstones, and conglomeratic beds that extended from Clallam Bay to east of Port Angeles. The Twin River Formation was reported to overlie the Lyre Formation and to be conformably overlain by the Clallam Formation (Brown and Gower, 1958). Brown and Gower (1958) divided the Twin River Formation into three mappable members (lower, middle, and upper), and later, Snavely et al. (1978) elevated each member to formation status, named each, and elevated the Twin River Formation to the Twin River Group (Fig. 2). They also extended the range of outcrop of the Twin River Group to include rocks extending from Neah Bay to east of Port Angeles (Snavely et al., 1978).

Hoko River Formation

The lowermost formation, the Hoko River Formation, is composed of massive- to thin-bedded siltstone and thinner beds of sandstones and conglomerates and ranges from 1600–2300 m in thickness (Snavely et al., 1978). Calcareous concretions have been collected throughout the Hoko River Formation, and they often contain decapods, gastropods, and wood fragments as their nuclei (Snavely et al., 1978). The Hoko River Formation conformably overlies the Lyre Formation and intertongues with it at some localities (Snavely et al., 1978). It is conformably overlain by the Makah Formation, the middle unit of the Twin River Group, in most localities but in some areas there is an unconformity between the two formations (Snavely et al., 1978). The Hoko River Formation is believed to be late Eocene (late Narizian Stage of Mallory) in age, based upon molluscan and foraminiferan assemblages (Snavely et al., 1978). Addicott (*in* Snavely et al., 1978) believed that crab occurrences placed the Hoko River Formation in the late Eocene, but Tucker (1995) reported that crab-bearing concretions were probably formed before their final deposition, making them somewhat older than the Hoko River sediments.

The depositional environment of the Hoko River Formation is thought to have been relatively deep and cool according to foraminiferal data (Rau, 1964). Depths may have ranged from bathyal to sublittoral, and the depth is estimated to have been 90–300 m (Rau, 1964). The Hoko River Formation is believed to have been deposited in a shallower environment than the Makah Formation, the middle unit of the Twin River Group, and much of the Pysht Formation, the uppermost unit of the Twin River Group, based on foraminiferal assemblages recovered from each unit (Rau, 1964).

Makah Formation

The middle formation of the Twin River Group, the Makah Formation, is composed chiefly of thin-bedded siltstone and turbiditic sandstone and includes six mappable members of differing lithologies (Snavely et al., 1978). The bulk of the formation is composed of siltstone beds ranging in thickness from one to ten centimeters interbedded with sandstones that display typical Bouma turbidite sequences (Snavely et al., 1980). The Makah Formation achieves an average thickness of 2800 m and is believed to be late Eocene to Oligocene in age based upon foraminiferal assemblages (Snavely et al., 1980).

Mappable members of the Makah Formation include four thick-bedded, turbiditic sandstones, an olistostromal unit of shallow-marine sandstone, and a bed of water-lain tuff (Snavely et al., 1978). Calcareous concretions may be found throughout the Makah Formation and these contain nuclei of calcite crystals, decapods, plant fragments, and worm burrows (Snavely et al., 1980). One of the mappable members of the Makah Formation, the olistostromal Jansen Creek Member, lies near the middle of the Makah Formation. It is believed to be an allocthonous unit resulting from erosion of uplifted, older rocks that bordered the deep marginal basin where the Makah Formation was being deposited (Snavely et al., 1980). The Jansen Creek Member is composed of shallow water conglomerate and fossiliferous sandstone and is enclosed by younger deepwater deposits according to foraminiferal data (Snavely et al., 1980). Snavely et al. (1978) believed the Jansen Creek Member to be late Eocene in age based upon molluscs and foraminifera and to be overlain by beds of Zemorrian Age (Oligocene). However, Squires and Goedert (1994) reported the Jansen Creek Member to be earliest Oligocene in age (p. 402). The fauna of this member represents a bathyal assemblage (Squires and Goedert, 1994). The Jansen Creek Member contains numerous fossiliferous calcareous concretions and contains the vast majority of the decapods found in the Makah Formation. The ctenochelid species *Callianopsis clallamensis* was collected from this unit.

Because the Makah Formation contains turbiditic sandstones, it is believed to represent a rapidly deposited submarine fan in the marginal Tofino–Fuca basin (Snavely et al., 1980). The Tofino–Fuca basin is thought to have been at its deepest during the late Eocene to Oligocene, when the Makah Formation was being deposited (Snavely et al., 1980:24). This interpretation is strengthened by the fact that foraminifera collected from the Makah Formation suggest a lower to middle bathyal, open water environment (Snavely et al., 1980:21). Rau (1964) believed the middle member of the Twin River Formation (Makah equivalent) to have been deposited at bathyal depths from 300–1830 m based on foraminiferal assemblages, which supports the interpretation of the Makah Formation as a deep basin deposit.

Pysht Formation

The Pysht Formation is the uppermost formation assigned to the Twin River Group. Every taxon herein described except *Macrocheira longirostra* was collected from the Pysht Formation. Unfortunately, the lithology and the stratigraphy of the Pysht Formation have not received comprehensive descriptive attention. Brown and Gower (1958) briefly described the lithology of the Twin River Formation and designated lower, middle, and upper members, of which the Pysht Formation is the upper member. They reported that the unit was composed chiefly of thin-bedded to massive, poorly indurated gray siltstones with occasional interbedded sandstones, and subsequent workers have concurred with this description for most of the Pysht Formation section (Rau, 1964; Addicott, 1976; Snavely et al., 1978; Armato, 1993; Squires and Goedert, 1994; Tucker, 1995). In addition to the work of Brown and Gower (1958), brief and/or limited lithologic and stratigraphic descriptions of the Pysht Formation have been provided by Rau (1964), Addicott (1976), Snavely et al., (1978), Snavely (1983), and Squires and Goedert (1994). An accurate thickness of the unit has yet to be determined due to structural complications, but it is estimated to be about 1100–1400 m thick (Snavely et al., 1978). The underlying Makah Formation has a gradational contact with the Pysht Formation in some areas but is unconformable in others (Snavely, 1983). The upper contact between the Pysht Formation and the Clallam Formation is gradational and conformable (Snavely et al., 1978).

Completion of detailed stratigraphic and lithologic descriptions of the Pysht Formation are hampered by several factors. First, there are structural complications in the area of outcrop. Numerous faults extend both north–south and east–west throughout the Pysht Formation (see Tabor and Cady, 1978). Second, much of the Pysht Formation section is covered by dense vegetation with occasional outcrops along the Strait of Juan de Fuca and streams, making it difficult to correlate between outcrops or even observe the rocks in many areas. Third, the Pysht Formation is composed of sandy siltstone and siltstone with interbedded sandstones throughout most of its vast thickness, and the occasional conglomerates appear to be similar in lithology. This monotonous and repetitive lithology with a lack of reliable key marker beds makes it difficult to correlate between localities.

Details of the stratigraphy and lithology of the Pysht Formation, beyond a general description, presented by various workers are brief and at times contradictory. Rau (1964) provided a lithologic description of each member of what was then known as the Twin River Formation. He described the probable ecologic setting of the depositional environment of the upper part of the upper member of the Twin River Group (= upper Pysht Formation) which he believed to have been deposited in cool, relatively deep waters that shallowed considerably near the top of the formation (Rau, 1964).

Addicott (1976) collected molluscs from what he believed to be the upper 400–500 m of the upper member of the Twin River Formation (= Pysht Formation), consisting of siltstone and sandy siltstone with an interbedded lens of fosssiliferous conglomerate. He reported that the fossiliferous conglomerate unit was exposed on a ridge south of Pearson Creek which is located between Slip Point and Pillar Point and that other exposures occurred at Pillar Point State Recreational Area and localities near Sekiu at the west end of Clallam Bay (Addicott, 1976). Gower (*in* Addicott, 1976) had mapped the conglomerate as being located in the lower part of the Clallam Formation, but Addicott (1976) reported that this conglomerate occurred about 1000 m above the base of the Pysht Formation. He assigned an early Miocene age based upon molluscan assemblages to the conglomerate and to overlying sandstones and siltstones of the upper 30–40 m.

Subsequently, Snavely et al. (1978) reported that conglomeratic channels occurred at the base of the Pysht Formation and that they were interbedded with siltstone and sandstone of the Makah Formation (Snavely et al., 1978). These conglomerate beds were observed along the coast between Sekiu and Kydaka Point and were reported to be composed of reworked cobble- and boulder-sized clasts of metamorphic and igneous rocks, felsic tuff, and mollusc-bearing sandstone (Snavely et al., 1978). These boulders are believed to have been derived from nearly lithified strata of approximately the same age located on Vancouver Island (Snavely et al., 1978). Snavely et al. (1978:A118) proposed that these conglomerates were similar to those located in the "western part of the Pysht Quadrangle." The conglomerates of the "western part of the Pysht Quadrangle" are the same conglomerates that Addicott (1976) believed to be located 1000 m above the base of Pysht Formation. Because of the lithologic similarity between the conglomerates of the Sekiu-Kydaka Point area which mark the basal contact of the Pysht and those of the "western part of the Pysht Quadrangle," Snavely et al. (1978) proposed that all of the conglomerates must indicate the base of

Pysht Formation. Oddly, they did not discuss the discrepancy between this conclusion and that of Addicott (1976), who placed the conglomerate of the "western part of the Pysht Quadrangle" 1000 m above the base of the Pysht Formation. Snavely et al. (1978) assigned the Pysht Formation a late Oligocene to early Miocene age based upon foraminifers and molluscs.

Armato (1993) reported that the base of the Pysht Formation was composed of conglomerate interbedded with siltstones of the upper Makah Formation. He did not report a conglomeratic unit to be located in the upper portion of the formation that could correspond to the conglomerate reported by Addicott (1976). However, Armato (1993) used the stratigraphic column of the Pysht Formation provided by Addicott (1976), which illustrates the conglomerate 1000 m from the base of the Pysht Formation but does not depict conglomerate at the base of the Pysht section.

In 1994, Squires and Goedert reported that the lower part of the Pysht Formation, just west of the mouth of Murdock Creek, was composed of mudstone with small, discontinuous sandstones at the localities they sampled. They assigned the lower Pysht Formation to the latest early or earliest late Oligocene, based upon the presence of gastropods transitional in morphology between *Liracassis rex* (Tegland) and *L. apta* (Tegland).

We are unable to provide a satisfactory solution to the question of the position of the conglomerate bed or beds in the Pysht Formation. At least two possibilities exist. One solution is that there is more than one conglomerate bed, with one (or more) near the base of the formation and one about 1000 m above the base. Obviously the other solution is that there is only one conglomerate bed near the base of the formation. Conglomeratic float observed by one of us at locality RB36 contained sedimentary concretions similar to those found in the siltstone layers and igneous clasts including granites. The RB36 locality is not located near any of the previously discussed conglomerate localities, so it is possible that this conglomeratic float represents still another conglomerate bed. However, since the conglomerate was observed as float, it is uncertain as to exactly where in the section it originated.

Another problem with the discrepancy of the conglomerate beds lies in the age determination. Addicott (1976) assigned the conglomerate he studied to the early Miocene; Snavely et al. (1978) appear to believe that this same conglomerate lies at the base of the formation. Squires and Goedert (1994) determined that localities near the base of the Pysht Formation just west of Murdock Creek were latest early or earliest late Oligocene in age. If the conglomerate described by Snavely et al. (1978) and Addicott (1976) is indeed the same bed and is located near the base, this creates a disturbing age discrepancy with two possible ages for the base of the formation. More detailed mapping, stratigraphic work, and collection of age-diagnostic fossils, all of which is beyond the scope of this study, will be necessary to resolve these discrepancies.

It is the opinion of the authors at the present time that there is most likely more than one conglomerate bed, with at least one being located near the contact with the Makah Formation at the base of the Pysht and one occurring near the top of the formation 1000 m above the base. This conclusion seems warranted for several reasons. First, based upon lithologic similarity only, Snavely et al. (1978) generalized that all of the conglomerates of the Pysht Formation must be located at the base; however, more convincing evidence, namely fossils, would be necessary to demonstrate that all of the conglomerates indeed represent the same bed. Second, because the conglomerate of Addicott was assigned an early Miocene age, it is more likely to be located near the top of the formation since the overlying Clallam Formation, with which the Pysht is conformable, is late early Miocene in age (Addicott, 1976). Third, the underlying Makah Formation is considered to be late Eocene to late Oligocene in age based upon foraminiferans (Snavely et al., 1980). Squires and Goedert (1994) reported that the lower Pysht Formation was latest early to earliest late Oligocene in age. This age determination for the base of the Pysht Formation is more consistent with the age reported for the Makah Formation than is an early Miocene age, especially because the Pysht and Makah formations are in many places conformable. Fourth, some of the outcrops sampled by Addicott (1976) are geographically near the contact between the Pysht Formation and the Clallam Formation, making it more likely that the conglomerate he sampled was near the top of the Pysht section unless faults or other structural complications exist near those localities.

The Pysht Formation contains the most diverse fauna of any of the formations of the Twin River Group (Feldmann et al., 1991). Megafossils include pelecypods, gastropods, scaphopods, pteropods, the nautiloid *Aturia* Bronn, the isopod *Bathynomus goedertorum* (Wieder and Feldmann), wood bored by *Teredo* Linnaeus, scleractinian corals, bryozoans, decapods, and vertebrates including cetaceans, a bird, and the shark *Heptranchias howelli* (Reed) (Weaver, 1942; Addicott, 1976; Olson, 1980; Kaler, 1989; Squires, 1989; Wieder and Feldmann, 1989; Feldmann et al., 1991; Squires and Goedert, 1994).

The age of the Pysht Formation is believed to be latest early or earliest late Oligocene (Zemmorian Stage) to early Miocene (Saucesian Stage) in age based on foraminiferans (Snavely, 1983) and molluscs (Addicott, 1976; Squires and Goedert, 1994). Addicott (1976) believed the upper 400–500 m of the Pysht Formation to be early Miocene in age, and he assigned the mollusc assemblage from this part of the section to the *Echinophoria apta* faunal zone, even though *Liracassis apta* (= *Echinophoria*) itself was not known to occur there at the time of his of study. *Liracassis apta* has been recovered from some localities of the Pysht Formation, including the exposures at RB18 and RB36 which are relatively close stratigraphically to locality A3678 of Addicott (1976). Locality A3678 is stratigraphically lower than the portion of the Pysht Formation assigned by Addicott (1976) to the early Miocene.

The Pysht Formation is interpreted to have been initially deposited in cool waters, approximately 300–1830 m deep, based on the foraminiferal assemblage collected from the lower portion of the upper member of the Twin River Formation (= Pysht) (Rau, 1964). Armato (1993) reported that the depositional environment near the central part of the Pysht Formation section was characterized by moderately deep sublittoral to bathyal depths and cool water temperatures, based on molluscan assemblages. The upper part of the Pysht Formation represents shallower but cool waters, probably inner sublittoral in depth, based upon foraminiferans (Rau, 1964) and molluscs (Armato, 1993). Addicott (1976) believed the upper part of the upper member of the Twin River Formation (= Pysht) to have been deposited in relatively shallow water, in part because of the absence of the deep-water genus *Liracassis*. Rau (1964) reported that the shallowing of the upper portion of the Pysht Formation represented a regional shallowing event that continued during deposition of the Miocene Clallam Formation, a sandy and conglomeratic formation interbedded with coal deposits (Addicott, 1976).

Table 1.—*Decapod collecting localities within the Twin River Group and Quimper Sandstone. Locality numbers are from the locality register of Ross Berglund. More detailed locality descriptions are given in the text.*

Locality numbers	Description of localities
RB15	Pysht Formation, W 1/2, Sec. 23, T31N, R10W, Twin River Quadrangle, 7.5′ series, Clallam County, Washington.
RB18	Pysht Formation, SW 1/4, Sec. 23, T31N, R10W, Twin River Quadrangle, 7.5′ series, Clallam County, Washington.
RB19	Makah Formation, SE 1/4, SE 1/4, Sec. 26, T33N, R14W of the Clallam Bay Quadrangle, 15′ series, Clallam County, Washington.
RB36	Pysht Formation, SE 1/4, Sec. 23, T31N, R10W, Twin River Quadrangle, 7.5′ series, Clallam County, Washington.
RB37	Pysht Formation, SW 1/4, NE 1/4, Sec. 21, T31N, R10W, Twin River Quadrangle, 7.5′ series, Clallam County, Washington.
RB38	Pysht Formation, NE 1/4, SE 1/4, Sec. 13, T31N, R11W, Pysht Quadrangle, 7.5′ series, Clallam County, Washington.
RB40	Quimper Sandstone, SW 1/4, NE 1/4, Sec. 18, T29N, R7E, Nordland Quadrangle, 7.5′ series, E. Jefferson County, Washington.
RB43	Pysht Formation, NE 1/4, NW 1/4, Sec. 21, T31N, R10W, Twin River Quadrangle, 7.5′ series, Clallam County, Washington.
RB89	Pysht Formation, N 1/2, SW 1/4, Sec. 18, T32N, R12W, Clallam Bay Quadrangle, 7.5′ series, Clallam County, Washington.

TWIN RIVER GROUP LOCALITIES

Although it is certain that the decapods were collected from rocks referrable to the Pysht Formation, stratigraphic assignment of the collecting localities (Table 1) within the Pysht Formation section is tentative because of the problems discussed. Decapods were collected from seven localities of the Pysht Formation (Fig. 1). Six of the localities occur along an approximately ten-kilometer section of the coast of the Strait of Juan de Fuca, and five of these localities crop out along approximately five kilometers of coast (Fig. 1). These six localities appear to be stratigraphically lower than the conglomerate described by Addicott (1976) as occurring about 400–500 km below the top of the Pysht Formation. The stratigraphic position of the seventh collecting locality is unknown.

Of the six easternmost localities, locality RB38 seems to be highest and RB36 to be lowest stratigraphically. Of these, RB37, RB38, and RB43 appear to be located stratigraphically higher than Addicott's A3678 locality and lower than his fossiliferous conglomerate. Localities RB15, RB18, and RB36 are believed to be very near locality A3678 of Addicott (1976). If the localities are indeed in these positions of the stratigraphic column relative to Addicott's localities, then the depositional environment of these six localities would correspond most closely to that described by Armato (1993) for the central part of the section. The age of the central part of the section appears to be late Oligocene based upon the work of Rau (1964), Addicott (1976), and Squires and Goedert (1994). The seventh and westernmost decapod collecting locality, RB89, crops out near Sekiu Point at the west end of Clallam Bay. The stratigraphic position, depositional environment, and relative age within the Pysht Formation of RB89 are unknown. According to Addicott (1976), this locality would be found in the upper conglomerate 1000 m from the base and, according to Snavely et al. (1978), would be located in the basal conglomerate near the contact with the Makah Formation.

At the RB15 locality, decapods were collected in concretions as float in the intertidal zone along the Strait of Juan de Fuca between the mouth of West Twin River and the loading dock of the West Twin Shale Quarry. A specimen of *Trichopeltarion berglundorum* n. sp. was collected in a concretion from this locality. The closely associated RB18 locality is located on an open hilltop overlooking the Strait of Juan de Fuca at the West Twin Shale Quarry. Fossils were collected as float in large expanses of quarried sandy siltstones and siltstones. This locality has yielded a decapod fauna dominated by *Callianopsis clallamensis* but includes *Trichopeltarion berglundorum*, *Mursia marcusana* Rathbun, *Macrocheira teglandi* Rathbun, *Asthenognathus cornishorum*, and possibly *Portunites triangulum* Rathbun. Associated fauna includes the gastropod *Liracassis apta*; the pelecypods *Acila gettysburgensis* (Reagan), *Portlandia* sp., *Archarax dalli* (Clark), *Thyasira* sp., *Macoma twinensis* Clark, *Modiolus* sp., and *Lucinoma acutilineata* (Conrad); scleractinian coral; vertebrate bone fragments; an echinoderm; *Teredo*-bored wood; and plant material. Most specimens were collected from concretions originating from medium- to thick-bedded siltstone blocks, but many were collected directly from the siltstone matrix.

At the Tegland Point locality (RB36), about 0.4 km east of the mouth of the East Twin River, fossils were collected along the Strait of Juan de Fuca from concretions occurring as float on a wave-cut terrace, and some concretions were collected in place from siltstone cliffs. Decapods from this locality include *Portunites triangulum*, *Mursia marcusana*, *Asthenognathus cornishorum*, and possibly *Macrocheira teglandi*. Associated fauna includes the gastropod *Liracassis apta*; the pelecypods *Katherinella etheringtoni* (Tegland), *Nucula* sp., *Portlandia* sp., *Archarax dalli*, and *Macoma twinensis*; and *Teredo*-bored wood.

Site RB37, located along the Strait of Juan de Fuca in the intertidal zone, yielded a large block of thin-bedded siltstone which occurred as float. This block contained large quantities of organic material on its bedding planes that included juvenile and adult decapods, molluscs, and large quantities of plant remains. Decapods recovered include *Portunites triangulum*, *Mursia marcusana*, *Macrocheira teglandi*, and *Asthenognathus cornishorum*.

Site RB38 is located in the intertidal zone along the Strait of Juan de Fuca east of the Silverking Fishing Resort near the mouth of Joe Creek. Decapods recovered from this locality include *Callianopsis clallamensis*, *Mursia marcusana*, and *Macrocheira teglandi*. Locality RB43, located along the Strait of Juan de Fuca approximately 3.0 km west–northwest of RB18 and about 0.60 km northwest of RB37, yielded one specimen of *Portunites triangulum*. Finally, one specimen of *Mursia marcusana* has been reported by amateurs from RB89 located at Sekiu Point at the west end of Clallam Bay; however, this specimen was not observed by the authors.

Locality RB19, the only locality from the late Eocene to Oligocene Makah Formation, is located at the mouth of Jansen Creek along the Strait of Juan de Fuca. It occurs in the Jansen Creek Member, an olistostromal unit believed to be somewhat older than the surrounding Makah Formation sediments, and yielded specimens of *Callianopsis clallamensis* preserved in concretions.

ABBREVIATIONS

The following abbreviations are used within the text of this paper: CM, Carnegie Museum of Natural History, Pittsburgh, Pennsylvania; USNM, United States National Museum, Washington, D.C.; RB, Collecting localities in the locality register of Ross Berglund, Bainbridge Island, Washington; H, Height (where there are more than one height dimension listed, they are denoted by numbers and explained where relevant); L, Length (numbers are used as for height); W, Width (numbers are used as for height). All other abbreviations are explained in the text where appropriate.

SYSTEMATIC PALEONTOLOGY

Order Decapoda Latreille, 1803
Infraorder Anomura H. Milne Edwards, 1832
Superfamily Thalassinoidea Latreille, 1831

Remarks.—As has been discussed by Hopkins and Feldmann (1997), identification and interpretation of fossil members of the Thalassinoidea, within both the Callianassidae Dana, 1852, and the Ctenochelidae Manning and Felder, 1991, have historically been hindered by the nature of preservation of fossil material. Because of the delicate nature of most of the cuticle, fossil thalassinoids are largely represented by isolated claws and fingers. Unfortunately, the diagnostic characters of extant taxa, including the nature of the pleopods, details of carapace architecture, and form of the abdomen, are not usually available for study in fossil specimens. The recent revision of the callianassids by Manning and Felder (1991), however, provided several morphological characters of the first pereiopods which, for the first time, permit recognition of more realistic relationships between fossil and recent taxa. Their clarification of the key characters necessary for recognition of genera has stimulated reassessment of several fossil taxa.

The two thalassinoid taxa described herein, *Callianassa* sensu lato cf. *C. porterensis* and *Callianassa* sensu lato sp. 1, do not possess sufficiently well-preserved material to permit referral to known taxa within the framework of Manning and Felder's (1991) revision.

Family Callianassidae? Dana, 1852

Diagnosis.—See Manning and Felder (1991).

Remarks.—In 1991, Manning and Felder revised the superfamily Thalassinoidea to include the Callianassidae Dana and the Ctenochelidae Manning and Felder, 1991. The two subfamilies are differentiated based upon characters not often preserved in the fossil record. The Ctenochelidae possess a cardiac prominence on the dorsal carapace and an appendix on the second pleopods of males. The uropodal exopod is longitudinally carinate on the dorsal surface and lacks a dorsal plate. The Callianassidae lack a cardiac prominence, appendix interna on the male second pleopods, and longitudinal dorsal keel on the uropodal exopods, and possess a dorsal plate on the uropods. None of these characters is preserved in the first two thalassinoid taxa herein described, the material for which consists only of portions of chelipeds. Nevertheless, they are assigned with some reservation to the Callianassidae because the cheliped material does not resemble that of species of any of the six genera assigned to the Ctenochelidae. Some members of the Ctenochelidae, such as *Ctenocheles* Kishinouye and *Dawsonius* Manning and Felder, have very distinctive major chelipeds. Additionally, two of the six genera of the Ctenochelidae are monotypic, including *Dawsonius* and *Paracalliax* de Saint Laurent (Manning and Felder, 1991), and the genus *Callianopsis* de Saint Laurent has few species, indicating that this family is less speciose and diverse than many genera of the Callianassidae. There are no ctenochelids besides *Cal-*

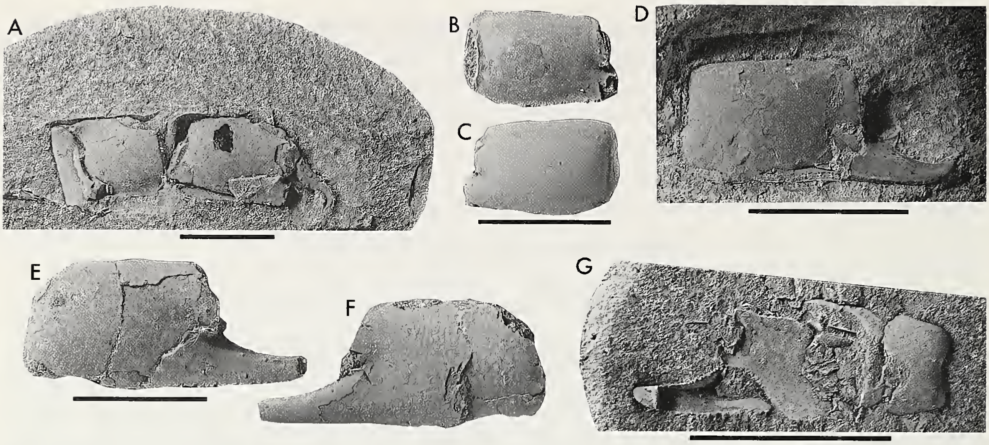

Fig. 3.—A. View of inner surface of cheliped of *Callianassa* cf. *C. porterensis*, CM 39654. B. Inner surface of manus of *Callianassa* cf. *C. porterensis*, CM 39655. C. Outer surface of manus of *Callianassa* cf. *C. porterensis*, CM 39655. D. Inner surface of manus of *Callianassa* sensu lato sp. 1, CM 39660. E. Inner surface of manus of *Callianassa* cf. *C. porterensis*, CM 39656. F. Outer surface of manus of *Callianassa* cf. *C. porterensis*, CM 39656. G. Outer surface of cheliped of *Callianassa* cf. *C. porterensis*, CM 39657. Scale bars = 1 cm. B/C and E/F share scales.

lianopsis found today on the North American coast of the Pacific Ocean (Manning and Felder, 1991). Callianassid genera found today in the eastern Pacific include *Neotrypaea* Manning and Felder, *Notiax* Manning and Felder, *Callichirus* Stimpson, *Corallianassa* Manning, *Glypturus* Stimpson, *Lepidophthalmus* Holmes, and *Cheramus* Bate (Manning and Felder, 1991). All of these factors suggest that the fossil material is most likely referrable to a genus of the Callianassidae; however, better-preserved and more-complete material is necessary to confidently assign these specimens to a family and genus.

Callianassa sensu lato
cf. *Callianassa porterensis* Rathbun, 1926
(Fig. 3A–C, E–G)

Callianassa porterensis Rathbun, 1926:119.

Diagnosis.—Callianassid with manus of cheliped nearly twice as long as high, widening towards proximal margin, distal margin with elongate, serrated projection and indentation just below serrations; fixed finger with serrated upper margin; movable finger with serrate occlusal surface and strongly curved tip (modified from Rathbun, 1926).

Description.—Merus longer than high, upper margin straight, proximal margin broken, distal margin rounded, lower margin nearly straight, broken at proximal end. Carpus of cheliped about as long as high; inner surface slightly convex; proximal margin with triangular, blunt projection at articulation with merus, concave just below projection and curving convexly to lowest extent of margin; upper margin broken; lower margin straight, rimmed; distal margin broken on upper and lower corners but remainder straight.

Manus of cheliped longer than high, widening posteriorly, outer surface smooth; proximal margin rimmed, slightly convex; upper margin straight, sharp; lower margin straight, serrate; outer surface convex longitudinally and transversely; distal margin sinuous, extending slightly obliquely from upper margin to lower margin, inflated region paralleling distal margin, margin incurved just below inflated region; fixed finger narrowing distally, finely serrate on both upper and lower margins, possessing a

Table 2.—*Measurements (in mm) taken on the manus of specimens of* Callianassa *sensu lato cf.* C. porterensis. *L1 = maximum length, H1 = maximum height, L2 = length of fixed finger.*

Specimen	L1	H1	L2	Locality
CM39655	14.6	7.1	—	RB36
CM39658	15.6	8.5	> 5.7	RB36
CM39656	21.0	> 9.4	> 7.8	RB36
CM39657	18.2	7.5	6.7	RB18
CM39654	>11.2	7.4	—	RB36

few scattered punctae; movable finger with finely serrate occlusal surface, wide proximally and narrowing distally, inner surface with two rows of small tubercles, distal tip strongly recurved to parallel distal margin of manus.

Inner surface of manus flattened on margins but convex centrally, smooth. Inner surface of fixed finger smooth, sometimes possessing a few small scattered tubercles, weakly developed keel extending from indentation in distal margin along fixed finger, appearing to disappear about two-thirds of the distance along the finger; upper surface of fixed finger serrated.

Remainder of animal unknown.

Measurements.—Measurements (in millimeters) taken on the manus of six specimens of *Callianassa* sensu lato cf. *Callianassa porterensis* are listed in Table 2. CM 39654: carpus, H (maximum) = 8.3, L (maximum) = 7.8; manus, H (maximum) = 2.8, L (maximum) > 7.8.

Referred Specimens.—Six specimens (CM 39654–39659) are deposited in the Carnegie Museum of Natural History.

Localities and Stratigraphic Position.—All of the specimens were collected as float in concretions along wave-cut terraces and shore cliffs of the Pysht Formation. CM 39654–39656 and CM 39658 and 39659 were recovered from RB36, and CM 39657 was collected from RB18.

Remarks.—Each of the six specimens referred to *Callianassa* sensu lato cf. *C. porterensis* was found in a concretion and consists of the manus of a cheliped. It is unknown as to whether they are major or minor chelae, and the incomplete nature of the material makes it impossible to assign it to a genus other than *Callianassa* sensu lato. Numerous similarities between the material described herein and *Callianassa porterensis* Rathbun permit tentative referral of the specimens to *C. porterensis*; however, the few discrepancies listed below do not allow the specimens to be assigned to that species with confidence.

The specimens described herein possess a manus that is longer than high, and higher proximally than distally, which is characteristic of *C. porterensis.* One specimen possesses a fixed finger with a serrated upper margin, another diagnostic character of *C. porterensis.* Rathbun's (1926) specimens were reported to be thicker near the proximal end of the manus and to have a smooth outer surface of the manus, true of the specimens studied herein. She also reported the presence of a few oblong tubercles on the outer surface of the manus in *C. porterensis* (Rathbun, 1926); the tubercles were not observed in this study. The inflated projection reported by Rathbun (1926) on the distal margin was serrated; in the specimens described herein the projection is not serrated.

Specimen CM 39654 is provisionally assigned to *Callianassa* cf. *C. porterensis.* CM 39654 possesses a movable finger, while the material assigned by Rathbun (1926) to *C. porterensis* does not, and Rathbun's (1926) material possesses the fixed finger while CM 39654 does not, making direct comparisons between the new specimen and Rathbun's material difficult. However, the manus of CM 39654 and specimens referred to *C. porterensis* are similarly shaped and both possess a shallow indentation in the distal margin just above the position of the fixed finger. Both possess a serrated lower margin of the manus. Because of the presence of the serrated lower margin in both CM 39654 and specimens referred by Rathbun (1926) to *C. porterensis*, which is a unique character among the thalassinoid specimens from the Pysht Formation, CM 39654 is provisionally assigned to *Callianassa* cf. *C. porterensis*. The description of *C. porterensis* will need to be broadened if it becomes clear that the specimens described here may all be assigned confidently to *C. porterensis*.

Characters of CM 39654, the most complete specimen referred to *Callianassa* cf. *C. porterensis*, may be compared with characters for species of several recent genera. Species of the genus *Callichirus* Stimpson are characterized by a strongly curved tip on the movable finger, but the carpus is much longer than the manus, a condition not seen in CM 39654. Species of the genus *Neocallichirus* Sakai possess a highly curved tip of the movable finger, but the carpus is narrower proportionally than that of CM 39654. Species of *Callianassa* Leach sensu stricto possess a highly curved movable finger, but the merus has a prominent spine which is not observable in CM 39654 due to the incomplete preservation of the merus. Species of the genus *Neotrypaea* have a very similar movable finger to CM 39654, but the manus of species of *Neotrypaea* is too short compared to the finger and to the carpus to accommodate CM 39654. Species of *Notiax* Manning and Felder have a movable finger, manus, and carpus that could be comparable to the new material, but species of *Notiax* possess a meral spine not observable in CM 39654. Consequently, characters of CM 39654 cannot permit tentative referral of *C.* cf. *C. porterensis* sensu lato to a known genus.

Callianassa sensu lato species 1
(Fig. 3D)

Diagnosis.—Callianassid with large, sharp, spinelike tooth on the fixed finger of the manus of the first pereiopod.

Description.—Manus about twice as long as high (H/L = 0.49), rectangular; inner surface smooth, weakly convex, flattening near base of fixed finger; proximal margin nearly straight, upper and lower margins parallel and straight; distal margin nearly straight, longitudinal inflated region paralleling distal margin.

Fixed finger weakly rimmed on lower margin, length of finger 0.32 total manus length, stout proximally and narrowing distally; inner surface with ridge extending from base to approximately two-thirds length of finger, ridge terminating rather abruptly, ridge projecting obliquely downward at about 120° angle from distal margin of manus; tip curving into small hook, finger bearing stout, sharp, triangular tooth about one-third distance from distal margin of manus.

Measurements.—All measurements are in millimeters. L (maximum of manus) = 18.2; H (maximum of manus) = 9.0; L (maximum of inner surface of fixed finger) = 5.9.

Referred Specimens.—The sole specimen, CM 39660, is deposited in the Carnegie Museum of Natural History.

Locality and Stratigraphic Position.—The specimen was collected in a concretion as float from RB36.

Remarks.—The specimen consists only of the inner surface of the manus and fixed finger of a cheliped; it is uncertain as to whether the cheliped is major or minor. The overall rectangular shape of the chela and the relatively short fixed finger indicate that it is more likely that the chela is a major claw rather than a minor one. This specimen is unlike any other previously described callianassid or ctenochelid from the Pacific Northwest, and no known extant genera possess a large, sharp tooth on the fixed finger such as is present in *Callianassa* sensu lato sp. 1. Some extant thalassinoid genera do possess a tooth or spine on the fixed finger, but none can be compared positively with *Callianassa* sensu lato sp. 1. The male of *Callianopsis* possesses a blunt tooth about midway along the fixed finger of the major chela, but the tooth on *Callianassa* sensu lato sp. 1 is positioned nearer the base of the finger and is much sharper and more toothlike. The major chela of the female *Callianopsis* possesses a sharp, triangular tooth at the base of the fixed finger, but the tooth is smaller and is not positioned as far along the fixed finger as the tooth in *Callianassa* sensu lato sp. 1. The minor chela of the male *Callianopsis* possesses a sharp, toothlike projection positioned near the base of the finger, but the hand and fingers of the minor chela of *Callianopsis* are of a different nature than those of *Callianassa* sensu lato sp. 1. The minor chela of *Callianopsis* tends to be more equidimensional and the fixed finger is much longer than the finger on the specimen under study. Specimens referred to the genus *Dawsonius* Manning and Felder possess a tooth on the fixed finger of the major chela, but the tooth is blunt and positioned just distally of the midlength of the finger (Manning and Felder, 1991). Specimens referred to the genus *Paracalliax* de Saint Laurent possesses a blunt tooth on the fixed finger of the minor chela, but the tooth is much smaller and less sharp than that of *Callianassa* sensu lato sp. 1 and the finger is much longer in specimens referred to *Paracalliax* (de Saint Laurent and Le Loeuff, 1979). Confident generic placement of the sole specimen of *Callianassa* sensu lato sp. 1 awaits the discovery of better material because only one specimen with this form was recovered from Pysht deposits, and there are no others like it, as far as is known, from Twin River Group deposits.

Family Ctenochelidae Manning and Felder, 1991
Subfamily Callianopsinae de Saint Laurent, 1973
Genus *Callianopsis* de Saint Laurent, 1973
Callianopsis clallamensis (Withers, 1924)

Callianassa clallamensis Withers, 1924:122; Rathbun, 1926:114; Berglund and Goedert, 1992:2–3.
Callianassa twinensis Rathbun, 1926:115; Berglund and Goedert, 1992:2–3.
Callianopsis clallamensis Hopkins and Feldmann, 1997.

Referred Specimens.—Several specimens are deposited in the Carnegie Museum of Natural History under the number CM 39691.

Localities and Stratigraphic Position.—Specimens referrable to this species were collected from RB18, RB19, and RB38. Most specimens were collected from RB18.

Remarks.—Hopkins and Feldmann (1997) referred both *Callianassa clallamensis* Withers and *Callianassa twinensis* Rathbun to the genus *Callianopsis* de Saint Laurent and synonymized the two species, with *Callianopsis twinensis* (Rathbun) being the junior synonym. Individuals originally referrable to *C. clallamensis* are males while those originally referrable to *C. twinensis* are females (Hopkins and Feldmann, 1997). Over 90 specimens referrable to this species have been collected from the Pysht Formation, and they are by far the most abundant of any of the decapods of the Pysht Formation.

Infraorder Brachyura Latreille, 1803
Section Heterotremata Guinot, 1977
Superfamily Calappoidea de Haan, 1833
Family Calappidae de Haan, 1833
Subfamily Calappinae de Haan, 1833
Genus *Mursia* Desmarest, 1823

Type Species.—*Mursia cristiata* H. Milne Edwards, 1837.

Diagnosis.—Calappid with transversely ovoid outline, strong lateral spines, and usually with rows of tubercles arranged on longitudinal ridges on the dorsal carapace. Chelae with row of small denticles on upper margin; merus of chelipeds sometimes possessing pronounced spine.

Description.—See Rathbun, 1937.

Remarks.—In addition to the characters commonly listed as diagnostic of the genus *Mursia*, almost every species possesses rows or ridges of tubercles, usually one medial and two or three on each branchial region. In the absence of rows of tubercles, the entire dorsal carapace surface may be coarsely granular as in *Mursia mcdowelli* Manning and Chace.

All species named on the basis of dorsal carapace morphology, except *Mursia obscura* Rathbun, possess lateral spines. Because of the absence of lateral spines and its narrow carapace, *M. obscura* was reassigned to *Paramursia* Karasawa by Karasawa (1991:14). The length of the lateral spines varies among authentic species of the genus *Mursia*, ranging from about half the total carapace width in *Mursia marcusana* Rathbun, to short denticles such as those of *Mursia microspina* Davie and Short. Lateral spine length may also vary among individuals within a species. For example, *Mursia armata* de Haan may possess lateral spines half as long as the total carapace width (Sakai, 1976); however, some specimens examined in the United States National Museum of Natural History (USNM 63715) possessed much shorter lateral spines.

Rathbun (1937:215) described the meri of the major chelipeds of *Mursia* as possessing a "distal ridge with one or more spines." The length of these meral spines appears to be highly variable within the genus. They are much reduced in *M. hawaiiensis* Rathbun, *M. microspina*, *M. flamma* Galil, *M. danigoi* Galil, *M. aspera* Alcock, and *M. armata*. In *M. africana* Galil, *M. musorstomia* Galil, *M. australiensis* Campbell, *M. curtispina* Miers, and *M. trispinosa* Parisi, they are intermediate in size. *Mursia spinimanus* Rathbun displays a prominent meral spine. There may be a weak correlation between lateral spine length and meral spine length, with those species possessing long lateral spines having somewhat longer meral spines.

Several genera are similar in dorsal carapace morphology to *Mursia*. The genus *Cycloes* de Haan possesses an overall narrower carapace than *Mursia* and shorter lateral spines than *Mursia*. In *Cycloes*, the lateral spines are directed posterolaterally while in *Mursia* those spines are directed laterally. Members of the genus *Cycloes* lack coarse carapace ornamentation which distinguishes them from species of *Mursia*. The genus *Paramursia* Karasawa was erected for fossil specimens possessing a round carapace with very short lateral spines which cannot be accommodated in *Mursia* (Karasawa, 1989). The genus *Acanthocarpus* Stimpson possesses a nearly equidimensional, ovate carapace while *Mursia* is transversely ovoid. In *Acanthocarpus*, the anterolateral and posterolateral margins are continuous while in members of the genus *Mursia*, the carapace possesses a convexly rounded anterolateral margin and a straighter, constricted, narrowing posterolateral margin. *Acanthocarpus* lacks strong ridges of tubercles on the dorsal carapace, which is characteristic of *Mursia*. Finally, the strong spine of *Acanthocarpus* is placed on the posterolateral margin and is directed posterolaterally while in *Mursia* the spine is positioned and directed laterally from the carapace. The genus *Platymera* H. Milne Edwards differs from *Mursia* in several aspects of the carapace and appendages, including possession of fine granules on the carapace instead of coarse granules as in *Mursia* (Galil, 1993:373). The genus *Platymera* had been synonymized with *Mursia* by many authors but was reinstated by Galil (1993).

The specimens described herein exhibit a suite of characters diagnostic of species of the genus *Mursia* including ridges with rows of tubercles; well-developed, lateral spines directed laterally; and a transversely ovoid carapace. They also possess a strong meral spine on the chelipeds, which has not been noted as characteristic of the genus *Mursia*. Therefore, the specimens herein described may be placed in the genus *Mursia*, and the diagnosis for the genus is therefore broadened to accommodate the strong meral spines of the specimens.

Mursia marcusana Rathbun, 1926
(Fig. 4, 5)

Mursia marcusana Rathbun, 1926:82; Feldmann et al., 1991:356.

Diagnosis.—Calappid with transversely ovoid outline, extremely long lateral spines, sinuous posterolateral margins, and five strong dorsal carapace ridges ornamented with tubercles in addition to two rows of tubercles not placed on ridges. Major cheliped with pronounced meral spine.

Emendation to Description.—Carapace transversely ovoid; vaulted longitudinally and laterally; maximum carapace width at position of long lateral spine at midlength, spines occupying about 55% maximum carapace width including spines; front narrow (frontal width/maximum carapace width without lateral spines = 0.10), downturned, sulcate, finely granular, projecting short distance beyond orbits; orbits large, subelliptical, closely spaced, rimmed on upper surface, bearing short fissure centrally on upper margin, bearing subtle outer orbital projection, orbital rim protruding slightly at inner orbital corner, fronto-orbital margin occupying 55% maximum carapace width excluding lateral spines; anterolateral margin convex, rounded, bearing rim of small rounded denticles; posterolateral margin somewhat sinuous and slightly concave; posterior margin narrow, approximately 20% maximum carapace width excluding lateral spines, bearing small blunt tooth on each corner.

Carapace ornamented with tubercles and tuberculate ridges; mesogastric, urogastric, and cardiac regions situated on medial ridge; mesogastric region narrow anteriorly and widening posteriorly, pair of small tubercles near middle, one large tubercle near posterior margin; urogastric region narrow, as wide as mesogastric region; cardiac region long, sinuous lateral margins, bearing three axial tubercles with posteriormost being smallest; all three medial regions inflated, bounded by distinct grooves.

Protogastric region bearing numerous small tubercles, delimited by shallow cervical groove on distal margin but demarcation between mesogastric region and protogastric region indistinct. Cervical groove curving convexly from anterolateral margin, outlining lateral and posterior margin of mesogastric region. Branchial region bearing row of three tubercles not situated on ridge, row closely paralleling anterolateral margin, most distal tubercle in row smallest, situated close to middle tubercle of row; branchial region bearing two major ridges with tubercles; first ridge paralleling anterolateral margin, extending from base of protogastric region, terminating at base of lateral spine, bearing about five tubercles; second extending obliquely from posterolateral margin to protogastric region, bearing about five tubercles of unequal size; ridge bifurcating about midway along second ridge, short bifurcating ridge extending obliquely towards front and bearing about two tubercles. Rounded tubercle present on either side of urogastric region; row of tiny tubercles paralleling groove outlining urogastric region and proximal portion of cardiac region; surfaces of the carapace between ridges finely granular.

Sternites finely granular; sternite 1 unknown; sternites 2, 3, and 4 fused; sternite 3 narrow with

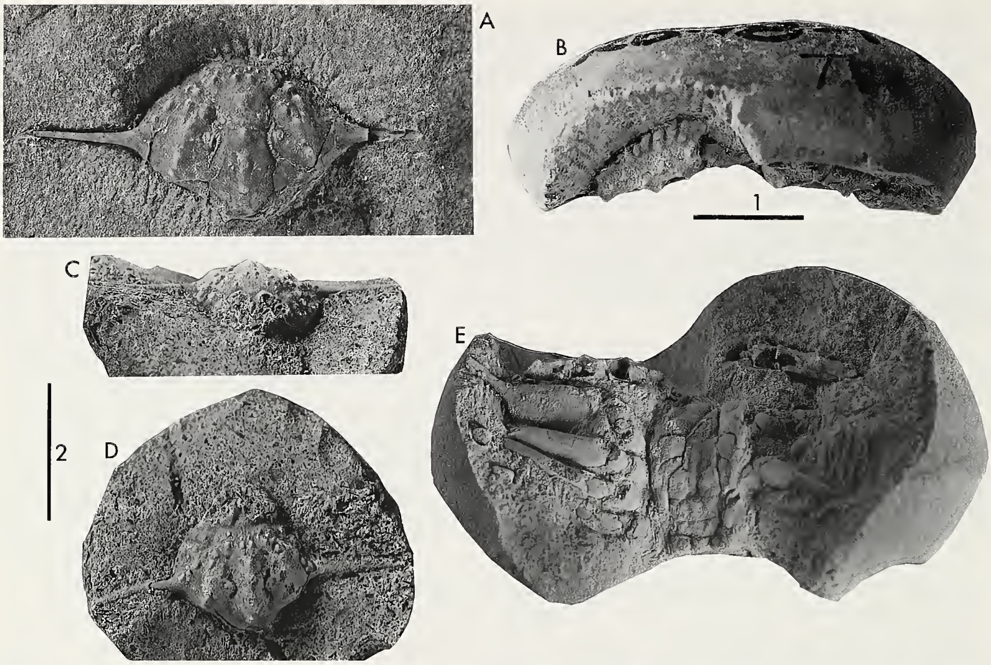

Fig. 4.—*Mursia marcusana* Rathbun. A. Dorsal view of nearly complete carapace, CM 39663. B. Lateral view of outer surface of major chela, CM 39665. C. Anterior view of nearly complete carapace, CM 39661. D. Dorsal view, CM 39661. E. Ventral view showing meral spine at upper left, CM 39665. Scale bar 1 for A, B, and E. Scale bar 2 for C and D. Scale bars = 1 cm.

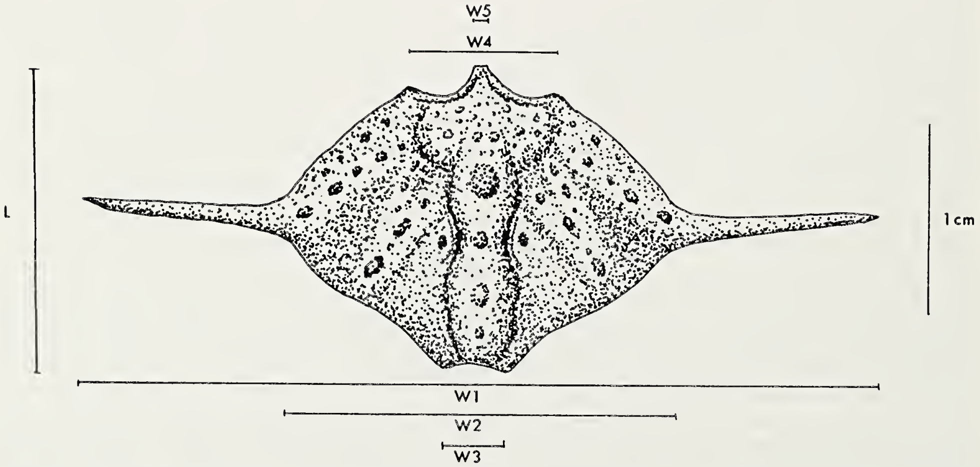

Fig. 5.—Reconstruction of *Mursia marcusana* Rathbun showing the position and orientation of measurements made.

small distal hook, directed anterolaterally; sternite 4 narrow, directed anterolaterally, long narrow distal hook; sternite 5 longest, directed laterally, distal hook long and narrow; sternite 6 directed posterolaterally, narrow, very long, stout distal hook; sternites 7 and 8 unknown. Abdomen slightly more than half as wide as sternum; telson isosceles triangular in shape; sixth somite as long as broad, slightly wider than telson and slightly shorter; fifth somite about two-thirds as long as sixth but about half again as wide; somites 1–4 becoming progressively shorter but maintaining same width.

Coxae of pereiopods 1–4 cylindrical, about as long as wide, about same size; ischia and bases of pereiopods 2–4 fused, slightly longer than wide; meri of pereiopods 2 and 3 much longer than wide, appearing to be flattened oval in cross section, margins not well known.

Carpus of major cheliped unknown; merus of major cheliped longer than high, margin articulating with ischium sinuous, bearing long spine on margin articulating with carpus, spine broken but appearing to be at least half as long as merus measured without meral spine. Major and minor chelae subequal, wide distally and narrowing proximally, bearing tuberculate crest on upper margin, lower margin with three to four small spines; outer surface of manus ornamented with numerous tubercles; fixed finger not known; movable finger short, stout, lower margin ornamented with three or four stout tubercles.

Measurements.—All measurements are in millimeters. CM 39663, W1 (maximum, including lateral spines) = 42.6, W2 (maximum, excluding lateral spines) = 19.4, W3 (posterior) = 3.6, L (maximum) = 15.8. CM 39661, W1 (maximum, including lateral spines) = 23.1, W2 (maximum, excluding lateral spines) = 10.0, W3 (posterior) = 2.6, W4 (fronto-orbital) = 5.5, W5 (frontal) = 1.0, L (maximum) = 9.8. CM39665, W (maximum of sternum) = 9.3, W (maximum width of sixth somite) = 3.6, L (maximum of sixth somite) = 3.6, W (maximum of fifth somite) = 5.1, L (maximum of fifth somite) = 2.4, L (maximum of abdomen) = 14.0, L (maximum of telson) = 3.9, W (maximum of telson) = 3.0. Merus of third pereiopod, L = 9.0. Merus of fourth pereiopod, L = 8.6. Major cheliped, L (merus) = 8.5, L (meral spine) > 4.3, L (maximum of manus) = 13.4, L (dactylus) = 5.1. Minor cheliped, L (maximum of manus) > 11.3. CM 39662, W (maximum excluding lateral spines) = 21.8 (based on half measures), L (maximum) > 15.8. Position and orientation of dorsal carapace measurements illustrated in Figure 5.

Referred Specimens.—Six specimens referred to this species, CM 39661–39666, are deposited in the Carnegie Museum of Natural History.

Localities and Stratigraphic Position.—CM 39662 was collected at site RB37 in thin-bedded siltstone. CM 39663 and CM 39664 were collected as float in concretions at RB38, and CM 39661 was collected as float in a concretion from RB36. CM 39665 and 39666 were collected as float in concretions from RB18.

Remarks.—Specimen CM 39663 possesses a dorsal carapace that is preserved mainly as a mold of the interior. The counterpart of this specimen retains some of the integument. Specimen CM 39661 consists of a dorsal carapace only and has remarkably well-preserved orbits and lateral spines. CM 39662 is a flattened dorsal carapace collected in a block of thin-bedded siltstone associated with large quantities of organic matter including molluscs, other decapods, and plant material. CM 39665 possesses a well-preserved venter including part of the abdomen and sternum, chelipeds, and other pereiopods. CM 39666 possesses part of the abdomen and sternum only, and CM 39664 possesses a fragment of the dorsal carapace.

The specimens are referrable to *Mursia marcusana* for several reasons. Although the specimen described by Rathbun (1926) is broken, ridges and arrangement of dorsal carapace tubercles can be observed, and the new material closely resembles the type material in these respects. Also, Rathbun (1926) reported that her specimens possessed a "strong lateral spine broken off at the base" (p. 82) as well as five well-developed ridges with strong tubercles, all of which the specimens referred to *M. marcusana* possess. The discovery of the material under study, preserving intact lateral spines, complete dorsal carapaces, a well-preserved venter, and chelae allows for a much more complete description of the species.

Specimens possessing only the ventral aspect are confidently referred to *Mursia marcusana* for several reasons. The venter and the chelipeds are typical of mursiids, both recent and fossil. *Mursia marcusana* is the only calappid and only mursiid recovered as yet from the Pysht Formation, and it seems unlikely that the venters would belong to a previously undescribed calappid from the Pysht Formation. Finally, the presence of extremely long lateral spines on the carapace and pronounced meral spines in the same animal is likely since the spines could be adapted for similar or identical functions.

In respect to the long meral spines, the specimens resemble species of the genus *Acanthocarpus*, which possess very pronounced meral spines. However, the material here assigned to *Mursia marcusana* differs from species of *Acanthocarpus* in several important aspects as has been discussed. Because the specimen possessing the venter and chelae is referrable to *M. marcusana*, the diagnosis for the genus *Mursia* must be broadened to accommodate the long meral spines.

This material from the Pysht Formation extends the geographic range of *Mursia marcusana* as reported by Rathbun (1926). She reported specimens from Bainbridge Island, Washington, from the upper Oligocene Blakely Formation and from Alki Point on Puget Sound, near Seattle, in upper Oligocene rocks. Feldmann et al. (1991) figured this species from the Pysht Formation of Washington but did not discuss it. Other species of *Mursia* have previously been reported from Oligocene rocks, including *M. yaquinensis* Rathbun of Oregon and *M. mcdonaldi* Rathbun of Panama.

Mursia marcusana can be distinguished from all other species of *Mursia* because of its extremely long lateral spines, long meral spines, and unique arrangement of tubercles on strong ridges. The species most similar to *M. marcusana* are *M. takahashii* Imaizumi from the Pliocene of Japan and *M. minuta* Karasawa from the Miocene of Japan. *Mursia takahashii* has shorter lateral spines and less pronounced tubercle-bearing ridges than *Mursia marcusana*. The arrangement of tubercles on *M. takahashii* is different because the most axially placed branchial ridge of tubercles of *M. takahashii* does not appear to bifurcate as seen in *M. marcusana*. The posterolateral margins of *M. takahashii* are relatively straight while those of *M. marcusana* are sinuous. Finally, the posterolateral margins of *M. marcusana* are much more constricted than those of *M. takahashii*.

Mursia marcusana can be distinguished from *M. minuta* Karasawa because *M. minuta* has a much more convex anterolateral margin, and the arrangement of carapace ridges is somewhat different in *M. minuta* because it does not possess a bifurcating ridge. The cardiac region of *M. minuta* possesses only two axial tubercles while *M. marcusana* possesses three on that region.

Among extant mursiids, *Mursia armata* most closely resembles *M. marcusana*. Both species possess long lateral spines, a convexly rounded anterolateral margin, highly constricted posterolateral margins, and short posterior margins with small denticles on each corner. The two species differ in several important ways, however. *Mursia armata* possesses seven ridges with tubercles while *M. marcusana* possesses five ridges of tubercles and two rows of tubercles not positioned on ridges. *Mursia armata* also lacks the numerous small tubercles on the protogastric

Table 3.—*Known species of* Mursia, *collecting locale, age, and depth at which specimens were collected.*

Taxon	Locality	Age	Depth (m)
M. africana Galil	East Africa	Recent	250–290
M. australiensis Campbell	West Pacific	Recent	40–320
M. danigoi Galil	Phillipines	Recent	143–204
M. flamma Galil	South Africa	Recent	35–510
M. musorstomia Galil	New Caledonia	Recent	420–575
M. cristimanus de Haan	South Atlantic	Recent	unknown
M. cristiata H. Milne Edwards	Indian Ocean	Recent	70–318
M. armata de Haan	Japan	Recent	50–150
M. spinimanus, Rathbun	Hawaii	Recent	95–435
M. bicristimana Alcock and Anderson	Indian Ocean	Recent	217–397
M. curtispina Miers	Japan	Recent	30–150
M. mcdowelli Manning and Chace	Ascension Island	Recent	122–152
M. hawaiiensis Rathbun	Hawaii	Recent	97–730
M. trispinosa Parisi	Japan	Recent	65–120
M. aspera Alcock	Japan	Recent	65–150
M. microspina Davie and Short	Australia	Recent	210
M. minuta Karasawa	Japan	early Pliocene	—
M. lienharti (Bachmayer)	Central Europe	Miocene	—
M. takahashii Imaizumi	Japan	Miocene	—
Mursia sp. Karasawa	Japan	mid-Miocene	—
Mursia sp. Förster	Poland	mid-Miocene	—
M. mcdonaldi Rathbun	Panama	Oligocene	—
M. yaquinensis Rathbun	Northwest United States	Oligocene	—
M. marcusana Rathbun	Northwest United States	Oligocene	—

region seen in *M. marcusana*, and the lateral spine of *M. armata* is shorter and more stout. Finally, *M. armata* lacks the strong meral spine seen in *M. marcusana*.

Species referred to *Mursia* are widely distributed geographically and inhabit a wide range of depths (Table 3). For example, *M. armata* has been reported from depths of 25–150 m, while *M. hawaiiensis* has been reported from 97–730 m in waters off Japan (Rathbun, 1893). Five species from Japan were collected from soft muddy or sandy bottoms at outer sublittoral depths (Sakai, 1976). *Mursia takahashii* was reported by Imaizumi (1952) to have been collected from the lower to middle Miocene Natori Group, which is characterized by fossils representing a warm-water fauna. Karasawa (1993) listed the Japanese *Carcinoplax prisca–M. minuta* assemblage as having inhabited a subtropical climate of the late Miocene and early Pliocene. Recent species are distributed from tropical to temperate climates, and those that are found in tropical climates inhabit deeper waters than those found in more temperate climates.

Superfamily Corystoidea Samouelle, 1819
Family Atelecyclidae Ortmann, 1893
Genus *Trichopeltarion* A. Milne Edwards, 1880

Type Species.—Trichopeltarion nobile A. Milne Edwards, 1880.

Remarks.—Many authors have discussed the fact that *Trichopeltarion* A. Milne Edwards and *Trachycarcinus* Faxon are closely related, if not indistinguishable from one another. The three most obvious similarities are the possession of numerous marginal spines, a tridentate rostrum, and a carapace ornamented with numerous tubercles. Most keys to the two genera fail to satisfactorily distinguish the two genera. For example, in his key to the Atelecyclidae, Sakai (1976) characterized *Trichopeltarion* as possessing an oval outline, tuberculate dorsal carapace, tridentate front, and toothed lateral margins (p. 311). *Trachycarcinus* was characterized as having the same characters except with a subpentagonal outline (Sakai, 1976:311), and many authors have argued that this similarity in characteristics makes the distinction between the two genera rather arbitrary (Dell, 1969; Guinot, 1986, 1989). Alcock and Anderson (1899) remarked that the separation of the two was "doubtful" (p. 10). Rathbun (1930) expressed doubt on the validity of the two genera by stating, "If the three genera *Peltarion*, *Trichopeltarion*, and *Trachycarcinus* be retained. . ." (p. 165). She described *Trichopeltarion* as possessing a subcircular carapace, spinose borders, and a tridentate front, among several other characters (Rathbun, 1930:168). She characterized *Trachycarcinus* as having a pentagonal carapace, toothed anterolateral margins, and a tridentate front, among several other characters (p. 164). Dell (1969) wrote that he, "preferred to unite *Trachycarcinus* with *Trichopeltarion*," because he believed that differences in tuberculation of the dorsal carapace were "differences of degree" and also that the use of length of the lateral spines to distinguish the two genera was arbitrary (p. 370). Guinot (1986, 1989) noted these concerns but did not offer a satisfactory solution to the problem of distinguishing the two genera. Although the specimens described herein conform well to the diagnosis for the genus *Trachycarcinus*, the overall difficulty associated with distinguishing *Trichopeltarion* and *Trachycarcinus* prompts us to follow Dell's (1969) suggestion to synonymize the two genera and to refer the new specimens to *Trichopeltarion*. All species that have been previously referred to *Trachycarcinus* are hereafter referred to the genus *Trichopeltarion*. A systematic revision of the genus *Trichopeltarion* and the family Atelecyclidae which will address the *Trichopeltarion–Trachycarcinus* problem in detail is in progress (Salva, personal communication).

Trichopeltarion berglundorum, **new species**
(Fig. 6, 7)

Trachycarcinus sp. Feldmann et al., 1991:356; Berglund and Goedert, 1992:3.

Diagnosis.—Atelecyclid with 15 simple carapace spines, oval to subpentagonal outline, well-developed carapace regions, and large granular tubercles.

Description.—Carapace oval to subpentagonal, slightly longer than wide, moderately vaulted both transversely and longitudinally, rather coarsely punctate in advance of cervical groove, finely punctate posteriorly; tumid carapace regions moderately well defined by grooves; carapace margin bearing 15 narrow triangular spines.

Fronto-orbital margin measured from tips of postorbital spines about 62% total carapace width measured between tips of posteriormost set of spines; anterolateral margin convex, long. Front moderately produced beyond orbits, bearing three spines, central spine stoutest. Orbits bounded by pre- and postorbital spines with intercalated spine; pre-orbital spine triangular, directed forward; intercalated spine narrow, sharp, directed anterolaterally; postorbital spine longest, directed anterolaterally. Anterolateral margin with three spines not including postorbital spine, first and third longest, narrow; second smaller, broadly triangular; all three directed laterally. Posterolateral margin convex; posterior margin not well known but appearing to be narrow.

Grooves moderately deep; cervical groove curving slightly posteriorly from just behind first anterolateral spine, continuing across carapace to medial region, then abruptly curving posteriorly, crossing medial region between mesogastric and urogastric regions; weak groove separating protogastric and hepatic region extends from between intercalated and postorbital spine to cervical groove; axial regions bounded by deep grooves.

Frontal region flattened with central shallow sulcus terminating at base of central rostral spine;

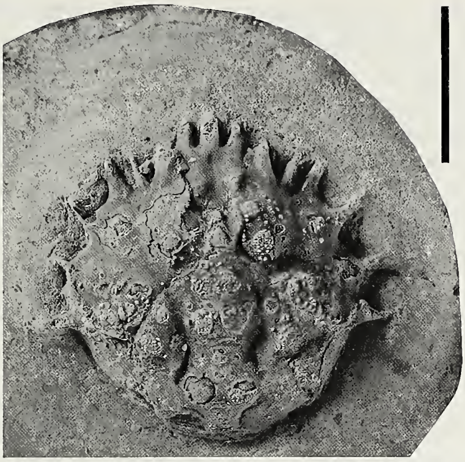

Fig. 6.—*Trichopeltarion berglundorum.* Dorsal view of holotype, CM 39667. Scale bar = 1 cm.

mesogastric region triangular, slightly granular, large tubercle situated anteriorly, granular bilobed swelling posteriorly; protogastric region granular, small, smooth tubercle near front on either side of medial sulcus, two large granular tubercles along axial margin; hepatic region small, triangular, granular, bearing one large granular tubercle; branchial region large, not subdivided, bearing numerous granules and four large granular tubercles, region elevated anteriorly, elevated region bearing large granular tubercles; urogastric region narrow, bearing pair of large granular tubercles; cardiac region pentagonal in shape, apex of pentagon directed posteriorly, bearing four granular tubercles arranged in diamond pattern with middle two tubercles largest; intestinal region obscure.

Venter and appendages unknown.

Measurements.—All measurements are in millimeters. CM 39667, carapace,

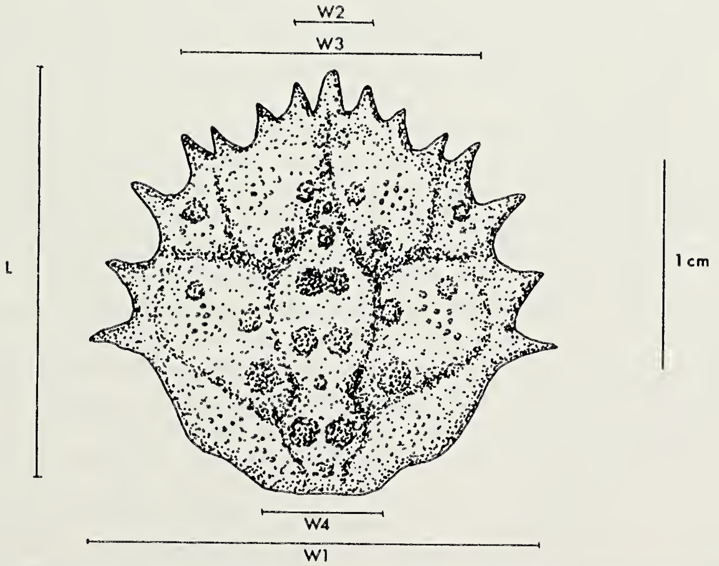

Fig. 7.—Reconstruction of *Trichopeltarion berglundorum* showing the position and orientation of measurements made.

W1 (maximum) = 22.1, L (maximum) = 21.0, W2 (frontal) = 7.0, W3 (fronto-orbital) = 13.8, W4 (posterior) = 5.8. CM 39668, carapace, W1 (maximum) > 13.9, L (maximum) = 15.1. Position and orientation of dorsal carapace measurements illustrated in Figure 7.

Types.—The holotype, CM 39667, and a paratype, CM 39668, are deposited in the Carnegie Museum of Natural History.

Localities and Stratigraphic Position.—CM 39667 was collected in a concretion as float at RB18 and CM 39668 was collected in a concretion as float at RB15.

Etymology.—The trivial name honors Ross and Marion Berglund of Bainbridge Island, Washington, who donated much of the material forming the basis of this study and whose contributions to the study of Tertiary decapods from the Pacific Northwest have been invaluable.

Remarks.—The two specimens referred to this new species were preserved in concretions. Both retain original carapace material with CM 39667 exhibiting a complete carapace and CM 39668 a broken carapace. The counterparts for each are not known.

Trichopeltarion berglundorum differs from *T. nobile*, *T. fantasticum* Richardson and Dell, *T. wardi* Dell, and *T. greggi* Dell in its possession of simple, small marginal spines as opposed to the complex spines of all of these species. The new species most closely resembles *T. huziokai* Imaizumi from the Miocene of Japan. Both species possess a rounded to subpentagonal carapace outline, similar spine shape and arrangement, and a similar arrangement of carapace regions. However, *T. huziokai* bears numerous prominent tubercles on the carapace while *T. berglundorum* bears small tubercles on some regions. *Trichopeltarion berglundorum* bears large granular tubercles on several regions which are absent in *T. huziokai*. *Trichopeltarion huziokai* Imaizumi bears numerous tubercles on the branchial region while *T. berglundorum* bears few if any on that region. The medial regions on *T. huziokai* are better differentiated than on *T. berglundorum*. *Trichopeltarion berglundorum* possesses better developed carapace spines, a less rounded carapace, and less inflated regions than does *T. inflatus* Kato. *Trichopeltarion berglundorum* differs from *T. decorus* Rathbun from the Miocene of Panama in several respects. *Trichopeltarion decorus* possesses very small carapace tubercles, carapace margins with numerous small spines, and slightly tumid carapace regions delimited by shallow grooves, while *T. berglundorum* has large granular carapace tubercles, large carapace spines, and tumid carapace regions.

Trichopeltarion berglundorum differs from nearly all recent species of *Trichopeltarion* in having a rounded to subpentagonal carapace instead of a pentagonal one. Many recent species including *T. foresti* Guinot, *T. glaucus* Alcock and Anderson, *T. balssi* Rathbun, *T. alcocki* Doflein, *T. crosnieri* Guinot, *T. sagamiensis* Rathbun, and *T. spinulifer* Rathbun, bear numerous intercalated spines between the larger anterolateral spines and some have spines which are themselves armed with small denticles; *Trichopeltarion berglundorum* exhibits neither condition. Several recent species have more ornamented carapaces and a more produced front than *T. berglundorum* including *T. foresti*, *T. glaucus*, *T. delli* Guinot, *T. crosnieri*, and *T. corallinus*. *Trichopeltarion berglundorum* is similar to many recent species of *Trichopeltarion* in possessing simple carapace spines and in the arrangement of large granular carapace tubercles, including *T. moosai* Guinot, *T. corallinus*, *T. hystricosus* Garth, *T. elegans* Guinot and Sakai, *T. delli*, and *T. intesi* Crosnier. *Trichopeltarion berglundorum* can be distinguished from *T. delli*

Table 4.—*All known species of* Trichopeltarion *and the collecting locale, age, and depth at which specimens were collected.*

Taxon	Geographic range	Age	Depth (m)
T. nobile Milne Edwards	Caribbean	Recent	150–400
T. fantasticum Dell and Richardson	New Zealand	Recent	180–730
T. wardi Dell	Southwest Pacific	Recent	80–140
T. hystricosus Garth	Southeast Pacific	Recent	200–1124
T. corallinus Faxon	Southeast Pacific	Recent	834–1280
T. crosnieri Guinot	Madagascar	Recent	480–700
T. spinulifer Rathbun	Gulf of Mexico	Recent	324–347
T. alcocki Doflein	Indo-Pacific	Recent	750–1650
T. ovalis (Anderson)	Indo-Pacific	Recent	100–397
T. moosai Guinot	Indo-Pacific	Recent	313
T. foresti Guinot	Indo-Pacific	Recent	395–450
T. delli Guinot	Indo-Pacific	Recent	425–595
T. balssi Rathbun	Japan	Recent	50–200
T. sagamiensis Rathbun	Japan	Recent	85–200
T. elegans Guinot and Sakai	Japan	Recent	100–150
T. intesi Crosnier	Ivory Coast	Recent	600
T. glaucus Alcock and Anderson	Indian Ocean	Recent	780
T. huziokai Imaizumi	Japan	Miocene	—
T. decorus Rathbun	Fiji	Miocene	—
Trachycarcinus berglundorum n. sp.	Northwest Washington USA	late Olig.–early Miocene	—
T. inflatus Kato	Japan	Miocene	—
T. greggi Dell	New Zealand	late Miocene	—

and *T. moosai* because it has a more oval outline and shorter spines. *Trichopeltarion berglundorum* does not possess fine perliform granules over the entire carapace as does *T. intesi*. *Trichopeltarion berglundorum* has a more circular carapace than does *T. hystricosus* and the spines of *T. berglundorum* are much less developed and produced than those of *T. hystricosus*. *Trichopeltarion elegans* has longer and more produced spines than does *T. berglundorum*. *Trichopeltarion corallinus* is much more distinctly pentagonal in shape than *T. berglundorum* and has somewhat different axial ornamentation than does *T. berglundorum*.

Trichopeltarion berglundorum, collected from the upper Oligocene to lower Miocene deposits of the Pysht Formation, represents one of the earliest known species of *Trichopeltarion*, suggesting a possible north Pacific origin. Several other fossil species are Miocene in age and include material from Fiji and Japan. *Trichopeltarion greggi* is known from the middle–late Miocene of New Zealand (Dell, 1969; Feldmann and Keyes, 1992). Recent species are known from the Caribbean Sea, the Gulf of Mexico, the Indo-Pacific and New Zealand (Table 4).

Most recent species of *Trichopeltarion* are found in very deep water (Table 4). Garth and Haig (1971) reported that specimens of *T. hystricosus* have several adaptations to deep water including eye size and pigmentation. A female specimen of *T. hystricosus* carried a small clutch of large eggs, while related species inhabiting shallower depths would be expected to have larger clutches of smaller eggs (Garth and Haig, 1971). Alcock and Anderson (1899) also reported that dredged females of the species *T. glaucus* carried a small number of large eggs. Garth and Haig (1971) speculated that this was an adaptation to deep water in which the larval stage would be abbreviated and there would be little exposure to pelagic dispersal. Recent species range widely in comparable depths (Table 4).

Karasawa (1993) inferred from the depths of recent species of *Trichopeltarion* found in Japan that *T. huziokai* must have inhabited the outer sublittoral to upper bathyal zones. His assertion was corroborated by the fact that living forms of *Carcinoplax* also inhabit deep waters, and a fossil species of *Carcinoplax* was found associated with specimens of *T. huziokai*. *Trichopeltarion glaucus* was reported by Alcock and Anderson (1899) in association with living and dead corals.

Superfamily Portunoidea Rafinesque, 1815
Family Portunidae Rafinesque, 1815
Subfamily Carcininae Macleay, 1838
Genus *Portunites* Bell, 1858

Type Species.—*Portunites incerta* Bell, 1858.

Remarks.—The specimens described here are conspecific with material Rathbun (1926) named *Portunites triangulum*. This species is retained in the genus *Portunites* at this time based on several criteria. According to Glaessner (1969), *Portunites* is defined as possessing a carapace that is not much broader than long, a front with four teeth, an anterolateral margin with three or four teeth excluding the outer-orbital spine, a posterolateral margin that is straight or slightly concave, well-marked gastrocardiac regions, an arcuate ridge extending from lateral tooth to medial area, and fifth pereiopods that are not flattened (p. R513). The specimens described in this study definitely possess all but one of these characters; the fifth pereiopods are unknown. The type species of *Portunites*, *Portunites incerta*, exhibits all of the characters noted by Glaessner, except that no fifth pereiopod was described for it. The only known species of *Portunites* to have been recovered with an intact fifth pereiopod, *P. alaskensis* Rathbun, has a paddlelike fifth pereiopod (Tucker and Feldmann, 1990) which contradicts Glaessner's (1969) diagnosis for the genus.

In addition to these criteria, the type species and *Portunites stintoni* Quayle, which was named based upon several paratypes of *P. incerta*, share several other characters. They possess a fronto-orbital margin that occupies two-thirds of the maximum carapace width and orbits with two fissures. Each possesses a longitudinal ridge on the branchial region extending from the posterior margin about three-quarters of the distance on the branchial region. Both species have a similar arrangement of anterolateral spines. The outer orbital spine is stout and directed forward and is similar in size to the third anterolateral spine. The second and fourth anterolateral spines are smaller than the first and third. The fifth anterolateral spine is the longest. The carapace shape of both *P. incerta* and *P. stintoni* is hexagonal. The cardiac regions of both species, especially *P. incerta*, are well defined, and, in *P. incerta* the cardiac region was reported to extend almost to the posterior margin. *Portunites incerta* possesses large stout chelipeds that are unequal in size (Quayle, 1984).

Specimens of *Portunites triangulum* differ from *P. incerta* and *P. stintoni* in several of these characters. They possesses a weak longitudinal branchial ridge that terminates in a strong tubercle; the ridge is not nearly as obvious as those on *P. incerta* or *P. stintoni*. *Portunites triangulum* possesses an anterolateral margin whose length is equal to one-half the maximum width of the carapace, not two-thirds of the width of the carapace. *Portunites triangulum* is almost half again as wide as long, while *P. incerta* and *P. stintoni* are less wide. The anterolateral teeth of *P. triangulum* become gradually larger laterally, with the fifth being the largest; this is different than the condition observed in either *P. incerta* or *P. stintoni*. The regions of *P. triangulum* are not as well defined, the overall carapace shape is less squarely hexagonal, and the chelipeds are narrower and longer than those of *P. incerta* or *P. stintoni*. However, these differences do not appear to be generic at this time and may constitute specific differences among species of *Portunites*. *Portunites triangulum* possesses all of the diagnostic characters for species of the genus and is therefore retained in it.

However, analysis of published plates of the Japanese fossil genera *Itoigawaia* and *Minohellenus* suggests that *P. triangulum* may be better accommodated in one of those two genera. Confirmation awaits examination of type material housed in Japan. Karasawa et al. (1992) erected the genus *Itoigawaia* for fossil material differing from *Portunites* in lacking a ridge separating the cephalic and branchial regions of the carapace. The type species of *Itoigawaia*, *I. minoensis*, was originally assigned to the genus *Portunites* and was later removed because of the lack of a transverse ridge (Karasawa et al., 1992). Examination of published plates of *Itoigawaia* shows that some specimens appear to have a very weakly developed ridge in the same position as that seen in species of *Portunites* (Karasawa et al., 1992; Karasawa, 1993). *Itoigawaia* possesses a length-to-width ratio, frontal margin, and carapace region configuration that could easily accommodate another taxon endemic to Japan, *Minohellenus*, which is superficially similar to *Portunites* and is quite similar to the genus *Itoigawaia*. The two genera, *Minohellenus* and *Itoigawaia*, possess similar carapace regions; a very weak tranverse ridge separating the cephalic and branchial regions; similar frontal, orbitofrontal, and anterolateral margins; and similar carapace size ratios. Both have chelae that appear to be fairly smooth with keels reported but not observable on the published plates of species of the two genera (Karasawa, 1990; Karasawa et al., 1992; Karasawa, 1993; Kato and Karasawa, 1994, 1996). The fifth lateral spine in *Itoigawaia* is the smallest, while in *Minohellenus*, the fifth anterolateral tooth is largest; this appears to be the only major difference between the two genera, and it is possible that they may be synonymous. The carapace of *Minohellenus* is more transversely ovoid than that of *P. triangulum* and the anterolateral margin is longer relative to the total length (*M. macrocheilus* = 0.62) than in *P. triangulum* (0.55–0.56). The abdomen of species of *Minohellenus* is strongly similar to that of *P. triangulum*; however, this may be a characteristic of the subfamily. *Portunites triangulum* is not referred to either genus at this time because it possesses fairly strong transverse ridges, chelae with a strong lateral keel, and strong tuberculate ornamentation on the branchial regions in the form of a triangle, none of which is possessed by species of either *Minohellenus* or *Itoigawaia* as far as can be discerned from published plates.

The sole species of the monospecific genus *Imaizumilia* Karasawa, *Imaizumila sexdentata* Karasawa, shares many similarities with species of *Portunites* including the presence of a ridge separating the cephalic and branchial regions and the arrangement of carapace regions and anterolateral spines. It differs from *Portunites* in possessing a wider carapace and a thin orbital margin (Karasawa, 1993). The genus *Imaizumila* possesses six frontal teeth, including the inner orbital teeth (Karasawa, 1993). This same arrangement occurs in many species of *Portunites*, except in *Imaizumila* the six teeth appear to be evenly spaced and well defined, while in species of *Portunites* the inner orbital teeth are smaller and closely spaced. Additionally, carapace regions in *Imaizumila* are much more clearly defined and inflated than those of most species of *Portunites*.

Other portunid genera possess characters similar to those of *Portunites* but are not easily confused with it. The monotypic genus *Pleolobites* was erected by Remy (1960) for specimens collected from Ivory Coast. *Pleolobites* can be immediately distinguished from *Portunites* because *Pleolobites* does not possess the transverse ridge separating the cephalic and branchial regions characteristic of *Portunites*. The genus *Pleolobites* is wider overall than *Portunites*, and the anterolateral spines appear to be more produced at the base and of an overall different shape than those of *Portunites*. Glaessner (1969) pointed out that *Pleolobites* resembles *Xanthilites*. However, examination of the type material would be necessary to confirm the reassignment *Pleolobites erinaceus* Remy.

The genus *Rhachiosoma* bears some resemblance to *Portunites*, but the two differ in several important aspects. *Rhachiosoma* has a more produced lateral spine that is situated posterior to the midpoint of the carapace; in *Portunites*, the spine is somewhat shorter and lies anterior to the midpoint of the carapace. Carapace regions on *Portunites* are somewhat better defined than on *Rhachiosoma*, and *Portunites* bears a ridge that separates the cephalic region from the branchial region; *Rhachiosoma* does not (Feldmann and Maxwell, 1990). One species of *Rhachiosoma* was originally assigned to *Portunites*, *Portunites granulifer* Glaessner. At that time, Glaessner (1960) felt that its closest relative might be *P. triangulum* but later removed it to the genus *Rhachiosoma*; Feldmann and Maxwell (1990) concurred and clarified the numerous differences between *R. granuliferum* and *P. triangulum*.

The species *Cancer araucana* Philippi was removed to *Portunites* by Glaessner (1960:33). Subsequently, Quayle (1984) reported that the species had too many characters that "fall beyond the characters shared by other described species of *Portunites* and it is doubtful if the species should be included in the genus" (p. 176). He based this conclusion on "*Portunites*" *araucana* having six instead of four frontal lobes, longer outer orbital spines, thin inner orbital spines, and an anterolateral margin with five spines, with the fourth and fifth equal in length. A specimen of "*Portunites*" *araucana* was examined by the authors at the United States National Museum of Natural History (USNM 496556), and it falls outside the diagnosis for the genus *Portunites* in several respects. The specimen possesses four frontal teeth, excluding the inner orbital spine, which is true of species of *Portunites*, and possesses four anterolateral spines, excluding the outer orbital spine, which is also characteristic of species of *Portunites*. However, in the specimen of "*P.*" *araucana* Philippi, the four frontal teeth and the inner orbital teeth are approximately the same size, while in species of *Portunites*, the inner orbital spines are smaller than the frontal teeth. The anterolateral teeth in "*P.*" *araucana* are stout at the base, broadly triangular, and are directed forward; anterolateral spine 4 is somewhat less stout but about as long as the other spines. In all *Portunites*, the last anterolateral spine is the longest and stoutest of all the spines, and anterolateral spines 1–3 are directed anterolaterally. The specimen of "*P.*" *araucana* is wider than long, and wider than species of *Portunites*. Finally, the dorsal carapace of the specimen of "*P.*" *araucana* is highly vaulted, especially posteriorly, which is not seen in species of *Portunites*.

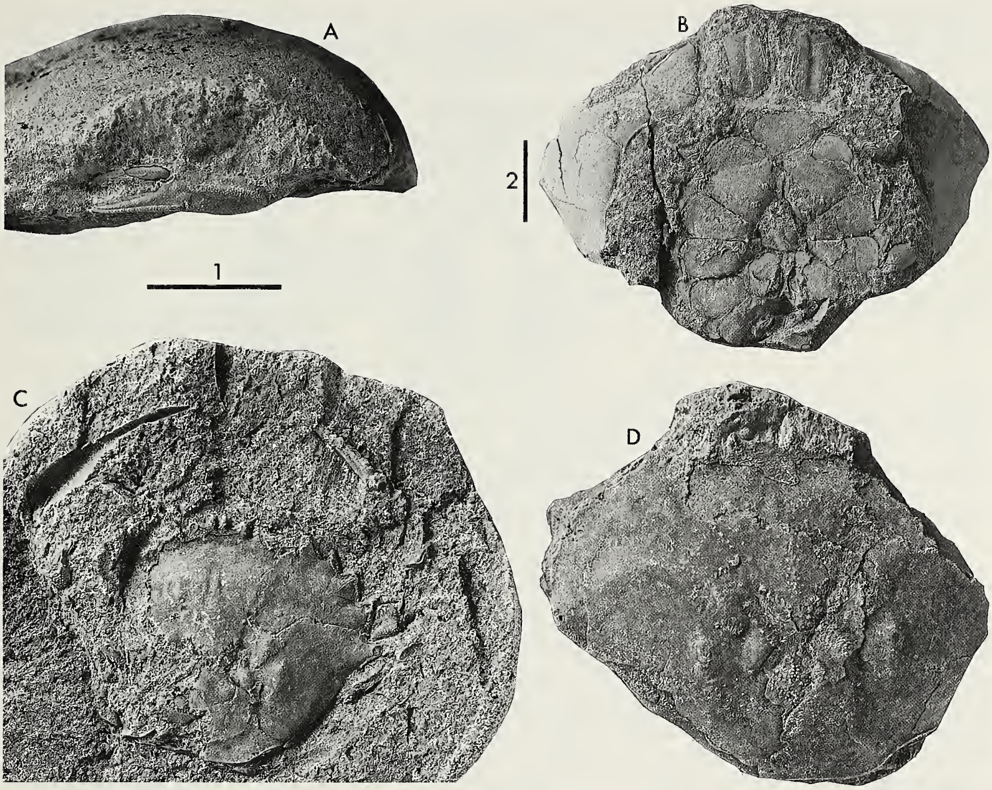

Fig. 8.—*Portunites triangulum* Rathbun. A. Lateral view of outer surface of major cheliped, CM 39669. B. Ventral view, CM 39676. C. Dorsal view of partially preserved carapace, CM 39669. D. Dorsal view of partially preserved carapace, CM 39670. Scale bar 1 for A, C, and D. Scale bar 2 for B. Scale bars = 1 cm.

Portunites triangulum Rathbun, 1926
(Fig. 8, 9)

Portunites triangulum Rathbun, 1926:68.

Diagnosis.—Portunid with three tubercles arranged in triangular pattern on branchial region just posterior of arcuate ridge; four frontal teeth excluding inner orbital tooth; four sharply triangular anterolateral teeth excluding outer orbital tooth, teeth gradually increasing in size posteriorly; carapace about 70% as long as wide; fronto-orbital margin occupying about 50% maximum carapace width.

Emendation to Description.—Carapace somewhat broader than long (L/W = 0.70); widest at position of the last and longest lateral spine; posterolateral margins somewhat longer than anterolateral margins; carapace moderately vaulted both transversely and longitudinally; longest lateral spine at midlength; carapace surface finely granular.

Front with four teeth, slightly projected in front of orbits; middle two frontal teeth closely spaced, projected slightly more than outer two frontal teeth; front occupying 23% of the maximum carapace width; orbits directed slightly anterolaterally, upper orbital margin with two fissures, inner fissure much longer and more pronounced than outer fissure; orbits bounded by inner and outer orbital spines, outer orbital spine longer, about as large as first anterolateral spine, directed forward; fronto-orbital margin occupying 50% maximum carapace width. Anterolateral margin with four teeth excluding outer orbital spine, teeth becoming progressively larger posteriorly; first directed forward; second and

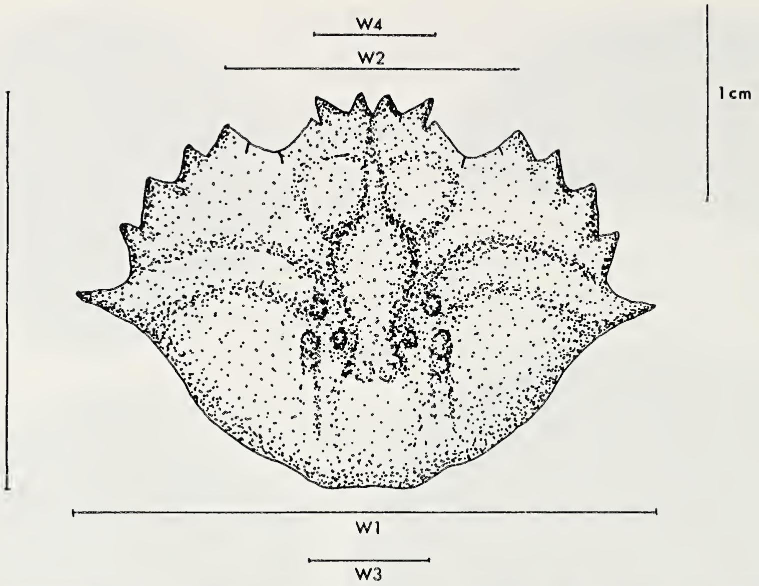

Fig. 9.—Reconstruction of *Portunites triangulum* Rathbun showing the position and orientation of measurements made.

third directed anterolaterally; first through third with slightly concave mesial margins and straight lateral margins; posteriormost longest, narrow, spinelike, directed laterally; posterolateral margin smooth, weakly convex, sinuous; posterior angle broad, concave, rimmed; posterior margin about 33% maximum carapace width, rimmed.

Carapace regions moderately elevated; frontal region slightly sulcate, possessing two low swellings on either side of sulcus, sulcus terminating between two inner frontal teeth; protogastric region tumid posteriorly and flattening near orbital rim; hepatic region slightly inflated; mesogastric region narrow, triangular anteriorly, and widening posteriorly into pentagonal region; cardiac region elevated, with two tubercles; subtle ridge extending in convexly forward arc from lateral spine toward midline, separating cephalic region from the branchial region, terminating in tubercle; mesobranchial region somewhat inflated, bearing three tubercles arranged in triangle pattern near edge of cardiac region, one tubercle of triangle is tubercle at termination of arcuate ridge; metabranchial region with poorly developed longitudinal ridge terminating anteriorly in large tubercle, tubercle included in triangle of tubercles, ridge extending towards posterior margin, gradually disappearing before reaching posterior margin; intestinal region indistinct.

Pterygostomial region finely granular anteriorly, smoother posteriorly; abdomen finely granular anteriorly and smooth posteriorly. Third maxillipeds longer than wide, endognath narrow anteriorly, widening slightly posteriorly, then narrowing and curving abruptly distally into narrow segment attaching to base of appendage; exognath wider than endognath, slightly constricted centrally, upper and lower margins not well known.

Sternum less than 48% maximum carapace width, ovate, narrowest anteriorly, widest at sternite 6, narrowing posteriorly but never as narrow as sternites 1–3; sternites 1–4 fused; sternites 1–3 broadly triangular in shape, apex directed distally, sutures between sternites not evident; sternite 4 petal-shaped, directed anterolaterally, straight axial margin, almost equidimensional, suture between sternites 3 and 4 distinct; sternite 5 petal-shaped, directed anterolaterally, with small peglike projection near lower inner angle; sternite 6 petal-shaped, directed laterally; sternite 7 petal-shaped, directed posterolaterally; sternite 8 poorly known. Sternites 4–7 with episternal projections curving posteriorly, bounding distal margin of next sternite. Abdomen of male extending approximately halfway on sternum, approximately 44% width of sternum, telson triangular, somite 6 about as long as telson but about 1.5 times as wide, remainder of abdomen poorly known.

Chelae unequal; outer surface of manus granular, narrow proximally and widening distally; outer surface with blunt keel extending from proximal margin almost the entire length of manus, keel gradually flattening near distal margin; lower margin of manus rounded, not keeled, granular; upper

Table 5.—*Measurements (in mm) taken on the dorsal carapace of specimens of* Portunites triangulum. *W1 = maximum width, W2 = fronto-orbital width, W3 = posterior width, W4 = frontal width, L1 = maximum length.*

Specimen number	W1	L1	W2	W3	W4
CM39669	26.4	18.5	13.2	6.2	6.4
CM39670	36.2[a]	26.6	16.4	13.8	7.9
CM39671	—	—	30.0	—	14.0
CM39672	60.0[a]	37.9	—	20.1	—
CM39673	45.0[a]	—	20.4[a]	—	8.1
CM39676	> 54.0	41.4	—	—	—

[a] Based on half measurements.

margin not well known; distal margin extending from upper to lower margin at about 50° angle, upper part of distal margin with rounded tubercles; inner surface of manus granular, not well known. Fixed finger narrow, long; possessing two keels, one paralleling lower margin and one paralleling upper margin, surface of keels granular, surface between keels and along occlusal surface smoother; occlusal surface armed with several blunt, rounded teeth of varying sizes. Movable finger long, slender, somewhat longer than fixed finger; upper margin granular, not well known; outer surface smoother than upper surface; occlusal surface with several blunt, rounded teeth of varying sizes.

Measurements.—See Table 5 for carapace measurements and Table 6 for measurements of chelae. All measurements are in millimeters. Position and orientation of carapace measurements illustrated in Figure 9. CM 39676, W (maximum of sternum) = 27.2, L (maximum of sternum) = 29.5, W (maximum of sixth somite) = 12.0, W (maximum of telson) = 4.7, L (maximum of telson) = 4.1, L (maximum of abdomen) > 15.3.

Referred Specimens.—Eight specimens, CM 39669–39676, are deposited in the Carnegie Museum of Natural History.

Localities and Stratigraphic Position.—CM 39669–39671 were collected from the RB36 locality. CM 39676 was collected in a concretion from site RB43. A claw fragment, CM 39674 was collected from RB37 as were several flattened specimens—CM 39672, 39673, and 39675. *Portunites triangulum* has also been reported by amateur collectors from sites RB15 and RB18, but these specimens were not seen by the authors.

Remarks.—Four of the specimens, CM 39669–39671 and 39676 were preserved in concretions, and all of the specimens retained the carapace cuticle. Several tiny specimens, CM 39675, as well as a claw fragment, CM 39674, were recovered along with other decapods, molluscs, and large amounts of organic material. The material herein described is more complete than that available to Rathbun (1926) when she erected the species *Portunites triangulum*, including a more complete venter and chelipeds, which permits a more complete description of the species.

Table 6.—*Measurements (in mm) taken on chelae of specimens of* Portunites triangulum *Rathbun.*

Specimen number	L major chela	L upper finger	L minor chela	L upper finger	L lower finger
CM39671	43.8	18.7	38.5	19.9	17.1
CM39669[a]	14.3	7.3	—	—	—

[a] Assuming preserved chela is major cheliped.

Table 7.—*All known species currently referred to* Portunites.

Taxon	Locality	Age
P. incerta Bell	England/Belgium	early Eocene
P. stintoni Quayle	England	early Eocene
P. sylviae Quayle and Collins	England	late Eocene
P. eocaenica Lörenthey and Beurlen	Hungary	Eocene
P. inculpta Rathbun	North America	mid-Eocene
P. alaskensis Rathbun	North America	Oligocene
P. triangulum Rathbun	North America	Oligocene–early Miocene
P. hexagonalis Nagao	Japan	late Eocene
P. kattachiensis Karasawa	Japan	mid-Eocene

Three species of *Portunites* have previously been described from Washington including *P. alaskensis*, *P. insculpta* Rathbun, and *P. triangulum* (Rathbun, 1926). All were described on the basis of well-preserved carapace material and some chela fragments. *Portunites triangulum* differs from all other species of the genus in bearing a triangular arrangement of tubercles near the axial regions. In addition to lacking a triangle of tubercles on the branchial region, *P. insculpta* has more well-developed carapace regions. Otherwise, *P. insculpta* is the species most similar to *P. triangulum.*

Upon examination of all known species of *Portunites* (Table 7), the main differences between the various species of *Portunites* include differences in the degree of granulation, position of tubercles, definition of carapace regions, and the number, length, and shape of anterolateral spines. Most species possess two orbital fissures in addition to the characters already listed as diagnostic for the genus. Examination of the type species of *Portunites* and all known species historically referred to the genus indicates that it embraces several species that differ in rather substantial aspects from the type species, *P. incerta. Portunites kuhni* Bachmayer cannot be retained in the genus because it possesses terraced ornamentation on the dorsal carapace; Karasawa (1991) reported that it belongs to the genus *Liocarcinus* Stimpson. *Portunites subovata* Quayle and Collins lacks the curved ridge separating the cephalic and branchial regions which is a diagnostic character of *Portunites*; this fact alone is sufficient to warrant removal of this taxon from the genus. *Portunites alaskensis*, which has been collected from localities of Oligocene age in Washington, Alaska, and Oregon, possesses a more square carapace and a shorter anterolateral margin than all other species in the genus (Tucker and Feldmann, 1990). The frontal margin of *P. alaskensis* is straighter than in other species of *Portunites. Portunites alaskensis* lacks the two orbital fissures common in other members of the genus, and has much larger and much more deeply excavated orbits than other members of the genus. Nagao (1932) observed that *P. hexagonalis* Nagao was most similar to *P. alaskensis*; therefore, in all likelihood, the two species are especially closely related. However, at this time these differences do not warrant removal of the two species from the genus *Portunites.* As has been discussed, *P. triangulum* differs from the type species of *Portunites* in several important features but these differences do not warrant removal of the species from the genus at this time.

All of the known species of *Portunites* have been reported from the Northern Hemisphere (Table 7). Two species from localities in England are early Eocene in age, suggesting that the genus arose in the early Eocene. Karasawa (1993) suggested that the genus has a Tethyan distributional pattern.

Superfamily Majoidea Samouelle, 1819
Family Majidae Samouelle, 1819
Subfamily Inachinae Alcock, 1895
Genus *Macrocheira* de Haan, 1839

Type Species.—*Maja kaempferi* Temminck, 1836.

Remarks.—The genus *Macrocheira* was erected by de Haan for one reported extant species, *Macrocheira kaempferi* (Temminck), which is known only from Japan. The genus is placed in the subfamily Inachinae, which is characterized by an overall rounded or pyriform dorsal carapace outline; long, unprotected eyestalks; long, spindly legs; a single or double rostrum; and poorly developed orbits, sometimes with a pre- and/or postocular spine (Griffin and Tranter, 1986).

Species of the genus *Macrocheira* are characterized by possessing a pyriform carapace; a hepatic spine; spindly legs; a double rostrum; a very poorly developed ocular eave; small pre-, intercalated, and postocular spines; and well-developed carapace regions (Miers, 1886; Rathbun, 1926; Sakai, 1976). The ocular eave and ocular spines are poorly developed and do not afford much protection for the eyestalk, making the orbit fundamentally different than those of the subfamily Majinae, which also have an orbital eave and three orbital spines. The protogastric and mesogastric regions of species of *Macrocheira* are inflated, the metagastric region is depressed, the epi- and mesobranchial regions are inflated, and the metabranchial region is depressed. The urogastric region of species of *Macrocheira* is poorly developed and the cardiac region is oblong and bounded by wide grooves with parallel crenulations positioned oblique to the axis of the grooves. Species of the genus *Macrocheira* are differentiated by the degree of inflation and overall shape of carapace regions, degree and nature of ornamentation on the regions, length of the rostrum, and size of the ocular spines and hepatic spine.

Several Miocene fossil species of *Macrocheira* are known from Japan including *M. ginzaensis* Imaizumi, *M. yabei* (Imaizumi), and *Macrocheira* sp. Imaizumi. *Macrocheira* sp. Karasawa is known from the Pliocene of Japan. One species, *M. teglandi* Rathbun, was previously known from the Oligocene of Washington, USA. The current study includes an emended description of *M. teglandi* from the late Oligocene to early Miocene Pysht Formation. Also described is the new species *Macrocheira longirostra* from the late Eocene Quimper Sandstone of Washington, marking the earliest known occurrence of the genus *Macrocheira*. Fossil species represented by dorsal carapace material, including *M. teglandi*, *M. longirostra*, and *M. yabei*, are considerably smaller than the very large recent species *M. kaempferi* which may attain a maximum width of 305 mm and a maximum length of 335 mm. *Macrocheira kaempferi* has been reported to inhabit bottoms of mud or sand at depths of 50–300 m and is endemic to Japan (Sakai, 1976).

Macrocheira teglandi Rathbun, 1926
(Fig. 10, 11)

Macrocheira teglandi Rathbun, 1926:148.

Diagnosis.—Carapace longer than wide, pyriform; rostrum bifid; carapace tubercles small, acute; regions moderately inflated; protogastric region continuous

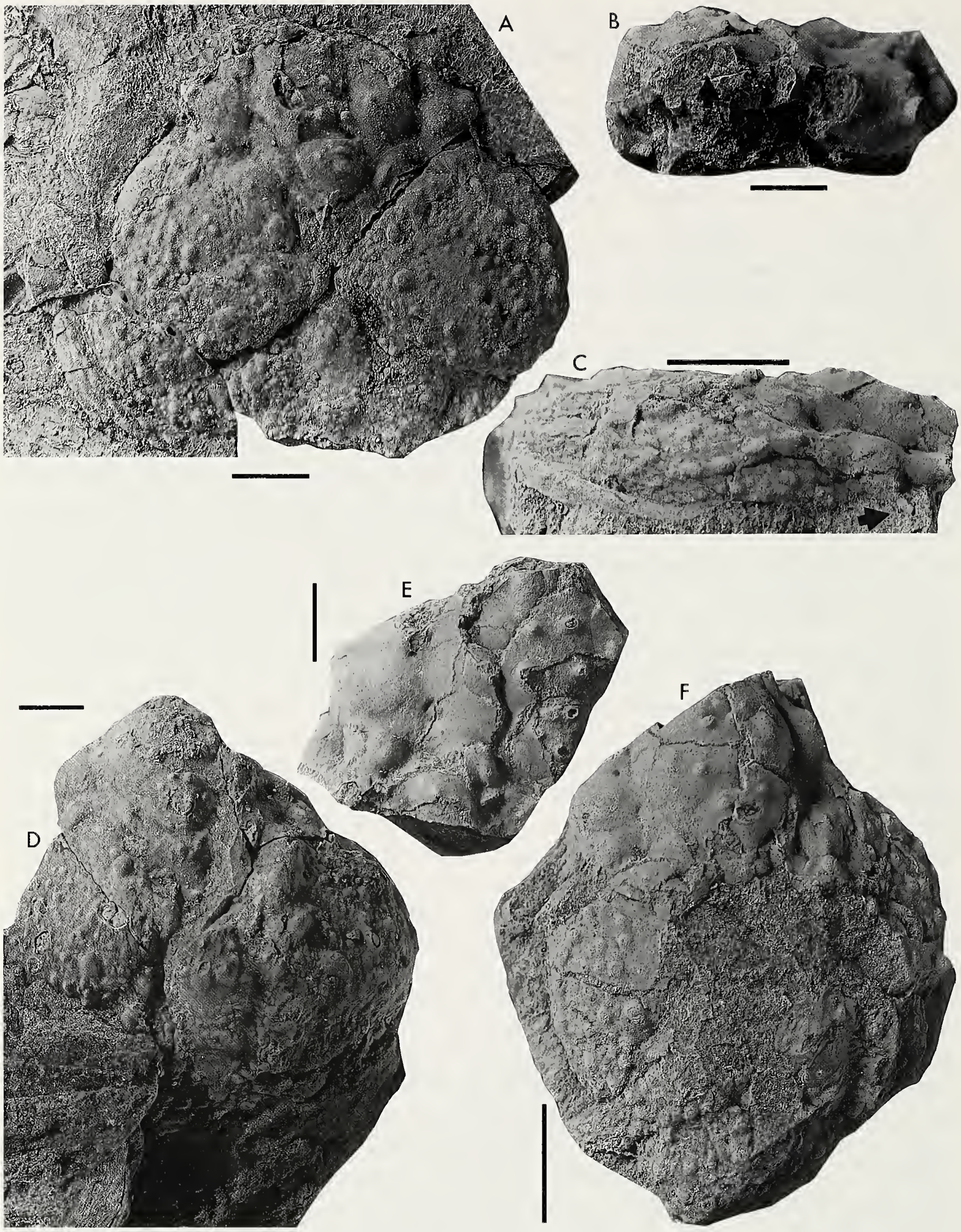

Fig. 10.—*Macrocheira teglandi* Rathbun. A. Dorsal view of partial carapace, CM 39679. B. Frontal view of carapace fragment, CM 39680. Arrow indicates broken base of double rostrum. C. Lateral view of partial carapace, CM 39677. Arrow indicates hepatic spine. D. Dorsal view of carapace fragment, CM 39680. E. Dorsal view of fractured carapace, CM 39678. F. Dorsal view of partial carapace, CM 39677. Scale bars = 1 cm.

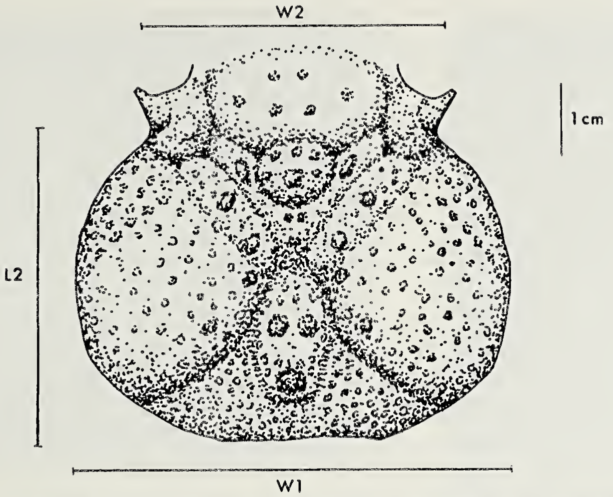

Fig. 11.—Reconstruction of *Macrocheira teglandi* Rathbun showing the position and orientation of measurements made.

unit, broadly subelliptical; hepatic region relatively smooth, with small spine; epi- and mesobranchial regions heavily ornamented, inflated.

Emendation to Description.—Carapace pyriform, widest about three-quarters of the distance from the front, vaulted both transversely and longitudinally; surface ornamented with numerous tubercles of varying sizes; regions inflated, bounded by wide, deep grooves.

Front and anterolateral margins poorly known; lateral margins rounded, convex, steep sided; posterior margin nearly straight.

Frontal region poorly known; ornamented with a few tubercles; rostrum bifid, broken at base. Protogastric region inflated; broadly subelliptical; convex proximal margin; concave distal margin; ornamented with several peaked tubercles. Hepatic region inflated; nearly smooth, bearing triangular marginal spine directed anterolaterally. Mesogastric region subelliptical, moderately inflated, bearing several small tubercles along proximal and lateral margins and one prominent tubercle centrally. Metagastric region U-shaped, extending between bases of hepatic regions, widest axially and narrowing distally, ornamented with a few tubercles axially and an oblong tubercle distally. Urogastric region depressed, possessing one central tubercle. Cardiac region elongate, diamond-shaped, ornamented with two broad tubercles anteriorly and large granular tubercle posteriorly, several small tubercles on remainder of region; region bounded by broad grooves with parallel crenulations slightly oblique to axis of groove. Intestinal region flattened, ornamented with numerous small tubercles.

Epibranchial region oblong; separated from metagastric region by broad cervical groove; demarcation between mesobranchial and epibranchial region weakly developed; possessing large tubercle axially; another large tubercle positioned centrally on region; remainder ornamented with small tubercles. Mesobranchial regions large; inflated; steep lateral margins; triangular in shape, apex directed axially; ornamented with numerous small tubercles, some arranged in rows roughly paralleling lateral margin; two large tubercles positioned along axial margin of region. Metabranchial region weakly inflated axially, flattened marginally; triangular in shape; ornamented with numerous small tubercles.

Venter and appendages unknown.

Measurements.—Measurements (in millimeters) taken on specimens of *Macrocheira teglandi* are presented in Table 8. Position and orientation of dorsal carapace measurements are illustrated in Figure 11.

Referred Specimens.—Specimens referred to *Macrocheira teglandi*, CM 39677–39682, are deposited in the Carnegie Museum of Natural History.

Localities and Stratigraphic Position.—Two specimens, CM 39677 and 39678,

Table 8.—*Measurements (in mm) taken on four specimens of* Macrocheira teglandi. *W1 = maximum width, L1 = maximum length, W2 = width measured between bases of hepatic spines, L2 = length measured from base of hepatic spine to posterior margin.*

Specimen number	Locality	W1	L1	W2	L2
CM39677	RB18	> 34.1	> 45.9	22.2	27.7
CM39680	RB37	—	—	58.8	—
CM39679	RB37	59.7	> 54.0	—	—
CM39678	RB18	65.6	> 69.1	39.8	49.4

were collected from RB18. Three specimens were collected from RB37, including CM 39679 and 39680, as well as CM 39681, a carapace fragment. One carapace fragment was recovered from RB38, CM 39682. Fragments that may be referrable to this species were collected at RB36.

Remarks.—The material herein referred to *Macrocheira teglandi* includes four broken carapaces. Three of the carapaces lack the front, rostrum, and orbits, and each are fractured in several places; one of these specimens does retain the hepatic spine. The fourth specimen (CM 39680) consists of only a fragment of the anterior portion of the carapace, but it retains the base of the rostrum indicating that it is bifid. Only one of the four specimens confidently referred to *M. teglandi* was preserved in a concretion.

Numerous fractures and the incomplete nature of the specimens herein referred to *Macrocheira teglandi* make recognition of some carapace regions difficult, and the description inherently reflects these deficiencies. Nevertheless, the specimens are confidently referred to *M. teglandi* based upon the overall shape of the carapace, hepatic spine, and shape and ornamentation of the gastric, branchial, cardiac, and intestinal regions of the carapace (see Rathbun, 1926). *Macrocheira teglandi* was named for material possessing the dorsal carapace, venter, and part of a cheliped (Rathbun, 1926). The specimens in this study consist only of dorsal carapace material; however, they are sufficiently well-preserved to allow for a more complete description of the dorsal carapace. The occurrence of *Macrocheira teglandi* in the Pysht Formation does not extend the geologic or geographic range of the species, since Rathbun's holotype was recovered from Tegland Point, a locality that corresponds with locality RB36 of this study.

Macrocheira teglandi is most similar to the extant species *M. kaempferi* of Japan, but *M. teglandi* differs from *M. kaempferi* in several respects. The tubercles ornamenting the surface of *M. teglandi* are somewhat larger and more variable in size than those of *M. kaempferi.* The cardiac region of *M. kaempferi* is longer and of an overall different ornamentation than that of *M. teglandi.* The metagastric region of *M. kaempferi* is more depressed and less ornamented than that of *M. teglandi.* The epigastric region of *M. kaempferi* is better developed than that of *M. teglandi,* and *M. kaempferi* is between five and six times as large as *M. teglandi. Macrocheira ginzaensis*, *Macrocheira* sp. Imaizumi, and *Macrocheira* sp. Karasawa are known only from claw fragments, making direct comparisons with *M. teglandi* impossible. *Macrocheira yabei* is known from several flattened specimens, so that direct comparison of that species to *M. teglandi* is difficult. *Macrocheira yabei* is longer and narrower than is *M. teglandi* and possesses different ornamentation on the carapace regions than does *M. teglandi. Macrocheira teglandi* possesses one spine on the hepatic region, while *M. yabei* possesses two

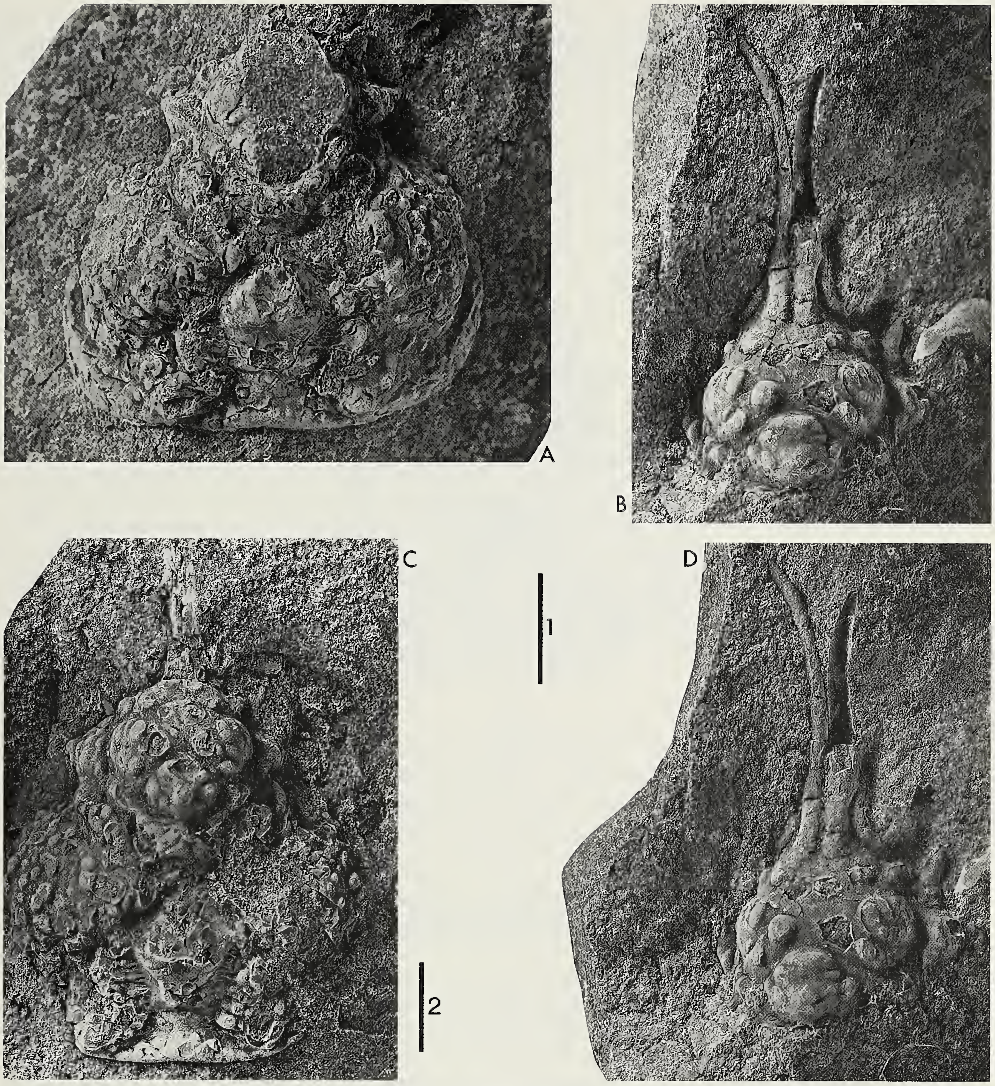

Fig. 12.—*Macrocheira longirostra*. A. Dorsal view of partial carapace, CM 39684. B. Dorsal view of partial specimen, CM 39685. C. Dorsal view of holotype, CM 39683. D. Oblique dorsal view of partial specimen, CM 39685. Arrow indicates preorbital spine on rudimentary ocular eave. Scale bar 1 for A, B, and D. Scale bar 2 for C. Scale bars = 1 cm.

spines on that region. Finally, the branchial regions of *M. teglandi* are more rounded and protrude farther laterally than do those regions of *M. yabei*.

Macrocheira longirostra, **new species**
(Fig. 12, 13)

Diagnosis.—Carapace longer than wide, pyriform; rostrum long, bifid; orbit with narrow eave, antorbital, intercalated, and postorbital spine; carapace regions inflated, bounded by wide grooves; protogastric region composed of two distinct,

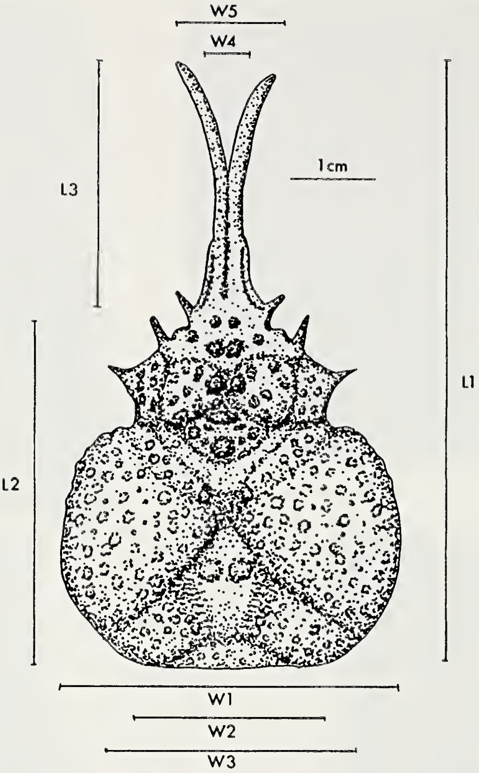

Fig. 13.—Reconstruction of *Macrocheira longirostra* showing the position and orientation of measurements made.

semispherical regions; hepatic region with rounded tubercles and spine; carapace surface ornamented with large, rounded tubercles.

Description.—Carapace pyriform, broadest about three-quarters of the distance from the front (W/L = approximately 0.80), highly vaulted transversely, moderately vaulted longitudinally; possessing inflated regions, regions bounded by broad grooves; surface ornamented with large, smoothly rounded tubercles; lateral margins of branchial regions round, highly convex; posterior margin nearly straight.

Rostrum long, bifid; rostral elements tubular, closely parallel basally, and diverging distally away from center line of carapace.

Ocular eave rudimentary, situated on basal portion of rostrum, eave rimmed, narrow, sinuous outer margin, terminating distally in narrow, attenuated antorbital spine, spine directed anterolaterally; intercalated spine short, blunt, directed more forward than antorbital spine; postorbital spine as long as but more stout than antorbital spine, directed more forward than antorbital spine.

Frontal region ornamented with two tubercles positioned at the outer basal edge of rostrum and two tubercles positioned at inner basal edge of rostrum. Protogastric region subround, inflated so as to be semispherical; ornamented with three large tubercles, round tubercle positioned axially, two oblong tubercles just distal to axial tubercle, several smaller tubercles on remainder of region. Hepatic region inflated, ornamented with several rounded tubercles; possessing rather stout, triangular marginal spine projecting anterolaterally.

Mesogastric region highly inflated, subelliptical, bearing an oblong tubercle centrally and proximally, large tubercle centrally and distally, smaller tubercles on either side of central two tubercles. Metagastric region U-shaped, extending between bases of hepatic regions; widest axially, and narrowest as it approaches margins; region not well known but appearing to be ornamented with numerous tubercles. Urogastric region depressed, not well known. Cardiac region diamond-shaped, inflated, ornamentation not well known but appearing to possess pair of large, rounded tubercles positioned

Table 9.—*Measurements (in mm) taken on specimens of* Macrocheira longirostra. *L1 = maximum length, L2 = maximum length (excl. rostrum), L3 = rostral length, W1 = maximum width, W2 = width measured at base of hepatic spine, W3 = width measured between tips of postorbital spines, W4 = rostral width measured at base midway along ocular eave, W5 = width measured between tips of antorbital spines.*

Specimen number	L1	L2	L3	W1	W2	W3	W4	W5
CM39683	> 54.6	40.0	> 14.6	> 38.4	23.1	16.1	5.5	11.4[a]
CM39686	> 40.2	—	> 11.7	> 34.4	23.0[a]	17.8[a]	4.8	13.8[a]
CM39685	—	—	26.6	—	22.0[a]	18.6[a]	6.5	13.2[a]
CM39684	—	38.4	—	39.0	20.7	16.2[a]	—	—

[a] = based on half measurements.

centrally on either side of the axial line; region delimited by very broad grooves, grooves with parallel crenulations positioned slightly oblique to axis of groove. Intestinal region flattened, broadly trapezoidal, ornamented with a few small tubercles.

Epibranchial region oblong, paralleling metagastric region, widest distally and narrowing axially, ornamented with numerous tubercles, very large tubercle along axial margin of region; separated from metagastric region by broad cervical groove; demarcation between epibranchial regions weakly developed. Mesobranchial region large; broadly triangular, apex of triangle directed axially; ornamented with numerous rounded tubercles of varying size, highly inflated axially, flattening somewhat along margins. Metabranchial region weakly inflated axially and flattened along margins, broadly triangular in shape, bearing several large tubercles along axial margin, remainder of region ornamented with smaller tubercles.

Venter and appendages unknown.

Measurements.—Measurements (in millimeters) taken on specimens of *Macrocheira longirostra* are presented in Table 9. Position and orientation of dorsal carapace measurements are illustrated in Figure 13.

Types.—The holotype, CM 39683, and three paratypes, CM 39684–39686, are deposited in the Carnegie Museum of Natural History.

Localities and Stratigraphic Position.—All of the specimens referred to *Macrocheira longirostra* were collected from site RB40 from the late Eocene Quimper Sandstone.

Etymology.—The trivial name is constructed from the Latin word *longus*, meaning long, and the Latin word *rostrum*, meaning beak, bill, snout, or muzzle, in reference to the extremely elongate rostrum exhibited by this species.

Remarks.—The material referred to *Macrocheira longirostra* consists solely of specimens preserved in concretions. All of the specimens retain dorsal carapace material, and all consist of dorsal carapaces only, suggesting that they may be molts. Each of the specimens is incomplete, but the preservation of the material is excellent and allows a detailed description of the dorsal carapace to be framed.

The new species, *Macrocheira longirostra*, can be referred to the genus *Macrocheira* based upon possession of several key characters including a pyriform carapace that is longer than wide and a bifid rostrum. The type and sole extant species, *M. kaempferi* possesses a rudimentary orbital eave, antorbital spine, intercalated spine, and postorbital spine. The type species also possesses inflated epi- and mesobranchial regions that are ornamented with numerous tubercles, inflated protogastric regions, an ovoid mesogastric region, a U-shaped metagastric region, a depressed urogastric region, a long, narrow cardiac region, and flattened metabranchial regions. The new species *M. longirostra* possesses all of the above-listed characters and is therefore referred to the genus *Macrocheira* with confidence.

The new species *Macrocheira longirostra* is congeneric with *M. teglandi* from the Pysht Formation, but is considered to be a distinct species based on several differences. *Macrocheira longirostra* possesses several rounded tubercles on the hepatic region while *M. teglandi* has a nearly smooth hepatic region. The carapace tubercles of *M. longirostra* are more rounded and larger than those of *M. teglandi*, which possesses tubercles that are smaller overall and are more acutely tipped. Carapace regions of *M. longirostra* are more inflated than those of *M. teglandi*. The branchial regions of *M. teglandi* possess smaller, more numerous tubercles, while those regions of *M. longirostra* have fewer, larger tubercles. Finally, the protogastric region of *M. longirostra* is composed of two distinct, rounded regions with several large tubercles while that of *M. teglandi* is a continuous region with smaller, more acute tubercles. Direct comparison of *M. longirostra* with *M. ginzaensis*, *Macrocheira* sp. Imaizumi, and *Macrocheira* sp. Karasawa is not possible because those three taxa are represented only by claw fragments, which are not present in the *M. longirostra* material. *Macrocheira yabei* was named for tiny, flattened specimens, so direct comparisons with *M. longirostra* are difficult although it appears to be longer and narrower overall than *M. longirostra*. The hepatic region of *M. yabei* was reported to possess two spines; *M. longirostra* possesses only one spine on that region. The branchial regions of *M. yabei* are not as rounded and do not protrude as far laterally as those of *M. longirostra*. Finally, the ornamentation reported for carapace regions of *M. yabei* differs from that seen on regions of *M. longirostra*.

Macrocheira longirostra differs from the recent species *M. kaempferi* because *M. longirostra* possesses larger, more rounded tubercles ornamenting the carapace, a shorter cardiac region, and a protogastric region that consists of two distinct, bulbous regions instead of one continuous region such as that of *M. kaempferi*. The hepatic regions of *M. longirostra* are more bulbous and more heavily ornamented than those of *M. kaempferi*. The rostrum of *M. longirostra* is much longer than that of *M. kaempferi*. The rostrum of *M. kaempferi* is quite short in adults, but it has been reported to attain lengths of more than one-half of the carapace length in juveniles (Sakai, 1976). Also, the adults of *M. kaempferi* are much larger than the fossil specimens of *M. longirostra*, at least six times as long based on measurements of *M. kaempferi* given in Sakai (1976). Possibly the fossil specimens are juveniles, but there is no clear indication that this is the case, because all of the specimens referred to the new species are approximately the same size, suggesting that they may be adults. However, each specimen consists only of dorsal carapace material, indicating that they may be molts, perhaps of younger individuals. Only one specimen has a complete rostrum preserved, and this particular specimen consists only of the rostrum, frontal, protogastric, and mesogastric regions. Consequently, it is not possible to compare rostral size with overall size for any of the specimens. Collection of additional fossil specimens will be necessary to determine whether the new species *M. longirostra* exhibits allometric growth in regards to the length of the rostrum and to determine whether the fossil specimens are adults or juveniles.

The occurrence of *Macrocheira longirostra* in the late Eocene rocks of the Quimper Sandstone marks the earliest known occurrence of this genus.

Section Thoracotremata Guinot, 1977
Superfamily Pinnotheroidea de Haan, 1833
Family Pinnotheridae de Haan, 1833

Remarks.—The specimens herein described superficially resemble members of both the families Pinnotheridae and Hexapodidae, based upon their small size, subrectangular carapace, small orbits, and simple carapace ornamentation. However, the specimens can be referred to the Pinnotheridae based upon several criteria. CM 39688 possesses the abdomen, sternum, and five pereiopods. The chelipeds are preserved only as the basal segments; however, pereiopods 2–5 are well preserved. Because of the presence of five pereiopods, assignment of the material to the Hexapodidae is impossible because that family possesses completely suppressed fifth pereiopods (Manning and Holthuis, 1981).

Other criteria support assignment of this material to the Pinnotheridae. Many hexapods, including *Pseudohexapus* Monod, *Parahexapus* Balss, and *Hexapus* de Haan, often have a ridge paralleling the lateral margins; this ridge is not apparent on previously described pinnotherids or the specimens from this study. Members of the Hexapodidae possess a long posterior border, often nearly as long as the widest part of the dorsal carapace. Our specimens possess a posterior border that is only half as long as the maximum carapace width in addition to highly concave posterolateral margins (called posterolateral facets by Sakai [1976]), a characteristic of the subfamily Asthenognathinae of the Pinnotheridae.

Evaluation of the abdomen of CM 39688 is somewhat problematic. The abdomen is more narrow than is typical for females, occupying about half the width of the sternum. However, it is wider than the abdomen of typical males, and possesses rounded lateral margins typical of females. Usually males of both the Hexapodidae and the Pinnotheridae have a straight-sided abdomen. No fusion of any of the abdominal somites is evident in specimen CM 39688. In hexapods, males possess fusion of some of the abdominal somites, often the third through fifth, third and fourth, fifth and sixth, or second through sixth (Manning and Holthuis, 1981). Some pinnotherids also may exhibit fusion of abdominal somites in males (Manning and Holthuis, 1981; Williams, 1984). Neither female hexapods nor female pinnotherids commonly exhibit fusion of any of the somites. Possibly the specimen under study is an immature female due to its rounded lateral margins, lack of fused somites, and intermediate width.

Subfamily Asthenognathinae Stimpson, 1858

Remarks.—The material herein described can be confidently referred to the subfamily Asthenognathinae because it possesses an overall trapezoidal dorsal carapace, a carapace that is moderately wider than long, highly concave posterolateral margins, and characteristic shape and arrangement of the carapace regions. The Asthenognathinae contains at least eight genera including *Asthenognathus* Stimpson, known from Japan, the Gulf of Thailand, France, and western Africa, and *Tritodynamia* Ortmann, known from Japan, China, and Korea. One species of *Tritodynamia*, *T. globosa* Karasawa, has been reported from the early–middle Miocene of Japan (Karasawa, 1993), and is herein referred to *Asthenognathus*. *Asthenognathus inaequipes* Stimpson has been reported from Holocene deposits near Osaka Bay, Japan (Schmitt et al., 1973).

Other pinnotherid subfamilies cannot accommodate the specimens described herein. Members of the subfamily Pinnotherinae possess a carapace that is globular in shape, unlike our specimens, and a carapace that is not wide enough to accommodate the new fossil material. Members of the subfamily Pinnotherellinae possess a broadly transverse carapace which the material studied here does not possess. Additionally, neither of the aforementioned subfamiles can accommodate specimens exhibiting either the trapezoidal shape of the material described herein or its highly concave posterolateral margins. Members of the subfamily Xenophthalminae White possess narrow orbits that are oriented parallel to the axis of the animal and extend posteriorly onto the dorsal carapace (Sakai, 1976), while the specimens of this study have small semicircular orbits.

Genus *Asthenognathus* Stimpson, 1858

Type Species.—*Asthenognathus inaequipes* Stimpson, 1858.

Remarks.—The material herein described is referred to the genus *Asthenognathus*. Species of that genus possess a trapezoidal carapace that is not much wider than long, extremely concave posterolateral margins (posterolateral facets of Sakai, 1976), and a weak rim paralleling the posterolateral and posterior margins. Additionally, members of the genus *Asthenognathus* possess a triangular mesogastric region, a small inflated area on the anterior portion of the protogastric region, slightly inflated branchial regions, and a subhexagonal cardiac region. The new specimens possess all of these characters and are therefore referred to that genus.

The Miocene Japanese species *Tritodynamia globosa* Karasawa very closely resembles the new pinnotherid species described below, and it is here referred to the genus *Asthenognathus*. At this time it seems best to assign the new material and the Japanese species to the genus *Asthenognathus* rather than *Tritodynamia* as explained below.

The specimens referred to the new species *Asthenognathus cornishorum* and *A. globosa* (Karasawa) can be differentiated from species of the genus *Tritodynamia* for several reasons. Species of the genus *Tritodynamia* possess a carapace that is wider than long and trapezoidal in shape with posterolateral facets, all characters of the new species and *A. globosa*. However, the shape of the carapace regions of species of *Tritodynamia* is somewhat different than that of the specimens described herein. The cardiac and mesogastric regions are not as well developed in species of *Tritodynamia* as in species of *Asthenognathus* and the new species. The protogastric region is semicircular in shape in species of *Tritodynamia*, while it is subtrapezoidal in species of *Asthenognathus* and the specimens described herein. The dorsal carapace of species of *Tritodynamia* is typically markedly wider than long, while the dorsal carapace of species of the genus *Asthenognathus* and the new species described below is not much wider than long.

Some species have been assigned at various times to both *Asthenognathus* and *Tritodynamia*. For example, *A. atlanticus* Monod has been assigned by some authors to *Tritodynamia*, and many authors have considered *T. japonica* and *A. inaequipes* to be synonymous (Yokoya, 1928; Monod, 1933; Bocquet, 1963, for example). Rathbun (1910) assigned *T. japonica* to *A. japonica*. Bocquet (1963) synonymized the two genera, but the two genera have been kept distinct by all other authors based upon differences between the two genera in the morphology of the third maxilliped (Sakai, 1976).

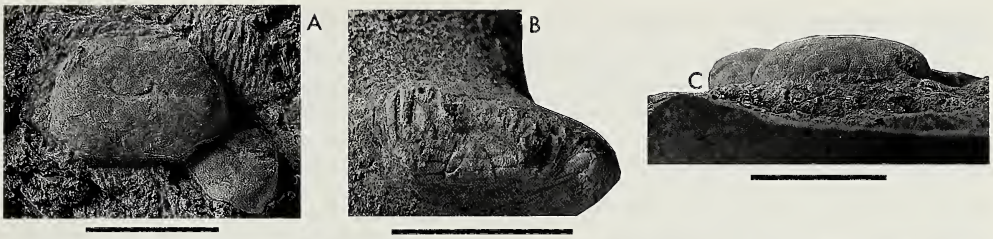

Fig. 14.—*Asthenognathus cornishorum*. A. Dorsal view of holotype, CM 39687. B. Ventral view, CM 39688. C. Anterior view of holotype, CM 39687. Scale bars = 1 cm.

Asthenognathus cornishorum, **new species**
(Fig. 14, 15)

Diagnosis.—Carapace wider than long, trapezoidal, regions weakly developed, surface finely granular laterally and smoother axially; protogastric region with small swellings anteriorly; orbits small, semi-oval; posterolateral margins highly incurved; row of granules paralleling posterior margin.

Description.—Carapace trapezoidal, widening posteriorly, maximum length about 75% the distance from front (L/W = 0.71); carapace regions poorly defined; carapace surface finely granular laterally, smoother axially; margins rounded and steep; highly vaulted both longitudinally and transversely.

Frontal margin straight; rostrum deflexed (rostral width/total width = 0.15), sulcate centrally, granular, projecting beyond orbits, distal extreme unknown. Orbits small, semi-oval, weakly rimmed, fronto-orbital width occupying 70% total frontal width. Anterolateral margin diverging distally, steeply rounded; posterolateral margin strongly concave, rimmed, converging distally; posterior margin straight, row of granules paralleling its total length, posterior width/total width = 0.51.

Protogastric region small, granular, small swelling anteriorly along axis, remainder of region weakly inflated, trapezoidal in shape; mesogastric region sulcate anteriorly, smoother than protogastric region, narrow anteriorly and broadening posteriorly into triangular area, bounded on distal margin by well-developed groove, groove interrupted centrally; urogastric region marked only by weakly developed incurved grooves on lateral margin; cardiac region weakly elevated, bounded by very weakly developed grooves, pentagonal in shape with apex directed posteriorly; urogastric and cardiac regions relatively smooth. Remainder of carapace not differentiated into regions.

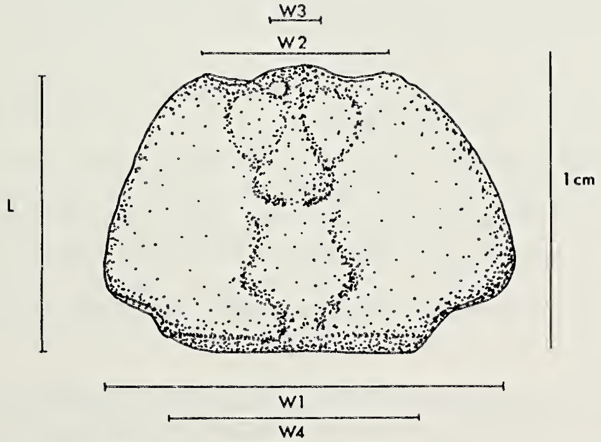

Fig. 15.—Reconstruction of *Asthenognathus cornishorum* showing the position and orientation of measurements made.

Carapace not bilaterally symmetrical, right half more inflated and protruding further laterally than left half.

Sternites 1–4 unknown; sternites 5–8 finely granular. Sternite 5 longer than wide, margins not well known. Sternite 6 wider than long; directed slightly anterolaterally; upper and lower margins straight and nearly parallel; outer margin rounded, with triangular, acutely tipped episternal projection. Sternite 7 similar in size and shape to sternite 6; directed slightly posterolaterally; sternite 8 narrower than 6 and 7; directed posterolaterally; upper margin straight; remainder unknown.

Telson equilaterally triangular; not well known. Somites 3–6 finely granular, with raised, smoother, rounded ridge extending centrally across all four somites; somites widening and becoming shorter distally. Somite 6 trapezoidal in shape; wider than long; upper and lower margins nearly straight and parallel; lateral margins converging proximally. Somite 5 wider than long, widest centrally; upper and lower margins slightly sinuous, nearly parallel; about as long as somite 6 but wider; lateral margins converging slightly proximally. Somite 4 nearly rectangular in shape; lateral margins converging very slightly proximally. Somite 3 rectangular in shape, not well known. Somites 1 and 2 unknown.

Chelipeds and third maxilliped poorly known. Pereiopods 2–4 similar in size and shape. Coxae of pereiopods 2–4 short, equidimensional, tubular. Basis and ischium appearing to be fused, poorly known, Merus of pereiopods 2–4 much longer than high; row of short spines on lower margin. Merus of pereiopod 5 longer than high; sinuous upper and lower margins; narrowing distally; carpus narrow proximally, widening distally, distal margin extending obliquely proximally from upper margin at about 45° angle; propodus longer than high, proximal margin extending obliquely proximally from upper to lower margin at about 45° angle, upper and lower margins appearing to be parallel and straight; remainder of propodus poorly known; dactylus much longer than high, appearing to be lanceolate.

Measurements.—All measurements are in millimeters. Position and orientation of dorsal carapace measurements are illustrated in Figure 15. CM 39687, large carapace, L (maximum) = 9.7, W1 (maximum) = 13.6, W2 (fronto-orbital) = 5.2, W3 (rostral) = 2.0, W4 (posterior) = 6.9; small carapace, L (maximum) = 6.9. CM 39689, carapace, L (maximum) = 5.7, W1 (maximum) = 8.5. CM 39688, venter, W (maximum) = 6.1; abdomen, W (maximum) = 2.9, L (maximum) = approximately 2.6; merus of pereiopod 3, L = approximately 2.1; merus of pereiopod 4, L = approximately 3.3; merus of pereiopod 5, L = approximately 3.8.

Types.—The holotype, CM 39687, and paratypes, CM 39688 and 39689, are deposited in the Carnegie Museum of Natural History.

Localities and Stratigraphic Position.—A concretion bearing two dorsal carapaces (CM 39687) was collected at RB36 and a flattened dorsal carapace (CM 39689) was collected at RB37. The venter, CM 39688, was collected from RB18. All localities are in the Pysht Formation of late Oligocene to early Miocene age.

Etymology.—The trivial name honors John and Gloria Cornish of Port Angeles, Washington, who graciously donated fossil material for this study.

Remarks.—Two specimens referred to this taxon consist only of dorsal carapaces. Two dorsal carapaces (CM 39687) are preserved in one concretion with one overlapping a portion of the other. The two carapaces retain some of the original carapace material but otherwise are internal molds of the carapace. CM 39689 consists of a flattened dorsal carapace that was recovered from medium-bedded siltstone associated with numerous decapods, molluscs, and a large amount of organic material. CM 39688 consists of a venter and portions of some of the appendages.

Asthenognathus cornishorum is most similar to *A. globosa* of the Miocene of Japan (Karasawa, 1992, 1993). *Asthenognathus cornishorum* can be distinguished from *A. globosa* in several ways. *Asthenognathus globosa* has very closely spaced orbits and the fronto-orbital width occupies about 27% of the total carapace width

(Karasawa, 1993). The orbits of *A. cornishorum* are less closely spaced and the fronto-orbital width occupies 38% of the total carapace width. The protogastric region of *A. cornishorum* possesses a small inflated area placed axially in the anteriormost portion of region while *A. globosa* does not. The granules of *A. cornishorum* are proportionately somewhat smaller than those of *A. globosa*. *Asthenognathus globosa* possesses a beaded rim on the posterior margin while *A. cornishorum* has a row of granules paralleling the posterior margin but not forming a rim. The cervical groove of *A. globosa* is better defined than that of *A. cornishorum.*

Asthenognathus cornishorum may be distinguished from the recent Japanese species *A. inaequipes* Stimpson because *A. inaequipes* has much more clearly defined carapace regions. *Asthenognathus cornishorum* differs from *A. atlanticus* because *A. atlanticus* possesses more inflated carapace regions than does *A. cornishorum* and a small ridge on the branchial region extending obliquely from the lateral margin toward the posterior margin, which *A. cornishorum* does not possess. *Asthenognathus hexagonum* Rathbun was reported to be strongly hexagonal in shape (Rathbun, 1909), while *A. cornishorum* is trapezoidal in shape.

The dorsal carapace of *Asthenognathus cornishorum* is asymmetrical, because the right half of the dorsal carapace is more inflated and protrudes further laterally than the left side. Interestingly, the dorsal carapaces of two specimens of *A. globosa* figured by Karasawa (1993:pl. 24, fig. 3, 8) also display a similar asymmetry. The asymmetry may be a result of a variety of factors. One possibility is that the crabs were infested by isopods of the family Bopyridae, a common parasite of decapods that causes swelling of the carapace in the area of infestation to accommodate the isopod (Glaessner, 1969; Hessler, 1969; Overstreet, 1983). Bopyrid infestation of decapods is known from as early as the Upper Jurassic and Cretaceous of England, Germany, France, and the former Czechoslovakia (Hessler, 1969). Another possibility is deformation of the dorsal carapace after death either by depositional forces or postdepositional factors such as compression by sediments.

The Recent Japanese species *Asthenognathus inaequipes* Stimpson is free living and inhabits bottoms of mud or sandy mud at depths of 10–65 m (Sakai, 1976). *Asthenognathus atlanticus* Monod is known from the coast of western Africa and France and has been reported to inhabit depths of 8–70 m in the sublittoral zone, at times commensal with tube worms (Monod, 1956; Schmitt et al., 1973). *Asthenognathus hexagonum* Rathbun was collected from the Gulf of Siam in mud at a depth of 15 m (Rathbun, 1909).

Assignment of the new material and the Japanese species to the genus *Asthenognathus* marks the first notice of the genus in the fossil record and one of the earliest known occurrences. The Japanese species *A. globosa* is known from the early Miocene of Japan, so the two species are of approximately the same age, with the Pysht specimens most likely being slightly older.

DISCUSSION

General

The decapod assemblage recovered from the Pysht Formation and the Quimper Sandstone can be used to help corroborate the previously reported depths and depositional environments for those formations. Taphonomy of the decapod specimens provides insight into conditions in the depositional area while the two formations were being deposited. Most importantly, the decapod fauna provides new evidence of a strong affinity between the late Eocene to early Miocene decapod fauna from the Pacific Northwest and the Cenozoic decapod fauna reported from Japan. Additionally, several species of the Pysht Formation and the Quimper Sandstone have modern congeners in the Pacific Ocean. The remarkable similarity of the Japanese and American faunas suggests that a distinct decapod fauna developed in the North Pacific as early as the late Eocene and that faunal exchange between the two areas was significant and may have continued until relatively recently.

Taphonomy of Pysht Formation Decapods

The decapod specimens of the Pysht Formation are almost all well preserved, although some specimens are fragmented or broken. In almost all cases, the cuticle of the specimens is present and well preserved. Some specimens appear to be corpses, including individuals of *Portunites triangulum*, *Mursia marcusana*, and *Asthenognathus cornishorum*, because they possess either the abdomen or both the abdomen and chelipeds. All other decapod specimens consist of portions of, or entire, carapaces or cheliped fragments, suggesting that the majority of the specimens may be molts. The excellent preservation of the thalassinoideans, especially *Callianopsis clallamensis*, suggests minimal reworking of the specimens in the depositional environment. Some specimens of *C. clallamensis* possess a well-preserved carapace, abdominal somites, and large portions of both the major and minor chelipeds, which is unusual in the fossil record because only the relatively well-calcified chelae of thalassinoideans are commonly preserved. The excellent preservation of the venter and appendages of *A. cornishorum*, *P. triangulum*, and *M. marcusana* supports the suggestion that the fossils experienced little reworking by depositional processes. Other supporting evidence includes one carapace of *Trichopeltarion berglundorum* and two carapaces of *M. marcusana* which are extremely well preserved, including nearly complete lateral spines and carapace morphology. Associated pelecypods are often articulated and gastropods are commonly unbroken.

However, several factors suggest that there was at least some degree of reworking and possible mixing of faunas in the depositional environment. Two specimens of *Mursia marcusana* and one specimen of *Trichopeltarion berglundorum* are preserved only as carapace fragments. Several specimens of *Portunites triangulum* are preserved as carapace fragments, and all of the specimens of *Macrocheira teglandi* are preserved as carapace fragments or broken carapaces. Many specimens of *Callianopsis clallamensis* and most of the other thalassinoid specimens are broken or incomplete. In some cases, associated pelecypods were broken or disarticulated and gastropods sometimes were broken, especially at the apex or near the aperture.

Additionally, many concretions, especially those collected from the RB18 locality, contain large quantities of dispersed organic material appearing to be mainly plant remains. This suggests that there were at least periodic influxes of organic matter from nearshore environments. The RB37 locality was the site of recovery of large blocks of siltstone that contain numerous decapods and molluscs and a large amount of organic material, mostly wood and leaves. Decapods, including *Portunites triangulum*, *Mursia marcusana*, and *Asthenognathus cornishorum*, and molluscs collected from this siltstone are preserved on bedding planes, flattened, and in some cases are crushed. Also preserved in the siltstone are a large number of what appear to be juvenile decapods, possibly of the species *Portunites triangulum*. The siltstone occurred as float in the intertidal zone, so it is not positive that the blocks originated in the Pysht Formation. However, several factors indicate that they did. First, the blocks contain decapods that are similar to those collected from other Pysht Formation localities. Second, the blocks contain large quantities of plant material and organic matter, and similar material is found at other localities of the Pysht Formation, albeit in smaller quantities. Third, the blocks are composed of well-indurated grey siltstone, and the other Pysht localities also contain grey siltstone, although it is less well-indurated. The siltstone blocks could represent a storm deposit, including a mix of plant material from nearshore environments and decapods and molluscs from both shallow- and deep-water environments.

Since the Pysht Formation contains evidence of quiet-water depositional conditions as well as evidence of some reworking of specimens, it is quite possible that elements of both conditions existed during Pysht Formation deposition. Possibly the depositional environment was primarily quiet with moderately rapid sedimentation, which is characteristic of steep and tectonically active continental slopes such as the northwest coast of North America. The excellent preservation of the carapace material of some of the decapod specimens suggests rapid sedimentation in the depositional area facilitating rapid burial of specimens. This could account for well-preserved decapod specimens. Periodic storm, seismic, or other catastrophic events could account for fragmentation of some decapod specimens and for deposits composed of large quantities of organic material and flattened decapods and molluscs. Periodic catastrophic events could also have facilitated downslope mixing of shallow- and deep-water fauna, thus accounting for the presence of species of the shallow-water genus *Asthenognathus* with a preponderance of species of deep-water genera such as *Callianopsis*, *Trichopeltarion*, *Mursia*, and *Macrocheira*.

Callianopsis clallamensis is by far the most abundant taxon of the decapod fauna of the Pysht Formation, with more than 90 individuals of that species having been collected (Hopkins and Feldmann, 1997). Relative abundances of decapod taxa could be related to preservation potential of each decapod taxon; however, note that thalassinoideans such as *C. clallamensis* are typically poorly preserved. It is likely that this taxon was both abundant and living under conditions favorable for excellent preservation. The burrowing habit of thalassinoideans would likely improve preservation potential of both molts and corpses, especially if the depositional area received large amounts of sedimentation to quickly fill and bury burrows. Since burial of the carapace would essentially be accomplished immediately after molting or death, it would be likely that specimens could be extremely well preserved and in great quantity. This is the case with the material in this study. Numerous burrows were observed in outcrops of the Pysht Formation, aligned both horizontally and vertically with respect to bedding, and some burrows were observed to contain fragments of thalassinoideans. However, most of the decapods were preserved in concretions, not burrows.

Other decapod taxa are represented by far fewer specimens. For instance, *Trichopeltarion berglundorum* is known from only two specimens and *Asthenognathus cornishorum* from only three. *Portunites triangulum* is known from eight specimens in addition to numerous tiny specimens that appear to be juveniles preserved on a bedding plane of siltstone associated with large quantities of or-

Table 10.—*Bathymetric range for Recent genera that have fossil representatives in the Pysht Formation and Quimper Sandstone.*

Decapod taxa	Depth in meters
Callianopsis sp.	350–650
Mursia spp.	25–730
Trichopeltarion spp.	0–1650
Macrocheira sp.	50–300
Asthenognathus spp.	8–70

ganic material. All other decapod taxa from the Pysht Formation are known from ten or fewer specimens. It is plausible that decapods other than *Callianopsis clallamensis* inhabited areas of the open shelf that were not necessarily conducive to rapid burial of corpses or molts and were therefore less often preserved. Specimens could have been disarticulated, swept away by currents, or ingested by scavengers before burial could occur. Probable swimmers, such as *Portunites triangulum*, would have likely inhabited more open water environments than thalassinoideans, which would have decreased their relative preservation potential. It is also possible that the relative abundances of the other decapod taxa preserved in the Pysht Formation were simply much lower than that of *C. clallamensis*.

Taphonomy of Quimper Sandstone Decapods

Specimens of *Macrocheira longirostra* consist only of carapaces, suggesting that they are molts. The cuticle is extremely well preserved, and all specimens are preserved in concretions, but all of the specimens are broken. This suggests that the specimens experienced at least some reworking during or after deposition. The Quimper Sandstone has been reported to have been initially deposited in a shallow-water, high-energy environment that subsequently deepened, resulting in deposition below wave base (Babcock et al., 1994). It is unknown whether the specimens were collected in the lower or upper part of the Quimper Sandstone; however, either condition could easily result in reworked fossil specimens. In either case, the taphonomy of the fossils does not suggest depositional conditions different than those previously reported for the Quimper Sandstone.

Bathymetry of the Pysht Formation

The bathymetric ranges for extant genera with congeners in the Pysht Formation show that the depositional environment of the Pysht Formation was more likely to be moderately deep than shallow (Table 10). The depth ranges for *Mursia* (Table 3), *Trichopeltarion* (Table 4), and *Macrocheira* overlap between depths of 50–300 m. The two genera *Callianopsis* and *Asthenognathus* fall outside of this range. The sole modern species of *Callianopsis* is found at depths of 350–650 m, slightly deeper than the 50–300 m range. Modern species of *Asthenognathus* inhabit a depth range of 8–70 m, which overlaps the shallow end of the range for *Mursia*, *Trichopeltarion*, and *Macrocheira*. However, the preponderance of the evidence corroborates the depth previously reported for the Pysht Formation. As has been discussed, mollusc and foraminiferal assemblages indicate that the Pysht Formation was initially deposited at bathyal depths of 300–1830 m (Rau, 1964), and subsequently shallowed to inner sublittoral depths, probably an outer-shelf environment, near the end of deposition of the formation (Addicott, 1976). The only genus that does not support this conclusion is *Asthenognathus*, species of which currently inhabit shallow-water inner- to middle-shelf environments. It is possible that this genus inhabited deeper waters in the past, rendering comparison with modern congeners inappropriate. It is also possible that the occurrence of *Asthenognathus* is a result of downslope mixing of a shallower-water taxon with deep-water taxa. It is more likely that the shallow-water genus *Asthenognathus* would be mixed with deeper-water genera as a result of downslope mixing than is a scenario where the deeper-water genus *Callianopsis* would be mixed with shallower-water genera, unless all the genera were washed downslope to the depth at which *Callianopsis* lived.

Bathymetry of the Quimper Sandstone

The depositional environment of the Quimper Sandstone is believed to initially have been an inner shelf in "upper sublittoral to sublittoral" conditions (Durham, 1942, 1944; Armentrout and Berta, 1977:225) that subsequently deepened to "sublittoral to upper bathyal depths" (Armentrout and Berta, 1977:225). The decapod species from this formation, *Macrocheira longirostra*, has a modern congener that inhabits depths of 50–300 m, which corroborates the previously reported depth for the Quimper Sandstone.

Paleobiogeography

Five of the decapod species of the Pysht Formation, including *Callianopsis clallamensis*, *Mursia marcusana*, *Trichopeltarion berglundorum*, *Macrocheira longirostra*, and *Asthenognathus cornishorum*, have Recent congeners that are known primarily or exclusively from the Pacific Ocean. Two species of presumably extinct genera of the Pysht Formation, including *Callianassa* sensu lato cf. *C. porterensis* and *Callianassa* sensu lato sp. 2 are known only from that formation, and one species, *Portunites triangulum*, is from an extinct genus known from both the Atlantic and Pacific oceans. The decapod from the Quimper Sandstone is known only from the Pacific Ocean. Three of the species from the Pysht Formation are members of genera that have been reported from high middle latitudes, including *Portunites*, *Macrocheira*, and *Callianopsis*. The genera *Trichopeltarion*, *Mursia*, and *Asthenognathus* are known from tropical, subtropical, and middle latitudes.

Five of the species herein described from the Pysht Formation were previously known from Oligocene rocks of Washington, including *Callianopsis clallamensis*, *Callianassa* sensu lato cf. *C. porterensis*, *Mursia marcusana*, *Portunites triangulum*, and *Macrocheira teglandi* (Rathbun, 1926). *Asthenognathus* was previously unknown from the Pacific Coast of North America, and only one extant species of *Trichopeltarion* was previously known from the Pacific Coast of North America. The genus *Macrocheira* was not previously known from the Quimper Sandstone. The species *Callianassa* sensu lato sp. 2 was not previously known from the Pacific Coast of North America, but it is not possible to comment on generic distribution of this species since generic placement of the species is unknown at this time.

The sole extant species of the genus *Callianopsis* is known from the west coast of North America from Alaska to Baja California (Rathbun, 1902). Fossil species are known from the upper Eocene to lower Oligocene and early to early middle Miocene of Japan (Karasawa, 1993; Kato and Karasawa, 1994). The species *Cal-*

lianopsis clallamensis (Withers) has been reported from the late Oligocene to early Miocene Pysht Formation of northwestern Washington (Hopkins and Feldmann, 1997). It seems reasonable to suggest that the genus arose in the Eocene, perhaps in the western Pacific, and was subsequently dispersed to other North Pacific localities.

Two genera from the Pysht Formation, *Mursia* and *Trichopeltarion*, are cosmopolitan in distribution (Tables 3 and 4, respectively). The earliest known occurrences of both genera are from Pacific localities. Three species of *Mursia* are known from the Oligocene and several Miocene species have been reported from central Europe and Japan (Table 3). It appears that this genus may have arisen in the eastern Pacific during the Oligocene and was subsequently dispersed to its current range (Table 3). Faunal exchange between the Pacific and Atlantic oceans could have occurred through the incomplete isthmus connecting North and South America until three to five million years ago (Briggs, 1987), accounting for dispersal of the genus into the Atlantic Ocean.

The genus *Trichopeltarion* is herein reported from the late Oligocene to early Miocene Pysht Formation. Other fossil species have been reported from Miocene deposits of Japan, Fiji, and New Zealand (Table 4). At this time it is not possible to comment on whether or not the new species of *Trichopeltarion* recovered from the Pysht Formation is the earliest known occurrence of that genus, because detailed and accurate stratigraphy and age of the collecting localities of *T. berglundorum* in the Pysht Formation are currently unknown. It appears that the genus arose during the Oligocene in the Pacific and was subsequently distributed to its current range throughout the entire Pacific and Indian oceans as well as localities in the Atlantic Ocean. As mentioned, faunal exchange between the Pacific and Atlantic oceans could have occurred through the incomplete Isthmus of Panama, accounting for the presence of species of *Trichopeltarion* in the Gulf of Mexico and Ivory Coast on the west coast of Africa.

The genus *Portunites* appears to have arisen in the early Eocene and interestingly, all occurrences of the genus are from high middle latitudes of the Northern Hemisphere (Table 7). Karasawa (1993) suggested that the genus has a Tethyan distribution. If this were the case, occurrences would be expected from Asia, India, South Pacific islands, and China, and confirmation of that hypothesis must await collection of more fossil material. Since species of the genus are currently known only from high middle latitudes, it might be expected that species of *Portunites* recovered from Tethyan areas would inhabit deep, cool water since the Tethys is closer to the subtropics than the localities at which species of the genus have previously been collected.

The new species *Macrocheira longirostra* marks the earliest known occurrence of the genus, having been collected from the late Eocene Quimper Sandstone. This suggests that the genus may have arisen in the Eocene in the eastern Pacific and been dispersed subsequently across the Pacific to Japan, where the sole extant species is currently found. Species of this genus, in addition to *Portunites*, are known solely from high middle latitude localities in the Northern Hemisphere, suggesting that species of the genus may have had difficulty surviving equatorial conditions during east–west dispersal in the Pacific Ocean unless they inhabited extremely deep environments. West–east dispersal of the genus would accommodate its apparent preference for high middle latitudes in the North Pacific, but the fossil record does not support this hypothesis at this time.

The genus *Asthenognathus* is known from Recent localities in France, Japan,

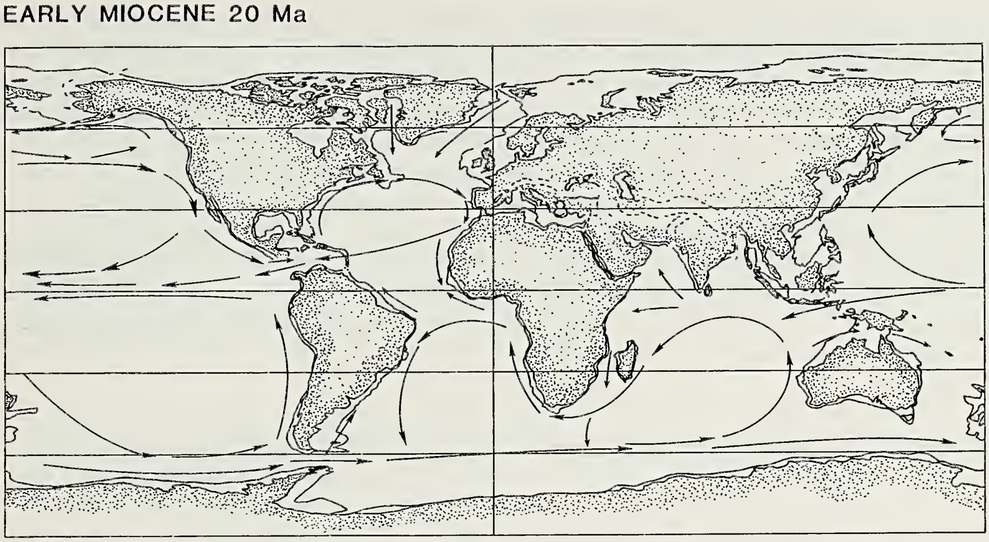

EARLY MIOCENE 20 Ma

Fig. 16.—Paleocirculation patterns for the late Oligocene depicted on an early Miocene map. Circulation patterns from B. U. Haq *in* J. P. Kennett (1982:726, fig. 19–16).

the Gulf of Siam, and the coast of northwest Africa. The latter two localities are near the subtropics, as opposed to many other decapod genera reported from the Pysht Formation which are known from high middle latitudes. The species referred here to *Asthenognathus* marks one of the earliest known occurrences of it with another species known from the Miocene of Japan. It seems reasonable to suggest that the genus may have arisen during the late Oligocene or early Miocene in the northeastern Pacific and subsequently been distributed, perhaps along equatorial currents, to localities in the southern Pacific and Japan. The genus could have been distributed to the Atlantic through the incomplete Isthmus of Panama or from the Indian Ocean around the southern tip of Africa to its Recent localities along the coast of northwest Africa. Alternatively, the genus may have arisen in the western Pacific and been subsequently dispersed to North America and other localities.

Perhaps the most important aspect of the assemblage of decapods of the Pysht Formation is the striking affinity with the Miocene decapod fauna of Japan. Every decapod species described from the Pysht Formation, with the exception of *Callianassa* sensu lato cf. *C. porterensis* and *Callianassa* sensu lato sp. 2. Five of the decapod taxa described from the Pysht Formation have extant congeners in the Pacific Ocean. This suggests that decapods were being freely dispersed between the east and west Pacific at least as early as the middle Tertiary and that evidence of this dispersal is preserved in the Recent fauna.

The similarity between the decapod fauna of the Pysht Formation and that of the Cenozoic of Japan suggests that a distinctive North Pacific decapod fauna developed as early as the late Eocene (Fig. 16). Decapod faunal affinities of Cretaceous and Paleogene localities in the Southern Hemisphere, including Antarctica, South America, and New Zealand, have been discussed by Feldmann et al. (1995), and it appears that broad faunal affinities also existed in the North Pacific as well. For example, faunal affinities exist between the middle Eocene

Manda Group decapod fauna of Japan and the lower Tertiary decapod fauna of Prince William Sound, Alaska. The genera *Raninoides*, *Portunites*, and *Branchioplax* each have species present in both faunas. In addition, the Eocene Hoko River Formation, which is part of the Twin River Group, possesses decapod genera including raninids and goneplacids, which may upon further study provide evidence of faunal similarity between the Japanese decapod fauna and the North American decapod fauna (Tucker, personal communication).

The Cenozoic decapod fauna described from Japan appears to be more diverse in terms of numbers of genera and species than the Cenozoic decapod fauna of the Northwest Coast of North America. However, research on currently unstudied specimens of the Twin River Group and other formations from Washington and Oregon may change that interpretation in the future (Tucker, personal communication).

Two of the species described from the Pysht Formation, *Macrocheira teglandi* and *Asthenognathus cornishorum*, have extant congeners inhabiting Japan but not the Pacific Coast of North America. *Mursia marcusana* and *Trichopeltarion berglundorum*, have extant congeners in both Japan and the Pacific Coast of North America. However, note that the apparent closest living relative of *M. marcusana*, *M. armata*, inhabits the seas of Japan. *Callianopsis clallamensis* has a recent congener from the Pacific Coast of North America and not Japan. Several possibilities for explaining this phenomenon exist. Perhaps the coast of Japan currently provides an environment more tolerable today for species of some genera found in the Pysht Formation than does the modern Pacific Coast of North America. Fossil species of Pysht genera may have originated in the eastern Pacific and been subsequently dispersed to Japan, where they were better able to thrive into the Recent. Conversely, fossil species may have originated in Japan and been dispersed to the eastern Pacific, where they lived until conditions became unsuitable. In the case of *Callianopsis*, it appears that the depositional environment of the Pysht Formation, a deep, cool continental shelf or slope, is almost identical to environments that the modern species now inhabits.

SUMMARY AND CONCLUSIONS

This study of the decapod fauna of the Pysht Formation first mentioned in 1926 by Rathbun has resulted in emended descriptions for four previously described taxa, *Mursia marcusana*, *Macrocheira teglandi*, *Portunites triangulum*, and *Callianassa* cf. *C. porterensis*, and descriptions of three previously undescribed taxa, *Trichopeltarion berglundorum*, *Asthenognathus cornishorum*, and *Callianassa* sensu lato sp. 2. One new decapod species from the Quimper Sandstone has been described, *Macrocheira longirostra*. The lower part of the Pysht Formation has been reported to have been deposited at depths of 300–1830 m but subsequently shallowed to inner sublittoral depths, and the Quimper Sandstone has been reported to have been initially deposited in littoral to sublittoral conditions that subsequently deepened to sublittoral to upper bathyal depths. Environmental and depth information on extant congeners of decapods from both the Pysht Formation and the Quimper Sandstone corroborate the previously reported depth and depositional environments for both formations.

The decapod fauna of the Pysht Formation and the Quimper Sandstone is remarkably similar to the decapod fauna of the Cenozoic of Japan. That similarity, along with the fact that five of the decapod species of the Pysht Formation have

Recent congeners in the Pacific Ocean, suggests that a distinctive decapod fauna developed in the North Pacific Ocean as early as the late Eocene and that evidence of this fauna persists into Recent times.

ACKNOWLEDGMENTS

R. E. and M. Berglund donated most of the material for this study and assisted in the field. J. and G. Goedert and J. and G. Cornish donated material to this study. A. B. Tucker and R. A. and B. J. Schweitzer assisted in the field. R. B. Manning, U. S. National Museum of Natural History, provided helpful comments regarding thalassinoid and pinnotherid taxa. A. H. Coogan, N. A. Wells, and two anonymous reviewers read earlier drafts of the manuscript and their comments improved it substantially. The Amoco Alumni Scholarship Fund partially funded fieldwork for Schweitzer. K. Smith, Department of Geology, Kent State University, assisted with word processing.

LITERATURE CITED

ADDICOTT, W. A. 1976. New molluscan assemblages from the upper member of the Twin River Formation, western Washington: Significance in Neogene chronostratigraphy. Journal of Research of the U. S. Geological Survey, 4:437–447.

ALCOCK, A. 1895. Materials for a carcinological fauna of India. No. 1. The Brachyura Oxyryncha. Journal of the Asiatic Society of Bengal, 64:157–291.

ALCOCK, A. A., AND A. R. S. ANDERSON. 1899. Natural history notes from the H. M. Royal Indian Marine Survey Ship "Investigator," Commander T. H. Heming, R. N. commanding. Series III. No. 2. An account of the deep-sea Crustacea dredged during the surveying season of 1897–1898, 7:1–27, 278–292.

ARMATO, P. J. 1993. Structure and habitat associations in molluscan assemblages from the Pysht and Clallam formations, Olympic Peninsula, Washington. Unpublished M. S. Thesis, Western Washington University, Bellingham, Washington.

ARMENTROUT, J. M., AND A. BERTA. 1977. Eocene–Oligocene foraminiferal sequence from the northeast Olympic Peninsula, Washington. Journal of Foraminiferal Research, 7:216–233.

ARNOLD, R., AND H. HANNIBAL. 1913. The marine Tertiary stratigraphy of the North Pacific coast of America. Proceedings of the American Philosophical Society, 52:559–605.

BABCOCK, R. S., C. A. SUCZEK, AND D. C. ENGEBRETSON. 1994. The Crescent "Terrane," Olympic Peninsula and southern Vancouver Island. Pp. 141–157, *in* Regional Geology of Washington State (R. Lasmanis and E. S. Cheney, eds.). Washington Division of Geology and Earth Resources Bulletin 80.

BELL, T. 1858. A monograph of the fossil malacostracous Crustacea of Great Britain, Part. 1, Crustacea of the London Clay. Palaeontographical Society, London, Great Britain.

BERGLUND, R. E., AND J. L. GOEDERT. 1992. A new species of *Cancer* (Decapoda: Brachyura) from the Miocene Astoria Formation in Washington. Burke Museum Contributions in Anthropology and Natural History, 9.

BOCQUET, C. 1963. Remarques morphologiques et systématiques sur le crabe *Tritodynamia atlantica* (Th. Monod) (= *Asthenognathus atlanticus* Th. Monod) présent dans la région de Roscoff. Cahiers de Biologie Marine, 4:65–79.

BRIGGS, J. C. 1987. Biogeography and Plate Tectonics. Elsevier, New York, New York.

BROWN, R. D., JR., AND H. D. GOWER. 1958. Twin River Formation (redefinition), northern Olympic Peninsula, Washington. Bulletin of the American Association of Petroleum Geologists, 42:2492–2512.

DANA, J. D. 1849. Geology. United States Exploring Expedition during the Years 1838, 1839, 1840, 1841, 1842, under the Command of Charles Wilkes, U. S. N. Volume X. Philadelphia, Pennsylvania.

———. 1852. Macroura. Conspectus Crustaceorum &. Conspectus of the Crustacea of the Exploring Expedition under Capt. C. Wilkes, U. S. N. Proceedings of the Academy of Natural Sciences of Philadelphia, 6:10–28.

DE HAAN, W. 1833–1850. Crustacea. Pp. 1–243, pl. A–Q, 1–55, circ. Table 2, *in* Fauna Japonica sive Descriptio Animalium, Quae in Itinere per Japoniam, Jussu et Auspiciis Superiorum, qui Summum in India Batava Imperium Tenent, Suscepto, Annis 1823–1830 Collegit, Notis, Observationibus et Adumbrationibus Illustravit, (P. F. Siebold). A. Arnz (Lugdunum Batavorum), Amsterdam, The Netherlands.

DE SAINT LAURENT, M. 1973. Sur la systématique et la phylogénie des Thalassinidea: Définition des familles des Callianassidae et des Upogebiidae et diagnose de cinq genres nouveaux (Crustacea Decapoda). Comptes Rendus Hebdomadaires des Séances de l'Académie des Sciences, Paris (Séries D), 277:513–516.

DE SAINT LAURENT, M., AND P. LE LOEUFF. 1979. Upogebiidae et Callianassidae. Crustacés Décapodes Thalassinidea, 1. Campagnes de la *Calypso* au large des côtes Atlantiques africaines (1956 et 1959) (suite), 22. Résultats Scientifiques des Campagnes de la *Calypso*, 11:29–101.

DELL, R. K. 1969. A new Pliocene fossil crab of the genus (*Trichopeltarion*) from New Zealand. Records of the Canterbury Museum, 8:367–371.

DESMAREST, A. G. 1823. Malacostracés: Dictionnaire des Sciences Naturelles, Volume 28. F. G. Levrault, Paris, France.

DURHAM, J. W. 1942. Notes on Pacific Coast Galeodeas. Journal of Paleontology, 16:183–191.

———. 1944. Megafaunal zones of the Oligocene of northwestern Washington. University of California Publications, Department of Geological Sciences Bulletin, 27:101–211.

FELDMANN, R. M., AND I. W. KEYES. 1992. Systematic and stratigraphic review with catalogue and locality index of the Mesozoic and Cenozoic decapod Crustacea of New Zealand. New Zealand Geological Survey Record, 45:1–73.

FELDMANN, R. M., AND P. A. MAXWELL. 1990. Late Eocene decapod Crustacea from North Westland, South Island, New Zealand. Journal of Paleontology, 64:779–797.

FELDMANN, R. M., A. B. TUCKER, AND R. E. BERGLUND. 1991. Paleobathymetry of decapod crustaceans, Washington. National Geographic Research and Exploration, 7:352–363.

FELDMANN, R. M., S. CASADIO, L. CHIRINO-GALVEZ, AND M. AGUIRRE-URRETA. 1995. Fossil decapod crustaceans from the Jaguel and Roca formations (Maastrichtian–Danian) of the Neuquén Basin, Argentina. Journal of Paleontology, 69 (supplement to number 5).

GABB, W. M. 1864. Description of the Cretaceous Fossils. Geological Survey of California: Palaeontology. Volume 1, Section 4.

GALIL, B. S. 1993. Crustacea Decapoda: A revision of the genus *Mursia* Desmarest, 1823 (Calappidae). Pp. 347–379, *in* Resultats des Campagnes MUSORSTOM, Volume 10 (A. Crosnier, ed.). Mémoires du Muséum National d'Histoire Naturelle 156.

GARTH, J. S., AND J. HAIG. 1971. Decapod Crustacea (Anomura and Brachyura) of the Peru–Chile Trench. Pp. 3–19, *in* Scientific Results of the Southeast Pacific Expedition (E. Chin ed.). Anton Bruun Reports, 6. Texas A and M University Marine Laboratory, Galveston, Texas.

GLAESSNER, M. F. 1960. The fossil decapod Crustacea of New Zealand and the evolution of the Order Decapoda. New Zealand Geological Survey Paleontological Bulletin 31.

———. 1969. Decapoda. Pp. R399–R533, *in* Treatise on Invertebrate Paleontology, Part R, Arthropoda 4(2) (Raymond C. Moore, ed.). Geological Society of America and University of Kansas Press, Lawrence, Kansas.

GRIFFIN, D. J. G., AND H. A. TRANTER. 1986. The Decapoda Brachyura of the Siboga Expedition. Part VIII. Majidae. Siboga Expedition Monographe 39.

GUINOT, D. 1977. Propositions pour une nouvelle classification des crustacés décapodes brachyoures. Compte Rendu, Academie Science Paris (D), 285:1049–1052.

———. 1986. Une nouvelle espèce du genre *Trachycarcinus*, *T. crosnieri* sp. nov., de Madagascar (Crustacea Decapoda Brachyura). Bulletin de Muséum National d'Histoire Naturelle, Paris, (Série 4), 7, 1985(1986), sect. A (4):805–817.

———. 1989. Les genres *Trachycarcinus* Faxon et *Trichopeltarion* A. Milne Edwards (Crustacea, Brachyura, Atelecyclidae). Pp. 347–385, *in* Résultats des Campagnes *Musorstom*, 5 (J. Forest, ed.). Mémoires de Muséum National d'Histoire Naturelle, (A) 144.

HESSLER, R. R. 1969. Peracarida. Pp. R360–R393, *in* Treatise on Invertebrate Paleontology, Part R, Arthropoda 4 (R. C. Moore, ed.). Geological Society of America and University of Kansas Press, Lawrence, Kansas.

HOPKINS, C. S., AND R. M. FELDMANN. 1997. Sexual dimorphism in fossil and extant species of *Callianopsis* de Saint Laurent. Journal of Crustacean Biology, 17:236–252.

IMAIZUMI, R. 1952. *Mursia takahashii* n. sp. (Brachyura) from Goishi in the Sendai area. Tohoku University, Institute of Geology and Paleontology Short Papers, 4:88–95.

KALER, K. L. 1989. Another cetacean (whale) fossil from the Olympic Peninsula. Washington Geologic Newsletter, 17:16–17.

KARASAWA, H. 1989. Decapod crustaceans from the Miocene Mizunami Group, central Japan. Part 1. Superfamily Thalassinoidea, Leucosioidea, and Grapsidoidea. Bulletin of the Mizunami Fossil Museum, 16:1–28.

———. 1990. Decapod crustaceans from the Miocene Mizunami Group, central Japan. Part 2. Section Oxyryncha, Cancridea, and Brachyryncha. Bulletin of the Mizunami Fossil Museum, 17:1–33.

———. 1991. Decapod crustaceans from the Miocene Mizunami Group, central Japan. Part 3. Decapod crustacean assemblage, paleoecology, with descriptions of two species. Bulletin of the Mizunami Fossil Museum, 18:1–18.

———. 1992. Fossil decapod crustaceans from the Manda Group (Middle Eocene), Kyushu, Japan. Transactions and Proceedings of the Palaeontological Society of Japan, New Series, 167:1247–1258.

———. 1993. Cenozoic decapod Crustacea from southwest Japan. Bulletin of the Mizunami Fossil Museum, 20:1–92.

KARASAWA, H., T. SAKUMOTO, AND K. TAKAYASU. 1992. A new portunid genus *Itoigawaia* (Decapoda: Crustacea) from the Miocene of southwest Japan. Bulletin of the Mizunami Fossil Museum, 19: 455–457.

KATO, H., AND H. KARASAWA. 1994. *Minohellenus macrocheilus* sp. nov. (Decapoda: Crustacea) from the Oligocene Ashiya Group, Kyushu, Japan. Bulletin of the Kitakyushu Museum of Natural History, 13:51–58.

———. 1996. An additional record of *Minohellenus macrocheilus* Kato and Karasawa, 1994 (Crustacea, Decapoda, Portunidae). Bulletin of the Kitakyushu Museum of Natural History, 15:31–33.

KENNETT, J. P. 1982. Marine Geology. Prentice-Hall, Englewood Cliffs, New Jersey.

LASMANIS, R., AND R. E. BERGLUND. 1991. Tertiary crustaceans: Collecting localities in western Washington state. Rocks and Minerals, 66:330–334.

LATREILLE, P. A. 1803. Histoire naturelle, générale et particuliére, des crustacés et des insectes. Volume 6. F. Dufart, Paris, France.

———. 1831. Cours d'Entomologie, ou de l'histoire naturelle des Crustacés, des Arachnides, des Myriapodes et des Insectes, etc. Annales I. Atlas, Roret, Paris, France.

MACLEAY, W. S. 1838. On the brachyurous decapod Crustacea brought from the Cape by Dr. Smith. Pp. 53–71, *in* Illustrations of the Zoology of South Africa, Invertebrata (A. Smith, ed.). Smith, Elder, and Co., London, Great Britain.

MANNING, R. B., AND D. L. FELDER. 1991. Revision of the American Callianassidae (Crustacea: Decapoda: Thalassinidea). Proceedings of the Biological Society of Washington, 104:764–792.

MANNING, R. B., AND L. B. HOLTHUIS. 1981. West African Brachyuran Crabs (Crustacea: Decapoda). Smithsonian Contributions to Zoology, 306.

MIERS, E. J. 1886. Report on the Brachyura collected by H. M. S. *Challenger* during the years 1873–76. Report on the Scientific Results of the Voyage of H. M. S. *Challenger*, Zoology, 17.

MILNE EDWARDS, A. 1880. Études préliminaires sur les Crustacés, Première Partie. Pp. 1–68, *in* Reports on the Results of Dredging under the Supervision of Alexander Agassiz, in the Gulf of Mexico, and in the Caribbean Sea, 1877, '78,'79, by the U. S. Coast Steamer "Blake," Lieutenant-Commander J. R. Bartlett, U. S. N., Commanding. Bulletin of the Museum of Comparative Zoology at Harvard College, 8.

MILNE EDWARDS, H. 1832. Recherches sur l'organisation et la classification naturelle des Crustacés Décapodes. Annales des Sciences Naturelles. Zoologie et Biologie Animale, 25:298–332.

———. 1837. Histoire Naturelle des Crustacés, comprenant l'anatomie, la physiologie et la classification de ces animaux, volume 2. Roret, Paris, France.

MONOD, T. 1933. Brachyura maroccana, I. Pinnoteridae, avec description d'*Asthenognathus atlanticus* nov. sp. Bulletin de la Societé de Sciences Naturelle de Maroc, 12:142–155.

———. 1956. Hippidea et Brachyura ouest-africains. Mémoires de l'institut Français d'Afrique Noire, 45.

NAGAO, T. 1932. Two Tertiary and one Cretaceous Crustacea from Hokkaido, Japan. Journal of the Faculty of Science, Hokkaido Imperial University, 2:15–22.

OLSON, S. L. 1980. A new genus of penguin-like pelecaniform bird from the Oligocene of Washington (Pelecaniformes: Plotopteridae). Contributions in Science: Natural History Museum of Los Angeles County, 330:51–57.

ORTMANN, A. E. 1893. Die Decapoden-Krebse des Strassburger Museums. VII Teil. Abtheilung: Brachyura (Brachyura genuina Boas) II. Unterabtheilung: Cancroidea, 2. Section: Cancrinea, 1. Gruppe: Cyclemotopa. Zoologischen Jahrbuchern. Abtheilung für Systematic, Geographie und Biologie der Thiere, 7:411–495.

OVERSTREET, R. M. 1983. Metazoan symbionts of crustaceans. Pp. 156–250, *in* The Biology of Crustacea. Volume 6. Pathobiology (A. J. Provenzano, Jr., ed.). Academic Press, New York, New York.

QUAYLE, J. 1984. A new crab, *Portunites stintoni* (Crustacea, Decapoda) from the London Clay. Tertiary Research, 5:173–178.

RAFINESQUE, C. S. 1815. Analyse de la nature, ou tableau de l'univers et des corps organisés. Palermo, Italy.

RATHBUN, M. J. 1893. Descriptions of new genera and species of crabs from the west coast of North America and the Sandwich Islands. Proceedings of the U. S. National Museum, 16:223–260.

———. 1902. Descriptions of new decapod crustaceans from the west coast of North America. Proceedings of the United States National Museum, 24:885–905.

———. 1909. New crabs from the Gulf of Siam. Proceedings of the Biological Society of Washington, 22:107–114.

———. 1910. Brachyura: The Danish Expedition to Siam 1899–1900, V. Pp. 301–367, *in* Det Kongelige Danske Videnskabernes Selskabs Skrifter, 7. Raekke, Naturvidenskabelig og Mathematisk Afdeling, Volume 4. Copenhagen, Denmark.

———. 1916. Description of a new genus and species of fossil crab from Port Townsend, Washington. American Journal of Science, 41:344–346.

———. 1926. The fossil stalk-eyed crustacea of the Pacific slope of North America. U. S. National Museum, Bulletin 138.

———. 1930. The cancroid crabs of America of the families Euryalidae, Portunidae, Atelecyclidae, Cancridae, and Xanthidae. Smithsonian Institution, United States National Museum Bulletin 152.

———. 1937. The oxystomatous and allied crabs of America. United States National Museum Bulletin 166.

RAU, W. W. 1964. Foraminifera from the Northern Olympic Peninsula, Washington. Geological Survey Professional Paper 374-G.

REMY, J. M. 1960. Études paléontologiques et géologiques sur les Falaises de Fresco (Côte d'Ivoire) 2. Crustacés. Annales de la Faculté des Sciences, Université de Dakar, 5:55–64.

SAKAI, T. 1976. Crabs of Japan and the Adjacent Seas. Tokyo Kodansha Ltd., Tokyo, Japan.

SAMOUELLE, G. 1819. The Entomologist's Useful Compendium, or an Introduction to the Knowledge of British Insects, etc. London, Great Britain.

SCHMITT, W. L., J. C. MCCAIN, AND E. S. DAVIDSON. 1973. Decapoda I, Brachyura I, Family Pinnotheridae. Pp. 1–160, *in* Crustaceorum Catalogus Part 3 (H.-E. Gruner and L. B. Holthuis, eds.). Dr. W. Junk B. V., Den Haag, The Netherlands.

SNAVELY, P. D., JR. 1983. Peripheral rocks: Tertiary geology of the northwestern part of the Olympic Peninsula, Washington. Pp. 6–31, *in* The Tertiary Olympic Terrane, Southwest Vancouver Island and Northwest Washington: Geological Association of Canada, Mineralogical Association of Canada, Canadian Geophysical Union Field Trip Guidebook (J. E. Muller, P. D. Snavely, Jr., and R. W. Tabor, eds.). Geological Association of Canada, Victoria, British Columbia, Canada.

———. 1987. Tertiary geologic framework, neotectonics, and petroleum potential of the Oregon–Washington continental margin. Pp. 305–335, *in* Geology and Resources Potential of the Continental Margin of Western North America and Adjacent Ocean Basins—Beaufort Sea to Baja California (D. W. Scholl, A. Grantz, and J. G. Vedder, eds.). Circum-Pacific Council for Energy and Mineral Resources, Earth Science Series 6.

SNAVELY, P. D., JR., A. R. NIEM, AND J. E. PEARL. 1978. Twin River Group (upper Eocene to lower Miocene)—Defined to include the Hoko River, Makah, and Pysht Formations, Clallam County, Washington. U. S. Geological Survey Bulletin, 1457:111–120.

SNAVELY, P. D., JR., A. R. NIEM, N. S. MACLEOD, J. E. PEARL, AND W. W. RAU. 1980. Makah Formation—A Deep Marginal Basin Sequence of Late Eocene and Oligocene Age in the Northwestern Olympic Peninsula, Washington. Geological Survey Professional Paper 1162-B.

SQUIRES, R. L. 1989. Pteropods (Mollusca: Gastropoda) from Tertiary formations of Washington and Oregon. Journal of Paleontology, 63:443–448.

SQUIRES, R. L., AND J. L. GOEDERT. 1994. A new species of the volutid gastropod *Fulgoraria* (*Musashia*) from the Oligocene of Washington. The Veliger, 37:400–409.

STIMPSON, W. 1858. Crustacea Ocypodoidea: Prodromus descriptionis animalium evertebratorum, quae in Expeditione ad Oceanum Pacificum Septentrionalem, a Republica Federata missa, Cadwaladaro Ringgold et Johanne Rodgers Ducibus, observavit et descripsit, Pars V. Proceedings of the Academy of Natural Sciences Philadelphia, 1858:93–110 (pages 39–56 on separate).

TABOR, R. W., AND W. M. CADY. 1978. Geologic Map of the Olympic Peninsula: Map 8-994, U. S. Geologic Survey, Reston, Virginia.

TEMMINCK, C. J. 1836. Coup-d'oeil sur la faune des Iles de la Sonde et de l'Empire du Japon. Discours préliminaire destiné à la Fauna du Japon. Musée du Pays-Bas, Leiden, The Netherlands.

TUCKER, A. B. 1995. A systematic evaluation of fossil Raninidae from the Twin River Group, Olympic Peninsula, Washington, and a re-examination of the Raninidae. Unpublished Ph.D. Dissert., Kent State University, Kent, Ohio.

TUCKER, A. B., AND R. M. FELDMANN. 1990. Fossil decapod crustaceans from the lower Tertiary of the Prince William Sound region, Gulf of Alaska. Journal of Paleontology, 64:409–427.

WEAVER, C. E. 1942. The paleontology of the marine Tertiary formations of Oregon and Washington. University of Washington Publications in Geology 5.

WIEDER, R. W., AND R. M. FELDMANN. 1989. *Palaega goedertorum*, a fossil isopod (Crustacea) from late Eocene to early Miocene rocks of Washington state. Journal of Paleontology, 63:73–80.

WILLIAMS, A. B. 1984. Shrimps, Lobsters, and Crabs of the Atlantic Coast of the Eastern United States, Maine to Florida. Smithsonian Institution Press, Washington, D. C.

WITHERS, T. H. 1924. Some decapod crustaceans (*Callianassa* and *Ranina*) from the Oligocene of Washington state, U.S.A. Annals and Magazine of Natural History, 14:121–127.

YOKOYA, Y. 1928. Report of the biological survey of Mutsu Bay. 10. Brachyura and crab-shaped Anomura. Scientific Report of Tohoku Imperial University, Series 4, 3:757–784.

ANNALS OF CARNEGIE MUSEUM

VOL. 68, NUMBER 4, PP. 275–287 18 NOVEMBER 1999

ARCHAEOLOGY OF TRANTS, MONTSERRAT. PART 5. PREHISTORIC AVIFAUNA

KELLEY R. REIS[1]

DAVID W. STEADMAN[2]

ABSTRACT

We report identifications of 225 bird bones from the Trants site, Montserrat, Lesser Antilles. The site was occupied by Saladoid peoples from ca. 500 BC to AD 400. The prehistoric bird assemblage represents 11 species and is dominated by pigeons, doves, and large passerines that probably were used as food by Saladoid peoples. The species of columbid found most commonly at Trants today (*Zenaida aurita*, characteristic of second-growth forest and edges) is uncommon in the bone assemblage, whereas bones of two other columbids not found at the site today (*Columba squamosa* and *Geotrygonmystacea*, both forest dwellers) are common. This suggests more forested conditions near Trants when Saladoid peoples occupied the site Three species of birds recorded from Trants (*Puffinus lherminieri*, *Porphyrio martinicus*, *Amazona* sp.) no longer occur on Montserrat. As on other West Indian islands, the avifauna of Montserrat has lost species to anthropogenic habitat destruction and predation by humans and introduced species. Catastrophic volcanic activity since 1995 has destroyed or degraded much of Montserrat's terrestrial ecosystems, undoubtedly with additional major negative impacts on the avifauna.

KEY WORDS: Montserrat, Saladoid, zooarchaeology, bird, human impact, faunal change

INTRODUCTION

Montserrat is a small (102 km^2), mountainous, volcanic island in the Lesser Antilles between 16°40′ and 16°49′ N latitude and 62°09′ and 62°15′ W longitude (Fig. 1). The nearest major islands are Antigua (43 km NE) and Guadeloupe (64 km SE). Montserrat is made up of seven coalesced volcanoes, three of which dominate the landscape; Silver Hill (north), Centre Hills (central), and Soufrière Hills (south). The rocky soils consist of protosols, young soils, latosolics, and smectoid clays (Lang, 1967). The youthful volcanic landscape of Montserrat has "few mangrove swamps, no significant estuaries, and limited sandy beaches" (Steadman et al., 1984*b*). Instead, rocky cliffs line the coast around most of the island. Steep inland ravines (called "ghauts") have been formed by streams through radial drainage from the volcanic mountains.

Large portions of the mountain slopes on Montserrat were cultivated by Europeans from the 17th to 19th centuries (Beard, 1949; Fergus, 1994). The high elevations of Soufrière and Centre hills had been dominated this century by secondary rainforest until the latest round of large-scale volcanic activity that began on 18 July 1995 (Montserrat Volcano Observatory Team, 1997). This activity, centered at Chance Peak in Soufrière Hills, continues in early 1998 and has destroyed or damaged most of Montserrat's forests.

Trants, a Saladoid occupation site on the eastern (windward) side of Montserrat, is the largest pre-Columbian site on the island (Watters, 1994). It is near sea level

---

[1] Department of Zoology, University of Florida, Gainesville, Florida 32611, USA. kreis@zoo.ufl.edu

[2] Florida Museum of Natural History, University of Florida, Gainesville, Florida 32611, USA. steadman@flmnh.ufl.edu

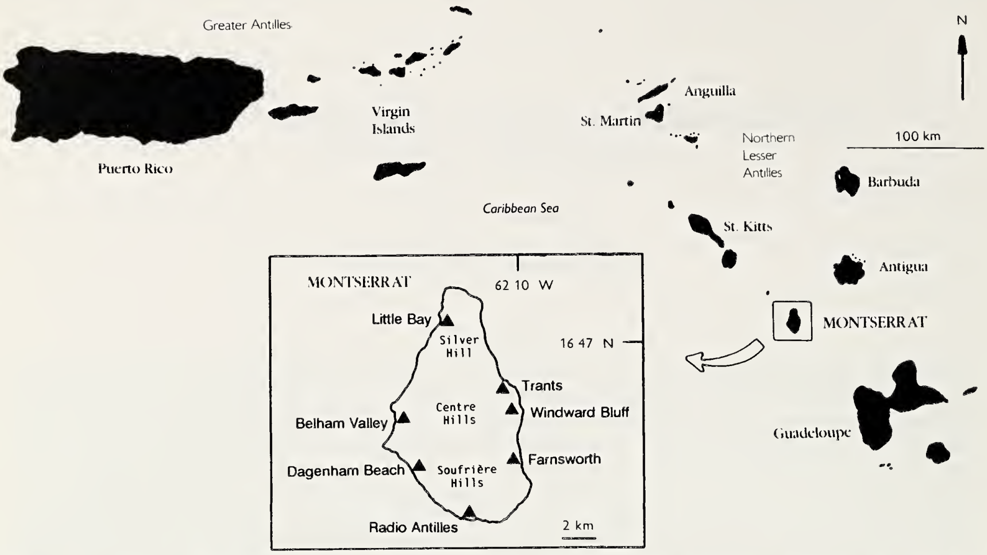

Fig. 1.—Islands of the West Indies, their relationship to Montserrat, and the location of Trants archaeological site (MS-G1). Two localities mentioned in the text are not depicted for lack of space. Chances Peak is a high peak in the Soufrière Hills. Galway's Estate is on the southwest slope of Chances Peak, 1 km from the ocean.

and occupies relatively flat terrain between the formerly forested slopes of Soufrière and Centre hills (to the west and north, respectively) and the Atlantic coast to the east (Fig. 1). The total area of Trants (ca. 600,000 m^2) is dominated today by pastures, garden plots, and an airstrip (Watters, 1994; Petersen, 1996).

The Saladoid people originated in South America and dispersed nearly throughout the West Indies, settling in Montserrat ca. 500 BC (Rouse; 1992; Keegan, 1994; Watters, 1994; Petersen, 1996). They produced a distinctive white-on-red (WOR) painted and zone-incised-crosshatched (ZIC) ceramic ware that has been excavated from many archaeological sites in the West Indies (Petersen and Watters, 1991; Siegel, 1991; Watters, 1994; Petersen, 1996). The Saladoid people were horticulturists who raised drought-resistant root crops that supplied little or no protein to their diet (Wing, 1989). They also exploited a variety of marine and terrestrial animals. The many thousands of bones from Saladoid sites on Montserrat and elsewhere suggest that these people had a dramatic effect on populations of terrestrial vertebrates, especially birds and rodents (Steadman et al., 1984*b*; Pregill et al., 1994; Reitz, 1994).

MATERIALS AND METHODS

D. R. Watters and J. B. Petersen excavated the Trants site (MS-G1) in 1979 and 1990 (Petersen and Watters, 1991; Watters, 1994; Petersen, 1996). The bones excavated in 1979 were reported by Steadman et al. (1984*b*). The vertebrate remains and their corresponding data (taxon, element, length measurement, provenience number, and stratum) from the 1990 excavations were described by Reitz (1994). The bird bones analyzed herein were excavated in 1990 from three 1 × 1-m excavation units within the site's core area: N396E571, N421/22E645, and N596E571. Each unit consisted of four quadrants: samples from quadrants

1–3 were screened through ¼-in mesh and those from quadrant 4 were screened through ⅛-in mesh. The ⅛-in mesh yielded twice as many bones as were recovered using ¼-in mesh, although the minimum number of individuals (MNI) recovered from both mesh sizes was similar (Reitz, 1994).

Excavation units were divided into four strata that were removed in 10-cm increments. Stratum A represents a mixture of historic and prehistoric artifacts and included post-Columbian species (*Rattus* sp.). Strata B and C were deposited ca. AD 0–200 and 500–0 BC, respectively; they represent the Saladoid occupation of Trants (Petersen, 1996). Bone samples from Stratum D are so limited that they are included with those from Stratum C. All four strata were depicted by Pregill et al. (1994:fig. 10) and in greater detail by Petersen (1996:fig. 5–9).

Our identifications are based on comparisons with modern bird skeletons from the Florida Museum of Natural History, University of Florida (UF) and the United States National Museum of Natural History, Smithsonian Institution (USNM). Our evaluations of the modern status of birds on Montserrat are based upon Steadman's collections and observations during 24–30 January 1983, supplemented by Danforth (1939), Bond (1956), and Evans (1990). Sadly, the modern avifauna of Montserrat had not been surveyed adequately before the major volcanic activity began in 1995. Some of our inferences on the habitat preferences of landbirds are based in part on the more thoroughly surveyed avifauna of St. Kitts, a nearby volcanic island with fairly similar habitats (Steadman et al., 1997).

RESULTS

General Collections

Columbids (pigeons and doves) and large passerines (mostly thrashers and thrushes) dominate the prehistoric avifauna from Trants (Table 1). Of the 225 bones we identified, 121 (54%) represent columbids and 82 (36%) represent large passerines. Of the 95 bones identified from the 1979 excavations, 79% are columbids and 16% are large passerines. The largest species of columbid, *Columba squamosa*, is the most common species in Stratum C/D, whereas the medium-sized columbid, *Geotrygon mystacea*, is the most common species in Strata A and B. Among the passerines, two species of thrashers (*Margarops fuscus*, *M. fuscatus*) far outnumber all other taxa. Only a single species of seabird (*Puffinus lherminieri*) and only two aquatic species (*Gallinula chloropus*, *Porphyrio martinicus*) are represented.

The columbids and large passerines that dominate the Trants bird assemblage are granivores or frugivores that are very palatable to humans. All of the bird bones from Trants are associated with Saladoid artifacts and cultural features, indicating that they probably were used as food. Approximately 20% of the bones show signs of burning. The element representation and breakage patterns in the bone assemblage are typical of those for landbirds from prehistoric cultural contexts on oceanic islands (Steadman et al., 1990).

Taxonomic Accounts

Order Procellariiformes

Family Procellariidae

Puffinus lherminieri (Audubon's Shearwater)

Material.—Stratum B: unit N596E571—mandible.

Comments.—No populations of *Puffinus lherminieri* are known to breed on

Table 1.—*Bird bones identified from the excavations conducted in 1990 at the Trants site, Montserrat. Numbers represent the number of identified specimens (NISP). Stratum A contained a mixture of prehistoric and historic artifacts. Strata B and C/D represent Saladoid occupation. "1979 total" is the bones identified by Steadman et al. (1984*b*) from the excavations conducted in 1979. †, species no longer occurs on Montserrat. *, taxa not necessarily different from others listed more specifically; such taxa are not included in "Total species."*

	Stratum			NISP	
Species	A	B	C/D	1990 total	1979 total
†*Puffinus lherminieri*	—	1	—	1	—
Gallinula chloropus	—	—	—	—	4
†*Porphyrio martinicus*	—	1	1	2	—
Columba squamosa	5	2	28	35	12
Zenaida aurita	4	2	3	9	9
Columbina passerina	—	—	—	—	1
Geotrygon mystacea	22	24	17	63	28
*Columbidae sp.	4	4	6	14	25
†*Amazona* sp.	—	—	1	1	—
Margarops fuscus	5	6	14	25	6
Margarops fuscatus	2	10	26	38	8
Cinclocerthia ruficauda	—	4	1	5	1
Cichlherminia lherminieri	1	—	4	5	—
*Mimidae/Turdidae sp.	1	4	4	9	—
Icterus oberi	—	2	—	2	—
*Passeriformes sp.	3	5	6	14	1
Total bones	47	65	111	223	95
Total species	6	9	9	11	8

Montserrat or nearby islands today. The nearest sighting of *P. lherminieri* at sea was near Redonda in 1931 (Danforth, 1939). This seabird nests in burrows in soil or in crevices. Predation at the nests by humans and introduced mammals (cats and rats) and habitat destruction have depleted or eliminated populations of this small shearwater on many islands in the tropical Pacific (Steadman et al., 1990; Steadman and Pahlavan, 1992), and the West Indian islands of Anguilla, Antigua, Barbados, Barbuda, and Grenada (Brodkorb, 1963; Steadman et al., 1984*a*; Watters et al., 1984; Pregill et al., 1994).

Order Gruiformes

Family Rallidae

Porphyrio (*Porphyrula*) *martinicus* (Purple Gallinule)

Material.—Stratum B: unit N596E571—sternum. Stratum C/D: unit N396E571—humerus.

Comments.—*Porphyrio martinicus* occurs locally on most islands in the Greater Antilles but is only a stray in the Lesser Antilles except for a possible resident population on Guadeloupe (Bond, 1974; Evans, 1990). It typically inhabits shrubby wetlands but can wander from these areas. We are aware of no previous records from Montserrat. *Porphyrio martinicus* has been recorded as well from archaeological sites on Antigua, Barbados, Martinique, and St. Kitts (Steadman et al., 1984*a*; Watters et al., 1984; Pregill et al., 1994). None of these islands currently sustains populations of *P. martinicus*. Use of the genus *Porphyrio* rather than *Porphyrula* follows Steadman (1988).

Order Columbiformes

Family Columbidae

The identification of bones of West Indian columbids is difficult, with size often being the only potentially diagnostic feature in many skeletal elements (Olson and Hilgartner, 1982; Steadman et al., 1984*b*). The West Indian species of *Geotrygon* and *Zenaida* are often similar in size. Species of *Columba* and *Columbina* tend to be markedly large and small, respectively, making them more easily identified. Six species of columbids are reported to occur in modern times on Montserrat or nearby Lesser Antillean islands. They are, in descending order of size, *Columba squamosa*, *C. leucocephala*, *Geotrygon mystacea*, *Zenaida aurita*, *G. montana*, and *Columbina passerina*. *Columba leucocephala* has been recorded on Montserrat only through sight records by Bond (1961) and Steadman et al. (1984*b*); it may not have a resident population there today. *Geotrygon montana* occurs on nearby Antigua and Guadeloupe, but not on Montserrat.

Columba squamosa (Scaly-necked Pigeon)

Material.—Stratum A: unit N396E571—femur; unit N421/22E645—carpometacarpus, pedal phalanx; unit N596E571—coracoid, pedal phalanx. Stratum B: unit N596E571—sternum, coracoid. Stratum C/D: unit N421/22E645—four coracoids, two scapulae, three humeri, five ulnae, four radii, four carpometacarpi, two femora, three tibiotarsi, tarsometatarsus.

Comments.—*Columba squamosa* is more commonly found in humid forests but may also occur in drier, wooded lowlands. This species is not found at Trants today but occurred on forested slopes above the site before the recent volcanic activity. Steadman et al. (1984*b*) reported that *C. squamosa* was also common in January 1983 in the forested ghauts on Montserrat. *Columba squamosa* has been recorded as well from archaeological and paleontological sites on Puerto Rico, Antigua, Barbuda, Martinique, and St. Eustatius (Wetmore,1952; Brodkorb, 1971; Steadman et al., 1984*b*; Pregill et al., 1994; Maíz, 1996). Especially relative to *Geotrygon mystacea*, the bones of *C. squamosa* are much more common in Stratum C/D than in strata A or B. This may suggest a preference for, and overexploitation of, *C. squamosa* early in the cultural sequence at Trants. Being large and frugivorous probably added to the desirability and palatability of *C. squamosa.*

Zenaida aurita (Zenaida Dove)

Material.—Stratum A: unit N421/22E645—two humeri; unit N596E571—coracoid, tibiotarsus. Stratum B: unit N596E571—two scapulae. Stratum C/D: unit N396E571—humerus; unit N421/22E645—coracoid, tibiotarsus.

Comments.—*Zenaida aurita* is a medium-sized columbid that prefers disturbed or second-growth forests. It is found as well in or around clearings, mangroves, arid scrub, and cultivated regions. *Zenaida aurita* was the most common columbid in the vicinity of Trants in January 1983. This species seems to profit from human-caused habitat disturbances, as long as some trees and shrubs remain. *Zenaida aurita* has been recorded from archaeological and paleontological sites on Puerto Rico, Anguilla, Antigua, Barbuda, Martinique, and St. Eustatius (Wetmore, 1952; Brodkorb, 1971; Steadman et al., 1984*b*; Pregill et al., 1994; Maíz, 1996).

Geotrygon mystacea (Bridled Quail-dove)

Material.—Stratum A: unit N421/22E645—two sterna, five coracoids, scapula, two humeri, two ulnae, ulnare, carpometacarpus, femur, three tibiotarsi; unit N596E571—coracoid, scapula, two humeri. Stratum B: unit N396E571—three coracoids, scapula; unit N421/22E645—coracoid, femur, tarsometatarsus; unit N596E571—sternum, six coracoids, five scapulae, two humeri, two carpometacarpi, femur. Stratum C/D: unit N421/22E645—three coracoids, scapula, humerus, carpometacarpus, two femora, two tibiotarsi, four tarsometatarsi; unit N596E571—coracoid, scapula, femur.

Comments.—*Geotrygon mystacea* inhabits mature forests and woodlands. It is not found at Trants at present but occurred on forested slopes above the site in January 1983. Other prehistoric records of *G. mystacea* are from Antigua, Barbuda, and St. Eustatius (Pregill et al., 1994).

Columbidae sp.

Material.—Stratum A: unit N421/22E645—two carpometacarpi; unit N596E571—humerus, manus phalanx. Stratum B: unit N596E571—ulna, ulnare, two carpometacarpi. Stratum C/D: unit N421/22E645—four ulnae, two carpometacarpi.

Comments.—These bones are in the approximate size range of *Zenaida aurita* or *Geotrygon mystacea* but lack diagnostic features to identify them further.

Order Psittaciformes

Family Psittacidae

Amazona sp.

Material.—Stratum C/D: unit N421/22E645—humerus.

Comments.—This specimen, a humerus lacking the proximal end, is referred to *Amazona* rather than to the other West Indian genera of Psittacidae (*Ara*, *Aratinga*) by having these characters: fossa olecrani relatively shallow; condylus ventralis craniocaudally compressed; shaft more dorsoventrally expanded, especially in distal portion. Within *Amazona*, the humerus from Montserrat is much smaller than in any living Lesser Antillean species (Table 2). Instead it resembles, in size and qualitative features, the smaller species of *Amazona* that occur today in the Greater Antilles. The specimen from Montserrat is most similar overall to the humerus of *A. agilis* of Jamaica. The Puerto Rican Parrot, *A. vittata*, has been reported from prehistoric sites on Antigua (Pregill et al., 1994). A comprehensive understanding of the natural distribution and diversity of West Indian *Amazona* will require the discovery and study of bones from prehuman contexts on a variety of islands. Nevertheless, that small "Greater Antillean" forms of *Amazona* occur in prehistoric sites on Antigua and Montserrat suggests either that these parrots were being moved between islands prehistorically or that the small forms were indigenous to, but extirpated in, the Lesser Antilles.

Order Passeriformes

Family Mimidae

Mimids (mockingbirds and thrashers) dominate the passerine bone assemblage at Trants. Mimids are much larger than most other Lesser Antillean passerines. Our comparisons included skeletons of all larger passerines that occur on Mont-

Table 2.—*Measurements (in mm) of the humerus of West Indian species of* Amazona. *The two five-digit catalogue numbers are UF. All six-digit catalogue numbers are USNM.*

Specimen	UF/USNM cat. #	Sex	Location	Least width of shaft	Least depth of shaft	Distal width
Montserrat:			Trants:			
specimen	—	?	Stratum C/D	3.8	3.2	8.8
A. agilis	559191	?	Jamaica	4.1	3.3	8.8
A. collaria	25803	♀	Jamaica	4.2	3.6	9.5
A. vittata	224002	?	Puerto Rico	4.2	3.6	8.9
A. vittata	573528	♀	Puerto Rico	4.3	3.8	10.0
A. ventralis	555753	♂	Hispanola	4.4	3.8	9.7
A. ventralis	555754	♂	Hispanola	4.4	3.8	9.8
A. ventralis	555755	♀	Hispanola	4.4	3.6	9.4
A. leucocephala	25796	♂	Cuba	4.5	3.8	9.7
A. versicolor	487664	?	St. Lucia	5.5	4.7	12.8
A. imperialis	321883	?	Dominica	5.9	5.0	13.7
A. imperialis	318792	♀	Dominica	6.1	5.4	15.4
A. arausiaca	321882	?	Dominica	5.7	5.0	13.6
A. arausiaca	346187	?	Dominica	5.5	5.0	13.5
A. guildingii	613763	♀	St. Vincent	5.9	5.2	14.5

serrat or nearby islands (*Mimus gundlachii*, *Mimus polyglottos*, *Mimus gilvus*, *Margarops fuscus*, *Margarops fuscatus*, *Cinclocerthia ruficauda*, *Turdus* [*Mimocichla*] *plumbeus*, *Cichlherminia lherminieri*, and *Myadestes genibarbis*).

Margarops fuscus (Scaly-breasted Thrasher)

Material.—Stratum A: unit N596E571—mandible, scapula, two carpometacarpi, humerus. Stratum B: unit N596E571—quadrate, scapula, carpometacarpus, ulna, two humeri. Stratum C/D: unit N421/22E645—two ulnae, three tibiotarsi, nine humeri.

Comments.—In January 1983, *Margarops fuscus* was common in forests and occurred in lower numbers in semi-arid woodlands. Overall, *M. fuscus* was less abundant on Montserrat than *M. fuscatus*. It was not found at Trants but on nearby forested slopes. Other prehistoric records are from Barbuda (Pregill et al., 1994).

Margarops fuscatus (Pearly-eyed Thrasher)

Material.—Stratum A: unit N421/22E645—manus phalanx; unit N596E571—manus phalanx. Stratum B: unit N596E571—coracoid, two scapulae, three ulnae, carpometacarpus, two tibiotarsi, tarsometatarsus. Stratum C/D: unit N396E571—tarsometatarsus; unit N421/22E645—quadrate, mandible, two coracoids, two scapulae, three ulnae, carpometacarpus, manus phalanx, femur, eight tibiotarsi, two tarsometatarsi; unit N596E571—humerus, ulna, carpometacarpus.

Comments.—*Margarops fuscatus* is the largest West Indian species of Mimidae. It inhabits forested mountains to scrubby woodlands. In January 1983, *M. fuscatus* was common in the ghauts above Trants, although not in the immediate vicinity of the site. Other prehistoric records are from Anguilla, Antigua, Barbuda, and St. Eustatius (Pregill et al., 1994) and St. Martin (E. S. Wing, personal communication).

Cinclocerthia ruficauda (Brown Trembler)

Material.—Stratum B: unit N596E571—quadrate, mandible, two humeri. Stratum C/D: unit N421/22E645—tibiotarsus.

Comments.—*Cinclocerthia ruficauda* typically is found in rainforest but can occur locally in drier wooded habitats (Zusi, 1969). This species did not occur at Trants in January 1983 but was found in nearby montane forests. It was most common in the moist forests surrounding Chance Peak, which now have been destroyed by volcanic eruptions. *Cinclocerthia ruficauda* also has been recorded from archaeological and paleontological sites on Antigua, Barbuda, and St. Eustatius (Olson, 1982; Steadman et al., 1984*b*), the first two of these islands no longer supporting the species.

Family Turdidae (Muscicapidae)

Cichlherminia lherminieri (Forest Thrush)

Material.—Stratum A: unit N596E571—mandible. Stratum C/D: unit N421/22E571—three coracoids, carpometacarpus.

Comments.—*Cichlherminia lhermineri* is found in semi-arid to humid forests (Bond, 1956; Diamond, 1973). The form on Montserrat is an endemic subspecies, *C. lherminieri lawrencii*. In January 1983, this thrush did not occur in habitats near Trants but was found in the since-devastated moist forests below Chance

Peak and Galway's Soufrière. *Cichlherminia lherminieri* also has been recorded from paleontological sites in Barbuda where it no longer occurs (Pregill et al., 1994).

Mimidae or Turdidae, genus and species indeterminate

Material.—Stratum A: unit N396E571—coracoid. Stratum B: unit N596E571—coracoid, carpometacarpus, two femora. Stratum C/D: unit N421/22E645—two coracoids, humerus, femur.

Comments.—These fragmentary bones lack diagnostic features to identify them further.

Family Icteridae

Icterus cf. *I. oberi* (Montserrat Oriole)

Material.—Stratum B: unit N596E571—humerus, tarsometatarsus.

Comments.—These specimens are referred to *Icterus* rather than other similarly sized genera of Icteridae (*Molothrus*, *Dolichonyx*) by the larger and more distinctly partitioned fossae pneumotricipitalis and the relatively broad but shallow fossa musculo brachialis (humerus), as well as the unique shape, size, and juxtaposition of the three trochleae (tarsometatarsus). Skeletons of *Icterus oberi* were not available, but the two specimens from Trants closely resemble specimens of the similarly sized *I. dominicensis* from Hispanola and Puerto Rico. These two species are larger than the two migrant species of orioles (*I. galbula*, *I. spurius*) that potentially might occur on Montserrat.

Icterus oberi was rare on Montserrat in January 1983. Steadman's only records of this endemic species were 1 km north of Salem Village at mature forest edge (elevation ca. 300 m) on 26 January 1983, and at mature forest edge (ca. 400 m) on the southwest slope (Upper Galway's Estate) of Chance Peak (an area now deforested by volcanic eruptions) on 28 January 1983. Known locally as the "Rainbird," *I. oberi* is the national bird of Montserrat and the island's only endemic species of bird. Wauer (1996) failed to find *I. oberi* during several days of birdwatching in February 1988, but did see the bird on another trip in May 1989, just before Montserrat's forests were damaged by Hurricane Hugo in September 1989. *Icterus oberi* still survived in 1994 (Arendt, 1994).

Passeriformes sp., family and species indeterminate

Material.—Stratum A: unit N421/22E645—coracoid, carpometacarpus; unit N596E571—carpometacarpus. Stratum B: unit N396E571—carpometacarpus; unit N596E571—coracoid, ulna, carpometacarpus, manus phalanx. Stratum C/D: unit 421/22E645—sternum, scapula, two tibiotarsi; unit N596E571—scapula, manus phalanx.

Comments.—These fragmentary bones lack diagnostic features to identify them further.

DISCUSSION

Precisely identified bones from prehistoric sites on tropical islands yield data that can be used to elucidate the related topics of long-term changes in habitat, human impact on the fauna, and human subsistence patterns (Pregill and Olson, 1981; Steadman et al., 1984*b*; Rea, 1986; Steadman, 1995). Our new data on birds from the Trants site are pertinent to each of these issues. Knowledge of these topics varies considerably between West Indian islands because of the intensity and quality of the research done thus far, as well as the timing and intensity of human occupation. Some islands, such as Grand Cayman, have no evidence at all of prehistoric occupation (Stokes and Keegan, 1996), whereas others, such as Antigua, have a long and relatively well-studied prehistoric record (see review in Pregill et al., 1994).

Human impact on island ecosystems typically is implemented through habitat degradation, introduction of predators, and direct predation by humans. We can assess this on Montserrat by comparing the distribution and abundance of prehistoric and modern faunas. *Columba squamosa*, *Geotrygon mystacea*, *Margarops fuscatus*, and *M. fuscus* were the most abundant species excavated from Trants in both 1979 and 1990 (Table 1). Along with *Cinclocerthia ruficauda* and *Cichlherminia lherminieri*, these six species occurred only in forested habitats on Montserrat in January 1983. This suggests either that the prehistoric habitat in the vicinity of Trants was more forested during Saladoid occupation of the island or that the Saladoid peoples preferred to hunt birds in forests, regardless of how far away these forests were from their settlement.

Zenaida aurita was common at Trants in January 1983 but was outnumbered in the bone assemblages by the two forest-dwelling columbids. *Zenaida aurita* prefers open habitats and clearings and thrives in places of high disturbance. That this species was common at Trants until the recent volcanic eruption but relatively uncommon in the bone assemblages adds further support to the notion that the Trants region was more forested when the site was occupied.

Two nonforest species of birds have been extirpated on Montserrat—the shearwater *Puffinus lherminieri*, and gallinule *Porphyrio martinicus*. The shearwater probably has been lost to predation in its nesting burrows by Saladoid peoples and introduced mammalian predators. Island populations of *Porphyrio martinicus* are vulnerable to habitat loss and predation from humans and introduced mammals (Steadman et al., 1984*a*). We should stress here that we do not know the precise time at which any of these species were lost on Montserrat.

The bones of procellariids, rallids, and columbids in Lesser Antillean cultural sites suggests that the Saladoid peoples used these species as food items. Birds from these same three families often make up most of species found in prehistoric sites in the tropical Pacific as well (Steadman, 1995). Shearwaters, rails, and pigeons furnished fat and protein for island peoples whose crops provided mostly carbohydrates. The presence at Trants as well of so many large passerines implies that these birds were also used as food, not surprising given that thrashers and thrushes are at least partially frugivorous and therefore have very tasty meat. The apparent absence of small passerines in the Trants faunal samples could be genuine, or perhaps is due to a preservational bias, or to the use of ¼-in mesh (in three of four quadrants in each excavation unit) rather than the ⅛-in mesh that would retain the smaller bones.

Six of the 11 species reported here were represented in the 95 bird bones from Trants reported by Steadman et al. (1984*b*). The five additional species (*Puffinus lherminieri*, *Porphyrio martinicus*, *Amazona* sp., *Cichlherminia lherminieri*, and *Icterus oberi*) were all recorded from either Stratum C/D of units N396E571 and N421/22E645 (near the 1979 excavation unit) or from unit N596E571 (located ca. 200 m north of the 1979 excavation unit). Excavations in 1990 reached greater depths (100–110 cm) than those in 1979 (80 cm). Radiocarbon dates from Stratum

C/D of the 1990 units indicate that this deposition occurred between ca. 500 BC and AD 400, which corresponds to the entire Saladoid occupation of Trants (Watters, 1994; Petersen, 1996). Therefore, species recovered in these units may represent a more complete sample of vertebrates used by the Saladoid people during their ca. 900-year occupation of Montserrat. Radiocarbon dates for Stratum C/D of the 1979 unit indicate that the first three centuries of Saladoid occupation are not represented in this unit (Watters, 1994). Steadman et al. (1984*b*) recorded two species (*Gallinula chloropus* and *Columbina passerina*) that were not found in the bone assemblage from 1990. The scarcity of *C. passerina* may be habitat related, as this species prefers fragmented or scrubby habitats rather than the large tracts of forest that may have occurred on Montserrat during the time of initial Saladoid occupation.

Finally, the bones from Trants provide a glimpse of past bird life on an island that is facing potential Krakatau-like biotic destruction from volcanic activity (see Thornton, 1995). If Montserrat's birdlife is lost in the current volcanic event, the study of recolonization will be more strongly rooted than on Krakatau in a knowledge of what lived there long before the devastation. Several thousand of Montserrat's only endemic species of bird, *Icterus oberi*, still survived in December 1997 (Atkinson and Gibbons, 1998). Should the volcanic activity continue and the oriole become critically endangered, an effort should be considered to capture individuals for captive breeding, thereby possibly preventing its extinction. This would be beneficial not just for the sake of the oriole, but also for the Montserratians, who are disheartened, displaced, and might take some consolation in knowing that their beloved "Rainbird" may return one day to the Emerald Isle.

ACKNOWLEDGMENTS

We thank E. J. Reitz and D. R. Watters for access to the prehistoric bird bones. S. L. Olson kindly provided access to the USNM bird collection. For comments that improved the manuscript we thank L. Carlson, J. W. Ferner, E. J. Reitz, J. K. Sailer, and E. S. Wing.

LITERATURE CITED

ARENDT, W. J. 1994. Effects of Hurricane Hugo on Montserrat's forest birds. El Pitirre, 7:5.

ATKINSON, P., AND D. GIBBONS. 1998. Status of the Montserrat Oriole *Icterus oberi* since the start of a volcanic eruption in July 1995. Bird Conservation International, 8:309.

BEARD, J. S. 1949. The natural vegetation of the Windward and Leeward islands. Oxford Forestry Memoirs, 21:1–92.

BOND, J. 1956. Check-list of Birds of the West Indies. Academy of Natural Sciences, Philadelphia, Pennsylvania.

———. 1961. Sixth Supplement to the Check-list of Birds of the West Indies. Academy of Natural Sciences, Philadelphia, Pennsylvania.

———. 1974. Nineteenth Supplement to the Check-list of Birds of the West Indies. Academy of Natural Sciences, Philadelphia, Pennsylvania.

BRODKORB, P. 1963. Catalogue of fossil birds: Part 1 (Archaeopterygiformes through Ardeiformes). Bulletin of Florida State Museum, Biological Sciences, 7:179–293.

———. 1971. Catalogue of fossil birds: Part 4 (Columbiformes through Piciformes). Bulletin of Florida State Museum, Biological Sciences, 15:163–266.

DANFORTH, S. T. 1939. The birds of Montserrat. Journal of Agriculture, University of Puerto Rico, 23:47–66.

DIAMOND, J. M. 1973. Ecology of St. Lucia forest birds. Ibis, 115:313–329.

EVANS, P. G. H. 1990. Birds of the Eastern Caribbean. MacMillan Education Ltd., London, United Kingdom.

FERGUS, H. A. 1994. Montserrat: History of a Caribbean Colony. Macmillan Press Ltd., London, United Kingdom.

KEEGAN, W. F. 1994. West Indian archaeology. 1. Overview and foragers. Journal of Archaeological Research, 2:255–284.

LANG, D. M. 1967. Soil and land-use survey no. 22: Montserrat. Regional Research Centre, University of the West Indies, St. Augustine, Trinidad.

MAÍZ, E. 1996. La fauna ornitológica de la familia Columbidae en el sito arqueológico Hernández Colón de Puerto Rico. Pp. 90–99, *in* Ponencias: Primer Seminariode Arqueología del Caribe (M. Veloz Maggiolo and A. Caba Fuentes, eds.). Museo Arqueológico Regional, Altos de Chavón, República Dominicana.

MONTSERRAT VOLCANO OBSERVATORY TEAM. 1997. The ongoing eruption in Montserrat. Science, 276: 371–372.

OLSON, S. L. 1982. Biological archeology in the West Indies. Florida Anthropologist, 35:162–168.

OLSON, S. L., AND W. B. HILGARTNER. 1982. Fossil and subfossil birds from the Bahamas. Pp. 22–56, *in* Fossil Vertebrates from the Bahamas (S. L. Olson, ed.). Smithsonian Contributions to Paleobiology, 48:1–65.

PETERSEN, J. B. 1996. Archaeology of Trants, Montserrat. Part 3. Chronological and settlement data. Annals of Carnegie Museum, 65:323–361.

PETERSEN, J. B., AND D. R. WATTERS. 1991. Archaeological testing at an early Saladoid Trants site, Montserrat, West Indies. Pp. 286–305, *in* Proceedings of the 14th International Congress for Caribbean Archaeology (A. Cummins and P. King, eds.). Barbados Museum and Historical Society, Barbados.

PREGILL, G. K., AND S. L. OLSON. 1981. Zoogeography of West Indian vertebrates in relation to Pleistocene climatic cycles. Annual Review of Ecology and Systematics, 12:75–98.

PREGILL, G. K., D. W. STEADMAN, AND D. R. WATTERS. 1994. Late Quaternary vertebrate faunas of the Lesser Antilles: Historical components of Caribbean biogeography. Bulletin of Carnegie Museum of Natural History no. 30.

REA, A. M. 1986. Verification and reverification: Problems in archaeofaunal studies. Journal of Ethnobiology, 6:9–18.

REITZ, E. J. 1994. Archaeology of Trants, Montserrat. Part 2. Vertebrate fauna. Annals of Carnegie Museum, 63:297–317.

ROUSE, I. 1992. The Tainos. Yale University Press, New Haven, C onnecticut.

SIEGEL, P. E. 1991. Migration research in Saladoid archaeology: A review. Florida Anthropologist, 44:79–91.

STEADMAN, D. W. 1988. New species of *Porphyrio* (Aves: Rallidae) from archaeological sites in the Marquesas Islands. Proceedings of Biological Society, Washington, 101:162–170.

———. 1995. Prehistoric extinctions of Pacific island birds: Biodiversity meets zooarchaeology. Science, 267:1123–1131.

STEADMAN, D. W., AND D. S. PAHLAVAN. 1992. Extinction and biogeography of birds on Huahine, Society Islands, French Polynesia. Geoarchaeology, 7:449–483.

STEADMAN, D. W., G. K. PREGILL, AND S. L. OLSON. 1984*a*. Fossil vertebrates from Antigua, Lesser Antilles: Evidence for the late Holocene human-caused extinctions in the West Indies. Proceedings of the National Academy of Sciences, U.S.A., 81:4448–4451.

STEADMAN, D. W., D. R. WATTERS, E. J. REITZ, AND G. K. PREGILL. 1984*b*. Vertebrates from archaeological sites on Montserrat, West Indies. Annals of Carnegie Museum, 53:1–29.

STEADMAN, D. W., D. S. PAHLAVAN, AND P. V. KIRCH. 1990. Extinction, biogeography, and human exploitation of birds on Tikopia and Anuta, Polynesian outliers in the Solomon Islands. Bishop Museum Occasional Papers, 30:118–153.

STEADMAN, D. W., R. L. NORTON, M. R. BROWNING, AND W. J. ARENDT. 1997. The birds of St. Kitts, Lesser Antilles. Caribbean Journal of Science, 33:1–20.

STOKES, A. V., AND W. F. KEEGAN. 1996. A reconnaissance for prehistoric archaeological sites on Grand Cayman. Caribbean Journal of Science, 32:425–430.

THORNTON, I. 1995. Krakatau: The Destruction and Reassembly of an Island Ecosystem. Harvard University Press, London, United Kingdom.

WATTERS, D. R. 1994. Archaeology of Trants, Montserrat. Part 1. Field methods and artifact density distributions. Annals of Carnegie Museum, 63:265–295.

WATTERS, D. R., E. J. REITZ, D. W. STEADMAN, AND G. K. PREGILL. 1984. Vertebrates from archaeological sites on Barbuda, West Indies. Annals of Carnegie Museum, 53:383–411.

WAUER, R. H. 1996. A Birder's West Indies. University of Texas Press, Austin, Texas.

WETMORE, A. 1952. A record of the Black-capped Petrel, *Pterodroma hasitata*, in Martinique. Auk, 69:460.

Wing, E. S. 1989. Human exploitation of animal resources in the Caribbean. Pp. 137–152, *in* Biogeography of the West Indies: Past, Present, and Future (C. A. Woods, ed.). Sandhill Crane Press, Gainesville, Florida.

Zusi, R. L. 1969. Ecology and adaptations of the Trembler on the island of Dominica. Living Bird, 8:137–164.

INDEX TO VOLUME 68

CONTENTS

ARTICLES

New karyotypes of shrews (Mammalia: Soricidae) from Cameroon and Somalia . . . . Duane A. Schlitter, Rainer Hutterer, Tiziano Maddalena, and Lynn W. Robbins 1

The head skeleton of *Amphisbaena alba* Linneaus . . . . Ricardo Montero and Carl Gans 15

New species and immature instars of crane flies of subgenus *Tipulodina* Enderlein from Sulawesi (Insecta: Diptera: Tipulidae: *Tipula*) . . . . Chen W. Young 81

Tournaisian (early Osagean) brachiopods from a bioherm in the St. Joe Formation near Kenwood, Oklahoma . . . . John L. Carter 91

Biology and immature stages of snail-killing flies belonging to the genus *Tetanocera* (Insecta: Diptera: Sciomyzidae). III. Life histories of the predators of aquatic snails . . . B. A. Foote 151

Revision of the Wind River faunas, Early Eocene of central Wyoming. Part 14. Postcranium of *Shoshonius cooperi* (Mammalia: Primates) . . . . Marian Dagosto, Daniel L. Gebo, and K. Christopher Beard 175

Fossil decapod crustaceans from the late Oligocene to early Miocene Pysht Formation and late Eocene Quimper Sandstone, Olympic Peninsula, Washington . . . . Carrie E. Schweitzer and Rodney M. Feldmann 215

Archaeology of Trants, Montserrat. Part 5. Prehistoric avifauna . . . . Kelley R. Reis and David W. Steadman 275

REVIEW

Rattlesnake: Portrait of a Predator (Manny Rubio) . . . . Travis J. LaDuc 213

NEW TAXA

NEW SPECIES

†*Asthenognathus cornishorum*, **new species** 259

†*Cranaena salinensis*, **new species** 143

†*Dielasma oklahomensis*, **new species** 145

†*Eomartiniopsis*, **new species** 124

†*Geniculifera siphuncula*, **new species** 99

†*Macrocheira longirostra*, **new species** 253

†*Pustula kenwoodensis*, **new species** 102

†*Pustula oklahomae*, **new species** 105

†*Rhynchopora kollari*, **new species** 116

†*Schizophoria mayesensis*, **new species** 109

Tipula (*Tipulodina*) *nettingi*, **new species** 82

Tipula (*Tipulodina*) *phasmatodes*, **new species** 88
†*Trichopeltarion berglundorum*, **new species** 238
† Fossil taxa

AUTHOR INDEX

Beard, K. Christopher 175
Carter, John L. 91
Dagosto, Marian 175
Feldmann, Rodney M. 215
Foote, B. A. 151
Gans, Carl 15
Gebo, Daniel L. 175
Hutterer, Rainer 1
LaDuc, Travis J. 213
Maddalena, Tiziano 1
Montero, Ricardo 15
Reis, Kelley R. 275
Robbins, Lynn W. 1
Schlitter, Duane A. 1
Schweitzer, Carrie E. 215
Steadman, David W. 275
Young, Chen W. 81

INSTRUCTIONS FOR AUTHORS

ANNALS OF CARNEGIE MUSEUM consist of contributions to the earth sciences (including paleontology), life sciences, and anthropology, in 30 by 46 picas format (127 by 195 mm or 5 by 7⅝ inches). Submit all manuscripts to the Office of Scientific Publications. Authors should give particular attention to scientific content, format, and general style for the ANNALS. **Manuscripts that do not conform to the style of the ANNALS will be returned to the author immediately.** Every manuscript will be subjected to external peer review. Authors should submit the names, addresses, phone and fax numbers, and e-mail addresses of at least four qualified potential reviewers for each manuscript. Authors will be asked to subsidize, if funds are available, any or all costs of publication (approximately $100/page printed). A detailed set of instructions to authors may be requested from the Office of Scientific Publications.

Manuscript Style.—Articles should include the following items in this order: title page, abstract, text (with desired headings), acknowledgments, literature cited, tables, figure captions, and copies of illustrations. All manuscripts must be typed ***double-spaced*** on standard 8½ by 11-inch white bond paper, with at least one-inch margins all around, and submitted ***in quadruplicate***—an original for the editors, and three review copies. All pages should be numbered, including tables, literature cited, and the list of figure captions. Only correspondence quality or better dot matrix printouts will be accepted; draft mode is unacceptable. A monospaced font, (e.g., Courier) is required. A disk in WordPerfect x.x or ASCII is helpful.

Title Page. The title should be brief, include the animal or plant group involved, be placed on a separate page, and appear two to three inches below the top margin. Include the author's name(s) and the affiliations of non-CMNH authors. In the case of multiple authorship, indicate the address to which proofs should be sent.

Abstracts. Abstracts should be short, but substantive, and included at the head of the first page of text.

Text. Do not right justify text or break (hyphenate) a word at the end of a line. ***Footnotes and acknowledgments as footnotes are unacceptable.*** All text is double-spaced in a monospaced font (e.g., Courier).

Tables and Figure Legends. The list of figure legends and each table should be typed consecutively on individual pages separate from the text. Tables must be double-spaced throughout with **no vertical lines**.

Measurements. Metric units should be used, if possible.

Literature Cited. All references to literature in text must appear in the Literature Cited section. The data (author, date, and page) in both citations must agree. ***Do not abbreviate the titles of periodicals or serials.*** The following style, double-spaced, should be used in Literature Cited:

1) Two authors in a journal series:

Soltis, D. E., and P. S. Soltis. 1992. The distribution of selfing rates in homosporous ferns. American Journal of Botany, 79:97–100.

2) Same authors repeated—use three-em dash:

———. 1923. The fauna of the Ardyn Obo Formation. American Museum of Natural History Novitates, 98:1–5.

3) Same authors plus a third author—repeat all authors:

Knutson, L. V., R. E. Orth, and W. L. Murphy. 1986. Catalog of Sciomyzidae (Diptera) of America north of Mexico. Entomography, 4: 1–53.

4) Chapter in an edited volume:

Rausch, R. L. 1963. A review of the distribution of Holarctic mammals. Pp. 29–43, *in* Pacific Basin Biogeography (J. L. Gressitt, ed.). Bishop Museum Press, Honolulu, Hawaii.

5) Unpublished dissertation:

Smith, J. P. 1976. Review of Eocene Mammals. Unpublished Ph.D. Dissert., University of California, Berkeley, California.

6) Book:

White, M. J. D. 1961. The Chromosomes. Metheuen and Co., Ltd., London, United Kingdom.

7) Journal articles with usual volume and issue number:

Anderson, W. I. 1969. Lower Mississippian conodonts from northern Iowa. Journal of Paleontology, 43:916–928.

Figures. Including all illustrative materials (line art, halftones, photographs), figures are to be numbered in Arabic numerals. Four sets of figures are required, one (original artwork) for reproduction, three for reviewers. Photocopies of photographs for reviewers are usually not acceptable but are adequate for line drawing review copies. Figures may not be larger than 17 by 12 inches. Reducing figures is the responsibility of the author. All figures must be reducible to a maximum of 127 by 195 mm (30 by 46 picas) without loss of clarity. Line copy should be designed for reduction to ⅔ or ½ or actual size. Typewritten figure copy will not be accepted. Photographic figures should be submitted at **actual reproduction size**, if possible.

Rectangular halftone figures should be abutted, without intervening spaces. The printer will insert narrow white spaces during the reproduction process. All figures must have **minimally** one-inch borders all around. Each figure should be given a protective cover and identified on the back side.

Lettering and/or a magnification scale (linear metric scale) for rectangular halftone figures should be placed directly on the photo, not in a blank space between photos. The scale or lettering for closely cropped photos can be placed in blank areas close to the figure.

Proof.—The author should answer all queried proof marks and check the entire proof copy. Return corrected page proof with the edited manuscript ***promptly*** to the Office of Scientific Publications.

If an author chooses to make extensive alterations to a paper in proof stage, the author will bear the cost. Original manuscripts will not be returned unless requested. Figures will be returned to the author only if requested prior to publication.

HECKMAN
BINDERY, INC.
Bound-To-Please®
JULY 01
N. MANCHESTER, INDIANA 46962

SMITHSONIAN INSTITUTION LIBRARIES
3 9088 00993 3714